

Distribution Agreement

In presenting this thesis or dissertation as a partial fulfillment of the requirements for an advanced degree from Emory University, I hereby grant to Emory University and its agents the non-exclusive license to archive, make accessible, and display my thesis or dissertation in whole or in part in all forms of media, now or hereafter known, including display on the world wide web. I understand that I may select some access restrictions as part of the online submission of this thesis or dissertation. I retain all ownership rights to the copyright of the thesis or dissertation. I also retain the right to use in future works (such as articles or books) all or part of this thesis or dissertation.

Signature:

Patrick Gross

Date

Development of Enantioselective C–N Bond Forming Reactions using Planar Chiral Rh(III) Indenyl

Catalysts

By

Patrick Gross

Doctor of Philosophy

Chemistry

Simon B. Blakey, Ph.D.
Advisor

Huw M. L. Davies, Ph.D.
Committee Member

Frank E. McDonald, Ph.D.
Committee Member

Accepted:

Kimberly J. Arriola, Ph.D.
Dean of the James T. Laney School of
Graduate Studies

Date

Development of Enantioselective C–N Bond-Forming Reactions using Planar Chiral Rh(III) Indenyl
Catalysts

By

Patrick Gross

B.S., College of Charleston, 2019

Advisor: Simon B. Blakey, Ph.D.

An abstract of
A dissertation submitted to the Faculty of the
James T. Laney School of Graduate Studies of Emory University
in partial fulfillment of the requirements for the degree of
Doctor of Philosophy
in Chemistry
2024

Abstract

Development of Enantioselective C–N Bond-Forming Reactions using Planar Chiral Rh(III) Indenyl

Catalysts

By: Patrick Gross

As drug designs exhibit increased three-dimensional complexity, the stereoselective formation of C–N bonds has become increasingly important in synthetic organic chemistry. To enable the rapid synthesis of chiral C–N containing motifs, the Blakey group developed a planar chiral Rh(III) indenyl catalyst to render a redox-neutral allylic C–H amidation enantioselective. Herein we report the application of this chiral catalyst platform to the development of two enantioselective methods for the synthesis of chiral aziridines and 2-aminotetralins. The enantioselective aziridination method uses a sulfonyl protected hydroxylamine nitrogen sources and demonstrates a previously unseen level of exclusive selectivity for unactivated alkenes. This transformation is proposed to operate via a migratory insertion mechanism and not via the more common metal nitrene intermediate typically reported for transition metal-catalyzed aziridinations of alkenes. Exchanging the sulfonyl protecting group of the hydroxylamine for a carbamate enabled the 1,2-arylamination of 4-phenylbutenes to form 2-aminotetralins, a drug scaffold of longstanding pharmaceutical interest. This transformation is a new example of a Group IX piano stool catalyzed activation of an electrophilic nitrogen source towards indirect nucleophilic attack. Optimization studies revealed the indenyl scaffold to be privileged, making our planar chiral catalysts ideal choice to render this transformation enantioselective. During our investigation of the scope of this method, competing 6-*endo* and 5-*endo* cyclization modes were observed leading to the formation of 2-aminotetralin regioisomers. The formation of a spirocyclic intermediate in the 5-*endo* pathway was confirmed through isolation; intentional trapping of this intermediate expanding the scope of this 1,2-arylamination to include a variety amine-substituted [4.5]- and [5.5]-carbospirocycles. Mechanistic investigations revealed an electrophilic aromatic substitution mechanism to be operative for the C–C bond formation. We propose a migratory insertion mechanism leading to the formation of an electrophilic four membered aza-metallocycle which is subjected to nucleophilic attack from the aromatic ring.

Development of Enantioselective C–N Bond-Forming Reactions using Planar Chiral Rh(III) Indenyl
Catalysts

By

Patrick Gross

B.S., College of Charleston, 2019

Advisors: Simon B. Blakey, Ph.D.

A dissertation submitted to the Faculty of the
James T. Laney School of Graduate Studies of Emory University
in partial fulfillment of the requirements for the degree of
Doctor of Philosophy
in Chemistry
2024

Acknowledgments

The journey to completing a PhD is often compared to the challenge of running a marathon. A long arduous journey filled with many highs and lows along the way. Requiring endurance, commitment, and mental fortitude to reach the finish line. While this PhD journey has been an individual race, there have been people in my life standing on the sidelines cheering me on. Without the constant support these people have given me over the years I am not sure if I would be completing this PhD journey. I would like to begin by thanking my advisor Dr. Simon Blakey. Throughout these five years you have been an incredible mentor and your support and encouragement have kept me going even when it felt like there was no way forward. I am grateful for the freedom you provided me to explore my ideas, while always having your office door open to discuss them. To my committee members, Dr. Huw Davies and Dr. Frank McDonald, thank you for the feedback and advice you have given me over these years. While the yearly milestones are stressful, I have always looked forward to sharing my chemistry with you and the scientific discussions we would have. I would also like to thank my College of Charleston undergraduate advisor Dr. Neal Tonks, my time in your lab was instrumental in discovering my passion for organic chemistry and I would have never considered pursuing a PhD had it not been for your guidance.

I would also like to thank the lab members of the Blakey lab both past and present. You have made this graduate experience so much more enjoyable, whether it was because of the many ridiculous jokes or the excellent chemistry discussions we would have. I have looked forward to coming to lab every day to work alongside you. To Michael, while we knew each other from CofC we became good friends in graduate school, and I will miss all the strange antics you were so well known for in lab. You are an incredible chemist that I learned so many skills from and I do not believe I would be the chemist I am today without the knowledge you shared with me. To Christina, our cohort was small when we joined Emory, and I am so happy we joined the Blakey lab together. Working next to you these past five years has brought me so much joy. You are one of the most impressive chemists I know, and I have learned so much about being an independent and driven scientist from seeing your amazing work.

Next, I would like to thank my family and friends for their endless and never wavering support. An meine Eltern I hätte diese Reise nie antreten können, wäre es nicht für eure Unterstützung. Ihr habt so viel Unglaubliches für mich getan, nicht nur in diese letzten fünf Jahre, sondern schon mein Leben lang. Die Erfahrungen, die ihr mir beschert habt, werde ich nie vergessen und sie werden mir mein Leben lang weiter helfen. Ich bin so unglaublich dankbar, euch also euch als Eltern zu haben. Ich liebe euch so sehr. To my sister Anna, I am incredibly proud of you for beginning your medical school journey. While my graduate journey is ending and yours is just beginning, I hope we will find time to spend together. To Jeremy, you have been a wonderful friend my whole life and we have shared many incredibly memories. I look forward to many more in the future. Last, but not least, I would like to thank Kim. I am so happy our paths crossed during our time at Emory. You have brought so much love and joy into my life. I cherish every day that we have spent together whether it has been on lovely hikes, kayak trips, or weekends spent cooking delicious meals. You have been incredibly supportive and have helped me through many difficult times. I am also incredibly proud of you for starting your PhD journey and I cannot wait to cheer for you when you cross the finish line. I love you so much.

Table of Contents

Chapter 1: Strategies for the Enantioselective Synthesis of Aziridines

| | |
|--|----|
| 1.1 Introduction to Aziridines | 1 |
| 1.2 Enantioselective Synthesis of Aziridines | 3 |
| 1.2.1 Overview of Aziridine Synthetic Strategies | 3 |
| 1.2.2 Enantioselective Synthesis of Aziridines via Intramolecular Condensation | 4 |
| 1.2.3 Enantioselective Synthesis of Aziridines via Carbon Addition to Imines | 5 |
| 1.2.4 Enantioselective Synthesis of Aziridines via Nitrogen Addition to Alkenes | 8 |
| 1.3 Transition Metal Catalyzed Enantioselective Aziridination of Unactivated Alkenes | 13 |
| 1.4 Conclusion | 15 |
| 1.5 References | 16 |

Chapter 2: Development of an Enantioselective Unactivated Alkene Aziridination Method using Planar Chiral Rh(III) Indenyl Catalysts and the Synthesis of Electron Rich Planar Chiral Indenyl Scaffolds

| | |
|---|----|
| 2.1 Introduction to Chiral Cyclopentadienyl Catalysts | 25 |
| 2.1.1 Overview of Chiral Cyclopentadienyl Transition Metal Catalysts | 25 |
| 2.1.2 Chiral Cp Ligands of C ₂ -Symmetry | 26 |
| 2.1.3 Planar Chiral Cp Transition Metal Complexes | 28 |
| 2.2 Development of Group IX Transition Metal Catalyzed Allylic C–H Functionalization Strategies in the Blakey Group | 29 |
| 2.2.1 Development of Group IX Catalyzed Oxidative Allylic C–H Functionalization Methods | 30 |
| 2.2.2 Development of Group IX Catalyzed Redox Neutral Allylic C–H Functionalization Methods | 32 |

| | |
|---|-----|
| 2.2.3 Development of a Planar Chiral Rh(III) Indenyl Catalyst for Enantioselective C–H Amidation | 33 |
| 2.3 Enantioselective Aziridination of Unactivated Alkenes Using A Planar Chiral Rh(III) Indenyl Catalyst | 38 |
| 2.3.1 Evaluation of Catalytic Activity of First- and Second-Generation Planar Chiral Catalysts | 39 |
| 2.3.2 Synthesis of Third-Generation Electron Rich Planar Chiral Catalysts | 40 |
| 2.3.3 Optimization of Reaction Conditions | 45 |
| 2.3.4 Reaction Scope | 47 |
| 2.3.5 Mechanistic Investigation | 51 |
| 2.4 Conclusion | 53 |
| 2.5 References | 55 |
| 2.6 Supporting Information | 63 |
| 2.6.1 General Information | 63 |
| 2.6.2 Experimental Procedures and Tabulated Data | 64 |
| 2.6.3 Supporting Information References | 125 |
| 2.6.4 NMR and HPLC Data | 128 |
| Chapter 3: Group IX Transition Metal Catalyzed Activation of Electrophilic Nitrogen Reagents Towards Direct and Indirect Nucleophilic Attack | |
| 3.1 Introduction to Transition Metal Catalyzed Activation of Electrophilic Nitrogen Reagents | 259 |
| 3.2 Direct Nucleophilic Attack | 261 |
| 3.3 Indirect Nucleophilic Attack | 265 |
| 3.4 Conclusion | 271 |
| 3.5 References | 272 |

Chapter 4: Enantioselective 1,2-Arylamination: Synthesis of 2-Aminotetralins and

2- Amino Carbospirocycles

| | | |
|--------------|---|------------|
| 4.1 | Introduction to 2-Aminotetralins | 276 |
| 4.1.1 | 2-Aminotetralins in Medicinal Chemistry | 276 |
| 4.1.2 | Enantioselective Synthesis of 2-Aminotetralins | 278 |
| 4.2 | Development of an Enantioselective 1,2-Arylamination | 280 |
| 4.2.1 | Reaction Discovery and Optimization | 280 |
| 4.2.2 | Regioselectivity and Scope of the Enantioselective 1,2-Arylamination | 286 |
| 4.2.3 | Mechanistic Investigations | 290 |
| 4.3 | Conclusion | 293 |
| 4.4 | References | 295 |
| 4.5 | Supporting Information | 302 |
| 4.5.1 | General Information | 302 |
| 4.5.2 | Experimental Procedures and Tabulated Data | 304 |
| 4.5.3 | Supporting Information References | 338 |
| 4.5.4 | NMR, HPLC and SFC Data | 341 |

List of Tables

| | |
|--|-----|
| Table 2.1 Optimization of Silver Halide Additive Loading | 46 |
| Table 4.1 Optimization of Base and Silver Salt Additives in the Racemic 1,2-Arylamination | 282 |
| Table 4.2 Screening of Catalyst and Solvent in the Racemic 1,2-Arylamination. | 283 |

List of Figures

| | |
|---|-----|
| Figure 1.1 Biologically Active Compounds of Natural and Synthetic Origin Containing Aziridines. | 1 |
| Figure 1.2 Nucleophilic Ring Opening of a Chiral Aziridines. | 2 |
| Figure 1.3 Overview of the Synthetic Disconnections to Access Aziridines. | 4 |
| Figure 1.4 Overview of Transition Metal Nitrene Intermediates in the Aziridination of Alkenes. | 10 |
| Figure 2.1 Overview of C_2 -Symmetric Chiral Cp Ligands and their Rhodium Complexes. | 26 |
| Figure 2.2 Overview of Planar Chiral Rhodium Complexes. | 28 |
| Figure 2.3 Overview of Ind Ligand Coordination and the Indenyl Effect. | 34 |
| Figure 2.4 Third Generation Electron Rich Planar Chiral Rh(III) Indenyl Catalysts | 41 |
| Figure 3.1 Overview of Mechanisms for Transition Metal Catalyzed C–N Bond Formations with Electrophilic Nitrogen Sources | 260 |
| Figure 4.1 Examples of 2-Aminotetralin Motifs Found in Biologically Active Compounds. | 277 |

List of Schemes

| | |
|---|----|
| Scheme 1.1 Application of Chiral Aziridines in Total Synthesis. | 3 |
| Scheme 1.2 Synthesis of Chiral Aziridine Building Blocks via Intramolecular Condensation. | 4 |
| Scheme 1.3 Enantioselective Addition of Diazo Reagents to Imines. | 6 |
| Scheme 1.4 Enantioselective Addition of Sulfonium Ylides to Imines. | 7 |
| Scheme 1.5 Synthesis of an Aziridine Intermediate Towards Epothilone B Analogues. | 8 |
| Scheme 1.6 Enantioselective Aziridinations via aza-Michael Initiated Ring Closures. | 9 |
| Scheme 1.7 Copper and Silver Catalyzed Enantioselective Aziridinations of Alkenes. | 11 |
| Scheme 1.8 Cobalt, Ruthenium, and Rhodium Catalyzed Enantioselective Aziridinations of Alkenes. | 12 |
| Scheme 1.9 Cobalt, and Ruthenium Catalyzed Enantioselective Aziridinations of Unactivated Alkenes. | 13 |
| Scheme 1.10 Rhodium Catalyzed Enantioselective Aziridinations of Unactivated Alkenes. | 14 |
| Scheme 2.1 Development of Rhodium Catalyzed Oxidative Allylic C–H Functionalization Strategies. | 30 |
| Scheme 2.2 First-Generation Allylic C–H Functionalization Mechanism. | 31 |
| Scheme 2.3 Development of Redox-Neutral Allylic C–H Functionalization Strategies. | 33 |
| Scheme 2.4 Baker’s Planar Chiral Indenyl Complex. | 35 |
| Scheme 2.5 Synthetic Route towards the First-Generation Planar Chiral Rh(III) Indenyl Catalyst. | 36 |
| Scheme 2.6 Planar Chiral Rh(III) Indenyl Catalyzed Enantioselective Allylic C-H Amidation. | 36 |
| Scheme 2.7 Mechanism of the Enantioselective Allylic C–H Amidation. | 37 |
| Scheme 2.8 Enantioselective Allylic C–H Amidation using Second-Generation Planar Chiral Indenyl Catalysts. | 38 |

| | |
|---|-----|
| Scheme 2.9 Synthesis of Pyrrolidines from Unactivated Alkenes | 39 |
| Scheme 2.10 Screen of First- and Second-Generation Planar Chiral Indenyl Catalyst in the Enantioselective Unactivated Alkene Aziridination | 40 |
| Scheme 2.11 Ligand Synthesis of the Third-Generation Electron Rich Planar Chiral Rh(III) Indenyl Catalyst | 42 |
| Scheme 2.12 Synthesis of Electron-Rich Ind ^X Rh(I)COD Complexes | 43 |
| Scheme 2.13 Synthesis of Racemic Third Generation Planar Chiral Rh(III) Precatalysts Dimers and Evaluation in the Unactivated Alkene Aziridination | 44 |
| Scheme 2.14 Chiral Resolution Attempts of Rh(I) and Rh(III) Planar Chiral Complexes | 45 |
| Scheme 2.15 Scope of Enantioselective Unactivated Alkene Aziridinations Bearing a Variety of Functional Groups | 47 |
| Scheme 2.16 Scope of Sterically Bulky Substrates in the Enantioselective Unactivated Alkene Aziridination | 48 |
| Scheme 2.17 Determination of the Effects of Carbon Linker Length in the Enantioselective Unactivated Alkene Aziridinations using Varied Linker Lengths | 49 |
| Scheme 2.18 Competition Substrate Scope in the Enantioselective Unactivated Alkene Aziridination | 51 |
| Scheme 2.19 Free Energy Diagram of Hydroxylamine Activation and Potential Metal-Nitrene Formation | 52 |
| Scheme 2.20 Free Energy Diagram of Alkene Migratory Insertion and Formation of Aziridine | 53 |
| Scheme 3.1 Ir(III) Catalyzed Synthesis of Aryl γ -Lactams and Spirocyclic γ -Lactams | 262 |
| Scheme 3.2 Co(III) Catalyzed Synthesis of Cyclic Arylcarbamates via Nucleophilic Attack | 263 |
| Scheme 3.3 Nucleophilic Attack of Enolates onto Co(V)-Nitrenes for the α -Amidation of Carbonyl Compounds. | 264 |

| | |
|---|-----|
| Scheme 3.4 Ir(III) Catalyzed Synthesis of Hydrazides via N–N Bond Formation | 265 |
| Scheme 3.5 Divergent Synthesis of Amine Substituted γ - and δ -Lactams via Indirect Amine Nucleophilic Attack onto Iridium Activated Electrophilic Nitrogen Reagents | 266 |
| Scheme 3.6 Ligand Controlled Indirect Carboxylate Nucleophilic Attack on to Iridium Activated Hydroxylamines. | 267 |
| Scheme 3.7 Synthesis of γ -Lactams via Iridium 1,3-Dipole Intermediates. | 268 |
| Scheme 3.8 Synthesis of γ -Lactams via Indirect Carboxylates Nucleophilic Attack onto Iridium Activated of Dioxazolones. | 269 |
| Scheme 3.9 Ir(III) Catalyzed Biomimetic Cascade Synthesis of Polycyclic δ -Lactams via Indirect Aryl Nucleophilic Attack. | 270 |
| Scheme 4.1 Enantioselective Synthesis of 2-Aminotetralins from β -Tetralones. | 278 |
| Scheme 4.2 Common Synthetic Routes Towards β -Tetralones. | 279 |
| Scheme 4.3 Enantioselective Syntheses of 2-Aminotetralins Involving Aziridines Intermediates. | 280 |
| Scheme 4.4 Discovery of the 1,2-Arylamination of 4-phenylbutene. | 281 |
| Scheme 4.5 Examination of Hydroxylamine Carbamate Nitrogen Sources for the 1,2-Arylamination. | 284 |
| Scheme 4.6 Catalyst Optimization of the Enantioselective 1,2-Arylamination. | 285 |
| Scheme 4.7 Observation of 2-aminotetralin Regioisomers and Proposed Mechanisms Leading to the Formation of both Regioisomers. | 286 |
| Scheme 4.8 Scope of Chiral 2-Aminotetralins for the Enantioselective 1,2-Arylamination. | 288 |
| Scheme 4.9 Scope of Chiral 2-Aminospirocycles for the Enantioselective 1,2-Arylamination. | 289 |
| Scheme 4.10 Attempted Synthesis of a 2-Aminotetrahydroazulene Leading to the Formation of a Bridged Bicyclic Azepine. | 290 |
| Scheme 4.11 Intramolecular Kinetic Isotope Effect Study | 291 |

Scheme 4.12 Mechanistic Investigations to Identify the Electrophilic Intermediate in the 1,2- Arylamination. 292

Scheme 4.13 Proposed Mechanism for the Enantioselective 1,2-Arylamination. 293

Table of Abbreviations

| | |
|--------------------|---|
| Ac | Acetyl |
| ACN <i>or</i> MeCN | Acetonitrile |
| Ar | Aryl |
| BINOL | 1,1'-Bi-2-naphthol |
| BINOL-Cp | BINOL-derived cyclopentadienyl |
| Bn | Benzyl |
| Boc | <i>tert</i> -Butoxycarbonyl |
| Bz | Benzoyl |
| Cbz | Carboxybenzyl |
| CDI | 1,1'-Carbonyldiimidazole |
| COD | 1,5-Cyclooctadiene |
| Cp | Cyclopentadienyl |
| Cp* | 1,2,3,4,5-Pentamethylcyclopentadienyl |
| Cp ^E | 1,3-bis(ethoxycarbonyl)cyclopentadienyl |
| Cp ^X H | Functionalized cyclopentadiene |
| DCE | 1,2-Dichloroethane |
| d | Day |
| DBU | 1,8-Diazabicyclo[5.4.0]undec-7-ene |
| DCM | Dichloromethane |
| DEAD | Diethyl azodicarboxylate |
| DFT | Density functional theory |
| DIAD | Diisopropyl azodicarboxylate |
| DIC | N, N'-Diisopropylcarbodiimide |
| DMAP | 4-Dimethylaminopyridine |

| | |
|---------------------------------|---|
| DMF | Dimethylformamide |
| d.r. | Diastereomeric ratio |
| EDCI | 1-Ethyl-3-(3-dimethylaminopropyl)carbodiimide |
| e.e. | Enantiomeric excess |
| e.r. | Enantiomeric ratio |
| Et | Ethyl |
| Et ₂ O | Diethyl Ether |
| EWG | Electron-withdrawing group |
| hr | Hour |
| HFIP | 1,1,1,3,3,3-Hexafluoro-2-propanol |
| HPLC | High-Performance Liquid Chromatography |
| Ind | Indenyl |
| Ind ^X | Functionalized Indenyl ligand |
| Ind* | 1,2,3,4,5,6,7-heptamethylindenyl |
| <i>i</i> Pr | <i>iso</i> -Propyl |
| KAIST | Korea Advanced Institute of Science and Technology |
| L | Ligand |
| M | Metal |
| <i>m</i> CPBA | <i>meta</i> -Chloroperbenzoic acid |
| Me | Methyl |
| min | Minute |
| Ms | Mesyl |
| M.S. | Molecular sieves |
| NaBAr ^F ₄ | Sodium tetrakis[3,5-bis(trifluoromethyl)phenyl]borate |
| NBS | <i>N</i> -Bromosuccinimide |

| | |
|--------------|---|
| NFTB | 1,1,1,3,3,3-Hexafluoro-2-trifluoromethyl-2-propanol |
| NMR | Nuclear Magnetic Resonance |
| Np | Neopentyl |
| <i>n</i> Pr | <i>n</i> -Propyl |
| Ns | Nosyl |
| Nu | Nucleophile |
| OAllyl | Allyl ether |
| OTf | Trifluoromethanesulfonate (triflate) |
| P or PG | Protecting group |
| Ph | Phenyl |
| Phth | Phthalimide |
| Pin | Pinacol |
| Piv | Pivaloyl |
| <i>p</i> TSA | <i>p</i> -Toluenesulfonic acid |
| TBAI | Tetra- <i>N</i> -butylammonium iodide |
| TBDPS | <i>tert</i> -Butyldiphenylsilyl |
| TBS | <i>tert</i> -Butyldimethylsilyl |
| <i>t</i> Bu | <i>tert</i> -Butyl |
| TEA | Triethylamine |
| TES | Triethylsilyl |
| Tf | Triflyl |
| TFA | Trifluoroacetic acid |
| TFE | 2,2,2-Trifluoroethan-1-ol |
| THF | Tetrahydrofuran |
| TMS | Trimethylsilyl |

| | |
|------|--|
| Troc | 2,2,2-Trichloroethoxycarbonyl |
| Ts | Tosyl |
| X | Halide (generally): also, carbon or heteroatom |

Chapter 1: Strategies for the Enantioselective Synthesis of Aziridines

In this chapter we will discuss the utility and synthesis of aziridines. Particular attention will be given towards enantioselective aziridination strategies. Emphasis will be placed on the discussion of transition metal-catalyzed enantioselective aziridinations with a particular focus centered upon the enantioselective aziridination of unactivated alkenes. The discussion of the literature precedents surrounding enantioselective aziridination strategies will lay the groundwork for Chapter 2.

1.1 Introduction to Aziridines

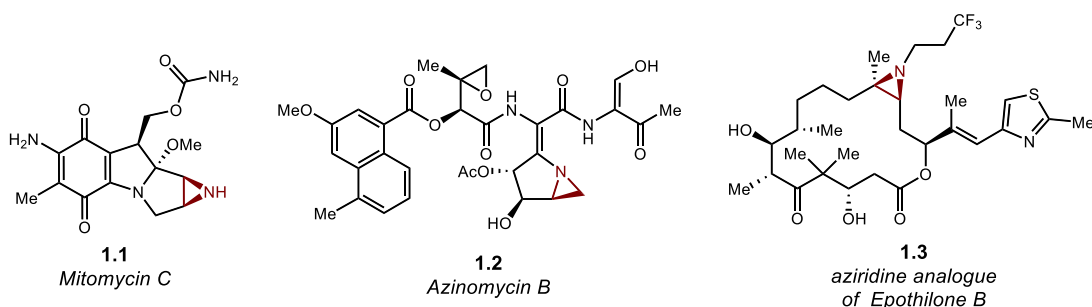


Figure 1.1 Biologically Active Compounds of Natural and Synthetic Origin Containing Aziridines.

Aziridines are the smallest and simplest class of nitrogen-containing heterocycles and are often compared to their oxygen containing counterparts, epoxides.¹ Aziridines have been found in a number of natural products and the strained three membered ring of aziridines is often implicated in their biological activity.^{2,3} The Mitosanes are the most well-known class of aziridine-containing natural products, Mitomycin C **1.1** has been found to be the most effective anti-cancer and antibiotic compound, due in part to the aziridine acting as the active DNA-crosslinking warhead (**Figure 1.1**).⁴ Azinomycin A and B **1.2** and are another class of anticancer compounds in which the bicyclic aziridine motif once again binds DNA.⁵ Aziridines have also found success as synthetic derivatives as the installation of the aziridine ring can increase the potency of the target compound, as observed in the synthesis of Epothilone B derivatives **1.3** by K.C. Nicolaou.^{6,7}

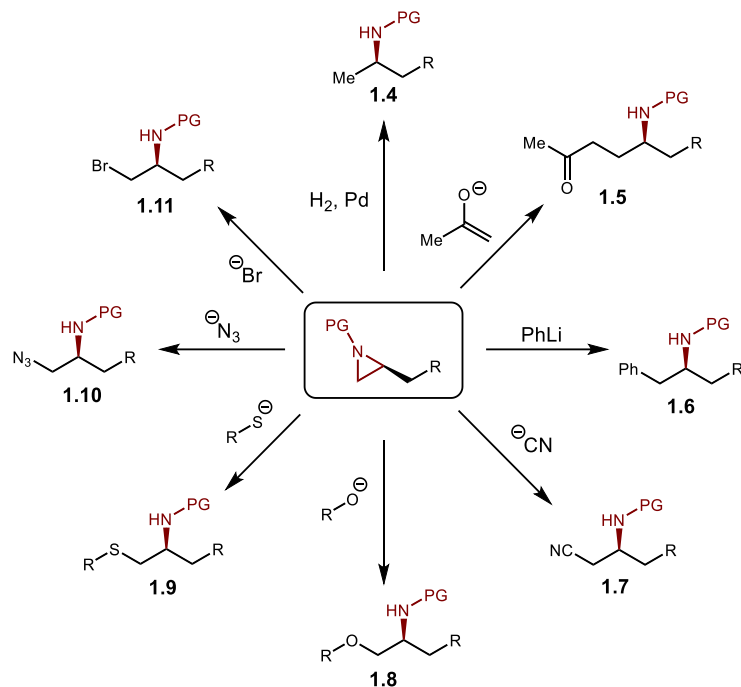
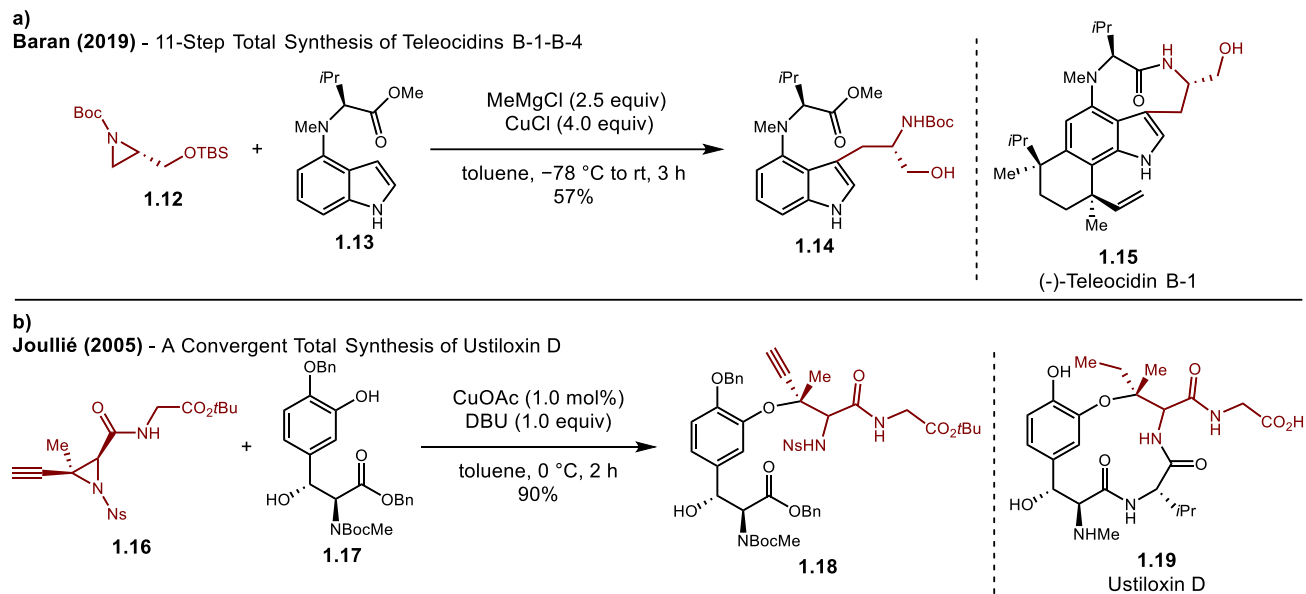


Figure 1.2 Nucleophilic Ring Opening of a Chiral Aziridines.

While aziridine motifs found in biologically active compounds have been of synthetic interest, aziridines have received the greatest amount of attention for their role as nitrogen building blocks. Like epoxides, the strained three-membered ring of aziridines may undergo ring opening reactions with a variety of nucleophiles (**Figure 1.2**).^{8,9} These transformations are often highly regio- and stereoselective and both selectivity parameters can be tuned using Lewis acid additives or through the formation of aziridinium cation intermediates.^{10,11} Furthermore, the often stereoretentive nature of these transformations allows for chiral aziridines to be transformed into valuable chiral nitrogen products such as amines, amino alcohols, halo-amines, and amino acids.¹² Aziridines have also found their way into more modern methodologies which have aimed to improve the selectivity in aziridine diversification often incorporating the use of transition metal catalysts. Extensive work by Doyle has employed a variety of nickel and metallaphotoredox methods aimed at the functionalization of aziridines.¹³⁻¹⁸

As result of their versatility as nitrogen building blocks, aziridines have been used extensively in the synthesis of complex molecules.² The following two examples highlight how aziridines have been employed in the context of total syntheses both in the early and later stages of a synthetic route. The 2019



Scheme 1.1 Application of Chiral Aziridines in Total Synthesis.

enantioselective synthesis of Teleocidins B1-B4 by Baran uses a small chiral aziridine block **1.12** in an early-stage copper-mediated coupling to furnish the desired chiral tryptophol intermediate **1.14** (**Scheme 1.1a**).¹⁹ In the synthesis of Ustiloxin D, Joullié used an advanced chiral aziridine **1.16** in another copper-catalyzed ring opening to furnish the key phenolic cross link of the macrocyclic natural product (**Scheme 1.1b**).^{20,21} It is this versatility in downstream diversification that has made aziridines and particularly chiral aziridines sought after building blocks for the stereoselective incorporation of nitrogen motifs.

1.2 Enantioselective Synthesis of Aziridines

1.2.1 Brief Overview of General Aziridine Synthetic Strategies

While the synthesis of epoxides has been well established, the synthesis of aziridines—particularly in an enantioselective fashion—has received less attention. Perhaps, unsurprisingly, this is attributed to the difference in reactivity of oxygen versus nitrogen. While many epoxidation strategies rely on the reactivity of O–O bonds of peroxide reagents to form the desired oxirane products, the analogous N–N bonded reagents (and even O–N bonded reagents) while still reactive, do not provide the same types of reactivity. Therefore,

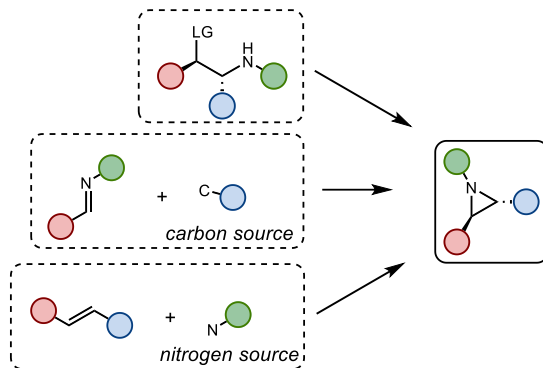
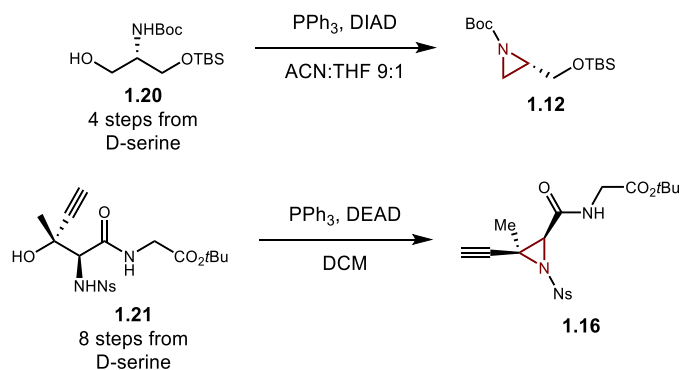


Figure 1.3 Overview of the Synthetic Disconnections to Access Aziridines.

many of the synthetic strategies that have been developed to access aziridines are often considered to be distinct from those used to access epoxides.¹ Three major synthetic strategies that exist to form aziridines include: 1) intramolecular condensation, 2) carbon addition to imines, and 3) nitrogen addition to alkenes (**Figures 1.3**). The growing interest in chiral aziridines as nitrogen building blocks has spurred the development of enantioselective methods in all three synthetic disconnections.²²

1.2.2 Enantioselective Synthesis of Aziridines via Intramolecular Condensation



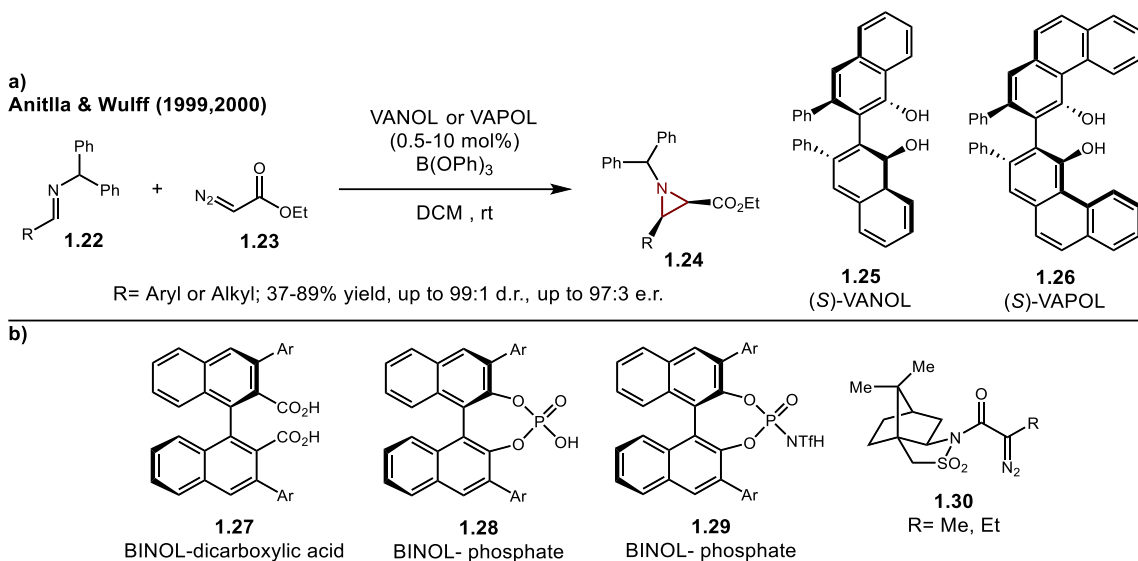
Scheme 1.2 Synthesis of Chiral Aziridine Building Blocks via Intramolecular Condensation.

The intramolecular condensation of chiral amines containing an alpha leaving group is the oldest and most commonly employed method for the synthesis of chiral aziridines. The popularity of this strategy arises from the accessibility of the necessary chiral amines which are often sourced from amino acids or epoxide ring-opening products. Chiral amino-alcohols are often the preferred starting material as the alcohol can easily be transformed *in-situ* into an excellent leaving group using Mitsunobu conditions or with tosylate and mesylate. The aziridine **1.12** used by Baran in the synthesis of Teleocidins B was readily

derived from D-serine in four steps in this manner using intramolecular Mitsunobu conditions.¹⁹ However, this reliance on chiral pool starting materials can be a considerable drawback in cases where more exotic and complex aziridine substituents are desired. This was the case with the synthesis of aziridine **1.16** needed for the synthesis of Ustiloxin D, a nine step synthesis from *D*-serine via an intermediate Garner's aldehyde was required to access the building block **1.21**.^{20,21,23} In cases where the derivatization of a chiral pool starting material cannot be achieved, other enantioselective methodologies must first be employed to synthesize the necessary chiral amines.^{24,25} While the synthesis of chiral aziridines via intramolecular condensation is considered to be robust, the challenges often encountered in the synthesis of the required chiral amine starting materials that cannot be derived from chiral pools has spurred increased interest in the development of more direct aziridination methods in the other two synthetic disconnections.

1.2.3 Enantioselective Synthesis of Aziridines via Carbon Addition to Imines

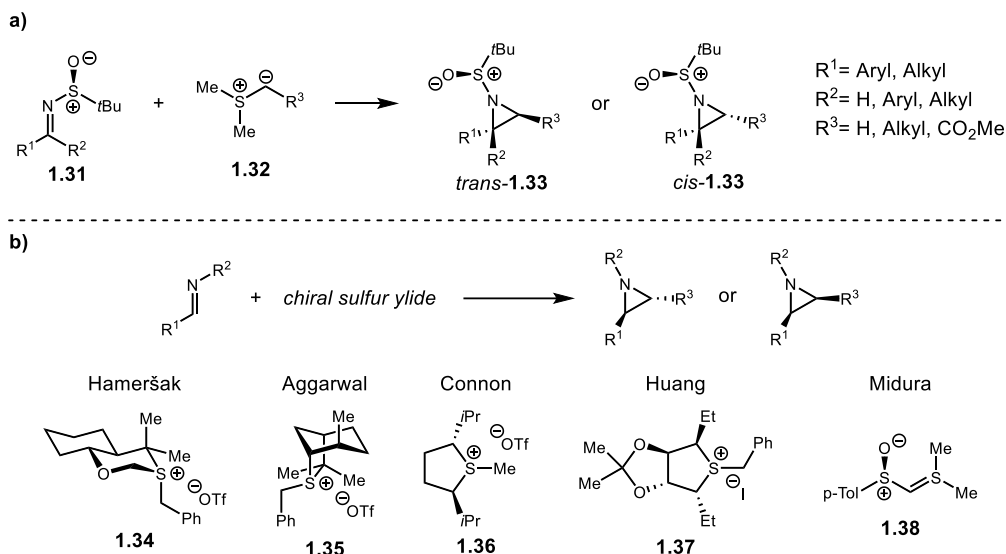
The second synthetic strategy to access chiral aziridines relies on the asymmetric addition of a carbon source across an imine. This synthetic disconnection uses ambiphilic carbon sources which upon addition to the imine can undergo intramolecular condensations to form the desired aziridines. However, unlike the intramolecular condensation strategies, this method is seen as a more direct enantioselective aziridination strategy as it does not rely on the preliminary synthesis of chiral starting materials. Furthermore, the convergent nature of the bond formation between C2 and C3 of the aziridine enables this method to excel at the formation of poly-substituted aziridines, which upon ring opening can provide highly valuable quaternary chiral amine centers. The types of enantioselective methods employed within this strategy depend on the different classes of carbon sources used. Diazo reagents have been commonly employed in the synthesis of aziridines through activation of the imine through Lewis or Brønsted acid catalysis. The first report of an asymmetric version by Antilla and Wulff utilized VANOL **1.25** and VAPOL **1.26** birayl ligands in conjunction with triphenylborate to catalyze the reaction of ethyl diazo acetate **1.23** with a variety of imines **1.22** to provide both chiral alkyl and aryl cis-aziridines **1.24** with excellent enantioselectivities (**Scheme 1.3a**).^{26,27} A wide range of chiral ligand scaffolds and discrete chiral acid



Scheme 1.3 *Enantioselective Addition of Diazo Reagents to Imines.*

catalysts **1.27-1.29** and chiral diazo reagents **1.30** have since been employed to improve following this first report (**Scheme 1.3b**).²⁸⁻³⁰ These improvements have enabled the chiral acid catalyzed addition of diazo reagents to imines to find success in synthetic applications such as in the synthesis of Dynobactin A by Baran where an early-stage chiral aziridine building block was crucial towards developing a rapid convergent synthesis.³¹ The activation of diazo reagents with chiral transition metal catalysts to form the corresponding metalcarbene has also been explored as a means to conduct enantioselective aziridinations. While initial work by Jacobsen³² and Jørgensen³³ using copper bisoxazoline catalysts showed enantioselective control was possible, more recent reports using Rh³⁴ and Ru^{35,36} have failed to improve upon the initial copper catalyzed reports, only achieving mild enantioselective control. As a result, the enantioselective synthesis of aziridines through the transfer of carbenes to imines has not received continued interest.

Sulfonium ylides have proven themselves to be excellent carbon sources for the synthesis of aziridines and their addition across imines is commonly known as the Johnson-Corey-Chaykovsky reaction.³⁷ Unlike diazo reagents, enantioselective methods utilizing ylides as carbon sources have relied heavily on substrate-controlled chiral induction using either *tert*-butylsulfinyl



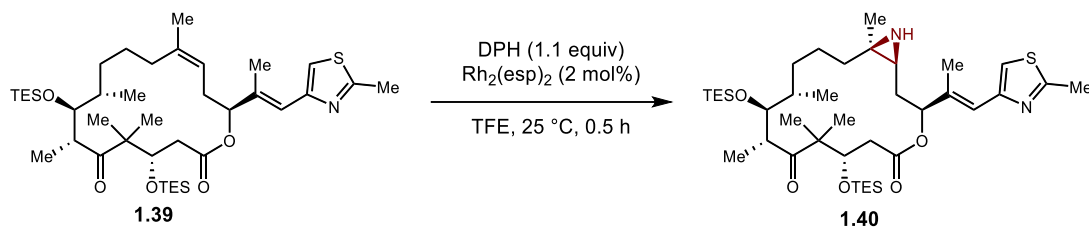
Scheme 1.4 Enantioselective Addition of Sulfonium Ylides to Imines.

imines or chiral sulfoxides **1.31**. Chiral *tert*-butylsulfinyl imines, also known as Ellman's auxiliary,³⁸ have received much attention as they are readily accessible and have been shown to provide access to many challenging poly-substituted aziridines (**Scheme 1.4a**).³⁹ Substrate control through chiral sulfoxides has spurred the development of a wide range of such chiral reagents **1.34-1.38** which allowed for the synthesis of both *cis*- and *trans*-substituted aziridines (**Scheme 1.4b**).⁴⁰⁻⁴⁴

The final class of carbon sources for the synthesis of aziridines are α -halo carbonyls species; their addition across imines allows for the *in-situ* formation of halo-amines which rapidly condense to the desired aziridine in what is known as an aza-Darzens reaction.⁴⁵ As with the use of ylides, enantioselective aza-Darzens have relied heavily on substrate controlled enantioinduction to provide chiral aziridines. Chiral *tert*-butylsulfinyl imine **1.31** once again prove to be the most commonly explored reagent for asymmetric aza-Darzens.^{39,46} While the α -halo carbonyls are the classic reagents for aza-Darzens, the use of other substitutions to form stabilized anions with α -halo leaving groups has allowed for the stereoselective synthesis of chiral aziridines bearing phosphonate esters,⁴⁷ nitro groups,⁴⁸ and even halides.⁴⁹ While the addition of carbon sources across imines is a more convergent synthesis towards chiral aziridines, the prevalent use of substrate control as means of enantioinduction, apart from chiral acid catalysis, has limited the synthetic utility of this synthetic disconnection.

1.2.4 Enantioselective Synthesis of Aziridines via Nitrogen Addition to Alkenes

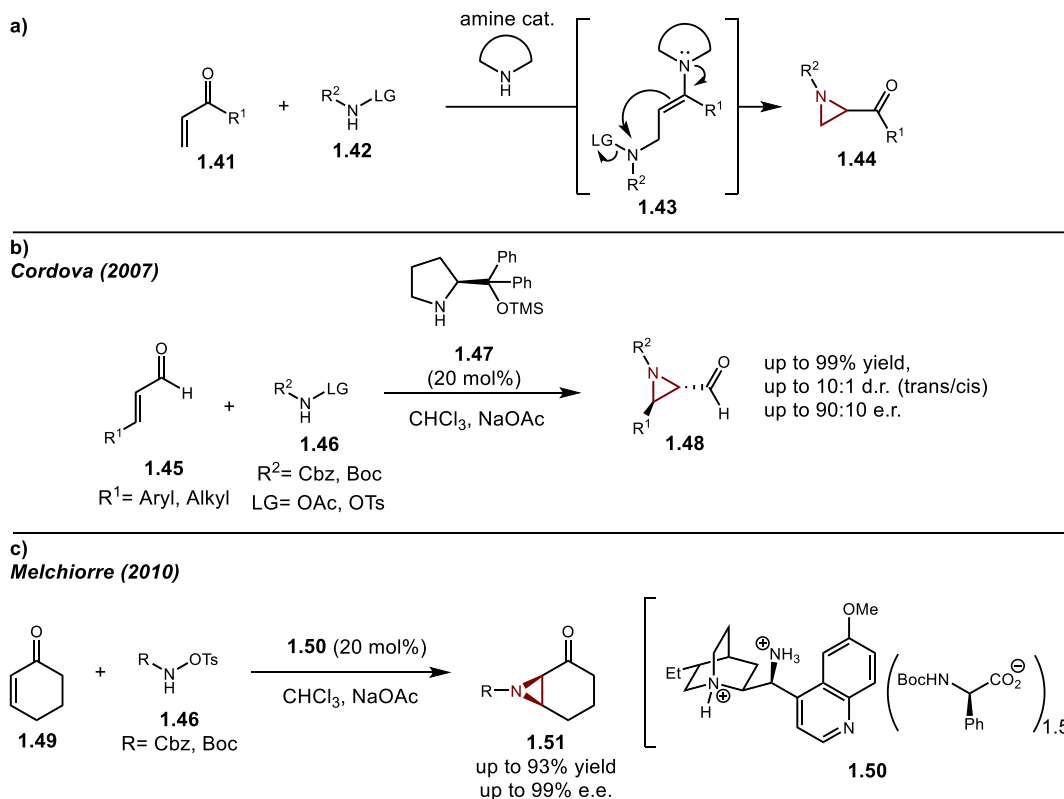
Nicolaou (2020)



Scheme 1.5 Synthesis of an Aziridine Intermediate Towards Epothilone B Analogues.

The third synthetic disconnection for the synthesis of aziridines is the addition of a nitrogen source across an alkene. This disconnection is considered to be the simplest and most direct means of accessing aziridines and the widespread availability of alkenes has made this disconnection the most extensively explored. It is analogous to the common epoxidation of alkenes, and from a retrosynthetic perspective is often the most desired. The synthetic utility of this disconnection was demonstrated in the synthesis of the aziridine analogues of Epothilone B **1.3**, where late-stage diastereoselective installation of the desired aziridine motifs was achieved with an rhodium catalyzed nitrene transfer to a complex alkene intermediate **1.39**.^{6,7,50} The resulting diastereoselectivity is attributed to substrate control from **1.39** as both the rhodium catalyst and nitrene precursor are achiral. In this case, the application of either the intramolecular condensation or carbon to imine addition strategies would not have enabled a modular synthesis of different analogues. Asymmetric aziridinations of alkenes have therefore been of great interest to the synthetic community, as these enable a more direct stereoselective synthesis of chiral aziridines without relying on substrate control as the means of stereocontrol. Two distinct strategies exist for the aziridination of alkenes, and each has seen significant development to render them enantioselective.

The first is the aza-Michael initiated ring closures (aza-MIRC) strategy. As the name suggests, conjugate addition of a nitrogen source containing a leaving group to an activated α - β -unsaturated carbonyl **1.41** is followed by intramolecular condensation of the resulting enolate or enamine **1.43** to provide the desired aziridine **1.44** (**Scheme 1.6a**). Amphiphilic nitrogen sources such as hydroxylamines or *N*-chloroamines are often used as they retain sufficient nucleophilicity to attack the chiral iminium ion or



Scheme 1.6 Enantioselective Aziridinations via aza-Michael Initiated Ring Closures.

enamine intermediates. This transformation has been rendered enantioselective using a range of organo-catalysts, and the choice of which depends upon the type of substrate. Enantioselective aziridination of α - β -unsaturated aldehydes **1.45** is commonly achieved using chiral prolinol **1.47** catalysts and was first reported by Cordova in 2007, in which a variety of trans-aziridines could be formed in with good enantiocontrol (**Scheme 1.6b**).⁵¹ Enantioselective aziridination of linear and cyclic α - β -unsaturated ketones **1.49** could not be achieved using the secondary amine prolinol catalysts **1.47** and this transformation was not realized until the use of chiral primary amine salts **1.50** by Melchiorre (**Scheme 1.6b**).²⁴ The combination of quinine with chiral amino acids enabled the enantioselective aziridination of both linear and cyclic α - β -unsaturated ketones. While these organocatalytic methods have demonstrated remarkable level of enantiocontrol with an excellent range of substitutions on the aziridine, they are limited to α - β -unsaturated systems.

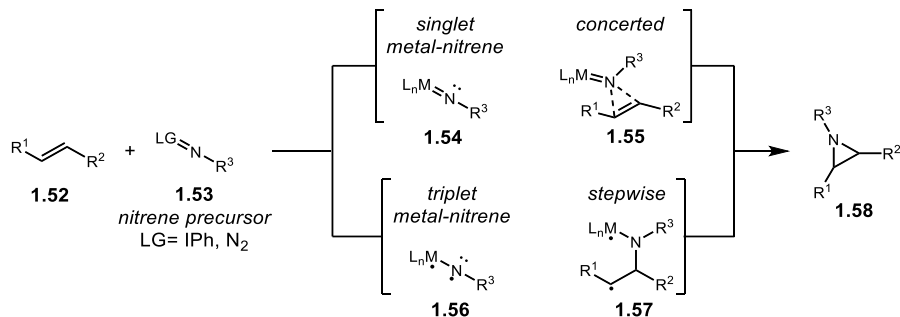
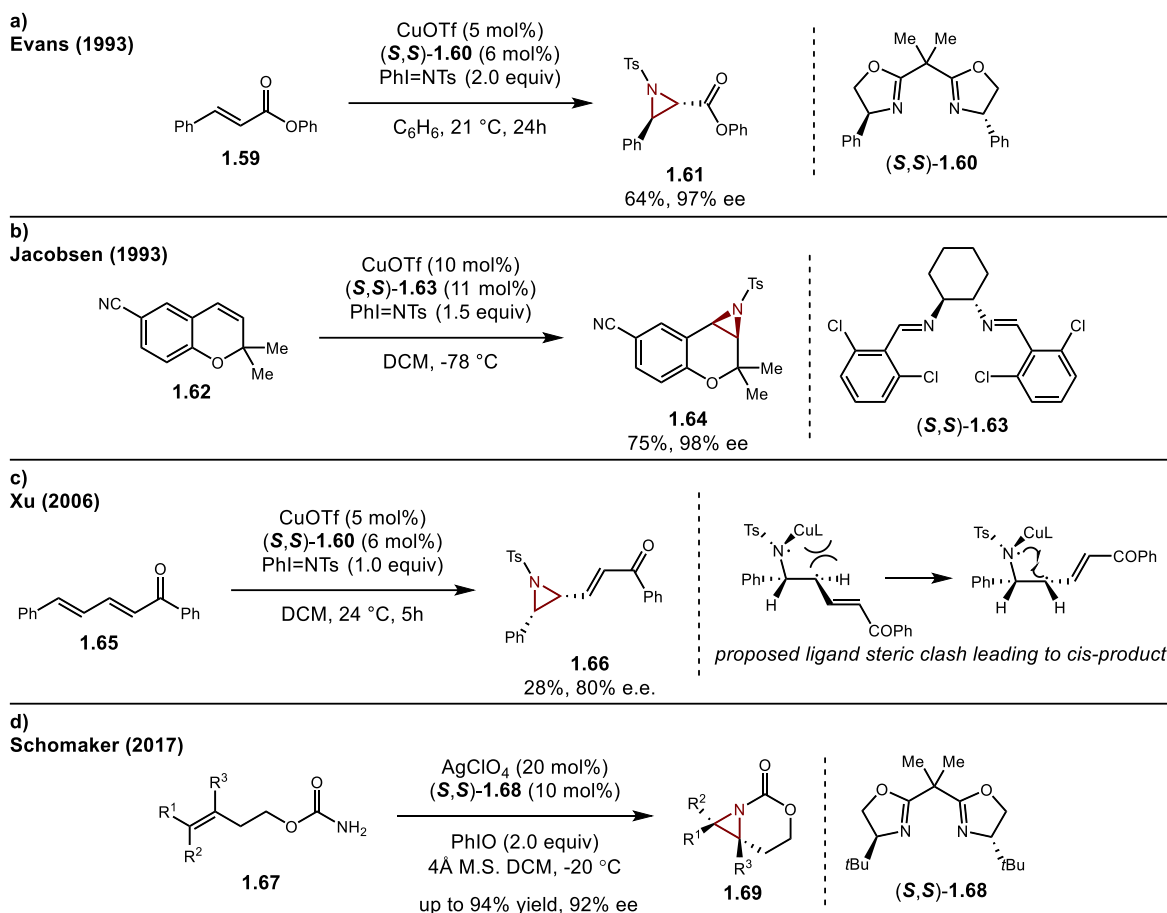


Figure 1.4 Overview of Transition Metal Nitrene Intermediates in the Aziridination of Alkenes.

The second aziridination strategy for nitrogen addition across an alkene is a transition metal catalyzed nitrene transfer (**Figure 1.4**). This strategy encompasses the greatest area of research into developing asymmetric aziridination methodologies across all three major aziridination strategies. To form the desired nitrenes iminoiodonanes or azides **1.53** have been the most frequently employed nitrene precursors. When paired with an appropriate metal catalyst these reagents decompose to form metal nitrenes whose spin state dictates the mechanism of the resulting aziridination. Closed shell singlet nitrenes **1.54** will react via concerted mechanism **1.55** to transfer the nitrogen to the alkene. Open shell triplet nitrenes **1.56** react in stepwise radical fashion **1.57** to form the desired aziridine **1.58**, which of the two pathways is heavily dependent upon the identity of the metal catalyst. Second and third row transition metals are typically implicated in singlet nitrene transfer reactions while first row transition metals often lead to the formation of triplet nitrene intermediates. Because the transition metal is heavily involved in the formation of both new bonds of the aziridine during the nitrene transfer, both open- and closed-shell mechanisms have been rendered enantioselective.

The first reports of an enantioselective transition metal-catalyzed aziridination of alkenes were disclosed by Evans^{52,53} and Jacobsen^{54,55} (**Scheme 1.7a&b**). Both reported the aziridination of styrene substrates (**1.59,1.62**) using Cu(I) salts, BOX **1.60** or Jacobsen diamine ligands **1.63**, and discrete sulfonyl iminoiodinane nitrene precursors. Following this seminal work, a variety of reports began to emerge seeking to improve the copper-catalyzed alkene aziridination by expanding the scope of the reaction to other conjugated alkenes⁵⁶ and intramolecular aziridiantions,⁵⁷ introducing new ligand scaffolds,^{58,59} and through

the use of *in-situ* generated iminoiodinanes. The majority of copper-catalyzed aziridinations are believed to operate via the closed-shell singlet metal nitrene concerted mechanism, although some methods have

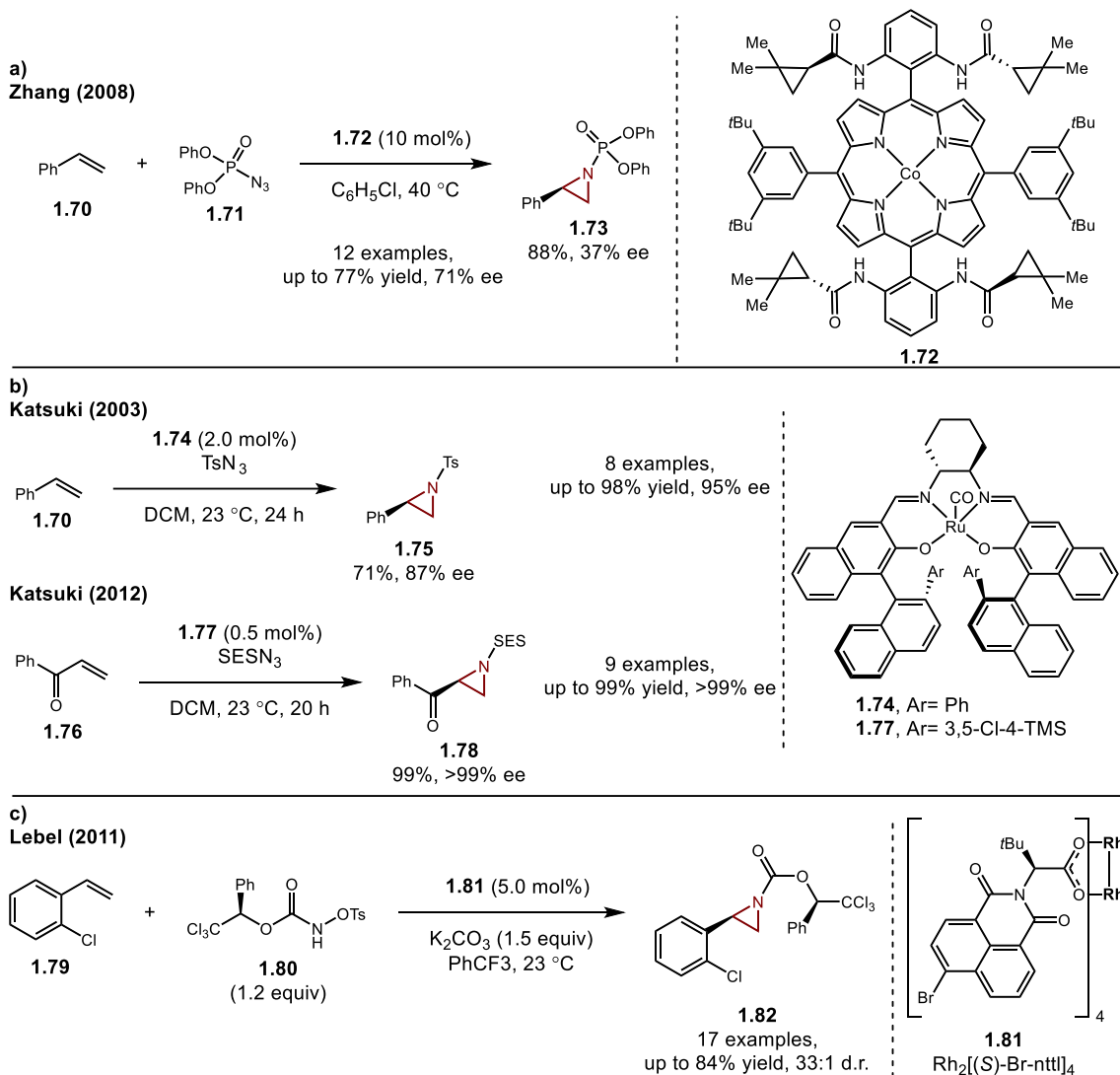


Scheme 1.7 Copper and Silver Catalyzed Enantioselective Aziridinations of Alkenes.

proposed singlet spin state nitrene intermediates as the active species (**Scheme 1.7c**).⁵⁶

The use of BOX ligands and derivate ligands have also found enormous success in the silver-catalyzed asymmetric aziridination of alkenes. A series of reports by Schomaker have demonstrated the ability to conduct intramolecular enantioselective aziridinations to form complex fused bicyclic aziridines with a variety of substitutions (**Scheme 1.7d**).^{60,61}

Following a series of racemic reports,⁶²⁻⁶⁴ Zhang demonstrated a Co(II) porphyrin **1.72** catalyzed asymmetric aziridination of styrenes **1.70** using diphenyl phosphoryl azide **1.71** for the formation of chiral N-phosphorylated aziridines **1.73** (**Scheme 1.8a**).⁶⁵ Since then a number of other reports using advanced



Scheme 1.8 Cobalt, Ruthenium, and Rhodium Catalyzed Enantioselective Aziridinations of Alkenes.

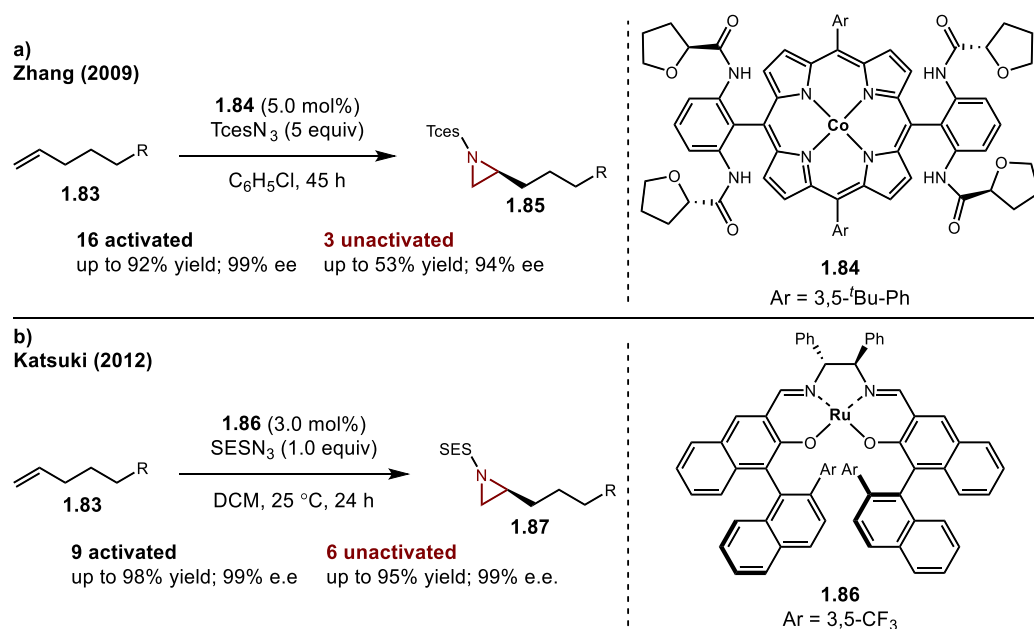
Co(II) porphyrin catalysts and azide nitrene precursors have been reported and the mechanistic investigations detailing an open-shell nitrene transfer mechanism for these systems.⁶⁶⁻⁶⁹ Chiral porphyrin catalysts have also been developed using a number of other transition metals such as Mn,⁷⁰ Fe,⁷¹ and Ru.^{72,73} Katsuki has also demonstrated the use of Ru[salen]CO catalyst platforms (**1.74**, **1.77**) for the enantioselective aziridination of both styrenes **1.70** and α - β -unsaturated ketones **1.76** (Scheme 1.8b).^{74,75}

Racemic rhodium-catalyzed aziridination of alkenes has been well established;⁷⁶ however, attempts to render these methods asymmetric have proven to be challenging, with many of the initial reports only providing low levels of enantiocontrol.⁷⁷⁻⁷⁹ The most promising result came from Lebel et al. who relied on

the use of chiral nitrene source **1.80** in conjunction with a chiral dirhodium(II) catalyst **1.81** to perform the diastereoselective aziridination of styrenes **1.79** (Scheme 1.8c).⁸⁰ Although a large number of transition metal-catalyzed intermolecular alkene aziridinations have been reported, notably absent from all of these methods are simple alkyl substituted *unactivated* alkenes. The methods reported so far have been limited to the functionalization of *activated* alkenes such as styrene and α - β -unsaturated carbonyls.

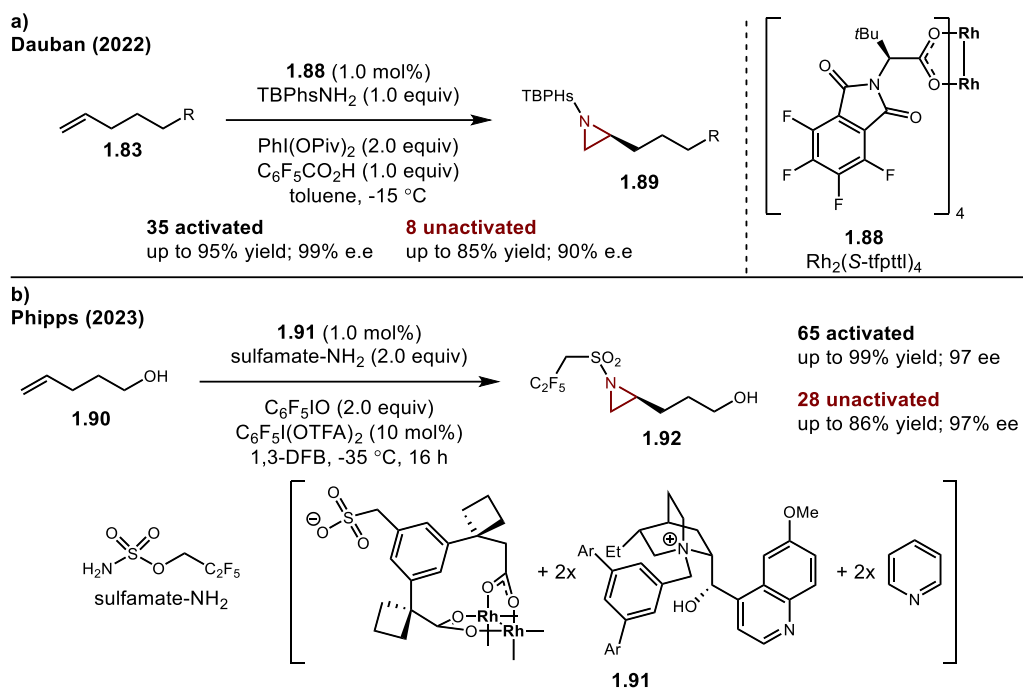
1.3 Transition Metal Catalyzed Enantioselective Aziridination of Unactivated Alkenes.

While simple alkyl-substituted alkenes are readily available as building blocks, their inertness to many reaction conditions has made their functionalization a challenging prospect, especially when considering simple monosubstituted alkenes which lack any of the steric or electronic biases often required for high levels of enantioselective control.⁸¹ As a result, the enantioselective aziridination of *unactivated* alkenes has only been reported in a select few cases. Early attempts to use the copper iminoiodinane catalyzed aziridination strategies were found to fall short of the desired results, only providing aziridines in low yields and with low enantioselectivities.⁸² In 2009, Zhang reported the first successful enantioselective aziridination of an unactivated alkene that could provide high levels of enantioselective control using the



Scheme 1.9 Cobalt, and Ruthenium Catalyzed Enantioselective Aziridinations of Unactivated Alkenes.

Co(II)por catalyst **1.84** (Scheme 1.9a).⁶⁹ However, this was limited to three examples in a substrate scope that consisted primarily of the more commonly observed activated substrates. In 2012, Katsuki was able to report the aziridination of a wider range of unactivated alkenes using the Ru[Salen]CO complex **1.86** (Scheme 1.9b).⁸³ While this scope still primarily contained styrenes, the unactivated alkenes demonstrated



Scheme 1.10 Rhodium Catalyzed Enantioselective Aziridinations of Unactivated Alkenes.

excellent levels of chemoselectivity with aziridination occurring solely at the terminal alkenes and with high levels of enantioselectivity.

The next report of an asymmetric unactivated alkene aziridination was not made until 2022 when Dauban et.al reported the use of a chiral dirhodium(II) catalysts **1.88** for the enantioselective aziridination of styrenes and unactivated alkenes (Scheme 1.10a).⁸⁴ This report proved to be a significant advance in the development of rhodium-catalyzed asymmetric aziridinations as previous attempts had not succeeded to provide sufficient enantiocontrol. However, once again the majority of the reported chiral aziridines were synthesized from activated alkenes. Lastly in 2023, Phipps et al. reported the successful aziridination of a large scope of unactivated alkenes (Scheme 1.10b).⁸⁵ This transformation required a pendant hydroxyl group to direct the achiral dirhodium(II) catalyst and chiral organocatalyst salt pair **1.91** to effect the desired

asymmetric aziridination. While this report was the first to extensively explore the aziridination of unactivated alkenes alongside styrenes, the reliance on a tethered hydroxyl directing group represents a significant limitation.

1.4 Conclusion

Chiral aziridines are valuable nitrogen-containing building blocks which have been used both for the early- and late-stage incorporation of chiral nitrogen motifs in synthetic targets. To meet the ever-growing demand for chiral aziridines, three major strategies have been used for their stereoselective synthesis: intramolecular condensation, carbon additions to imines, and nitrogen addition to alkenes. While the intramolecular condensation of chiral amines is still used today, it is limited to simple aziridine substitutions. The stereoselective synthesis of aziridines from imines has enabled the synthesis of more complex aziridines, yet it is frequently limited to the use of chiral auxiliaries and has therefore found limited synthetic applications. The asymmetric synthesis of aziridines from alkenes has been the most attractive synthetic disconnection as it mirrors the common synthetic strategy of the epoxidation of alkenes. Transition metal catalyzed methods have dominated this area for the stereoselective transfer of metal nitrenes to alkenes. A variety of unique chiral ligand scaffolds and metal catalysts have been developed. However, most methods have been limited to the aziridination of activated alkenes such as styrenes and α - β -unsaturated carbonyls, whereas alkyl substituted unactivated alkenes have remained a challenging class of substrates. Furthermore, many existing enantioselective alkene aziridination methods rely on the use of highly reactive azide or iminoiodinane nitrene precursors which can pose significant safety risks as well as chemoselectivity challenges. Chapter 2 of this dissertation will discuss the development of an enantioselective aziridination method for unactivated alkene using a mild hydroxylamine nitrogen source.

1.5 References

- (1) Sweeney, J. B. Aziridines: epoxides' ugly cousins? *Chem. Soc. Rev.* **2002**, *31* (5), 247.
- (2) Botuha, C.; Chemla, F.; Ferreira, F.; Pérez-Luna, A. In *Heterocycles in Natural Product Synthesis*, 2011, DOI:10.1002/9783527634880.ch1.
- (3) Ismail, F. M.; Levitsky, D. O.; Dembitsky, V. M. Aziridine alkaloids as potential therapeutic agents. *Eur. J. Med. Chem.* **2009**, *44* (9), 3373.
- (4) Hata, T.; Sano, Y.; Sugawara, R.; Matsumae, A.; Kanamori, K.; Shima, T.; Hoshi, T. Mitomycin, a New Antibiotic From Streptomyces. I. *The Journal of Antibiotics, Series A* **1956**, *9* (4), 141.
- (5) Yokoi, K.; Nagaoka, K.; Nakashima, T. Azinomycins A and B, new antitumor antibiotics. II. Chemical structures. *Chem Pharm Bull (Tokyo)* **1986**, *34* (11), 4554.
- (6) Nicolaou, K. C.; Shelke, Y. G.; Dherange, B. D.; Kempema, A.; Lin, B.; Gu, C.; Sandoval, J.; Hammond, M.; Aujay, M.; Gavrilyuk, J. Design, Synthesis, and Biological Investigation of Epothilone B Analogues Featuring Lactone, Lactam, and Carbocyclic Macrocycles, Epoxide, Aziridine, and 1,1-Difluorocyclopropane and Other Fluorine Residues. *J. Org. Chem.* **2020**, *85* (5), 2865.
- (7) Nicolaou, K. C.; Rhoades, D.; Wang, Y.; Bai, R.; Hamel, E.; Aujay, M.; Sandoval, J.; Gavrilyuk, J. 12,13-Aziridinyl Epothilones. Stereoselective Synthesis of Trisubstituted Olefinic Bonds from Methyl Ketones and Heteroaromatic Phosphonates and Design, Synthesis, and Biological Evaluation of Potent Antitumor Agents. *J. Am. Chem. Soc.* **2017**, *139* (21), 7318.
- (8) Akhtar, R.; Naqvi, S. A. R.; Zahoor, A. F.; Saleem, S. Nucleophilic ring opening reactions of aziridines. *Molecular Diversity* **2018**, *22* (2), 447.
- (9) Hu, X. E. Nucleophilic ring opening of aziridines. *Tetrahedron* **2004**, *60* (12), 2701.
- (10) Stankovic, S.; D'Hooghe, M.; Catak, S.; Eum, H.; Waroquier, M.; Van Speybroeck, V.; De Kimpe, N.; Ha, H. J. Regioselectivity in the ring opening of non-activated aziridines. *Chem. Soc. Rev.* **2012**, *41* (2), 643.

- (11) Lu, P. F. Recent developments in regioselective ring opening of aziridines. *Tetrahedron* **2010**, *66* (14), 2549.
- (12) Beresford, K. J.; Church, N. J.; Young, D. W. Synthesis of alpha-amino acids by reaction of aziridine-2-carboxylic acids with carbon nucleophiles. *Org Biomol Chem* **2006**, *4* (15), 2888.
- (13) Dongbang, S.; Doyle, A. G. Ni/Photoredox-Catalyzed C(sp³)–C(sp³) Coupling between Aziridines and Acetals as Alcohol-Derived Alkyl Radical Precursors. *J. Am. Chem. Soc.* **2022**, *144* (43), 20067.
- (14) Estrada, J. G.; Williams, W. L.; Ting, S. I.; Doyle, A. G. Role of Electron-Deficient Olefin Ligands in a Ni-Catalyzed Aziridine Cross-Coupling To Generate Quaternary Carbons. *J. Am. Chem. Soc.* **2020**, *142* (19), 8928.
- (15) Huang, C.-Y.; Doyle, A. G. Electron-Deficient Olefin Ligands Enable Generation of Quaternary Carbons by Ni-Catalyzed Cross-Coupling. *J. Am. Chem. Soc.* **2015**, *137* (17), 5638.
- (16) Kalow, J. A.; Doyle, A. G. Enantioselective fluoride ring opening of aziridines enabled by cooperative Lewis acid catalysis. *Tetrahedron* **2013**, *69* (27), 5702.
- (17) Steiman, T. J.; Liu, J.; Mengiste, A.; Doyle, A. G. Synthesis of β-Phenethylamines via Ni/Photoredox Cross-Electrophile Coupling of Aliphatic Aziridines and Aryl Iodides. *J. Am. Chem. Soc.* **2020**, *142* (16), 7598.
- (18) Woods, B. P.; Orlandi, M.; Huang, C.-Y.; Sigman, M. S.; Doyle, A. G. Nickel-Catalyzed Enantioselective Reductive Cross-Coupling of Styrenyl Aziridines. *J. Am. Chem. Soc.* **2017**, *139* (16), 5688.
- (19) Nakamura, H.; Yasui, K.; Kanda, Y.; Baran, P. S. 11-Step Total Synthesis of Teleocidins B-1-B-4. *J. Am. Chem. Soc.* **2019**, *141* (4), 1494.
- (20) Li, P.; Evans, C. D.; Joullié, M. M. A Convergent Total Synthesis of Ustiloxin D via an Unprecedented Copper-Catalyzed Ethynyl Aziridine Ring-Opening by Phenol Derivatives. *Org. Lett.* **2005**, *7* (23), 5325.

- (21) Li, P.; Evans, C. D.; Wu, Y.; Cao, B.; Hamel, E.; Joullié, M. M. Evolution of the Total Syntheses of Ustiloxin Natural Products and Their Analogues. *J. Am. Chem. Soc.* **2008**, *130* (7), 2351.
- (22) Degennaro, L.; Trinchera, P.; Luisi, R. Recent advances in the stereoselective synthesis of aziridines. *Chem. Rev.* **2014**, *114* (16), 7881.
- (23) Campbell, A. D.; Raynham, T. M.; Taylor, R. J. K. A Simplified Route to the (R)-Garner Aldehyde and (S)-Vinyl Glycinol. *Synthesis* **1998**, *1998* (12), 1707.
- (24) Bartoli, G.; Bosco, M.; Carlone, A.; Locatelli, M.; Melchiorre, P.; Sambri, L. Asymmetric Catalytic Synthesis of Enantiopure N-Protected 1,2-Amino Alcohols. *Org. Lett.* **2004**, *6* (22), 3973.
- (25) Fadeyi, O. O.; Schulte, M. L.; Lindsley, C. W. General Access to Chiral N-Alkyl Terminal Aziridines via Organocatalysis. *Org. Lett.* **2010**, *12* (14), 3276.
- (26) Antilla, J. C.; Wulff, W. D. Catalytic Asymmetric Aziridination with a Chiral VAPOL–Boron Lewis Acid. *J. Am. Chem. Soc.* **1999**, *121* (21), 5099.
- (27) Antilla, J. C.; Wulff, W. D. Catalytic Asymmetric Aziridination with Arylborate Catalysts Derived from VAPOL and VANOL Ligands. *Angew. Chem. Int. Ed.* **2000**, *39* (24), 4518.
- (28) Hashimoto, T.; Nakatsu, H.; Yamamoto, K.; Maruoka, K. Chiral Brønsted Acid-Catalyzed Asymmetric Trisubstituted Aziridine Synthesis Using α -Diazoacyl Oxazolidinones. *J. Am. Chem. Soc.* **2011**, *133* (25), 9730.
- (29) Hashimoto, T.; Nakatsu, H.; Watanabe, S.; Maruoka, K. Stereoselective Synthesis of Trisubstituted Aziridines with N- α -Diazoacyl Camphorsultam. *Org. Lett.* **2010**, *12* (8), 1668.
- (30) Hashimoto, T.; Nakatsu, H.; Yamamoto, K.; Watanabe, S.; Maruoka, K. Asymmetric Trisubstituted Aziridination of Aldimines and Ketimines using N- α -Diazoacyl Camphorsultams. *Chemistry – An Asian Journal* **2011**, *6* (2), 607.
- (31) Schneider, F.; Guo, Y.; Lin, Y.-C.; Eberle, K. J.; Chiodi, D.; Greene, J. A.; Lu, C.; Baran, P. S. Total Synthesis of Dynobactin A. *J. Am. Chem. Soc.* **2024**, DOI:10.1021/jacs.3c11560
10.1021/jacs.3c11560.

- (32) Hansen, K. B.; Finney, N. S.; Jacobsen, E. N. Carbenoid Transfer to Imines: A New Asymmetric Catalytic Synthesis of Aziridines. *Angewandte Chemie International Edition in English* **1995**, *34* (6), 676.
- (33) Rasmussen, K. G.; Jørgensen, K. A. Catalytic formation of aziridines from imines and diazoacetate. *J. Chem. Soc., Chem. Commun.* **1995**, *0* (14), 1401.
- (34) Krumper, J. R.; Gerisch, M.; Suh, J. M.; Bergman, R. G.; Tilley, T. D. Monomeric Rhodium(II) Catalysts for the Preparation of Aziridines and Enantioselective Formation of Cyclopropanes from Ethyl Diazoacetate at Room Temperature. *The Journal of Organic Chemistry* **2003**, *68* (25), 9705.
- (35) Egloff, J.; Ranocchiari, M.; Schira, A.; Schotes, C.; Mezzetti, A. Highly Enantioselective Ruthenium/PNNP-Catalyzed Imine Aziridination: Evidence of Carbene Transfer from a Diazoester Complex. *Organometallics* **2013**, *32* (16), 4690.
- (36) Ranocchiari, M.; Mezzetti, A. Ru/PNNP-Catalyzed Asymmetric Imine Aziridination by Diazo Ester Activation. *Organometallics* **2009**, *28* (13), 3611.
- (37) Caiuby, C. A. D.; Furniel, L. G.; Burtoloso, A. C. B. Asymmetric transformations from sulfoxonium ylides. *Chemical Science* **2022**, *13* (5), 1192.
- (38) Liu, G.; Cogan, D. A.; Ellman, J. A. Catalytic Asymmetric Synthesis of tert-Butanesulfinamide. Application to the Asymmetric Synthesis of Amines. *J. Am. Chem. Soc.* **1997**, *119* (41), 9913.
- (39) Robak, M. T.; Herbage, M. A.; Ellman, J. A. Synthesis and Applications of tert-Butanesulfinamide. *Chem. Rev.* **2010**, *110* (6), 3600.
- (40) Solladié-Cavallo, A.; Roje, M.; Welter, R.; Šunjić, V. Two-Step Asymmetric Synthesis of Disubstituted N-Tosyl Aziridines Having 98–100% ee: Use of a Phosphazene Base. *The Journal of Organic Chemistry* **2004**, *69* (4), 1409.
- (41) Stipetić, I.; Roje, M.; Hameršak, Z. Highly Enantioselective Aziridination of N-Protected Imines: Comparison of the Phosphazene EtP2 and Sodium Hydride as Bases. *Synlett* **2008**, *2008* (20), 3149.
- (42) Illa, O.; Arshad, M.; Ros, A.; McGarrigle, E. M.; Aggarwal, V. K. Practical and Highly Selective Sulfur Ylide Mediated Asymmetric Epoxidations and Aziridinations Using an Inexpensive, Readily

- Available Chiral Sulfide. Applications to the Synthesis of Quinine and Quinidine. *J. Am. Chem. Soc.* **2010**, *132* (6), 1828.
- (43) Gui, Y.; Shen, S.; Wang, H.-Y.; Li, Z.-Y.; Huang, Z.-Z. Synthesis of C₂-Symmetric Sulfide and Its First Application in Highly Enantioselective Synthesis of Chiral Aziridines. *Chem. Lett.* **2007**, *36* (12), 1436.
- (44) Midura, W. H. Highly stereoselective aziridination of imines with (S)-dimethylsulfonium-(p-tolylsulfinyl)methylide. *Tetrahedron Lett.* **2007**, *48* (22), 3907.
- (45) Sweeney, J. Aziridine Synthesis via Nucleophilic Attack of Carbene Equivalents on Imines: the Aza-Darzens Reaction. *Eur. J. Org. Chem.* **2009**, *2009* (29), 4911.
- (46) Solá, T. M.; Churcher, I.; Lewis, W.; Stockman, R. A. Stereoselective aza-Darzens reactions of tert-butanesulfinimines: convenient access to chiral aziridines. *Organic & Biomolecular Chemistry* **2011**, *9* (14), 5034.
- (47) Davis, F. A.; Ramachandar, T.; Wu, Y. Improved Asymmetric Synthesis of Aziridine 2-Phosphonates Using (S)-(+)-2,4,6-Trimethylphenylsulfonamide. *The Journal of Organic Chemistry* **2003**, *68* (18), 6894.
- (48) Yadav, L. D. S.; Garima; Kapoor, R. The first diastereoselective nitroaziridination of N-tosylaldimines with 1-bromonitroalkanes. *Tetrahedron Lett.* **2009**, *50* (38), 5420.
- (49) Boulwood, T.; Affron, D. P.; Trowbridge, A. D.; Bull, J. A. Synthesis of cis-C-Iodo-N-Tosyl-Aziridines using Diiodomethyl lithium: Reaction Optimization, Product Scope and Stability, and a Protocol for Selection of Stationary Phase for Chromatography. *The Journal of Organic Chemistry* **2013**, *78* (13), 6632.
- (50) Jat, J. L.; Paudyal, M. P.; Gao, H.; Xu, Q. L.; Yousufuddin, M.; Devarajan, D.; Ess, D. H.; Kurti, L.; Falck, J. R. Direct stereospecific synthesis of unprotected N-H and N-Me aziridines from olefins. *Science* **2014**, *343* (6166), 61.
- (51) Vesely, J.; Ibrahim, I.; Zhao, G. L.; Rios, R.; Cordova, A. Organocatalytic enantioselective aziridination of alpha,beta-unsaturated aldehydes. *Angew. Chem. Int. Ed. Engl.* **2007**, *46* (5), 778.

- (52) Evans, D. A.; Faul, M. M.; Bilodeau, M. T.; Anderson, B. A.; Barnes, D. M. Bis(Oxazoline) Copper-Complexes as Chiral Catalysts for the Enantioselective Aziridination of Olefins. *J. Am. Chem. Soc.* **1993**, *115* (12), 5328.
- (53) Evans, D. A.; Bilodeau, M. T.; Faul, M. M. Development of the Copper-Catalyzed Olefin Aziridination Reaction. *J. Am. Chem. Soc.* **1994**, *116* (7), 2742.
- (54) Li, Z.; Quan, R. W.; Jacobsen, E. N. Mechanism of the (Diimine)Copper-Catalyzed Asymmetric Aziridination of Alkenes - Nitrene Transfer Via Ligand-Accelerated Catalysis. *J. Am. Chem. Soc.* **1995**, *117* (21), 5889.
- (55) Li, Z.; Conser, K. R.; Jacobsen, E. N. Asymmetric alkene aziridination with readily available chiral diimine-based catalysts. *J. Am. Chem. Soc.* **1993**, *115* (12), 5326.
- (56) Ma, L.; Du, D. M.; Xu, J. Asymmetric aziridination of 1,3-dienes catalyzed by bisoxazoline-copper complexes. *Chirality* **2006**, *18* (8), 575.
- (57) Estéoule, A.; Durán, F.; Retailleau, P.; Dodd, R. H.; Dauban, P. Enantioselective Intramolecular Copper-Catalyzed Aziridination of Sulfamates. *Synthesis* **2007**, *2007* (08), 1251.
- (58) Wang, X.; Ding, K. One-pot enantioselective aziridination of olefins catalyzed by a copper(I) complex of a novel diimine ligand by using $\text{PhI}(\text{OAc})_2$ and sulfonamide as nitrene precursors. *Chemistry* **2006**, *12* (17), 4568.
- (59) Ma, L.; Jiao, P.; Zhang, Q.; Du, D.-M.; Xu, J. Ligand and substrate π -stacking interaction controlled enantioselectivity in the asymmetric aziridination. *Tetrahedron: Asymmetry* **2007**, *18* (7), 878.
- (60) Ju, M.; Weatherly, C. D.; Guzei, I. A.; Schomaker, J. M. Chemo- and Enantioselective Intramolecular Silver-Catalyzed Aziridinations. *Angew. Chem. Int. Ed. Engl.* **2017**, *56* (33), 9944.
- (61) Alderson, J. M.; Corbin, J. R.; Schomaker, J. M. Tunable, Chemo- and Site-Selective Nitrene Transfer Reactions through the Rational Design of Silver(I) Catalysts. *Acc. Chem. Res.* **2017**, *50* (9), 2147.
- (62) Gao, G.-Y.; Harden, J. D.; Zhang, X. P. Cobalt-Catalyzed Efficient Aziridination of Alkenes. *Org. Lett.* **2005**, *7* (15), 3191.

- (63) Gao, G.-Y.; Jones, J. E.; Vyas, R.; Harden, J. D.; Zhang, X. P. Cobalt-Catalyzed Aziridination with Diphenylphosphoryl Azide (DPPA): Direct Synthesis of N-Phosphorus-Substituted Aziridines from Alkenes. *The Journal of Organic Chemistry* **2006**, *71* (17), 6655.
- (64) Ruppel, J. V.; Jones, J. E.; Huff, C. A.; Kamble, R. M.; Chen, Y.; Zhang, X. P. A Highly Effective Cobalt Catalyst for Olefin Aziridination with Azides: Hydrogen Bonding Guided Catalyst Design. *Org. Lett.* **2008**, *10* (10), 1995.
- (65) Jones, J. E.; Ruppel, J. V.; Gao, G. Y.; Moore, T. M.; Zhang, X. P. Cobalt-catalyzed asymmetric olefin aziridination with diphenylphosphoryl azide. *J. Org. Chem.* **2008**, *73* (18), 7260.
- (66) Jin, L. M.; Xu, X.; Lu, H.; Cui, X.; Wojtas, L.; Zhang, X. P. Effective synthesis of chiral N-fluoroaryl aziridines through enantioselective aziridination of alkenes with fluoroaryl azides. *Angew. Chem. Int. Ed. Engl.* **2013**, *52* (20), 5309.
- (67) Tao, J.; Jin, L. M.; Zhang, X. P. Synthesis of chiral N-phosphoryl aziridines through enantioselective aziridination of alkenes with phosphoryl azide via Co(II)-based metalloradical catalysis. *Beilstein J Org Chem* **2014**, *10* (li), 1282.
- (68) Riart-Ferrer, X.; Sang, P.; Tao, J.; Xu, H.; Jin, L.-M.; Lu, H.; Cui, X.; Wojtas, L.; Zhang, X. P. Metalloradical activation of carbonyl azides for enantioselective radical aziridination. *Chem* **2021**, *7* (4), 1120.
- (69) Subbarayan, V.; Ruppel, J. V.; Zhu, S.; Perman, J. A.; Zhang, X. P. Highly asymmetric cobalt-catalyzed aziridination of alkenes with trichloroethoxysulfonyl azide (TcesN3). *Chem. Commun.* **2009**, DOI:10.1039/B905727G 10.1039/B905727G(28), 4266.
- (70) Lai, T.-S.; Che, C.-M.; Kwong, H.-L.; Peng, S.-M. Catalytic and asymmetric aziridination of alkenes catalysed by a chiral manganese porphyrin complex. *Chem. Commun.* **1997**, DOI:10.1039/a706395d 10.1039/a706395d(24), 2373.
- (71) Simonato, J. P.; Pecaut, J.; Scheidt, W. R.; Marchon, J. C. Antagonistic metal-directed inductions in catalytic asymmetric aziridination by manganese and iron tetramethylchiroporphyrins. *Chem. Commun.* **1999**, *1* (11), 989.

- (72) Liang, J. L.; Huang, J. S.; Yu, X. Q.; Zhu, N.; Che, C. M. Metalloporphyrin-mediated asymmetric nitrogen-atom transfer to hydrocarbons: aziridination of alkenes and amidation of saturated C-H bonds catalyzed by chiral ruthenium and manganese porphyrins. *Chemistry* **2002**, *8* (7), 1563.
- (73) Chan, K. H.; Guan, X.; Lo, V. K.; Che, C. M. Elevated catalytic activity of ruthenium(II)-porphyrin-catalyzed carbene/nitrene transfer and insertion reactions with N-heterocyclic carbene ligands. *Angew. Chem. Int. Ed. Engl.* **2014**, *53* (11), 2982.
- (74) Omura, K.; Murakami, M.; Uchida, T.; Irie, R.; Katsuki, T. Enantioselective aziridination and amination using p-toluenesulfonyl azide in the presence of Ru(salen)(CO) complex. *Chem. Lett.* **2003**, *32* (4), 354.
- (75) Fukunaga, Y.; Uchida, T.; Ito, Y.; Matsumoto, K.; Katsuki, T. Ru(CO)-salen-catalyzed synthesis of enantiopure aziridinyl ketones and formal asymmetric synthesis of (+)-PD 128907. *Org. Lett.* **2012**, *14* (17), 4658.
- (76) Müller, P.; Baud, C.; Jacquier, Y. A method for rhodium(II)-catalyzed aziridination of olefins. *Tetrahedron* **1996**, *52* (5), 1543.
- (77) Fruit, C.; Muller, P. Asymmetric transfer of nitrenes catalyzed by chiral dirhodium(II) using aromatic sulfamate esters. *Tetrahedron-Asymmetry* **2004**, *15* (6), 1019.
- (78) Liang, J. L.; Yuan, S. X.; Chan, P. W. H.; Che, C. M. Chiral rhodium(II,II) dimers catalyzed enantioselective intramolecular aziridination of sulfonamides and carbamates. *Tetrahedron Lett.* **2003**, *44* (31), 5917.
- (79) Yamawaki, M.; Tanaka, M.; Abe, T.; Anada, M.; Hashimoto, S. Catalytic enantioselective aziridination of alkenes using chiral dirhodium(II) carboxylates. *Heterocycles* **2007**, *72* (1i), 709.
- (80) Lebel, H.; Spitz, C.; Leogane, O.; Trudel, C.; Parmentier, M. Stereoselective rhodium-catalyzed amination of alkenes. *Org. Lett.* **2011**, *13* (20), 5460.
- (81) Coombs, J. R.; Morken, J. P. Catalytic Enantioselective Functionalization of Unactivated Terminal Alkenes. *Angew. Chem. Int. Ed. Engl.* **2016**, *55* (8), 2636.

- (82) Cho, D.-J.; Jeon, S.-J.; Kim, H.-S.; Cho, C.-S.; Shim, S.-C.; Kim, T.-J. Chiral C₂-symmetric bisferrocenyldiamines as ligands for transition metal catalyzed asymmetric cyclopropanation and aziridination. *Tetrahedron: Asymmetry* **1999**, *10* (19), 3833.
- (83) Kim, C.; Uchida, T.; Katsuki, T. Asymmetric olefin aziridination using a newly designed Ru(CO)(salen) complex as the catalyst. *Chem Commun (Camb)* **2012**, *48* (57), 7188.
- (84) Boquet, V.; Nasrallah, A.; Dana, A. L.; Brunard, E.; Di Chenna, P. H.; Duran, F. J.; Retailleau, P.; Darses, B.; Sircoglou, M.; Dauban, P. Rhodium(II)-Catalyzed Enantioselective Intermolecular Aziridination of Alkenes. *J. Am. Chem. Soc.* **2022**, *144* (37), 17156.
- (85) Fanourakis, A.; Hodson, N. J.; Lit, A. R.; Phipps, R. J. Substrate-Directed Enantioselective Aziridination of Alkenyl Alcohols Controlled by a Chiral Cation. *J. Am. Chem. Soc.* **2023**, *145* (13), 7516.

Chapter 2: Development of an Enantioselective Unactivated Alkene Aziridination Method using Planar Chiral Rh(III) Indenyl Catalysts and the Synthesis of Electron Rich Planar Chiral Indenyl Scaffolds

In this chapter we provide an overview of the scope of chiral cyclopentadienyl (Cp) ligands and how the state of the field in 2018 influenced the Blakey groups development of a planar chiral Rh(III) indenyl catalyst for an enantioselective allylic C–H amidation. We will discuss the subsequent development of an enantioselective unactivated alkene aziridination method and the attempts to synthesize electron-rich planar chiral Rh(III) indenyl catalysts. This work was published in collaboration with the Baik group in JACS in 2024.¹

2.1 Introduction to Chiral Cyclopentadienyl Catalysts

2.1.1 Overview of Chiral Cyclopentadienyl Transition Metal Catalysts

Since the discovery of the sandwich complex ferrocene in 1951, cyclopentadienyl (Cp) ligands have become some of the most widely used ligands in transition metal catalysis.² The strong σ - and π -donation of Cp ligands and their η^5 -coordination provides many of the resulting transition metal complexes with exceptional levels of stability, which has made their synthesis and handling an accessible feature for many laboratories. Furthermore, the stability imparted by Cp ligands through their η^5 -coordination allows for the removal of other ligands from the metal center exposing open coordination sites for catalytic activity. While the ability to modulate both steric and electronic parameters of Cp ligands, has enabled the creation of a wide range of tunable transition metal catalysts.³ Late transition metals have particularly benefited from the use of Cp ligands in the realm of C–H functionalization. As the development of Cp transition metal catalyzed reactions began to progress the demand to develop enantioselective version.⁴ While the use of achiral ancillary chelating ligands⁵⁻⁸ or the attachment of chiral tethers⁹ to Cp ligands has enabled the development of enantioselective transformations both strategies occupy coordination sites on the metal and therefore do not display the same types of reactivity as their achiral

counterparts. As a result, the development of truly chiral Cp ligands that retain open coordination sites for catalytic activity has been of great interest.

2.1.2 Chiral Cp Ligands of C_2 -Symmetry

The earliest reports of chiral Cp ligands were made by Vollhardt (**2.01**)^{10,11} and Halterman (**2.02**),¹² each developing unique ligand designs; however, none of these were successful at achieving high levels of enantioselective control (**Figure 2.1**). Although chiral Cp ligands continued to be developed in the following decades,¹³⁻¹⁵ the breakthrough development in chiral Cp catalysis came in 2012 when Cramer et al. introduced a new scaffold (**2.03**) inspired by Vollhardt's design,^{10,11} but which incorporated increased

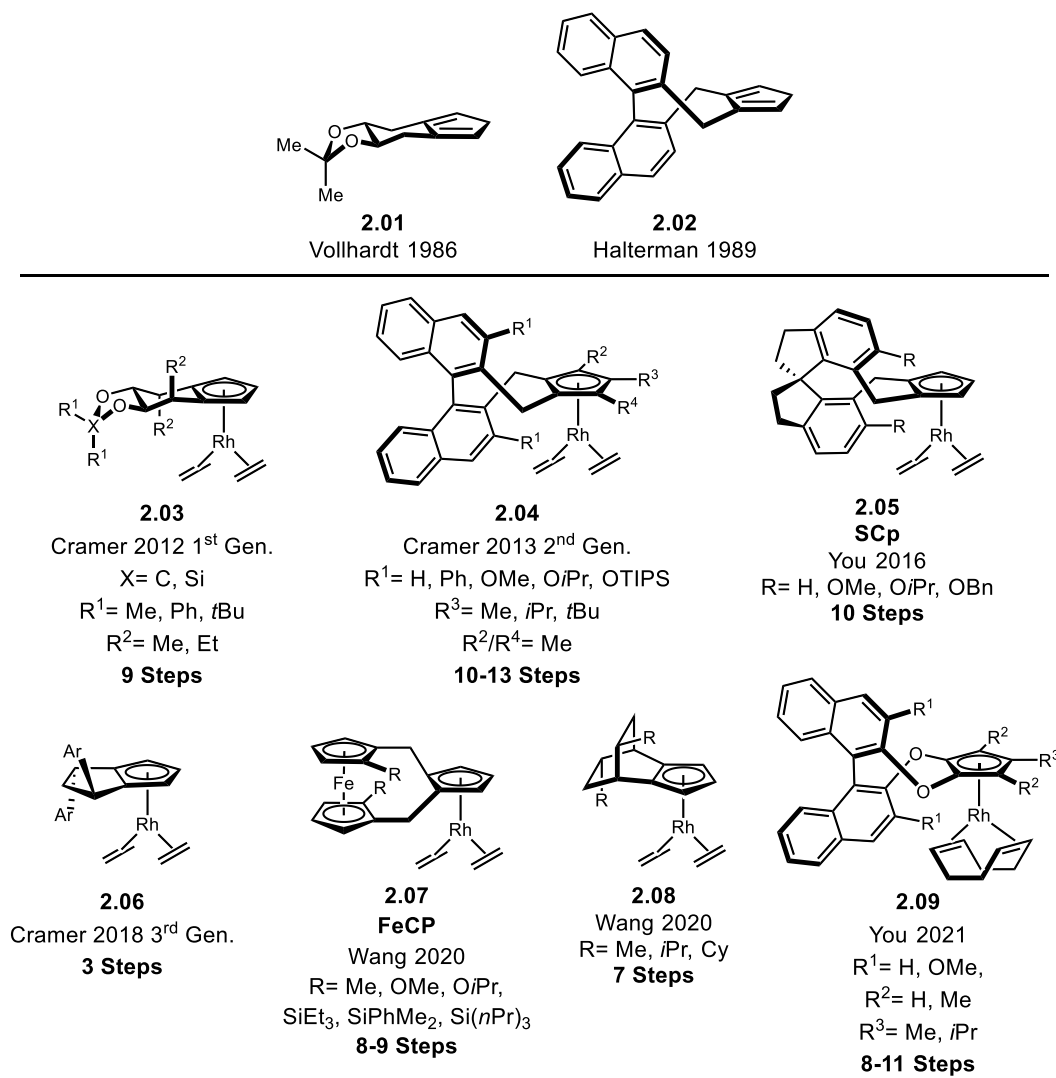


Figure 2.1 Overview of C_2 -Symmetric Chiral Cp Ligands and their Rhodium Complexes.

steric blocking elements.¹⁶ While its catalytic activity, tunability, and accessibility from *D*-mannitol in eight steps were a significant advantage over previous designs, the ligand crucially is of a C_2 -symmetric design. This allows for a single catalyst enantiomer to be formed upon metal coordination to either face of the ligand. This is a significant advantage over many previous chiral Cp designs and chiral tether Cp design which required the enantiomeric resolution of either ligands prior to metal coordination, or the metal complexes post ligand coordination.

Cramer followed upon his first design with his second-generation ligand (**2.04**) which introduced more steric blocking elements to the BINAP scaffolds first developed by Halterman.¹⁷ This ligand design has seen the greatest level of success, becoming the gold standard in chiral Cp catalysis with a number of derivatives being developed and finding applications using Co,¹⁸⁻²⁰ Ir,²¹⁻²⁵ Ru,^{26,27} Sc,²⁸⁻³⁰ and a number of other rare earth metals.³¹⁻³³ Cramer's first- and second-generation chiral Cp ligands reinvigorated synthetic interest into the development of chiral Cp ligands. In 2016 You et al. developed the SCp **2.05** scaffold which, like Cramer's BINOL-Cp design, is a C_2 -symmetric design, now based on the axially chiral SPINOL ligands.³⁴ In 2018 Cramer developed a new ligand scaffold (**2.05**) which, unlike his previous designs, did not rely on a lengthy synthetic sequence to access the desired ligands.³⁵ The cPent-Cp ligand was accessible in two steps using an organocatalyzed enantioselective ene-type reaction to provide the C_2 -symmetric ligand. The C_2 -symmetric FcCp ligand **2.07** was developed in 2020 by Wang et al. and the alternate ligand geometry proved to be advantageous in providing complementary reactivity compared to the BINOL-Cp and SCp ligand designs, often outperforming these scaffolds in both yield and enantioselectivity.³⁶ The same year, Wang also developed the fused bicyclo[2.2.2]octane Cp rhodium complex **2.08**.³⁷ This was followed by the development of a oxo-bridged derivative **2.09** of Cramer's second-generation ligand design in 2021.³⁸

2.1.3 Planar Chiral Cp Transition Metal Complexes

Following the development of many C_2 -symmetric ligand scaffolds, a number of planar chiral Cp scaffolds began to emerge. Unlike C_2 -symmetric ligand designs, these designs are considerably more challenging to access in an enantiopure fashion as complexation to either face of the prochiral Cp ring will provide a mixture of planar chiral enantiomers. To overcome this challenge many of the following designs have sought to bias one face of the Cp ring towards complexation by introducing steric blocking elements. Others have relied on chromatographic or crystallographic resolution strategies to separate enantiomeric or diastereomeric pairs.³⁹

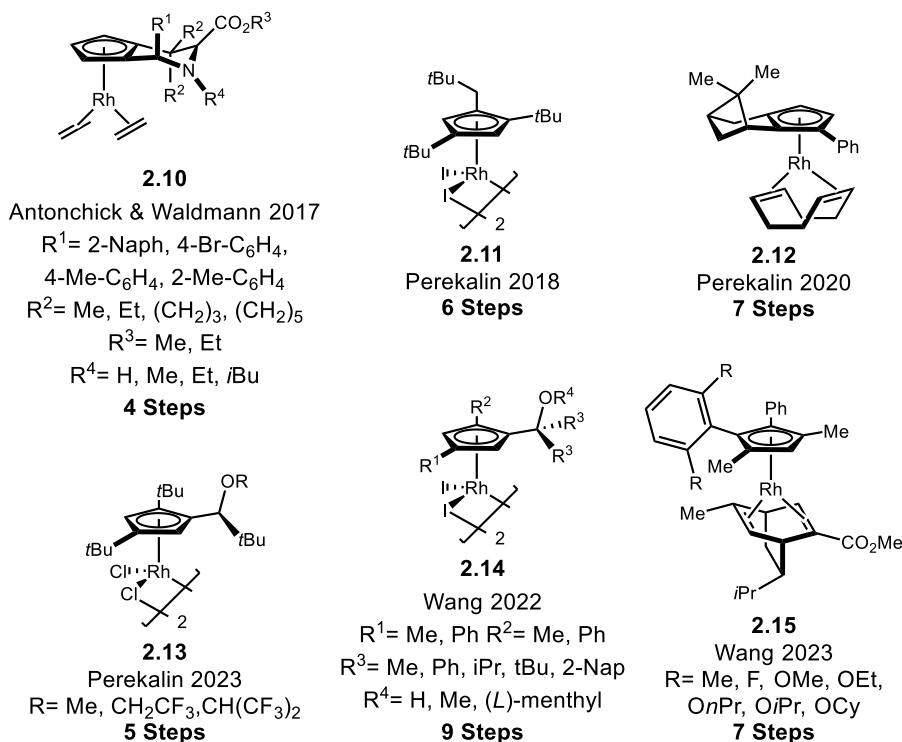


Figure 2.2 Overview of Planar Chiral Rhodium Complexes.

One of the first reports of a planar chiral transition metal catalyst came from Antonchick and Waldmann who developed a ligand scaffold (**2.10**) which unlike the previous design did not rely on chiral pool starting materials. Rather a copper catalyzed enantioselective [6+3] cycloaddition of imino esters to fulvenes to give the desired JasCp ligands (**Figure 2.2**).⁴⁰ In 2018, Perekalin reported a trisubstituted Cp ligand which formed a planar chiral complex upon coordination to rhodium metal center (**2.11**).⁴¹

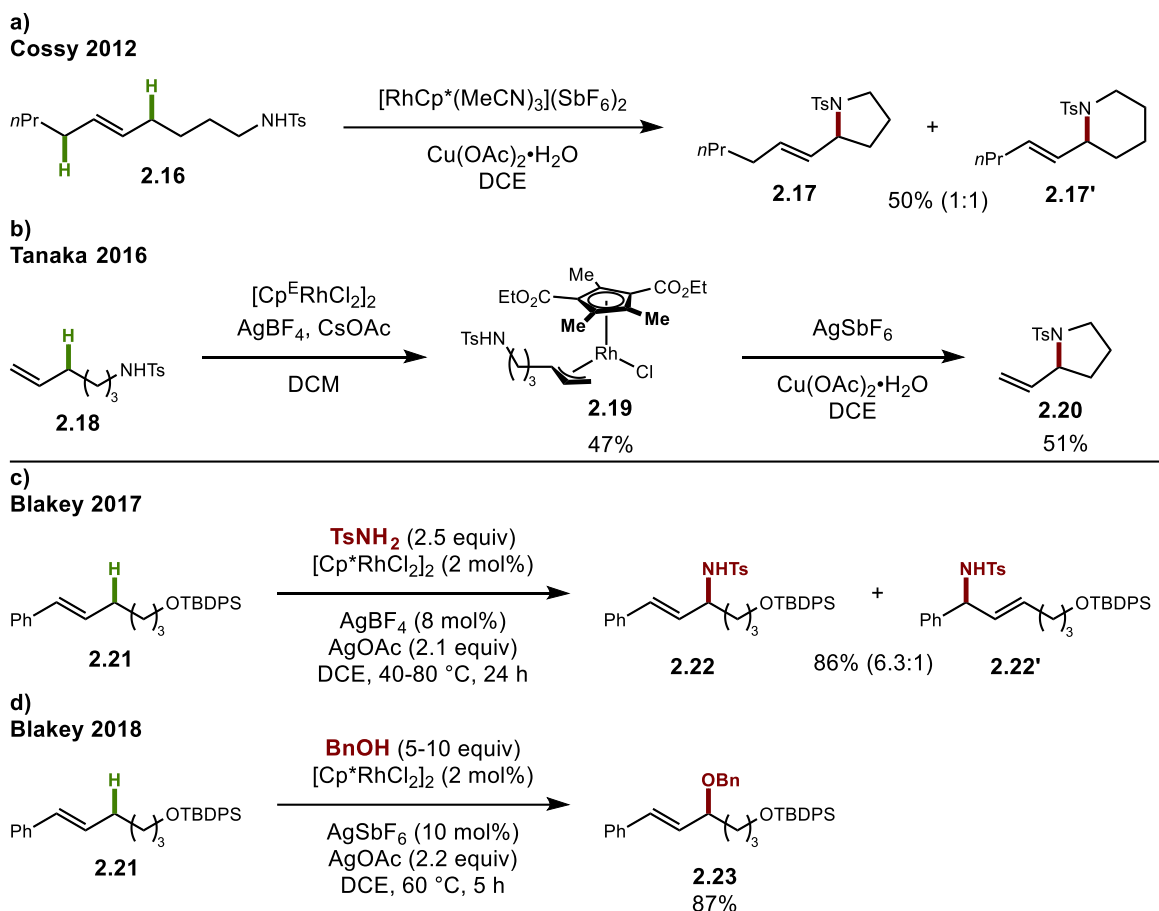
Resolution of **2.11** into its enantiopure form was achieved by forming an (*S*)-proline adduct; subsequent crystallization and removal of the proline ligand gave the desired complex in its enantiopure form. Perekalin subsequently developed a second planar chiral scaffold (**2.12**) which was derived from myrtenal.⁴² This design utilized the geminal dimethyl bridge head of myrtenal to bias metal coordination to one face of the Cp ring and provide **2.12** as single enantiomer. Unfortunately, this scaffold proved to be ineffective as a chiral catalyst and could only provide low levels of enantioselectivity. Perekalin developed a third ligand design in 2023. The planar chiral complex **2.13** could be resolved through silica gel chromatography after chelation with a chiral amino-alcohol, providing **2.13** in moderate enantiopurity.⁴³ As a result of this incomplete chiral resolution, low levels of enantioselective were observed when **2.13** was applied as a catalyst. In 2022, Wang developed a scaffold which could be resolved via diastereomeric crystallization of an intermediate *L*-menthol-ester-Cp rhodium complex and enabled the synthesis of twelve different scaffolds (**2.14**).⁴⁴ To improve enantiomer resolution of planar chiral catalysts Wang developed a second series of planar chiral complexes (**2.15**), where the use of a chiral diene allowed for diastereomeric resolution through flash column chromatography.⁴⁵

2.2 Development of Group IX Transition Metal Catalyzed Allylic C–H Functionalization Strategies in the Blakey Group

Allylic functionalization has emerged as a powerful synthetic tool for the rapid synthesis of complex molecular scaffolds. Initial work by Tsuji and Trost lead to the development of allylic substitutions using palladium as the primary choice of transition metal.^{46,47} While the development of allylic substitutions has flourished, allowing for the introduction of wide range of nucleophiles and in a stereoselective fashion, this strategy often requires prefunctionalization, which necessitates additional synthetic steps. This limitation has led to increasing interest in the development of allylic C–H functionalization as a faster means to access substituted allylic motifs. Once again, palladium transition metal catalysis was the first to demonstrate this type of reactivity and allowed for the installation of a variety of strong carbon and nitrogen nucleophiles to provide branched allylic products.⁴⁸ The development of Group IX-catalyzed methods

sought to expand the breadth of nucleophiles which could be employed as well as develop methods with enhanced levels of stereoselectivity.^{49,50}

2.2.1 Development of Group IX Catalyzed Oxidative Allylic C–H Functionalization Methods

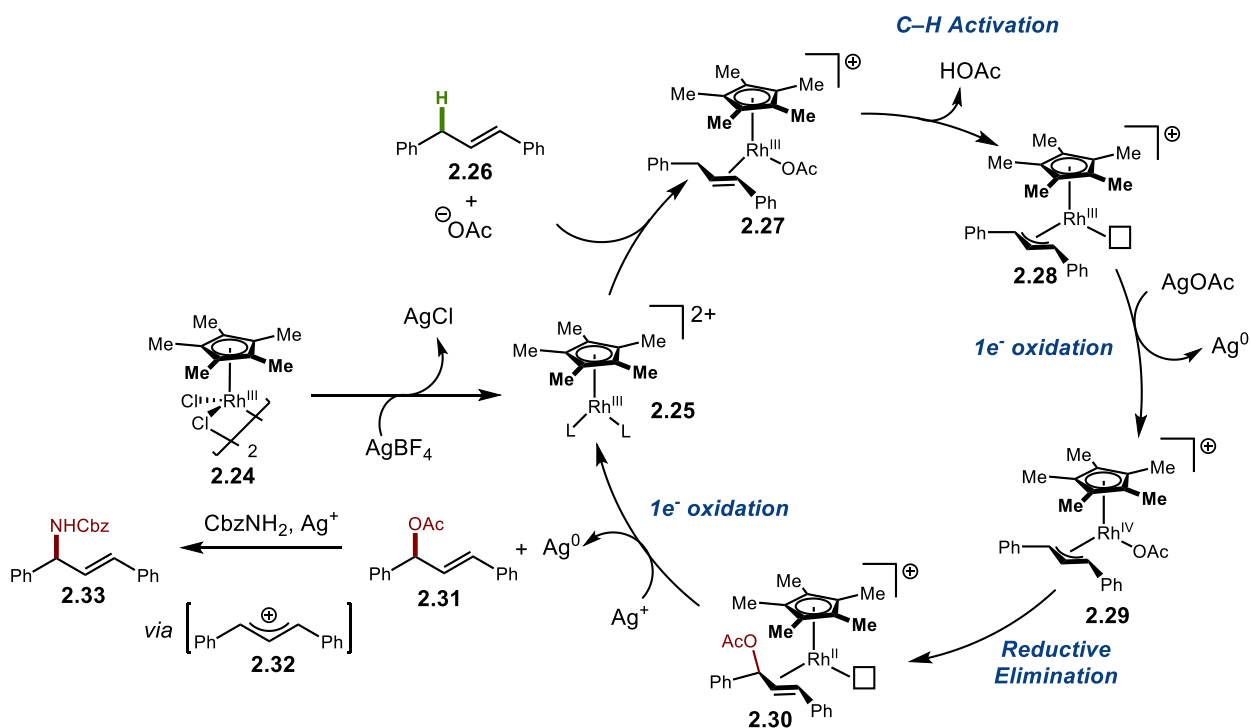


Scheme 2.1 Development of Rhodium Catalyzed Oxidative Allylic C–H Functionalization Strategies.

Initial stoichiometric work by Cossy and Tanaka demonstrated that RhCp* π -allyl complexes could be formed and subjected to nucleophilic attack from amines to form allylic amines products (**2.17**, **2.20**) (**Scheme 2.1a-b**).^{51,52} These initial reports laid the groundwork for the development of catalytic allylic C–H functionalization reactions. In 2017, the Blakey group disclosed an oxidative allylic C–H functionalization of internal olefins (**2.21**) using primary and secondary amines containing only one electron withdrawing group (**Scheme 2.1c**).⁵³ The reaction was found to be highly selective for the conjugated allylic products (**2.22** vs. **2.22'**) when functionalizing internal olefins. Following the development of a Rh-catalyzed allylic amination, the Blakey group disclosed the development of an allylic

etherification (**Scheme 2.1d**).⁵⁴ Prior to this report the use of oxygen nucleophiles had been limited to the use of carboxylates, while alcohols were considered to be oxidatively sensitive under the oxidative conditions required for allylic C-H functionalization. Nevertheless, the Blakey group was able to use a wide range of oxygen nucleophiles and was once again able to demonstrate excellent levels of regioselectivity for the conjugated allylic products (**2.24**). Following these initial reports by the Blakey group, other groups employed similar methodologies, expanding the catalytic activity to $[\text{Cp}^*\text{IrCl}_2]_2$ and utilizing aryl and triarylborylene nucleophiles.⁵⁵⁻⁵⁷

Following the Blakey group's first report of an allylic amination, work began to render this transformation enantioselective. In collaboration with the Cramer group, Dr. Jacob Burman evaluated the first- and second-generation C_2 -symmetric chiral Cp Cramer catalysts in the allylic amination. Unfortunately, no enantioinduction was observed, prompting a closer investigation of the mechanism of the allylic amination. In 2020, and in collaboration with the Macbeth and Baik groups, the Blakey group disclosed detailed kinetic and computational investigations into the mechanism of the rhodium catalyzed

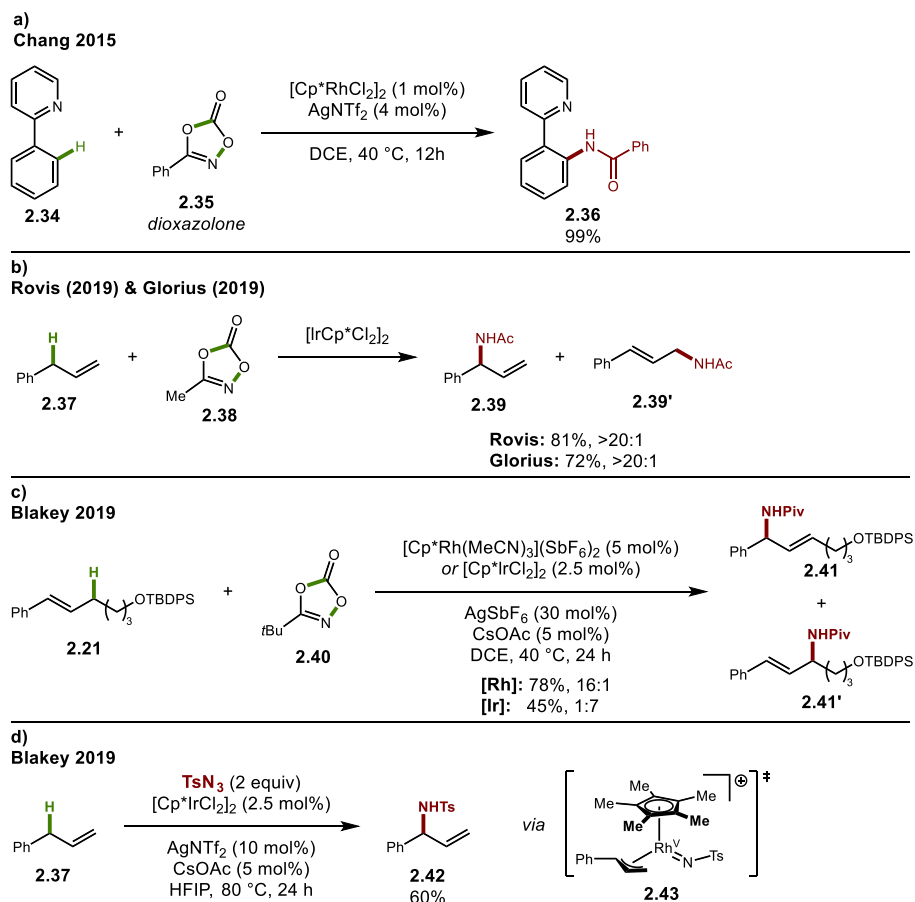


Scheme 2.2 First-Generation Allylic C-H Functionalization Mechanism.

oxidative allylic C–H amination.⁵⁸ Previous reports had proposed a Rh(III)-Rh(I)-Rh(III) catalytic cycle; however, it was determined that a Rh(III)-Rh(IV)-Rh(II)-Rh(III) cycle was likely operative (**Scheme 2.2**). The added AgOAc oxidant was proposed to be responsible for the two single electron oxidations and served as a source of acetate, which would lead to the formation of an intermediate allylic acetate **2.32**. This species would then undergo a disproportionation event, and the subsequent allylic cation **2.33** would undergo an S_N1 reaction with the amine nucleophile. This off-metal reaction explained the lack of enantioinduction when using a chiral Cp catalyst, as the transition metal was not directly involved in the key C–N bond formation step.

2.2.2 Development of Group IX Catalyzed Redox Neutral Allylic C–H Functionalization Methods

In an effort to continually expand the scope of possible nucleophiles for allylic C–H functionalization the Blakey,⁵⁸ Rovis,⁵⁹ and Glorius⁶⁰ groups independently and in rapid succession reported on the use of dioxazolones as amidating reagents. Dioxazolones had been first employed by the Chang group as bench-stable amidating reagents which could be safely handled unlike the more commonly employed azide reagents (**Scheme 2.3a**).⁶¹ The Chang group had shown that the N–O bond could serve as an internal oxidant for a metal catalyst through the liberation of carbon dioxide and lead to the formation of a metal nitrene, which would allow for an inner-sphere C–N bond formation. Inspired by Chang's work, Rovis and Glorius each utilized [Cp*IrCl₂]₂ and demonstrated the allylic functionalization on a variety of terminal alkenes with excellent regioselectivity for the branched products (**Scheme 2.3b**). The Blakey group followed up with a more detailed investigation of both terminal and internal olefins and demonstrated excellent catalyst controlled divergent regioselectivity. The use of [Cp*Rh(MeCN)₃](SbF₆)₂ with internal olefins **2.21** showed a greater selectivity towards benzylic C–N bond formation **2.41**, while the use of [Cp*IrCl₂]₂ with **2.21** showed a greater regioselectivity for the branched functionalized C–H amidation product **2.41'**. The redox neutral reactivity was further extended by the Blakey group through the use of TsN₃ as a nitrogen source to enable the branch-selective allylic sulfamidation of terminal olefins (**Scheme 2.3d**).⁶² These allylic C–H functionalizations are proposed to operate with a Rh(III)-Rh(V)-Rh(III) catalytic



Scheme 2.3 Development of Redox-Neutral Allylic C–H Functionalization Strategies.

cycle; through the cleavage of the dioxazolone N–O bond, or azide N–N bond, formation of the Rh(V) intermediate **2.43**, which then allows for reductive elimination, closing the redox-neutral catalytic pathway.

2.2.3 Development of a Planar Chiral Rh(III) Indenyl Catalyst for Enantioselective C–H Amidation

With an improved understanding of the limitations of the first-generation oxidative allylic C–H functionalization and with a means of conducting allylic C–H functionalization in a redox-neutral fashion using dioxazolones and azides, the Blakey group returned to previous efforts of developing an enantioselective reaction. While a renewed attempt could have been made using the catalyst developed by Cramer and others, the long and difficult synthesis required to access the C_2 -symmetric ligands (**2.01-2.06**) and planar chiral complexes (**2.10-2.11**), prompted the Blakey group to explore an alternative Cp scaffold.

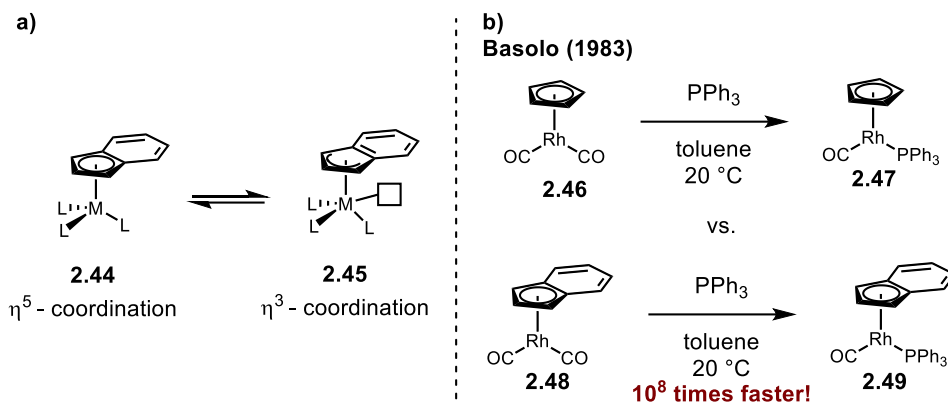
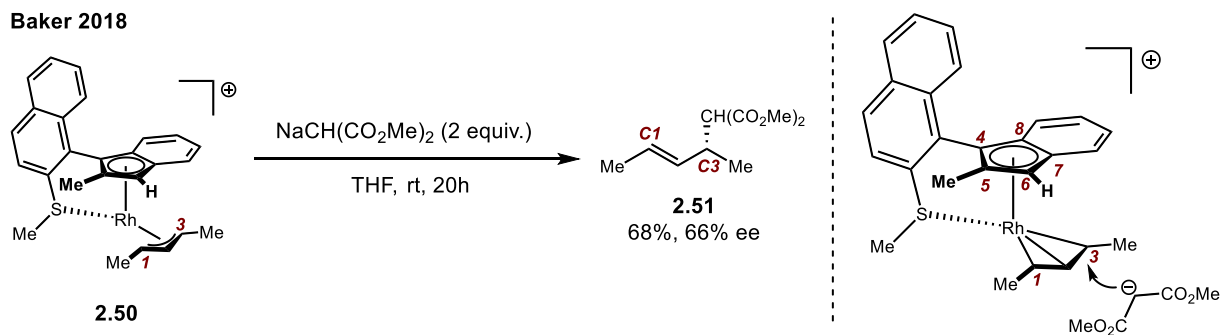


Figure 2.3 Overview of Ind Ligand Coordination and the Indenyl Effect.

One appealing alternative to a Cp scaffold is the indenyl (Ind) scaffold. Although structurally similar to the Cp scaffold with an η^5 -coordination and a 6π electron count, the fused aromatic ring of the Ind ligand produces unique reactivity characteristics once complexed to a metal.⁶³ Indenyl ligands are capable of changing their coordination to metal centers in a ring slip from η^5 **2.44** to a more η^3 -like coordination **2.45**, and in some extreme cases to a true η^3 -coordination (**Figure 2.3a**).⁶⁴ The fused aromatic ring of the Ind ligands provides additional aromatic stabilization in the η^3 -coordination.^{65,66} As the Ind ligand undergoes a ring slip, the η^3 -binding reduces the electron count on the metal, effectively opening a coordination site for additional ligand coordination. The ring slip of Ind complexes can lead to increased reaction rates and is known as the *indenyl effect*. Hart-Davis and Mawby were the first to describe this effect in 1969 when they observed an increase in rates of carbonyl migratory insertion by one of magnitude for a Ind molybdenum complex over the Cp variant.⁶⁷ Significantly larger increases in reaction rates have also been observed by Basolo where the substitution of carbon monoxide was found to occur 10^8 times faster with an Ind rhodium-complex **2.48** than with the Cp variant **2.46** (**Figure 2.3b**).⁶⁸

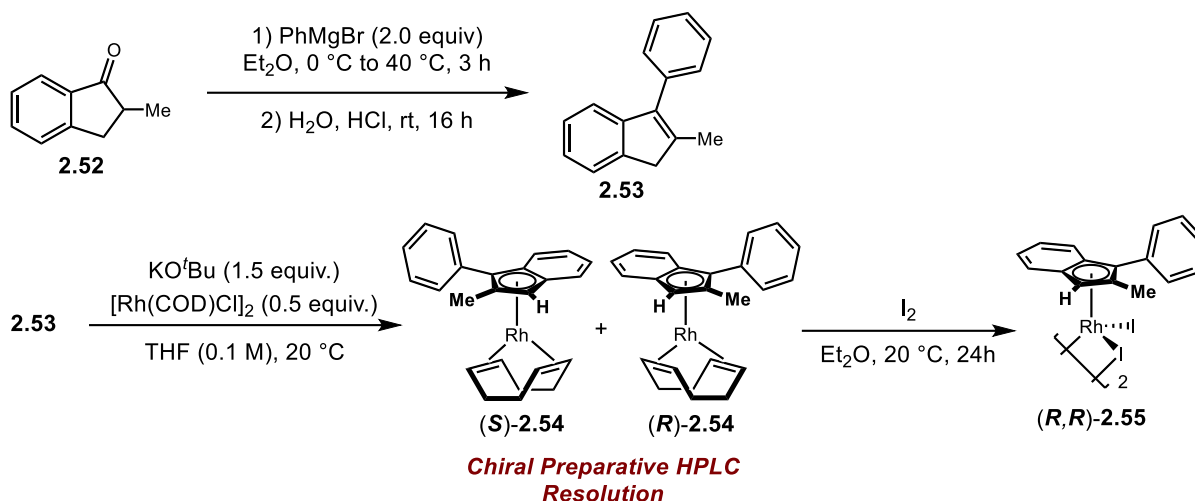


Scheme 2.4 Baker's Planar Chiral Indenyl Complex.

The Blakey group was inspired to pursue a Ind-based chiral catalyst following a report from Baker in 2018 in which he disclosed the development of a planar chiral Rh(III) π -allyl complex **2.50** (Scheme 2.4).⁶⁹ Exposing **2.50** to a dimethyl malonate nucleophile lead to the formation of the allylic product **2.51** in a moderate yield of 68% and with moderate enantioselectivity (66% e.e.). Computational and crystallographic analysis of **2.50** revealed that the asymmetric scaffold of the Ind ligand was responsible for the observed enantioinduction in the outer sphere mechanism. The asymmetric ring slip of the indenyl ligand towards a more η^3 -like coordination results in a trans-effect where the distal Rh–C7 and Rh–C8 bonds begin to lengthen, causing the Rh–C1 bond to shorten and strengthen. The shortening of the Rh–C1 favors nucleophilic attack at the weaker and longer C3 position of the π -allyl ligand.

While this precedent from Baker demonstrated a unique case of electronic asymmetry leading to enantioinduction, the Rh complex was not catalytically active due to the thioether tether occupying a coordination space. In order to develop a catalytic enantioselective allylic C–H functionalization reaction, the Blakey group set out to simplify the Baker complex design by removing the thioether tether. The resulting indene ligand **2.53** was a simple design that could be accessed in a one-pot synthetic sequence through the addition of phenyl magnesium bromide to the indanone **2.52** and elimination of the intermediate alcohol adduct using HCl (Scheme 2.5).⁷⁰ Complexation of **2.53** to $[\text{Rh}(\text{COD})\text{Cl}]_2$ provided racemic $\text{Ind}^X\text{Rh}(\text{I})(\text{COD})$ intermediate **2.54** whose planar chiral enantiomers could be easily separated using chiral preparative HPLC. Once the enantiomers of **2.54** were separated, simple oxidation using molecular iodine provided the Rh(III) diiodide dimer **2.55**. Although this synthetic sequence toward **2.55** requires the use of

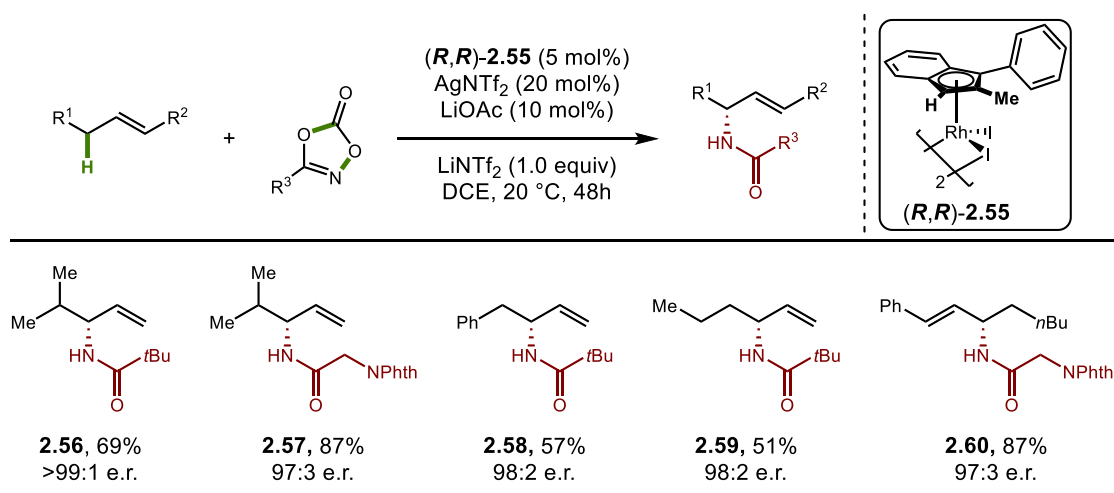
Blakey (2020)



Scheme 2.5 Synthetic Route towards the First-Generation Planar Chiral Rh(III) Indenyl Catalyst.

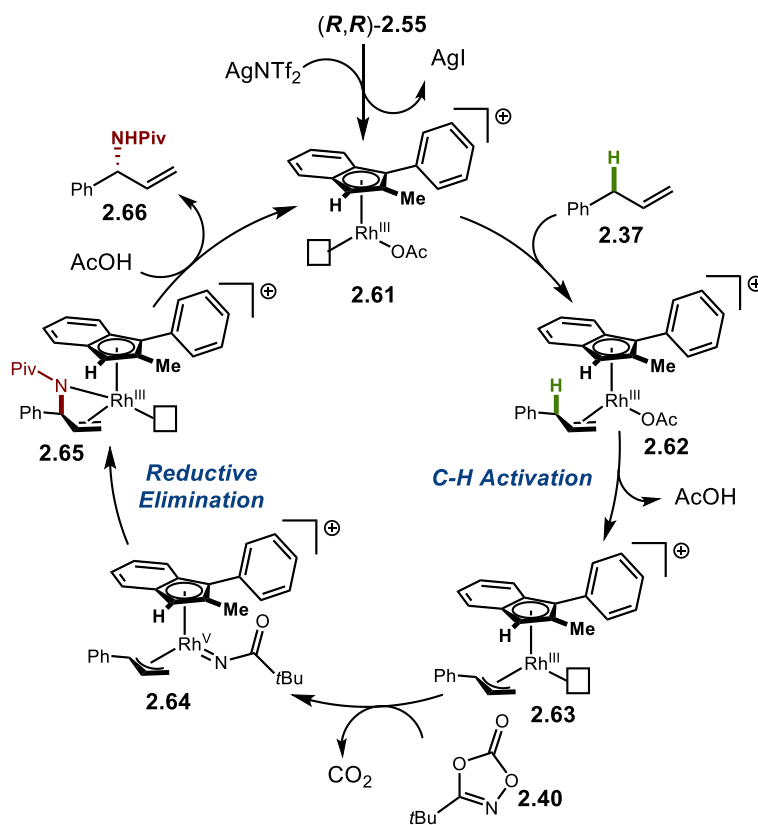
preparative HPLC, it still represents one of the shortest synthetic sequences towards a chiral Cp-like catalyst.

With a new chiral catalyst in hand, development of an enantioselective allylic C–H amidation was undertaken. Following optimization of the Blakey conditions for the use of dioxazolone nitrene precursors, catalyst **2.55** was found to be highly effective allowing for the enantioselective C–H amidation using a variety of dioxazolone reagents on a number of both terminal and internal olefins (**Scheme 2.6**).⁵⁸ The



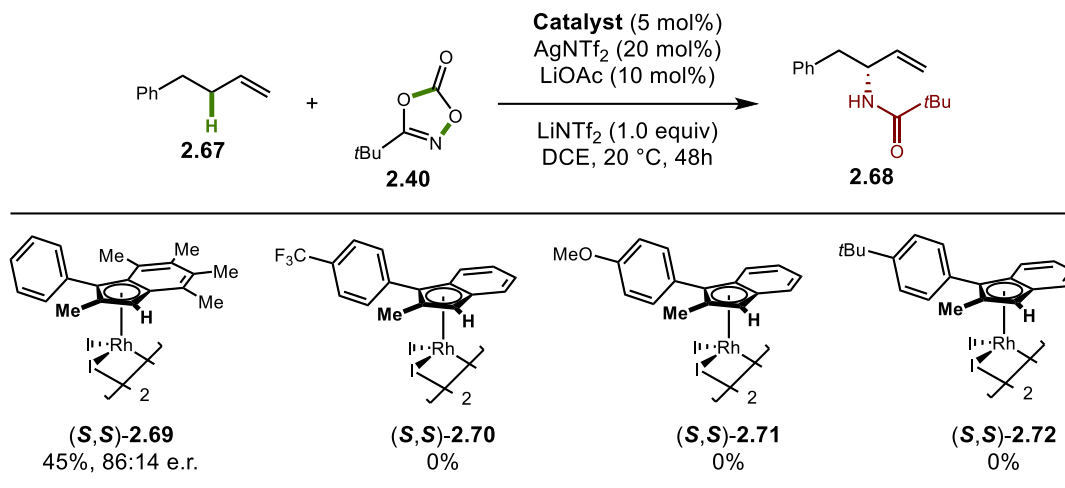
Scheme 2.6 Planar Chiral Rh(III) Indenyl Catalyzed Enantioselective Allylic C–H Amidation.

reaction was found to be highly regioselective for the formation of branched products from terminal olefins and conjugated products from internal olefins.



Scheme 2.7 Mechanism of the Enantioselective Allylic C–H Amidation.

Computational mechanistic investigations were conducted in collaboration with the Baik group to elucidate the role of the Ind ligand in this transformation. The initial allylic C–H functionalization step was determined to be the rate- and enantiodetermining step, with the asymmetric design of the planar chiral catalyst controlling the formation of the resulting π -allyl **2.63** through steric blocking (**Scheme 2.7**). As previously hypothesized, formation of a high-valent Rh(V)-metal-nitrene **2.65** was found to be the lowest energy pathway and would allow for a facile reductive elimination to form the C–N bond. The location of reductive elimination to either the terminal or branched position of the π -allyl is dictated by electronic bias brought forth by the indenyl ligand's asymmetric binding to the π -allyl.

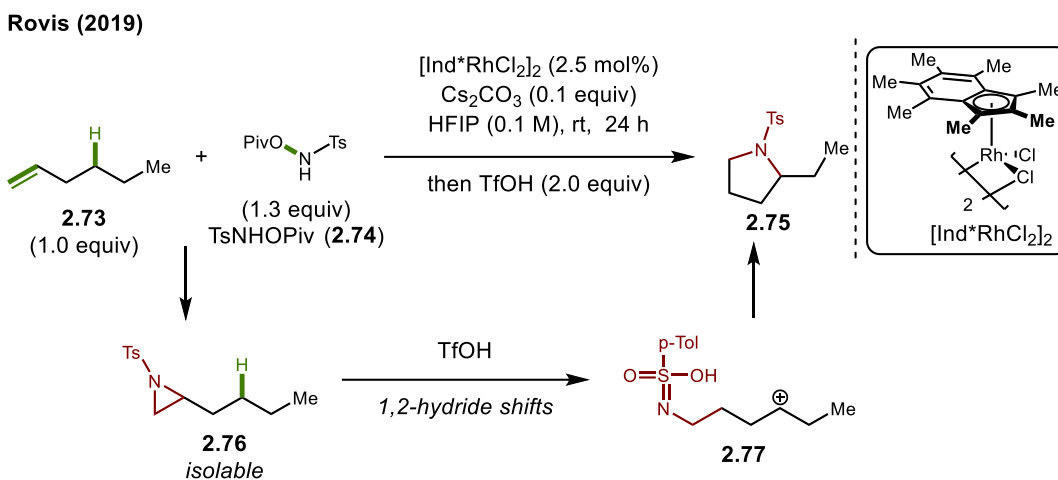


Scheme 2.8 Enantioselective Allylic C–H Amidation using Second-Generation Planar Chiral Indenyl Catalysts.

Recognizing that the ligand electronics were key to indenyl ligands unique reactivity profiles, a pentamethylated version **2.69** was also developed in the course of this work but was found to be less effective in the allylic amidation. Following the publication of this work, further development of electronically tuned second-generation planar chiral catalysts was conducted by Dr. David Laws III to identify the role of ligand electronics in catalyst reactivity. The facile synthetic sequence of the indene ligand enabled the rapid synthesis of electronically varied catalyst **2.70-2.72** (Scheme 2.8). Unfortunately, these second-generation catalysts were not found to be catalytically active in the enantioselective allylic C–H amidation.

2.3 Enantioselective Aziridination of Unactivated Alkenes Using A Planar Chiral Rh(III) Indenyl Catalyst

While the first- and second-generation indenyl catalysts had been developed in the context of allylic C–H functionalization, their unique reactivity profile of asymmetric steric and electronic induction and the possibility of increased rates of reaction through ring slippage led us to explore their application in other catalytic reactions. We were drawn to a report from the Rovis group which demonstrated the synthesis of substituted pyrrolidines **2.75** from terminal unactivated alkenes **2.73** (Scheme 2.9).⁷¹ Notably, this reaction was found to be more effectively catalyzed by the heptamethylindenyl (Ind*) catalyst [Ind*RhCl₂]₂ than

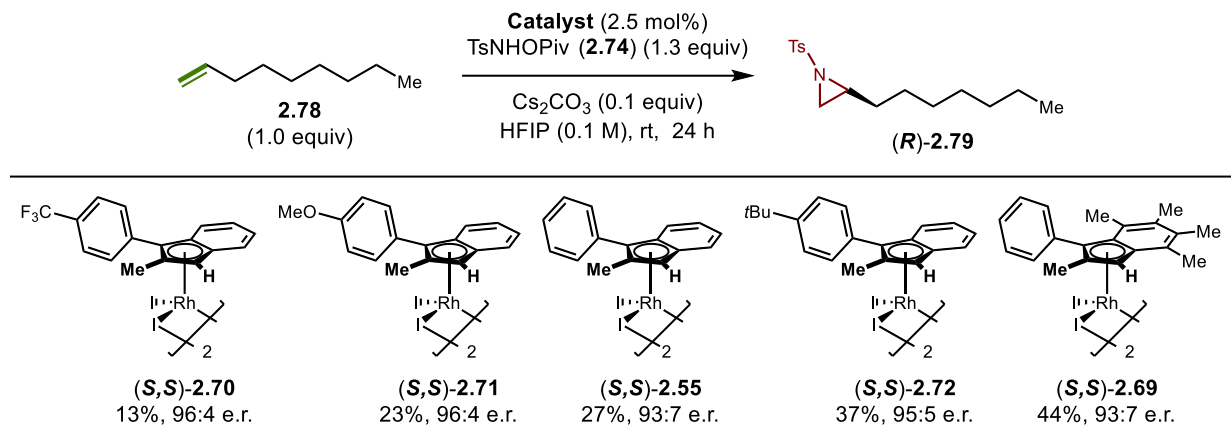


Scheme 2.9 Synthesis of Pyrrolidines from Unactivated Alkenes

with the more common $[Cp^*RhCl_2]_2$ catalyst. Furthermore, during mechanistic investigations, it was determined that the key isolable intermediate was an aziridine **2.76** which upon exposure to triflic acid would undergo a series of 1,2-hydride shifts to form the pyrrolidines. While aziridines had been frequently invoked as intermediates in Group IX-catalyzed nitrogen transfers to alkenes, prior to this report, none had been isolated.^{72,73} The authors proposed either a classic metal-nitrene intermediate which could transfer the nitrogen to the alkene, or a migratory insertion mechanism with an addition of the nitrogen and rhodium across the alkene followed by intramolecular cyclization. While the pyrrolidines could not be accessed in an enantioselective fashion due to the cationic 1,2-hydride shift mechanism, the aziridine intermediates could potentially be accessed asymmetrically using the planar chiral indenyl catalyst developed in the Blakey group. We were further motivated by synthetic utility of chiral aziridines as chiral nitrogen building blocks and the lack of asymmetric methods for the enantioselective aziridination of unactivated alkenes (**Chapter 1**). We therefore set out to develop an enantioselective unactivated alkene aziridination using the Blakey group's planar chiral Rh(III) indenyl catalysts.

2.3.1 Evaluation of Catalytic Activity of First- and Second-Generation Planar Chiral Catalysts

We began by determining whether enantioinduction was feasible with the catalyst scaffolds on hand. The first- and second-generation catalysts **2.55**, **2.69-2.72** were evaluated in the enantioselective



Scheme 2.10 Screen of First- and Second-Generation Planar Chiral Indenyl Catalyst in the Enantioselective Unactivated Alkene Aziridination

aziridination of nonene **2.79** using hydroxylamine **2.74** and reaction conditions first reported by Rovis (**Scheme 2.10**). The trifluoromethyl-substituted catalyst **2.70** provided the aziridine **2.79** in a 13% yield and with 96:4 e.r. The methoxy-substituted catalyst **2.71** was found to provide **2.79** in a 23% yield and with a 96:4 e.r. While methoxy substituents are typically considered activating groups, the out-of-plane orientation of the aryl substituent prevents the methoxy from donating electron density to the metal center via resonance. Instead, the oxygen acts as an electron withdrawing group through inductive effects leading to a similar level of reactivity as the trifluoromethyl-substituted catalyst **2.70**. The first-generation catalyst **2.55** provided **2.79** in a 27% yield and 93:7 e.r, while the use of the electron-donating *tert*-butyl catalyst **2.72** increased the yield of **2.79** to 37% and still provided excellent levels of enantioselectivity (95:5 e.r.). The pentamethylated catalyst **2.69** was found to be the most effective and provided **2.79** in a 44% yield and with 93:7 e.r.. The observed greater reactivity of the electron-rich catalysts **2.72** and **2.69** was hypothesized to arise from the autoionization of the dimeric precatalysts structure to the 16-electron monomeric Rh(III) species, which would receive greater inductive stabilizing effects from the electron-rich ligands.

2.3.2 Synthesis of Third-Generation Electron Rich Planar Chiral Catalysts

Recognizing an opportunity to further develop the planar chiral indenyl catalysts, a series of third-generation electron-rich planar chiral designs **2.80-2.85** were envisioned (**Figure 2.4**). These catalysts

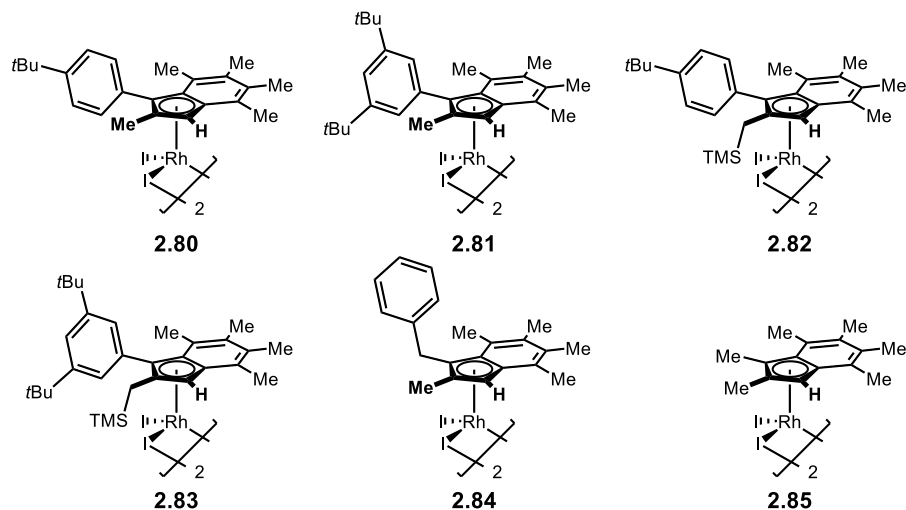
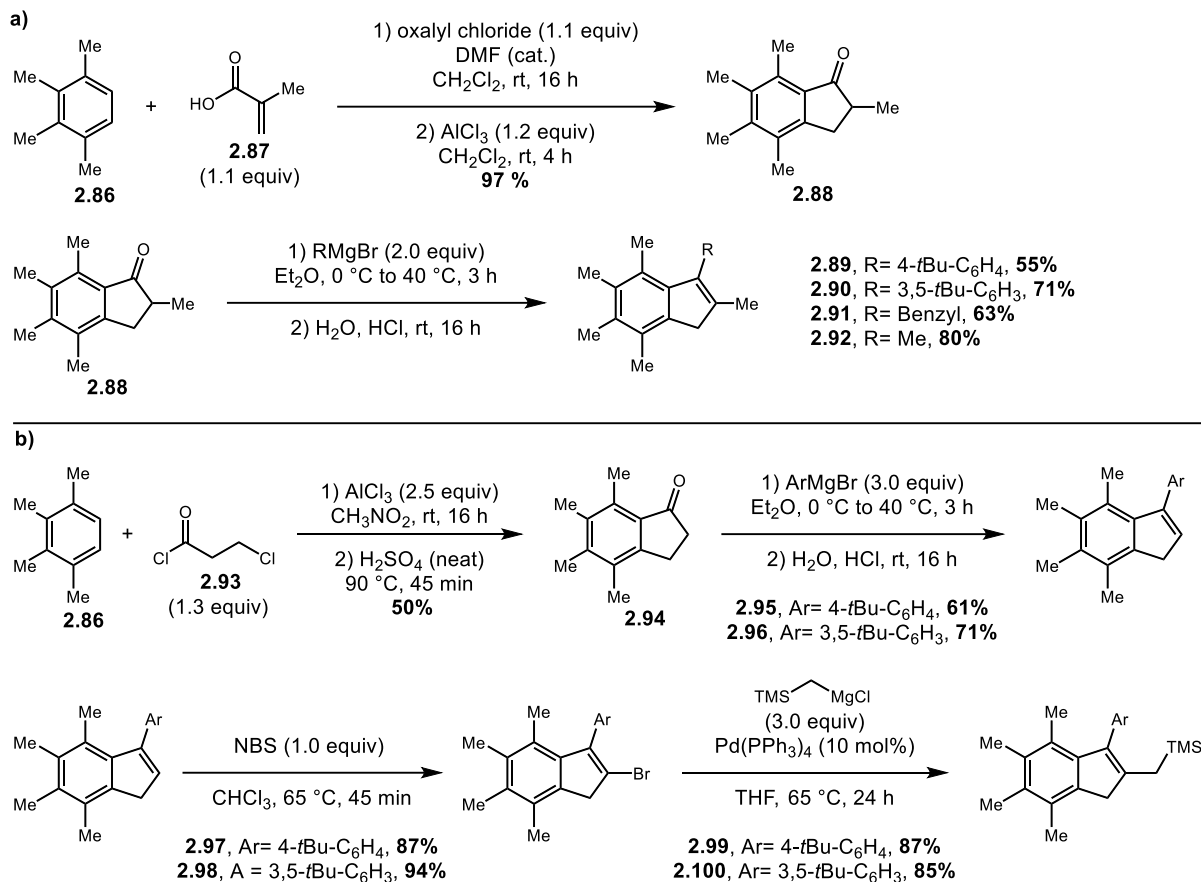


Figure 2.4 Third Generation Electron Rich Planar Chiral Rh(III) Indenyl Catalysts

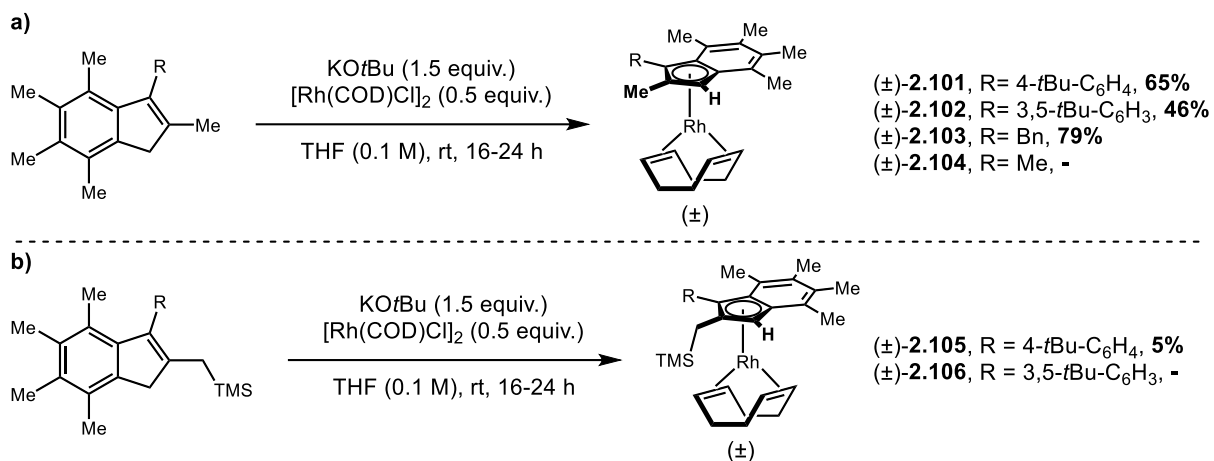
incorporated design elements from previous catalysts and introduced new ones. All six catalysts contained the methylation of the aromatic backbone used in the successful catalyst **2.69**. The electron-donating *tert*-butyl substitution from catalyst **2.72** was introduced to the four catalysts **2.80-2.83**. The addition of a silicon substituent at the 2-position of the indenyl ligand for catalysts **2.82** and **2.83** was envisioned to harness the β -silicon effect. This effect describes silicon's ability to stabilize the buildup of cationic charge through donation of electron density from its low-lying C–Si σ -bond into neighboring empty high energy σ^* -orbital. The β -silicon effect was used by Rovis to achieve similar electronic properties as a Cp* ligand while retaining the reduced steric properties of a monosubstituted Cp ring.⁷⁴ We therefore envisioned that the silicon substitution of **2.82** and **2.83** would further stabilize the build-up of cationic charge on the rhodium metal center. The final two catalysts **2.84** and **2.85** exchanged the phenyl substitution of **2.69** for methyl and benzyl substitutions to probe different steric blocking elements and potentially match the similar steric and electronic properties of Ind*.

As with the first- and second-generation designs, the synthesis of ligands required for the third-generation could be achieved in relatively few steps. The synthetic sequence towards the ligands for the pentamethylated catalyst began with a tandem Friedel-Crafts acylation and Nazarov cyclization on 1,2,3,4-tetramethylbenzene **2.86** using methacrylic acid **2.87** to provide the indanone **2.88** (Scheme 2.11a).



Scheme 2.11 Ligand Synthesis of the Third-Generation Electron Rich Planar Chiral Rh(III) Indenyl Catalyst

In a one-pot procedure, **2.88** was subjected to the appropriate Grignard reagent followed by the elimination of the intermediate alcohol using HCl to provide the desired ligands **2.89-2.92** (Scheme 2.11b). The synthesis of the silicon substituted ligands also began with a Friedel-Crafts acylation of **2.86**, this time using the acid chloride **2.93** which allowed for an acid-catalyzed cyclization to the indanone **2.94**; this intermediate could be subjected to the same one-pot procedure to provide indenenes **2.95** and **2.96**. To install the desired silicon substituents, bromination of the indene at the 2-position using freshly recrystallized NBS, and short reaction times to prevent over bromination, gave the 2-bromoindenenes **2.97** and **2.98**. These could then be subjected to Kumada coupling conditions to forge the desired silicon substituted ligands **2.99** and **2.100**.

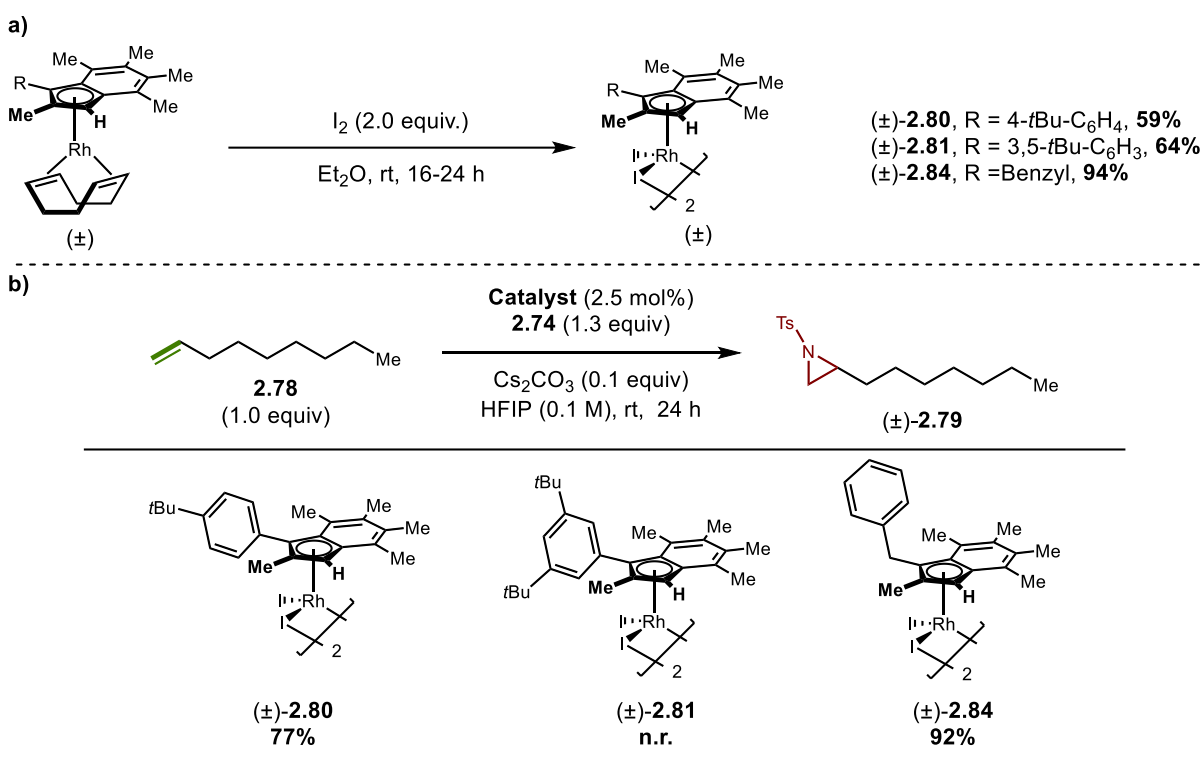


Scheme 2.12 Synthesis of Electron-Rich Ind^XRh(I)COD Complexes

With the new indene ligands in hand, complexation to form the intermediate Ind^XRh(I)COD complexes were attempted using the same conditions as were used for the previous catalyst synthesis. Beginning with the pentamethylated ligands Ind^XRh(I)COD complexes **2.101-2.103** were synthesized (**Scheme 2.12a**). These complexes were found to be very nonpolar and required rigorous purification to remove any unreacted indene ligand starting material. Furthermore, they were found to be highly sensitive to acidic media, decomposing on silica and in CDCl₃. Basification of the silica prior to purification allowed for their isolation and the use of C₆D₆ enabled their characterization by NMR. The hexamethylene complex **2.104** could only be formed in trace amounts and was found to decompose rapidly. Both silicon complexes **2.105** and **2.106** were also found to be unstable with **2.105** only being isolated in a 5% yield (**Scheme 2.12b**).

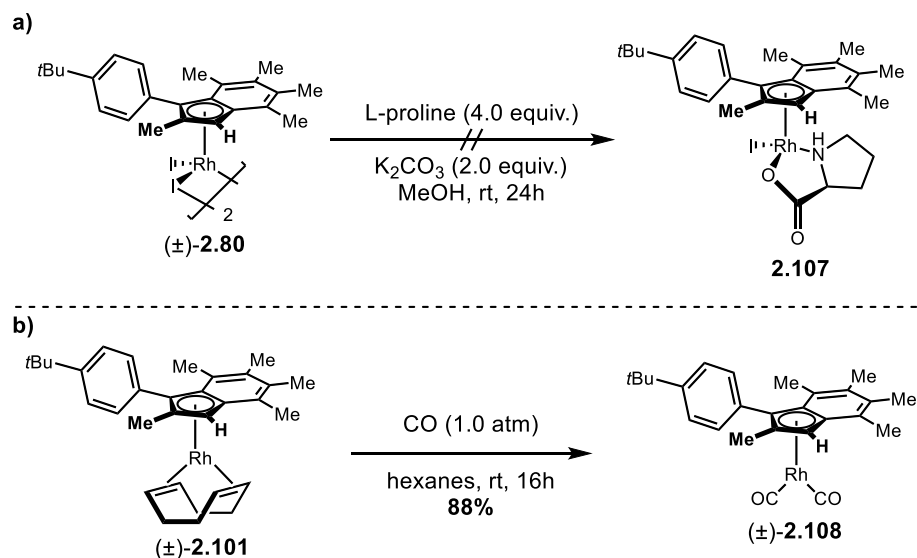
With three of the initial six complexes having been successfully synthesized, they were oxidized using molecular iodine to the racemic Rh(III) diiodide dimers **2.80**, **2.81**, **2.84** to begin testing their initial racemic reactivity in the aziridination (**Scheme 2.13a**). The pentamethylated mono-*tert*-butyl catalyst **2.80** was found to significantly improve the yield of **2.79** to 77% (**Scheme 2.13b**). Unfortunately, the di-*tert*-butyl variant **2.81** was entirely unreactive, and only returned unreacted starting materials. The benzyl-substituted catalyst **2.84** proved to be highly effective in the aziridination providing the aziridine **2.79** in a

92% yield. These racemic tests using the new third-generation catalysts proved to be promising in demonstrating how the increased electron donation improved the reactivity of the catalyst.



Scheme 2.13 Synthesis of Racemic Third Generation Planar Chiral Rh(III) Precatalysts Dimers and Evaluation in the Unactivated Alkene Aziridination

To continue the development of the third generation of catalysts, the racemic Ind^XRh(I)COD complexes of **2.101** and **2.103** needed to be resolved into their single enantiomers. Initial investigation on normal phase chiral analytical HPLC, however, was not promising. While the enantiomers of **2.101** began to separate on an OD-H Chiralcel column at 100% hexanes, baseline resolution could not be achieved. The enantiomers of the benzyl substituted complex **2.103** did not separate and the decision was made to not pursue this complex further due to its highly nonpolar nature. Still motivated by the promising racemic aziridination results using **2.80**, attempts were made to access **2.101** in an enantiopure form via alternative purification techniques. Promising results at the time of this work from the Perekalin group in the synthesis of planar chiral complexes showed the use of ancillary ligands to separate planar chiral enantiomers of Rh(III) complexes, either through the crystallization of diastereomeric proline complexes or the chromatographic separation⁴¹ of chiral amine adducts.⁷⁵ However, these methods failed when applied to the



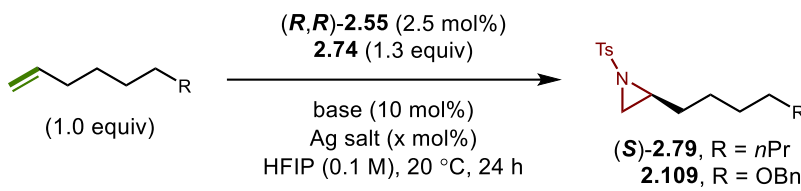
Scheme 2.14 Chiral Resolution Attempts of Rh(I) and Rh(III) Planar Chiral Complexes

Rh(III) indenyl complex **2.101** with the discrete proline adduct complex **2.107** never being formed (**Scheme 2.14a**). In an attempt to alter the polarity of the racemic Ind^xRh(I)COD complex ligand substitution of COD with carbon monoxide provided the Ind^xRh(I)(CO)₂ complex **2.108** (**Scheme 2.14b**). This compound did show improved separation on an analytic instrument with baseline resolution between enantiomeric peaks; however, once separation began on a preparative scale the complex proved to be too unstable and insufficient separation of the enantiomers was observed. The challenges faced in the separation of planar chiral complexes are inherent to their design and were exacerbated in this study by the nonpolar characteristic of the Ind^xRh(I) intermediates.

2.3.3 Optimization of Reaction Conditions

Although our attempts at developing a third generation of planar chiral indenyl catalysts for an enantioselective aziridination did bear fruit, we were still interested in the development of the enantioselective reaction. Following our hypothesis of ligand electronics enhancing autoionization, we investigated the use of Ag halide scavengers to activate the catalyst. The initial attempt using AgNTf₂ (10 mol%) in the aziridination of 1-nonene did not prove successful, leading to a reduction in yield (19%, 94:6 e.r.) (**Table 2.1, Entry 1**). A change in base from Cs₂CO₃, to CsOPiv proved to be key, with an improved

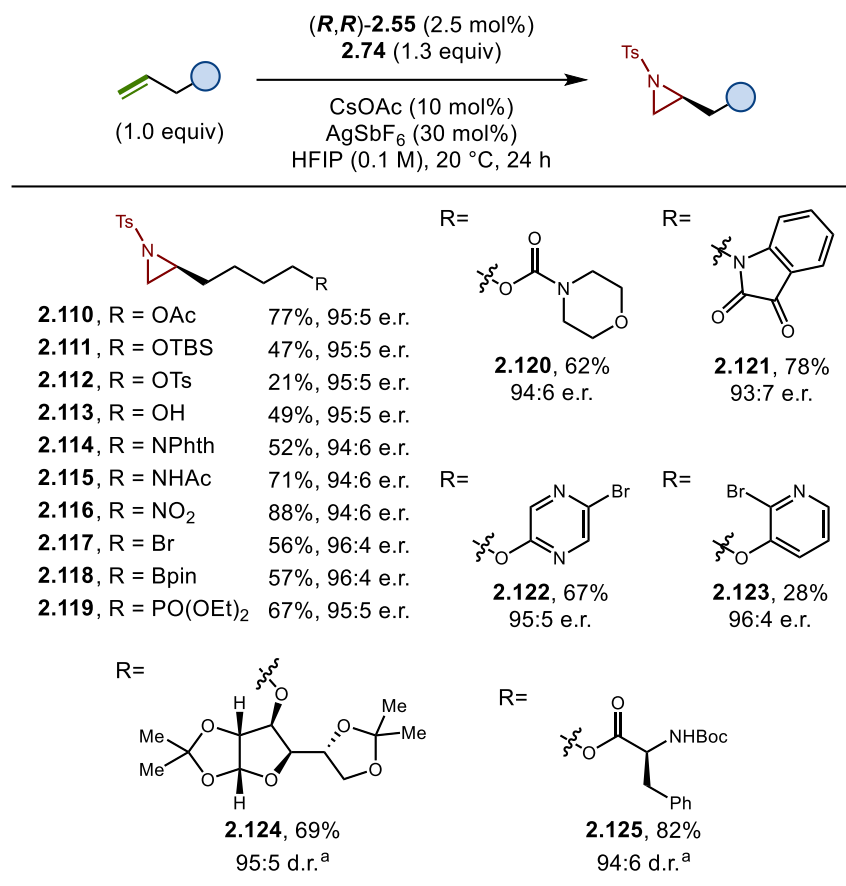
Table 2.1 Optimization of Silver Halide Additive Loading



| entry | R | Ag salt | base | % yield ^a | e.r. ^b |
|-------|-------------|------------------------------|---------------------------------|----------------------|-------------------|
| 1 | <i>n</i> Pr | AgNTf ₂ (10 mol%) | Cs ₂ CO ₃ | 19 | 94:6 |
| 2 | <i>n</i> Pr | AgNTf ₂ (10 mol%) | CsOPiv | 65 | 94:6 |
| 3 | <i>n</i> Pr | AgNTf ₂ (10 mol%) | CsOAc | 74 | 96:4 |
| 4 | <i>n</i> Pr | AgSbF ₆ (10 mol%) | CsOAc | 83 | 95:5 |
| 5 | OBn | AgSbF ₆ (10 mol%) | CsOAc | 35 | 95:5 |
| 6 | OBn | AgSbF ₆ (20 mol%) | CsOAc | 49 | 95:5 |
| 7 | OBn | AgSbF ₆ (30 mol%) | CsOAc | 66 | 95:5 |
| 8 | OBn | AgSbF ₆ (40 mol%) | CsOAc | 55 | 95:5 |
| 9 | OBn | AgSbF ₆ (50 mol%) | CsOAc | 28 | 95:5 |
| 10 | OBn | AgSbF ₆ (60 mol%) | CsOAc | 27 | 95:5 |

yield of 65% while still achieving excellent enantioselectivity (95:5 e.r.), due to improved stabilization of catalytic intermediate by the pivalate anion over the carbonate (**Table 2.1, Entry 2**). Further improvements were achieved by using AgSbF₆ (10 mol%) and CsOAc (10 mol%) allowing for the formation of **2.79** in 83% with excellent enantioselectivity (95:5 e.r.) (**Table 2.1, Entry 4**). We next explored the loading of AgSbF₆ as we observed a significant decrease in yield when using an alkene other than **2.78** (**Table 2.1, Entry 5**). Switching to the benzoyl protected 5-hexen-1-ol, we discovered that a loading of 30 mol% of AgSbF₆ was required to provide the aziridine **2.109** in a 66% yield with the same excellent enantioselectivity (95:5 e.r.) (**Table 2.1, Entry 7**). Loadings of AgSbF₆ above or below 30 mol% were found to be detrimental to the yield of **2.109** (**Table 2.1, Entry 8-10**). The increased loading of silver halide scavenger is hypothesized to recover the catalyst from decomposition pathways.

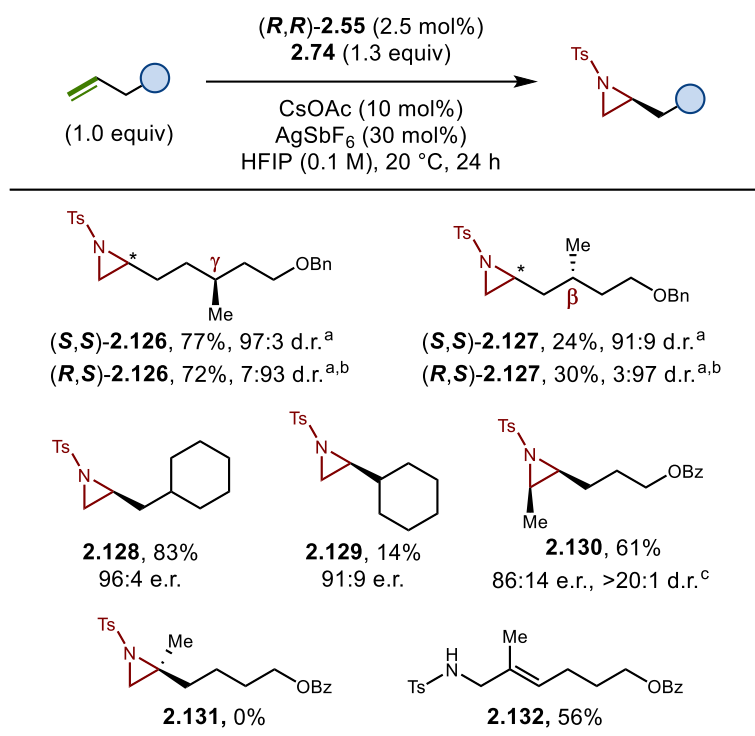
2.3.4 Reaction Scope



Scheme 2.15 Scope of Enantioselective Unactivated Alkene Aziridinations Bearing a Variety of Functional Groups

With newly optimized reaction conditions that enabled the use of the first-generation catalyst **2.55**, the scope of the enantioselective aziridination was explored (**Scheme 2.15**). We first examined protected 5-hexen-1-ol derivatives which were well tolerated and provided the aziridine products **2.110-2.112** in low to good yields (21-77%) with excellent enantioselectivities (93:7-95:5 e.r.). The unprotected alcohol of 5-hexen-1-ol could also be tolerated and gave the aziridine **2.113** in a 49% and 95:5 e.r.. The phthalimide-protected alkyl amine was found to be robust, with the aziridine **2.114** forming in a 52% yield and 95:5 e.r.. The free N-H of an N-alkyl acetamide was not found to inhibit the reaction and provided the aziridine **2.115** in a 71% yield with excellent enantioselectivity (94:6 e.r.). An alkyl nitro was also found to be well tolerated and gave access to the aziridine **2.116** in a 64% yield with a 95:5 e.r. while an alkyl halide was found not to inhibit the catalyst through oxidative addition and provided aziridine **2.117** in 56% yield. An alkyl

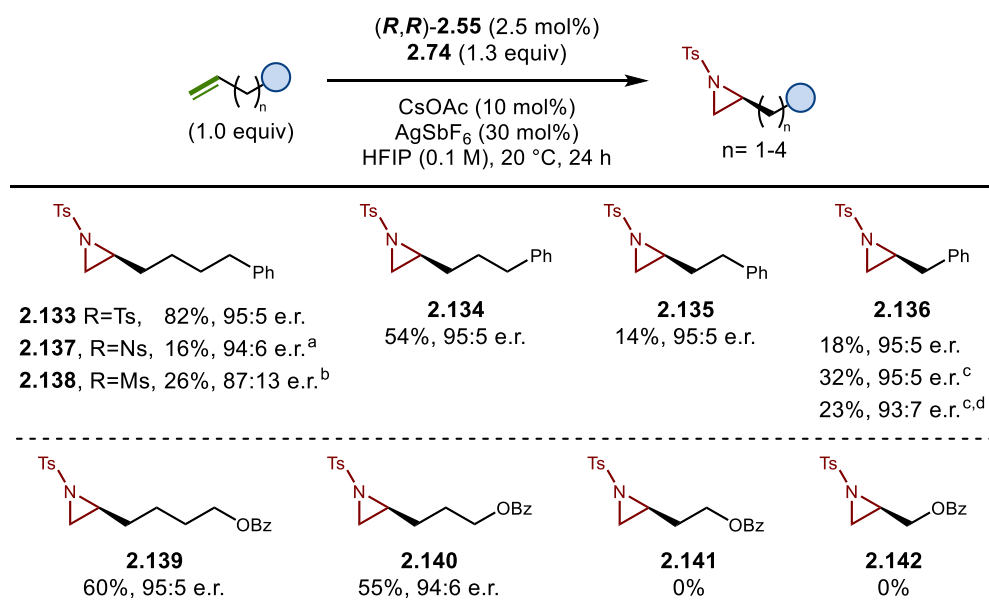
boronic ester also did not inhibit the catalyst through potential transmetalation and gave the aziridine **2.118** in a 57% yield with 96:4 e.r. A phosphonate ester was also well tolerated giving the aziridine **2.119** in a 67% yield with a 95:5 e.r. With good tolerance for a variety of heteroatoms established, we next explored a small heterocycle scope which provided the aziridine products **2.120-2.123** in low to good yields (28-82%) with excellent enantioselectivities (94:6-95:5 e.r.). Aziridination of *D*-glucofuranose and *L*-phenylalanine derivatives were successful in providing aziridines **2.124** and **2.125** in 69% yield, 95% d.r., and 81% yield, 95:5 d.r., respectively.



Scheme 2.16 Scope of Sterically Bulky Substrates in the Enantioselective Unactivated Alkene Aziridination

Having established a broad scope highlighting the functional group tolerance of this reaction, we were interested in gaining insight into substrate steric effects. We began by exploring matched and mismatched substrate catalyst pairings in the aziridination of *L*-citronellol-derived alkenes. Beginning with a stereogenic center at the γ -position relative to the alkene, the use of catalyst (R,R) -**2.55** provided the aziridine (S,S) -**2.126** in 77% yield with a 97:3 d.r., and constitutes the matched pairing, while the use of catalyst (S,S) -**2.55** gave the aziridine diastereomer (R,S) -**2.126** in a 72% yield with a 93:7 d.r. and

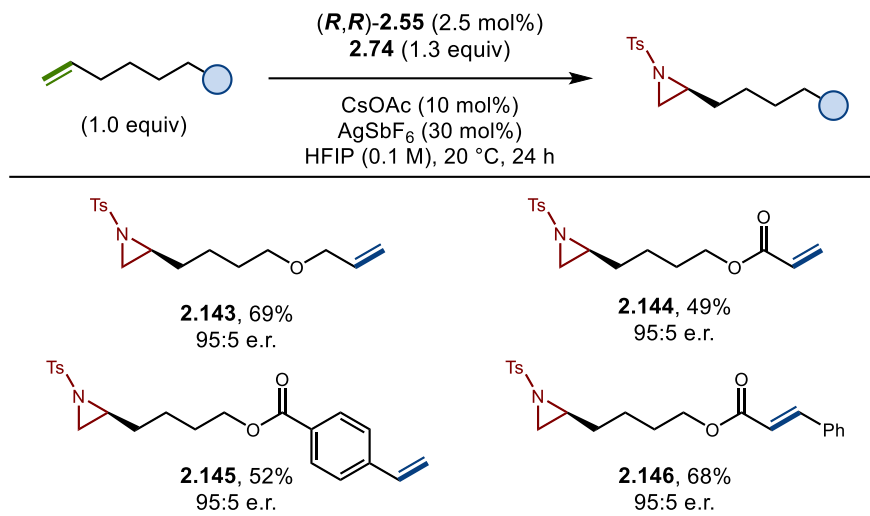
represents the mismatched case (**Scheme 2.16**). The minor effect of a stereogenic center at the γ -position allows for both diastereomers to be accessed in high yield with excellent diastereomeric control. Moving the stereogenic center to the β -position, catalyst (*S,S*)-**2.55** gave the aziridine (*R,S*)-**2.127** in a 30% yield with a 96:4 d.r. in the matched pairing. The mismatched case using (*R,R*)-**2.55** provided the aziridine (*S,S*)-**2.127** in a reduced 24% yield with a 92:8 d.r., The pronounced steric effect of a β -chiral center significantly reduces the yield of the aziridinations but does not decrease diastereoselectivity. Rigidification of steric bulk at the β -positions using allyl cyclohexane allowed for recovery of reactivity, providing the corresponding aziridine **2.128** in 83% yield and with an excellent enantioselectivity of 96:4 e.r.. Substitution of the α -position proved to be too challenging for this catalytic system with vinyl cyclohexane only providing the corresponding aziridine **2.129** in a significantly reduced 14% yield and 91:9 e.r. Attempts to conduct aziridinations on internal unactivated alkenes were also found to be hampered through strong steric interactions. While the *cis*-aziridine **2.130** could be formed in a 61% yield, with a >20:1 d.r. and 86:14 e.r. from the corresponding *Z*-alkene, the *E*-alkene was found to be unreactive. Aziridination of a 1,1-disubstituted alkene did not provide the desired aziridine **2.131** and instead formed the allylic amine **2.132** in a 56% yield (3:1 d.r.).



Scheme 2.17 Determination of the Effects of Carbon Linker Length in the Enantioselective Unactivated Alkene Aziridinations using Varied Linker Lengths

The investigation of substrate steric and electronic effects was continued by exploring the effects of shortened alkyl chains. Beginning with a series of aryl substituted substrates the longer chain lengths of four carbons did not hamper the aziridination and provided aziridine **2.133** in 82% yield (95:5 e.r.) (**Scheme 2.17a**). Reducing the chain length to three showed a slight decrease in yield for the formation of aziridine **2.134** (54% yield) with no effect on the enantioselectivity (95:5 e.r.). However, a significant drop in yield was observed in both homoallylic and allylic substrates which only provided the aziridines **2.135** and **2.136** in 14% yield, 95:5 e.r., and 18% yield, 95:5 e.r., respectively. This reduction in reactivity is primarily attributed to an increase in steric bulk near the site of aziridination, yet an electronic effect cannot be ruled out. Attempts to improve the yield of **2.136** using extended reaction times or heating to 60 °C were found to be ineffective. The stereochemistry of **2.136** was assigned to be (*S*) by comparing the HPLC trace of **2.136** to chiral standards (*R*)-**2.136** and (*S*)-**2.136** which were synthesized via intramolecular condensation from the commercially available chiral amino alcohols (see SI for details). All other chiral aziridine products synthesized using catalyst (*R,R*)-**2.55** were assigned the (*S*) configuration by analogy. Next, the effect of electronic perturbation near the site of aziridination was assessed using *O*-benzoyl substrates (**Scheme 2.17b**). Once again, longer carbon chains of four and three carbons were well tolerated providing the aziridines **2.139** and **2.140** in 60% yield, 95:5 e.r, and 55% yield, 95:5 e.r, respectively. However, in this series neither the homoallylic nor allylic substrates were found to be reactive and the aziridines **2.141** and **2.142** could not be formed due to proximity of an electron withdrawing substitution deactivating the alkene towards aziridination.

To further investigate electronic effects and demonstrate the chemoselectivity of the reaction towards unactivated alkenes, competition reactions were conducted using substrates containing both activated and unactivated alkenes. The presence of a terminal allylic ether was shown to have no effect on the aziridination and provided **2.143** in 69% yield and 95:5 e.r. (**Scheme 2.18**). An acrylic ester was also tolerated and provided aziridine **2.144** in 49% yield with 95:5 e.r. The styrene motif commonly employed as aziridination substrates, was well tolerated and aziridine **2.145** was formed in 52% yield and 95:5 e.r.

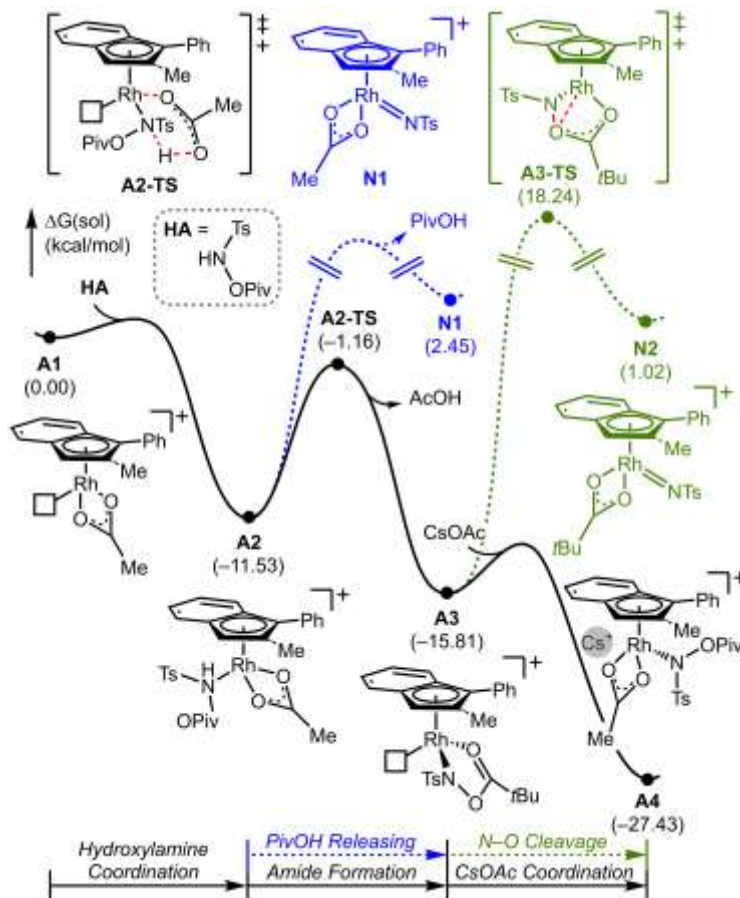


Scheme 2.18 Competition Substrate Scope in the Enantioselective Unactivated Alkene Aziridination

Finally, the doubly activated cinnamate derived substrate was also well tolerated and gave aziridine **2.146** in a 68% yield and 95:5 e.r. In all four competition reactions, aziridination was found to occur exclusively at the unactivated alkenes, with the activated alkenes remaining intact. This level of selectivity has been previously unseen for enantioselective alkene aziridination strategies.

2.3.5 Mechanistic Investigation

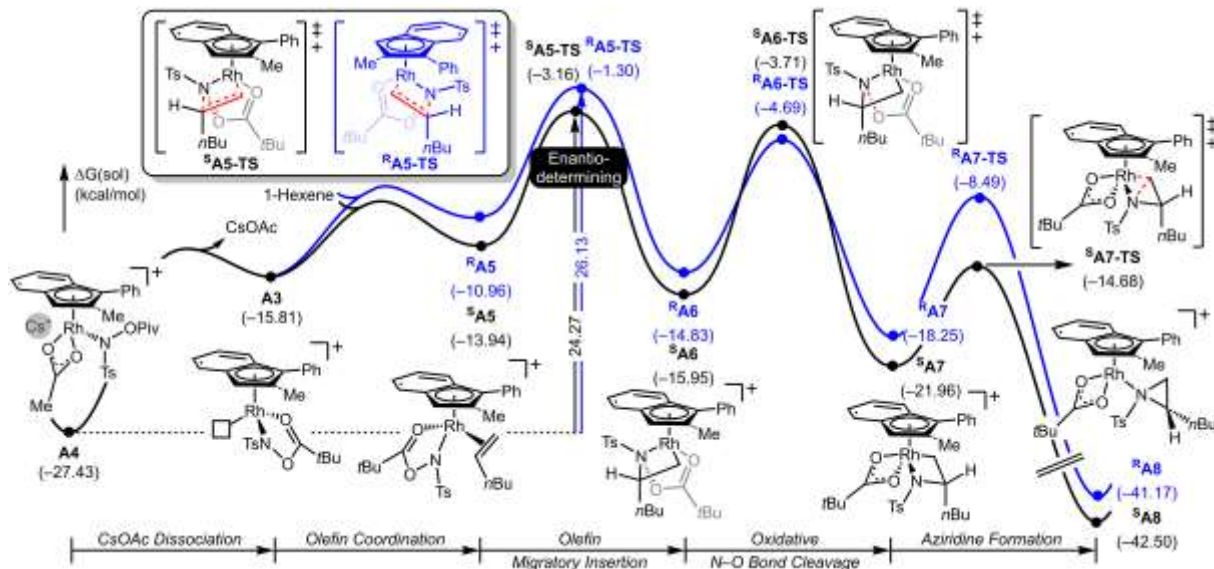
With a broad scope of enantioselective aziridinations, we became interested in elucidating the mechanism of this transformation. While the initial publication from Rovis had done mechanistic investigations to determine the formation of the pyrrolidine products from the intermediate aziridines, no investigations had been undertaken to elucidate the mechanism of the aziridination. To better understand the mechanism, extensive computational investigations through density functional theory (DFT) calculations were performed by Hoyoung Im and Bohyun Park from the Baik group. Initial hypotheses considered a metal-nitrene formation from the hydroxylamine **2.74** and subsequent concerted aziridination of the alkene. However, these were quickly dismissed, as the energy barriers and resulting free energies of the metal-nitrene species **N1** and **N2** were too high (**Scheme 2.19**). Allylic C–H functionalization was also quickly dismissed as the coordination of hydroxylamine **2.74** was found to occur more readily than the alkene coordination. This explains the divergent reactivity observed from previous mechanisms.



Scheme 2.19 Free Energy Diagram of Hydroxylamine Activation and Potential Metal-Nitrene Formation

Considering an alternative mechanism, the resting state intermediate **A4** could allow for alkene coordination following dissociation of acetate ligand as CsOAc. The alkene coordination can occur in two orientations and the resulting migratory insertion to form the four-member aza-metallacycle **A6** is the enantiodetermining step of the transformation (**Scheme 2.20**). The enantioselectivity of this step is dictated purely by the steric interactions between the indenyl ligand, the sulfonyl group, and the alkyl chain of the substrate. Following migratory insertion, cleavage of the N–O bond leads to the formation of Rh(V) intermediate which can then readily undergo the reductive elimination to form the aziridine.

Shortly after publication of this work a complimentary report for an enantioselective aziridination of unactivated alkenes was made by Wang.⁷⁶ This method was also inspired by the seminal report from Rovis but utilizes a Cramer C_2 -symmetryic ligand scaffold. An extensive scope of chiral aziridines was



Scheme 2.20 Free Energy Diagram of Alkene Migratory Insertion and Formation of Aziridine

reported, including many of the aziridines discussed above, such as the competition substrates **2.143**, **2.144**, and **2.146** which also demonstrated the selectivity of this transformation for unactivated alkenes. Deuterium labeling studies led the authors of this work to also propose a migratory insertion pathway excluding the formation of a metal nitrene intermediate.

2.4 Conclusion

The Blakey group developed a planar chiral Rh(III) indenyl catalysts, building upon the developments in chiral Cp catalysis and inspired by a planar chiral rhodium indenyl complex developed by Baker. This new catalyst, in combination with increased mechanistic understanding of oxidative allylic C–H functionalization enabled the development of an redox neutral enantioselective allylic C–H amidation. Following a report from Rovis detailing the isolation of a Rh(III) catalyst aziridine intermediate, we saw an opportunity to apply our catalyst platform in the development of enantioselective aziridination of unactivated alkenes. Initial screening of electronically varied catalysts, which had been developed by Dr. David Laws III, in the enantioselective aziridination revealed a trend in catalyst reactivity favoring electron-rich scaffolds. Following this trend, new electron-rich planar chiral Rh(III) catalysts were developed; while improvements were seen in reactivity, these catalyst could not be synthesized in an

enantiopure fashion. Further optimization of enantioselective aziridination conditions using a simpler catalyst revealed the importance of base and halide scavenger selection, enabling synthetically useful yields of an extensive scope of aziridines with unprecedented levels of selectivity for unactivated alkenes over activated alkenes. Computational investigation into the mechanism of this aziridination were conducted Hoyoung Im and Dr. Bohyun Park from the Baik and led to a proposed mechanism which operates through a migratory insertion and does not include commonly proposed metal nitrene intermediates. Chapter 3 of this dissertation will discuss the examples of Group IX piano stool catalyzed activations of electrophilic nitrogen reagents towards nucleophilic attack and will serve as a background for the chemistry discussed in Chapter 4.

2.5 References

- (1) Gross, P.; Im, H.; Laws, D., III; Park, B.; Baik, M.-H.; Blakey, S. B. Enantioselective Aziridination of Unactivated Terminal Alkenes Using a Planar Chiral Rh(III) Indenyl Catalyst. *J. Am. Chem. Soc.* **2024**, *146* (2), 1447.
- (2) Kealy, T. J.; Pauson, P. L. A New Type of Organo-Iron Compound. *Nature* **1951**, *168* (4285), 1039.
- (3) Piou, T.; Romanov-Michailidis, F.; Romanova-Michaelides, M.; Jackson, K. E.; Semakul, N.; Taggart, T. D.; Newell, B. S.; Rithner, C. D.; Paton, R. S.; Rovis, T. Correlating Reactivity and Selectivity to Cyclopentadienyl Ligand Properties in Rh(III)-Catalyzed C-H Activation Reactions: An Experimental and Computational Study. *J. Am. Chem. Soc.* **2017**, *139* (3), 1296.
- (4) Liu, C.-X.; Yin, S.-Y.; Zhao, F.; Yang, H.; Feng, Z.; Gu, Q.; You, S.-L. Rhodium-Catalyzed Asymmetric C-H Functionalization Reactions. *Chem. Rev.* **2023**, *123* (16), 10079.
- (5) Wang, H.; Park, Y.; Bai, Z.; Chang, S.; He, G.; Chen, G. Iridium-Catalyzed Enantioselective C(sp³)-H Amidation Controlled by Attractive Noncovalent Interactions. *J. Am. Chem. Soc.* **2019**, *141* (17), 7194.
- (6) Kim, S.; Kim, D.; Hong, S. Y.; Chang, S. Tuning Orbital Symmetry of Iridium Nitrenoid Enables Catalytic Diastereo- and Enantioselective Alkene Difunctionalizations. *J. Am. Chem. Soc.* **2021**, *143* (10), 3993.
- (7) Lee, E.; Hwang, Y.; Kim, Y. B.; Kim, D.; Chang, S. Enantioselective Access to Spirolactams via Nitrenoid Transfer Enabled by Enhanced Noncovalent Interactions. *J. Am. Chem. Soc.* **2021**, *143* (17), 6363.
- (8) Böge, M.; Heck, J. Catalytic sugar-assisted transfer hydrogenation with Ru(II), Rh(III) and Ir(III) halfsandwich complexes. *J. Mol. Catal. A: Chem.* **2015**, *408*, 107.
- (9) Trost, B. M.; Rao, M.; Dieskau, A. P. A Chiral Sulfoxide-Ligated Ruthenium Complex for Asymmetric Catalysis: Enantio- and Regioselective Allylic Substitution. *J. Am. Chem. Soc.* **2013**, *135* (49), 18697.

- (10) Halterman, R. L.; Vollhardt, K. P. C. Practical synthesis of two annelated optically active cyclopentadienes from the chiral pool and their transition metal complexes. *Tetrahedron Lett.* **1986**, 27 (13), 1461.
- (11) Halterman, R. L.; Vollhardt, K. P. C. Synthesis and asymmetric reactivity of enantiomerically pure cyclopentadienylmetal complexes derived from the chiral pool. *Organometallics* **1988**, 7 (4), 883.
- (12) Colletti, S. L.; Halterman, R. L. Binaphthylcyclopentadiene: A C₂-symmetric annulated cyclopentadienyl ligand with axial chirality. *Tetrahedron Lett.* **1989**, 30 (27), 3513.
- (13) Erker, G.; van der Zeijden, A. A. H. Enantioselective Catalysis with a New Zirconium Trichloride Lewis Acid Containing a “Dibornacyclopentadienyl” Ligand. *Angewandte Chemie International Edition in English* **1990**, 29 (5), 512.
- (14) Matsushima, Y.; Onitsuka, K.; Kondo, T.; Mitsudo, T.-a.; Takahashi, S. Asymmetric Catalysis of Planar-Chiral Cyclopentadienylruthenium Complexes in Allylic Amination and Alkylation. *J. Am. Chem. Soc.* **2001**, 123 (42), 10405.
- (15) Gutnov, A.; Heller, B.; Fischer, C.; Drexler, H.-J.; Spannenberg, A.; Sundermann, B.; Sundermann, C. Cobalt(I)-Catalyzed Asymmetric [2+2+2] Cycloaddition of Alkynes and Nitriles: Synthesis of Enantiomerically Enriched Atropoisomers of 2-Arylpyridines. *Angew. Chem. Int. Ed.* **2004**, 43 (29), 3795.
- (16) Ye, B.; Cramer, N. Chiral cyclopentadienyl ligands as stereocontrolling element in asymmetric C-H functionalization. *Science* **2012**, 338 (6106), 504.
- (17) Ye, B.; Cramer, N. A tunable class of chiral Cp ligands for enantioselective rhodium(III)-catalyzed C-H allylations of benzamides. *J. Am. Chem. Soc.* **2013**, 135 (2), 636.
- (18) Ozols, K.; Jang, Y.-S.; Cramer, N. Chiral Cyclopentadienyl Cobalt(III) Complexes Enable Highly Enantioselective 3d-Metal-Catalyzed C–H Functionalizations. *J. Am. Chem. Soc.* **2019**, 141 (14), 5675.
- (19) Herraiz, A. G.; Cramer, N. Cobalt(III)-Catalyzed Diastereo- and Enantioselective Three-Component C–H Functionalization. *ACS Catalysis* **2021**, 11 (19), 11938.

- (20) Ozols, K.; Onodera, S.; Woźniak, Ł.; Cramer, N. Cobalt(III)-Catalyzed Enantioselective Intermolecular Carboamination by C–H Functionalization. *Angew. Chem. Int. Ed.* **2021**, *60* (2), 655.
- (21) Dieckmann, M.; Jang, Y.-S.; Cramer, N. Chiral Cyclopentadienyl Iridium(III) Complexes Promote Enantioselective Cycloisomerizations Giving Fused Cyclopropanes. *Angew. Chem. Int. Ed.* **2015**, *54* (41), 12149.
- (22) Jang, Y.-S.; Dieckmann, M.; Cramer, N. Cooperative Effects between Chiral Cpx–Iridium(III) Catalysts and Chiral Carboxylic Acids in Enantioselective C–H Amidations of Phosphine Oxides. *Angew. Chem. Int. Ed.* **2017**, *56* (47), 15088.
- (23) Jang, Y.-S.; Woźniak, Ł.; Pedroni, J.; Cramer, N. Access to P- and Axially Chiral Biaryl Phosphine Oxides by Enantioselective CpxIrIII-Catalyzed C–H Arylations. *Angew. Chem. Int. Ed.* **2018**, *57* (39), 12901.
- (24) Mas-Roselló, J.; Smejkal, T.; Cramer, N. Iridium-catalyzed acid-assisted asymmetric hydrogenation of oximes to hydroxylamines. *Science* **2020**, *368* (6495), 1098.
- (25) Woźniak, Ł.; Cramer, N. Atropo-Enantioselective Oxidation-Enabled Iridium(III)-Catalyzed C–H Arylations with Aryl Boronic Esters. *Angew. Chem. Int. Ed.* **2021**, *60* (34), 18532.
- (26) Kossler, D.; Cramer, N. Chiral Cationic CpxRu(II) Complexes for Enantioselective Yne-Enone Cyclizations. *J. Am. Chem. Soc.* **2015**, *137* (39), 12478.
- (27) Kossler, D.; Cramer, N. Neutral chiral cyclopentadienyl Ru(ii)Cl catalysts enable enantioselective [2+2]-cycloadditions. *Chemical Science* **2017**, *8* (3), 1862.
- (28) Song, G.; O, W. W. N.; Hou, Z. Enantioselective C–H Bond Addition of Pyridines to Alkenes Catalyzed by Chiral Half-Sandwich Rare-Earth Complexes. *J. Am. Chem. Soc.* **2014**, *136* (35), 12209.
- (29) Lou, S.-J.; Mo, Z.; Nishiura, M.; Hou, Z. Construction of All-Carbon Quaternary Stereocenters by Scandium-Catalyzed Intramolecular C–H Alkylation of Imidazoles with 1,1-Disubstituted Alkenes. *J. Am. Chem. Soc.* **2020**, *142* (3), 1200.

- (30) Zhan, G.; Teng, H.-L.; Luo, Y.; Lou, S.-J.; Nishiura, M.; Hou, Z. Enantioselective Construction of Silicon-Stereogenic Silanes by Scandium-Catalyzed Intermolecular Alkene Hydrosilylation. *Angew. Chem. Int. Ed.* **2018**, *57* (38), 12342.
- (31) Luo, Y.; Teng, H.-L.; Nishiura, M.; Hou, Z. Asymmetric Yttrium-Catalyzed C(sp³)-H Addition of 2-Methyl Azaarenes to Cyclopropenes. *Angew. Chem. Int. Ed.* **2017**, *56* (31), 9207.
- (32) Teng, H.-L.; Ma, Y.; Zhan, G.; Nishiura, M.; Hou, Z. Asymmetric C(sp)-H Addition of Terminal Alkynes to Cyclopropenes by a Chiral Gadolinium Catalyst. *ACS Catalysis* **2018**, *8* (5), 4705.
- (33) Teng, H.-L.; Luo, Y.; Wang, B.; Zhang, L.; Nishiura, M.; Hou, Z. Synthesis of Chiral Aminocyclopropanes by Rare-Earth-Metal-Catalyzed Cyclopropene Hydroamination. *Angew. Chem. Int. Ed.* **2016**, *55* (49), 15406.
- (34) Zheng, J.; Cui, W. J.; Zheng, C.; You, S. L. Synthesis and Application of Chiral Spiro Cp Ligands in Rhodium-Catalyzed Asymmetric Oxidative Coupling of Biaryl Compounds with Alkenes. *J. Am. Chem. Soc.* **2016**, *138* (16), 5242.
- (35) Wang, S. G.; Park, S. H.; Cramer, N. A Readily Accessible Class of Chiral Cp Ligands and their Application in Ru(II) -Catalyzed Enantioselective Syntheses of Dihydrobenzoindoles. *Angew. Chem. Int. Ed. Engl.* **2018**, *57* (19), 5459.
- (36) Liang, H.; Vasamsetty, L.; Li, T.; Jiang, J.; Pang, X.; Wang, J. A New Class of C₂-Symmetric Chiral Cyclopentadienyl Ligand Derived from Ferrocene Scaffold: Design, Synthesis and Application. *Chemistry – A European Journal* **2020**, *26* (64), 14546.
- (37) Li, G.; Yan, X.; Jiang, J.; Liang, H.; Zhou, C.; Wang, J. Chiral Bicyclo[2.2.2]octane-Fused CpRh Complexes: Synthesis and Potential Use in Asymmetric C-H Activation. *Angew. Chem. Int. Ed. Engl.* **2020**, *59* (50), 22436.
- (38) Pan, C.; Yin, S.-Y.; Wang, S.-B.; Gu, Q.; You, S.-L. Oxygen-Linked Cyclopentadienyl Rhodium(III) Complexes-Catalyzed Asymmetric C-H Arylation of Benzo[h]quinolines with 1-Diazonaphthoquinones. *Angew. Chem. Int. Ed.* **2021**, *60* (28), 15510.

- (39) Laws, D.; Poff, C. D.; Heyboer, E. M.; Blakey, S. B. Synthesis, stereochemical assignment, and enantioselective catalytic activity of late transition metal planar chiral complexes. *Chem. Soc. Rev.* **2023**, *52* (17), 6003.
- (40) Jia, Z. J.; Merten, C.; Gontla, R.; Daniliuc, C. G.; Antonchick, A. P.; Waldmann, H. General Enantioselective C-H Activation with Efficiently Tunable Cyclopentadienyl Ligands. *Angew. Chem. Int. Ed. Engl.* **2017**, *56* (9), 2429.
- (41) Trifonova, E. A.; Ankudinov, N. M.; Mikhaylov, A. A.; Chusov, D. A.; Nelyubina, Y. V.; Perekalin, D. S. A Planar-Chiral Rhodium(III) Catalyst with a Sterically Demanding Cyclopentadienyl Ligand and Its Application in the Enantioselective Synthesis of Dihydroisoquinolones. *Angew. Chem. Int. Ed. Engl.* **2018**, *57* (26), 7714.
- (42) Pototskiy, R. A.; Kolos, A. V.; Nelyubina, Y. V.; Perekalin, D. S. Rhodium Catalysts with a Chiral Cyclopentadienyl Ligand Derived from Natural R-Myrtenal. *Eur. J. Org. Chem.* **2020**, *2020* (37), 6019.
- (43) Kolos, A. V.; Nelyubina, Y. V.; Podyacheva, E. S.; Perekalin, D. S. Rhodium complexes with planar-chiral cyclopentadienyl ligands: synthesis from tert-butylacetylene and catalytic performance in C–H activation of arylhydroxamates. *Dalton Transactions* **2023**, *52* (45), 17005.
- (44) Yan, X.; Jiang, J.; Wang, J. A Class of Readily Tunable Planar-Chiral Cyclopentadienyl Rhodium(III) Catalysts for Asymmetric C-H Activation. *Angew. Chem. Int. Ed. Engl.* **2022**, *61* (23), e202201522.
- (45) Zhang, C.; Jiang, J.; Huang, X.; Wang, J. Planar-Chiral Cyclopentadienyl Rhodium Catalysts: Design Concept, Chiral Resolution Strategy, and Applications. *ACS Catalysis* **2023**, *13* (15), 10468.
- (46) Tsuji, J.; Takahashi, H.; Morikawa, M. Organic syntheses by means of noble metal compounds XVII. Reaction of π -allylpalladium chloride with nucleophiles. *Tetrahedron Lett.* **1965**, *6* (49), 4387.
- (47) Trost, B. M.; Fullerton, T. J. New synthetic reactions. Allylic alkylation. *J. Am. Chem. Soc.* **1973**, *95* (1), 292.

- (48) Chen, M. S.; White, M. C. A Sulfoxide-Promoted, Catalytic Method for the Regioselective Synthesis of Allylic Acetates from Monosubstituted Olefins via C–H Oxidation. *J. Am. Chem. Soc.* **2004**, *126* (5), 1346.
- (49) Nelson, T. A. F.; Hollerbach, M. R.; Blakey, S. B. Allylic C–H functionalization via group 9 π -allyl intermediates. *Dalton Transactions* **2020**, *49* (40), 13928.
- (50) Kazerouni, A. M.; McKoy, Q. A.; Blakey, S. B. Recent advances in oxidative allylic C–H functionalization via group IX-metal catalysis. *Chem. Commun.* **2020**, *56* (87), 13287.
- (51) Cochet, T.; Bellosta, V.; Roche, D.; Ortholand, J.-Y.; Greiner, A.; Cossy, J. Rhodium(iii)-catalyzed allylic C–H bond amination. Synthesis of cyclic amines from ω -unsaturated N-sulfonylamines. *Chem. Commun.* **2012**, *48* (87), 10745.
- (52) Shibata, Y.; Kudo, E.; Sugiyama, H.; Uekusa, H.; Tanaka, K. Facile Generation and Isolation of π -Allyl Complexes from Aliphatic Alkenes and an Electron-Deficient Rh(III) Complex: Key Intermediates of Allylic C–H Functionalization. *Organometallics* **2016**, *35* (10), 1547.
- (53) Burman, J. S.; Blakey, S. B. Regioselective Intermolecular Allylic C–H Amination of Disubstituted Olefins via Rhodium/ π -Allyl Intermediates. *Angew. Chem. Int. Ed.* **2017**, *56* (44), 13666.
- (54) Nelson, T. A. F.; Blakey, S. B. Intermolecular Allylic C–H Etherification of Internal Olefins. *Angew. Chem. Int. Ed.* **2018**, *57* (45), 14911.
- (55) Sihag, P.; Jeganmohan, M. Iridium(III)-Catalyzed Intermolecular Allylic C–H Amidation of Internal Alkenes with Sulfonamides. *The Journal of Organic Chemistry* **2019**, *84* (20), 13053.
- (56) Lerchen, A.; Knecht, T.; Koy, M.; Ernst, J. B.; Bergander, K.; Daniliuc, C. G.; Glorius, F. Non-Directed Cross-Dehydrogenative (Hetero)arylation of Allylic C(sp³)–H bonds enabled by C–H Activation. *Angew. Chem. Int. Ed.* **2018**, *57* (46), 15248.
- (57) Knecht, T.; Pinkert, T.; Dalton, T.; Lerchen, A.; Glorius, F. Cp*RhIII-Catalyzed Allyl–Aryl Coupling of Olefins and Arylboron Reagents Enabled by C(sp³)–H Activation. *ACS Catalysis* **2019**, *9* (2), 1253.

- (58) Burman, J. S.; Harris, R. J.; Farr, C. M. B.; Bacsa, J.; Blakey, S. B. Rh(III) and Ir(III)Cp* Complexes Provide Complementary Regioselectivity Profiles in Intermolecular Allylic C–H Amidation Reactions. *ACS Catalysis* **2019**, *9* (6), 5474.
- (59) Lei, H.; Rovis, T. Ir-Catalyzed Intermolecular Branch-Selective Allylic C–H Amidation of Unactivated Terminal Olefins. *J. Am. Chem. Soc.* **2019**, *141* (6), 2268.
- (60) Knecht, T.; Mondal, S.; Ye, J.-H.; Das, M.; Glorius, F. Intermolecular, Branch-Selective, and Redox-Neutral Cp*Ir(III)-Catalyzed Allylic C–H Amidation. *Angew. Chem. Int. Ed.* **2019**, *58* (21), 7117.
- (61) Park, Y.; Park, K. T.; Kim, J. G.; Chang, S. Mechanistic Studies on the Rh(III)-Mediated Amido Transfer Process Leading to Robust C–H Amination with a New Type of Amidating Reagent. *J. Am. Chem. Soc.* **2015**, *137* (13), 4534.
- (62) Kazerouni, A. M.; Nelson, T. A. F.; Chen, S. W.; Sharp, K. R.; Blakey, S. B. Regioselective Cp*Ir(III)-Catalyzed Allylic C–H Sulfamidation of Allylbenzene Derivatives. *The Journal of Organic Chemistry* **2019**, *84* (20), 13179.
- (63) Trost, B. M.; Ryan, M. C. Indenylmetal Catalysis in Organic Synthesis. *Angew. Chem. Int. Ed.* **2017**, *56* (11), 2862.
- (64) Merola, J. S.; Kacmarcik, R. T.; Van Engen, D. The .eta.5 to .eta.3 conversion in indenyliridium complexes. *J. Am. Chem. Soc.* **1986**, *108* (2), 329.
- (65) Westcott, S. A.; Kakkar, A. K.; Stringer, G.; Taylor, N. J.; Marder, T. B. Flexible coordination of indenyl ligands in sandwich complexes of transition metals. Molecular structures of [(η-C₉H₇)₂M] (M = Fe, R = H, Me; M = Co, Ni, R = H): Direct measurement of the degree of slip-fold distortion as a function of d-electron count. *J. Organomet. Chem.* **1990**, *394* (1), 777.
- (66) Marder, T. B.; Calabrese, J. C.; Roe, D. C.; Tulip, T. H. The slip-fold distortion of π-bound indenyl ligands. Dynamic NMR and x-ray crystallographic studies of (η⁵-indenyl)RhL₂ complexes. *Organometallics* **1987**, *6* (9), 2012.

- (67) Hart-Davis, A. J.; Mawby, R. J. Reactions of π -indenyl complexes of transition metals. Part I. Kinetics and mechanisms of reactions of tricarbonyl- π -indenylmethylmolybdenum with phosphorus(III) ligands. *J. Chem. Soc. A* **1969**, 0 (0), 2403.
- (68) Rerek, M. E.; Ji, L.-N.; Basolo, F. The indenyl ligand effect on the rate of substitution reactions of $\text{Rh}(\eta\text{-C}_9\text{H}_7)(\text{CO})_2$ and $\text{Mn}(\eta\text{-C}_9\text{H}_7)(\text{CO})_3$. *J. Chem. Soc., Chem. Commun.* **1983**, (21), 1208.
- (69) Baker, R. W. Asymmetric Induction via the Structural Indenyl Effect. *Organometallics* **2018**, 37 (3), 433.
- (70) Farr, C. M. B.; Kazerouni, A. M.; Park, B.; Poff, C. D.; Won, J.; Sharp, K. R.; Baik, M.-H.; Blakey, S. B. Designing a Planar Chiral Rhodium Indenyl Catalyst for Regio- and Enantioselective Allylic C–H Amidation. *J. Am. Chem. Soc.* **2020**, 142 (32), 13996.
- (71) Lee, S.; Lei, H.; Rovis, T. A Rh(III)-Catalyzed Formal [4+1] Approach to Pyrrolidines from Unactivated Terminal Alkenes and Nitrene Sources. *J. Am. Chem. Soc.* **2019**, 141 (32), 12536.
- (72) Lei, H.; Conway, J. H., Jr.; Cook, C. C.; Rovis, T. Ligand Controlled Ir-Catalyzed Regiodivergent Oxyamination of Unactivated Alkenes. *J. Am. Chem. Soc.* **2019**, 141 (30), 11864.
- (73) Conway, J. H., Jr.; Rovis, T. Regiodivergent Iridium(III)-Catalyzed Diamination of Alkenyl Amides with Secondary Amines: Complementary Access to γ - or δ -Lactams. *J. Am. Chem. Soc.* **2018**, 140 (1), 135.
- (74) Lei, H.; Rovis, T. A site-selective amination catalyst discriminates between nearly identical C–H bonds of unsymmetrical disubstituted alkenes. *Nature Chemistry* **2020**, 12 (8), 725.
- (75) Kolos, A. V.; Nelyubina, Y. V.; Sundararaju, B.; Perekalin, D. S. Synthesis of Overloaded Cyclopentadienyl Rhodium(III) Complexes via Cyclotetramerization of tert-Butylacetylene. *Organometallics* **2021**, 40 (22), 3712.
- (76) Wang, J.; Luo, M. P.; Gu, Y. J.; Liu, Y. Y.; Yin, Q.; Wang, S. G. Chiral Cp(x) Rhodium(III)-Catalyzed Enantioselective Aziridination of Unactivated Terminal Alkenes. *Angew. Chem. Int. Ed. Engl.* **2024**, DOI:10.1002/anie.202400502.

2.6 Supporting Information

2.6.1 General Information

All reactions were conducted under nitrogen atmosphere with anhydrous solvents in oven- or flame-dried glassware using standard Schlenk technique, unless otherwise stated. Anhydrous dichloromethane (DCM), diethyl ether (Et₂O), tetrahydrofuran (THF), and were obtained by passage through activated alumina using a *Glass Contours* solvent purification system. 1,1,1,3,3,3-hexafluoroisopropanol (HFIP) was distilled over activated 4Å molecular sieves and stored over activated 4Å molecular sieves. Solvents for workup, extraction, and column chromatography were used as received from commercial suppliers without further purification. All catalysts were stored and weighed in a nitrogen-filled glovebox. All other chemicals were purchased from Millipore Sigma, Strem Chemicals, Oakwood Chemicals, Alfa Aesar, TCI, Combi Blocks, or Ambeed and used as received without further purification, unless otherwise stated.

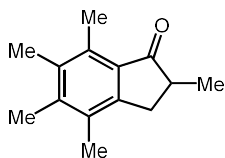
¹H and ¹³C nuclear magnetic resonance (NMR) spectra were recorded on a Varian Inova 600 spectrometer (600 MHz ¹H, 151 MHz ¹³C), ¹³C 600 spectrometer (600 MHz ¹H, 151 MHz ¹³C), a Varian Inova 500 spectrometer (500 MHz ¹H, 126 MHz ¹³C), a Bruker 400 spectrometer (400 MHz ¹H, 126 MHz), and a Varian Inova 400 spectrometer (400 MHz ¹H, 126 MHz ¹³C). Chemical shifts δ values were reported in parts per million (ppm) relative to CHCl₃ (7.26 ppm for ¹H, 77.16 ppm for ¹³C) for CDCl₃, relative to C₆H₆ ((7.16 ppm for ¹H, 128.06 ppm for ¹³C) for C₆D₆, relative to DMSO (2.50 ppm for ¹H, 39.52 ppm for ¹³C) for DMSO-*d*₆. Coupling constants (*J* values) were reported in Hz and multiplicities were indicated using the following abbreviations: s = singlet, d = doublet, t = triplet, q = quartet, qn = quintet, m = multiplet, br = broad. High resolution mass spectra (HRMS) were obtained using a Thermo Electron Corporation Finigan LTQFTMS (at the Mass Spectrometry Facility, Emory University). High Pressure Liquid Chromatography (HPLC) was performed on an Agilent 1100 series HPLC utilizing CHIRALPAK[®] AD-H, AS-H, CHIRALCEL[®] OD-H and OJ-H 4.6 x 150 mm analytical columns or on an Agilent 1260 Infinity II series HPLC utilizing CHIRALPAK[®] IA, IB, IH, IJ, and IK 4.6 x 150 mm analytical columns. Semi preparative

HPLC was performed on an Agilent 1260 Infinity II series preparative HPLC using a CHIRALCEL[®] OD-H 20 x 250 mm column. Optical rotations were measured on a PerkinElmer 341 polarimeter. Analytical thin layer chromatography (TLC) was performed on precoated glass-backed Silicycle SiliaPureR 0.25 mm silica gel 60 plates and visualized with UV light or ethanolic *p*-anisaldehyde. Silica gel column chromatography was performed using Silicycle SiliaFlashR F60 silica gel (40- 63 μm). Flash column chromatography was performed using Silicycle SiliaFlashR F60 silica gel (40- 63 μm) on a Biotage Isolera One system. Preparatory TLC was performed on precoated glass backed Silicycle SiliaPureR 1.0 mm silica gel 60 plates.

2.6.2 Experimental Procedures and Tabulated Data

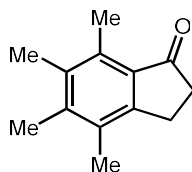
Ligand and Catalyst Synthesis

[Ind*RhCl₂]₂ catalyst was synthesized following a reported literature procedure¹.



2,4,5,6,7-pentamethyl-2,3-dihydro-1H-inden-1-one (**2.88**): Using an adapted procedure from by O'Hare². Under a N₂ atmosphere, dry CH₂Cl₂ (50 mL) was added to 250 mL round bottom flask equipped with a stir bar. Oxalyl chloride (3.0 mL 34.4 mmol, 1.1 equiv.), methacrylic acid (2.9 mL, 34.4 mmol, 1.1 equiv.), and five drops of DMF were sequentially added and the reaction was left to stir vigorously overnight at room temperature. The reaction was placed in an ice bath before quickly adding AlCl₃ (5.7 g, 43.0 mmol, 1.4 equiv.). After five minutes, 1,2,3,4-tetramethylbenzene (4.5 mL, 30.2 mmol, 1.0 equiv.) was slowly added rapidly turning the reaction to a dark red orange. The reaction was allowed to stir at room temperature for an additional 4 hours before pouring into a (1:1) HCl: ice slurry. The resulting biphasic solution was extracted with CH₂Cl₂ 3x. The combined organic layers were washed with DI H₂O 3x and dried over Na₂SO₄. The solvent was removed under reduced pressure and the crude product purified using silica gel column chromatography (0-5% EtOAc in hexanes) to afford **2.88** (5.79 g, 98% yield) as an off-white solid.

¹H NMR (400 MHz, CDCl₃) δ 3.22 (dd, *J* = 16.8, 8.0 Hz, 1H), 2.69 – 2.58 (m, 4H), 2.51 (dd, *J* = 16.8, 4.0 Hz, 1H), 2.29 (s, 3H), 2.24 (d, *J* = 2.4 Hz, 6H), 1.29 (d, *J* = 7.4 Hz, 3H). **¹³C NMR** (151 MHz, CDCl₃) δ 211.18, 150.57, 142.06, 135.29, 134.54, 131.13, 130.74, 42.53, 33.68, 17.14, 16.94, 15.50, 15.28, 13.93. **HRMS** (+APCI) calculated for C₁₄H₁₉O [M+H]⁺ 203.14304, found 203.1427

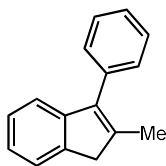


4,5,6,7-tetramethyl-2,3-dihydro-1H-inden-1-one (2.94): A 100 mL round bottom flask equipped with a stir bar and septum cap was flame dried under vacuum and purged with N₂ (3X). Opening the reaction vessel, AlCl₃ (10.3432 g, 77.6 mmol, 2.5 equiv.) was quickly added and the vessel was purged with N₂ again (3x). CH₃NO₂ (30 mL) was slowly added to the reaction vessel and let stir until the complete dissolution of AlCl₃ occurred. To the yellow-grey solution, 3-chloropropanoyl chloride (3.8 mL, 40.0 mmol, 1.3 equiv.) was added and the reaction vessel was placed in an ice bath and allowed to cool to 0 °C. Once cool, 1,2,3,4-tetramethylbenzene (4.5 mL, 30.0 mmol, 1.0 equiv.) was added dropwise over five minutes after which the reaction was left to stir at room temperature overnight. After 16 hours, the reaction was carefully poured into a slurry of concentrated HCl and ice (50 mL, 1:1 (v/v)). The slurry was extracted with DCM (3 x 50 mL) and the combined organic layers were washed with 1M HCl (1 x 50 mL) and brine (2 x 50 mL). The organic layers were dried over Na₂SO₄ before concentrating under reduced pressure to yield a forest green crude oil residue which was carried forward with no further purification. To the crude material, neat H₂SO₄ (60 mL) was added and placed in a preheated alumina block set to 95 °C. After 45 minutes the reaction was cooled to room temperature before being poured into an ice slurry (50 mL). The slurry was extracted with toluene (5 x 75 mL) and the combined organic layers washed with saturated NaHCO₃ (3 x 50 mL), DI H₂O (1 x 50 mL), and brine (2 x 50 mL). The organic layer was dried over Na₂SO₄ and concentrated under reduced pressure. The crude material was purified via flash chromatography (5% EtOAc in Hexanes) to yield **2.94** as a white solid (2.8721 g, 50% yield). **¹H NMR** (600 MHz, CDCl₃) δ 2.95 – 2.89 (m, 2H), 2.67

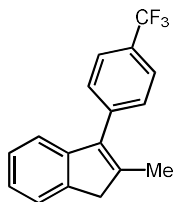
– 2.60 (m, 5H), 2.29 (s, 3H), 2.24 (d, $J = 8.8$ Hz, 6H). ^{13}C NMR (151 MHz, CDCl_3) δ 208.83, 152.43, 142.03, 135.17, 134.33, 131.87, 130.88, 37.33, 24.38, 17.14, 15.48, 15.21, 13.90. HRMS (+APCI) calculated for $\text{C}_{13}\text{H}_{16}\text{O}$ $[\text{M}+\text{H}]^+$ 189.12739, found 189.12704

General Procedure A: Indene Synthesis

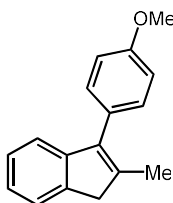
A three neck round bottom flask equipped with a stir bar and a condenser was placed under a N_2 atmosphere. The corresponding indanone (1.0 equiv.) was transferred as a solution in THF (0.3-0.5M) and the reaction vessel was placed in an ice bath to cool to 0 °C. Once cooled, the corresponding Grignard reagent (3.0 equiv.) was slowly added to the reaction. Once the addition was complete the ice bath was removed and replaced with a heating block to reflux the reaction for 16 hours. The reaction was cooled to room temperature and placed in an ice bath before carefully quenching with DI H_2O . Concentrated HCl was added to the reaction vessel and stirred for an additional 24 hours at room temperature. The layers of the biphasic solution were separated, and the aqueous layer extracted with Et_2O 3x. The combined organic layers were sequentially washed with NaHCO_3 , DI H_2O and brine before being dried over MgSO_4 . The solvent was removed under reduced pressure and the resulting crude product purified via silica gel column chromatography (0-5% EtOAc in hexanes).



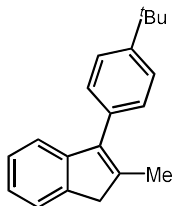
2-methyl-3-phenyl-1H-indene (**2.53**) Prepared according to **General Procedure A** using 2-methylindan-1-one³ (3.94 g, 26.9 mmol, 1.0 equiv) and phenyl magnesium bromide (36 mL, 2.0M, 75 mmol, 2.8 equiv.). (**2.53**) (4.78 g, 86% yield) Spectroscopic data for **2.53** matches those previously reported in the literature⁴.



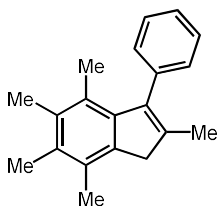
2-methyl-3-(4-(trifluoromethyl)phenyl)-1H-indene (S1) Prepared according to **General Procedure A** using 2-methylindan-1-one³ (0.290 g, 2.0 mmol, 1.0 equiv) and freshly prepared (4-(trifluoromethyl)phenyl)magnesium bromide (1.09 g, 4.4 mmol, 2.2 equiv.). **(S1)** (0.361 g, 66% yield) **¹H NMR** (600 MHz, CDCl₃) δ 7.73 (d, *J* = 8.2 Hz, 2H), 7.52 (d, *J* = 8.2 Hz, 1H), 7.49 – 7.44 (m, 1H), 7.28 – 7.22 (m, 1H), 7.22 – 7.14 (m, 2H), 3.50 (s, 2H), 2.15 (s, 3H). **¹³C NMR** (151 MHz, CDCl₃) δ 145.83, 142.42, 142.17, 139.47, 137.69, 129.59, 129.14 (q, *J* = 32.2 Hz), 126.47, 125.55 (q, *J* = 3.7 Hz), 124.49, 124.47 (q, *J* = 271.9 Hz), 123.70, 43.40, 14.95. **¹⁹F NMR** (564 MHz, CDCl₃) δ -62.40. **HRMS** (+APCI) calculated for C₁₇H₁₄F₃ [M+H]⁺ 275.10421, found 275.10404. **Prepared by Dr. David Laws III**



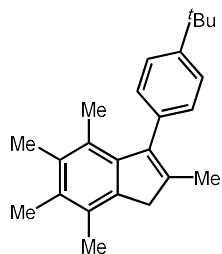
3-(4-methoxyphenyl)-2-methyl-1H-indene (S2) Prepared according to **General Procedure A** using 2-methylindan-1-one³ (0.500 g, 3.42 mmol, 1.0 equiv) and freshly prepared (4-methoxyphenyl)magnesium bromide (1.45 g, 6.84 mmol, 2.0 equiv.). **(S2)** (0.537 g, 66% yield) **¹H NMR** (600 MHz, CDCl₃) δ 7.44 (d, *J* = 7.3 Hz, 1H), 7.36 (d, *J* = 8.4 Hz, 2H), 7.25 (d, *J* = 4.2 Hz, 2H), 7.17 (dq, *J* = 7.8, 4.0 Hz, 1H), 7.02 (d, *J* = 8.6 Hz, 2H), 3.88 (s, 3H), 3.45 (s, 2H), 2.15 (s, 3H). **¹³C NMR** (151 MHz, CDCl₃) δ 158.69, 146.71, 142.55, 140.15, 138.25, 130.37, 127.95, 126.26, 124.01, 123.49, 119.36, 113.99, 55.41, 43.14, 15.00. **HRMS** (+APCI) calculated for C₁₇H₁₇O [M+H]⁺ 237.12739, found 237.12732. **Prepared by Dr. David Laws III**



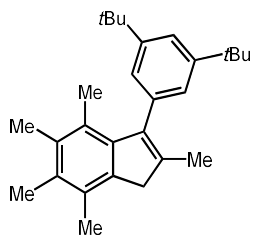
3-(4-(tert-butyl)phenyl)-2-methyl-1H-indene (S3) Prepared according to **General Procedure A** 2-methylindan-1-one³ (0.500 g, 3.42 mmol, 1.0 equiv) and freshly prepared (4-(tert-butyl)phenyl)magnesium bromide (3.25 g, 13.7 mmol, 4.0 equiv.). **(S3)** (0.440 g, 49% yield) ¹H NMR (600 MHz, CDCl₃) δ 7.49 (d, *J* = 8.3 Hz, 2H), 7.44 (d, *J* = 7.3 Hz, 1H), 7.36 (d, *J* = 8.3 Hz, 2H), 7.29 (d, *J* = 7.5 Hz, 1H), 7.24 (t, *J* = 7.4 Hz, 1H), 7.16 (td, *J* = 7.3, 1.2 Hz, 1H), 3.46 (s, 2H), 2.17 (s, 3H), 1.40 (s, 9H). ¹³C NMR (151 MHz, CDCl₃) δ 149.85, 146.63, 142.58, 140.45, 138.50, 132.56, 128.89, 126.22, 125.40, 123.98, 123.47, 119.56, 43.25, 34.76, 31.56, 15.10. **HRMS** (+APCI) calculated for C₂₀H₂₃ [M+H]⁺ 263.17943, found 263.17932. **Prepared by Dr. David Laws III**



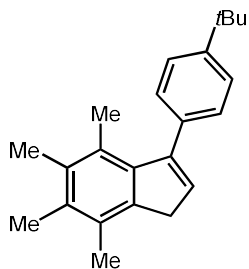
2,4,5,6,7-pentamethyl-3-phenyl-1H-indene (S4): Prepared according to **General Procedure A** using **2.88** (0.608 g, 3.0 mmol, 1.0 equiv) and phenyl magnesium bromide (11.5 mL, 0.8 M, 9.2 mmol, 3.0 equiv.). **(S4)** (0.415 g, 57% yield) ¹H NMR (400 MHz, CDCl₃) δ 7.42 (tt, *J* = 8.1, 1.6 Hz, 4H), 7.35 (t, *J* = 7.3 Hz, 1H), 7.27 – 7.22 (m, 2H), 3.35 (s, 2H), 2.33 (s, 3H), 2.29 (s, 3H), 2.20 (s, 3H), 1.92 (s, 3H), 1.83 (s, 3H). ¹³C NMR (101 MHz, CDCl₃) δ 141.48, 140.80, 140.44, 139.68, 139.11, 134.17, 130.88, 129.70, 128.67, 128.23, 126.80, 126.69, 42.28, 16.56, 16.38, 16.28, 16.20, 14.84. **HRMS** (+APCI) calculated for C₂₀H₂₃ [M+H]⁺ 263.17943, found 263.18007.



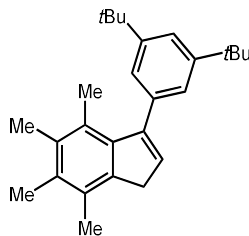
3-(4-(tert-butyl)phenyl)-2,4,5,6,7-pentamethyl-1H-indene (2.89): Prepared according to **General Procedure A** using **2.88** (1.17 g, 5.8 mmol, 1.0 equiv) and (4-(tert-butyl)phenyl)magnesium bromide (23 mL, 0.75 M, 17 mmol, 3.0 equiv.). (**S7**) (0.987 g, 53% yield) **¹H NMR** (400 MHz, CDCl₃) δ 7.41 (d, *J* = 8.3 Hz, 2H), 7.16 (d, *J* = 8.3 Hz, 2H), 3.33 (s, 2H), 2.33 (s, 3H), 2.28 (s, 3H), 2.20 (s, 3H), 1.93 (s, 3H), 1.84 (s, 3H), 1.39 (s, 9H). **¹³C NMR** (101 MHz, CDCl₃) δ 149.47, 141.63, 140.74, 140.36, 139.14, 136.38, 134.14, 130.75, 129.25, 128.59, 126.93, 125.00, 42.25, 34.67, 31.62, 16.55, 16.41, 16.27, 16.19, 14.96. **HRMS** (+APCI) calculated for C₂₄H₃₁ [M+H]⁺ 319.24203, found 319.24142



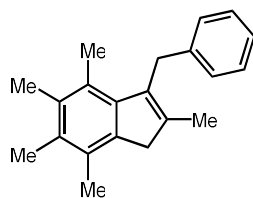
3-(3,5-di-tert-butylphenyl)-2,4,5,6,7-pentamethyl-1H-indene (2.90): Prepared according to **General Procedure A** using **2.88** (1.07 g, 4.9 mmol, 1.0 equiv) and (3,5-di-tert-butylphenyl)magnesium bromide, (100% Pentane). Flakey white powder. (1.3214 g, 71% yield). **¹H NMR** (600 MHz, CDCl₃) δ 7.34 (t, *J* = 1.9 Hz, 1H), 7.06 (d, *J* = 1.8 Hz, 2H), 3.32 (s, 2H), 2.31 (s, 3H), 2.26 (s, 3H), 2.17 (s, 3H), 1.93 (s, 3H), 1.77 (s, 3H), 1.33 (s, 18H). **¹³C NMR** (151 MHz, CDCl₃) δ 150.33, 141.81, 141.70, 139.73, 139.23, 138.31, 134.18, 130.76, 128.64, 126.93, 124.05, 119.99, 42.27, 34.97, 31.69, 16.54, 16.29, 16.20, 14.98. **HRMS** (+APCI) calculated for C₂₈H₃₈ [M+H]⁺ 375.30463, found 375.30402.



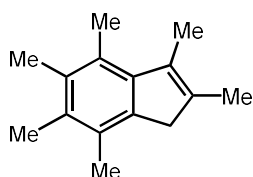
3-(4-(tert-butyl)phenyl)-4,5,6,7-tetramethyl-1H-indene (2.95): Prepared according to **General Procedure A** using **2.94** (1.17 g, 6.2 mmol, 1.0 equiv) and (4-(tert-butyl)phenyl)magnesium bromide (100% Pentane) Flakey white powder. (1.1602g, 61% yield). **¹H NMR** (600 MHz, CDCl₃) δ 7.39 (d, *J* = 8.0 Hz, 2H), 7.28 (d, *J* = 8.2 Hz, 2H), 6.29 (t, *J* = 2.2 Hz, 1H), 3.35 (d, *J* = 2.1 Hz, 2H), 2.34 (s, 3H), 2.30 (s, 3H), 2.22 (s, 3H), 1.99 (s, 3H), 1.37 (s, 9H). **¹³C NMR** (151 MHz, CDCl₃) δ 149.89, 147.63, 141.30, 139.96, 137.14, 134.25, 132.26, 131.98, 129.15, 128.47, 127.96, 124.87, 37.49, 34.69, 31.60, 17.17, 16.53, 16.30, 16.28. **HRMS** (+APCI) calculated for C₂₃H₂₉ [M+H]⁺ 305.22638, found 305.22598.



3-(3,5-di-tert-butylphenyl)-4,5,6,7-tetramethyl-1H-indene (2.96) Prepared according to **General Procedure A** using **2.94** (0.995 g, 5.3 mmol, 1.0 equiv) (3,5-di-*tert*-butylphenyl)magnesium bromide (100% Pentane) Flakey white powder. (1.3447g, 71% yield). **¹H NMR** (400 MHz, CDCl₃) δ 7.38 (t, *J* = 1.9 Hz, 1H), 7.21 (d, *J* = 1.9 Hz, 2H), 6.33 (t, *J* = 2.2 Hz, 1H), 3.37 (d, *J* = 2.2 Hz, 2H), 2.34 (s, 3H), 2.30 (s, 3H), 2.22 (s, 3H), 1.93 (s, 3H), 1.34 (s, 19H). **¹³C NMR** (101 MHz, CDCl₃) δ 150.27, 148.54, 141.34, 140.05, 139.05, 134.30, 131.99, 131.74, 129.20, 127.94, 123.22, 120.67, 37.47, 35.00, 31.67, 16.98, 16.54, 16.32, 16.29. **HRMS** (+APCI) calculated for C₂₇H₃₇ [M+H]⁺ 361.289, found 361.2888.



3-benzyl-2,4,5,6,7-pentamethyl-1H-indene (2.91) Prepared according to **General Procedure A** using **2.88** (0.755g, 3.73 mmol, 1.0 equiv) and benzylmagnesium bromide (100% Hexanes). White powder. (0.6542 g, 63% yield). $^1\text{H NMR}$ (600 MHz, CDCl_3) δ 7.24 (t, $J = 7.6$ Hz, 2H), 7.15 (d, $J = 7.5$ Hz, 3H), 4.09 (s, 2H), 3.29 (s, 2H), 2.28 (s, 3H), 2.24 (s, 3H), 2.17 (d, $J = 13.0$ Hz, 6H), 2.08 (s, 3H). $^{13}\text{C NMR}$ (151 MHz, CDCl_3) δ 141.29, 140.64, 140.62, 139.50, 135.85, 133.84, 130.79, 128.54, 128.47, 128.20, 126.43, 125.82, 42.32, 33.39, 16.51, 16.40, 16.32, 15.67, 14.41. **HRMS** (+APCI) calculated for $\text{C}_{21}\text{H}_{25}$ $[\text{M}+\text{H}]^+$ 277.19508, found 277.1949.

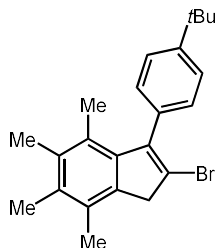


2,3,4,5,6,7-hexamethyl-1H-indene (2.92): Prepared according to **General Procedure A** using **2.88** (1.17 g, 5.8 mmol, 1.0 equiv) and methylmagnesium bromide (100% Hexanes). Off white powder (0.5995 g, 80%). $^1\text{H NMR}$ (600 MHz, CDCl_3) δ 3.13 (s, 2H), 2.51 (s, 3H), 2.24 (s, 12H), 2.03 (s, 3H). $^{13}\text{C NMR}$ (151 MHz, CDCl_3) δ 142.03, 139.26, 137.32, 134.12, 133.72, 130.43, 128.36, 126.45, 42.12, 16.41, 16.39, 16.24, 15.86, 15.31, 14.23.

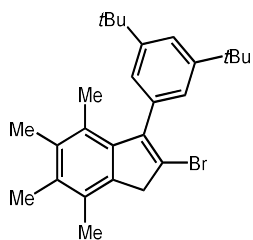
General Procedure B: Indene Bromination

The indene (3.30 mmol, 1.0 equiv.) was added to an oven-dried three neck 50 mL round bottom flask equipped with an oven-dried stir bar and condenser. The atmosphere was exchanged with N_2 (3x) and freshly recrystallized NBS (3.30 mmol, 1.0 equiv.) was added and the reaction vessel atmosphere exchanged with N_2 once again. CHCl_3 (12 mL) was added and the reaction was placed into a preheated

aluminum block to reflux for 45 minutes. After cooling to room temperature, the reaction was concentrated under reduced pressure and the crude material redissolved in DI H₂O and EtOAc before extracting with Et₂O (4 x 15 mL). The combined organic layers were dried over Na₂SO₄ and the solvent removed under reduced pressure. The crude product was then purified via flash chromatography using 100% Hexanes to yield the brominated indene.



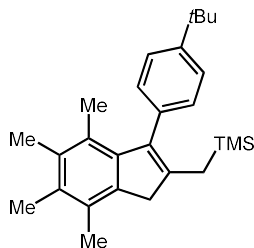
2-bromo-3-(4-(tert-butyl)phenyl)-4,5,6,7-tetramethyl-1H-indene (2.97): Off white solid. (1.0954 g, 87% yield). ¹H NMR (600 MHz, CDCl₃) δ 7.44 (d, *J* = 7.6 Hz, 2H), 7.19 (d, *J* = 7.7 Hz, 2H), 3.63 (s, 2H), 2.29 (s, 3H), 2.25 (s, 3H), 2.18 (s, 3H), 1.79 (s, 3H), 1.37 (s, 9H). ¹³C NMR (151 MHz, CDCl₃) δ 150.55, 145.32, 139.58, 139.00, 134.85, 134.69, 132.21, 128.79, 128.66, 127.54, 125.29, 122.81, 44.67, 34.79, 31.58, 16.47, 16.34, 16.30, 16.29. HRMS (+APCI) calculated for C₂₃H₂₈Br [M+H]⁺ 383.13689, found 383.13608.



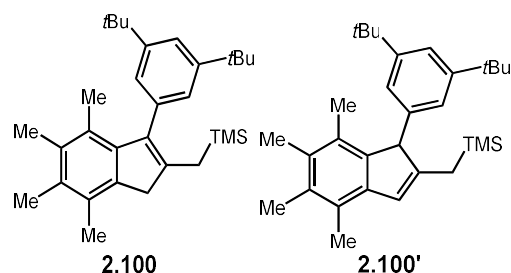
2-bromo-3-(3,5-di-tert-butylphenyl)-4,5,6,7-tetramethyl-1H-indene (2.98): Off white solid. (1.1489 g, 94% yield). ¹H NMR (600 MHz, CDCl₃) δ 7.39 (t, *J* = 1.8 Hz, 1H), 7.12 (d, *J* = 1.9 Hz, 2H), 3.63 (s, 2H), 2.30 (s, 3H), 2.26 (s, 3H), 2.18 (s, 3H), 1.76 (s, 3H), 1.34 (s, 18H). ¹³C NMR (151 MHz, CDCl₃) δ 150.54, 146.18, 139.62, 139.11, 136.70, 134.72, 132.18, 128.69, 127.52, 123.70, 122.30, 120.95, 44.67, 35.04, 31.64, 16.47, 16.32, 16.29, 16.24. HRMS (+APCI) calculated for C₂₇H₃₆Br [M+H]⁺ 439.19949, found 439.19949.

General Procedure C: Kumada Coupling

The bromoindene (1.0 equiv.) was added to an oven-dried three neck 50 ml round bottom flask equipped with an oven-dried stir bar and condenser. The flask was placed under vacuum and the atmosphere was exchanged with N₂ (3x). Inside a N₂ filled glove box Pd(PH₃)₄ (10 mol%) was added to a 7 mL vial and brought out of the box and transferred to the reaction using THF (3 x 5 mL). The yellow solution was allowed to stir for 15min before adding the ((trimethylsilyl)methyl)magnesium chloride (3.0 equiv.) at room temperature and placing into a preheated aluminum block set to 65 °C to reflux for 24 hours. The reaction was allowed to cool to room temperature, and excess Grignard was quenched with the addition of DI H₂O (10 mL). The quenched reaction was extracted with Et₂O (5 x 10 mL) and the combined organic layers dried over Na₂SO₄ before removing the solvent under reduced pressure. The crude ligand was purified via flash chromatography using 100% pentane.



((3-(4-(tert-butyl)phenyl)-4,5,6,7-tetramethyl-1H-inden-2-yl)methyl)trimethylsilane (2.99): Synthesized from **2.97** and a prepared solution of ((trimethylsilyl)methyl)magnesium chloride. (100% Hexanes). White crystalline solid (0.3563 g, 87%) ¹H NMR (600 MHz, CDCl₃) δ 7.38 (d, *J* = 8.3 Hz, 2H), 7.12 (d, *J* = 8.3 Hz, 2H), 3.28 (s, 2H), 2.30 (s, 3H), 2.26 (s, 3H), 2.17 (s, 3H), 1.80 (s, 2H), 1.78 (s, 3H), 1.36 (s, 9H), -0.04 (s, 9H). ¹³C NMR (151 MHz, CDCl₃) δ 149.43, 143.01, 141.97, 138.73, 138.48, 136.62, 134.18, 130.26, 129.65, 128.39, 126.46, 124.99, 42.20, 34.67, 31.63, 20.36, 16.56, 16.32, 16.28, 16.16, -0.51. HRMS (+APCI) calculated for C₂₇H₃₉Si [M+H]⁺ 391.28155, found 391.2814.

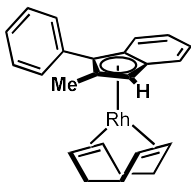


((3-(3,5-di-tert-butylphenyl)-4,5,6,7-tetramethyl-1H-inden-2-yl)methyl)trimethylsilane (2.100):

Synthesized from **2.99** and a prepared solution of ((trimethylsilyl)methyl)magnesium chloride. (100% Hexanes). White crystalline solid, mixture of two inseparable regioisomers (0.3541 g, 85%, (4:1, **2.100:2.100'**) (**2.100**) ¹H NMR (600 MHz, CDCl₃) δ 7.31 (t, *J* = 1.9 Hz, 1H), 7.06 (d, *J* = 1.8 Hz, 2H), 3.29 (s, 2H), 2.30 (s, 3H), 2.26 (s, 3H), 2.17 (s, 3H), 1.84 (s, 2H), 1.74 (s, 4H), 1.32 (s, 18H), -0.05 (s, 9H). (**2.100'**) ¹H NMR (600 MHz, CDCl₃) δ 7.19 (d, *J* = 1.9 Hz, 1H), 6.78 (s, 2H), 6.37 (s, 1H), 4.24 (s, 1H), 2.36 (s, 3H), 2.24 (s, 3H), 2.15 (s, 3H), 1.89 (s, 3H), 1.34 (s, 2H), 1.25 (s, 18H), -0.00 (s, 9H). ¹³C NMR (151 MHz, CDCl₃) δ 150.56, 150.29, 142.36, 142.01, 139.46, 138.80, 138.53, 134.22, 130.27, 128.44, 126.45, 124.49, 119.79, 42.20, 34.98, 31.68, 31.65, 22.81, 20.37, 20.12, 16.56, 16.30, 16.17, 16.14, 14.27, -1.07.

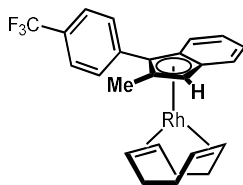
General Procedure D: Catalyst Complexation

In a nitrogen filled glovebox, indene ligand (2.2 equiv.), KO^tBu (3.0 equiv.) and [Rh(COD)Cl]₂ (1.0 equiv.) were weighed out into a 15 mL vial equipped with a stir bar. The vial was sealed with a Teflon septum screw capped and brought out of the box. Outside the glovebox, anhydrous THF (0.3-0.5M) was added, and the reaction was stirred overnight under a N₂ balloon at room temperature. The reaction was filtered through a celite pipette plug flushing with hexanes and the filtrate concentrated under reduced pressure. The resulting crude product was columned via silica gel column chromatography using deacidified silica gel (1% Et₃N in hexanes, flushing with 100% hexanes before loading and eluting the yellow product band with 100% hexanes) to provide the Rh(I)Indenyl complex. Separation of the planar chiral enantiomers was conducted via chiral semipreparative HPLC.



(±)-1,5-cyclooctadiene(η^5 -2-methyl-3-phenylinden-1H-yl)rhodium(I)(±-**2.54**). Prepared according to **General Procedure D** using 2-methyl-3-phenyl-1H-indene⁴ (120 mg, 0.58 mmol, 2.2 equiv.), KO^tBu (97 mg, 0.86 mmol, 3.2 equiv.), and [Rh(COD)Cl]₂ (128 mg, 0.26 mmol, 1.0 equiv.). (±-**2.54**) (0.2069 g, 96% yield) yellow oil. Spectroscopic data for (±)-**2.54** matches those previously reported in the literature.⁴

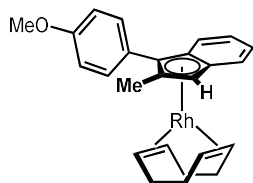
Chiral Resolution: Analytical HPLC: (OD-H column 0% 2-propanol in hexanes, 1.0 mL/min) ((**S**)-**S8**): $t_1 = 14.3$ min, ((**R**)-**S8**): $t_2 = 21.1$ min, **Semi-prep HPLC:** 20 x 250 mm Chiracel OD-H column, 0% 2-Propanol in Hexanes, 20 mL/min 900 μ L injections of 22 mg/mL solutions were made to resolve the complex.



(±)-1,5-cyclooctadiene(η^5 -2-methyl-3-(4-(trifluoromethyl)phenyl)inden-1H-yl)rhodium(I) (±-**S5**). Prepared according to **General Procedure D** using **S1** (175 mg, 0.64 mmol, 2.1 equiv.), KO^tBu (85 mg, 0.76 mmol, 2.5 equiv.), and [Rh(COD)Cl]₂ (150 mg, 0.30 mmol, 1.0 equiv.). (±-**S5**) (0.0852 g, 75% yield). ¹H NMR (600 MHz, C₆D₆) δ 7.45 (d, $J = 8.2$ Hz, 2H), 7.27 (d, $J = 7.8$ Hz, 2H), 7.19 (ddt, $J = 9.2, 8.2, 1.1$ Hz, 2H), 7.11 – 7.05 (m, 2H), 4.62 (s, 1H), 3.82 (qd, $J = 4.8, 2.2$ Hz, 2H), 3.62 (ddd, $J = 8.0, 5.6, 2.5$ Hz, 2H), 2.23 (d, $J = 1.3$ Hz, 3H), 1.87 – 1.77 (m, 4H), 1.71 – 1.60 (m, 4H). ¹³C NMR (151 MHz, C₆D₆) δ 139.67, 129.68, 125.73 (q, $J = 3.8$ Hz), 124.32 (q, $J = 271.6$ Hz), 123.57, 122.78, 119.77, 117.37, 112.81 (d, $J_{C-Rh} = 2.1$ Hz), 112.49 (d, $J_{C-Rh} = 2.8$ Hz), 108.08 (d, $J_{C-Rh} = 5.0$ Hz), 94.09 (d, $J_{C-Rh} = 3.8$ Hz), 77.50 (d, $J_{C-Rh} = 4.8$ Hz), 72.51 (d, $J_{C-Rh} = 13.7$ Hz), 69.67 (d, $J_{C-Rh} = 13.7$ Hz), 31.78, 31.64, 14.69. ¹⁹F NMR (564 MHz, C₆D₆) δ -61.98. **HRMS** (+APCI) calculated for C₂₅H₂₄F₃Rh [M]⁺ 484.08797, found 484.0894. **Prepared by Dr.**

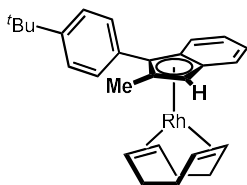
David Laws III

Chiral Resolution: Analytical HPLC (Chiracel AD-H column 100% Hexanes, 1.0 mL/min) ((*S*)-**S5**): $t_1 = 4.6$ min, ((*R*)-**S5**): $t_2 = 7.1$ min, **Semi-prep HPLC** (20 x 250 mm Chiracel OD-H column, 100% Hexanes, 10 mL/min 250 μ L injections of 20 mg/mL solutions were made to resolve the complex.



(±)-1,5-cyclooctadiene(η^5 -3-(4-methoxyphenyl)-2-methylinden-1H-yl)rhodium(I)(±-**S6**): Prepared according to **General Procedure D** using **S2** (53 mg, 0.23 mmol, 2.2 equiv.), KO^tBu (39 mg, 0.35 mmol, 3.4 equiv.), and [Rh(COD)Cl]₂ (59 mg, 0.12 mmol, 1.0 equiv.). (±-**S6**) (0.0731 g, 80% yield). **¹H NMR** (600 MHz, C₆D₆) δ 7.43 – 7.39 (m, 1H), 7.38 (d, $J = 8.2$ Hz, 2H), 7.25 – 7.21 (m, 1H), 7.13 – 7.08 (m, 2H), 6.88 (d, $J = 8.2$ Hz, 2H), 4.68 (s, 1H), 3.94 (td, $J = 7.5, 3.4$ Hz, 2H), 3.77 (tt, $J = 7.6, 3.1$ Hz, 2H), 3.37 (s, 3H), 2.38 (s, 3H), 1.96 – 1.83 (m, 4H), 1.78 – 1.65 (m, 4H). **¹³C NMR** (151 MHz, C₆D₆) δ 158.78, 130.77, 127.43, 123.15, 122.41, 119.66, 117.96, 114.42, 112.97 (d, $J_{C-Rh} = 2.3$ Hz), 112.07 (d, $J_{C-Rh} = 2.7$ Hz), 107.69 (d, $J_{C-Rh} = 5.0$ Hz), 96.06 (d, $J_{C-Rh} = 3.7$ Hz), 76.77 (d, $J_{C-Rh} = 4.9$ Hz), 72.03 (d, $J_{C-Rh} = 13.7$ Hz), 69.12 (d, $J_{C-Rh} = 13.8$ Hz), 54.86, 31.91, 31.78, 14.82. **HRMS** (+APCI) calculated for C₂₅H₂₇ORh [M]⁺ 446.11115, found 446.1111. *Prepared by Dr. David Laws III*

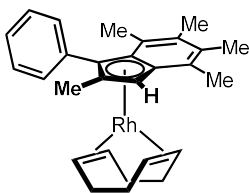
Chiral Resolution: Analytical HPLC: Chiracel OD-H column 100% Hexanes, 1.0 mL/min ((*S*)-**S6**): $t_1 = 34.2$ min, ((*R*)-**S6**): $t_2 = 50.9$ min, **Semi-prep HPLC:** 20 x 250 mm Chiracel OD-H column, 100% Hexanes, 20 mL/min 900 μ L injections of 20 mg/mL solutions were made to resolve the complex



(±)-1,5-cyclooctadiene(η^5 -3-(4-(tert-butyl)phenyl)-2-methylinden-1H-yl)rhodium(I)(±-**S7**). Prepared according to **General Procedure D** using **S3** (67 mg, 0.25 mmol, 2.2 equiv.), KO^tBu (41mg, 0.37 mmol,

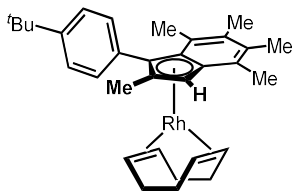
3.2 equiv.), and [Rh(COD)Cl]₂ (68 mg, 0.14 mmol, 1.0 equiv.). (**±-S7**) (0.0852 g, 78% yield). ¹H NMR (600 MHz, C₆D₆) δ 7.47 – 7.45 (m, 2H), 7.45 – 7.41 (m, 1H), 7.41 – 7.37 (m, 2H), 7.24 – 7.20 (m, 1H), 7.12 – 7.06 (m, 2H), 4.67 (s, 1H), 3.94 (dp, *J* = 7.2, 3.0 Hz, 2H), 3.77 (ddt, *J* = 7.8, 6.2, 1.9 Hz, 2H), 2.40 (d, *J* = 1.4 Hz, 3H), 1.92 – 1.82 (m, 4H), 1.75 – 1.63 (m, 4H), 1.29 (s, 9H). ¹³C NMR (151 MHz, C₆D₆) δ 149.19, 132.57, 129.47, 125.77, 123.18, 122.43, 119.68, 113.04 (d, *J*_{C-Rh} = 2.3 Hz), 112.18 (d, *J*_{C-Rh} = 2.7 Hz), 107.81 (d, *J*_{C-Rh} = 5.0 Hz), 96.04 (d, *J*_{C-Rh} = 3.8 Hz), 76.95 (d, *J*_{C-Rh} = 4.9 Hz), 72.09 (d, *J*_{C-Rh} = 13.8 Hz), 69.19 (d, *J*_{C-Rh} = 13.6 Hz), 34.62, 31.81 (d, *J*_{C-Rh} = 2.2 Hz), 31.50, 14.91. HRMS (+APCI) calculated for C₂₈H₃₃Rh [M]⁺ 472.16318, found 472.16426. *Prepared by Dr. David Laws III*

Chiral Resolution: Analytical HPLC: Chiracel OD-H column 100% Hexanes, 0.5 mL/min (**(S)-S7**): *t*₁ = 13.0 min, (**(R)-S7**): *t*₂ = 16.7 min, **Semi-prep HPLC:** 20 x 250 mm Chiracel OD-H column, 100% Hexanes, 20 mL/min 900 μL injections of 20 mg/mL solutions were made to resolve the complex.



(**±**)-1,5-cyclooctadiene(η⁵-2,4,5,6,7-pentamethyl-3-phenylinden-1H-yl)rhodium(I)(**±-S8**). Prepared according to **General Procedure D** using **2.88** (115 mg, 0.44 mmol, 2.2 equiv.), KO^tBu (67 mg, 0.60 mmol, 3.0 equiv.), and [Rh(COD)Cl]₂ (118 mg, 0.24 mmol, 1.0 equiv.). (**±-S8**) (0.109 g, 58% yield). ¹H NMR (600 MHz, C₆D₆) δ 7.77 (d, *J* = 7.7 Hz, 1H), 7.36 – 7.30 (m, 1H), 7.27 – 7.21 (m, 1H), 4.83 (s, 1H), 4.10 (tt, *J* = 7.8, 3.1 Hz, 2H), 3.88 (tt, *J* = 7.9, 2.9 Hz, 2H), 2.29 (s, 3H), 2.18 (s, 3H), 2.13 (d, *J* = 1.2 Hz, 3H), 2.12 (s, 3H), 1.99 (s, 3H), 1.99 – 1.88 (m, 4H), 1.84 – 1.73 (m, 4H). ¹³C NMR (151 MHz, C₆D₆) δ 137.80, 132.56, 131.04, 130.39, 126.78, 123.60, 122.87, 111.43 (d, *J*_{C-Rh} = 2.7 Hz), 109.15 (d, *J*_{C-Rh} = 2.4 Hz), 107.78 (d, *J*_{C-Rh} = 4.9 Hz), 99.37 (d, *J*_{C-Rh} = 4.2 Hz), 75.64 (d, *J*_{C-Rh} = 4.8 Hz), 69.25 (d, *J*_{C-Rh} = 13.8 Hz), 68.95 (d, *J*_{C-Rh} = 13.9 Hz), 32.56, 31.98, 18.14, 16.56, 16.51, 16.24, 13.84. HRMS (+APCI) calculated for C₂₈H₃₃Rh [M]⁺ 472.16318, found 472.16342.

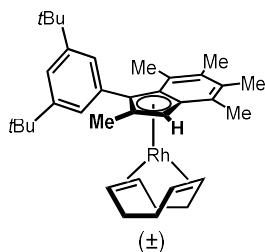
Chiral Resolution: Analytical HPLC (Chiracel OD-H column 100% Hexanes, 1.0 mL/min) ((*R*)-**S8**): $t_1 = 4.5$ min, ((*S*)-**S8**): $t_2 = 5.7$ min, **Semi-prep HPLC** (20 x 250 mm Chiracel OD-H column, 100% Hexanes, 20 mL/min 250 μ L injections of 20 mg/mL solutions were made to resolve the complex.



(±)-1,5-cyclooctadiene(η^5 -3-(4-(*tert*-butyl)phenyl)-2,4,5,6,7-pentamethylinden-1*H*-yl)rhodium(I)

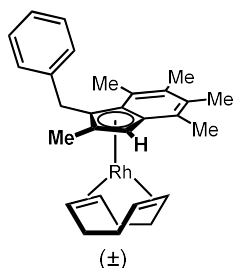
(±-**2.101**). Prepared according to **General Procedure D** using **2.89** (115 mg, 0.44 mmol, 2.2 equiv.), KO^tBu (64 mg, 0.60 mmol, 3.0 equiv.), and [Rh(COD)Cl₂] (118 mg, 0.24 mmol, 1.0 equiv.). (±-**2.101**) (0.108 g, 58% yield). ¹H NMR (600 MHz, CDCl₃) δ 7.75 (dd, $J = 8.0, 1.9$ Hz, 1H), 7.45 (dd, $J = 8.0, 2.1$ Hz, 1H), 7.29 (qd, $J = 8.1, 2.0$ Hz, 2H), 4.85 (s, 1H), 4.14 (td, $J = 7.5, 3.7$ Hz, 2H), 3.92 (ddd, $J = 10.6, 7.7, 2.9$ Hz, 2H), 2.30 (s, 3H), 2.19 (s, 3H), 2.17 (d, $J = 1.2$ Hz, 3H), 2.12 (s, 3H), 2.04 (s, 3H), 2.03 – 1.99 (m, 2H), 1.99 – 1.91 (m, 2H), 1.86 – 1.76 (m, 4H), 1.29 (s, 9H). ¹³C NMR (151 MHz, CDCl₃) δ 149.39, 134.78, 132.32, 130.82, 130.32, 125.00, 124.91, 123.74, 122.84, 111.41 (d, $J_{C-Rh} = 2.6$ Hz), 109.26 (d, $J_{C-Rh} = 2.6$ Hz), 107.77 (d, $J_{C-Rh} = 4.6$ Hz), 99.21 (d, $J_{C-Rh} = 4.3$ Hz), 75.63 (d, $J_{C-Rh} = 4.9$ Hz), 69.12 (d, $J_{C-Rh} = 13.8$ Hz), 68.98 (d, $J_{C-Rh} = 13.8$ Hz), 34.61, 32.58, 32.06, 31.57, 18.20, 16.56, 16.52, 16.25, 14.02. **HRMS** (+APCI) calculated for C₃₂H₄₂Rh [M+H]⁺ 529.23361, found 529.2339.

The planar chiral enantiomers of (±-**2.101**) were not found to separate sufficiently on chiral HPLC to allow for the clean chiral resolution of this complex.



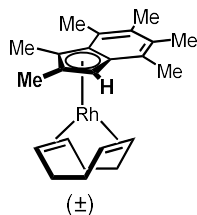
(±)-1,5-cyclooctadiene(η^5 -3-(3,5-di-tert-butylphenyl)-2,4,5,6,7-pentamethyl-1H-inden-1-yl)rhodium(I):

(2.102) Canary Yellow residue (0.0275g, 46% yield). $^1\text{H NMR}$ (600 MHz, C_6D_6) δ 7.83 (t, $J = 1.7$ Hz, 1H), 7.54 (t, $J = 1.9$ Hz, 1H), 7.36 (t, $J = 1.7$ Hz, 1H), 4.86 (s, 1H), 4.18 (td, $J = 7.7, 3.8$ Hz, 2H), 3.92 (td, $J = 7.6, 3.7$ Hz, 2H), 2.33 (s, 3H), 2.22 (s, 3H), 2.20 (s, 3H), 2.12 (s, 3H), 2.10 (s, 3H), 2.10 – 1.93 (m, 4H), 1.90 – 1.78 (m, 4H), 1.49 (s, 9H), 1.30 (s, 9H). $^{13}\text{C NMR}$ (151 MHz, C_6D_6) δ 150.11, 149.90, 136.52, 130.59, 126.90, 126.71, 123.58, 123.07, 120.28, 111.23 (d, $J_{\text{C-Rh}} = 2.7$ Hz), 109.18 (d, $J_{\text{C-Rh}} = 2.4$ Hz), 107.68 (d, $J_{\text{C-Rh}} = 4.8$ Hz), 101.14 (d, $J_{\text{C-Rh}} = 4.2$ Hz), 75.48 (d, $J_{\text{C-Rh}} = 4.8$ Hz), 69.55 (d, $J_{\text{C-Rh}} = 13.8$ Hz), 69.18 (d, $J_{\text{C-Rh}} = 13.8$ Hz), 35.24, 34.94, 32.52, 32.30, 31.84, 31.69, 18.19, 16.61, 16.50, 16.26, 14.06. **HRMS** (+APCI) calculated for $\text{C}_{36}\text{H}_{50}^{103}\text{Rh}$ $[\text{M}+\text{H}]^+$ 585.29621, found 585.29673.



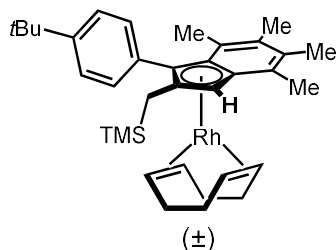
(±)-1,5-cyclooctadiene(η^5 -3-benzyl-2,4,5,6,7-pentamethyl-1H-inden-1-yl)rhodium(I) **(2.103)**: Yellow Residue (0.0313 g, 79% yield). $^1\text{H NMR}$ (600 MHz, C_6D_6) δ 7.11 – 7.00 (m, 5H), 5.04 (s, 1H), 4.15 (td, $J = 7.3, 6.8, 3.3$ Hz, 2H), 3.95 (d, $J = 17.3$ Hz, 1H), 3.77 (d, $J = 17.3$ Hz, 1H), 3.73 (dt, $J = 7.7, 4.0$ Hz, 2H), 2.28 (s, 3H), 2.21 (s, 3H), 2.17 (d, $J = 1.4$ Hz, 3H), 2.11 (s, 3H), 2.02 (s, 3H), 1.99 – 1.84 (m, 7H), 1.78 (dq, $J = 11.3, 6.7, 5.2$ Hz, 2H). $^{13}\text{C NMR}$ (151 MHz, C_6D_6) δ 141.38, 129.36, 128.96, 128.83, 128.81, 128.44, 126.19, 123.77, 122.22, 111.71 (d, $J_{\text{C-Rh}} = 2.6$ Hz), 110.36 (d, $J_{\text{C-Rh}} = 2.2$ Hz), 107.75 (d, $J_{\text{C-Rh}} = 5.3$ Hz), 89.47 (d, $J_{\text{C-Rh}} = 4.5$ Hz), 77.03 (d, $J_{\text{C-Rh}} = 4.5$ Hz), 70.42 (d, $J_{\text{C-Rh}} = 13.8$ Hz), 67.08 (d, $J_{\text{C-Rh}} = 13.7$ Hz),

32.73, 32.62, 31.78, 16.68, 16.49, 16.18, 16.09, 13.44. **HRMS** (+APCI) calculated for $C_{29}H_{36}^{103}Rh$ $[M+H]^+$ 487.18666, found 487.18754.

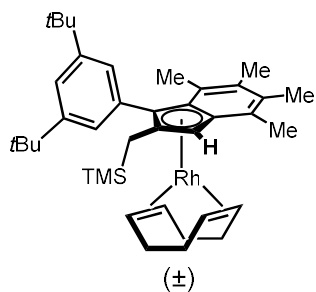


(±)-1,5-cyclooctadiene(η^5 -2,3,4,5,6,7-hexamethyl-1H-inden-1-yl)rhodium(I) (**2.104**)

Could not be separated from reaction impurities, too impure to properly assign all NMR signals.



(±)-1,5-cyclooctadiene(η^5 -3-(4-(tert-butyl)phenyl)-4,5,6,7-tetramethyl-2-((trimethylsilyl)methyl)-1H-inden-1-yl)rhodium(I) (**2.105**): Yellow-orange residue. (0.0026 g, 5%) **1H NMR** (600 MHz, C_6D_6) δ 7.96 (d, $J = 8.1$ Hz, 1H), 7.43 (d, $J = 8.1$ Hz, 1H), 7.30 (t, $J = 12.1$ Hz, 2H), 4.88 (s, 1H), 4.23 – 4.15 (m, 2H), 3.75 (dt, $J = 7.8, 4.2$ Hz, 2H), 2.35 (s, 3H), 2.20 (s, 3H), 2.15 (s, 3H), 2.00 (s, 3H), 2.00 – 1.78 (m, 10H), 1.28 (s, 9H), -0.20 (s, 9H). **^{13}C NMR** (151 MHz, C_6D_6) δ 149.44, 134.33, 133.17, 130.74, 130.30, 127.42, 124.88, 124.75, 123.41, 122.84, 111.66 (d, $J_{C-Rh} = 4.2$ Hz), 111.24 (d, $J_{C-Rh} = 2.7$ Hz), 107.81 (d, $J_{C-Rh} = 2.5$ Hz), 98.80 (d, $J_{C-Rh} = 4.1$ Hz), 74.10 (d, $J_{C-Rh} = 5.0$ Hz), 70.49 (d, $J_{C-Rh} = 14.0$ Hz), 68.65 (d, $J_{C-Rh} = 13.8$ Hz), 34.61, 32.53, 32.33, 31.54, 18.70, 17.89, 16.55, 16.43, 16.21, -1.16. **HRMS** (+APCI) calculated for $C_{35}H_{50}^{103}Rh^{28}Si$ $[M+H]^+$ 601.27313, found 601.27314.

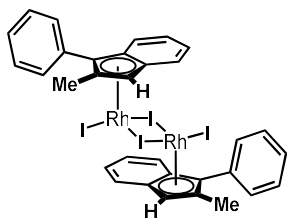


(±)-1,5-cyclooctadiene(η^5 -3-(3,5-di-tert-butylphenyl)-4,5,6,7-tetramethyl-2-((trimethylsilyl)methyl)-1H-inden-1-yl)rhodium(I) (**2.106**): Could not be separated from reaction impurities, too impure to properly assign all NMR signals.

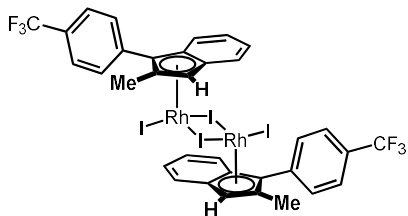
General Procedure E: Precatalysts Synthesis

With no precautions against air or moisture exposure, I_2 crystals (2.5 equiv.) were added to an 8 dram vial equipped with a stir bar and containing a solution of resolved (*S,S*)-Ind^XRh(I)(COD) complex (1.0 equiv.) in Et₂O (0.03M). The vial was capped to prevent solvent evaporation and the black solution was stirred for 24 hours. The reaction was filtered through a Buchner funnel washing with excess Et₂O until the filtrate was clear. The fine black powder was carefully collected from the filter paper to give the (*S,S*)-[Ind^XRh(III)I₂]₂ precatalyst which was stored in a nitrogen filled glovebox.

(*R,R*)-[Ind^XRh(III)I₂]₂ precatalysts and (±)-[Ind^XRh(III)I₂]₂ precatalysts were synthesized in the same manner.

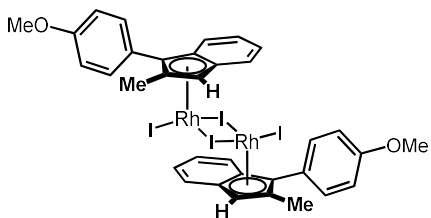


(S,S)-(η^5 -2-methyl-3-phenylinden-1H-yl) rhodium(III) diiodide dimer (**(S,S)-2.55**): Prepared according to **General Procedure E** using (**S**)-**2.54** (97 mg, 0.23 mmol, 1.0 equiv.) and I₂ (148 mg, 0.58 mmol, 2.5 equiv.). **(S,S)-2.55** (120 mg, 93% yield) Fine black powder. Spectroscopic data for **(S,S)-2.55** matches those previously reported in the literature⁴.

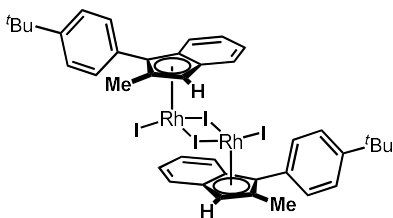


(S,S)-(η^5 -2-methyl-3-(4-(trifluoromethyl)phenyl)inden-1H-yl) rhodium(III) diiodide dimer (**(S,S)-2.70**): Prepared according to **General Procedure E** using (**S**)-**XX** (49 mg, 0.10 mmol, 1.0 equiv.) and I₂ (64 mg, 0.25 mmol, 2.5 equiv.). **(S,S)-2.70** (37 mg, 58% yield) Fine black powder. ¹H NMR (600 MHz, DMSO-d₆) δ 8.06 (d, *J* = 8.0 Hz, 4H), 7.88 (d, *J* = 8.0 Hz, 4H), 7.71 (d, *J* = 8.5 Hz, 2H), 7.63 (t, *J* = 7.5 Hz, 2H), 7.59 (t, *J* = 7.6 Hz, 2H), 7.44 (d, *J* = 8.4 Hz, 2H), 6.54 (s, 2H), 2.27 (s, 6H). ¹³C NMR (151 MHz, DMSO-d₆) δ 134.06, 133.73, 132.67, 129.01 (q, *J* = 31.9 Hz), 127.62, 125.39, 125.31 (q, *J* = 4.0 Hz), 124.18 (q, *J* = 272.1 Hz), 112.10 (d, *J*_{C-Rh} = 5.4 Hz), 107.09 (d, *J*_{C-Rh} = 3.7 Hz), 104.34 (d, *J*_{C-Rh} = 4.1 Hz), 92.91 (d, *J*_{C-Rh} = 5.6 Hz), 78.28 (d, *J*_{C-Rh} = 6.7 Hz), 13.46. ¹⁹F NMR (565 MHz, DMSO-d₆) δ -61.09. **HRMS** (+APCI) calculated for C₁₇H₁₂F₃¹²⁷I₃¹⁰³Rh [M-C₁₇H₁₂I₃Rh]⁻ 756.70857, found 756.70865 **Prepared by Dr. David Laws**

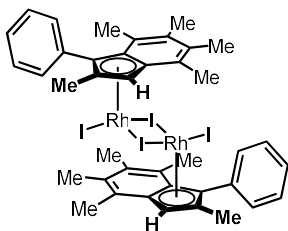
III



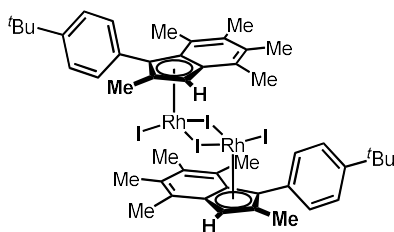
(S,S)-(η^5 -3-(4-methoxyphenyl)-2-methylinden-1H-yl) rhodium(III) diiodide dimer (**(S,S)**-2.71): Prepared according to **General Procedure E** using **(S)**-XX (52 mg, 0.12 mmol, 1.0 equiv.) and I₂ (74 mg, 0.29 mmol, 2.5 equiv.). **(S,S)**-2.71 (51 mg, 71% yield) Fine black powder. ¹H NMR (600 MHz, DMSO-d₆) δ 7.80 (d, *J* = 8.7 Hz, 4H), 7.70 – 7.65 (m, 2H), 7.58 (tt, *J* = 6.7, 5.2 Hz, 4H), 7.47 – 7.41 (m, 2H), 7.06 (d, *J* = 8.7 Hz, 4H), 6.43 (s, 2H), 3.83 (s, 6H), 2.23 (s, 6H). ¹³C NMR (151 MHz, DMSO-d₆) δ 159.64, 133.48, 132.35, 132.21, 127.83, 125.55, 120.95, 113.98, 110.83 (d, *J*_{C-Rh} = 5.4 Hz), 107.29 (d, *J*_{C-Rh} = 3.9 Hz), 103.45 (d, *J*_{C-Rh} = 4.7 Hz), 95.23 (d, *J*_{C-Rh} = 5.6 Hz), 77.58 (d, *J*_{C-Rh} = 7.2 Hz), 55.23, 13.58. **HRMS** (+APCI) calculated for C₁₇H₁₄OI₂Rh [M-C₁₇H₁₆OI₂Rh]⁻ 590.81725, found 590.81689 **Prepared by Dr. David Laws III**



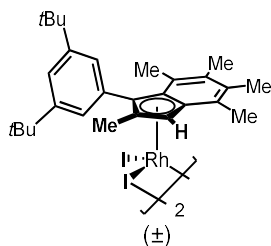
(S,S)-(η^5 -3-(4-(tert-butyl)phenyl)-2-methylinden-1H-yl) rhodium(III) diiodide dimer (**(S,S)**-2.72): Prepared according to **General Procedure E** using **(S)**-S11 (43 mg, 0.90 mmol, 1.0 equiv.) and I₂ (57 mg, 0.23 mmol, 2.5 equiv.). **(S,S)**-2.72 (39 mg, 72% yield) Fine black powder. ¹H NMR (600 MHz, DMSO-d₆) δ 7.79 (d, *J* = 8.3 Hz, 4H), 7.68 (dd, *J* = 8.4, 1.2 Hz, 2H), 7.62 – 7.58 (m, 2H), 7.58 – 7.55 (m, 2H), 7.51 (d, *J* = 8.0 Hz, 4H), 7.45 (d, *J* = 8.5 Hz, 2H), 6.44 (s, 2H), 2.25 (s, 6H), 1.34 (s, 18H). ¹³C NMR (151 MHz, DMSO-d₆) δ 151.29, 133.48, 130.55, 127.75, 125.67, 125.28, 111.32 (d, *J*_{C-Rh} = 5.7 Hz), 107.36 (d, *J*_{C-Rh} = 3.8 Hz), 103.62 (d, *J*_{C-Rh} = 4.5 Hz), 94.93 (d, *J*_{C-Rh} = 5.9 Hz), 77.63 (d, *J*_{C-Rh} = 7.0 Hz), 34.59, 31.03, 13.74. **HRMS** (+APCI) calculated for C₂₀H₂₁I₂Rh [M-C₂₀H₂₁I₂Rh]⁺ 490.97375, found 490.9738 **Prepared by Dr. David Laws III**



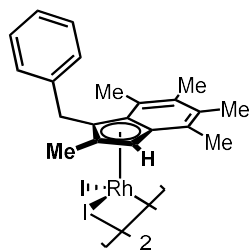
(S,S)-(η^5 -2,4,5,6,7-pentamethyl-3-phenylinden-1H-yl) rhodium(III) diiodide dimer (**(S,S)-2.69**): Prepared according to **General Procedure E** using **(S)-XX** (32 mg, 0.069 mmol, 1.0 equiv.) and I₂ (44 mg, 0.17 mmol, 2.5 equiv.). **(S,S)-2.69** (42 mg, 98% yield) Fine black powder. ¹H NMR (600 MHz, DMSO) δ 8.27 – 8.22 (m, 2H), 7.48 – 7.41 (m, 4H), 7.40 – 7.35 (m, 2H), 7.29 – 7.24 (m, 2H), 6.44 (s, 2H), 2.46 (s, 6H), 2.18 (s, 6H), 2.11 (s, 6H), 2.02 (s, 6H), 1.87 (s, 6H). ¹³C NMR (151 MHz, DMSO) δ 142.65, 141.60, 133.53, 131.02, 130.69, 129.88, 129.22, 128.47, 128.08, 127.73, 112.53 (d, J_{C-Rh} = 6.0 Hz), 107.15 (d, J_{C-Rh} = 2.9 Hz), 104.92 (d, J_{C-Rh} = 3.7 Hz), 95.91 (d, J_{C-Rh} = 6.9 Hz), 75.08 (d, J_{C-Rh} = 7.0 Hz), 18.25, 17.77, 17.46, 17.27, 13.97. **HRMS** (+APCI) calculated for C₄₀H₄₂I₃Rh₂ [M-I]⁺ 1108.85251, found 1108.85571



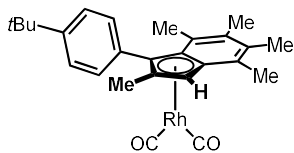
*(η^5 -3-(4-(tert-butyl)phenyl)-2,4,5,6,7-pentamethylinden-1H-yl) rhodium(III) diiodide dimer (**2.80**): Prepared according to **General Procedure E** using **2.101** (97 mg, 0.23 mmol, 1.0 equiv.) and I₂ (148 mg, 0.58 mmol, 2.5 equiv.). **2.80** (120 mg, 93% yield) Fine black powder. ¹H NMR (600 MHz, DMSO) δ 8.16 (dd, J = 8.2, 2.1 Hz, 1H), 7.48 (dd, J = 8.2, 2.1 Hz, 1H), 7.39 (dd, J = 8.1, 2.1 Hz, 1H), 7.18 (dd, J = 8.1, 2.0 Hz, 1H), 6.42 (s, 1H), 2.46 (s, 3H), 2.18 (s, 3H), 2.11 (s, 3H), 2.01 (s, 3H), 1.88 (s, 3H), 1.33 (s, 9H). ¹³C NMR (151 MHz, DMSO) δ 150.82, 142.51, 141.62, 133.11, 130.90, 129.52, 129.09, 127.97, 124.84, 124.45, 112.55 (d, J_{C-Rh} = 5.7 Hz), 107.34 (d, J_{C-Rh} = 2.6 Hz), 104.78 (d, J_{C-Rh} = 3.5 Hz), 96.06 (d, J_{C-Rh} = 6.7 Hz), 74.83 (d, J_{C-Rh} = 6.9 Hz), 34.47, 31.12, 18.30, 17.72, 17.44, 17.24, 14.02. **HRMS** (+APCI) calculated for C₄₈H₅₈I₃Rh₂ [M-I]⁺ 1220.97772, found 1220.98175.*



(±)-(η⁵-3-(3,5-di-tert-butylphenyl)-2,4,5,6,7-pentamethyl-1H-inden-1-yl)rhodium(III) diiodide dimer (**2.81**): Dirt Brown powder (0.0225 g, 64% yield). ¹H NMR (600 MHz, DMSO-*d*₆) δ 8.21 (t, *J* = 1.7 Hz, 2H), 7.38 (t, *J* = 1.8 Hz, 2H), 7.06 (t, *J* = 1.7 Hz, 2H), 6.39 (s, 2H), 2.46 (s, 6H), 2.18 (s, 6H), 2.11 (s, 6H), 2.03 (s, 6H), 1.88 (s, 6H), 1.35 (s, 18H), 1.27 (s, 18H). HRMS (+APCI) calculated for C₅₆H₇₄¹²⁷I₃¹⁰³Rh₂ [M-I]⁺ 1333.10544, found 1333.10292.

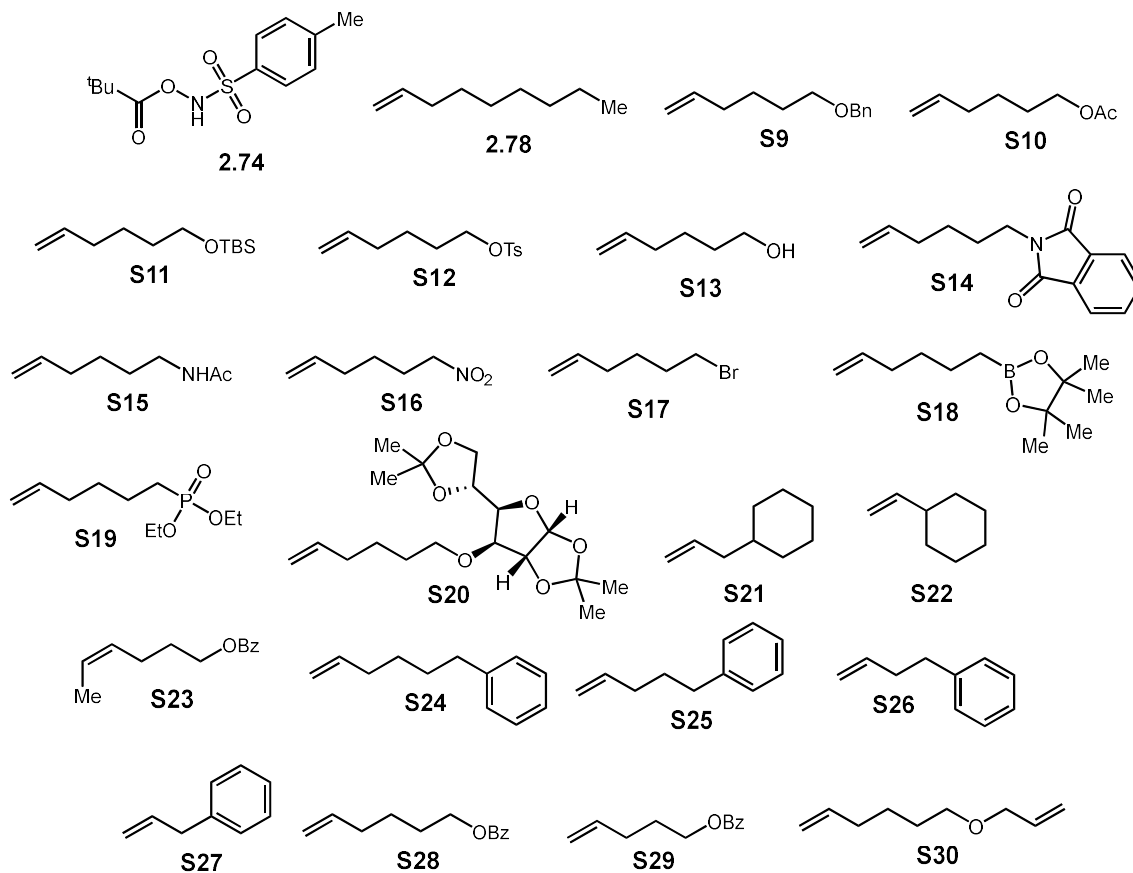


(±)-(η⁵-3-benzyl-2,4,5,6,7-pentamethyl-1H-inden-1-yl)rhodium(III) diiodide dimer (**2.84**): Dirt brown powder (0.0336 g, 94% yield) ¹H NMR (600 MHz, DMSO-*d*₆) δ 7.28 (t, *J* = 7.6 Hz, 4H), 7.21 (t, *J* = 7.4 Hz, 2H), 7.03 (d, *J* = 7.6 Hz, 4H), 6.45 (s, 2H), 4.49 (d, *J* = 17.6 Hz, 2H), 3.89 (d, *J* = 17.6 Hz, 2H), 2.42 (s, 6H), 2.27 (s, 6H), 2.17 (s, 6H), 2.16 (s, 6H), 2.10 (s, 6H). ¹³C NMR (151 MHz, DMSO-*d*₆) δ 142.52, 141.43, 137.70, 130.09, 129.84, 128.90, 127.29, 126.54, 112.66 (d, *J*_{C-Rh} = 6.3 Hz), 106.89 (d, *J*_{C-Rh} = 4.3 Hz), 105.34 (d, *J*_{C-Rh} = 3.6 Hz), 90.68 (d, *J*_{C-Rh} = 6.5 Hz), 75.64 (d, *J*_{C-Rh} = 6.2 Hz), 32.25, 17.85, 17.47, 16.60, 12.66. HRMS (+APCI) calculated for C₄₂H₄₆¹²⁷I₃¹⁰³Rh₂ [M-I]⁺ 1136.88381, found 1136.88522



(±)-di-carbonyl-(η^5 -3-(4-(tert-butyl)phenyl)-2,4,5,6,7-pentamethylinden-1H-yl)rhodium(I) (**2.108**): In a 10 mL Schlenk flask under an N_2 atmosphere, **2.101** (45.6 mg, 0.086 mmol) was dissolved in a Hexanes (6 mL). A balloon of CO was attached with a long needed and the solution was sparged. This process was repeated an additional two times before a fresh CO balloon was attached and the solution was left to stir overnight at room temperature. Once the reaction was complete, the hexanes was evaporated and the crude material purified by passing through a neutral alumina column using 100% Pentane to provide **2.108** as yellow residue (36.3 mg, 88% yield). **1H NMR** (600 MHz, C_6D_6) δ 7.91 (dd, $J = 8.0, 2.1$ Hz, 1H), 7.35 (dd, $J = 8.0, 2.1$ Hz, 1H), 7.30 (dd, $J = 8.1, 2.2$ Hz, 1H), 7.18 (dd, $J = 8.1, 2.1$ Hz, 1H), 5.33 (s, 1H), 2.16 (s, 3H), 1.97 (s, 3H), 1.95 (s, 3H), 1.89 (s, 3H), 1.87 (d, $J = 2.1$ Hz, 3H), 1.25 (s, 9H). **^{13}C NMR** (151 MHz, C_6D_6) δ 192.53, 191.97, 150.77, 133.91, 133.19, 132.97, 131.82, 130.77, 125.82, 125.21, 123.88, 122.02, 115.27 (d, $J_{C-Rh} = 2.3$ Hz), 115.17 (d, $J_{C-Rh} = 6.4$ Hz), 115.01 (d, $J_{C-Rh} = 1.9$ Hz), 104.01 (d, $J_{C-Rh} = 3.8$ Hz), 72.60 (d, $J_{C-Rh} = 3.5$ Hz), 34.63, 31.47, 16.91, 16.35, 16.30, 15.49, 14.57.

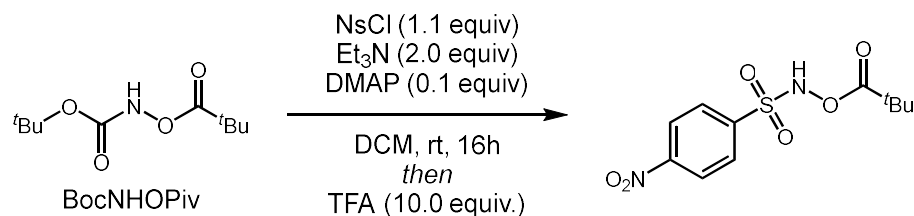
Preparation of Starting Materials



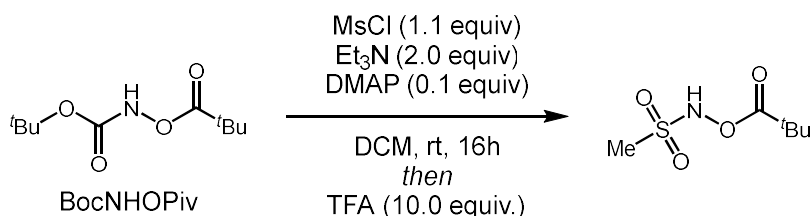
2.78, S13, S17, S21, S22, S26, and S27 were obtained commercially and used without further purification.

2.74,⁵ S9,⁶ S10,⁷ S11,⁸ S12,⁹ S14,¹⁰ S15,¹¹ S16,¹² S18,¹³ S19,¹⁴ S20,¹⁵ S23,¹⁶ S24,¹⁷ S25,¹⁹ S28,¹⁸ S29,¹⁹ and S30²⁰ were synthesized following reported literature procedures.

Synthesis of Nitrogen Sources



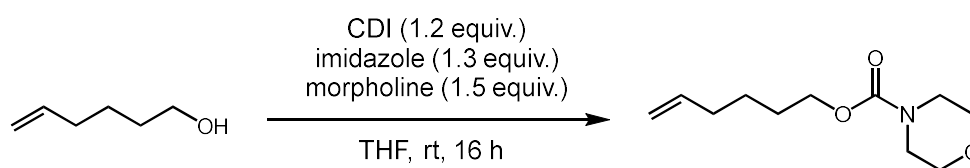
4-nitro-N-(pivaloyloxy)benzenesulfonamide (S31): To a solution of BocNHOPiv (0.55 g, 2.5 mmol, 1.0 equiv.) and DMPA (0.040 g, 0.33 mmol, 0.13 equiv.) in DCM (10 mL) was added Et₃N (0.70 mL, 5.0 mmol, 2.0 equiv.) followed by the addition of NsCl (0.61 g, 2.8 mmol, 1.1 equiv.) . The solution was left to stir at room temperature for 16 hours. To the solution, TFA (2.0 mL, 25.0 mmol, 10.0 equiv.) was slowly added and the solution was continued to stir for one hour. The reaction was then diluted with DCM and washed with 1M HCl once. The aqueous layer was extracted a further two times with DCM before the combined organic layers were dried over MgSO₄ and the solvent was removed under reduced pressure. The crude product was purified using silica gel column chromatography (10% EtOAc in Hexanes) to obtain **S31** as an off white solid (0.423 g, 55 % yield). ¹H NMR (400 MHz, CDCl₃) δ 9.08 (s, 1H), 8.42 (d, J = 8.9 Hz, 2H), 8.15 (d, J = 8.9 Hz, 2H), 1.16 (s, 9H). ¹³C NMR (101 MHz, CDCl₃) δ 176.75, 151.21, 141.64, 130.35, 124.52, 38.47, 26.90. HRMS (+APCI) calculated for C₁₁H₁₃O₆N₂S [M-H]⁻ 301.04998, found 301.0487.



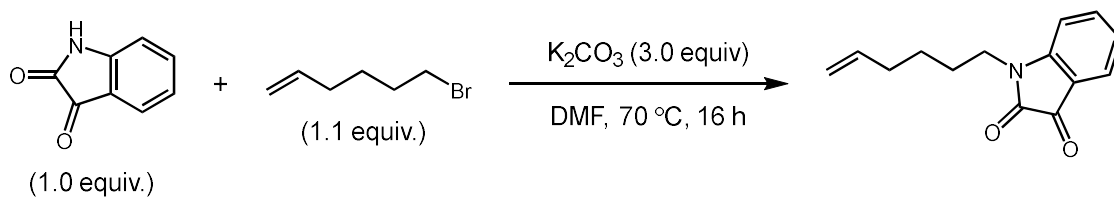
N-(pivaloyloxy)methanesulfonamide (S32): To a solution of BocNHOPiv (0.55 g, 2.5 mmol, 1.0 equiv.) and DMPA (0.030 g, 0.25mmol, 0.10 equiv.) in DCM (10 mL) was added Et₃N (0.70 mL, 5.0 mmol, 2.0 equiv.) followed by the addition of MsCl (0.21 mL, 2.7 mmol, 1.1 equiv.) . The solution was left to stir at room temperature for 16 hours. To the solution TFA, (2.0 mL, 25.0 mmol, 10.0 equiv.) was slowly added and the solution was continued to stir for one hour. The reaction was then diluted with DCM and washed

with 1M HCl once. The aqueous layer was extracted a further two times with DCM before the combined organic layers were dried over MgSO₄ and the solvent was removed under reduced pressure. The crude product was purified using silica gel column chromatography (10% EtOAc in Hexanes) to obtain **S32** as a white solid (0.226 g, 46 % yield). ¹H NMR (400 MHz, CDCl₃) δ 8.71 (s, 1H), 3.07 (s, 3H), 1.32 (s, 9H). ¹³C NMR (101 MHz, CDCl₃) δ 177.16, 38.99, 38.56, 26.98. HRMS (+APCI) calculated for C₆H₁₂O₄NS [M-H]⁻ 194.0493, found 194.0494.

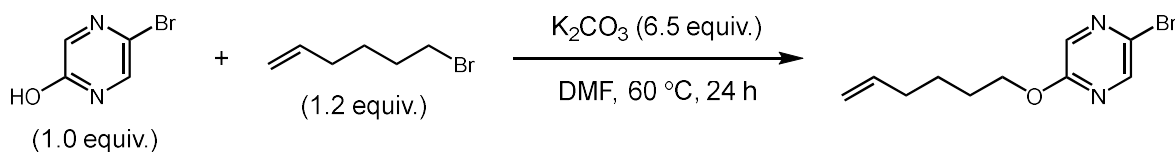
Synthesis of Alkene Substrates



hex-5-en-1-yl morpholine-4-carboxylate (S33): To a solution of CDI (0.98 g, 6.0 mmol, 1.2 equiv.) in THF (10 mL) was added hex-5-en-1-ol (0.60 mL, 5.0 mmol, 1.0 equiv.) and solution was stirred for two hours at room temperature. After which, imidazole (0.45 g, 6.6 mmol, 1.3 equiv.) and morpholine (0.66 mL, 7.6 mmol, 1.5 equiv.) were added sequentially before letting the reaction stir for 16 hours. The reaction was diluted with EtOAc and washed with 1M HCl twice, DI H₂O once, and sat. brine once. The organic layer was dried over anhydrous Na₂SO₄, and the solvent removed under reduced pressure to obtain **S33** as colorless oil that did not require further purification (1.10 g, quant.). ¹H NMR (400 MHz, CDCl₃) δ 5.79 (ddt, *J* = 16.9, 10.3, 6.6 Hz, 1H), 5.01 (dt, *J* = 17.1, 1.7 Hz, 1H), 4.96 (ddd, *J* = 10.2, 2.2, 1.1 Hz, 1H), 4.09 (t, *J* = 6.6 Hz, 2H), 3.65 (s, 4H), 3.46 (t, *J* = 4.8 Hz, 4H), 2.08 (q, *J* = 7.2 Hz, 2H), 1.70 – 1.59 (m, 2H), 1.52 – 1.38 (m, 2H). ¹³C NMR (101 MHz, CDCl₃) δ 155.60, 138.42, 114.83, 66.63, 65.52, 44.01, 33.34, 28.43, 25.23. HRMS (+APCI) calculated for C₁₁H₂₀O₃N [M+H]⁺ 214.14377, found 214.14361

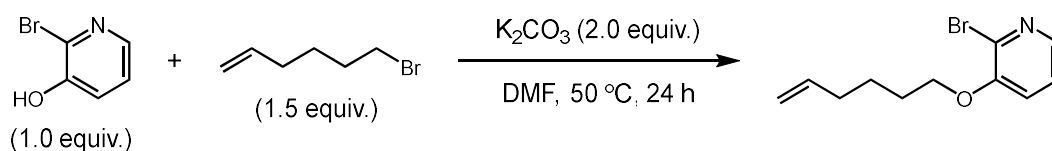


1-(hex-5-en-1-yl)indoline-2,3-dione (S34): Indoline-2,3-dione (0.77, 5.2 mmol, 1.0 equiv.) and K_2CO_3 (2.1 g, 15.4 mmol, 3.0 equiv.) were added to a flame dried 24mL reaction vial equipped with a stir bar and the atmosphere was exchanged with N_2 three times. DMF (10 mL) was added to the vial and the reaction stirred for 5 minutes before adding 6-bromohex-1-ene (0.84 mL, 6.0 mmol, 1.1 equiv.). The reaction was placed in an aluminium heating block and stirred at 70 °C for 16 hours. The reaction was cooled to room temperature and diluted with EtOAc before washing with DI H_2O four times. The organic layer was dried over anhydrous Na_2SO_4 , and the solvent removed under reduced pressure. The crude product was purified using silica gel column chromatography (20% EtOAc in Hexanes) to obtain **S34** as a colorless oil (1.104 g, 92 % yield). $^1\text{H NMR}$ (400 MHz, CDCl_3) δ 7.66 – 7.53 (m, 2H), 7.11 (td, $J = 7.5, 0.8$ Hz, 1H), 6.89 (dt, $J = 7.8, 0.8$ Hz, 1H), 5.77 (ddt, $J = 16.9, 10.2, 6.7$ Hz, 1H), 5.07 – 4.92 (m, 2H), 3.77 – 3.67 (m, 2H), 2.15 – 2.08 (m, 2H), 1.79 – 1.65 (m, 2H), 1.55 – 1.40 (m, 2H). $^{13}\text{C NMR}$ (101 MHz, CDCl_3) δ 183.76, 158.26, 151.13, 138.45, 138.08, 125.63, 123.77, 117.72, 115.36, 110.26, 40.20, 33.33, 26.74, 26.17. **HRMS** (+APCI) calculated for $\text{C}_{14}\text{H}_{16}\text{O}_2\text{N}$ $[\text{M}+\text{H}]^+$ 230.11756, found 230.11746

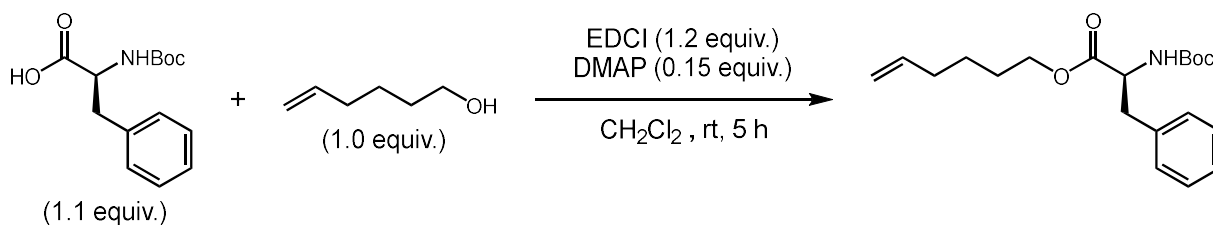


2-bromo-5-(hex-5-en-1-yloxy)pyrazine (S35): Following a modified procedure²¹, 5-bromopyrazin-2-ol (0.88, 5.0 mmol, 1.0 equiv.) and K_2CO_3 (4.5 g, 33 mmol, 6.5 equiv.) were added to a flame dried 22 mL reaction vial equipped with a stir bar and the atmosphere was exchanged with N_2 three times. DMF (10 mL) was added to the vial and the reaction stirred for 20 minutes before adding 6-bromohex-1-ene (0.80 mL, 6.0 mmol, 1.5 equiv.). The reaction was placed in an aluminium heating block and stirred at 60 °C for 24 hours. The reaction was cooled to room temperature and diluted with EtOAc before washing with DI H_2O

three times and sat. LiCl once. The organic layer was dried over anhydrous Na₂SO₄ and the solvent removed under reduced pressure. The crude product was purified using silica gel column chromatography (5% EtOAc in Hexanes) to obtain **S35** as a colorless oil (0.64 g, 50 % yield). ¹H NMR (400 MHz, CDCl₃) δ 8.16 (d, *J* = 1.3 Hz, 1H), 7.99 (d, *J* = 1.4 Hz, 1H), 5.81 (ddt, *J* = 17.0, 10.2, 6.7 Hz, 1H), 5.03 (dq, *J* = 17.1, 1.7 Hz, 1H), 4.97 (ddt, *J* = 10.2, 2.2, 1.2 Hz, 1H), 4.29 (t, *J* = 6.6 Hz, 2H), 2.12 (dtd, *J* = 7.6, 6.3, 1.4 Hz, 2H), 1.79 (dq, *J* = 8.1, 6.6 Hz, 2H), 1.54 (p, *J* = 8.0 Hz, 2H). ¹³C NMR (101 MHz, CDCl₃) δ 159.82, 142.94, 138.44, 135.58, 129.98, 115.05, 67.13, 33.47, 28.26, 25.28. HRMS (+APCI) calculated for C₁₀H₁₄ON₂Br [M+H]⁺ 257.0284, found 257.02895

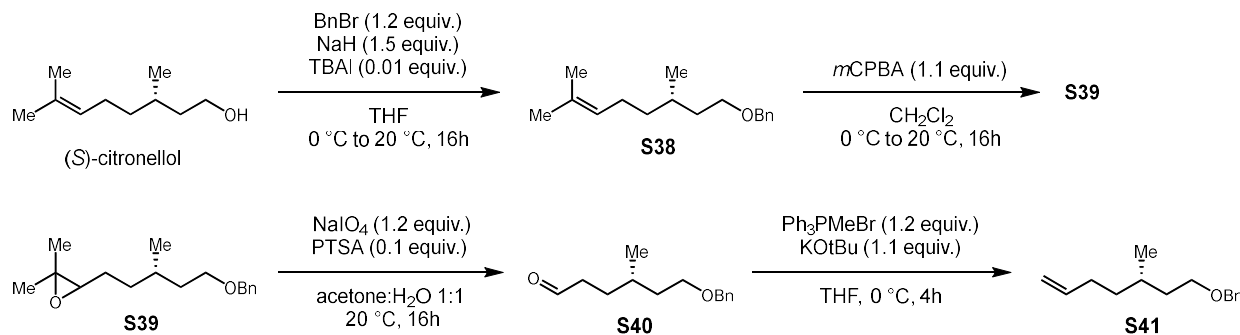


2-bromo-3-(hex-5-en-1-yloxy)pyridine (**S36**): Following a modified procedure²¹, 2-bromopyridin-3-ol (0.89, 5.1 mmol, 1.0 equiv.) and K₂CO₃ (1.4 g, 10 mmol, 2.0 equiv.) were added to a flame dried 22 mL reaction vial equipped with a stir bar and the atmosphere was exchanged with N₂ three times. DMF (10 mL) was added to the vial and the reaction stirred for 20 minutes before adding 6-bromohex-1-ene (1.0 mL, 7.5 mmol, 1.5 equiv.). The reaction was placed in an aluminum heating block and stirred at 50 °C for 24 hours. The reaction was cooled to room temperature and diluted with EtOAc before washing with DI H₂O three times and sat. LiCl once. The organic layer was dried over anhydrous Na₂SO₄ and the solvent removed under reduced pressure. The crude product was purified using silica gel column chromatography (10% EtOAc in Hexanes) to obtain **S36** as a colorless oil (1.19 g, 91 % yield). ¹H NMR (400 MHz, CDCl₃) δ 7.96 (dd, *J* = 4.6, 1.6 Hz, 1H), 7.19 (dd, *J* = 8.1, 4.6 Hz, 1H), 7.11 (dd, *J* = 8.1, 1.6 Hz, 1H), 5.83 (ddt, *J* = 16.9, 10.2, 6.6 Hz, 1H), 5.05 (dq, *J* = 17.1, 1.7 Hz, 1H), 4.98 (ddt, *J* = 10.2, 2.2, 1.3 Hz, 1H), 4.04 (t, *J* = 6.3 Hz, 2H), 2.15 (qt, *J* = 6.6, 1.4 Hz, 2H), 1.87 (dq, *J* = 8.4, 6.4 Hz, 2H), 1.62 (dq, *J* = 10.1, 7.5 Hz, 2H). ¹³C NMR (101 MHz, CDCl₃) δ 152.61, 141.21, 138.46, 133.31, 123.46, 119.61, 115.08, 69.26, 33.41, 28.44, 25.31. HRMS (+APCI) calculated for C₁₁H₁₅ONBr [M+H]⁺ 256.03315, found 256.03311



hex-5-en-1-yl (tert-butoxycarbonyl)-L-phenylalaninate (S37): In a 24 mL reaction vial equipped with a stir bar under an N_2 atmosphere, hex-5-en-1-ol (0.42 mL, 3.5 mmol, 1.0 equiv.) was added to a solution of (tert-butoxycarbonyl)-L-phenylalanine (1.0 g, 3.8 mmol, 1.1 equiv.) and DMAP (0.06 g, 0.5 mmol, 0.14 equiv.) in CH_2Cl_2 (15 mL). After stirring for five minutes EDCI (0.81 g, 4.3 mmol, 1.2 equiv.) was added and the reaction stirred at room temperature for five hours until complete consumption of the starting material was observed via TLC. The reaction was diluted with EtOAc and washed with 1M HCl, sat. NaHCO_3 , and brine. The organic layer was dried over anhydrous Na_2SO_4 and the solvent removed under reduced pressure to give **S37** as colorless oil that did not require further purification. (1.21 g, 99% yield.). $^1\text{H NMR}$ (400 MHz, CDCl_3) δ 7.33 – 7.20 (m, 3H), 7.13 (d, $J = 6.6$ Hz, 2H), 5.77 (ddt, $J = 16.9, 10.2, 6.7$ Hz, 1H), 5.09 – 4.88 (m, 3H), 4.57 (q, $J = 6.1$ Hz, 1H), 4.09 (td, $J = 6.7, 2.5$ Hz, 2H), 3.08 (t, $J = 6.0$ Hz, 2H), 2.05 (q, $J = 7.3$ Hz, 2H), 1.69 – 1.52 (m, 2H), 1.45 – 1.34 (m, 11H). $^{13}\text{C NMR}$ (101 MHz, CDCl_3) δ 172.11, 155.20, 138.33, 136.21, 129.46, 128.64, 127.12, 115.07, 79.99, 65.40, 54.60, 38.60, 33.35, 28.44, 28.01, 25.18. **HRMS** (+APCI) calculated for $\text{C}_{20}\text{H}_{30}\text{O}_4\text{N}$ $[\text{M}+\text{H}]^+$ 348.21693, found 348.21711. $[\alpha]_{\text{D}}^{22} +28.2^\circ$ ($c = 7.3$, CHCl_3)

Synthetic sequence for *(S)*-(((3-methylhept-6-en-1-yl)oxy)methyl)benzene (**S41**):



(S)-(((3,7-dimethyloct-6-en-1-yl)oxy)methyl)benzene (**S38**)²²:

To a 250 mL round bottom flask equipped with a stir bar NaH (60% wt, 1.8 g, 45 mmol, 1.8 equiv.) was added and the atmosphere exchanged with N₂ 3x followed by the addition of THF (100 mL). The reaction was placed in an ice bath and *(S)*-citronellol (4.6 mL, 25 mmol, 1.0 equiv.) was slowly added. The reaction was stirred in the ice bath for one hour after which BnBr (3.6 mL, 30 mmol, 1.2 equiv.) and TBAI (92 mg, 0.25 mmol, 0.01 equiv.) were added. The reaction was warmed to room temperature and stirred overnight. After which, the reaction was again placed in an ice bath and quenched with sat. NH₄Cl. The reaction was extracted with EtOAc and washed with DI H₂O and sat. brine. The combined organic layers were dried over anhydrous Na₂SO₄ and solvent removed under reduced pressure to obtain **S38** which was used crude in the next reaction.

3-(((*S*)-5-(benzyloxy)-3-methylpentyl)-2,2-dimethyloxirane (**S39**)²³:

A 100 mL round bottom flask equipped with a stir bar and containing solution of **S38** (4.25 g, 17.3 mmol, 1.0 equiv.) in CH₂Cl₂ (60 mL) was placed in an ice bath. Once cooled, mCPBA (77 wt%, 4.34 g, 19 mmol, 1.1 equiv.) was added and the reaction left to stir at room temperature overnight. The reaction was diluted with CH₂Cl₂ and washed with sat. NaHCO₃. The organic layer was dried over Na₂SO₄ and the solvent removed to yield **S39** which was used crude in the next reaction.

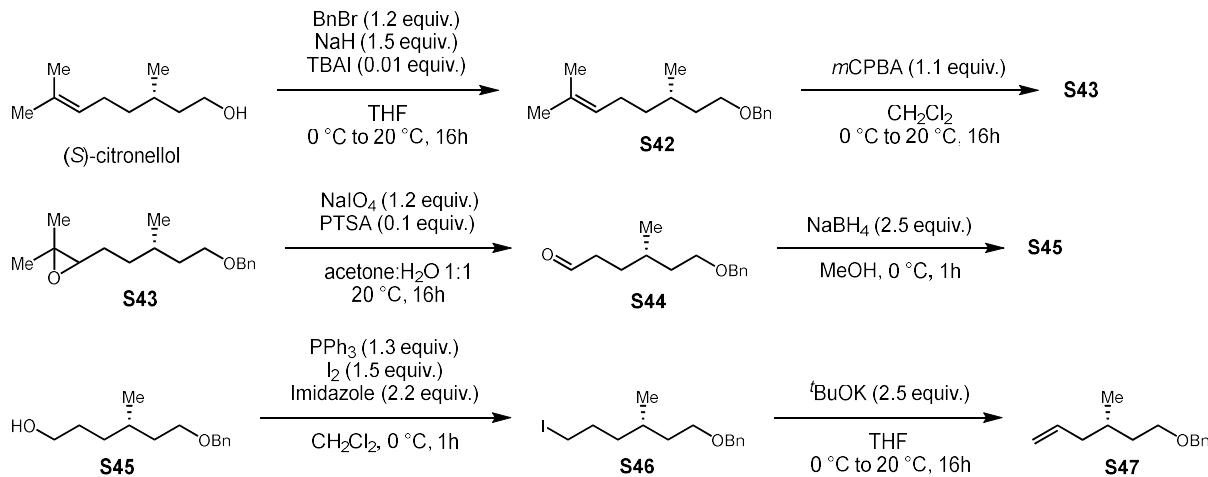
(S)-6-(benzyloxy)-4-methylhexanal (**S40**)²³:

To solution of **S39** (3.94 g, 15.0 mmol, 1.0 equiv.) in acetone (40 mL) in a 250mL round bottom flask equipped with a stir bar was sequentially added NaIO₄ (3.8 g, 18 mmol, 1.2 equiv.), DI H₂O (40 mL), and PTSA (0.328 g, 1.5 mmol, 0.1 equiv.). The reaction mixture was left to stir open to air at room temperature overnight. After which the reaction was filtered to remove the white solid that had formed washing with hexanes. The filtrate was washed with DI H₂O and the organic layer was dried over anhydrous Na₂SO₄. The solvent removed to obtain **S40** which was used without further purification.

(S)-(((3-methylhept-6-en-1-yl)oxy)methyl)benzene (**S41**)²³:

A 250 mL round bottom flask equipped with a stir bar and containing a solution of MePPh₃Br (6.44 g, 18 mmol, 1.2 equiv.) in THF (80 mL) was placed in an ice bath. Once cooled, added KO^tBu (1.93 g, 17 mmol, 1.1 equiv.) and the yellow suspension was stirred in the ice bath for two hours. After which, a solution of **S40** (3.31 g, 15.0 mmol, 1.0 equiv.) in THF (20 mL) was added slowly and continued to be stirred in the ice bath. After an additional two hours the reaction was filtered and the filtrate concentrated under reduced pressure. The crude product was purified by silica gel column chromatography (0-5% EtOAc in hexanes) to yield **S41** as a colorless oil (1.75g, 32% yield over 4 steps). ¹H NMR (400 MHz, CDCl₃) δ 7.38 – 7.26 (m, 5H), 5.81 (ddt, *J* = 16.9, 10.2, 6.6 Hz, 1H), 5.00 (dq, *J* = 17.1, 1.7 Hz, 1H), 4.93 (ddt, *J* = 10.2, 2.3, 1.2 Hz, 1H), 4.51 (s, 2H), 3.51 (ddd, *J* = 9.3, 6.8, 3.0 Hz, 2H), 2.16 – 1.97 (m, 2H), 1.76 – 1.54 (m, 2H), 1.52 – 1.34 (m, 2H), 1.23 (dddd, *J* = 13.4, 9.7, 7.8, 5.8 Hz, 1H), 0.90 (d, *J* = 6.5 Hz, 3H). ¹³C NMR (101 MHz, CDCl₃) δ 139.34, 138.82, 128.49, 127.75, 127.62, 114.27, 73.05, 68.78, 36.82, 36.41, 31.40, 29.59, 19.63. HRMS (+APCI) calculated for C₁₅H₂₃O [M+H]⁺ 219.17434, found 219.17457. [α]_D²² -1.5° (*c* = 2.1, CHCl₃)

Synthetic sequence for *(S)*-(((3-methylhex-5-en-1-yl)oxy)methyl)benzene (**S47**):



(S)-(((3,7-dimethyloct-6-en-1-yl)oxy)methyl)benzene (**S42**)²²:

To a 250 mL round bottom flask equipped with a stir bar NaH (60% wt, 2.1 g, 53 mmol, 2.1 equiv.) was added and the atmosphere exchanged with N₂ 3x followed by the addition of THF (100 mL). The reaction was placed in an ice bath and *(S)*-citronellol (4.6 mL, 25 mmol, 1.0 equiv.) was slowly added. The reaction was stirred in the ice bath for one hour after which BnBr (3.4 mL, 29 mmol, 1.1 equiv.) and TBAI (105 mg, 0.28 mmol, 0.01 equiv.) were added. The reaction was warmed to room temperature and stirred overnight. After which, the reaction was again placed in an ice bath and quenched with sat. NH₄Cl. The reaction was extracted with EtOAc and washed with DI H₂O and sat. brine. The combined organic layers were dried over anhydrous Na₂SO₄ and solvent removed under reduced pressure to obtain **S42** which was used crude in the next reaction.

3-(((*S*)-5-(benzyloxy)-3-methylpentyl)-2,2-dimethyloxirane (**S43**)²³:

A 100 mL round bottom flask equipped with a stir bar and containing solution of **S42** (4.89 g, 19.8 mmol, 1.0 equiv.) in CH₂Cl₂ (60 mL) was placed in an ice bath. Once cooled, mCPBA (77 wt%, 4.96 g, 22 mmol, 1.1 equiv.) was added and the reaction left to stir at room temperature overnight. The reaction was diluted with CH₂Cl₂ and washed with sat. NaHCO₃. The organic layer was dried over Na₂SO₄ and the solvent removed to yield **S43** which was used crude in the next reaction.

(S)-6-(benzyloxy)-4-methylhexanal (**S44**)²³:

To solution of **S43** (5.21 g, 19.8 mmol, 1.0 equiv.) in acetone (60 mL) in a 250mL round bottom flask equipped with a stir bar was sequentially added NaIO₄ (5.1 g, 23 mmol, 1.2 equiv.), DI H₂O (60 mL), and PTSA (0.38 g, 2.0 mmol, 0.1 equiv.). The reaction mixture was left to stir open to air at room temperature overnight. After which the reaction was filtered to remove the white solid that had formed washing with hexanes. The filtrate was washed with DI H₂O and the organic layer was dried over anhydrous Na₂SO₄. The solvent removed to obtain **S44** which was used without further purification.

(S)-6-(benzyloxy)-4-methylhexan-1-ol (**S45**)²⁴:

A 250 mL round bottom flask equipped with a stir bar and containing a solution of **S44** (4.37 g, 19.8 mmol, 1.0 equiv.) in MeOH (100 mL) was placed in an ice bath. Once cooled, NaBH₄ (1.87 g, 49 mmol, 2.5 equiv.) was slowly added, and the reaction was left to stir in the ice bath for one hour. The solvent was removed under reduced pressure and the remaining residue redissolved in EtOAc before being sequentially washed with DI H₂O and sat. brine. The organic layer was dried over anhydrous Na₂SO₄ and the solvent removed under reduced pressure to yield **S45** which was sufficiently clean to use in the next step without further purification.

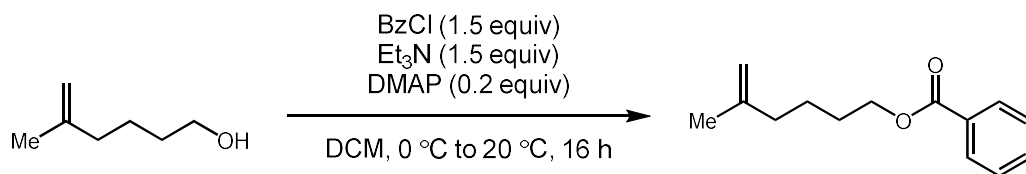
(S)-(((6-iodo-3-methylhexyl)oxy)methyl)benzene (**S46**)²⁴:

To 100 mL three neck round bottom flask equipped with a stir bar imidazole (1.84 g, 27 mmol, 2.0 equiv.) and PPh₃ (4.51 g, 17 mmol, 1.3 equiv.) were added. The atmosphere was exchanged with N₂ three times and a solution of **S45** (3.0 mL, 13.5 mmol, 1.0 equiv.) in CH₂Cl₂ (60mL) was added. The reaction vessel was placed in an ice bath and I₂ crystals (4.46 g, 17 mmol, 1.3 equiv.) were added in small portions. The reaction was left to stir in the ice bath for one hour before being quenched with sat. Na₂S₂O₃ (20mL). The biphasic reaction was extracted with CH₂Cl₂, and the combines organic layers washed with sat. brine. The organic layer was dried over anhydrous MgSO₄ and the solvent removed under reduced pressure. Hexanes was added to the crude residue and the resulting solid was filtered off using short silica plug

flushing with more 5% EtOAc in hexanes. The solvent was removed from the filtrate to yield **S46** which was immediately used crude in the next step.

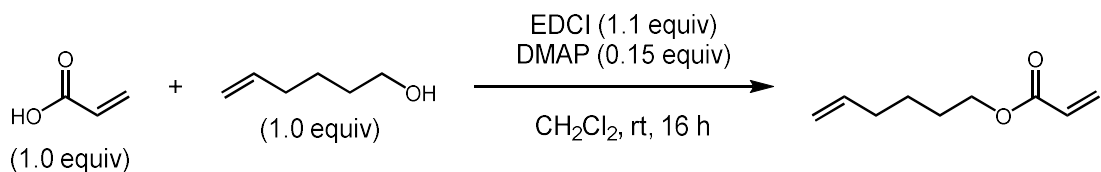
*(S)-(((3-methylhex-5-en-1-yl)oxy)methyl)benzene (S47)*²⁵:

A 100 mL two neck round bottom flask containing **S46** (4.49 g, 13.5 mmol, 1.0 equiv.) in THF (50mL) was placed in an ice bath. To the reaction, KO^tBu (3.89 g, 34 mmol, 2.5 equiv.) was slowly added forming a white suspension. The reaction was removed from the ice bath and left to stir at room temperature overnight. The reaction was quenched using sat. NH₄Cl and extracted three times with Et₂O. The combined organic layers were then washed with sat. Na₂S₂O₃ and sat. brine. The organic layer was dried over anhydrous MgSO₄ the solvent removed under reduced pressure. The crude product was purified by silica gel column chromatography (5% EtOAc in hexanes) to yield **S47** as a colorless oil (2.715 g, 54% yield over 6 steps). ¹H NMR (400 MHz, CDCl₃) δ 7.39 – 7.32 (m, 4H), 7.32 – 7.26 (m, 1H), 5.78 (ddt, *J* = 16.2, 11.2, 7.1 Hz, 1H), 5.01 (ddt, *J* = 5.1, 2.3, 1.3 Hz, 1H), 4.98 (t, *J* = 1.3 Hz, 1H), 4.51 (d, *J* = 0.8 Hz, 2H), 3.51 (ddd, *J* = 9.3, 6.7, 3.0 Hz, 2H), 2.09 (dddt, *J* = 13.8, 6.8, 5.4, 1.3 Hz, 1H), 1.92 (dtt, *J* = 13.8, 7.3, 1.2 Hz, 1H), 1.76 – 1.62 (m, 2H), 1.50 – 1.36 (m, 1H), 0.90 (d, *J* = 6.5 Hz, 3H). ¹³C NMR (101 MHz, CDCl₃) δ 138.79, 137.41, 128.49, 127.75, 127.62, 115.97, 73.04, 68.69, 41.57, 36.38, 29.91, 19.56. HRMS (+APCI) calculated for C₁₄H₂₁O [M+H]⁺ 205.15869, found 205.15888. [α]_D²² +2.6° (*c* = 3.6, CHCl₃)

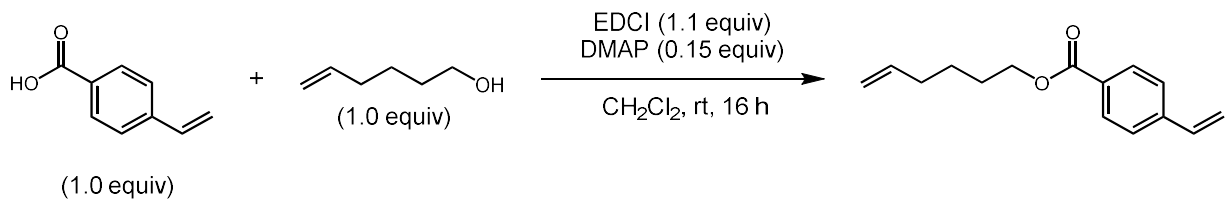


5-methylhex-5-en-1-yl benzoate (S48): To a solution of 5-methylhex-5-en-1-ol (0.68 mL, 5.0 mmol, 1.0 equiv) and DMAP (0.130 g, 1.0 mmol, 0.2 equiv.) in DCM (10 mL) was added Et₃N (1.0 mL, 7.5 mmol, 1.5 equiv.). The reaction was placed in an ice bath and BzCl (0.87 mL, 7.5 mmol, 1.5 equiv.) was added dropwise at 0 °C. The reaction was allowed to warm to room temperature and stirred for 16 hours. The reaction was quenched with the addition of DI H₂O and the layers were separated followed by extraction

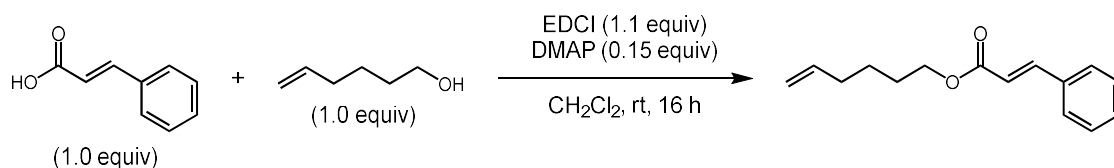
of the aqueous phase with DCM three times. The combined organic layers were dried over MgSO₄ and the solvent was removed under reduced pressure. The crude product was purified using silica gel column chromatography (0-2% EtOAc in Hexanes) to obtain **S48** as a colorless oil (1.062 g, 97%). ¹H NMR (400 MHz, CDCl₃) δ 8.09 – 8.00 (m, 2H), 7.60 – 7.52 (m, 1H), 7.48 – 7.39 (m, 2H), 4.76 – 4.71 (m, 1H), 4.71 – 4.66 (m, 1H), 4.33 (t, J = 6.6 Hz, 2H), 2.09 (t, J = 7.5 Hz, 2H), 1.83 – 1.74 (m, 2H), 1.73 (s, 3H), 1.66 – 1.54 (m, 2H). ¹³C NMR (101 MHz, CDCl₃) δ 166.82, 145.56, 132.97, 130.59, 129.67, 128.47, 110.37, 65.07, 37.45, 28.43, 24.06, 22.44. HRMS (+APCI) calculated for C₁₄H₁₉O₂ [M+H]⁺ 219.13796, found 219.13805.



hex-5-en-1-yl acrylate (S49): In a 24 mL reaction vial equipped with a stir bar under an N₂ atmosphere, hex-5-en-1-ol (0.60 mL, 5.0 mmol, 1.0 equiv.) was added to a solution of acrylic acid (0.35 mL, 5.1 mmol, 1.0 equiv.) and DMAP (0.08 g, 0.7 mmol, 0.12 equiv.) in CH₂Cl₂ (15 mL). After stirring for five minutes EDCI (1.17 g, 6.0 mmol, 1.2 equiv.) was added and the reaction stirred at room temperature overnight until complete consumption of the starting material was observed via TLC. The reaction was diluted with CH₂Cl₂ and washed with 1M HCl, sat. NaHCO₃, DI H₂O, and brine. The organic layer was dried over anhydrous Na₂SO₄ and the solvent removed under reduced pressure. The crude product was purified using silica gel column chromatography (10% EtOAc in Hexanes) to obtain **S49** as a colorless oil (0.250 g, 32 % yield) ¹H NMR (400 MHz, CDCl₃) δ 6.39 (dd, J = 17.4, 1.5 Hz, 1H), 6.11 (dd, J = 17.3, 10.4 Hz, 1H), 5.86 – 5.72 (m, 2H), 5.01 (dq, J = 17.1, 1.7 Hz, 1H), 4.96 (ddt, J = 10.2, 2.2, 1.2 Hz, 1H), 4.15 (t, J = 6.6 Hz, 2H), 2.09 (tdt, J = 7.8, 6.7, 1.4 Hz, 2H), 1.75 – 1.62 (m, 2H), 1.53 – 1.40 (m, 2H). ¹³C NMR (101 MHz, CDCl₃) δ 166.44, 138.46, 130.66, 128.70, 114.97, 64.59, 33.41, 28.16, 25.31. HRMS (+APCI) calculated for C₉H₁₅O₂ [M+H]⁺ 155.10666, found 155.1069.



hex-5-en-1-yl 4-vinylbenzoate (**S50**): In a 24 mL reaction vial equipped with a stir bar under an N₂ atmosphere, hex-5-en-1-ol (0.60 mL, 5.0 mmol, 1.0 equiv.) was added to a solution of 4-vinylbenzoic acid (0.76 g, 5.1 mmol, 1.0 equiv.) and DMAP (0.08 g, 0.7 mmol, 0.15 equiv.) in CH₂Cl₂ (15 mL). After stirring for five minutes EDCI (1.10 g, 5.8 mmol, 1.2 equiv.) was added and the reaction stirred at room temperature overnight until complete consumption of the starting material was observed via TLC. The reaction was diluted with CH₂Cl₂ and washed with 1M HCl, sat. NaHCO₃, DI H₂O, and brine. The organic layer was dried over anhydrous Na₂SO₄ and the solvent removed under reduced pressure. The crude product was purified using silica gel column chromatography (10% EtOAc in Hexanes) to obtain **S50** as a colorless oil (0.722g, 67 % yield) ¹H NMR (400 MHz, CDCl₃) δ 8.00 (d, *J* = 8.4 Hz, 2H), 7.46 (d, *J* = 8.1 Hz, 2H), 6.75 (dd, *J* = 17.6, 10.9 Hz, 1H), 5.91 – 5.75 (m, 2H), 5.38 (dd, *J* = 10.9, 0.7 Hz, 1H), 5.04 (dq, *J* = 17.1, 1.6 Hz, 1H), 4.98 (ddt, *J* = 10.2, 2.2, 1.2 Hz, 1H), 4.32 (t, *J* = 6.6 Hz, 2H), 2.13 (tdt, *J* = 7.8, 6.7, 1.4 Hz, 2H), 1.85 – 1.73 (m, 2H), 1.62 – 1.49 (m, 2H). ¹³C NMR (101 MHz, CDCl₃) δ 166.56, 141.96, 138.50, 136.16, 129.98, 129.69, 126.21, 116.56, 115.02, 65.00, 33.46, 28.30, 25.44. HRMS (+APCI) calculated for C₁₅H₁₉O₂ [M+H]⁺ 231.13796, found 231.13813.



hex-5-en-1-yl cinnamate (**S51**): In a 24 mL reaction vial equipped with a stir bar under an N₂ atmosphere, hex-5-en-1-ol (0.60 mL, 5.0 mmol, 1.0 equiv.) was added to a solution of *trans*-cinnamic acid (0.79 g, 5.3 mmol, 1.1 equiv.) and DMAP (0.07 g, 0.7 mmol, 0.12equiv.) in CH₂Cl₂ (15 mL). After stirring for five minutes EDCI (1.18 g, 6.0 mmol, 1.2 equiv.) was added and the reaction stirred at room temperature overnight until complete consumption of the starting material was observed via TLC. The reaction was

diluted with CH₂Cl₂ and washed with 1M HCl, sat. NaHCO₃, DI H₂O, and brine. The organic layer was dried over anhydrous Na₂SO₄ and the solvent removed under reduced pressure. The crude product was purified using silica gel column chromatography (10% EtOAc in Hexanes) to obtain **S51** as a colorless oil (0.766 g, 66 % yield) ¹H NMR (400 MHz, CDCl₃) δ 7.57 (d, *J* = 16.0 Hz, 1H), 7.46 – 7.37 (m, 2H), 7.31 – 7.23 (m, 3H), 6.33 (d, *J* = 16.0 Hz, 1H), 5.70 (ddt, *J* = 16.9, 10.2, 6.7 Hz, 1H), 4.92 (dq, *J* = 17.1, 1.7 Hz, 1H), 4.86 (ddt, *J* = 10.2, 2.3, 1.2 Hz, 1H), 4.10 (t, *J* = 6.6 Hz, 2H), 2.00 (tdt, *J* = 7.7, 6.6, 1.4 Hz, 2H), 1.67 – 1.55 (m, 2H), 1.46 – 1.34 (m, 2H). ¹³C NMR (101 MHz, CDCl₃) δ 167.20, 144.75, 138.50, 134.56, 130.36, 129.00, 128.18, 118.33, 114.98, 64.61, 33.45, 28.28, 25.36. HRMS (+APCI) calculated for C₁₅H₁₉O₂ [M+H]⁺ 231.13796, found 231.13814.

Enantioselective Aziridination Procedures

General Procedure F: Optimization of Enantioselective Aziridination using **1-nonene (2.78)**

An oven-dried 4 dram reaction vial, with Teflon tape wrapped threads, and equipped with an oven dried stir bar was brought into the glovebox. The nitrogen source **2.74** (0.13 mmol, 1.3 equiv.), base, silver salt additive and catalyst (2.5 mol%) were added to the reaction vial. The vial was sealed with a Teflon septum screw cap and brought out of the box to complete the reaction. Under an N₂ atmosphere, HFIP (1.0 mL, 0.1M) was added directly to the reaction vial followed by 1-nonene **2.78** (17.0 μL, 0.10 mmol, 1.0 equiv.) using a micro syringe. The reaction was left to stir at the indicated temperature under a N₂ balloon for the indicated time. After which, the crude reaction was filtered through a Celite pipette plug using DCM. The solvent was removed under reduced pressure and a crude NMR sample was prepared using dibromomethane as an internal standard. The crude material purified via preparative TLC (5% EtOAc in hexanes) to yield the corresponding aziridine product which was analyzed via chiral HPLC (AD-H column 3% 2-propanol in hexanes, 1.0 mL/min) to determine the enantiomeric ratio.

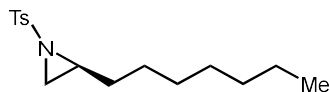
General Procedure G: Aziridination Procedure for substrates with known densities.

An oven-dried 4dram reaction vial, with Teflon tape wrapped threads, and equipped with an oven dried stir bar was brought into the glovebox. The nitrogen source **2.74** (0.13 mmol, 1.3 equiv.), CsOAc (0.01mmol, 0.1 equiv.), AgSbF₆ (0.30 mmol, 0.3 equiv.), and **2.55** (2.5 mol%) were added to the reaction vial. The vial was sealed with a Teflon septum screw cap and brought out of the box to complete the reaction. Under an N₂ atmosphere, HFIP (1.0 mL, 0.1M) was added directly to the reaction vial followed by the olefin (0.10 mmol, 1.0 equiv.) using a micro syringe. The reaction was left to stir at room temperature under a N₂ balloon for 24 hours. After 24 hours the crude reaction was filtered through a Celite pipette plug using DCM to flush. The solvent was removed under reduced pressure and the crude material purified via preparative TLC using the indicated eluent to yield the corresponding aziridine product.

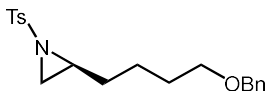
General Procedure H: Aziridination Procedure for substrates with unknown densities.

An oven-dried 4dram reaction vial, with Teflon tape wrapped threads, and equipped with an oven dried stir bar was brought into the glovebox. The nitrogen source **2.74** (0.13 mmol, 1.3 equiv.), CsOAc (0.01mmol, 0.1 equiv.), AgSbF₆ (0.30 mmol, 0.3 equiv.), and **2.55** (2.5 mol%) were added to the reaction vial. The vial was sealed with a Teflon septum screw cap and brought out of the box to complete the reaction. The olefin (0.10 mmol 1.0 equiv.) was added as a stock solution in HFIP (1.0 mL, 0.1M) and the reaction was left to stir at room temperature under a N₂ balloon for 24 hours. After 24 hours the crude reaction was filtered through a Celite pipette plug using DCM to flush. The solvent was removed under reduced pressure and the crude material purified via preparative TLC using the indicated eluent to yield the corresponding aziridine product.

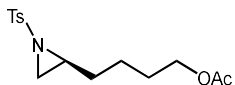
All racemic reactions were conducted using [Ind*RhCl₂]₂ as the catalyst using either **General Procedure G** or **H**.



(*S*)-2-heptyl-1-tosylaziridine (**2.79**): Prepared using **General Procedure H** using 1-nonene (**2.78**) and (*R,R*)-**2.55**. Purified via preparative TLC using (5% EtOAc in Hexanes) to provide **4** (0.0245 g, 83% yield, 95:5 e.r.) as colorless oil. $^1\text{H NMR}$ (600 MHz, CDCl_3) δ 7.82 (d, $J = 8.2$ Hz, 2H), 7.33 (d, $J = 8.2$ Hz, 2H), 2.71 (tt, $J = 7.5, 4.8$ Hz, 1H), 2.64 (d, $J = 7.0$ Hz, 1H), 2.44 (s, 3H), 2.05 (d, $J = 4.6$ Hz, 1H), 1.53 (ddd, $J = 9.6, 6.6, 3.4$ Hz, 1H), 1.36 – 1.09 (m, 12H), 0.86 (t, $J = 7.3$ Hz, 3H). $^{13}\text{C NMR}$ (151 MHz, CDCl_3) δ 144.53, 135.36, 129.74, 128.13, 40.64, 33.91, 31.76, 29.20, 29.11, 26.89, 22.74, 21.75, 14.20. **HRMS** (+APCI) calculated for $\text{C}_{16}\text{H}_{26}\text{O}_2\text{NS}$ $[\text{M}+\text{H}]^+$ 296.16788, found 296.16864. **HPLC** (AD-H column 3% 2-propanol in hexanes, 1.0 mL/min) $t_{\text{M}} = 11.9$ min $t_{\text{m}} = 10.5$ min, 95:5 e.r.

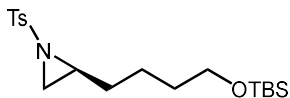


(*S*)-2-(4-(benzyloxy)butyl)-1-tosylaziridine (**2.109**): Prepared using **General Procedure H** using **S9** and (*R,R*)-**2.55**. Purified via preparative TLC using (20% EtOAc in Hexanes) to provide **2.109** (0.0218 g, 61% yield, 95:5 e.r.) as colorless oil. $^1\text{H NMR}$ (600 MHz, CDCl_3) δ 7.82 (d, $J = 8.3$ Hz, 2H), 7.38 – 7.27 (m, 7H), 4.46 (s, 2H), 3.38 (t, $J = 6.4$ Hz, 2H), 2.73 (tt, $J = 7.0, 4.8$ Hz, 1H), 2.62 (d, $J = 6.9$ Hz, 1H), 2.42 (s, 3H), 2.05 (d, $J = 4.6$ Hz, 1H), 1.65 – 1.48 (m, 4H), 1.43 – 1.31 (m, 3H). $^{13}\text{C NMR}$ (151 MHz, CDCl_3) δ 144.55, 138.64, 135.29, 129.76, 128.51, 128.11, 127.73, 73.04, 70.05, 40.34, 33.92, 31.21, 29.26, 23.64, 21.75. **HRMS** (+APCI) calculated for $\text{C}_{20}\text{H}_{26}\text{O}_3\text{N}^{\text{32}}\text{S}$ $[\text{M}+\text{H}]^+$ 360.16279, found 360.16254. **HPLC** (AD-H column 5% 2-propanol in hexanes, 1.0 mL/min) $t_{\text{M}} = 22.2$ min $t_{\text{m}} = 18.7$ min, 95:5 e.r.

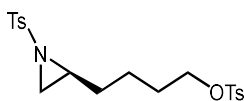


(*S*)-4-(1-tosylaziridin-2-yl)butyl acetate (**2.110**): Prepared using **General Procedure H** using **S10** and (*R,R*)-**2.55**. Purified via preparative TLC using (20% EtOAc in Hexanes) to provide **2.110** (0.0240 g, 77% yield, 95:5 e.r.) as colorless oil. $^1\text{H NMR}$ (400 MHz, CDCl_3) δ 7.82 (d, $J = 8.3$ Hz, 2H), 7.38 – 7.30 (m,

2H), 3.95 (t, $J = 6.6$ Hz, 2H), 2.73 (tt, $J = 7.1, 4.5$ Hz, 1H), 2.63 (d, $J = 7.0$ Hz, 1H), 2.44 (s, 3H), 2.06 (d, $J = 4.6$ Hz, 1H), 2.03 (s, 3H), 1.68 – 1.48 (m, 3H), 1.38 – 1.27 (m, 3H). ^{13}C NMR (101 MHz, CDCl_3) δ 171.24, 144.69, 135.15, 129.78, 128.11, 64.17, 40.10, 33.92, 30.98, 28.05, 23.40, 21.77, 21.10. **HRMS** (+APCI) calculated for $\text{C}_{15}\text{H}_{22}\text{O}_4\text{NS}$ $[\text{M}+\text{H}]^+$ 312.12641, found 312.12625. **HPLC** (AD-H column 8% 2-propanol in hexanes, 1.0 mL/min) $t_{\text{M}} = 15.1$ min $t_{\text{m}} = 13.4$ min, 95:5 e.r.

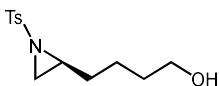


(S)-2-(4-((*tert*-butyldimethylsilyl)oxy)butyl)-1-tosylaziridine (**2.111**): Prepared using **General Procedure H** using **S11** and (*R,R*)-**2.55**. Purified via preparative TLC using (20% EtOAc in Pentane) to provide **2.111** (0.0181 g, 47% yield, 95:5 e.r.) as colorless oil. ^1H NMR (600 MHz, CDCl_3) δ 7.82 (d, $J = 8.3$ Hz, 2H), 7.33 (dd, $J = 8.6, 0.7$ Hz, 2H), 3.51 (t, $J = 6.4$ Hz, 2H), 2.77 – 2.67 (m, 1H), 2.63 (d, $J = 7.0$ Hz, 1H), 2.44 (s, 3H), 2.06 (d, $J = 4.6$ Hz, 1H), 1.61 – 1.52 (m, 1H), 1.49 – 1.42 (m, 2H), 1.41 – 1.34 (m, 1H), 1.34 – 1.27 (m, 2H), 0.88 (s, 10H), 0.02 (s, 6H). ^{13}C NMR (151 MHz, CDCl_3) δ 144.53, 135.36, 129.77, 128.12, 62.86, 40.47, 33.91, 32.27, 31.22, 26.09, 23.23, 21.77, 18.47, -5.18. **HRMS** (+APCI) calculated for $\text{C}_{19}\text{H}_{34}\text{O}_3\text{NSSi}$ $[\text{M}+\text{H}]^+$ 384.20232, found 384.2021. **HPLC** (OJ-H column 5% 2-propanol in hexanes, 1.0 mL/min) $t_{\text{M}} = 6.0$ min $t_{\text{m}} = 8.8$ min, 95:5 e.r.

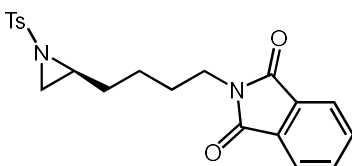


(S)-4-(1-tosylaziridin-2-yl)butyl 4-methylbenzenesulfonate (**2.112**): Prepared using **General Procedure H** using **S12** and (*R,R*)-**2.55**. Purified via preparative TLC using (60% EtOAc in Hexanes) to provide **2.112** (0.0087 g, 21% yield, 95:5 e.r.) as colorless oil. ^1H NMR (400 MHz, CDCl_3) δ 7.80 (d, $J = 8.3$ Hz, 2H), 7.77 (d, $J = 8.3$ Hz, 2H), 7.38 – 7.30 (m, 4H), 3.92 (t, $J = 6.3$ Hz, 2H), 2.67 (tt, $J = 7.0, 4.5$ Hz, 1H), 2.59 (d, $J = 7.0$ Hz, 1H), 2.45 (s, 6H), 2.02 (d, $J = 4.5$ Hz, 1H), 1.66 – 1.52 (m, 4H), 1.37 – 1.20 (m, 4H). ^{13}C NMR (101 MHz, CDCl_3) δ 144.94, 144.82, 135.08, 133.18, 130.02, 129.86, 128.11, 128.00, 70.16, 39.81, 33.85, 30.67, 28.25, 22.95, 21.79. **HRMS** (+APCI) calculated for $\text{C}_{20}\text{H}_{26}\text{O}_5\text{NS}_2$ $[\text{M}+\text{H}]^+$ 424.12469, found

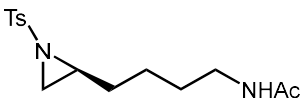
424.12426. **HPLC** (IA column 30% 2-propanol in hexanes, 1.0 mL/min) $t_M = 14.5$ min $t_m = 13.5$ min, 95:5 e.r



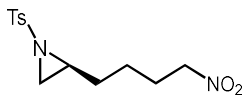
(*S*)-4-(1-tosylaziridin-2-yl)butan-1-ol (**2.113**): Prepared using **General Procedure G** using hex-5-en-1-ol and (*R,R*)-**2.55**. Purified via preparative TLC using (60% EtOAc in Hexanes) to provide **2.113** (0.0132 g, 49% yield, 95:5 e.r.) as colorless oil. **¹H NMR** (400 MHz, CDCl₃) δ 7.82 (d, $J = 8.3$ Hz, 2H), 7.34 (dd, $J = 8.6, 0.8$ Hz, 2H), 3.56 (td, $J = 6.4, 5.0$ Hz, 2H), 2.75 (tt, $J = 7.0, 4.6$ Hz, 1H), 2.62 (d, $J = 7.0$ Hz, 1H), 2.44 (s, 3H), 2.06 (d, $J = 4.6$ Hz, 1H), 1.68 – 1.57 (m, 1H), 1.57 – 1.47 (m, 2H), 1.39 – 1.33 (m, 3H). **¹³C NMR** (101 MHz, CDCl₃) δ 144.68, 135.16, 129.80, 128.14, 62.66, 40.23, 34.04, 32.05, 31.09, 23.19, 21.78. **HRMS** (+APCI) calculated for C₁₃H₂₀O₃NS [M+H]⁺ 270.11584, found 270.11587. (IK column 30% 2-propanol in hexanes, 1.0 mL/min) $t_M = 16.5$ min $t_m = 19.3$ min, 95:5 e.r.



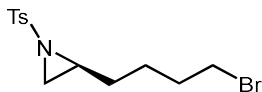
(*S*)-2-(4-(1-tosylaziridin-2-yl)butyl)isoindoline-1,3-dione (**2.114**): Prepared using **General Procedure H** using **S14** and (*R,R*)-**2.55**. Purified via preparative TLC using (20% EtOAc in Hexanes) to provide **2.115** (0.0209 g, 52% yield, 94:6 e.r.) as colorless oil. **¹H NMR** (400 MHz, CDCl₃) δ 7.87 – 7.78 (m, 4H), 7.71 (dd, $J = 5.5, 3.0$ Hz, 2H), 7.34 (s, 2H), 3.63 – 3.54 (m, 2H), 2.71 (tt, $J = 7.2, 4.7$ Hz, 1H), 2.63 (d, $J = 6.9$ Hz, 1H), 2.44 (s, 3H), 2.07 (d, $J = 4.5$ Hz, 1H), 1.69 – 1.54 (m, 3H), 1.44 – 1.18 (m, 4H). **¹³C NMR** (101 MHz, CDCl₃) δ 168.49, 144.65, 135.17, 134.08, 132.20, 129.82, 128.11, 123.34, 40.15, 37.60, 33.83, 30.82, 28.05, 24.06, 21.79. **HRMS** (+APCI) calculated for C₂₁H₂₃O₄N₂S [M+H]⁺ 399.1373, found 399.13749 **HPLC** (IA column 35% 2-propanol in hexanes, 1.0 mL/min) $t_M = 15.0$ min $t_m = 12.6$ min, 94:6 e.r.



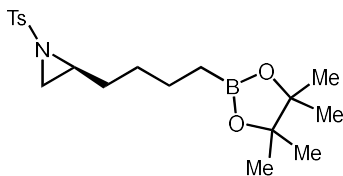
(S)-*N*-(4-(1-tosylaziridin-2-yl)butyl)acetamide (**2.115**): Prepared using **General Procedure H** using **S15** and **(R,R)**-**2.55**. Purified via preparative TLC using (100% EtOAc) to provide **2.115** (0.0221 g, 71% yield, 94:6 e.r.) as colorless oil. **¹H NMR** (400 MHz, CDCl₃) δ 7.80 (d, *J* = 8.4 Hz, 2H), 7.34 (d, *J* = 8.1 Hz, 2H), 5.70 (s, 1H), 3.17 (hept, *J* = 6.6 Hz, 2H), 2.81 – 2.69 (m, 1H), 2.57 (d, *J* = 7.0 Hz, 1H), 2.44 (s, 3H), 2.05 (d, *J* = 4.6 Hz, 1H), 1.96 (d, *J* = 0.9 Hz, 3H), 1.73 – 1.61 (m, 1H), 1.56 – 1.45 (m, 2H), 1.43 – 1.20 (m, 4H). **¹³C NMR** (101 MHz, CDCl₃) δ 170.35, 144.77, 135.03, 129.84, 128.09, 39.87, 39.40, 34.33, 30.75, 28.62, 24.31, 23.39, 21.78. **HRMS** (+APCI) calculated for C₁₅H₂₃O₃N₂S [M+H]⁺ 311.14239, found 311.14236. **HPLC** (IH column 30% acetonitrile in H₂O, 0.75 mL/min) *t*_M = 20.5 min *t*_m = 18.0 min, 94:6 e.r.



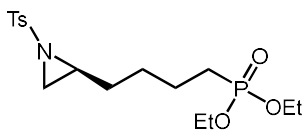
(S)-2-(4-nitrobutyl)-1-tosylaziridine (**2.116**): Prepared using **General Procedure H** using **S16** and **(R,R)**-**2.55**. Purified via preparative TLC using (40% EtOAc in Hexanes) to provide **2.116** (0.0261 g, 88% yield, 94:6 e.r.) as colorless oil. **¹H NMR** (400 MHz, CDCl₃) δ 7.81 (d, *J* = 8.3 Hz, 2H), 7.35 (d, *J* = 7.8 Hz, 2H), 4.28 (td, *J* = 6.9, 2.3 Hz, 2H), 2.71 (ddt, *J* = 8.4, 7.1, 4.3 Hz, 1H), 2.64 (d, *J* = 7.0 Hz, 1H), 2.46 (s, 3H), 2.07 (d, *J* = 4.4 Hz, 1H), 2.01 – 1.89 (m, 2H), 1.78 – 1.65 (m, 1H), 1.40 – 1.22 (m, 3H). **¹³C NMR** (101 MHz, CDCl₃) δ 144.94, 134.93, 129.87, 128.12, 39.57, 33.86, 30.56, 26.60, 23.80, 21.78. **HRMS** (+APCI) calculated for C₁₃H₁₉O₄N₂S [M+H]⁺ 299.10600, found 299.10601 **HPLC** (IB column 40% 2-propanol in hexanes, 1.0 mL/min) *t*_M = 11.8 min *t*_m = 11.2 min, 94:6 e.r.



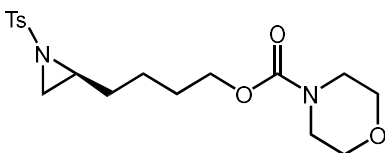
(*S*)-2-(4-bromobutyl)-1-tosylaziridine (**2.117**): Prepared using **General Procedure G** using 6-bromohex-1-ene (**S17**) and (*R,R*)-**2.55**. Purified via preparative TLC using (7:2:1, Hex:EtOAc:Et₃N) to provide **2.117** (0.0196 g, 59% yield, 96:4 e.r.) as colorless oil. ¹H NMR (400 MHz, CDCl₃) δ 7.82 (d, *J* = 8.3 Hz, 2H), 7.35 (d, *J* = 7.8 Hz, 2H), 3.29 (td, *J* = 6.7, 1.6 Hz, 2H), 2.71 (tt, *J* = 7.1, 4.5 Hz, 1H), 2.64 (d, *J* = 7.0 Hz, 1H), 2.45 (s, 3H), 2.07 (d, *J* = 4.5 Hz, 1H), 1.85 – 1.70 (m, 2H), 1.69 – 1.57 (m, 1H), 1.46 – 1.21 (m, 3H). ¹³C NMR (101 MHz, CDCl₃) δ 144.74, 135.14, 129.84, 128.13, 40.04, 33.84, 33.36, 32.01, 30.54, 25.60, 21.79. HRMS (+APCI) calculated for C₁₃H₁₉O₂NBrS [M+H]⁺ 332.03144, found 332.03157. HPLC (IH column 20% 2-propanol in hexanes, 1.0 mL/min) *t*_M = 23.5 min *t*_m = 21.5 min, 96:4 e.r.



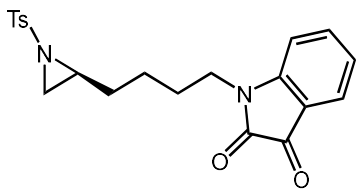
(*S*)-2-(4-(4,4,5,5-tetramethyl-1,3,2-dioxaborolan-2-yl)butyl)-1-tosylaziridine (**2.118**): Prepared using **General Procedure H** using **S18** and (*R,R*)-**2.55**. Purified via preparative TLC using (10% Acetone in Pentane) to provide **2.118** (0.0216 g, 57% yield, 96:4 e.r.) as colorless oil. ¹H NMR (400 MHz, CDCl₃) δ 7.81 (d, *J* = 8.3 Hz, 2H), 7.32 (d, *J* = 7.8 Hz, 2H), 2.71 (tt, *J* = 7.1, 4.9 Hz, 1H), 2.62 (d, *J* = 7.0 Hz, 1H), 2.44 (s, 3H), 2.05 (d, *J* = 4.6 Hz, 1H), 1.58 – 1.44 (m, 1H), 1.41 – 1.27 (m, 3H), 1.23 (s, 14H), 0.66 (t, *J* = 7.8 Hz, 2H). ¹³C NMR (101 MHz, CDCl₃) δ 144.52, 135.37, 129.75, 128.10, 83.08, 40.60, 33.89, 31.18, 29.48, 24.94, 23.62, 21.77. HRMS (+APCI) calculated for C₁₉H₃₁O₄NBS [M+H]⁺ 379.20977, found 379.20968. HPLC (IH column 5% 2-propanol in hexanes, 1.0 mL/min) *t*_M = 18.7 min *t*_m = 16.8 min, 96:4 e.r.



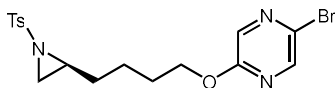
diethyl (S)-4-(1-tosylaziridin-2-yl)butylphosphonate (2.119): Prepared using **General Procedure H** using **S19** and **(R,R)-2.55**. Purified via preparative TLC using (80% EtOAc in Hexanes) to provide **2.119** (0.0259 g, 67%yield, 95:5 e.r.) as colorless oil. $^1\text{H NMR}$ (400 MHz, CDCl_3) δ 7.80 (d, $J = 8.3$ Hz, 2H), 7.33 (d, $J = 8.3$ Hz, 2H), 4.15 – 3.98 (m, 4H), 2.71 (tt, $J = 6.7, 4.9$ Hz, 1H), 2.60 (d, $J = 6.9$ Hz, 1H), 2.43 (s, 3H), 2.04 (d, $J = 4.5$ Hz, 1H), 1.70 – 1.48 (m, 5H), 1.40 – 1.25 (m, 9H). $^{13}\text{C NMR}$ (101 MHz, CDCl_3) δ 144.62, 135.17, 129.79, 128.09, 61.60, 61.54, 39.95, 33.97, 30.94, 30.92, 27.93, 27.76, 26.32, 24.91, 22.12, 22.07, 21.75, 16.62, 16.56. $^{31}\text{P NMR}$ (162 MHz, CDCl_3) δ 31.80 (tp, $J = 17.0, 9.0$ Hz). **HRMS** (+APCI) calculated for $\text{C}_{17}\text{H}_{29}\text{O}_5\text{NPS}$ $[\text{M}+\text{H}]^+$ 390.14986, found 390.14991. **HPLC** (IH column 50% acetonitrile in water, 0.75 mL/min) $t_M = 10.2$ min $t_m = 9.3$ min, 95:5 e.r.



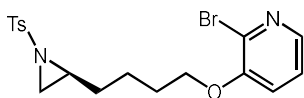
(S)-4-(1-tosylaziridin-2-yl)butyl morpholine-4-carboxylate (2.120): Prepared using **General Procedure H** using **S33** and **(R,R)-2.55**. Purified via preparative TLC using (50% EtOAc in Hexanes) to provide **2.120** (0.0236 g, 62%yield, 94:6 e.r.) as colorless oil. $^1\text{H NMR}$ (400 MHz, CDCl_3) δ 7.81 (d, $J = 8.3$ Hz, 2H), 7.33 (d, $J = 8.1$ Hz, 2H), 3.99 (t, $J = 6.6$ Hz, 2H), 3.64 (d, $J = 4.7$ Hz, 4H), 3.45 (d, $J = 4.9$ Hz, 4H), 2.74 (tt, $J = 6.9, 4.5$ Hz, 1H), 2.61 (d, $J = 7.0$ Hz, 1H), 2.44 (s, 3H), 2.05 (d, $J = 4.6$ Hz, 1H), 1.68 – 1.53 (m, 3H), 1.41 – 1.29 (m, 3H). $^{13}\text{C NMR}$ (101 MHz, CDCl_3) δ 155.47, 144.60, 135.06, 129.69, 127.99, 66.61, 65.14, 39.91, 33.94, 30.90, 28.35, 23.31, 21.68. **HRMS** (+APCI) calculated for $\text{C}_{18}\text{H}_{27}\text{O}_5\text{N}_2\text{S}$ $[\text{M}+\text{H}]^+$ 383.16352, found 383.16338. **HPLC** (IH column 50% 2-propanol in hexanes, 1.0 mL/min) $t_M = 17.8$ min $t_m = 15.4$ min, 94:6 e.r.



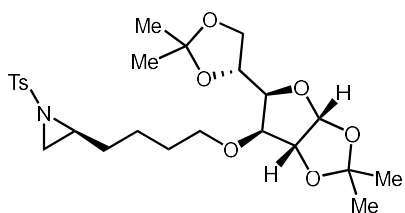
(*S*)-1-(4-(1-tosylaziridin-2-yl)butyl)indoline-2,3-dione (**2.121**): Prepared using **General Procedure H** using **S34** and (*R,R*)-**2.55**. Purified via preparative TLC using (50% EtOAc in Hexanes) to provide **2.121** (0.0310 g, 78 % yield, 93:7 e.r.) as colorless oil. **¹H NMR** (400 MHz, CDCl₃) δ 7.79 (d, *J* = 8.3 Hz, 2H), 7.59 (d, *J* = 7.6 Hz, 2H), 7.33 (d, *J* = 7.8 Hz, 2H), 7.11 (td, *J* = 7.6, 0.8 Hz, 1H), 6.90 (dt, *J* = 7.6, 0.9 Hz, 1H), 3.66 (hept, *J* = 7.2 Hz, 2H), 2.74 (tt, *J* = 7.1, 4.5 Hz, 1H), 2.58 (d, *J* = 6.9 Hz, 1H), 2.44 (s, 3H), 2.05 (d, *J* = 4.6 Hz, 1H), 1.70 (ddd, *J* = 13.2, 9.1, 6.1 Hz, 3H), 1.48 – 1.30 (m, 3H). **¹³C NMR** (101 MHz, CDCl₃) δ 183.63, 158.24, 150.94, 144.78, 138.56, 134.95, 129.85, 128.07, 125.58, 123.83, 117.66, 110.34, 39.96, 39.67, 34.08, 30.75, 26.61, 24.26, 21.78. **HRMS** (+ESI) calculated for C₂₁H₂₃O₄N₂S [M+H]⁺ 399.1373, found 399.13772. **HPLC** (IH column 50% acetonitrile in water, 0.75 mL/min) *t*_M = 21.2 min *t*_m = 19.6 min, 93:7 e.r.



(*S*)-2-bromo-5-(4-(1-tosylaziridin-2-yl)butoxy)pyrazine (**2.122**): Prepared using **General Procedure H** using **S35** and (*R,R*)-**2.55**. Purified via preparative TLC using (7:2:1, Hex:EtOAc:Et₃N) to provide **2.122** (0.0284 g, 67% yield, 95:5 e.r.) as colorless oil. **¹H NMR** (400 MHz, CDCl₃) δ 8.15 (d, *J* = 1.4 Hz, 1H), 7.97 (d, *J* = 1.3 Hz, 1H), 7.82 (d, *J* = 8.3 Hz, 2H), 7.33 (d, *J* = 8.0 Hz, 2H), 4.18 (t, *J* = 6.5 Hz, 2H), 2.76 (tt, *J* = 7.0, 4.6 Hz, 1H), 2.63 (d, *J* = 6.9 Hz, 1H), 2.07 (d, *J* = 4.6 Hz, 1H), 1.80 – 1.59 (m, 3H), 1.51 – 1.30 (m, 3H). **¹³C NMR** (101 MHz, CDCl₃) δ 159.66, 144.67, 142.92, 135.50, 135.16, 130.08, 129.78, 128.12, 66.80, 40.04, 33.98, 31.02, 28.13, 23.43, 21.76. **HRMS** (+APCI) calculated for C₁₇H₂₁O₃N₃BrS [M+H]⁺ 426.04815, found 426.04952. **HPLC** (IA column 10% 2-propanol in hexanes, 1.0 mL/min) *t*_M = 19.8 min *t*_m = 18.5 min, 95:5 e.r.

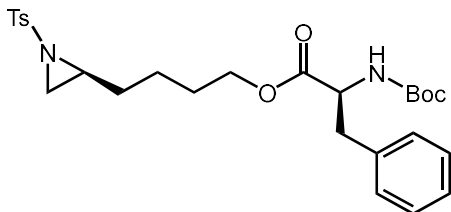


(*S*)-2-bromo-3-(4-(1-tosylaziridin-2-yl)butoxy)pyridine (**2.123**): Prepared using **General Procedure H** using **S36** and (*R,R*)-**2.55**. Purified via preparative TLC using (50% EtOAc in Hexanes) to provide **2.123** (0.0120 g, 28 % yield, 96:4 e.r.) as colorless oil. $^1\text{H NMR}$ (400 MHz, CDCl_3) δ 8.00 (dd, $J = 4.6, 1.5$ Hz, 1H), 7.85 (d, $J = 8.3$ Hz, 2H), 7.35 (d, $J = 7.7$ Hz, 2H), 7.22 (dd, $J = 8.1, 4.6$ Hz, 1H), 7.10 (dd, $J = 8.1, 1.6$ Hz, 1H), 3.96 (td, $J = 6.2, 2.0$ Hz, 2H), 2.81 (ddt, $J = 7.7, 7.0, 4.6$ Hz, 1H), 2.66 (d, $J = 7.0$ Hz, 1H), 2.41 (s, 3H), 2.12 (d, $J = 4.6$ Hz, 1H), 1.84 (ddd, $J = 13.8, 7.3, 6.1$ Hz, 2H), 1.79 – 1.68 (m, 1H), 1.62 – 1.36 (m, 3H). $^{13}\text{C NMR}$ (101 MHz, CDCl_3) δ 152.45, 144.66, 141.32, 135.12, 133.20, 129.83, 128.14, 123.52, 119.55, 68.99, 40.10, 34.01, 30.96, 28.28, 23.60, 21.74. **HRMS** (+ESI) calculated for $\text{C}_{18}\text{H}_{22}\text{O}_3\text{N}_2\text{BrS}$ $[\text{M}+\text{H}]^+$ 425.0529, found 425.05288. **HPLC** (IJ column 50% 2-propanol in hexanes, 1.5 mL/min) $t_{\text{M}} = 19.6$ min $t_{\text{m}} = 17.3$ min, 96:4 e.r.

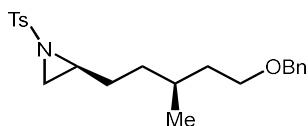


(*S*)-2-(4-(((3*aR*,5*R*,6*S*,6*aR*)-5-((*R*)-2,2-dimethyl-1,3-dioxolan-4-yl)-2,2-dimethyltetrahydrofuro[2,3-*d*][1,3]dioxol-6-yl)oxy)butyl)-1-tosylaziridine (**2.124**): Prepared using **General Procedure H** using **S20** and (*R,R*)-**2.55**. Purified via preparative TLC using (20% EtOAc in Hexanes) to provide **2.124** (0.0355 g, 69% yield, 95:5 d.r.) as colorless oil. $^1\text{H NMR}$ (400 MHz, CDCl_3) δ 7.81 (d, $J = 8.3$ Hz, 2H), 7.33 (d, $J = 8.2$ Hz, 2H), 5.85 (d, $J = 3.7$ Hz, 1H), 4.49 (d, $J = 3.8$ Hz, 1H), 4.26 (dt, $J = 7.7, 5.9$ Hz, 1H), 4.13 – 4.01 (m, 2H), 3.97 (dd, $J = 8.6, 5.7$ Hz, 1H), 3.80 (d, $J = 3.0$ Hz, 1H), 3.52 (dt, $J = 9.1, 6.3$ Hz, 1H), 3.44 (dt, $J = 9.3, 6.3$ Hz, 1H), 2.74 (tt, $J = 6.4, 4.6$ Hz, 1H), 2.59 (d, $J = 7.0$ Hz, 1H), 2.44 (s, 3H), 2.04 (d, $J = 4.6$ Hz, 1H), 1.62 – 1.50 (m, 3H), 1.48 (s, 3H), 1.41 (s, 3H), 1.39 – 1.33 (m, 3H), 1.32 (s, 3H), 1.31 (s, 3H). $^{13}\text{C NMR}$ (101 MHz, CDCl_3) δ 144.59, 135.27, 129.77, 128.10, 111.87, 109.05, 105.36, 82.63, 82.25, 81.26, 72.58, 70.24, 67.38, 40.11, 34.00, 31.07, 29.16, 26.96, 26.94, 26.37, 25.55, 23.46, 21.76. **HRMS** (+APCI)

calculated for $C_{25}H_{38}O_8NS$ $[M+H]^+$ 512.23126, found 512.23097 **HPLC** (OJ-H column 20% 2-propanol in hexanes, 1.0 mL/min) $t_M = 12.3$ min $t_m = 17.7$ min, 95:5 d.r.



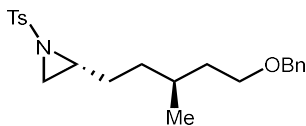
4-((*S*)-1-tosylaziridin-2-yl)butyl (*tert*-butoxycarbonyl)-*L*-phenylalaninate (**2.125**): Prepared using **General Procedure H** using **S37** and (*R,R*)-**2.55**. Purified via preparative TLC using (30% EtOAc in Hexanes) to provide **2.125** (0.0423 g, 82% yield, 94:6 d.r.) as a yellow oil. 1H NMR (400 MHz, $CDCl_3$) δ 7.81 (d, $J = 8.3$ Hz, 2H), 7.33 (d, $J = 8.0$ Hz, 2H), 7.32 – 7.19 (m, 3H), 7.12 (d, $J = 6.5$ Hz, 2H), 4.99 (d, $J = 8.3$ Hz, 1H), 4.54 (dt, $J = 8.4, 6.2$ Hz, 1H), 3.97 (t, $J = 6.6$ Hz, 2H), 3.05 (ddd, $J = 20.9, 14.0, 6.4$ Hz, 2H), 2.71 (tt, $J = 7.2, 4.8$ Hz, 1H), 2.62 (d, $J = 7.0$ Hz, 1H), 2.43 (s, 3H), 2.05 (d, $J = 4.5$ Hz, 1H), 1.64 – 1.46 (m, 3H), 1.41 (s, 9H), 1.36 – 1.19 (m, 3H). ^{13}C NMR (101 MHz, $CDCl_3$) δ 172.03, 155.16, 144.70, 136.14, 135.12, 129.79, 129.40, 128.62, 128.09, 127.10, 79.99, 64.99, 54.56, 39.91, 38.56, 33.90, 30.86, 28.40, 27.86, 23.24, 21.74. **HRMS** (+ESI) calculated for $C_{27}H_{36}O_6N_2NaS$ $[M+Na]^+$ 539.21863, found 539.21969. **HPLC** (IH column 60% acetonitrile in water, 0.75 mL/min) $t_M = 16.6$ min $t_m = 15.5$ min, 94:6 d.r.



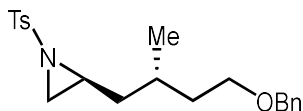
(*S*)-2-((*S*)-5-(benzyloxy)-3-methylpentyl)-1-tosylaziridine (*S,S*)-**2.126**: Prepared using **General Procedure H** using **S41** and (*R,R*)-**2.55**. Purified via preparative TLC using (7:2:1, Hex:EtOAc:Et₃N) to provide (*S,S*)-**2.126** (0.0300 g, 77% yield, 97:3 d.r.) as colorless oil. 1H NMR (400 MHz, $CDCl_3$) δ 7.82 (d, $J = 8.3$ Hz, 2H), 7.39 – 7.27 (m, 7H), 4.48 (s, 2H), 3.44 (tq, $J = 6.1, 2.8$ Hz, 2H), 2.68 (tt, $J = 7.2, 4.6$ Hz, 1H), 2.62 (d, $J = 7.0$ Hz, 1H), 2.43 (s, 3H), 2.05 (d, $J = 4.5$ Hz, 1H), 1.59 – 1.46 (m, 3H), 1.41 – 1.18 (m, 3H), 1.09 – 0.96 (m, 1H), 0.80 (d, $J = 6.4$ Hz, 3H). ^{13}C NMR (101 MHz, $CDCl_3$) δ 144.54, 138.70, 135.26, 129.73,

128.48, 128.14, 127.74, 127.65, 73.05, 68.44, 40.68, 36.66, 33.95, 33.94, 29.48, 28.89, 21.73, 19.37.

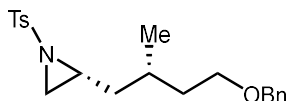
HRMS (+APCI) calculated for $C_{22}H_{30}O_3NS$ $[M+H]^+$ 388.19409, found 388.19394. **HPLC** (IH column 15% 2-propanol in hexanes, 1.0 mL/min) $t_M = 17.0$ min $t_m = 19.8$ min, 97:3 d.r.



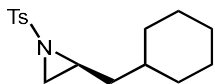
(R,S)-2-((S)-5-(benzyloxy)-3-methylpentyl)-1-tosylaziridine (R,S)-2.126: Prepared using **General Procedure H** using **S41** and **(S,S)-2.55**. Purified via preparative TLC using (7:2:1, Hex:EtOAc:Et₃N) to provide **(R,S)-2.126** (0.0280 g, 72% yield, 7:93 d.r.) as colorless oil. **¹H NMR** (400 MHz, CDCl₃) δ 7.82 (d, $J = 8.3$ Hz, 2H), 7.39 – 7.26 (m, 7H), 4.47 (s, 2H), 3.43 (td, $J = 6.8, 6.3, 2.7$ Hz, 2H), 2.68 (tt, $J = 7.2, 4.7$ Hz, 1H), 2.62 (d, $J = 7.0$ Hz, 1H), 2.44 (s, 3H), 2.05 (d, $J = 4.5$ Hz, 1H), 1.65 – 1.43 (m, 3H), 1.40 – 1.15 (m, 3H), 1.07 (dddd, $J = 13.3, 10.9, 7.4, 5.4$ Hz, 1H), 0.80 (d, $J = 6.5$ Hz, 3H). **¹³C NMR** (101 MHz, CDCl₃) δ 144.54, 138.69, 135.31, 129.74, 128.49, 128.14, 127.73, 127.66, 73.06, 68.46, 40.75, 36.51, 33.99, 33.89, 29.49, 28.90, 21.75, 19.57. **HRMS** (+APCI) calculated for $C_{22}H_{30}O_3NS$ $[M+H]^+$ 388.19409, found 388.19386. **HPLC** (IH column 15% 2-propanol in hexanes, 1.0 mL/min) $t_M = 19.7$ min $t_m = 17.2$ min, 7:93 d.r.



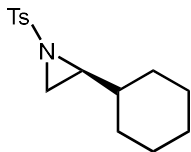
(S,S)-2-((S)-4-(benzyloxy)-2-methylbutyl)-1-tosylaziridine (S,S)-2.127: Prepared using **General Procedure H** using **S47** and **(R,R)-2.55**. Purified via preparative TLC using (7:2:1, Hex:EtOAc:Et₃N) to provide **(S,S)-2.127** (0.0090 g, 24% yield, 9:91 d.r.) as colorless oil. **¹H NMR** (400 MHz, CDCl₃) δ 7.82 (d, $J = 8.3$ Hz, 2H), 7.38 – 7.26 (m, 7H), 4.46 (s, 2H), 3.43 (td, $J = 6.6, 2.6$ Hz, 2H), 2.79 (tdd, $J = 7.1, 5.8, 4.6$ Hz, 1H), 2.64 (d, $J = 6.9$ Hz, 1H), 2.42 (s, 3H), 2.04 (d, $J = 4.6$ Hz, 1H), 1.73 – 1.53 (m, 3H), 1.51 – 1.37 (m, 2H), 1.35 – 1.22 (m, 2H), 0.89 (d, $J = 6.6$ Hz, 3H). **¹³C NMR** (101 MHz, CDCl₃) δ 144.56, 138.66, 135.32, 129.80, 129.77, 128.52, 128.10, 127.72, 127.68, 73.07, 68.31, 38.85, 38.81, 36.84, 34.40, 28.84, 21.77, 19.31. **HRMS** (+APCI) calculated for $C_{21}H_{28}O_3N^{32}S$ $[M+H]^+$ 374.17844, found 374.1784. **HPLC** (IK column 15% 2-propanol in hexanes, 1.0 mL/min) $t_M = 22.3$ min $t_m = 19.9$ min, 9:91 d.r.



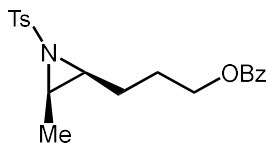
(*R*)-2-((*S*)-4-(benzyloxy)-2-methylbutyl)-1-tosylaziridine (**(*R,S*)-2.127**): Prepared using **General Procedure H** using **S47** and (***S,S*-2.55**). Purified via preparative TLC using (7:2:1, Hex:EtOAc:Et₃N) to provide (***R,S*-2.127**) (0.0110 g, 30% yield, 97:3 d.r.) as colorless oil. **¹H NMR** (400 MHz, CDCl₃) δ 7.82 (d, *J* = 8.3 Hz, 2H), 7.38 – 7.27 (m, 7H), 4.47 (s, 2H), 3.51 – 3.33 (m, 2H), 2.81 (tdd, *J* = 6.9, 6.0, 4.6 Hz, 1H), 2.60 (d, *J* = 7.0 Hz, 1H), 2.43 (s, 3H), 1.99 (d, *J* = 4.6 Hz, 1H), 1.75 – 1.60 (m, 2H), 1.51 – 1.31 (m, 3H), 0.90 (d, *J* = 6.6 Hz, 3H). **¹³C NMR** (101 MHz, CDCl₃) δ 144.55, 138.65, 135.35, 129.80, 128.53, 128.10, 127.76, 127.70, 73.11, 68.27, 38.95, 38.77, 36.13, 33.88, 28.91, 21.78, 19.74. **HRMS** (+APCI) calculated for C₂₁H₂₈O₃NS [M+H]⁺ 374.17844, found 374.17833. **HPLC** (IK column 15% 2-propanol in hexanes, 1.0 mL/min) *t*_M = 19.9 min *t*_m = 22.4 min, 97:3 d.r.



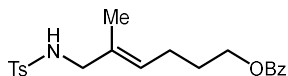
(*S*)-2-(cyclohexylmethyl)-1-tosylaziridine (**2.128**): Prepared using **General Procedure H** using allylcyclohexane (**S21**) and (***R,R*-2.55**). Purified via preparative TLC using (20% EtOAc in Hexanes) to provide **2.128** (0.0247 g, 83% yield, 96:4 e.r.) as a colorless oil. **¹H NMR** (400 MHz, CDCl₃) δ 7.83 (d, *J* = 8.3 Hz, 2H), 7.34 (d, *J* = 7.7 Hz, 2H), 2.80 – 2.72 (m, 1H), 2.65 (d, *J* = 7.0 Hz, 1H), 2.44 (s, 3H), 2.03 (d, *J* = 4.6 Hz, 1H), 1.72 – 1.50 (m, 5H), 1.39 – 1.22 (m, 2H), 1.21 – 0.99 (m, 4H), 0.91 – 0.75 (m, 2H). **¹³C NMR** (101 MHz, CDCl₃) δ 144.57, 135.32, 129.77, 128.14, 39.25, 39.13, 36.20, 34.01, 33.51, 32.70, 26.42, 26.24, 26.10, 21.77. **HRMS** (+APCI) calculated for C₁₆H₂₄O₂NS [M+H]⁺ 294.15223, found 294.15201. **HPLC** (IK column 10% 2-propanol in hexanes, 1.0 mL/min) *t*_M = 21.1 min *t*_m = 19.0 min, 96:4 e.r.



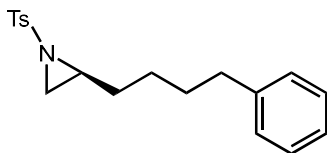
(S)-2-cyclohexyl-1-tosylaziridine (**2.129**): Prepared using **General Procedure G** using vinylcyclohexane (**S22**) and (*R,R*)-**2.55**. Purified via preparative TLC using (20% EtOAc in Hexanes) to provide **2.129** (0.0039 g, 14% yield, 91:9 e.r.) as colorless oil. $^1\text{H NMR}$ (400 MHz, CDCl_3) δ 7.82 (d, $J = 8.3$ Hz, 2H), 7.33 (d, $J = 7.9$ Hz, 2H), 2.60 (d, $J = 7.0$ Hz, 1H), 2.53 (td, $J = 7.2, 4.6$ Hz, 1H), 2.45 (s, 3H), 2.10 (d, $J = 4.6$ Hz, 1H), 1.74 – 1.45 (m, 6H), 1.27 – 0.85 (m, 7H). $^{13}\text{C NMR}$ (101 MHz, CDCl_3) δ 144.53, 135.27, 129.74, 128.23, 45.31, 39.54, 32.81, 30.34, 29.77, 26.16, 25.70, 25.52, 21.81. **HRMS** (+APCI) calculated for $\text{C}_{15}\text{H}_{22}\text{O}_2\text{NS}$ $[\text{M}+\text{H}]^+$ 280.13658, found 280.13654. **HPLC** (AS-H column 5% 2-propanol in hexanes, 1.0 mL/min) $t_{\text{M}} = 22.9$ min $t_{\text{m}} = 18.2$ min, 91:9 e.r.



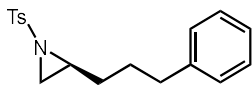
3-((*2S,3R*)-3-methyl-1-tosylaziridin-2-yl)propyl benzoate (**2.130**): Prepared using **General Procedure H** using **S23** and (*R,R*)-**2.55**. Purified via preparative TLC using (7:2:1, Hex:EtOAc:Et₃N) to provide **2.130** (0.0226 g, 61% yield, 86:14 e.r., >20:1 d.r.) as colorless oil. $^1\text{H NMR}$ (400 MHz, CDCl_3) δ 8.00 (dd, $J = 8.4, 1.4$ Hz, 2H), 7.82 (d, $J = 8.3$ Hz, 2H), 7.61 – 7.51 (m, 1H), 7.49 – 7.40 (m, 2H), 7.32 (dd, $J = 8.7, 0.8$ Hz, 2H), 4.33 – 4.17 (m, 2H), 2.95 (dq, $J = 7.3, 5.9$ Hz, 1H), 2.81 (ddd, $J = 8.3, 7.3, 4.9$ Hz, 1H), 2.40 (s, 3H), 1.77 – 1.61 (m, 3H), 1.56 – 1.45 (m, 1H), 1.22 (d, $J = 5.9$ Hz, 3H). $^{13}\text{C NMR}$ (101 MHz, CDCl_3) δ 166.55, 144.51, 135.45, 133.12, 130.25, 129.78, 129.63, 128.51, 127.97, 64.16, 44.46, 40.47, 26.59, 23.31, 21.73, 12.11. **HRMS** (+APCI) calculated for $\text{C}_{20}\text{H}_{24}\text{O}_4\text{N}^32\text{S}$ $[\text{M}+\text{H}]^+$ 374.14206, found 374.14319. **HPLC** (IB column 10% 2-propanol in hexanes, 1.0 mL/min) $t_{\text{M}} = 16.9$ min $t_{\text{m}} = 15.4$ min, 86:14 e.r. >20:1 d.r.



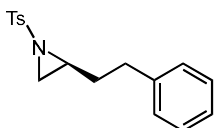
5-methyl-6-((4-methylphenyl)sulfonamido)hex-4-en-1-yl benzoate (2.132): Prepared using **General Procedure H** using **S48** and **(R,R)-2.55**. Purified via preparative TLC using (20% EtOAc in Hexanes) to provide **2.132** (0.0215 g, 56% yield) as a colorless oil. $^1\text{H NMR}$ (400 MHz, CDCl_3) δ 8.06 – 7.98 (m, 2H), 7.75 – 7.69 (m, 2H), 7.59 – 7.53 (m, 1H), 7.44 (dd, $J = 8.5, 7.0$ Hz, 2H), 7.30 (d, $J = 8.1$ Hz, 2H), 5.35 – 5.20 (m, 1H), 4.44 (s, 1H), 4.26 (t, $J = 6.5$ Hz, 2H), 3.44 (d, $J = 6.4$ Hz, 2H), 2.42 (s, 3H), 2.11 (q, $J = 7.4$ Hz, 2H), 1.81 – 1.71 (m, 2H), 1.56 (s, 3H). $^{13}\text{C NMR}$ (101 MHz, CDCl_3) δ 166.71, 143.50, 137.18, 133.08, 131.60, 130.41, 129.79, 129.63, 128.52, 127.33, 127.25, 64.34, 51.14, 28.38, 24.33, 21.65, 14.44. **HRMS** (+APCI) calculated for $\text{C}_{21}\text{H}_{26}\text{O}_4\text{N}^{32}\text{S}$ $[\text{M}+\text{H}]^+$ 388.15771, found 388.15732.



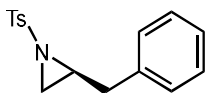
(S)-2-(4-phenylbutyl)-1-tosylaziridine (2.133): Prepared using **General Procedure H** using **S24** and **(R,R)-2.55**. Purified via preparative TLC using (20% EtOAc in Hexanes) to provide **2.133** (0.0215 g, 82% yield, 94:6 e.r.) as colorless oil. $^1\text{H NMR}$ (400 MHz, CDCl_3) δ 7.82 (d, $J = 8.3$ Hz, 2H), 7.33 (d, $J = 7.9$ Hz, 2H), 7.30 – 7.23 (m, 2H), 7.22 – 7.15 (m, 1H), 7.12 (d, $J = 6.7$ Hz, 2H), 2.72 (tt, $J = 7.3, 4.8$ Hz, 1H), 2.63 (d, $J = 7.0$ Hz, 1H), 2.52 (t, $J = 7.7$ Hz, 2H), 2.45 (s, 3H), 2.06 (d, $J = 4.6$ Hz, 1H), 1.64 – 1.48 (m, 3H), 1.44 – 1.21 (m, 3H). $^{13}\text{C NMR}$ (101 MHz, CDCl_3) δ 144.55, 142.32, 135.30, 129.77, 128.45, 128.41, 128.11, 125.87, 40.42, 35.79, 33.93, 31.31, 30.92, 26.54, 21.77. **HRMS** (+APCI) calculated for $\text{C}_{19}\text{H}_{24}\text{O}_2\text{NS}$ $[\text{M}+\text{H}]^+$ 330.15223, found 330.15195. **HPLC** (AD-H column 5% 2-propanol in hexanes, 1.0 mL/min) $t_{\text{M}} = 16.8$ min $t_{\text{m}} = 13.2$ min, 94:6 e.r.



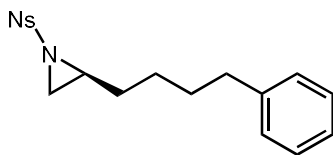
(S)-2-(3-phenylpropyl)-1-tosylaziridine (**2.134**): Prepared using **General Procedure H** using **S25** and **(R,R)-2.55**. Purified via preparational TLC using (20% EtOAc in Hexanes) to provide **2.134** (0.0170 g, 54%yield, 94:6 e.r.) as colorless oil. **¹H NMR** (400 MHz, CDCl₃) δ 7.83 (d, *J* = 8.3 Hz, 2H), 7.32 (d, *J* = 8.0 Hz, 2H), 7.29 – 7.21 (m, 2H), 7.21 – 7.11 (m, 1H), 7.11 – 7.01 (m, 2H), 2.79 – 2.69 (m, 1H), 2.64 (d, *J* = 6.9 Hz, 1H), 2.55 (t, *J* = 7.5 Hz, 2H), 2.42 (s, 3H), 2.06 (d, *J* = 4.5 Hz, 1H), 1.68 – 1.48 (m, 3H), 1.39 – 1.24 (m, 1H). **¹³C NMR** (101 MHz, CDCl₃) δ 144.64, 141.78, 135.24, 129.78, 128.43, 128.13, 125.98, 40.29, 35.19, 33.93, 30.88, 28.47, 21.75. **HRMS** (+APCI) calculated for C₁₈H₂₂O₂NS [M+H]⁺ 316.13658, found 316.13643. **HPLC** (IA column 10% 2-propanol in hexanes, 1.0 mL/min) *t*_M = 10.1 min *t*_m = 8.9 min, 94:6 e.r.



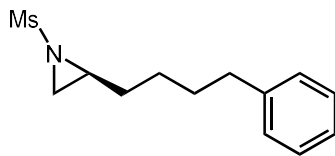
(S)-2-phenethyl-1-tosylaziridine (**2.135**): Prepared using **General Procedure A** using but-3-en-1-ylbenzene and **(R,R)-XX**. Purified via preparational TLC using (7:2:1, Hex:EtOAc:Et₃N) to provide **(2.135)** (0.0033 g, 11%yield, 96:4 e.r.) as colorless oil. **¹H NMR** (400 MHz, CDCl₃) δ 7.83 (d, *J* = 8.3 Hz, 2H), 7.34 (d, *J* = 7.9 Hz, 2H), 7.30 – 7.24 (m, 4H), 7.23 – 7.14 (m, 1H), 7.14 – 7.06 (m, 2H), 2.77 (tt, *J* = 7.4, 4.8 Hz, 1H), 2.69 – 2.50 (m, 3H), 2.45 (s, 3H), 2.05 (d, *J* = 4.6 Hz, 1H), 1.88 (dddd, *J* = 13.8, 8.9, 7.4, 5.0 Hz, 1H), 1.67 (dtd, *J* = 14.0, 7.9, 6.4 Hz, 2H). **¹³C NMR** (101 MHz, CDCl₃) δ 144.68, 140.85, 135.18, 129.82, 128.62, 128.47, 128.17, 126.28, 39.88, 34.06, 33.30, 33.14, 21.81. **HRMS** (+APCI) calculated for C₁₇H₂₀O₂NS [M+H]⁺ 302.12093, found 302.12104. **HPLC** (IA column 10% 2-propanol in hexanes, 1.0 mL/min) *t*_M = 10.0 min *t*_m = 9.2 min, 96:4 e.r.



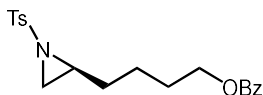
(S)-2-benzyl-1-tosylaziridine (**2.136**): Prepared using **General Procedure G** using allylbenzene (**S27**) and **(R,R)**-**2.55**. Purified via preparative TLC using (7:2:1, Hex:EtOAc:Et₃N) to provide **2.136** (0.0051 g, 18% yield, 95:5 e.r.) as white crystalline solid. ¹H NMR (400 MHz, CDCl₃) δ 7.68 (d, *J* = 8.3 Hz, 2H), 7.21 (d, *J* = 7.9 Hz, 2H), 7.16 (dd, *J* = 4.9, 2.0 Hz, 3H), 7.04 (td, *J* = 4.9, 4.2, 3.2 Hz, 2H), 2.95 (tt, *J* = 7.0, 4.9 Hz, 1H), 2.81 (dd, *J* = 14.5, 5.2 Hz, 1H), 2.74 – 2.65 (m, 2H), 2.42 (s, 3H), 2.16 (d, *J* = 4.5 Hz, 1H). ¹³C NMR (101 MHz, CDCl₃) δ 144.45, 137.14, 135.00, 129.73, 128.86, 128.60, 128.02, 126.65, 41.32, 37.64, 32.97, 21.77. HRMS (+APCI) calculated for C₁₆H₁₈O₂N³²S [M+H]⁺ 288.10528, found 288.10601. HPLC (IA column 5% 2-propanol in hexanes, 1.0 mL/min) *t*_M = 14.7 min *t*_m = 13.0 min, 95:5 e.r.



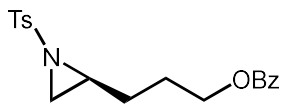
(S)-1-((4-nitrophenyl)sulfonyl)-2-(4-phenylbutyl)aziridine (**2.137**): Prepared using **General Procedure H** using **S24** and **(R,R)**-**2.55**. Purified via preparative TLC using (20% EtOAc in Hexanes) to provide **2.137** (0.0057 g, 16% yield, 94:6 e.r.) as a colorless oil. ¹H NMR (400 MHz, CDCl₃) δ 8.36 (d, *J* = 8.9 Hz, 2H), 8.13 (d, *J* = 8.8 Hz, 2H), 7.30 – 7.24 (m, 2H), 7.21 – 7.15 (m, 1H), 7.14 – 7.08 (m, 2H), 2.88 (tt, *J* = 7.2, 4.8 Hz, 1H), 2.74 (d, *J* = 7.0 Hz, 1H), 2.55 (t, *J* = 7.6 Hz, 2H), 2.15 (d, *J* = 4.7 Hz, 1H), 1.69 – 1.53 (m, 3H), 1.46 – 1.26 (m, 3H). ¹³C NMR (101 MHz, CDCl₃) δ 150.69, 144.21, 142.05, 129.36, 128.48, 128.44, 126.00, 124.37, 41.38, 35.70, 34.73, 31.28, 30.80, 26.48. HRMS (+APCI) calculated for C₁₈H₂₁O₄N₂S [M+H]⁺ 361.12165, found 361.12133. HPLC (IB column 20% 2-propanol in hexanes, 1.0 mL/min) *t*_M = 22.8 min *t*_m = 19.7 min, 94:6 e.r.



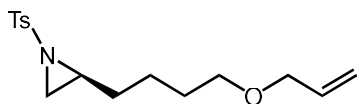
(*S*)-1-(methylsulfonyl)-2-(4-phenylbutyl)aziridine (**2.138**): Prepared using **General Procedure H** using **S24** and (*R,R*)-**2.55**. Purified via preparative TLC using (20% EtOAc in Hexanes) to provide **2.138** (0.0067 g, 26% yield, 87:13 e.r.) as a colorless oil. $^1\text{H NMR}$ (400 MHz, CDCl_3) δ 7.31 – 7.26 (m, 2H), 7.21 – 7.14 (m, 3H), 3.01 (s, 3H), 2.72 (tt, $J = 7.0, 4.9$ Hz, 1H), 2.63 (t, $J = 7.6$ Hz, 2H), 2.59 (d, $J = 7.0$ Hz, 1H), 2.09 (d, $J = 4.6$ Hz, 1H), 1.75 – 1.56 (m, 3H), 1.55 – 1.45 (m, 3H). $^{13}\text{C NMR}$ (101 MHz, CDCl_3) δ 142.27, 128.54, 128.49, 125.96, 39.77, 39.61, 35.85, 33.55, 31.37, 31.08, 26.63. **HRMS** (+APCI) calculated for $\text{C}_{13}\text{H}_{20}\text{O}_2\text{NS}$ $[\text{M}+\text{H}]^+$ 254.12093, found 254.12082. **HPLC** (IB column 20% 2-propanol in hexanes, 1.0 mL/min) $t_{\text{M}} = 11.3$ min $t_{\text{m}} = 10.0$ min, 87:13 e.r.



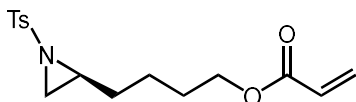
(*S*)-4-(1-tosylaziridin-2-yl)butyl benzoate (**2.139**): Prepared using **General Procedure H** using **S28** and (*R,R*)-**2.55**. Purified via preparative TLC using (7:2:1, Hex:EtOAc:Et₃N) to provide **2.139** (0.0225 g, 60% yield, 95:5 e.r.) as colorless oil. $^1\text{H NMR}$ (400 MHz, CDCl_3) δ 8.02 (d, $J = 7.0$ Hz, 2H), 7.82 (d, $J = 8.3$ Hz, 2H), 7.57 (t, $J = 7.4$ Hz, 1H), 7.45 (t, $J = 7.6$ Hz, 2H), 7.30 (d, $J = 7.6$ Hz, 2H), 4.20 (td, $J = 6.5, 1.4$ Hz, 2H), 2.75 (tt, $J = 7.1, 4.5$ Hz, 1H), 2.66 (d, $J = 6.9$ Hz, 1H), 2.40 (s, 3H), 2.09 (d, $J = 4.5$ Hz, 1H), 1.78 – 1.58 (m, 3H), 1.47 – 1.31 (m, 3H). $^{13}\text{C NMR}$ (101 MHz, CDCl_3) δ 166.69, 144.73, 135.15, 133.08, 130.41, 129.79, 129.66, 128.51, 128.12, 64.66, 40.20, 33.92, 31.03, 28.19, 23.57, 21.74. **HRMS** (+APCI) calculated for $\text{C}_{20}\text{H}_{24}\text{O}_4\text{NS}$ $[\text{M}+\text{H}]^+$ 374.14206, found 374.1431. **HPLC** (IA column 10% 2-propanol in hexanes, 1.0 mL/min) $t_{\text{M}} = 17.5$ min $t_{\text{m}} = 15.6$ min, 95:5 e.r.



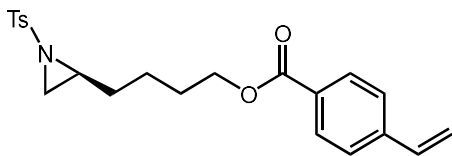
(*S*)-3-(1-tosylaziridin-2-yl)propyl benzoate (**2.140**): Prepared using **General Procedure H** using **29** and (*R,R*)-**2.55**. Purified via preparational TLC using (20% EtOAc in Hexanes) to provide **2.140** (0.0198 g, 55 %yield, 94:6 e.r.) as colorless oil. $^1\text{H NMR}$ (400 MHz, CDCl_3) δ 8.00 (d, $J = 7.1$ Hz, 2H), 7.83 (d, $J = 8.3$ Hz, 2H), 7.56 (t, $J = 7.4$ Hz, 1H), 7.44 (t, $J = 7.6$ Hz, 2H), 7.34 (s, 2H), 4.25 (td, $J = 6.3, 2.4$ Hz, 2H), 2.80 (ddt, $J = 8.0, 6.9, 4.4$ Hz, 1H), 2.66 (d, $J = 7.0$ Hz, 1H), 2.41 (s, 3H), 2.11 (d, $J = 4.5$ Hz, 1H), 1.84 – 1.68 (m, 3H), 1.51 – 1.40 (m, 1H). $^{13}\text{C NMR}$ (101 MHz, CDCl_3) δ 166.57, 144.76, 135.05, 133.13, 130.24, 129.84, 129.65, 128.51, 128.13, 64.06, 39.74, 34.01, 28.13, 26.24, 21.76. **HRMS** (+APCI) calculated for $\text{C}_{19}\text{H}_{22}\text{O}_4\text{N}^{\text{32}}\text{S}$ $[\text{M}+\text{H}]^+$ 360.12641, found 360.1272. **HPLC** (IA column 10% 2-propanol in hexanes, 1.0 mL/min) $t_M = 19.1$ min $t_m = 17.0$ min, 94:6 e.r.



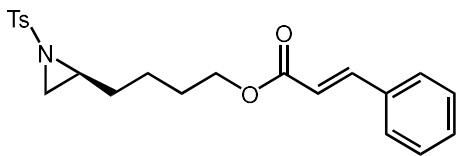
(*S*)-2-(4-(allyloxy)butyl)-1-tosylaziridine (**2.143**): Prepared using **General Procedure H** using **S30** and (*R,R*)-**2.55**. Purified via preparative TLC using (7:2:1, Hex:EtOAc:Et₃N) to provide **2.143** (0.0214 g, 69 % yield, 95:5 e.r.) as colorless oil. $^1\text{H NMR}$ (400 MHz, CDCl_3) δ 7.82 (d, $J = 8.3$ Hz, 2H), 7.33 (d, $J = 8.2$ Hz, 2H), 5.89 (ddt, $J = 17.2, 10.3, 5.6$ Hz, 1H), 5.25 (dq, $J = 17.3, 1.7$ Hz, 1H), 5.16 (dq, $J = 10.3, 1.4$ Hz, 1H), 3.92 (dt, $J = 5.6, 1.4$ Hz, 2H), 3.33 (t, $J = 6.5$ Hz, 2H), 2.73 (tt, $J = 7.0, 4.8$ Hz, 1H), 2.62 (d, $J = 7.0$ Hz, 1H), 2.44 (s, 3H), 2.06 (d, $J = 4.6$ Hz, 1H), 1.64 – 1.46 (m, 3H), 1.45 – 1.27 (m, 3H). $^{13}\text{C NMR}$ (101 MHz, CDCl_3) δ 144.55, 135.30, 135.06, 129.77, 128.13, 116.92, 71.96, 70.05, 40.35, 33.92, 31.24, 29.27, 23.64, 21.77. **HRMS** (+ESI) calculated for $\text{C}_{16}\text{H}_{24}\text{O}_3\text{NS}$ $[\text{M}+\text{H}]^+$ 310.14714, found 310.14709. **HPLC** (IH column 20% 2-propanol in hexanes, 1.0 mL/min) $t_M = 14.0$ min $t_m = 18.1$ min, 95:5 e.r.



(*S*)-4-(1-tosylaziridin-2-yl)butyl acrylate (**2.144**): Prepared using **General Procedure H** using **S49** and (*R,R*)-**2.55**. Purified via preparative TLC using (7:2:1, Hex:EtOAc:Et₃N) to provide **2.144** (0.0159 g, 49 % yield, 95:5 e.r.) as colorless oil. ¹H NMR (400 MHz, CDCl₃) δ 7.82 (d, *J* = 8.3 Hz, 2H), 7.33 (d, *J* = 7.9 Hz, 2H), 6.39 (dd, *J* = 17.3, 1.5 Hz, 1H), 6.10 (dd, *J* = 17.3, 10.4 Hz, 1H), 5.82 (dd, *J* = 10.4, 1.5 Hz, 1H), 4.04 (t, *J* = 6.6 Hz, 2H), 2.73 (tt, *J* = 7.0, 4.6 Hz, 1H), 2.64 (d, *J* = 7.0 Hz, 1H), 2.44 (s, 3H), 2.07 (d, *J* = 4.5 Hz, 1H), 1.69 – 1.53 (m, 3H), 1.41 – 1.28 (m, 3H). ¹³C NMR (101 MHz, CDCl₃) δ 166.32, 144.70, 135.23, 130.79, 129.79, 128.59, 128.13, 64.24, 40.13, 33.89, 30.99, 28.08, 23.44, 21.76. HRMS (+ESI) calculated for C₁₆H₂₂O₄NS [M+H]⁺ 324.12641, found 324.1266. HPLC (IA column 10% 2-propanol in hexanes, 1.0 mL/min) *t*_M = 13.6 min *t*_m = 12.5 min, 95:5 e.r.

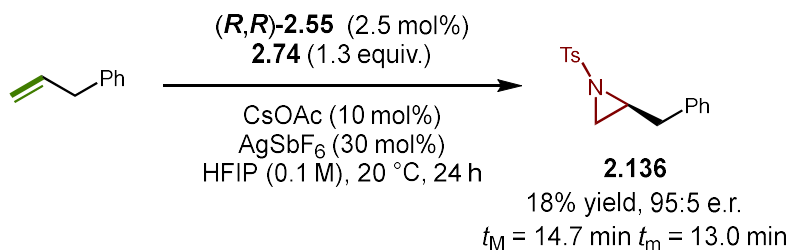


(*S*)-4-(1-tosylaziridin-2-yl)butyl 4-vinylbenzoate (**2.145**): Prepared using **General Procedure H** using **S50** and (*R,R*)-**2.55**. Purified via preparative TLC using (7:2:1, Hex:EtOAc:Et₃N) to provide **2.145** (0.0206 g, 52 % yield, 95:5 e.r.) as colorless oil. ¹H NMR (400 MHz, CDCl₃) δ 7.98 (d, *J* = 8.4 Hz, 2H), 7.82 (d, *J* = 8.3 Hz, 2H), 7.47 (d, *J* = 8.2 Hz, 2H), 7.30 (dd, *J* = 8.6, 0.7 Hz, 2H), 6.76 (dd, *J* = 17.6, 10.9 Hz, 1H), 5.87 (dd, *J* = 17.6, 0.8 Hz, 1H), 5.39 (dd, *J* = 10.9, 0.7 Hz, 1H), 4.20 (td, *J* = 6.6, 1.4 Hz, 2H), 2.75 (tt, *J* = 7.1, 4.5 Hz, 1H), 2.66 (d, *J* = 7.0 Hz, 1H), 2.41 (s, 3H), 2.08 (d, *J* = 4.5 Hz, 1H), 1.76 – 1.60 (m, 3H), 1.46 – 1.33 (m, 4H). ¹³C NMR (101 MHz, CDCl₃) δ 166.46, 144.71, 142.10, 136.15, 135.24, 130.00, 129.83, 129.80, 129.56, 128.14, 126.26, 116.67, 64.64, 40.19, 33.93, 31.04, 28.21, 23.58, 21.74. HRMS (+ESI) calculated for C₂₂H₂₆O₄NS [M+H]⁺ 400.15771, found 400.158. HPLC (IH column 70% acetonitrile in water, 0.75 mL/min) *t*_M = 12.0 min *t*_m = 11.0 min, 95:5 e.r.



(*S*)-4-(1-tosylaziridin-2-yl)butyl cinnamate (**2.146**): Prepared using **General Procedure H** using **S51** and (*R,R*)-**2.55**. Purified via preparative TLC using (7:2:1, Hex:EtOAc:Et₃N) to provide **2.146** (0.0272 g, 68 % yield, 95:5 e.r.) as colorless oil. ¹H NMR (400 MHz, CDCl₃) δ 7.83 (d, *J* = 8.3 Hz, 2H), 7.68 (d, *J* = 16.0 Hz, 1H), 7.57 – 7.48 (m, 2H), 7.44 – 7.35 (m, 3H), 7.32 (dd, *J* = 8.6, 0.8 Hz, 2H), 6.42 (d, *J* = 16.0 Hz, 1H), 4.10 (td, *J* = 6.6, 0.8 Hz, 2H), 2.75 (tt, *J* = 6.9, 4.5 Hz, 1H), 2.65 (d, *J* = 7.0 Hz, 1H), 2.43 (s, 3H), 2.08 (d, *J* = 4.6 Hz, 1H), 1.73 – 1.57 (m, 3H), 1.44 – 1.31 (m, 3H). ¹³C NMR (101 MHz, CDCl₃) δ 167.08, 144.90, 144.69, 135.24, 134.51, 130.44, 129.78, 129.04, 128.20, 128.13, 118.18, 64.25, 40.15, 33.92, 31.01, 28.18, 23.48, 21.75. HRMS (+ESI) calculated for C₂₂H₂₆O₄NS [M+H]⁺ 400.15771, found 400.15807. HPLC (IA column 70% acetonitrile in water, 0.75 mL/min) *t*_M = 16.7 min *t*_m = 19.2 min, 95:5 e.r.

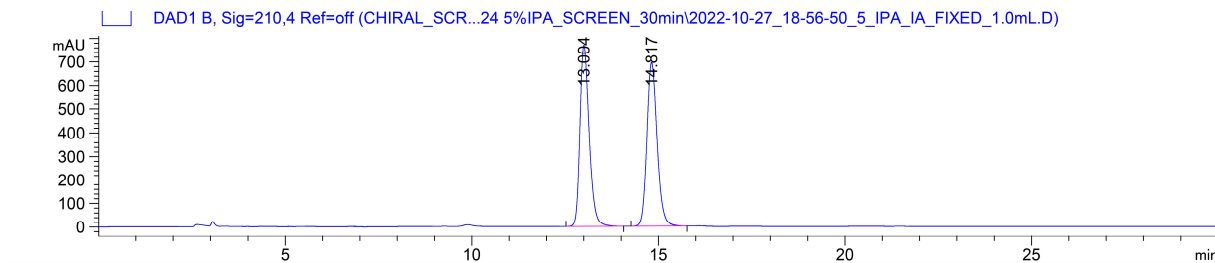
Determination of Aziridine Stereochemistry



Stereochemistry of 2-benzyl-1-tosylaziridine **2.136** was assigned by synthesizing (*R*)-2-benzyl-1-tosylaziridine from (*R*)-2-amino-3-phenylpropan-1-ol and synthesizing (*S*)-2-benzyl-1-tosylaziridine from (*S*)-2-amino-3-phenylpropan-1-ol then comparing HPLC data to the reaction HPLC data for the same substrate, shown below.

(*S*)-2-benzyl-1-tosylaziridine (**2.136**): See **Enantioselective Aziridine Scope** for full experimental. HPLC (IA column 5% 2-propanol in hexanes, 1.0 mL/min) *t*_M = 14.7 min *t*_m = 13.0 min, 95:5 e.r.

(±)-2-benzyl-1-tosylaziridine (±-2.136):

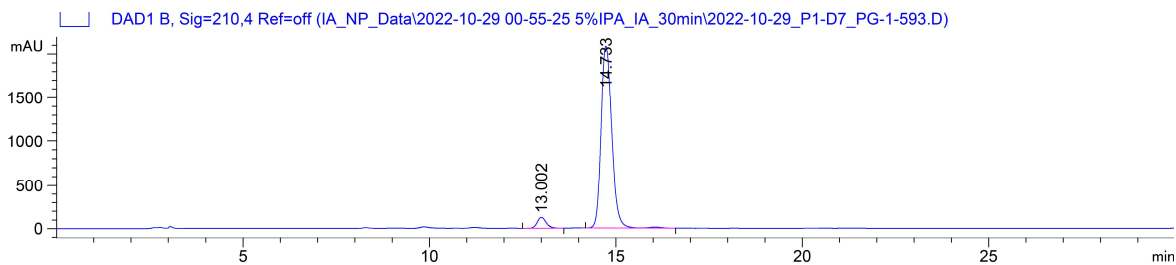


Signal 2: DAD1 B, Sig=210,4 Ref=off

| Peak # | RetTime [min] | Type | Width [min] | Area [mAU*s] | Height [mAU] | Area % |
|--------|---------------|------|-------------|--------------|--------------|---------|
| 1 | 13.004 | BB | 0.2642 | 1.32316e4 | 769.17761 | 49.9148 |
| 2 | 14.817 | BB | 0.2935 | 1.32768e4 | 694.65857 | 50.0852 |

Totals : 2.65083e4 1463.83618

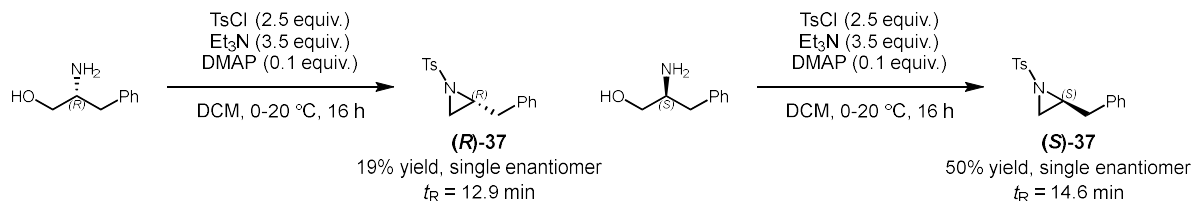
(S)-2-benzyl-1-tosylaziridine (2.136):



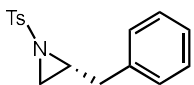
Signal 2: DAD1 B, Sig=210,4 Ref=off

| Peak # | RetTime [min] | Type | Width [min] | Area [mAU*s] | Height [mAU] | Area % |
|--------|---------------|------|-------------|--------------|--------------|---------|
| 1 | 13.002 | BB | 0.2471 | 2112.04272 | 127.29562 | 4.8152 |
| 2 | 14.733 | BV R | 0.2419 | 4.17496e4 | 2081.45728 | 95.1848 |

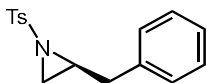
Totals : 4.38617e4 2208.75290



*Synthesis of chiral 2-benzyl-1-tosylaziridine from amino alcohols*²⁶: To a solution of chiral amino alcohol (0.76 g, 5.0 mmol, 1.0 equiv.) in dry CH_2Cl_2 (20 mL) at 0 °C was added Et_3N (2.4 mL, 18 mmol, 3.5 equiv.), and TsCl (2.4 g, 13 mmol, 2.5 equiv.). After 10 minutes, DMAP (61 mg, 0.5 mmol, 0.1 equiv.) was added and the reaction was allowed to stir under a N_2 balloon at room temperature overnight. After which, the reaction was quenched with H_2O and extracted with CH_2Cl_2 three times. The combined organic layers were dried with Na_2SO_4 and the solvent removed under reduced pressure. The crude product was purified using silica gel column chromatography (5-10% EtOAc) and further purified via recrystallization from EtOAc and hexanes to yield (*R*)- **2.136** or (*S*)- **2.136** as a white solid.

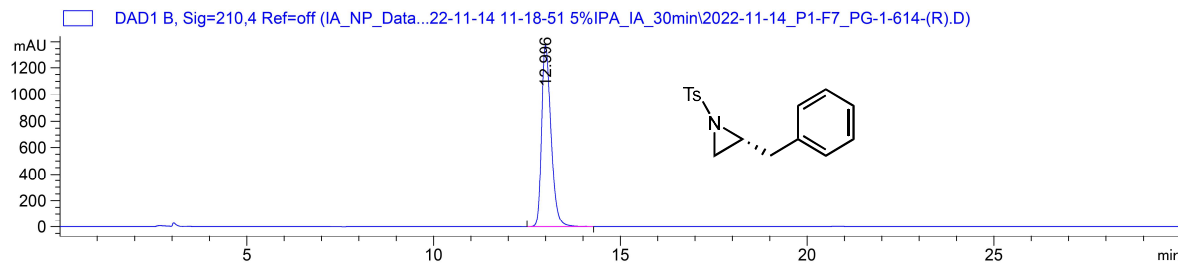


(*R*)-2-benzyl-1-tosylaziridine ((*R*)-**2.136**): (0.275 g, 19% yield, single enantiomer) $^1\text{H NMR}$ (400 MHz, CDCl_3) δ 7.69 (d, $J = 8.3 \text{ Hz}$, 2H), 7.21 (d, $J = 8.0 \text{ Hz}$, 2H), 7.16 (dd, $J = 4.9, 2.0 \text{ Hz}$, 3H), 7.09 – 6.99 (m, 2H), 2.95 (tt, $J = 7.0, 4.8 \text{ Hz}$, 1H), 2.81 (dd, $J = 14.5, 5.2 \text{ Hz}$, 1H), 2.75 – 2.64 (m, 2H), 2.42 (s, 3H), 2.16 (d, $J = 4.5 \text{ Hz}$, 1H). $^{13}\text{C NMR}$ (101 MHz, CDCl_3) δ 144.45, 137.13, 134.93, 129.72, 128.85, 128.59, 128.01, 126.63, 41.33, 37.63, 32.96, 21.77. **HRMS** (+APCI) calculated for $\text{C}_{16}\text{H}_{18}\text{O}_2\text{N}^{\text{32}}\text{S}$ $[\text{M}+\text{H}]^+$ 288.10528, found 288.10601. **HPLC** (IA column 5% 2-propanol in hexanes, 1.0 mL/min) $t_R = 12.9 \text{ min}$ $[\alpha]_D^{22} -16.3^\circ$ ($c = 2.3$, CHCl_3)



(*S*)-2-benzyl-1-tosylaziridine ((*S*)-**2.136**)²⁶ (0.712 g, 50% yield) **¹H NMR** (400 MHz, CDCl₃) δ 7.68 (d, *J* = 8.3 Hz, 2H), 7.21 (d, *J* = 7.9 Hz, 2H), 7.19 – 7.11 (m, 3H), 7.09 – 7.00 (m, 2H), 2.95 (tt, *J* = 7.1, 4.9 Hz, 1H), 2.81 (dd, *J* = 14.4, 5.2 Hz, 1H), 2.74 – 2.64 (m, 2H), 2.42 (s, 3H), 2.17 (d, *J* = 4.5 Hz, 1H). **¹³C NMR** (¹³C NMR (101 MHz, CDCl₃) δ 144.45, 137.13, 134.93, 129.72, 128.84, 128.58, 128.00, 126.63, 41.33, 37.62, 32.96, 21.77. **HPLC** (IA column 5% 2-propanol in hexanes, 1.0 mL/min) *t*_R = 14.6 [α]_D²² 16.6° (*c* = 2.3, CHCl₃)

(R)-2-benzyl-1-tosylaziridine ((*R*)-2.136):

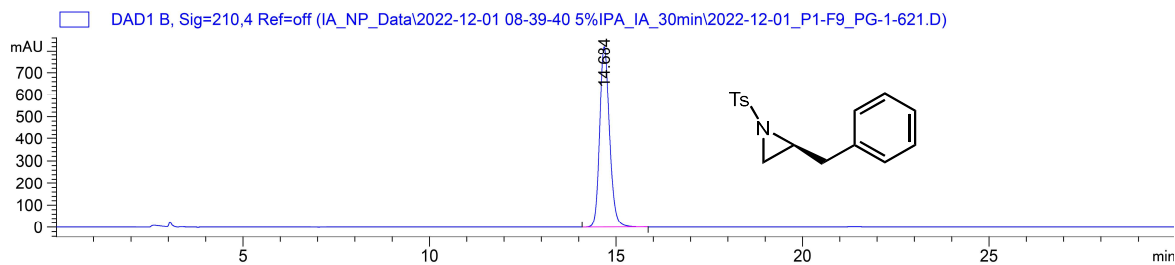


Signal 2: DAD1 B, Sig=210,4 Ref=off

| Peak # | RetTime [min] | Type | Width [min] | Area [mAU*s] | Height [mAU] | Area % |
|--------|---------------|------|-------------|--------------|--------------|----------|
| 1 | 12.996 | BB | 0.2626 | 2.39854e4 | 1370.93250 | 100.0000 |

Totals : 2.39854e4 1370.93250

(S)-2-benzyl-1-tosylaziridine ((*S*)-2.136):



Signal 2: DAD1 B, Sig=210,4 Ref=off

| Peak # | RetTime [min] | Type | Width [min] | Area [mAU*s] | Height [mAU] | Area % |
|--------|---------------|------|-------------|--------------|--------------|----------|
| 1 | 14.684 | BB | 0.2811 | 1.50120e4 | 820.03436 | 100.0000 |

Totals : 1.50120e4 820.03436

2.6.3 Supplemental Information References

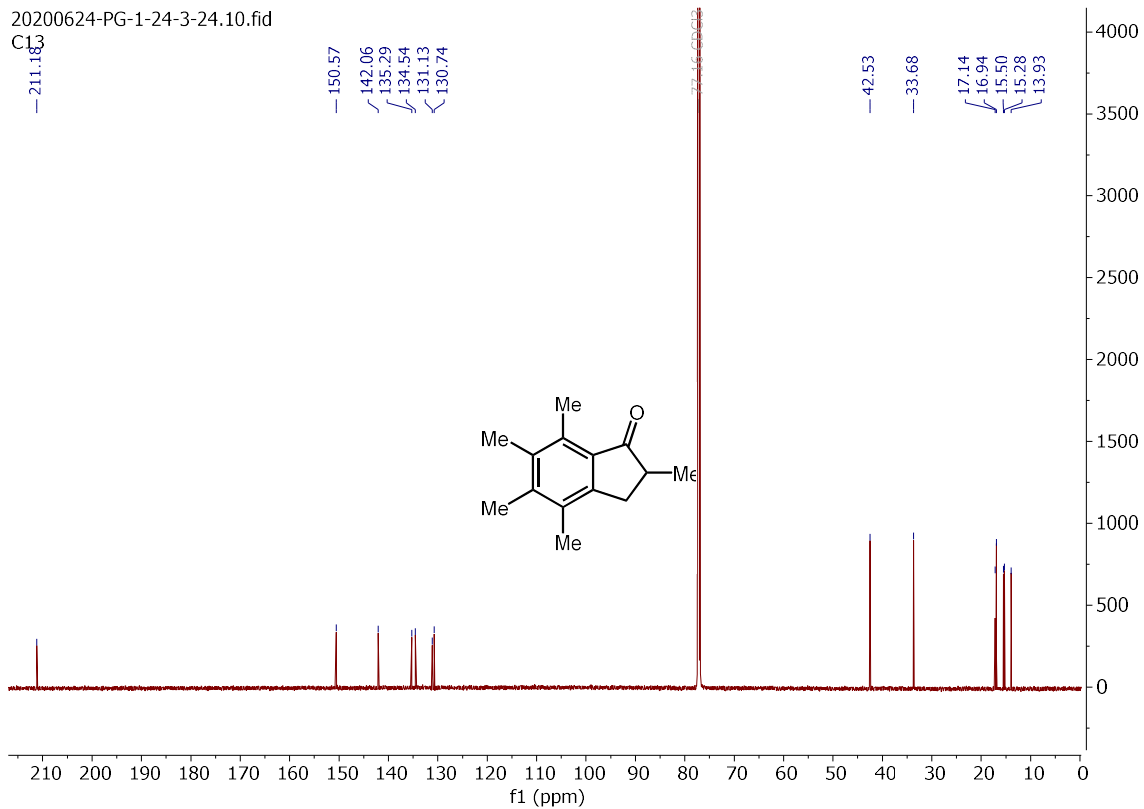
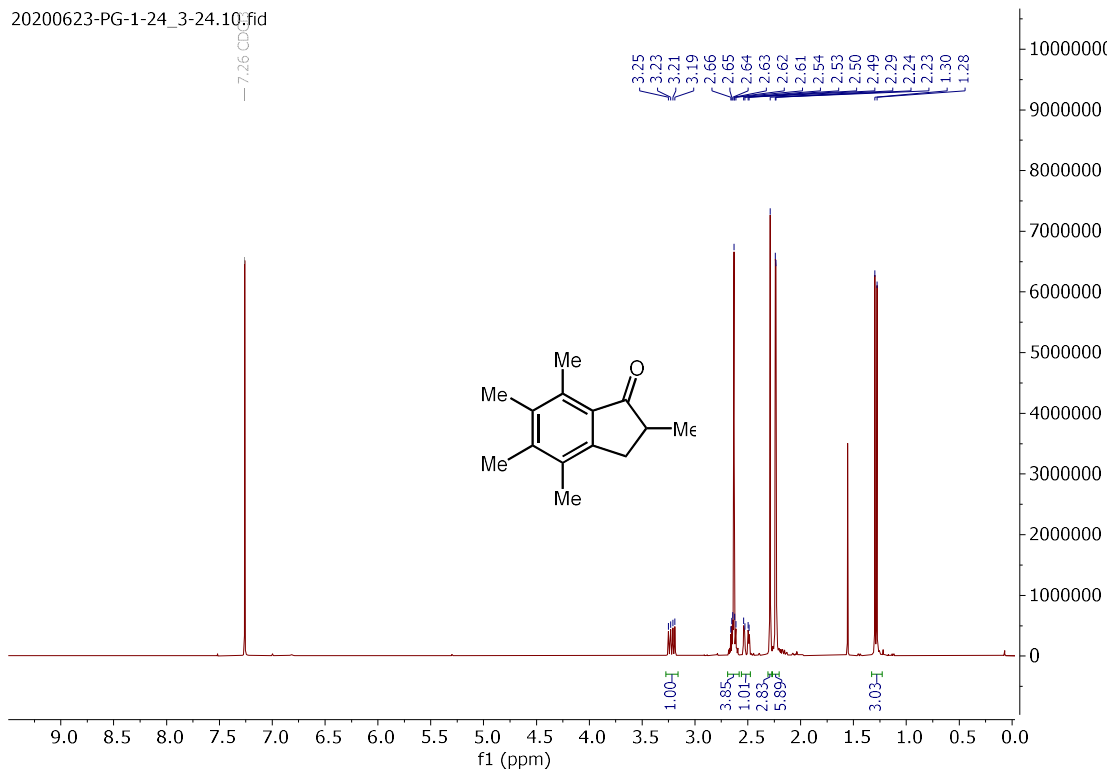
- (1) Semakul, N.; Jackson, K. E.; Paton, R. S.; Rovis, T. Heptamethylindenyl (Ind*) enables diastereoselective benzamidation of cyclopropenes via Rh(iii)-catalyzed C-H activation. *Chem Sci* **2017**, *8* (2), 1015.
- (2) Arnold, T. A. Q.; Buffet, J. C.; Turner, Z. R.; O'Hare, D. Synthesis, characterisation, and polymerisation studies of hexamethylindenyl zirconocenes and hafnocenes. *J. Organomet. Chem.* **2015**, *792*, 55.
- (3) Yan, Z.; Chong, S.; Lin, H.; Yang, Q.; Wang, X.; Zhang, W.; Zhang, X.; Zeng, Z.; Su, Y. Design, synthesis and biological evaluation of tetrazole-containing RXR α ligands as anticancer agents. *Eur. J. Med. Chem.* **2019**, *164*, 562.
- (4) Farr, C. M. B.; Kazerouni, A. M.; Park, B.; Poff, C. D.; Won, J.; Sharp, K. R.; Baik, M. H.; Blakey, S. B. Designing a Planar Chiral Rhodium Indenyl Catalyst for Regio- and Enantioselective Allylic C-H Amidation. *J. Am. Chem. Soc.* **2020**, *142* (32), 13996.
- (5) Wang, A.; Venditto, N. J.; Darcy, J. W.; Emmert, M. H. Nondirected, Cu-Catalyzed sp³ C-H Aminations with Hydroxylamine-Based Amination Reagents: Catalytic and Mechanistic Studies. *Organometallics* **2017**, *36* (7), 1259.
- (6) Matsumoto, K.; Usuda, K.; Okabe, H.; Hashimoto, M.; Shimada, Y. Synthesis of optically active heterocyclic compounds via deracemization of 1,2-diol monotosylate derivatives bearing a long aliphatic chain by a combination of enzymatic hydrolysis with Mitsunobu inversion. *Tetrahedron: Asymmetry* **2013**, *24* (2), 108.
- (7) Brown, H. C.; Lynch, G. J. Solvomercuration-demercuration. 8. Oxymercuration-demercuration of methoxy-, hydroxy- and acetoxy-substituted alkenes. *The Journal of Organic Chemistry* **1981**, *46* (3), 531.
- (8) Kalyankar, K. B.; Das, S. First total synthesis of 5(S)-hydroxyrecifeiolide. *Synth. Commun.* **2020**, *50* (3), 322.

- (9) Karabiyikoglu, S.; Boon, B. A.; Merlic, C. A. Cycloaddition Reactions of Cobalt-Complexed Macrocyclic Alkynes: The Transannular Pauson–Khand Reaction. *The Journal of Organic Chemistry* **2017**, *82* (15), 7732.
- (10) Smith, B. J.; Sulikowski, G. A. Total Synthesis of (±)-Haliclonyclamine C. *Angew. Chem. Int. Ed.* **2010**, *49* (9), 1599.
- (11) Bender, T. A.; Bergman, R. G.; Raymond, K. N.; Toste, F. D. A Supramolecular Strategy for Selective Catalytic Hydrogenation Independent of Remote Chain Length. *J. Am. Chem. Soc.* **2019**, *141* (30), 11806.
- (12) Marsh, G. P.; Parsons, P. J.; McCarthy, C.; Corniquet, X. G. An Efficient Synthesis of Nitroalkenes by Alkene Cross Metathesis: Facile Access to Small Ring Systems. *Org. Lett.* **2007**, *9* (14), 2613.
- (13) Yang, C.; Gao, Y.; Bai, S.; Jiang, C.; Qi, X. Chemoselective Cross-Coupling of gem-Borazirconocene Alkanes with Aryl Halides. *J. Am. Chem. Soc.* **2020**, *142* (26), 11506.
- (14) Basauri-Molina, M.; Verhoeven, D. G. A.; van Schaik, A. J.; Kleijn, H.; Klein Gebbink, R. J. M. Ring-Closing and Cross-Metathesis with Artificial Metalloenzymes Created by Covalent Active Site-Directed Hybridization of a Lipase. *Chemistry – A European Journal* **2015**, *21* (44), 15676.
- (15) Li, Y.-G.; Li, L.; Yang, M.-Y.; He, G.; Kantchev, E. A. B. A Bulky Disulfoxide Ligand for Pd-Catalyzed Oxidative Allylic C–H Amination with 2,2,2-Trichloroethyl Tosyl Carbamate. *The Journal of Organic Chemistry* **2017**, *82* (9), 4907.
- (16) Buslov, I.; Becouse, J.; Mazza, S.; Montandon-Clerc, M.; Hu, X. Chemoselective Alkene Hydrosilylation Catalyzed by Nickel Pincer Complexes. *Angew. Chem. Int. Ed.* **2015**, *54* (48), 14523.
- (17) Meng, Q.-Y.; Schirmer, T. E.; Katou, K.; König, B. Controllable Isomerization of Alkenes by Dual Visible-Light-Cobalt Catalysis. *Angew. Chem. Int. Ed.* **2019**, *58* (17), 5723.
- (18) Li, X.; He, S.; Song, Q. Diethylzinc-Mediated Radical 1,2-Addition of Alkenes and Alkynes. *Org. Lett.* **2021**, *23* (8), 2994.

- (19) Cruz, D. A.; Sinka, V.; de Armas, P.; Steingruber, H. S.; Fernández, I.; Martín, V. S.; Miranda, P. O.; Padrón, J. I. Iron(II) and Copper(I) Control the Total Regioselectivity in the Hydrobromination of Alkenes. *Org. Lett.* **2021**, *23* (15), 6105.
- (20) Cleveland, A. H.; Fronczek, F. R.; Kartika, R. Synthesis of Vicinal Dichlorides via Activation of Aliphatic Terminal Epoxides with Triphosgene and Pyridine. *The Journal of Organic Chemistry* **2018**, *83* (6), 3367.
- (21) Maust, M. C.; Hendy, C. M.; Jui, N. T.; Blakey, S. B. Switchable Regioselective 6-endo or 5-exo Radical Cyclization via Photoredox Catalysis. *J. Am. Chem. Soc.* **2022**, *144* (9), 3776.
- (22) Yadav, J. S.; Kumar, G. G. K. S. N. A concise stereoselective formal total synthesis of the cytotoxic macrolide (+)-Neopeltolide via Prins cyclization. *Tetrahedron* **2010**, *66* (2), 480.
- (23) Breitenbach, R.; Chiu, C. K. F.; Massett, S. S.; Meltz, M.; Murtiashaw, C. W.; Pezzullo, S. L.; Staigers, T. A practical synthesis of 3(S)-methyl-heptanoic acid from (S)-citronellol. *Tetrahedron-Asymmetry* **1996**, *7* (2), 435.
- (24) Wu, B.; Woodward, R.; Wen, L.; Wang, X.; Zhao, G.; Wang, P. G. Synthesis of a Comprehensive Polyprenol Library for Evaluation of Bacterial Enzyme Lipid Substrate Specificity. *European J Org Chem* **2013**, *2013* (36), 8162.
- (25) Kumar, S. M.; Prasad, K. R. Enantiospecific formal total synthesis of iriomoteolide 3a. *Chem Asian J* **2014**, *9* (12), 3431.
- (26) Perez, S. J.; Purino, M. A.; Cruz, D. A.; Lopez-Soria, J. M.; Carballo, R. M.; Ramirez, M. A.; Fernandez, I.; Martin, V. S.; Padron, J. I. Enantiodivergent Synthesis of (+)- and (-)-Pyrrolidine 197B: Synthesis of trans-2,5-Disubstituted Pyrrolidines by Intramolecular Hydroamination. *Chemistry* **2016**, *22* (43), 15529.

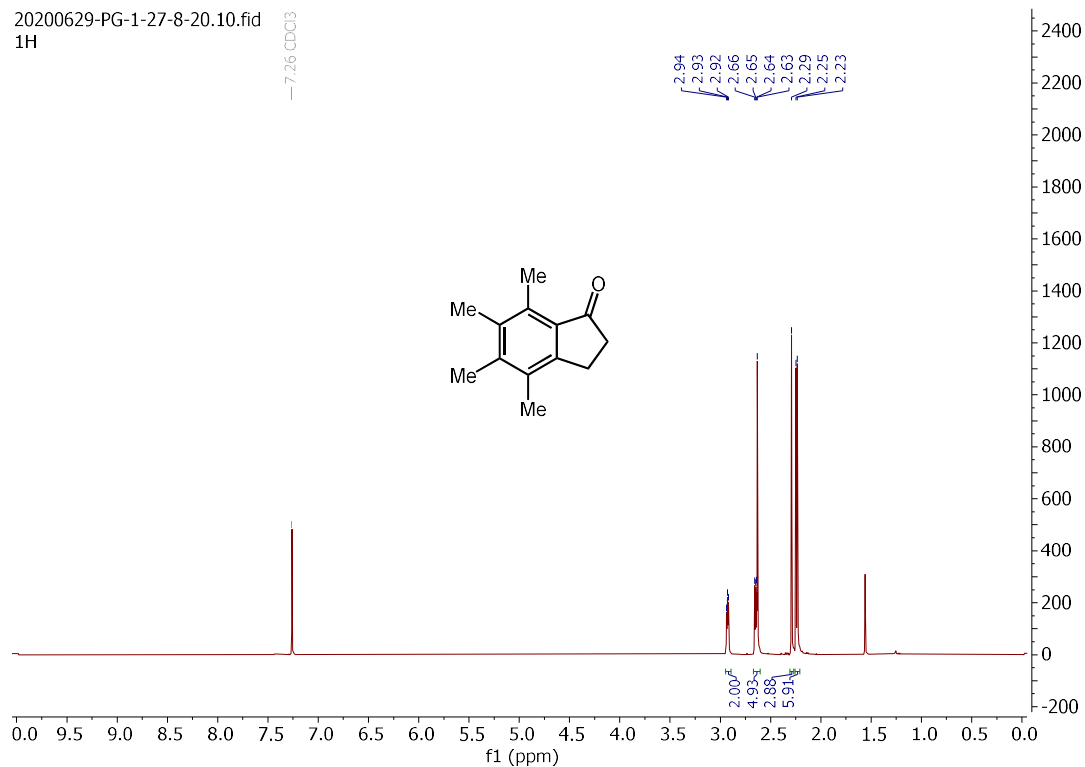
2.6.4 NMR and HPLC Data

2,4,5,6,7-pentamethyl-2,3-dihydro-1H-inden-1-one (2.88):

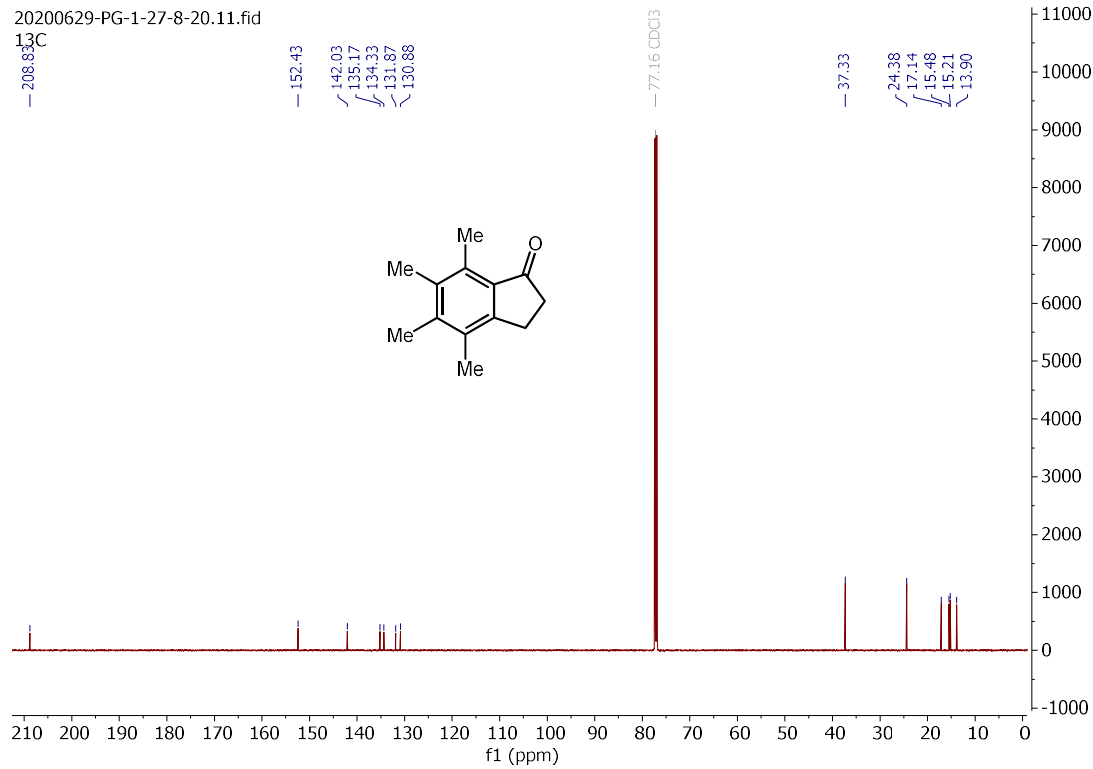


4,5,6,7-tetramethyl-2,3-dihydro-1H-inden-1-one (2.94):

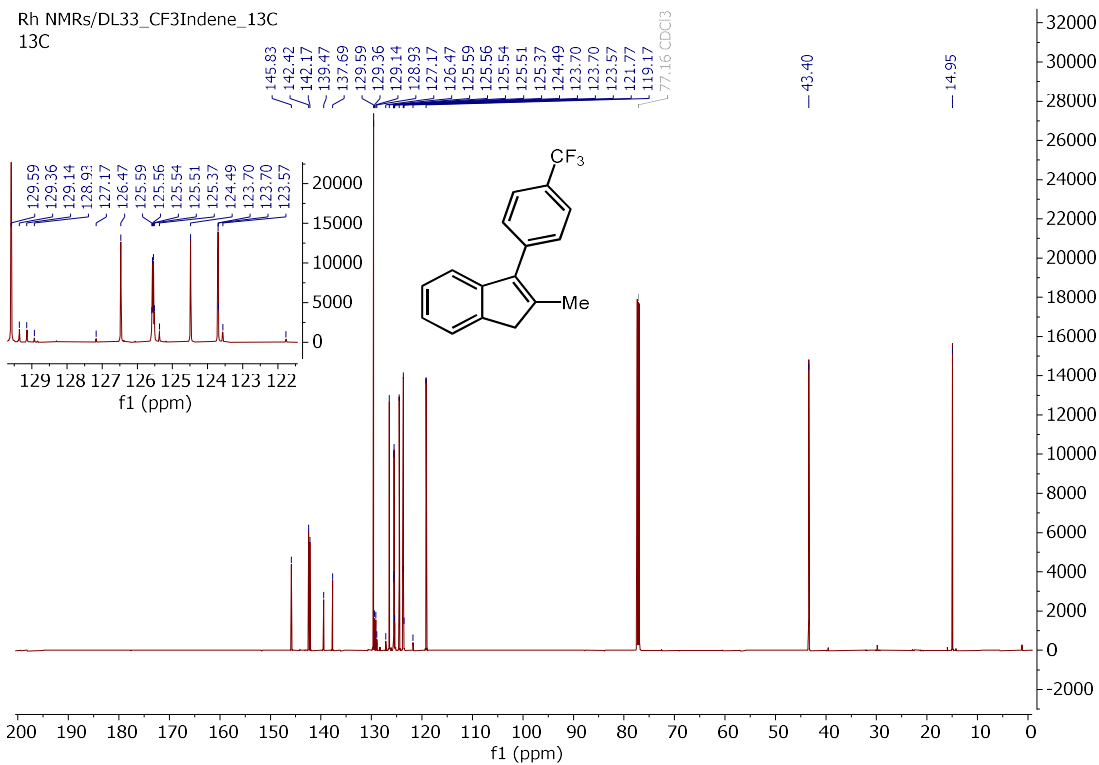
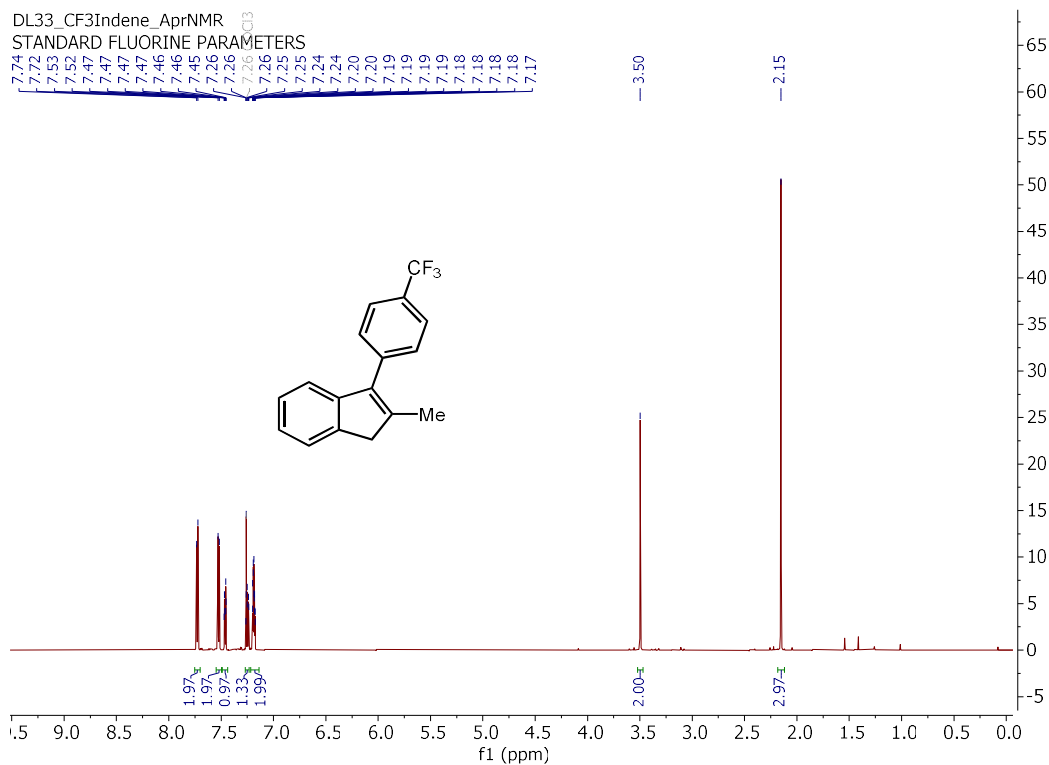
20200629-PG-1-27-8-20.10.fid
1H



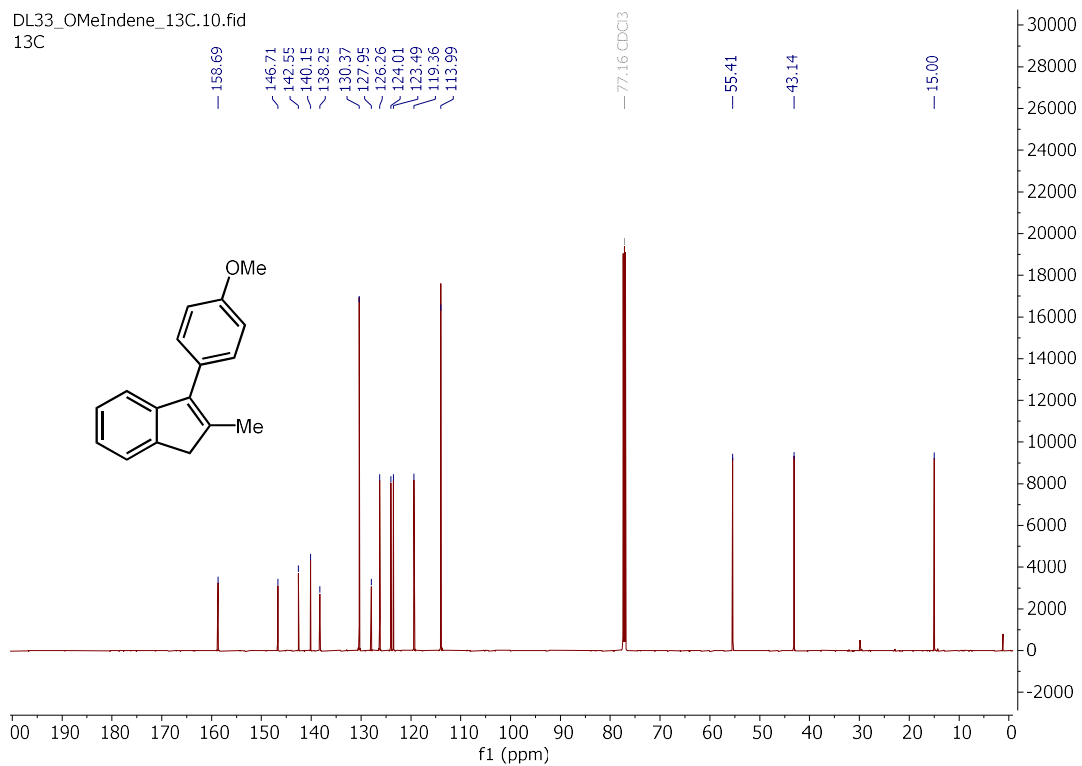
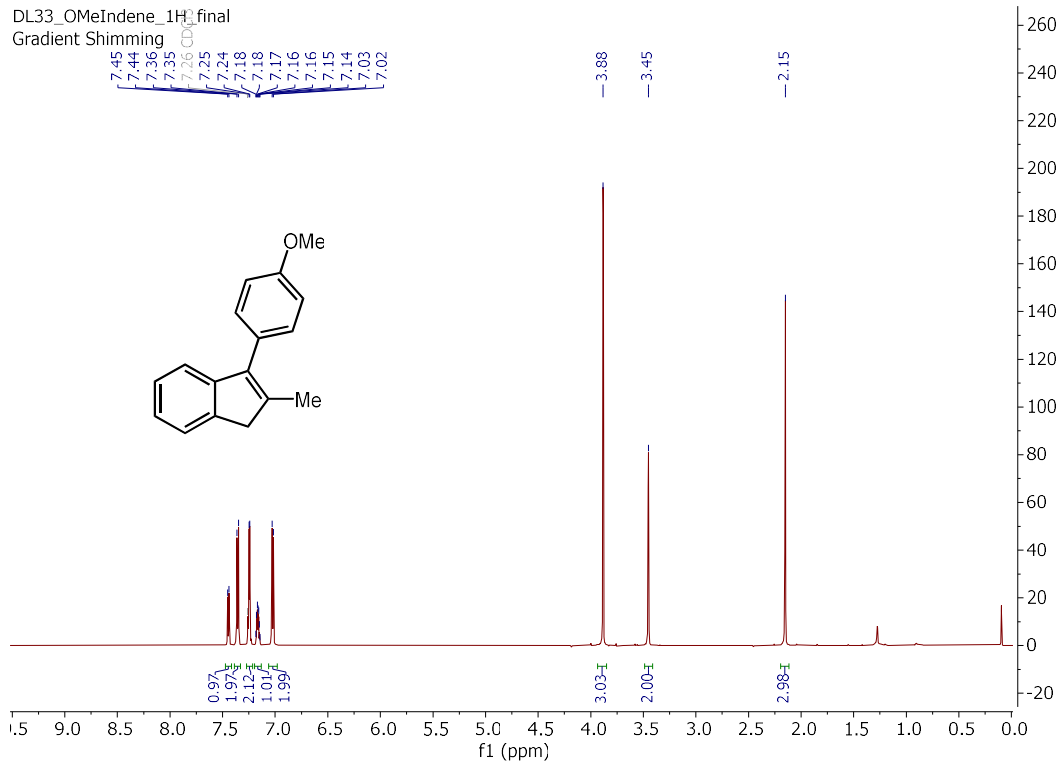
20200629-PG-1-27-8-20.11.fid
13C



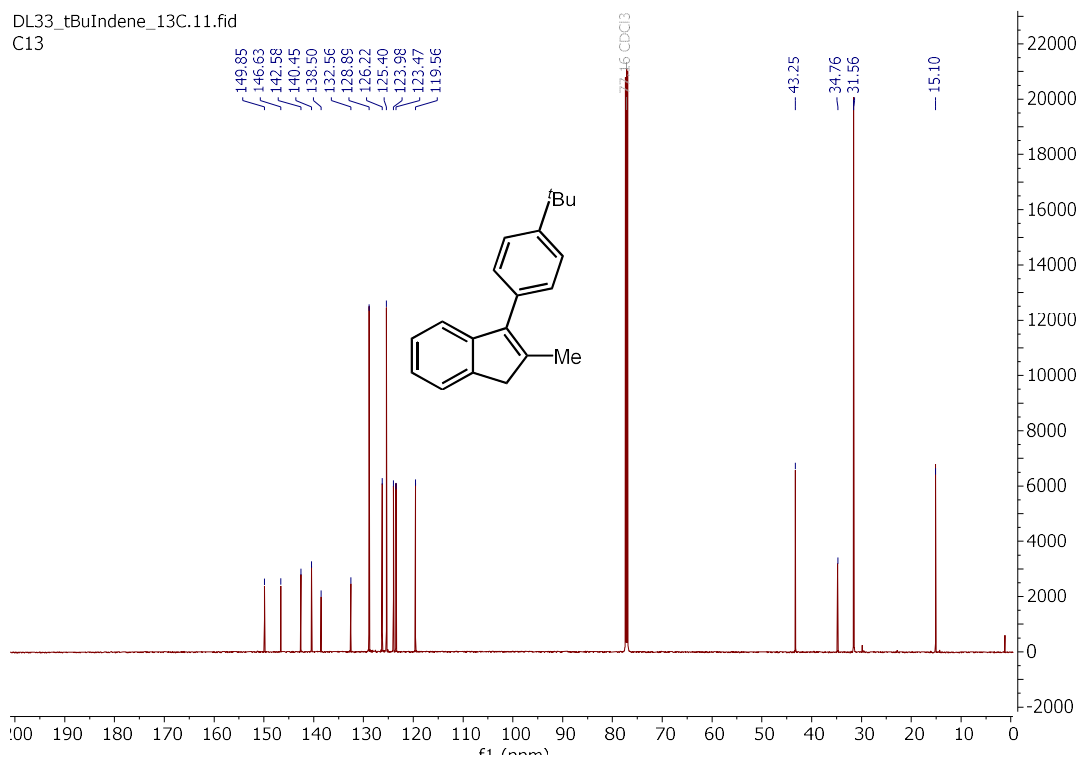
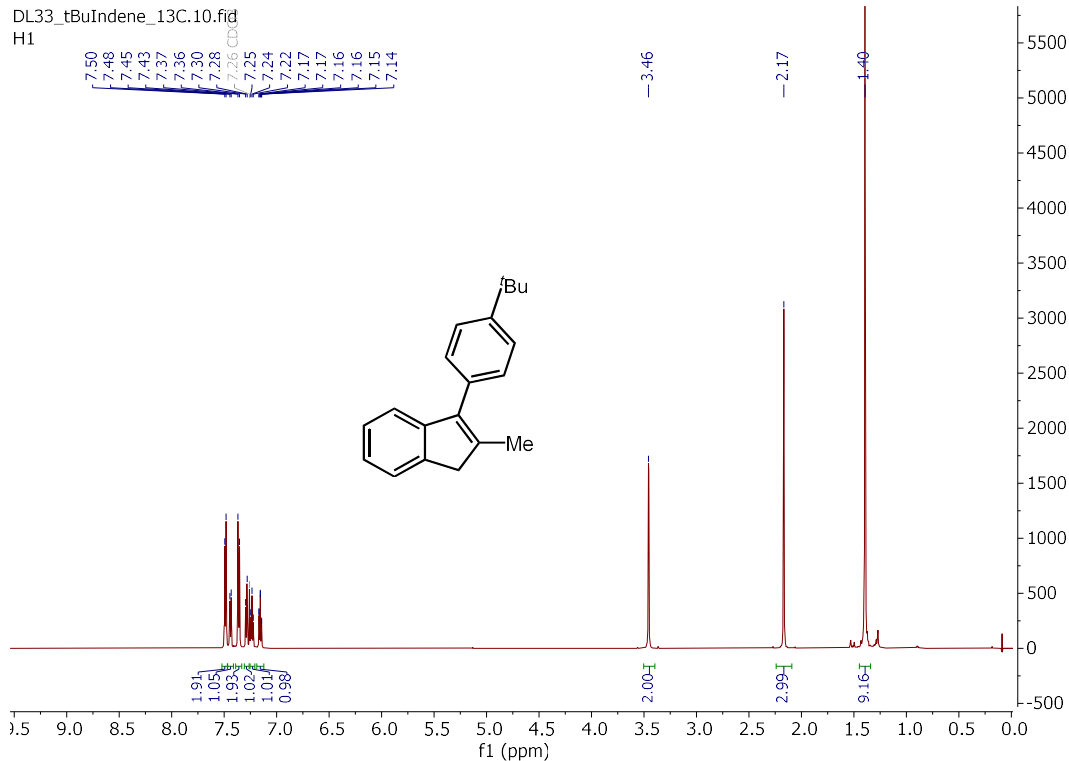
2-methyl-3-(4-(trifluoromethyl)phenyl)-1H-indene (S1):



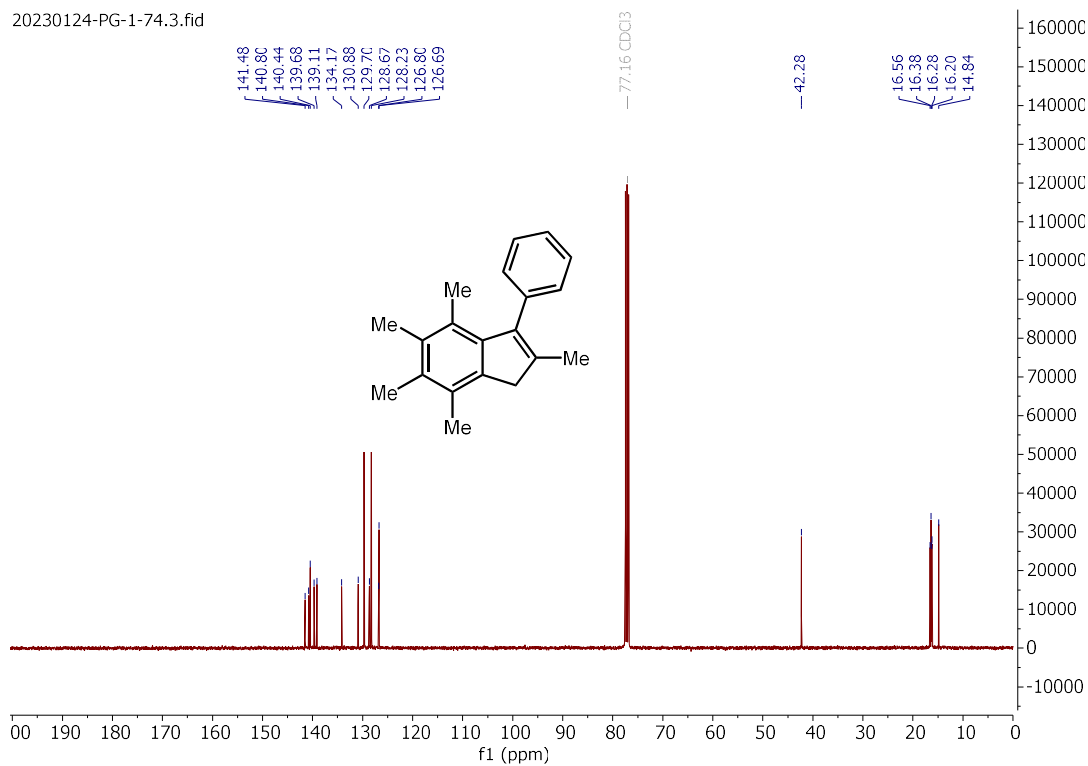
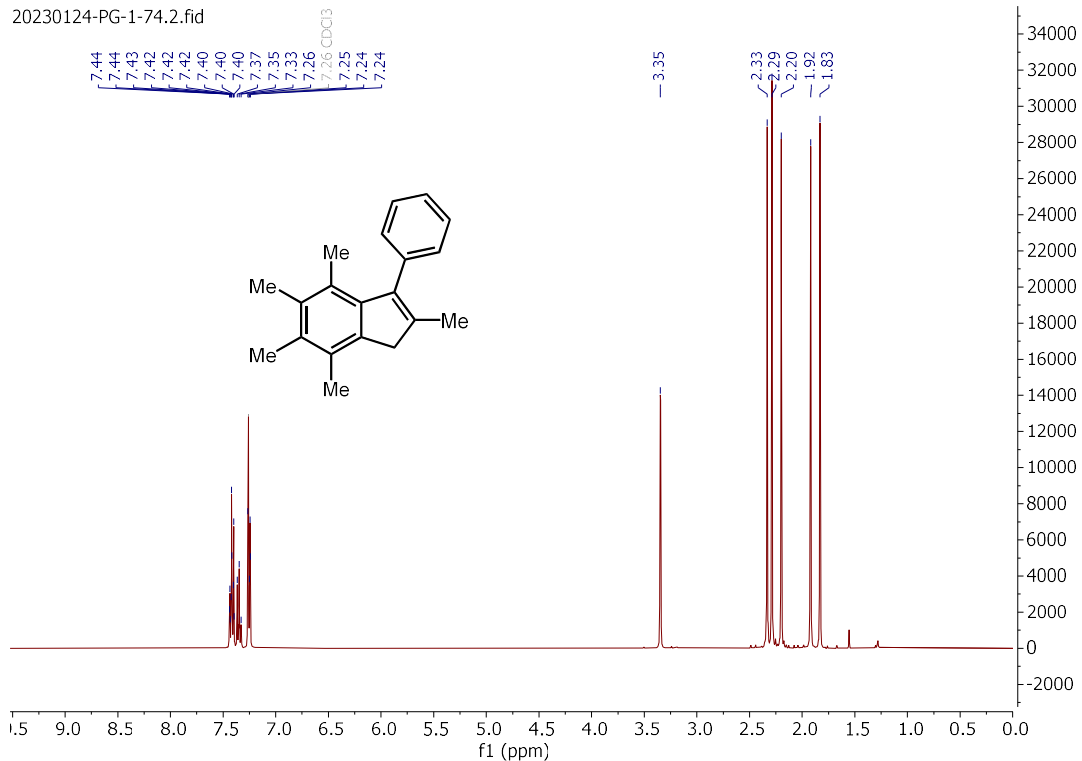
3-(4-methoxyphenyl)-2-methyl-1H-indene (**S2**):



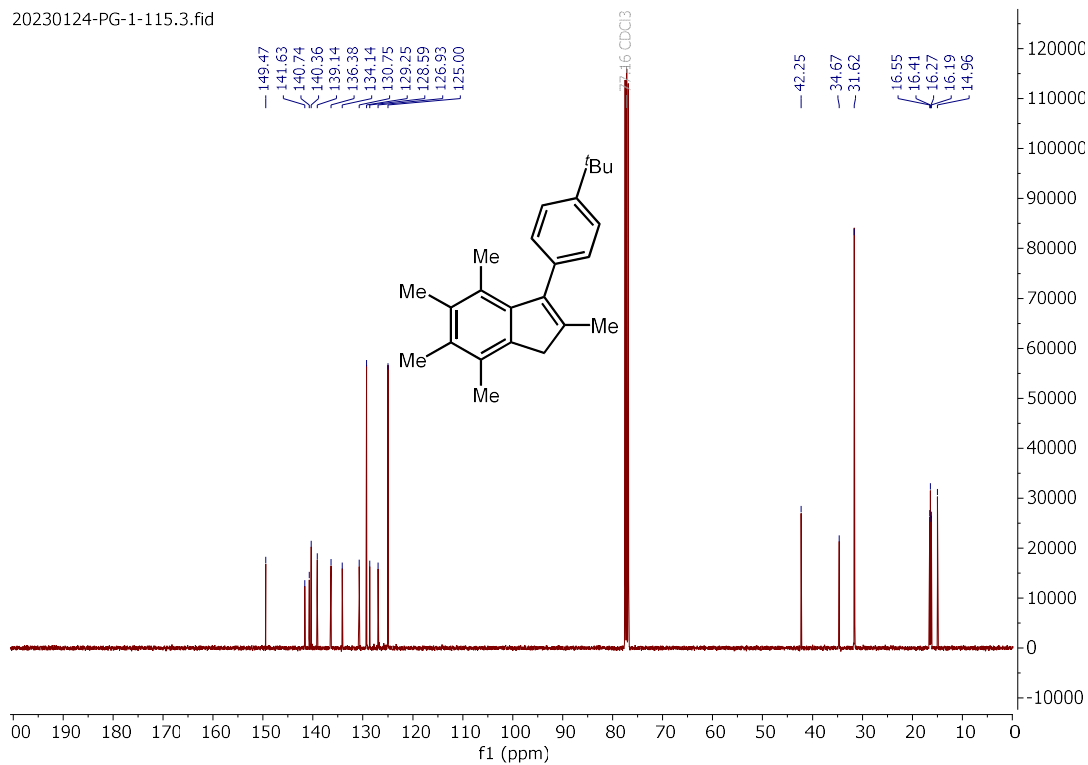
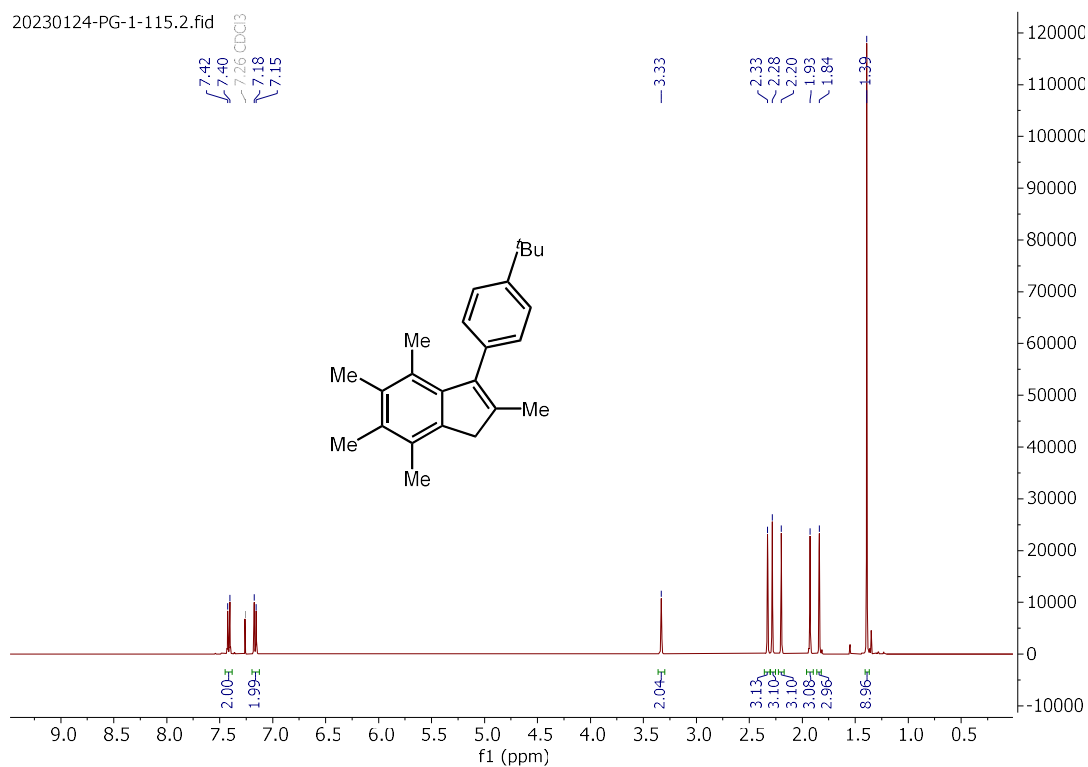
3-(4-(*tert*-butyl)phenyl)-2-methyl-1*H*-indene (**S3**):



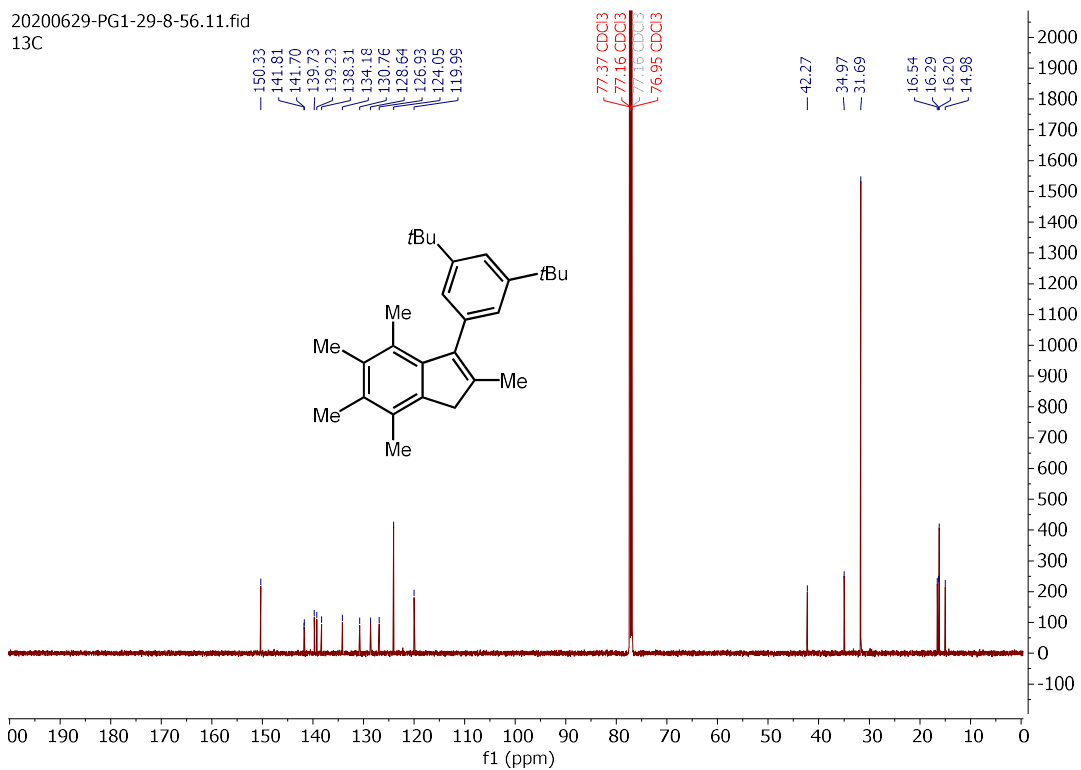
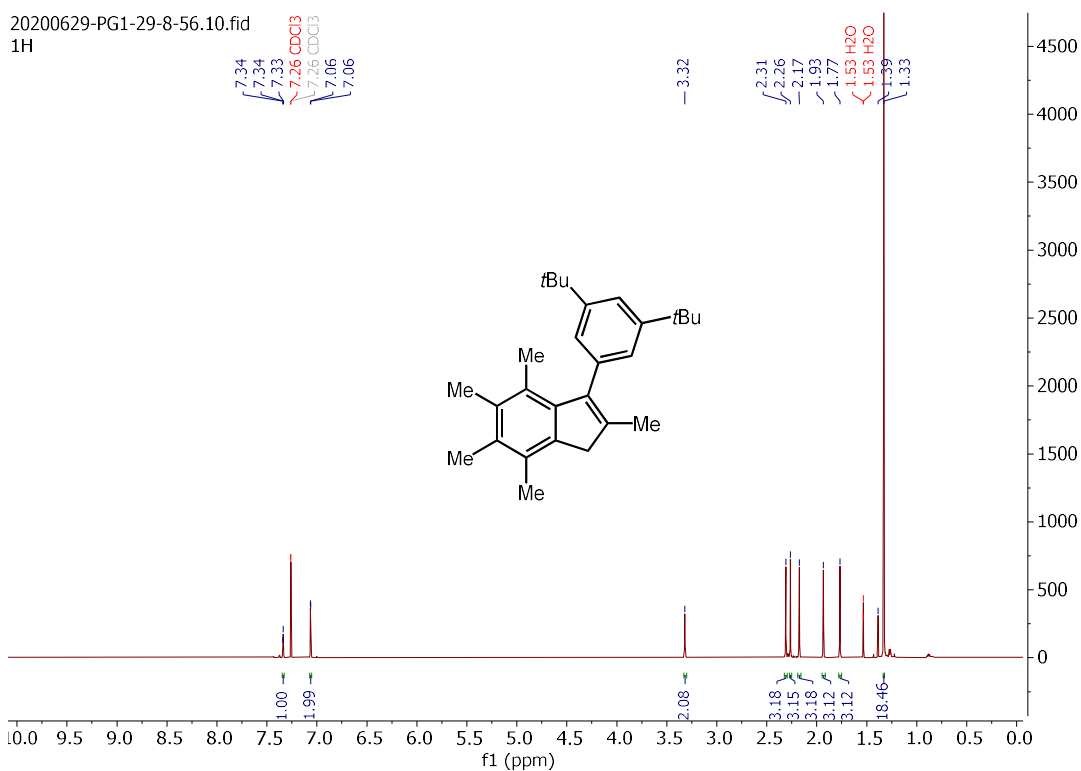
2,4,5,6,7-pentamethyl-3-phenyl-1H-indene (**S4**):



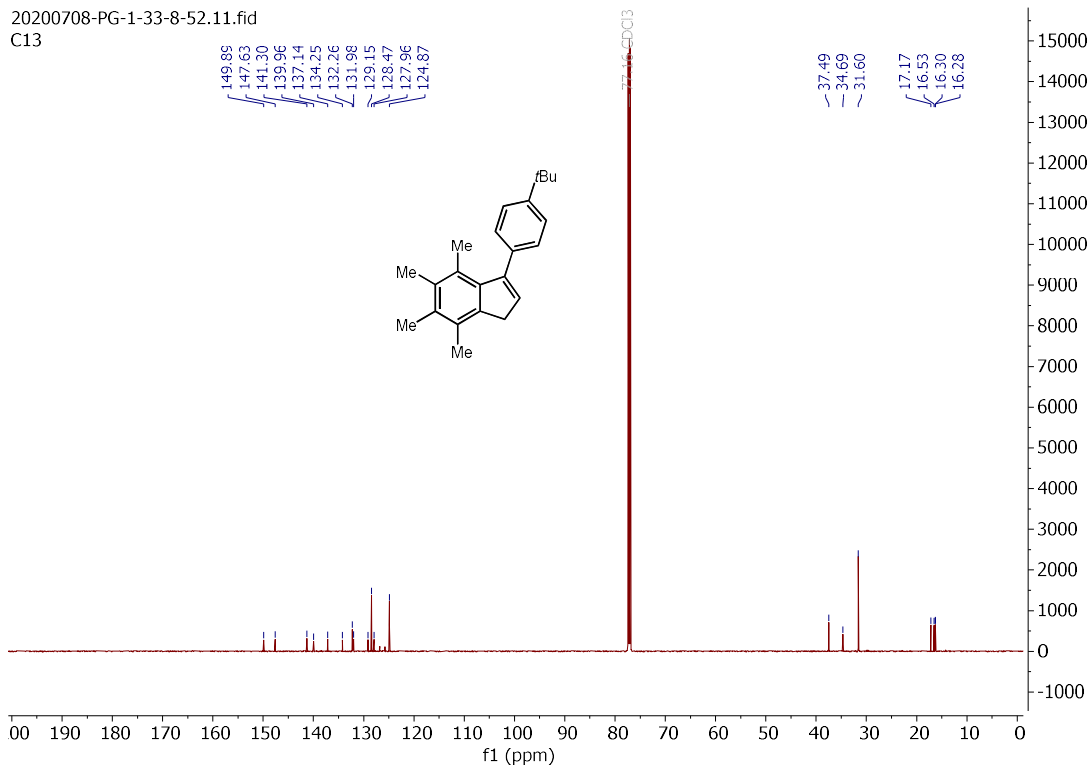
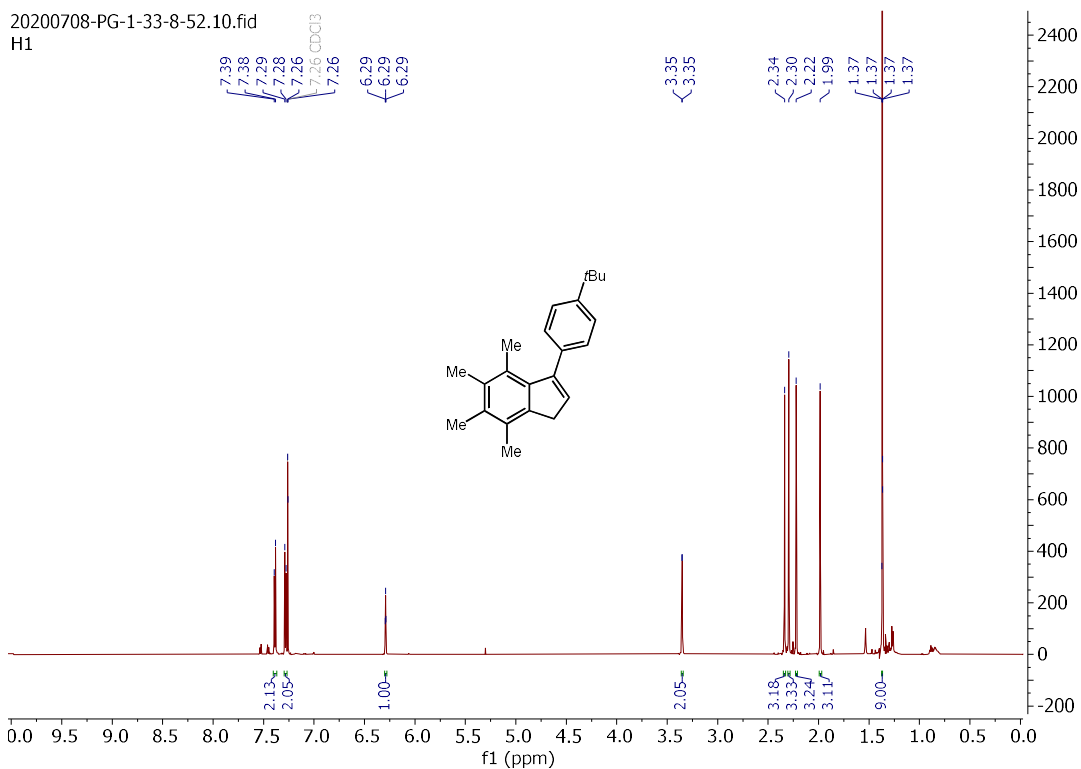
3-(4-(tert-butyl)phenyl)-2,4,5,6,7-pentamethyl-1H-indene (**2.89**):



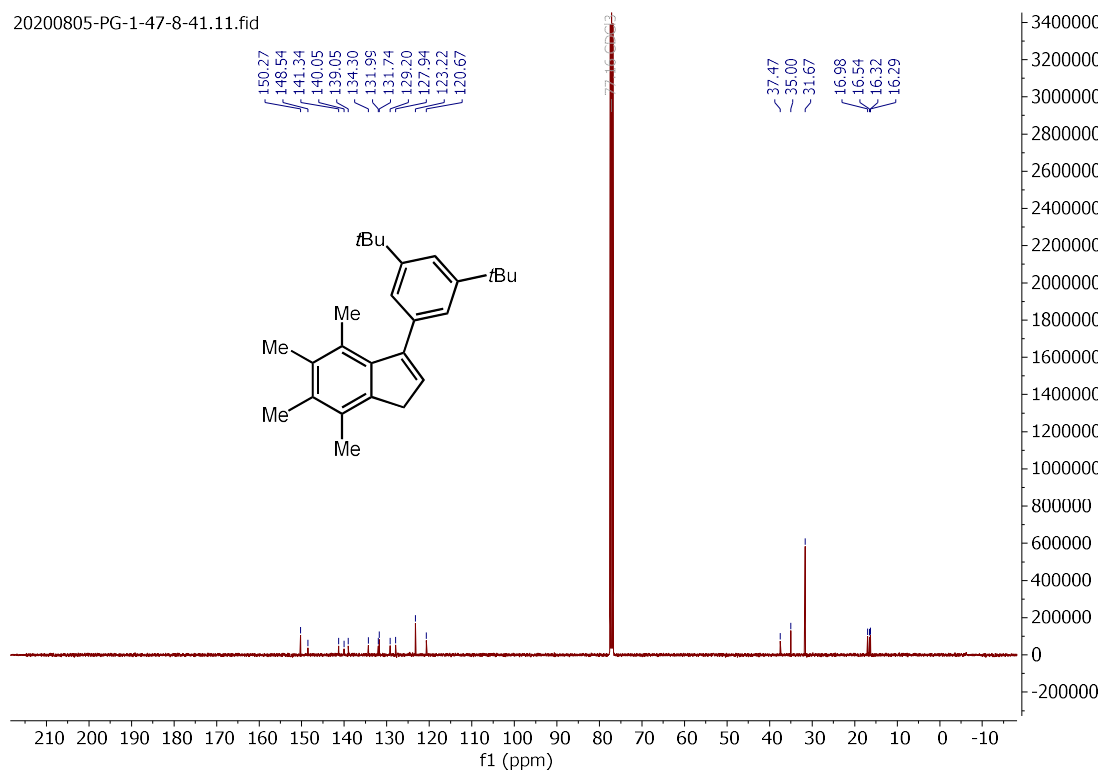
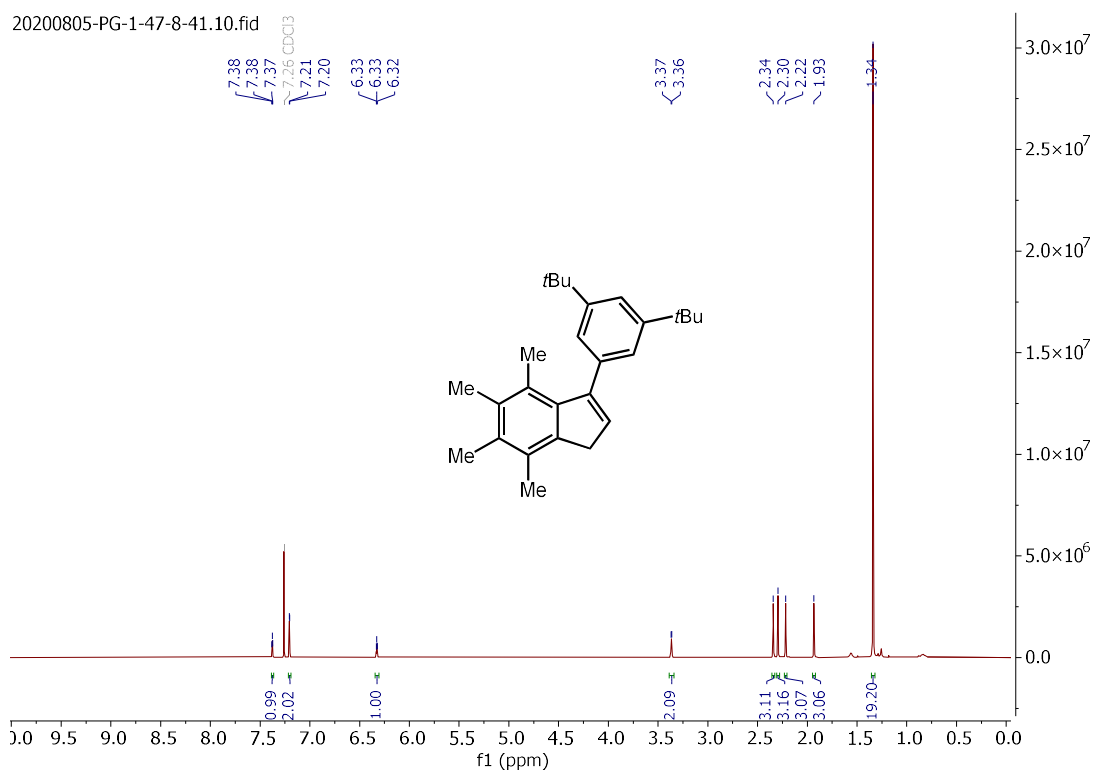
3-(3,5-di-tert-butylphenyl)-2,4,5,6,7-pentamethyl-1H-indene (2.90):



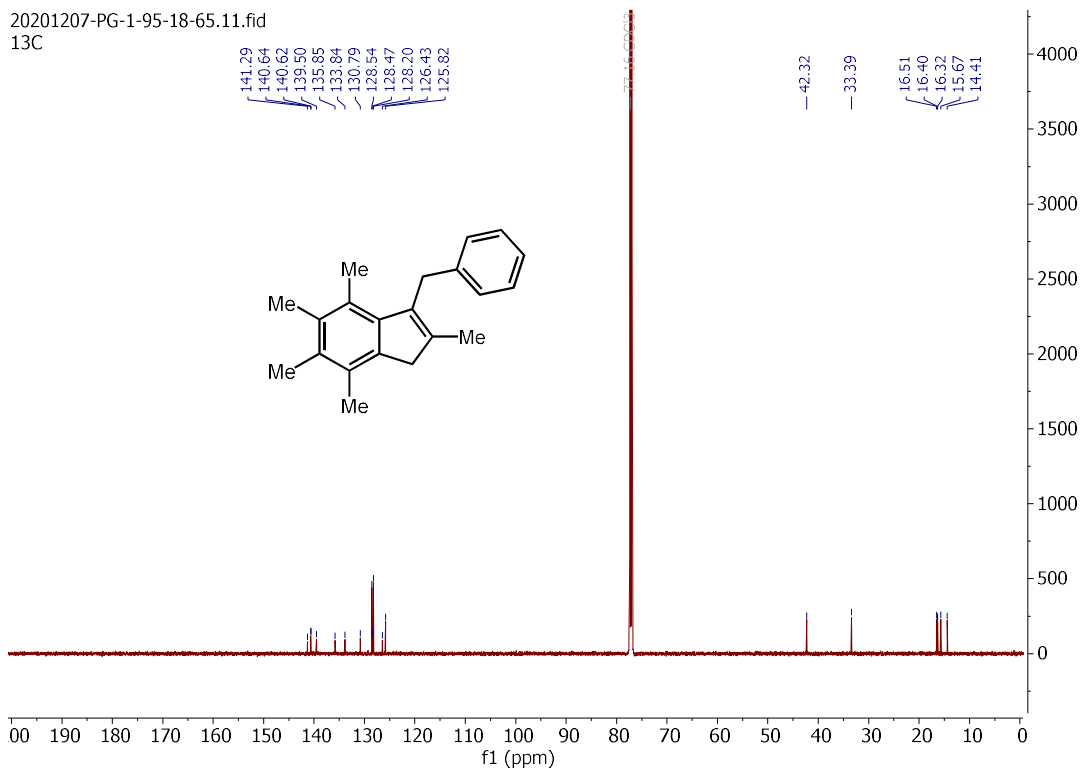
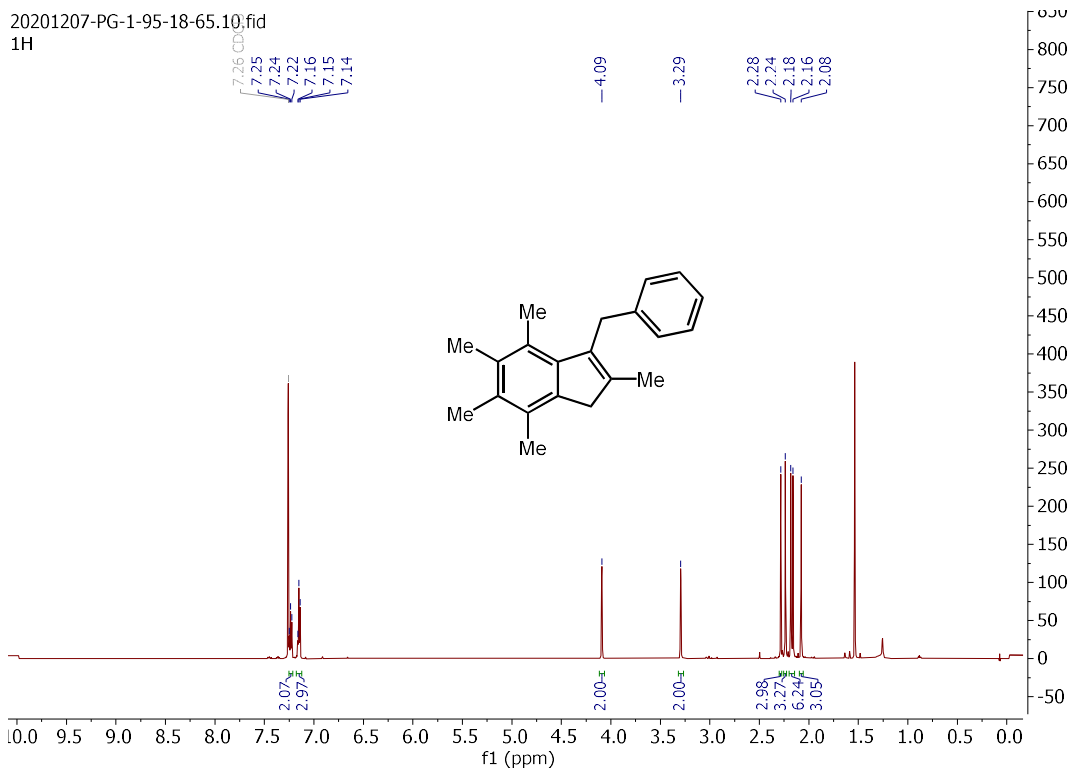
3-(4-(*tert*-butyl)phenyl)-4,5,6,7-tetramethyl-1*H*-indene (**2.95**):



3-(3,5-di-tert-butylphenyl)-4,5,6,7-tetramethyl-1H-indene (2.96):

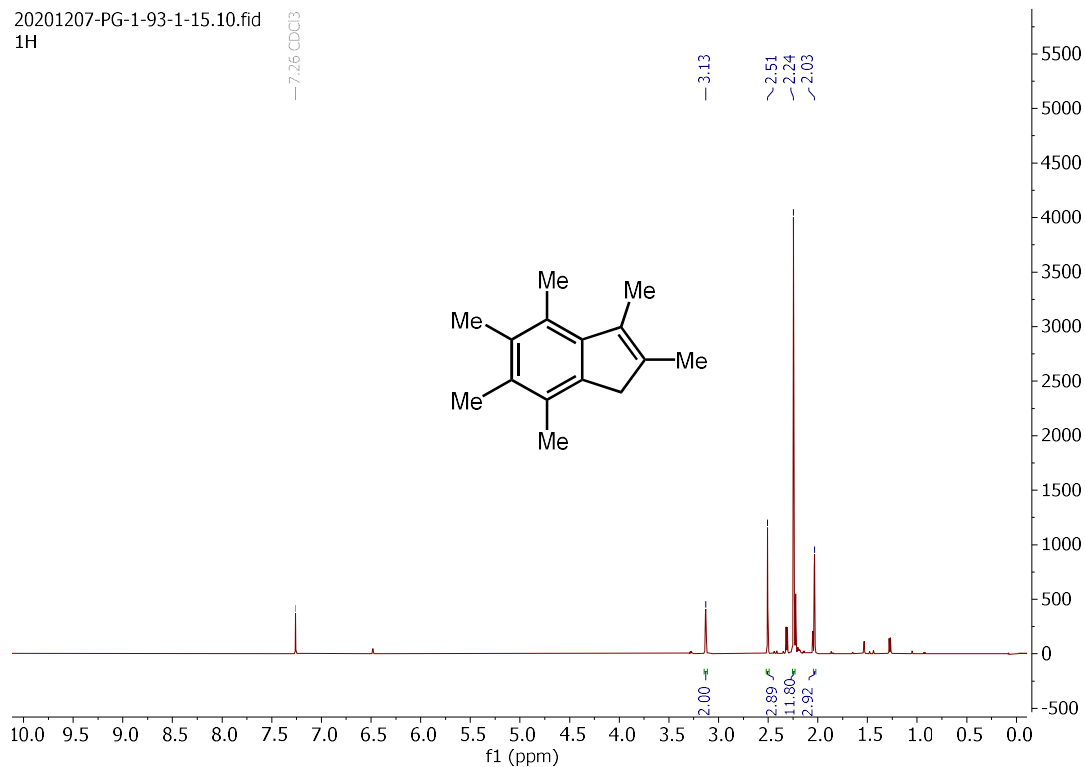


3-benzyl-2,4,5,6,7-pentamethyl-1H-indene (**2.91**):

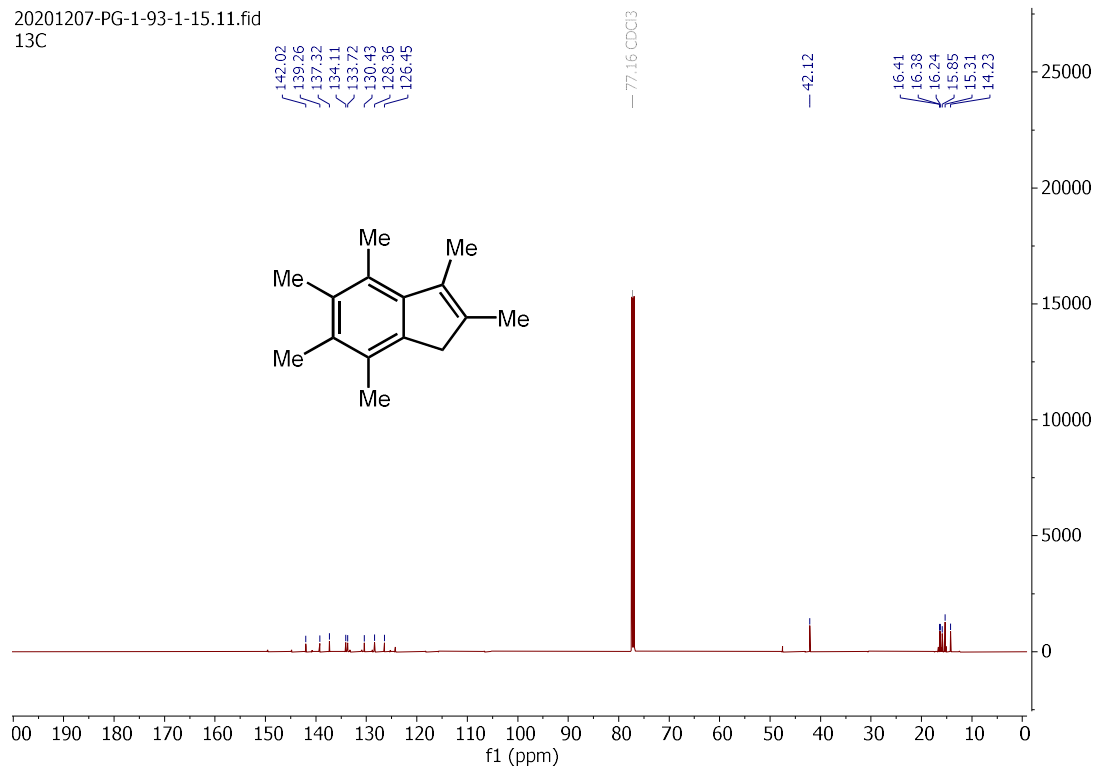


2,3,4,5,6,7-hexamethyl-1H-indene (2.92):

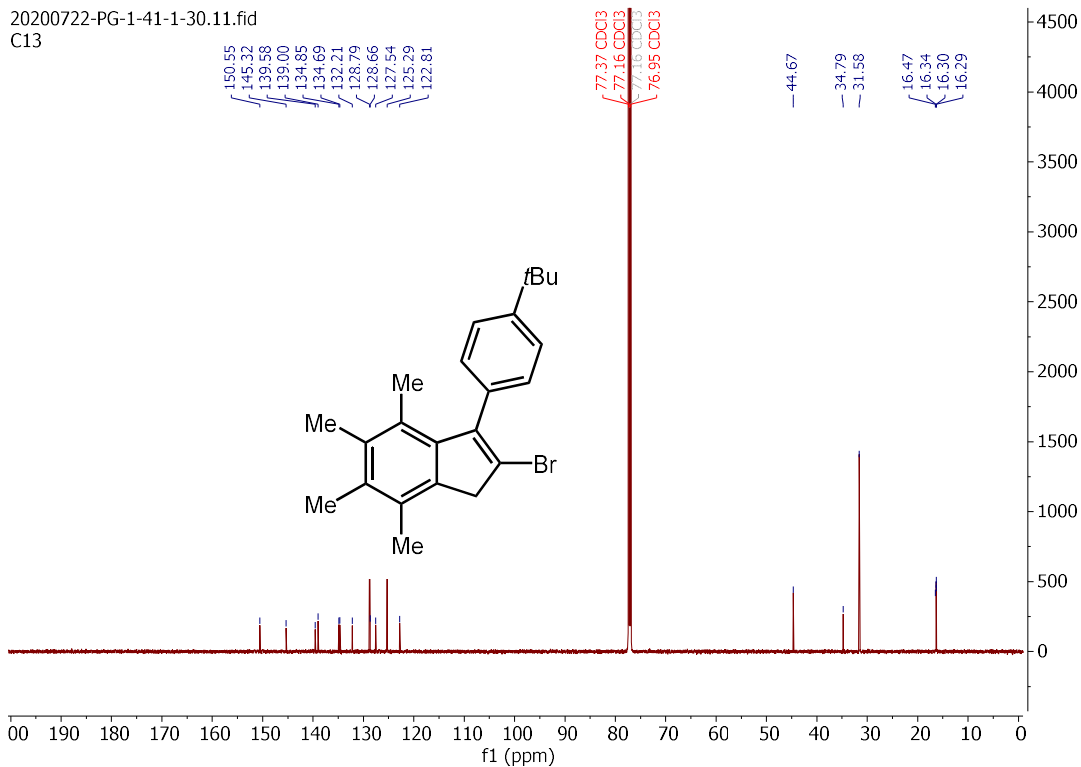
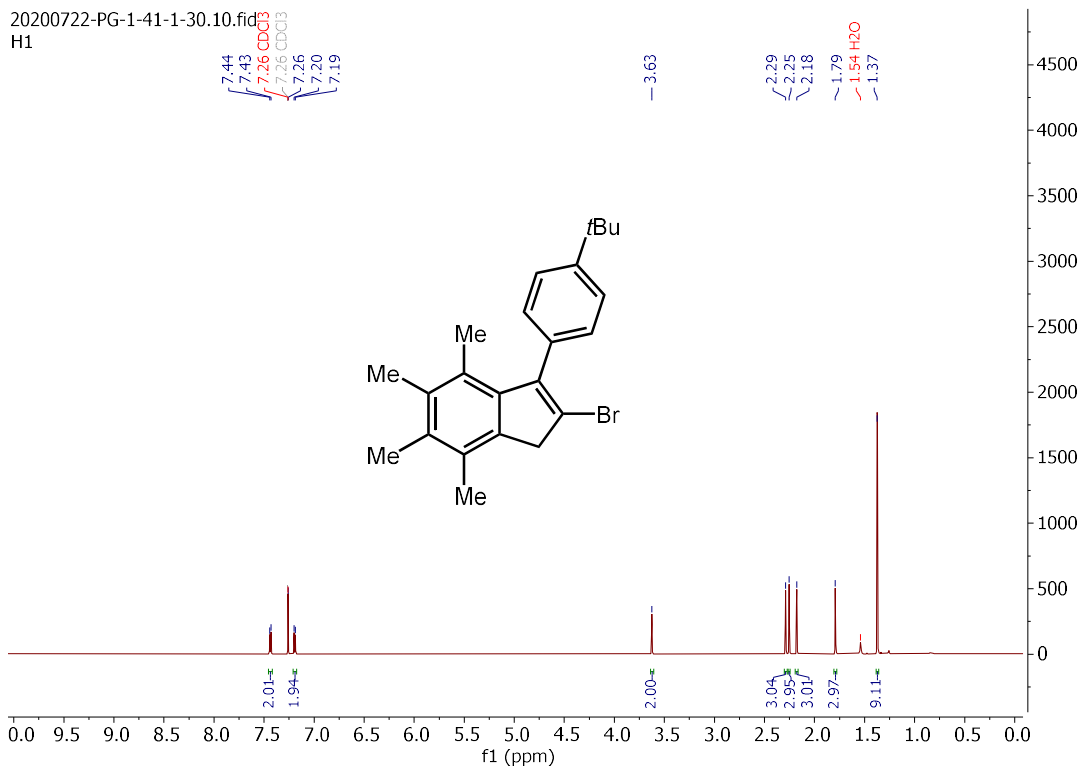
20201207-PG-1-93-1-15.10.fid
1H



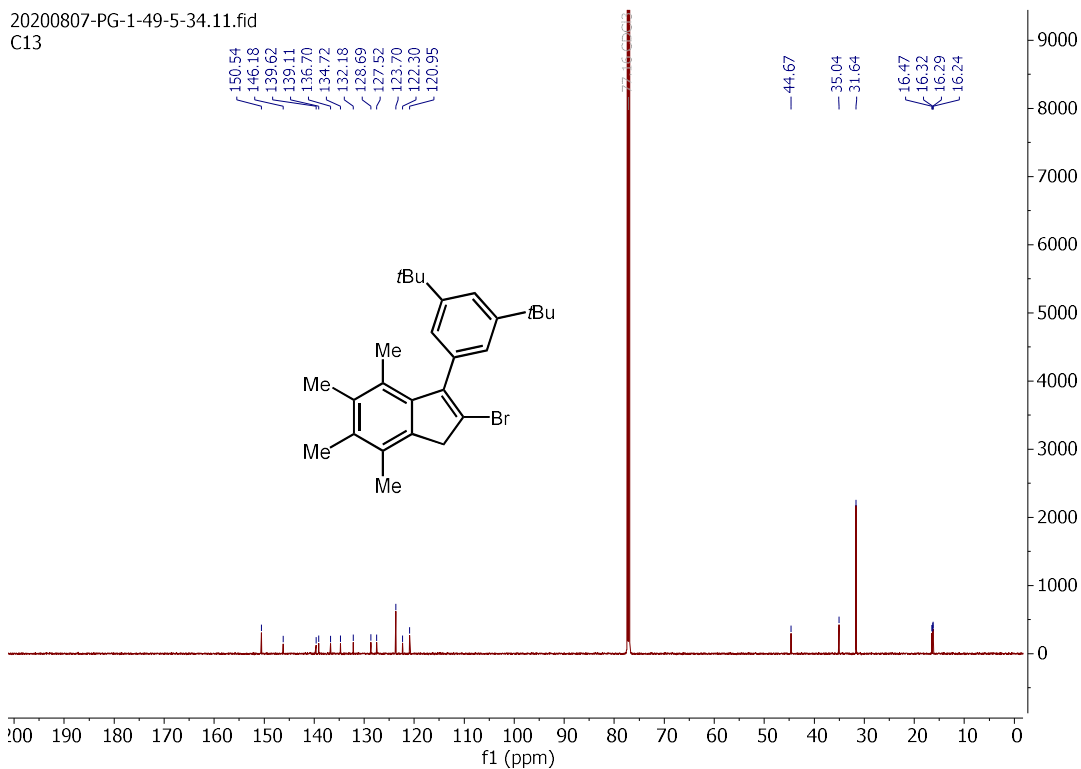
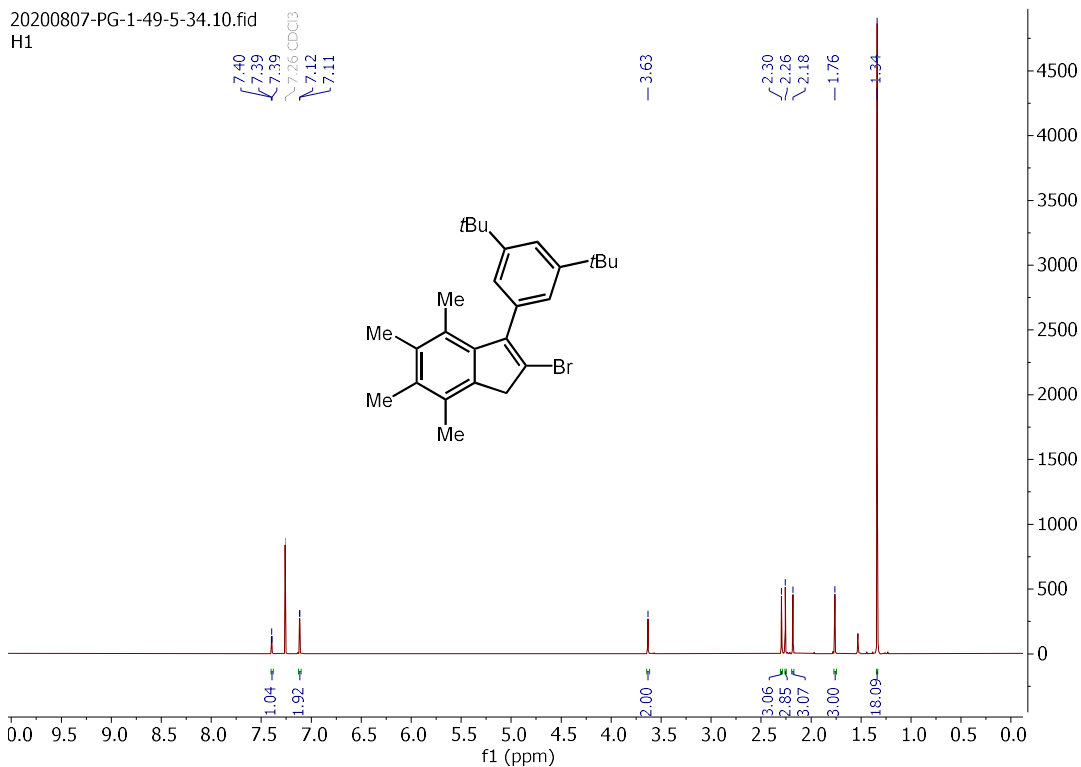
20201207-PG-1-93-1-15.11.fid
13C



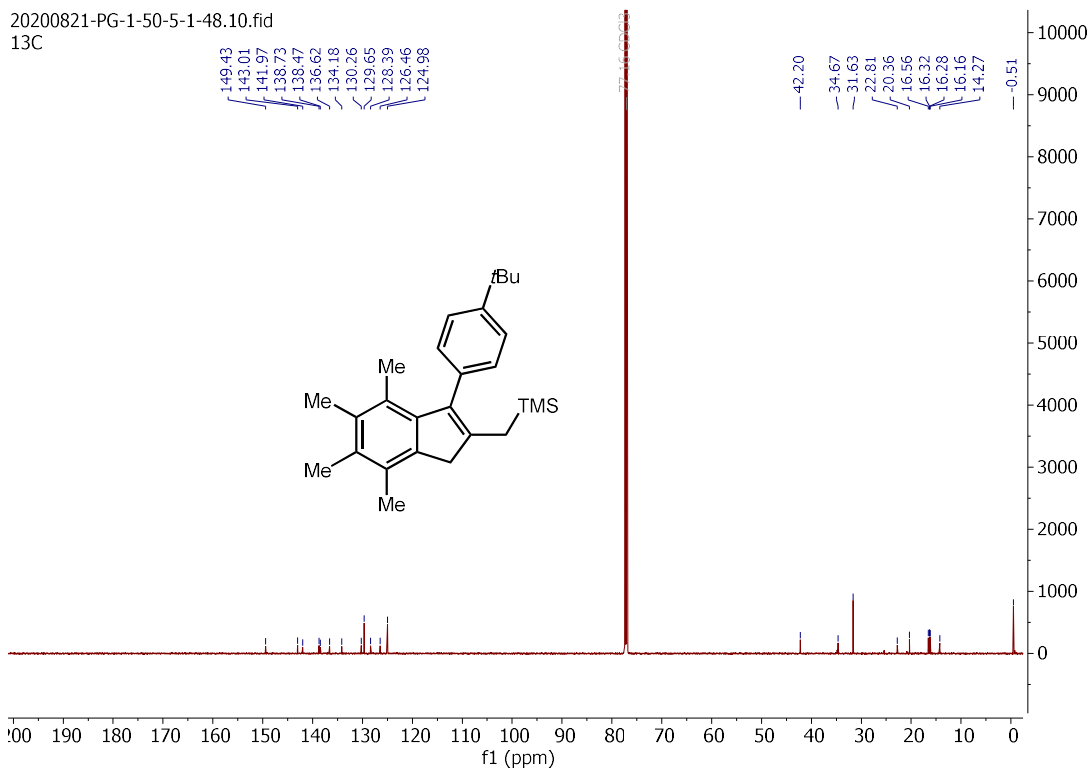
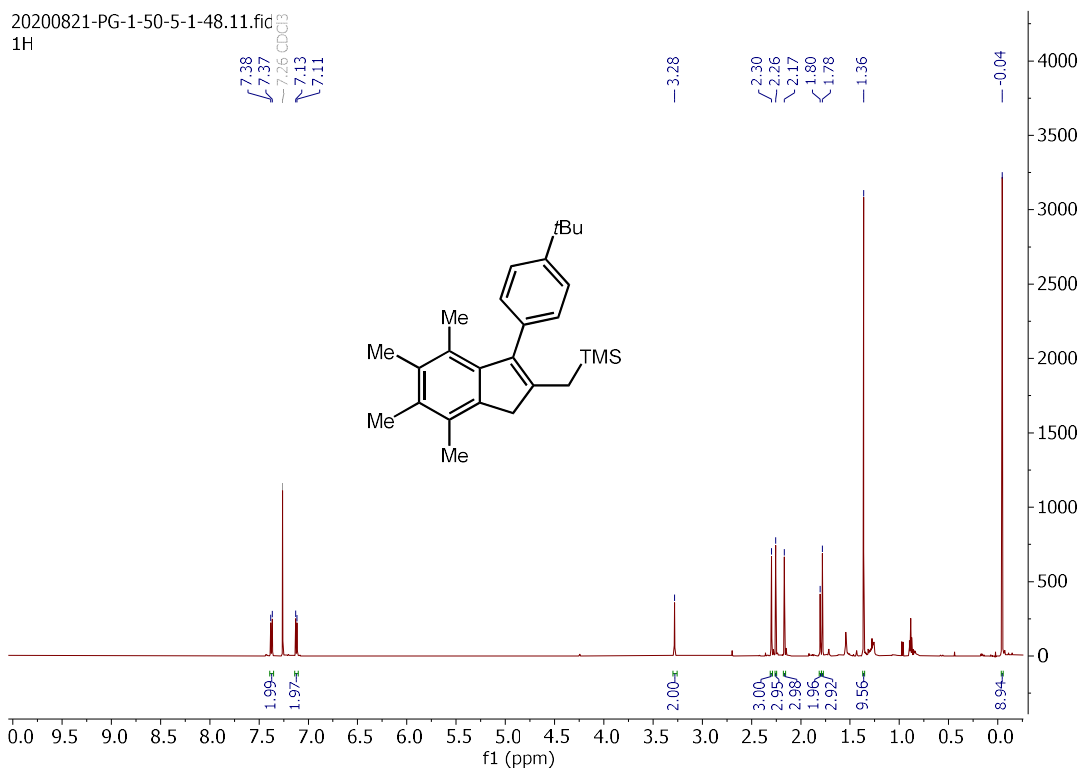
2-bromo-3-(4-(tert-butyl)phenyl)-4,5,6,7-tetramethyl-1H-indene (**2.97**):



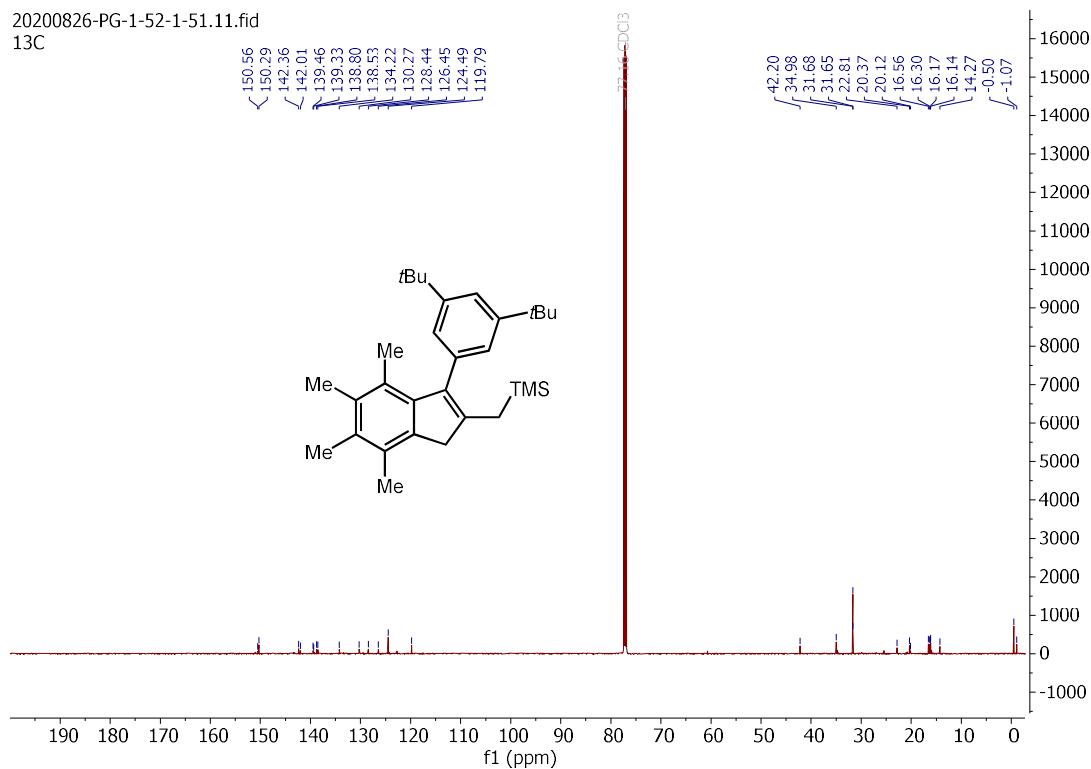
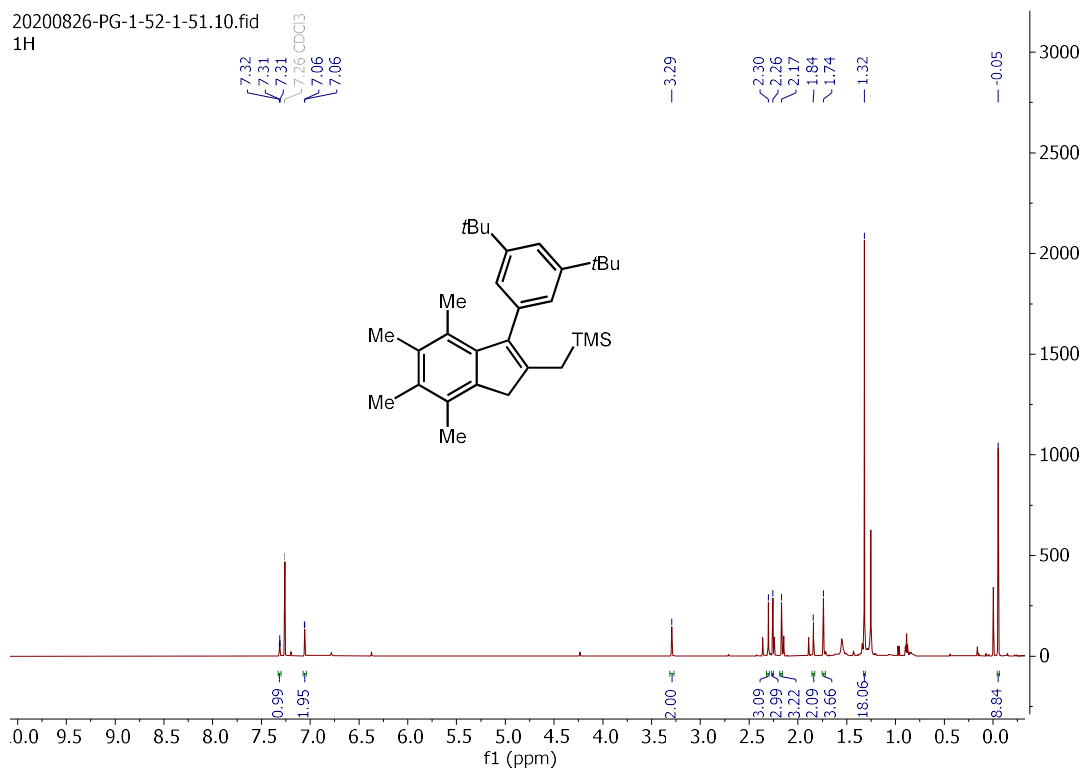
2-bromo-3-(3,5-di-tert-butylphenyl)-4,5,6,7-tetramethyl-1H-indene (2.98):



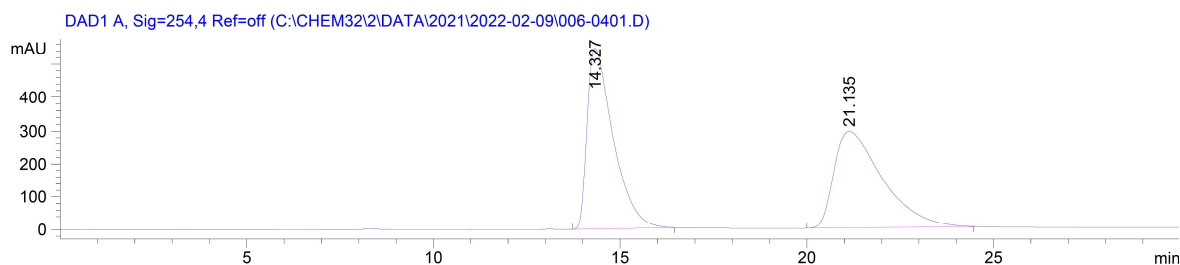
((3-(4-(tert-butyl)phenyl)-4,5,6,7-tetramethyl-1H-inden-2-yl)methyl)trimethylsilane (2.99):



((3-(3,5-di-tert-butylphenyl)-4,5,6,7-tetramethyl-1H-inden-2-yl)methyl)trimethylsilane (2.100):



(±)-1,5-cyclooctadiene(η^5 -2-methyl-3-phenylinden-1H-yl)rhodium(I)(±-2.54):

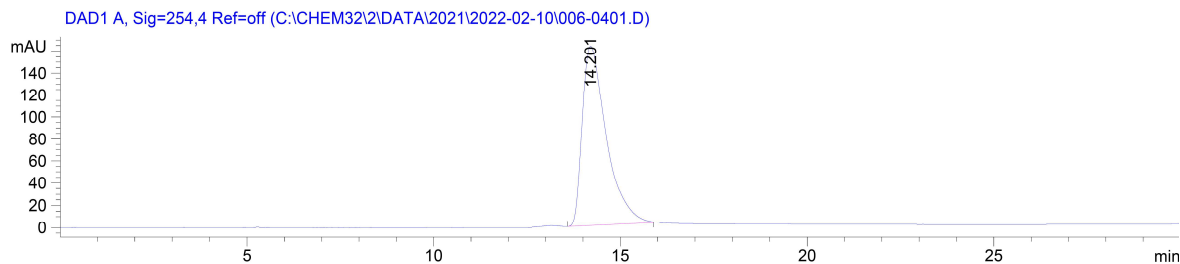


Signal 1: DAD1 A, Sig=254,4 Ref=off

| Peak # | RetTime [min] | Type | Width [min] | Area [mAU*s] | Height [mAU] | Area % |
|--------|---------------|------|-------------|--------------|--------------|---------|
| 1 | 14.327 | BB | 0.7227 | 2.65512e4 | 546.65851 | 50.0758 |
| 2 | 21.135 | BB | 1.3366 | 2.64708e4 | 293.38287 | 49.9242 |

Totals : 5.30221e4 840.04138

(S)-1,5-cyclooctadiene(η^5 -2-methyl-3-phenylinden-1H-yl)rhodium(I) ((S)-2.54):

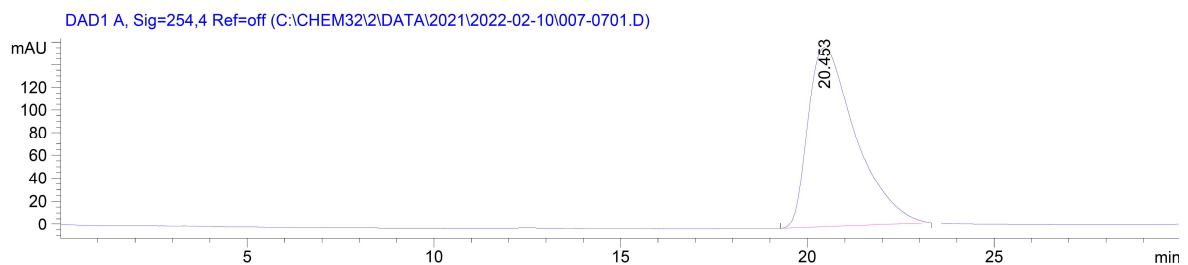


Signal 1: DAD1 A, Sig=254,4 Ref=off

| Peak # | RetTime [min] | Type | Width [min] | Area [mAU*s] | Height [mAU] | Area % |
|--------|---------------|------|-------------|--------------|--------------|----------|
| 1 | 14.201 | BB | 0.6687 | 7259.47119 | 162.66116 | 100.0000 |

Totals : 7259.47119 162.66116

(R)-1,5-cyclooctadiene(η^5 -2-methyl-3-phenylinden-1H-yl)rhodium(I) ((*R*)-2.54):

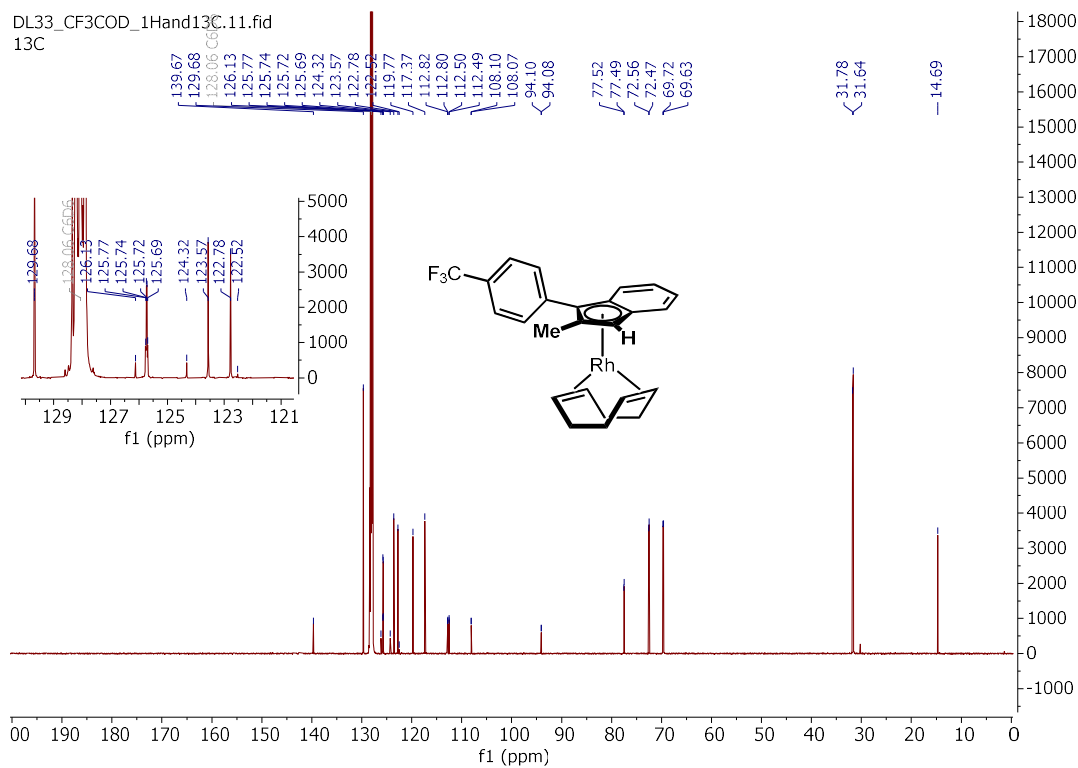
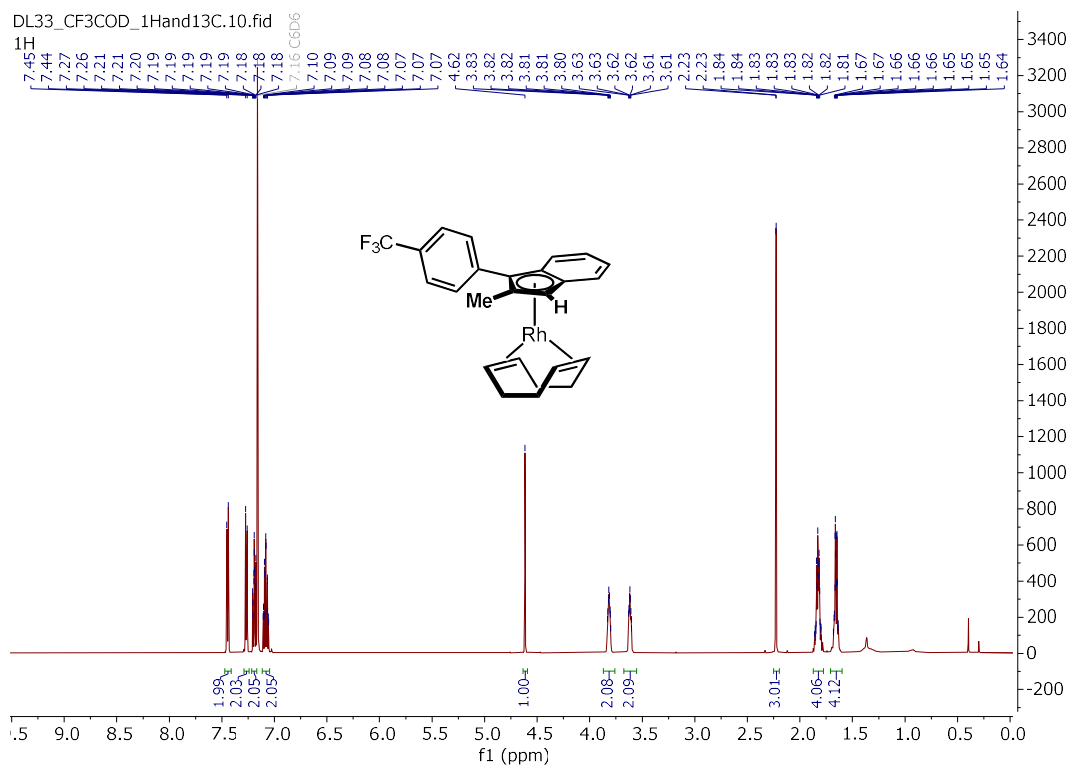


Signal 1: DAD1 A, Sig=254,4 Ref=off

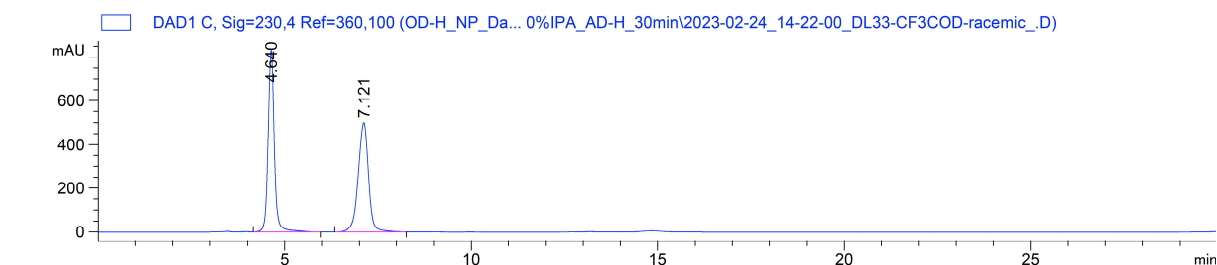
| Peak # | RetTime [min] | Type | Width [min] | Area [mAU*s] | Height [mAU] | Area % |
|--------|---------------|------|-------------|--------------|--------------|----------|
| 1 | 20.453 | BB | 1.3022 | 1.39726e4 | 157.62514 | 100.0000 |

Totals : 1.39726e4 157.62514

(±)-1,5-cyclooctadiene(η^5 -2-methyl-3-(4-(trifluoromethyl)phenyl)inden-1H-yl)rhodium(I) (±-S5):



(±)-1,5-cyclooctadiene(η^5 -2-methyl-3-(4-(trifluoromethyl)phenyl)inden-1H-yl)rhodium(I) (±-S5):

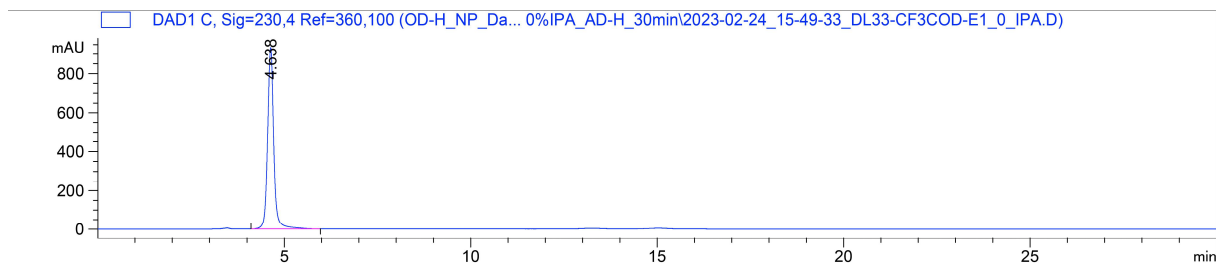


Signal 3: DAD1 C, Sig=230,4 Ref=360,100

| Peak # | RetTime [min] | Type | Width [min] | Area [mAU*s] | Height [mAU] | Area % |
|--------|---------------|------|-------------|--------------|--------------|---------|
| 1 | 4.640 | BB | 0.1779 | 9718.68945 | 831.37299 | 50.1056 |
| 2 | 7.121 | BB | 0.2947 | 9677.72656 | 499.10626 | 49.8944 |

Totals : 1.93964e4 1330.47925

(S)-1,5-cyclooctadiene(η^5 -2-methyl-3-(4-(trifluoromethyl)phenyl)inden-1H-yl)rhodium(I) ((S)-S5):

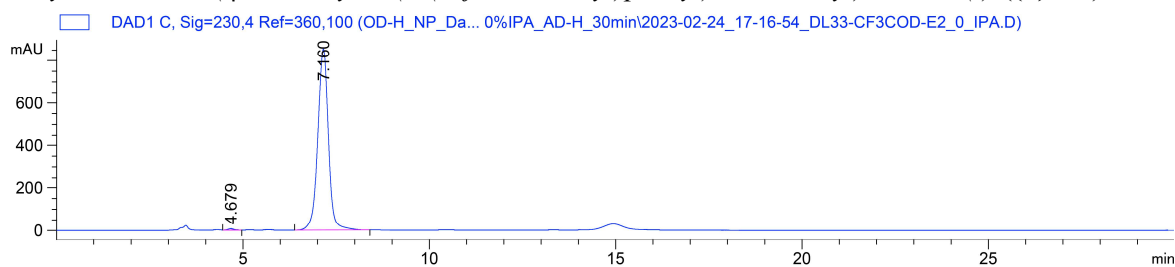


Signal 3: DAD1 C, Sig=230,4 Ref=360,100

| Peak # | RetTime [min] | Type | Width [min] | Area [mAU*s] | Height [mAU] | Area % |
|--------|---------------|------|-------------|--------------|--------------|----------|
| 1 | 4.638 | BB | 0.1743 | 1.07581e4 | 934.78265 | 100.0000 |

Totals : 1.07581e4 934.78265

(R)-1,5-cyclooctadiene(η^5 -2-methyl-3-(4-(trifluoromethyl)phenyl)inden-1H-yl)rhodium(I) (**(R)-S5**):

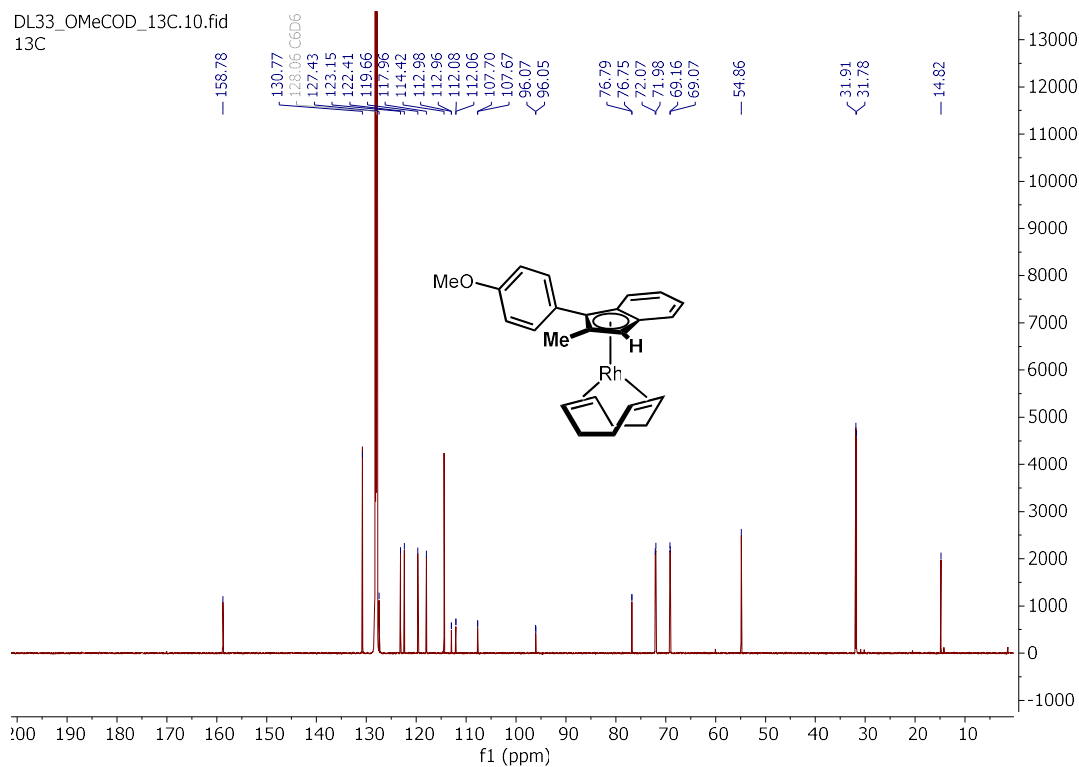
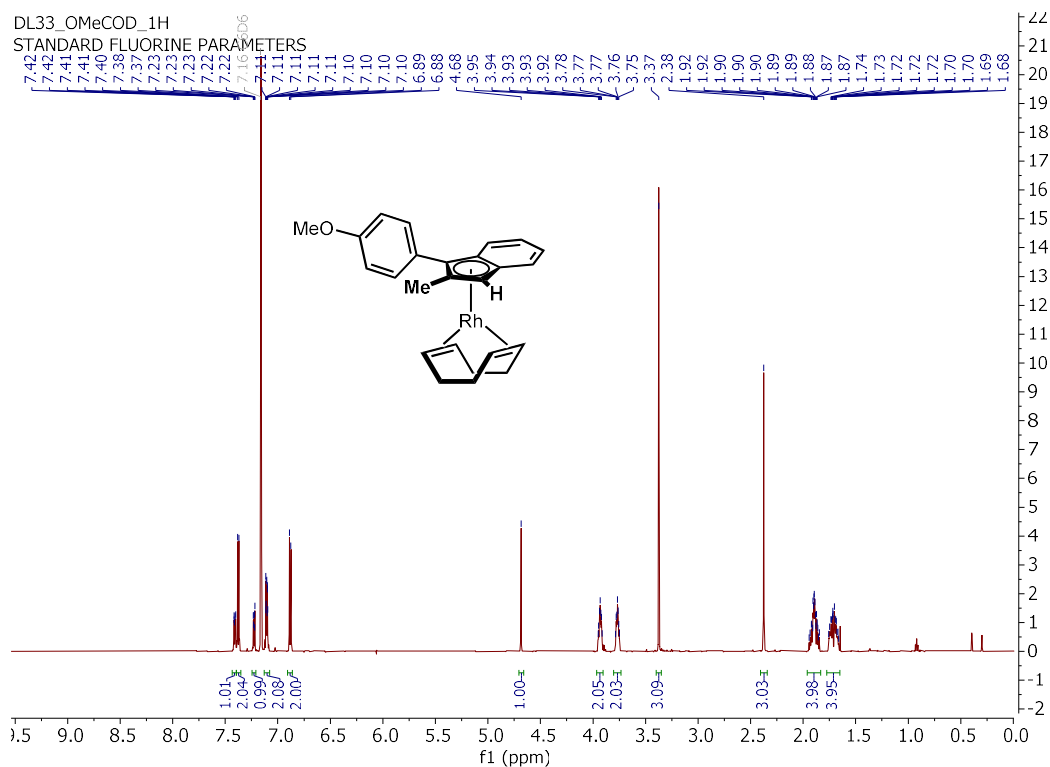


Signal 3: DAD1 C, Sig=230,4 Ref=360,100

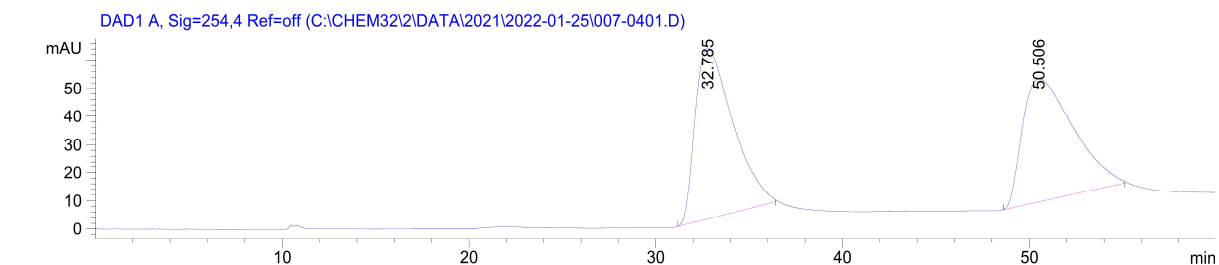
| Peak # | RetTime [min] | Type | Width [min] | Area [mAU*s] | Height [mAU] | Area % |
|--------|---------------|------|-------------|--------------|--------------|---------|
| 1 | 4.679 | VB | 0.1404 | 74.39933 | 6.50820 | 0.4384 |
| 2 | 7.160 | BB | 0.3026 | 1.68954e4 | 854.68109 | 99.5616 |

Totals : 1.69698e4 861.18930

(±)-1,5-cyclooctadiene(η^5 -3-(4-methoxyphenyl)-2-methylinden-1H-yl)rhodium(I) (±-S6):



(±)-1,5-cyclooctadiene(η^5 -3-(4-methoxyphenyl)-2-methylinden-1H-yl)rhodium(I) (±-S6):

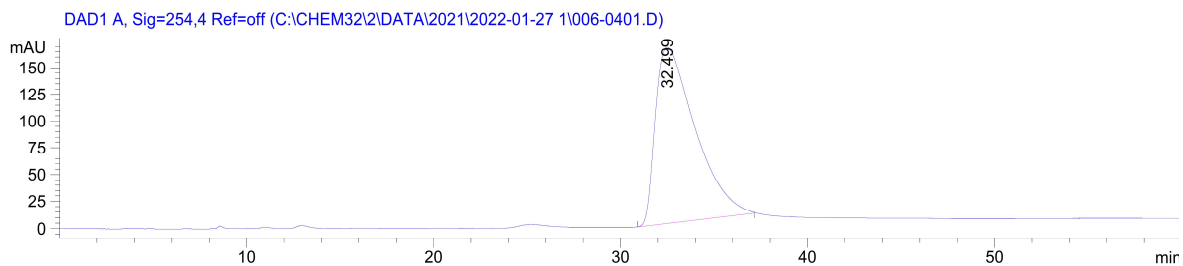


Signal 1: DAD1 A, Sig=254,4 Ref=off

| Peak # | RetTime [min] | Type | Width [min] | Area [mAU*s] | Height [mAU] | Area % |
|--------|---------------|------|-------------|--------------|--------------|---------|
| 1 | 32.785 | BB | 1.9017 | 8497.05078 | 60.90253 | 50.7854 |
| 2 | 50.506 | BB | 2.2075 | 8234.23340 | 43.87610 | 49.2146 |

Totals : 1.67313e4 104.77863

(S)-1,5-cyclooctadiene(η^5 -3-(4-methoxyphenyl)-2-methylinden-1H-yl)rhodium(I) ((S)-S6):

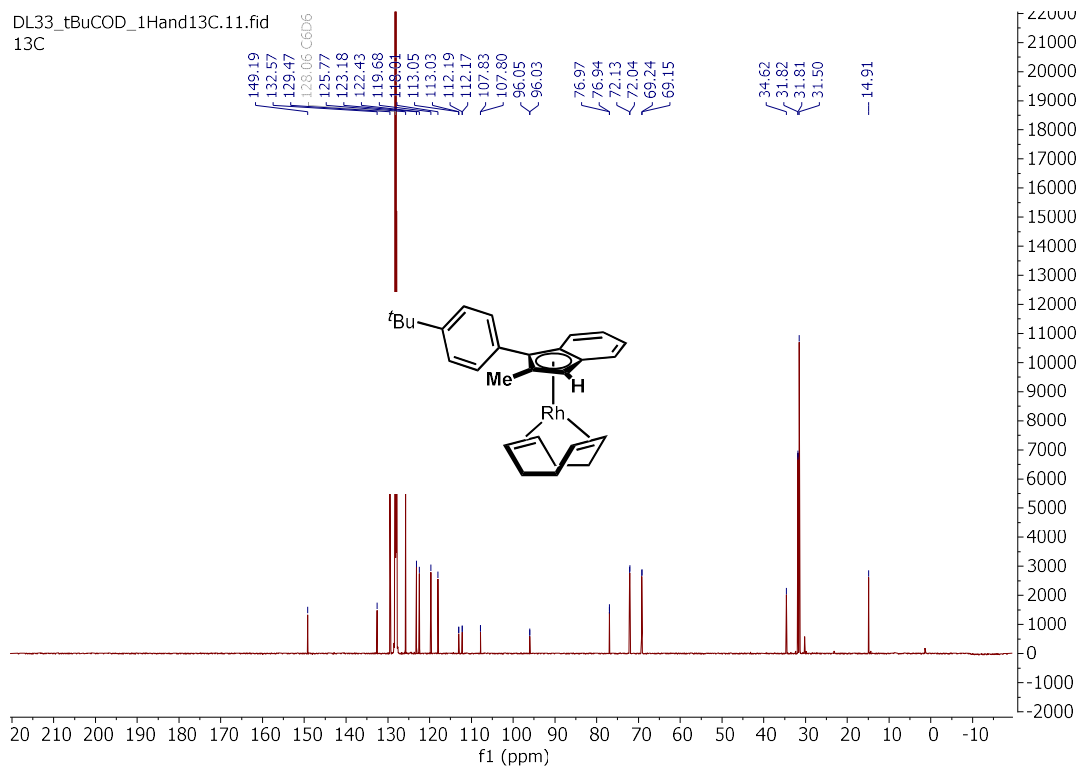
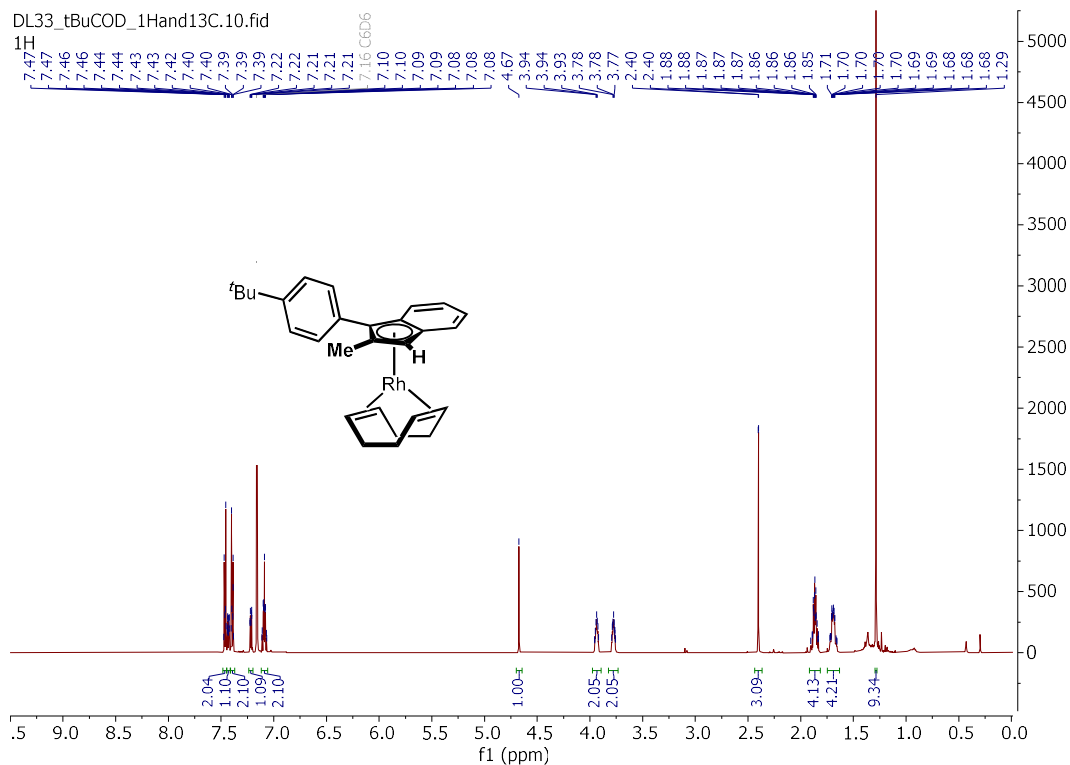


Signal 1: DAD1 A, Sig=254,4 Ref=off

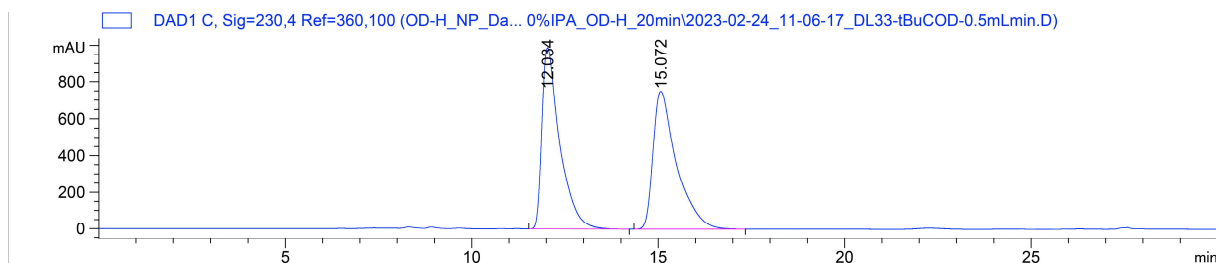
| Peak # | RetTime [min] | Type | Width [min] | Area [mAU*s] | Height [mAU] | Area % |
|--------|---------------|------|-------------|--------------|--------------|----------|
| 1 | 32.499 | BB | 2.0821 | 2.42883e4 | 164.54539 | 100.0000 |

Totals : 2.42883e4 164.54539

(±)-1,5-cyclooctadiene(η^5 -3-(4-(tert-butyl)phenyl)-2-methylinden-1H-yl)rhodium(I) (±-S7):



(±)-1,5-cyclooctadiene(η^5 -3-(4-(tert-butyl)phenyl-2-methylinden-1H-yl)rhodium(I) (±)-S7):

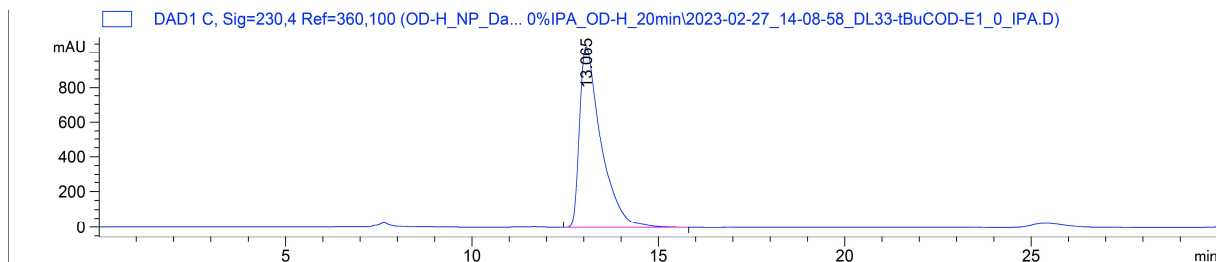


Signal 3: DAD1 C, Sig=230,4 Ref=360,100

| Peak # | RetTime [min] | Type | Width [min] | Area [mAU*s] | Height [mAU] | Area % |
|--------|---------------|------|-------------|--------------|--------------|---------|
| 1 | 12.034 | BB | 0.4709 | 3.27591e4 | 989.06738 | 49.9359 |
| 2 | 15.072 | BB | 0.5844 | 3.28431e4 | 750.77612 | 50.0641 |

Totals : 6.56021e4 1739.84351

(S)-1,5-cyclooctadiene(η^5 -3-(4-(tert-butyl)phenyl-2-methylinden-1H-yl)rhodium(I) ((S)-S7):

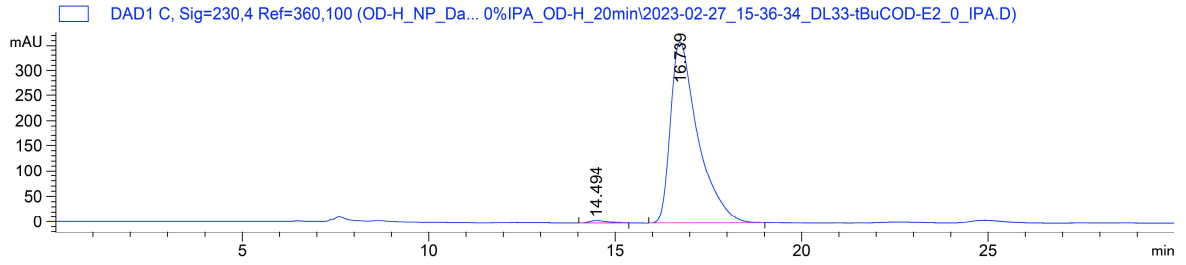


Signal 3: DAD1 C, Sig=230,4 Ref=360,100

| Peak # | RetTime [min] | Type | Width [min] | Area [mAU*s] | Height [mAU] | Area % |
|--------|---------------|------|-------------|--------------|--------------|----------|
| 1 | 13.065 | BB | 0.5320 | 4.10621e4 | 1035.77551 | 100.0000 |

Totals : 4.10621e4 1035.77551

(R)-1,5-cyclooctadiene(η^5 -3-(4-(*tert*-butyl)phenyl-2-methylinden-1*H*-yl)rhodium(I) (**(R)**-S7):

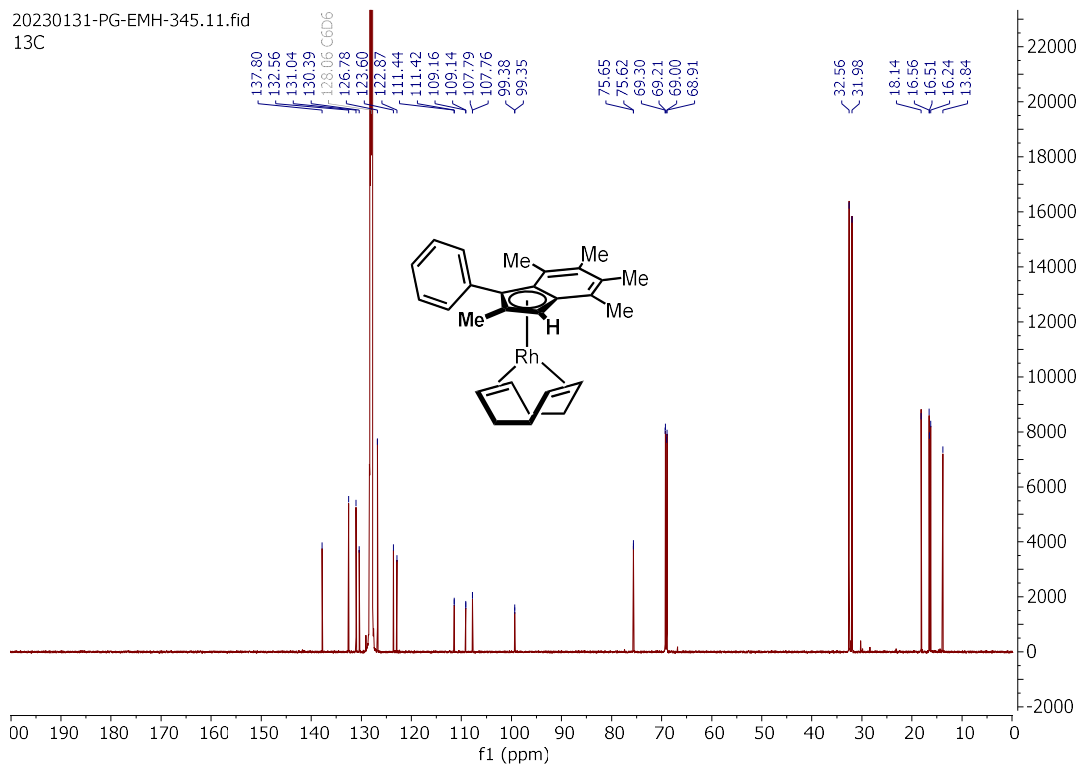
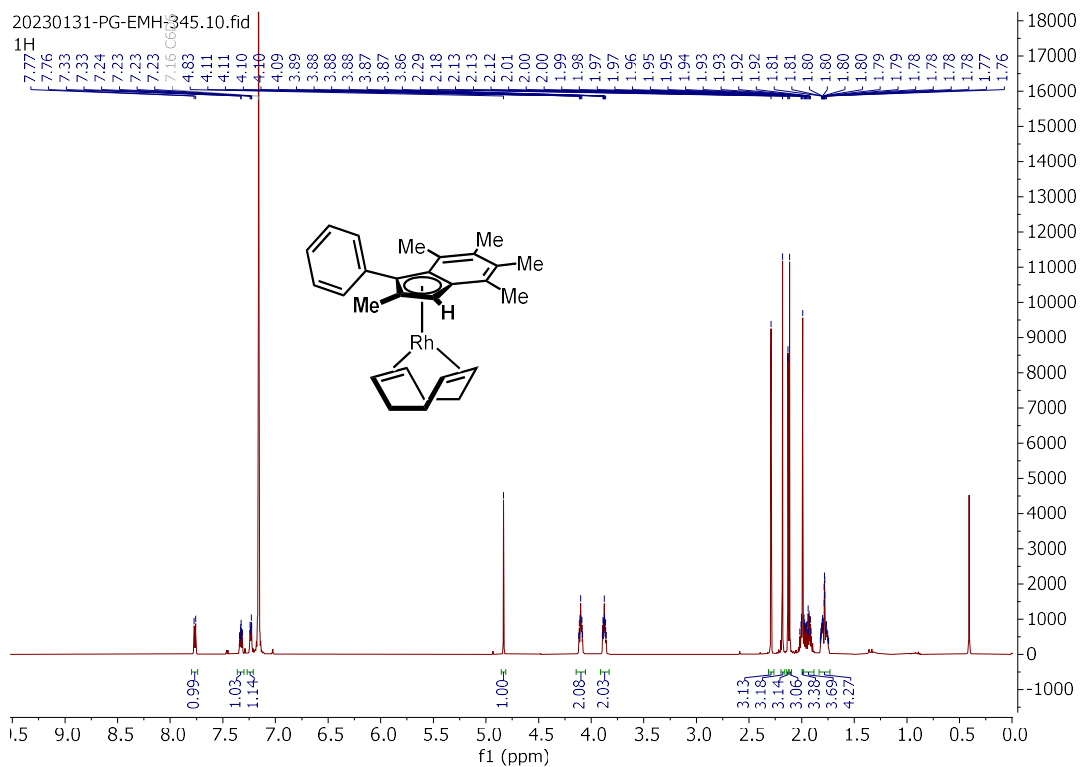


Signal 3: DAD1 C, Sig=230,4 Ref=360,100

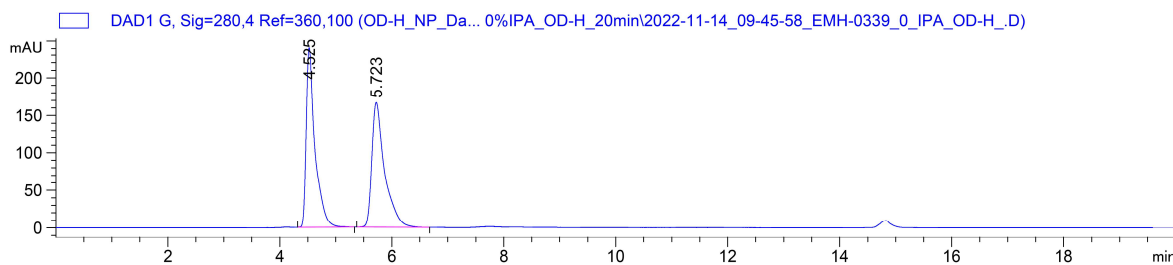
| Peak # | RetTime [min] | Type | Width [min] | Area [mAU*s] | Height [mAU] | Area % |
|--------|---------------|------|-------------|--------------|--------------|---------|
| 1 | 14.494 | BB | 0.3794 | 147.94838 | 4.57352 | 0.8020 |
| 2 | 16.739 | BB | 0.6538 | 1.83004e4 | 360.19049 | 99.1980 |

Totals : 1.84484e4 364.76401

(±)-1,5-cyclooctadiene(η^5 -2,4,5,6,7-pentamethyl-3-phenylinden-1H-yl)rhodium(I)(±-S8).



(±)-1,5-cyclooctadiene(η^5 -2,4,5,6,7-pentamethyl-3-phenylinden-1H-yl)rhodium(I)(±-S8).

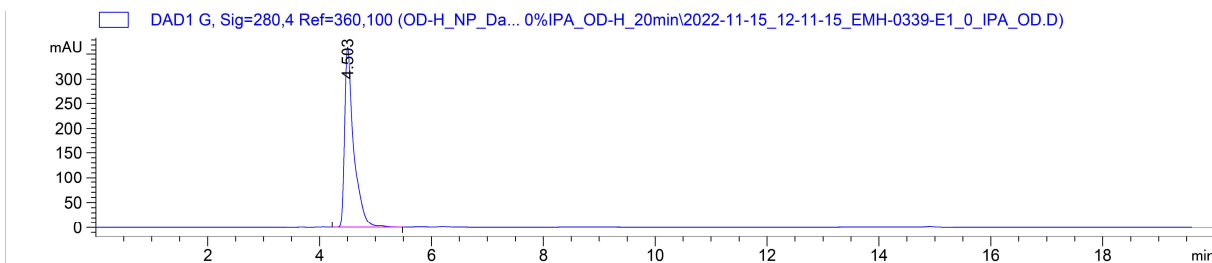


Signal 7: DAD1 G, Sig=280,4 Ref=360,100

| Peak # | RetTime [min] | Type | Width [min] | Area [mAU*s] | Height [mAU] | Area % |
|--------|---------------|------|-------------|--------------|--------------|---------|
| 1 | 4.525 | BB | 0.1554 | 2594.72900 | 240.36707 | 49.6225 |
| 2 | 5.723 | BB | 0.2273 | 2634.20874 | 166.34329 | 50.3775 |

Totals : 5228.93774 406.71036

(R)-1,5-cyclooctadiene(η^5 -2,4,5,6,7-pentamethyl-3-phenylinden-1H-yl)rhodium(I) ((R)-S8):

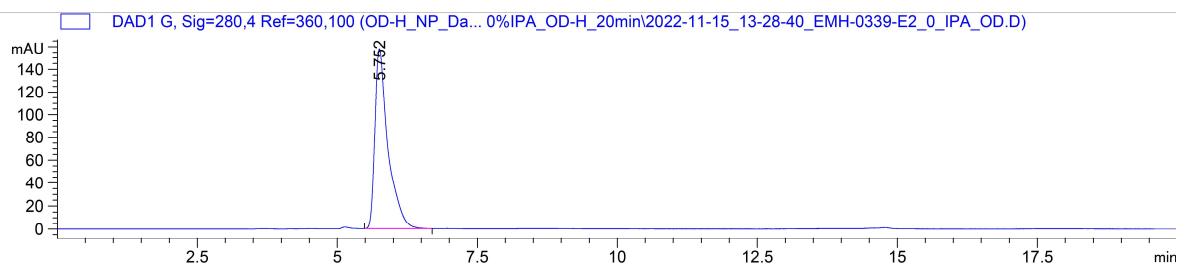


Signal 7: DAD1 G, Sig=280,4 Ref=360,100

| Peak # | RetTime [min] | Type | Width [min] | Area [mAU*s] | Height [mAU] | Area % |
|--------|---------------|------|-------------|--------------|--------------|----------|
| 1 | 4.503 | BV R | 0.1599 | 4102.95166 | 365.32794 | 100.0000 |

Totals : 4102.95166 365.32794

(S)-1,5-cyclooctadiene(η^5 -2,4,5,6,7-pentamethyl-3-phenylinden-1H-yl)rhodium(I) ((S)-S8):

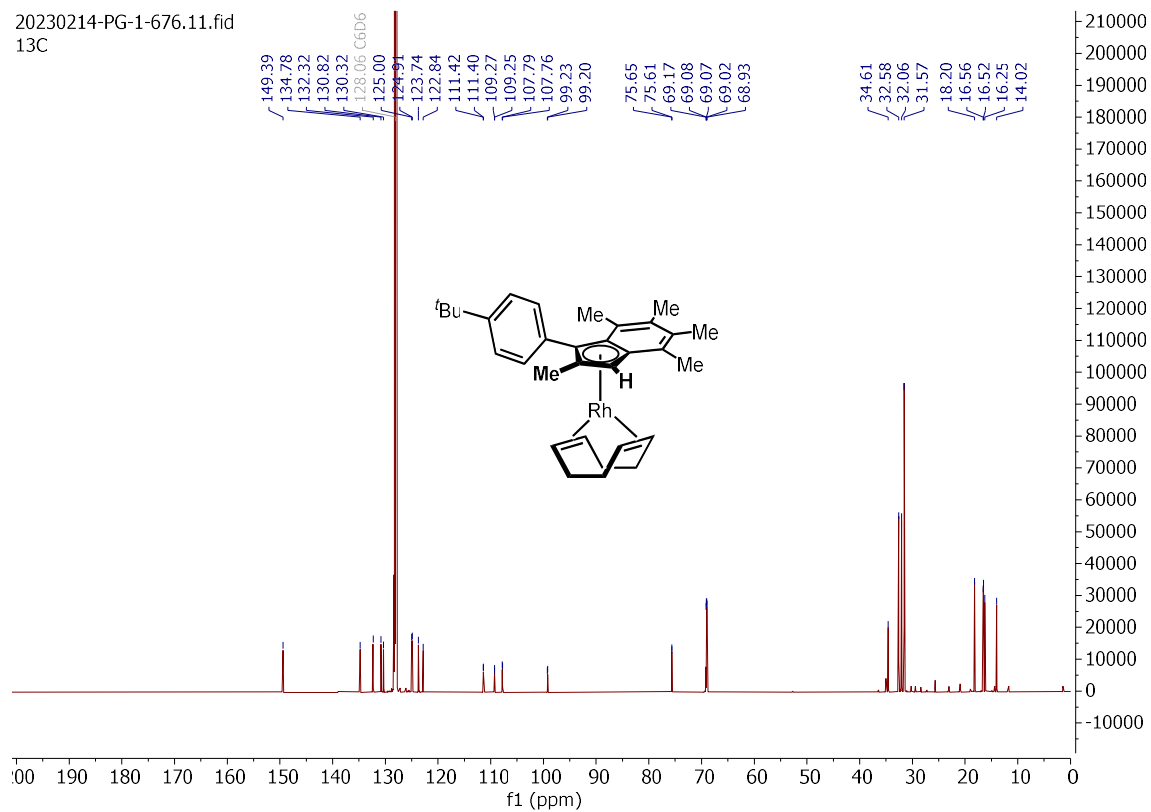
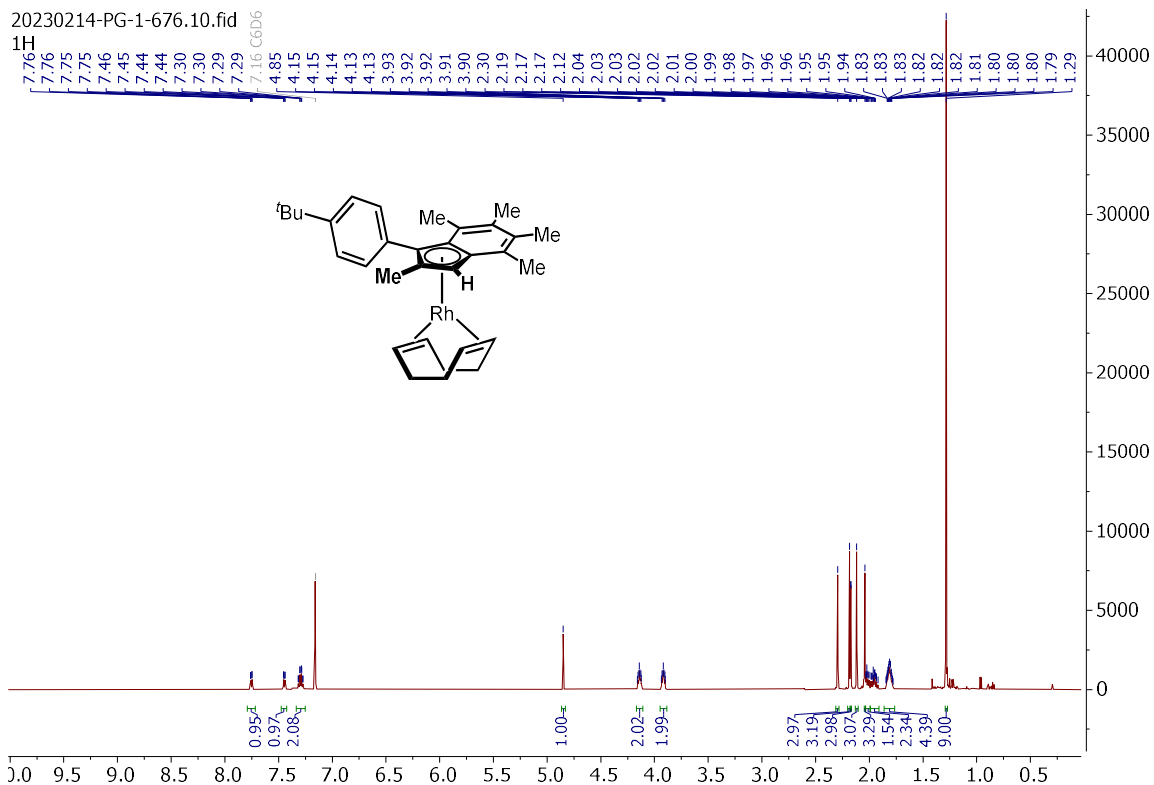


Signal 7: DAD1 G, Sig=280,4 Ref=360,100

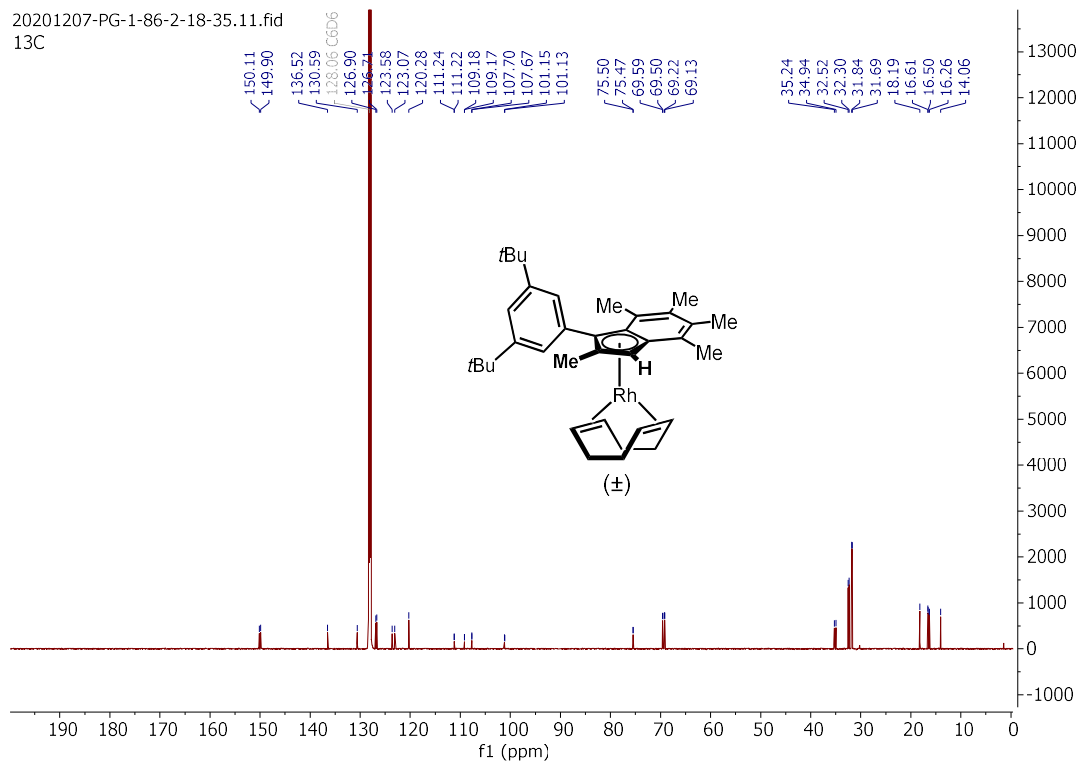
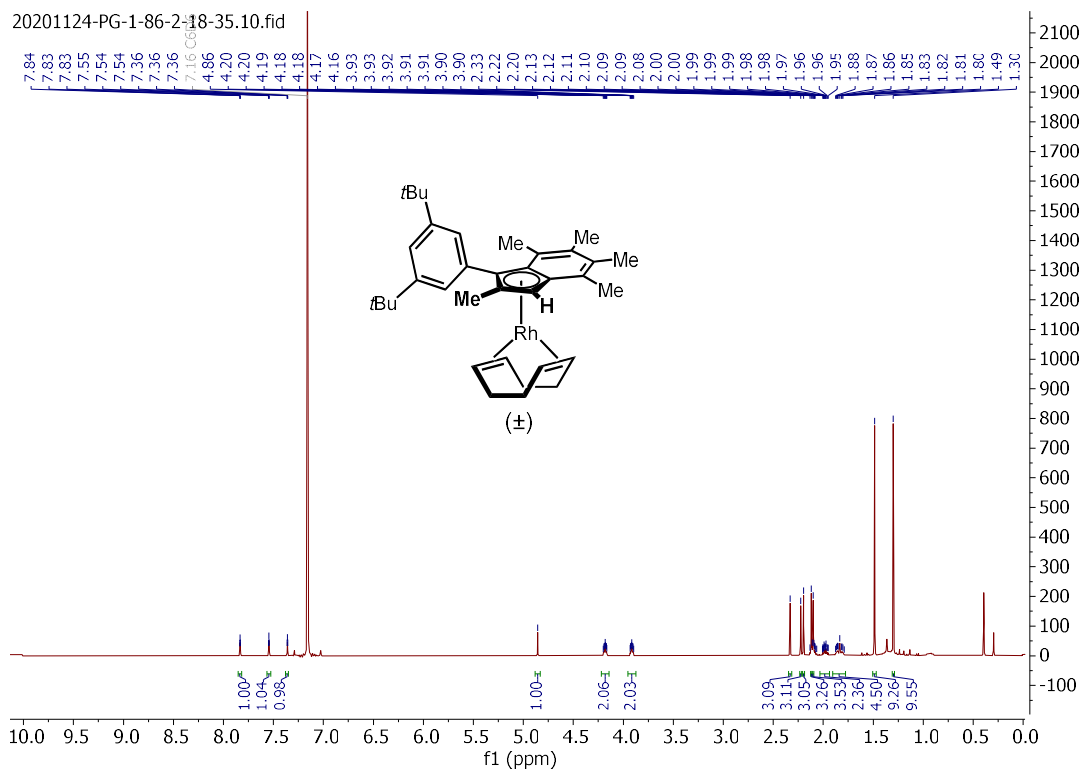
| Peak # | RetTime [min] | Type | Width [min] | Area [mAU*s] | Height [mAU] | Area % |
|--------|---------------|------|-------------|--------------|--------------|----------|
| 1 | 5.752 | BB | 0.2317 | 2548.04932 | 157.92233 | 100.0000 |

Totals : 2548.04932 157.92233

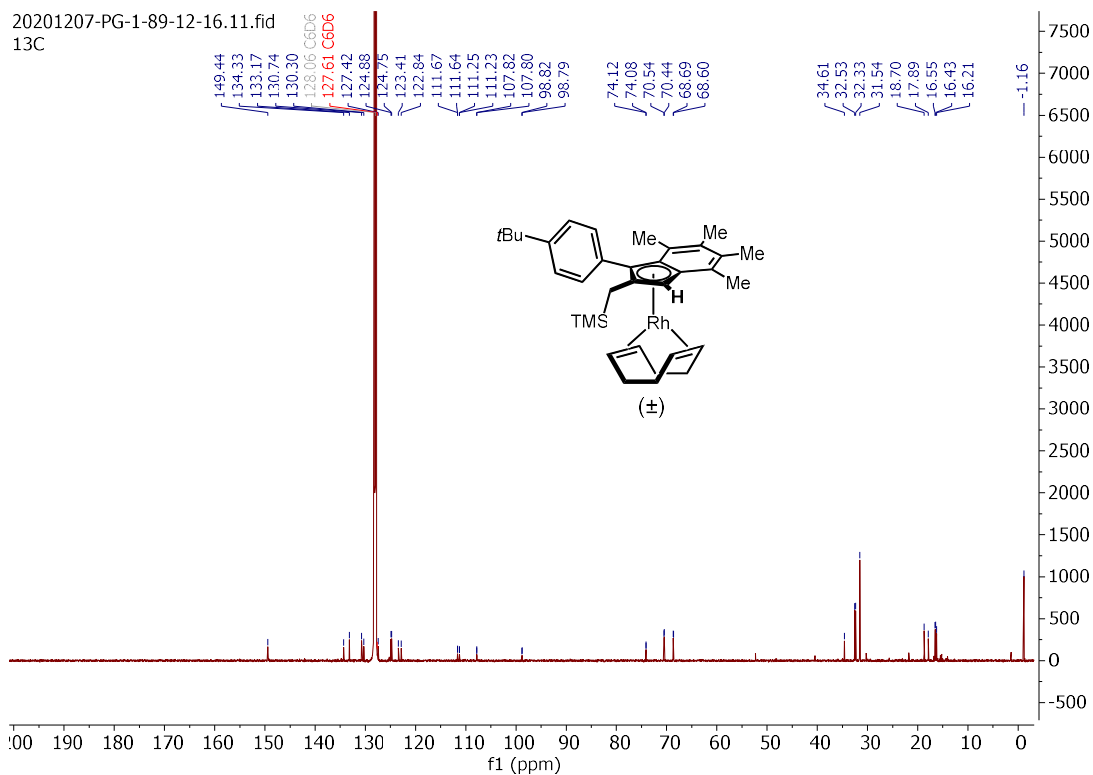
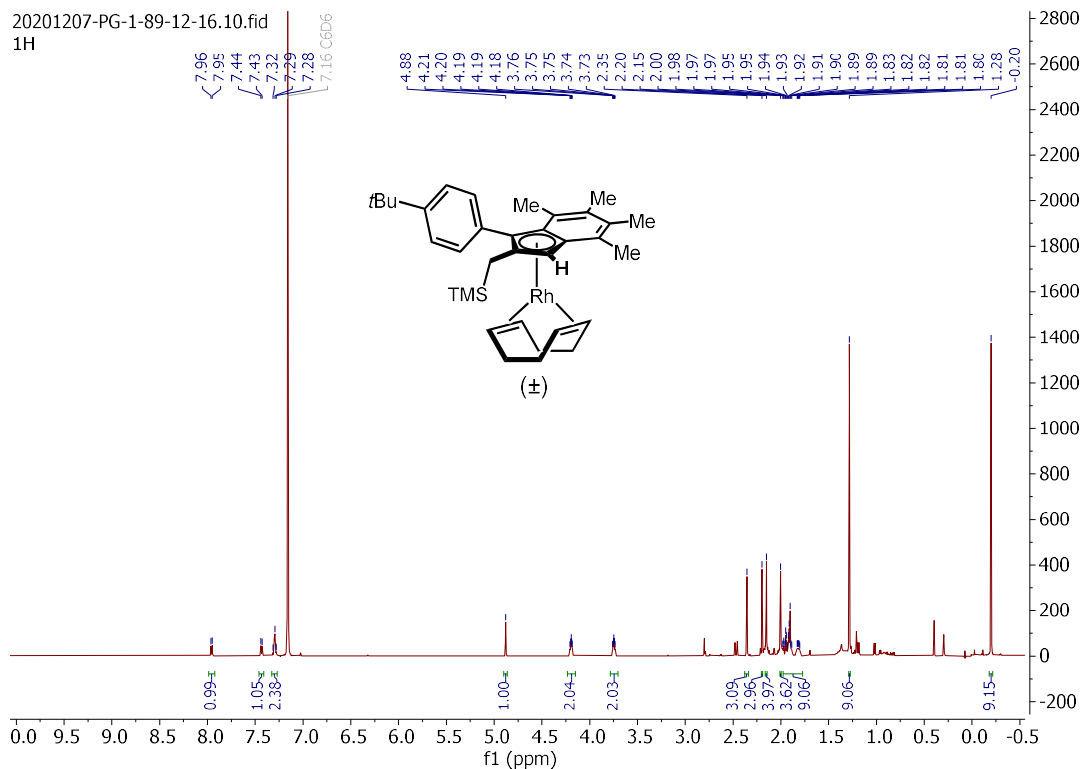
(±)-1,5-cyclooctadiene(η^5 -3-(4-(*tert*-butyl)phenyl)-2,4,5,6,7-pentamethylinden-1*H*-yl)rhodium(I) (±-**2.101**)



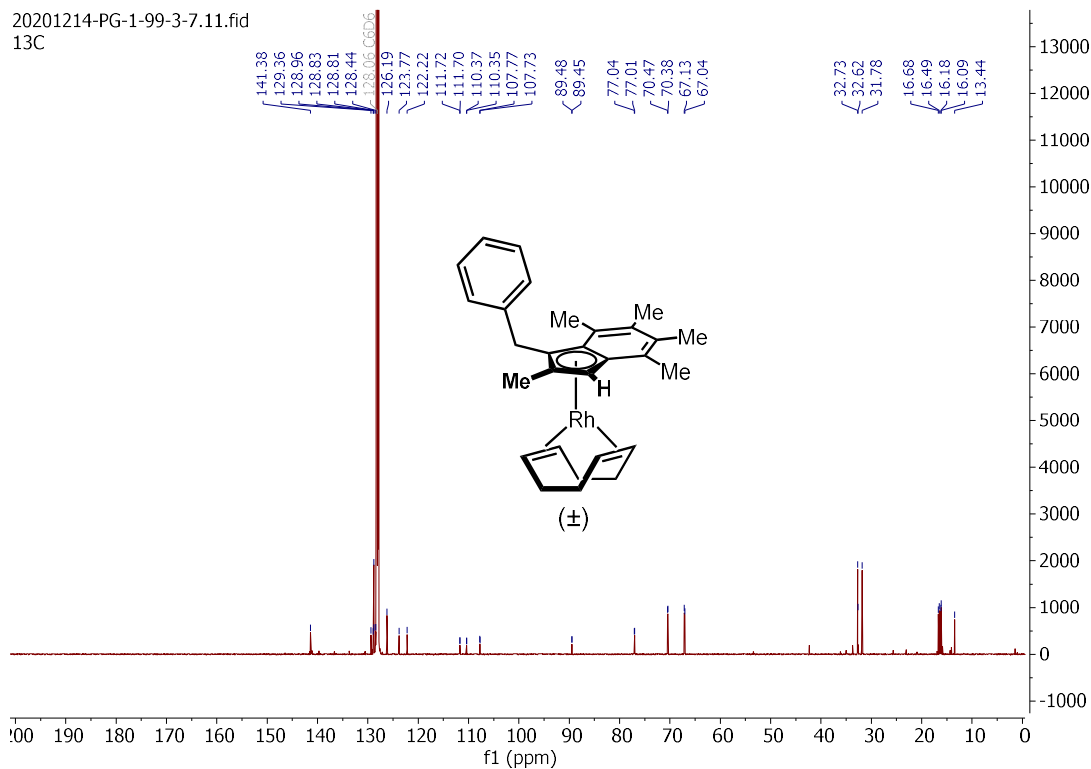
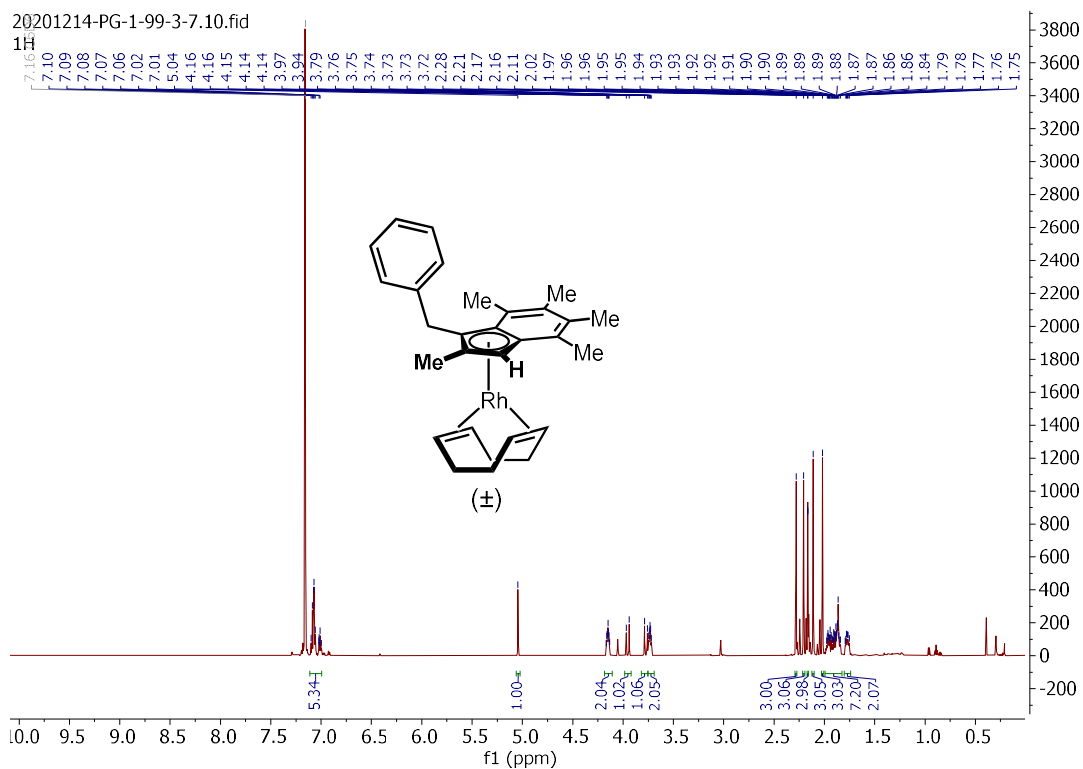
(±)-1,5-cyclooctadiene(η^5 -3-(3,5-di-tert-butylphenyl)-2,4,5,6,7-pentamethyl-1H-inden-1-yl)rhodium(I)
(2.102):



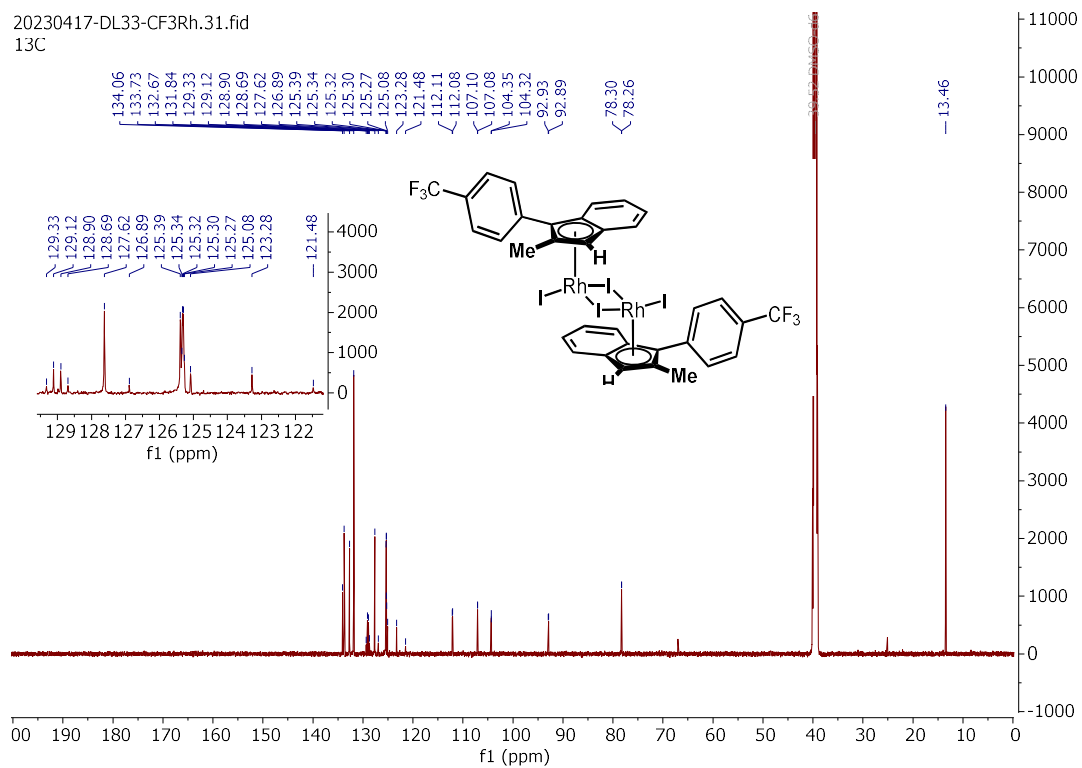
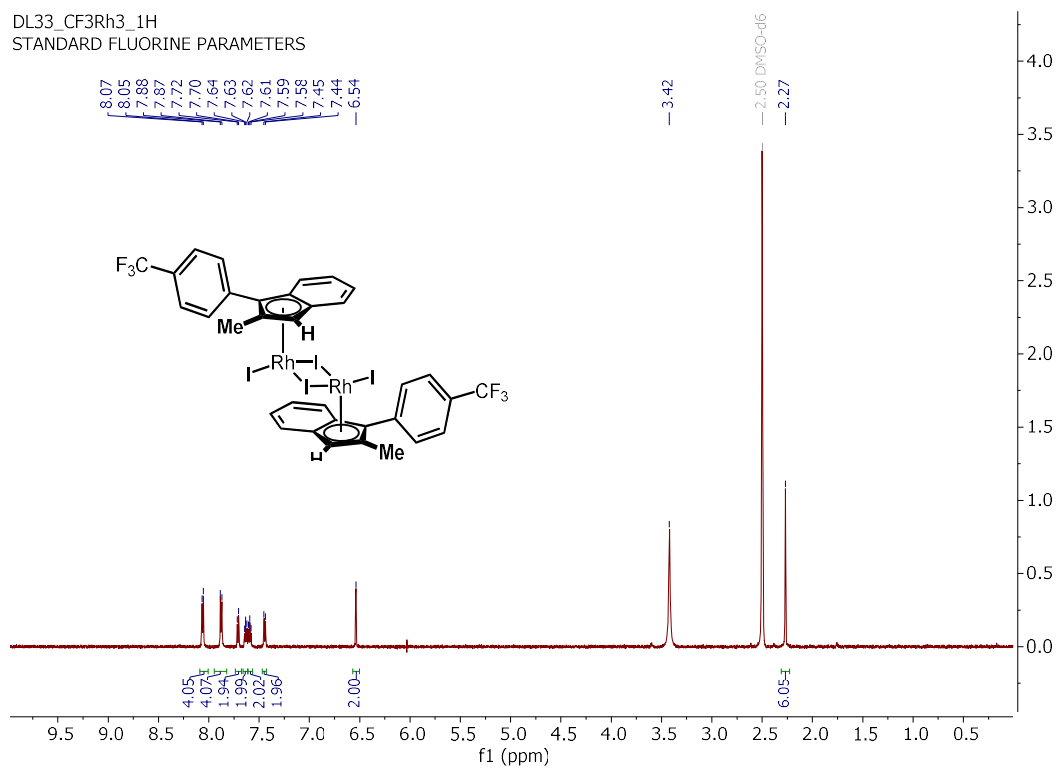
(±)-1,5-cyclooctadiene(η^5 -3-(4-(*tert*-butyl)phenyl)-4,5,6,7-tetramethyl-2-((trimethylsilyl)methyl)-1H-inden-1-yl)rhodium(I) (**2.105**):



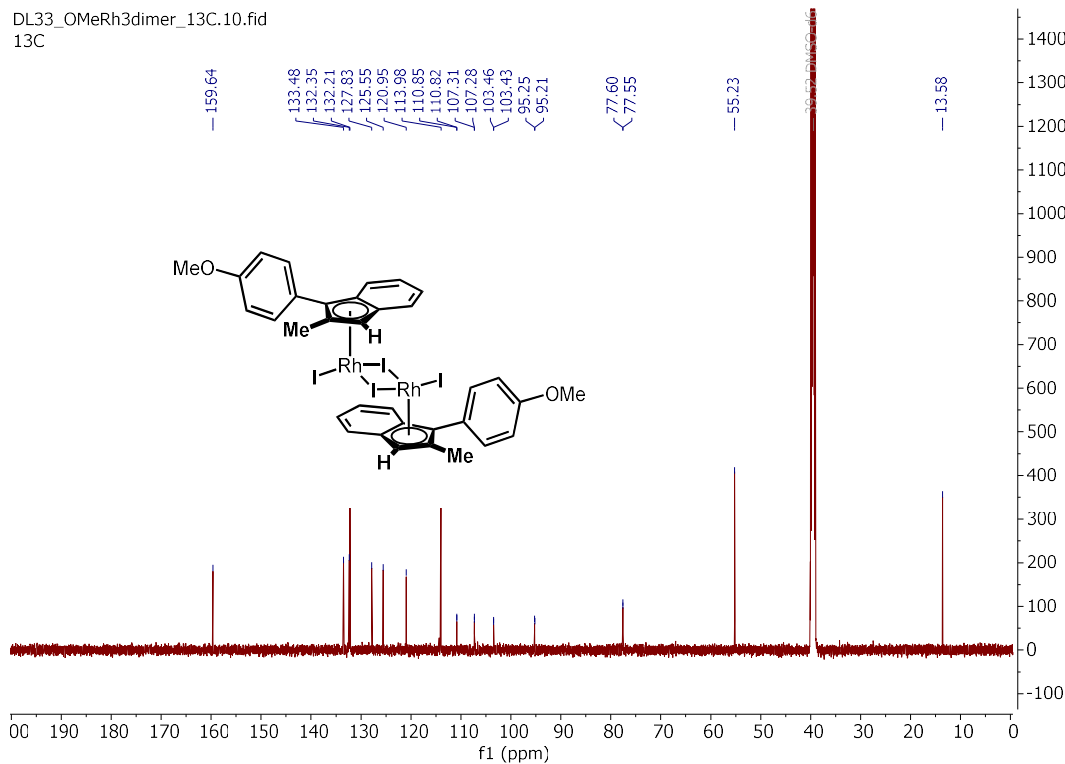
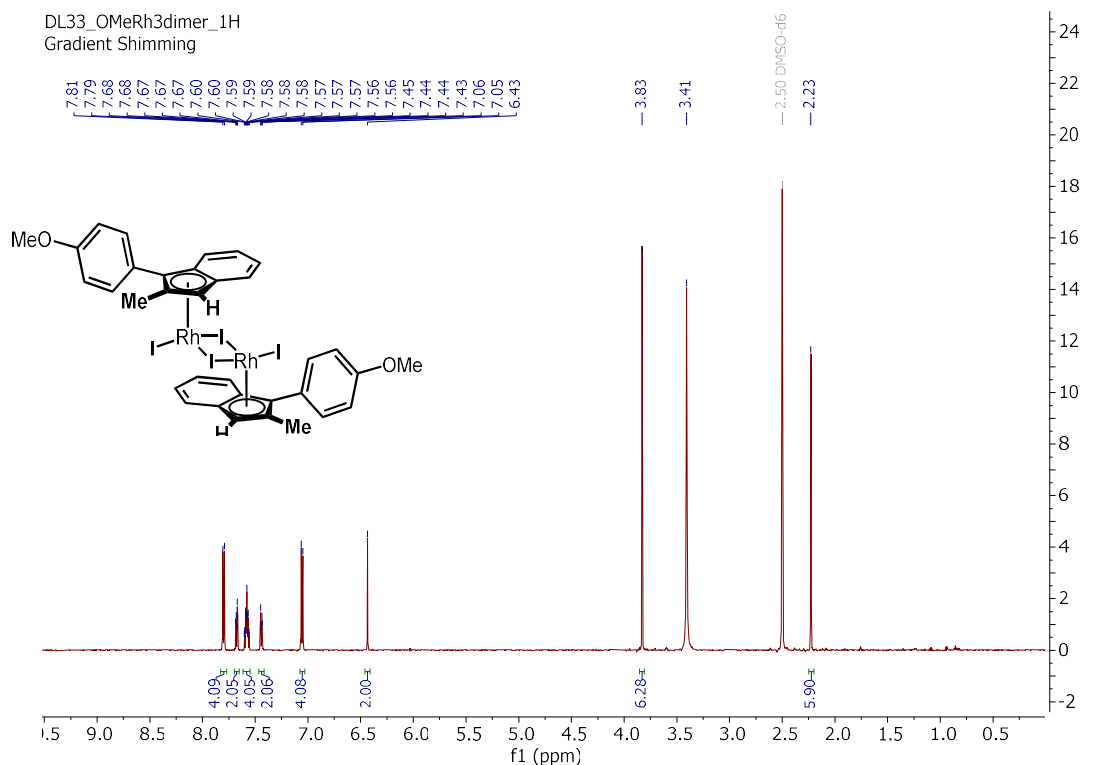
(±)-1,5-cyclooctadiene(η^5 -3-benzyl-2,4,5,6,7-pentamethyl-1H-inden-1-yl)rhodium(I) (**2.103**):



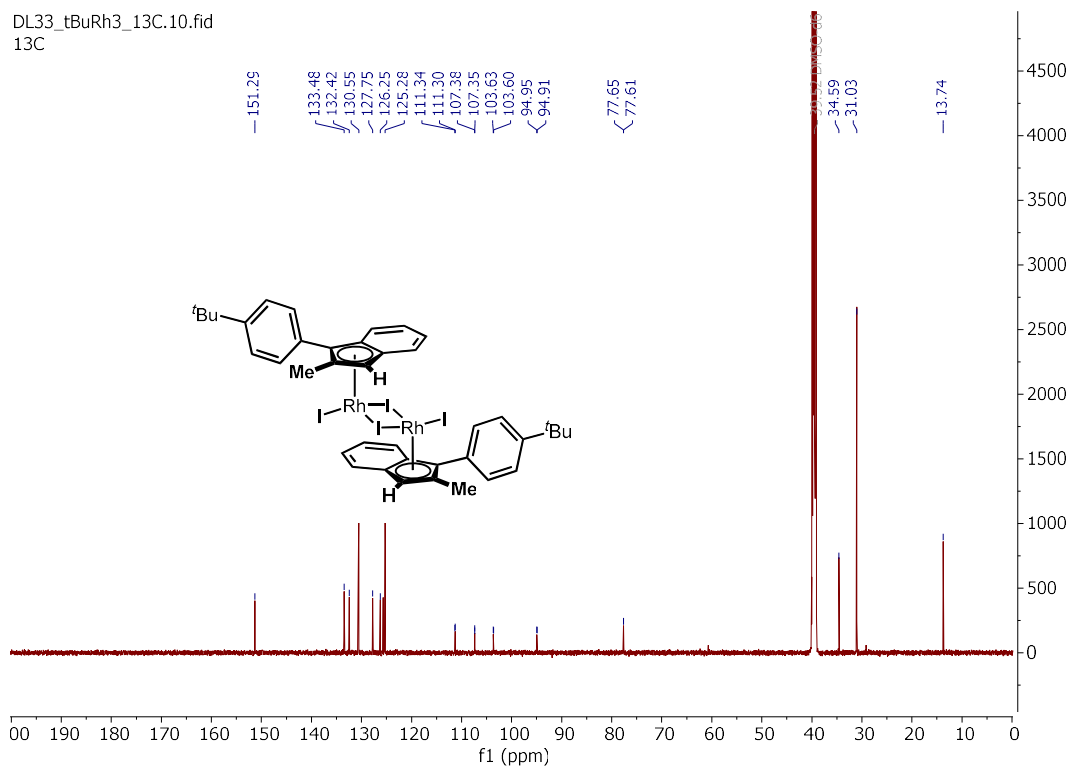
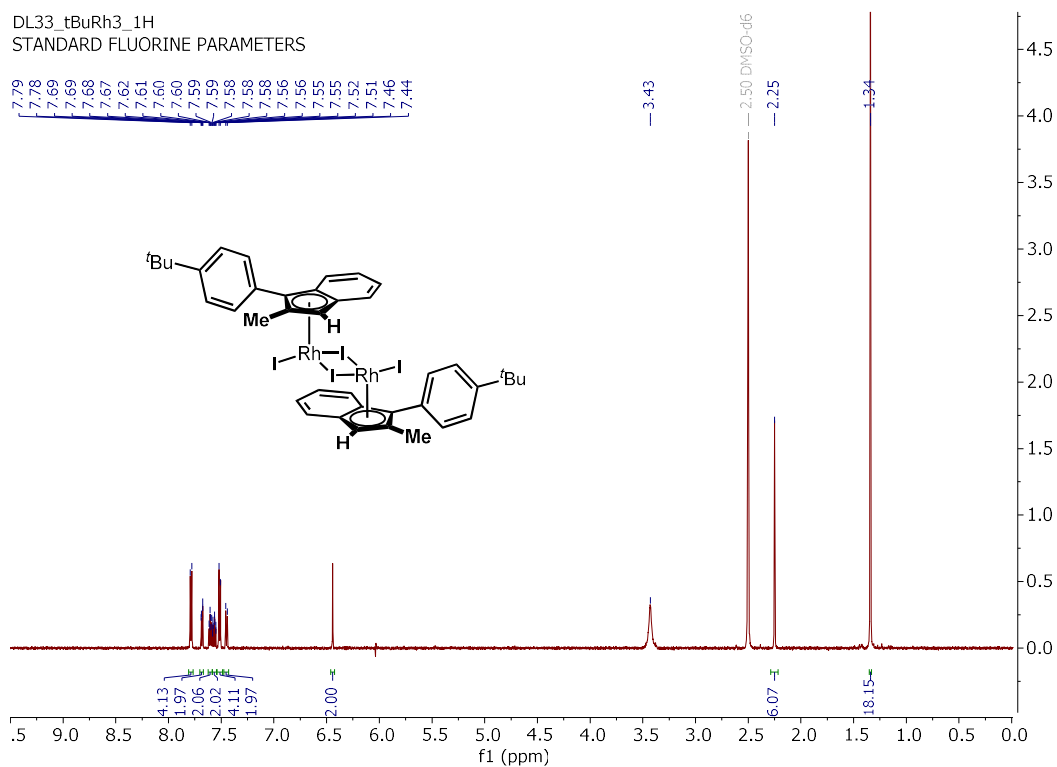
(S,S)-(η^5 -2-methyl-3-(4-(trifluoromethyl)phenyl)inden-1H-yl) rhodium(III) diiodide dimer (**(S,S)**-**S5**):



(S,S)-(η^5 -3-(4-methoxyphenyl)-2-methylinden-1H-yl) rhodium(III) diiodide dimer (**(S,S)**-6):

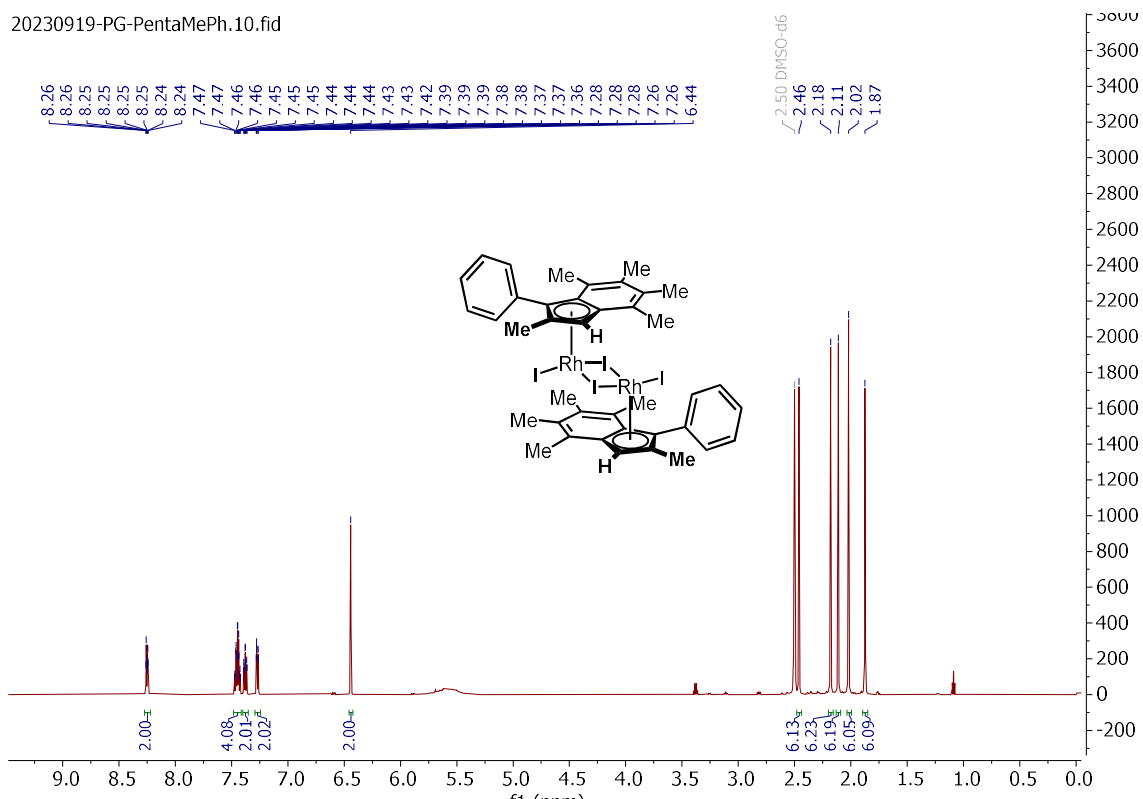


(S,S)-(η^5 -3-(4-(*tert*-butyl)phenyl)-2-methylinden-1*H*-yl) rhodium(III) diiodide dimer (**(S,S)**-**7**):

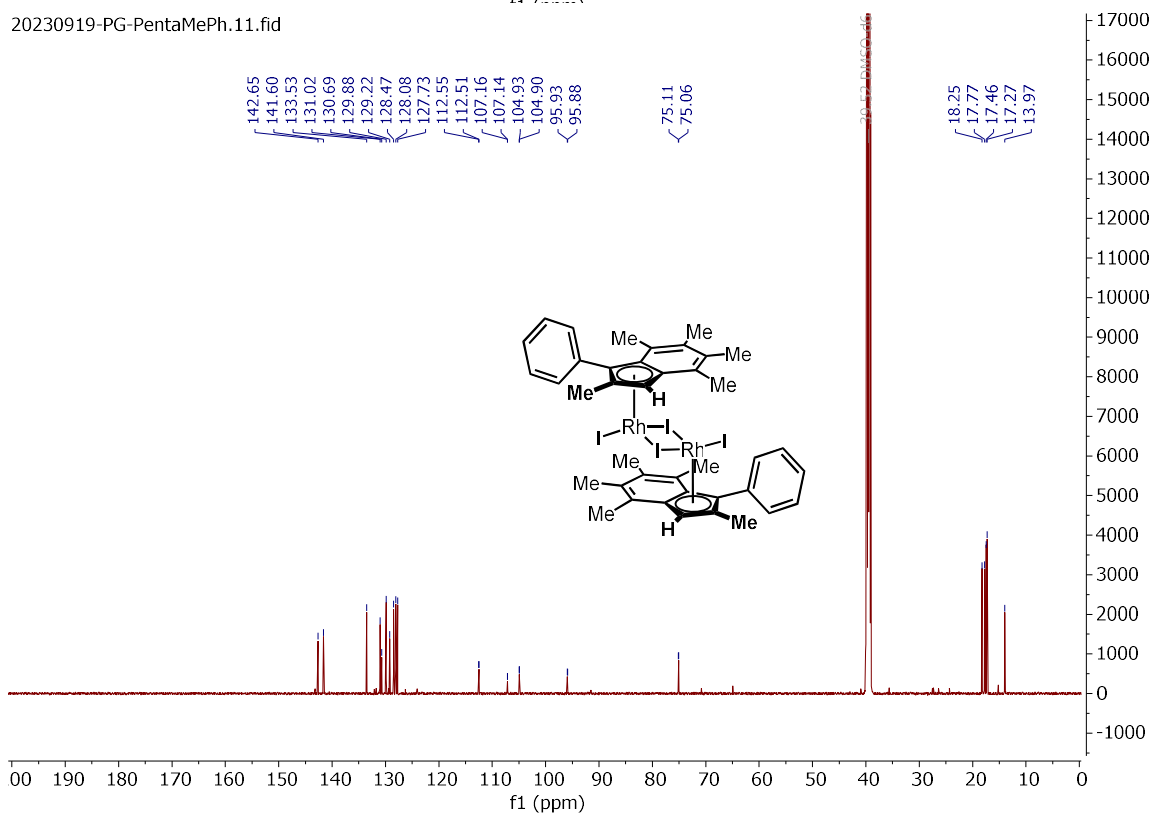


(S,S)-(η^5 -2,4,5,6,7-pentamethyl-3-phenylinden-1H-yl) rhodium(III) diiodide dimer (**(S,S)-8**):

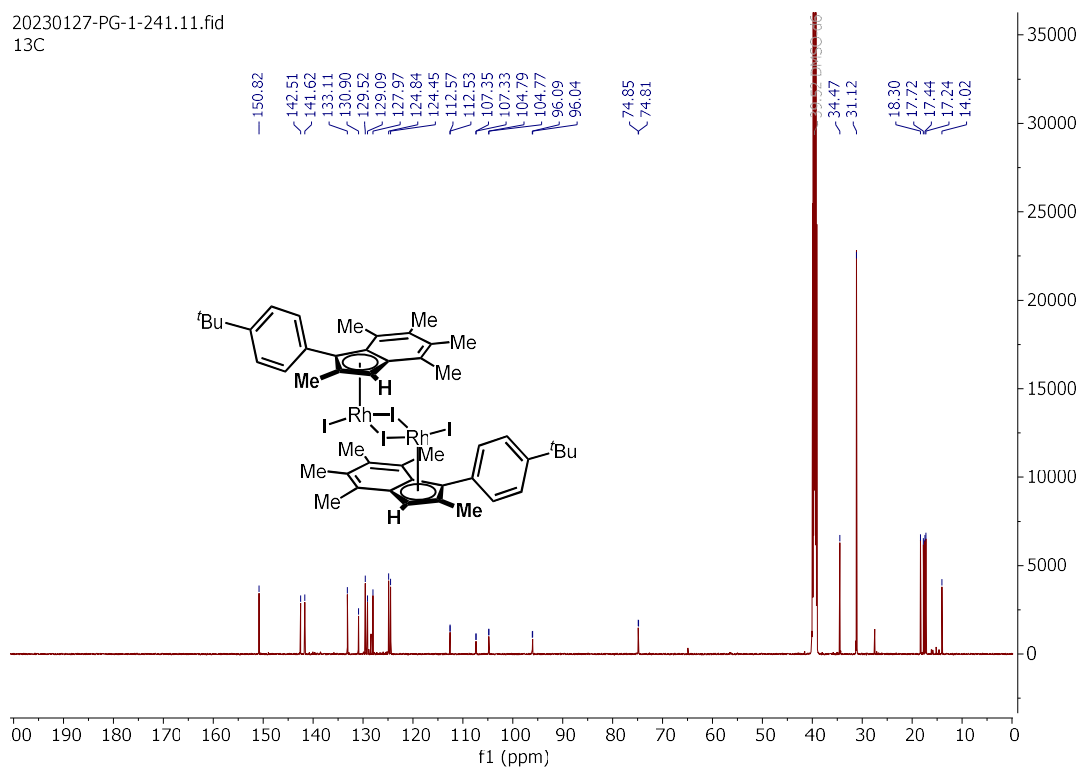
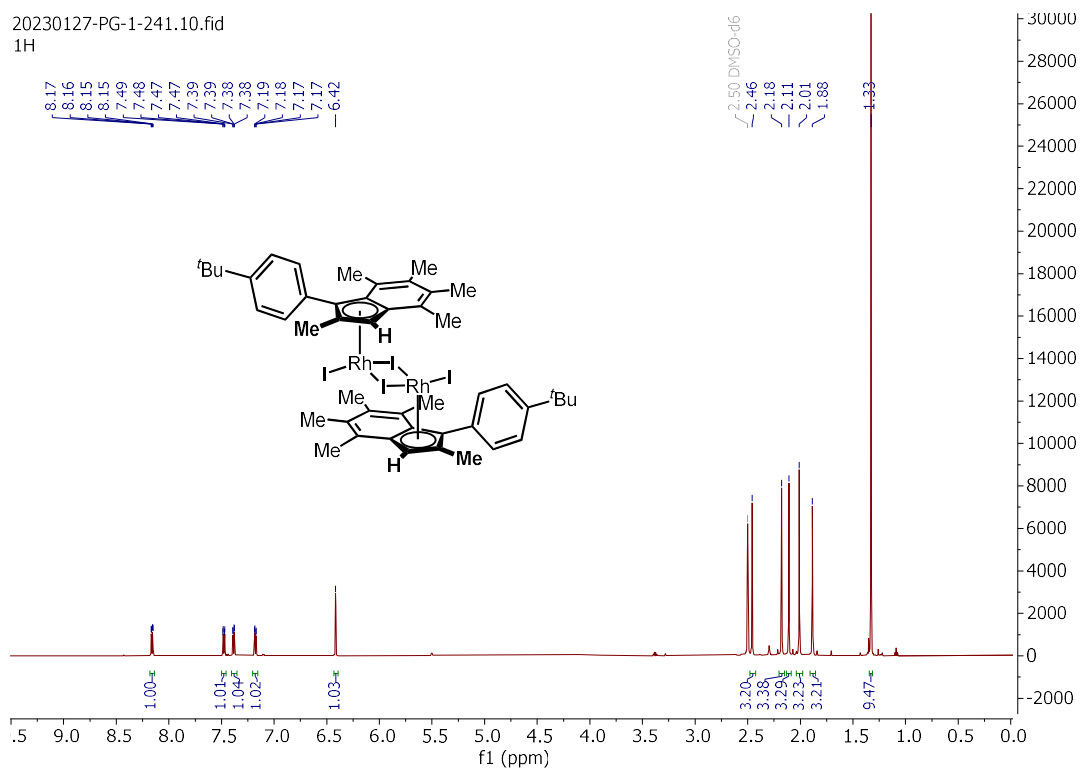
20230919-PG-PentaMePh.10.fid



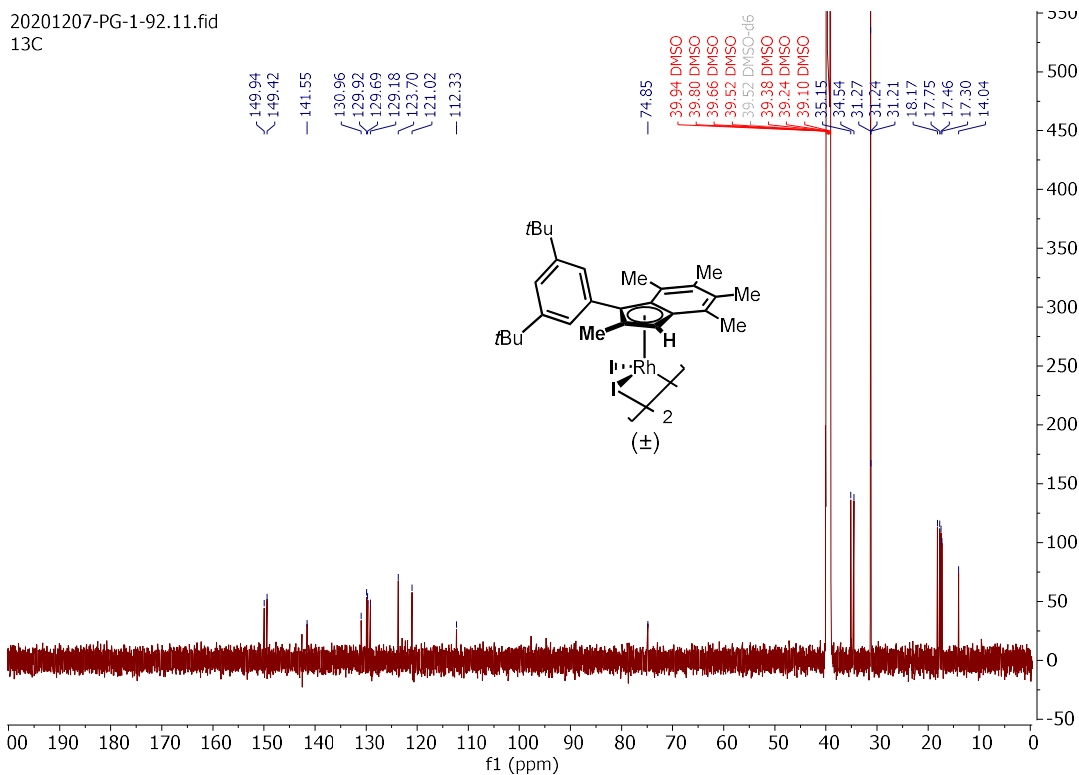
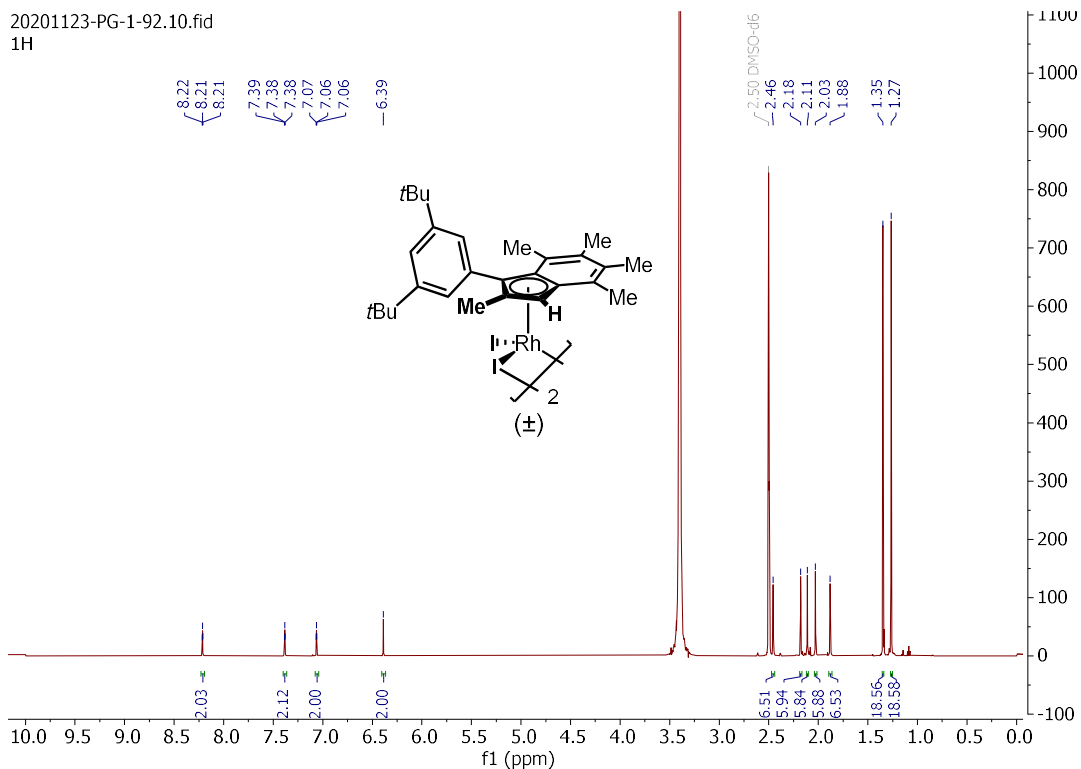
20230919-PG-PentaMePh.11.fid



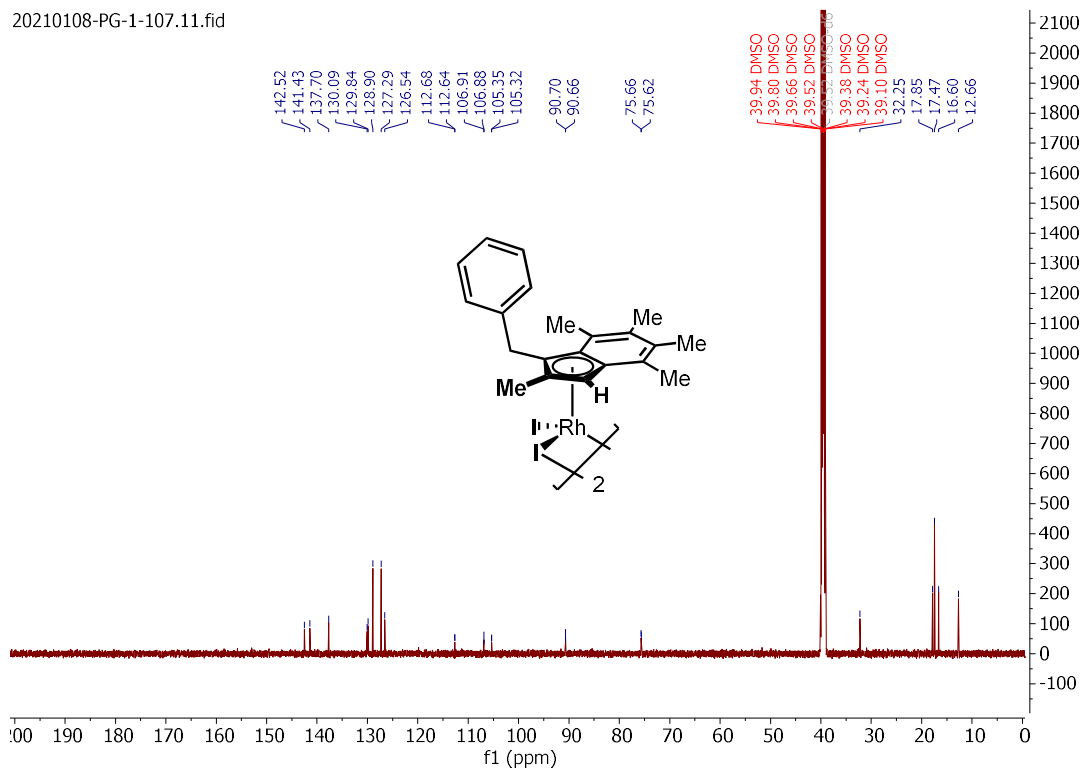
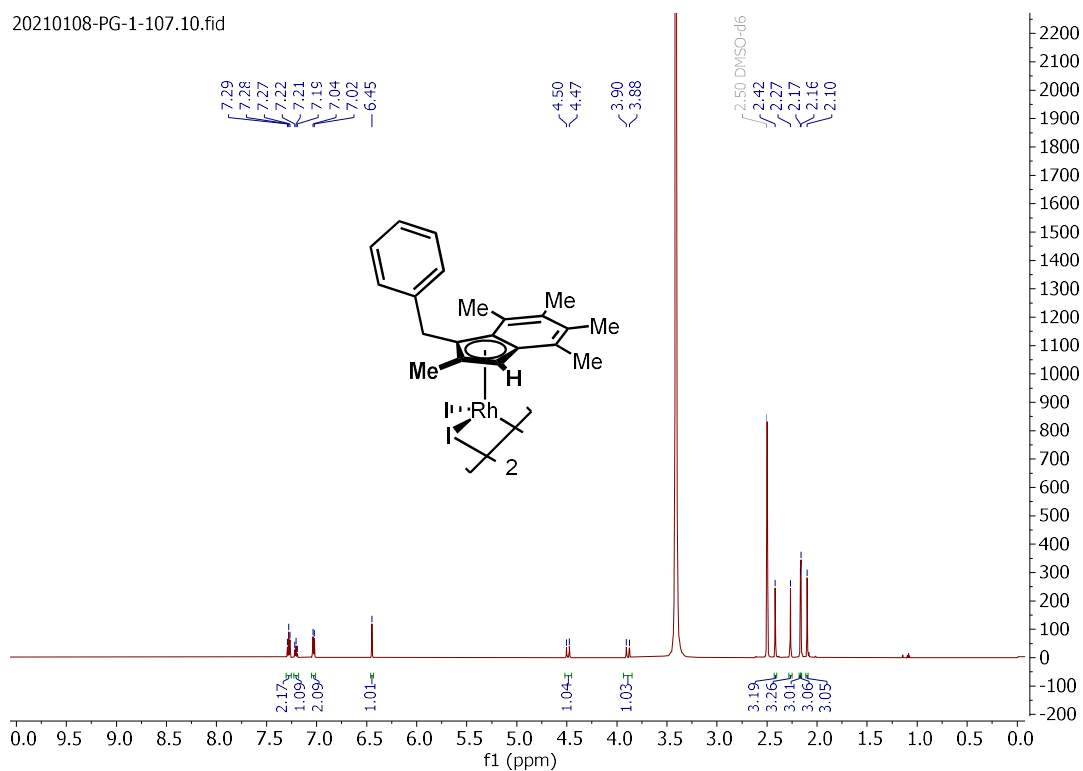
$(\eta^5-3-(4-(tert\text{-butyl})phenyl)-2,4,5,6,7\text{-pentamethylinden-1H-yl})$ rhodium(III) diiodide dimer (**2.80**)



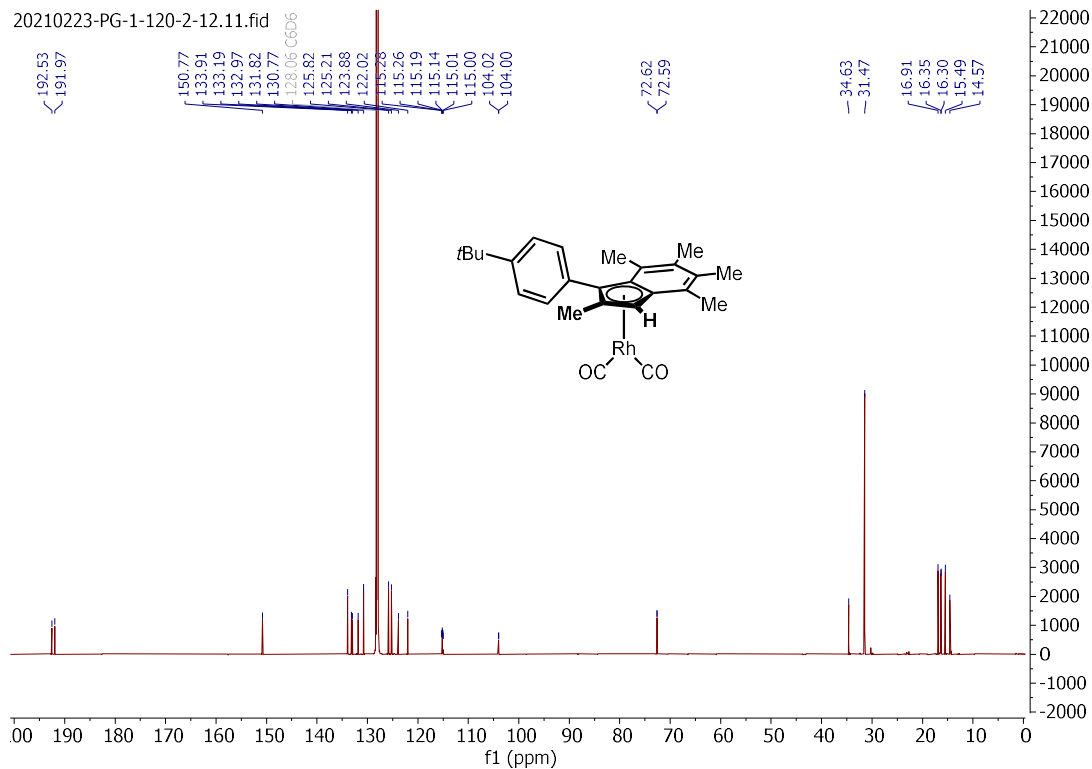
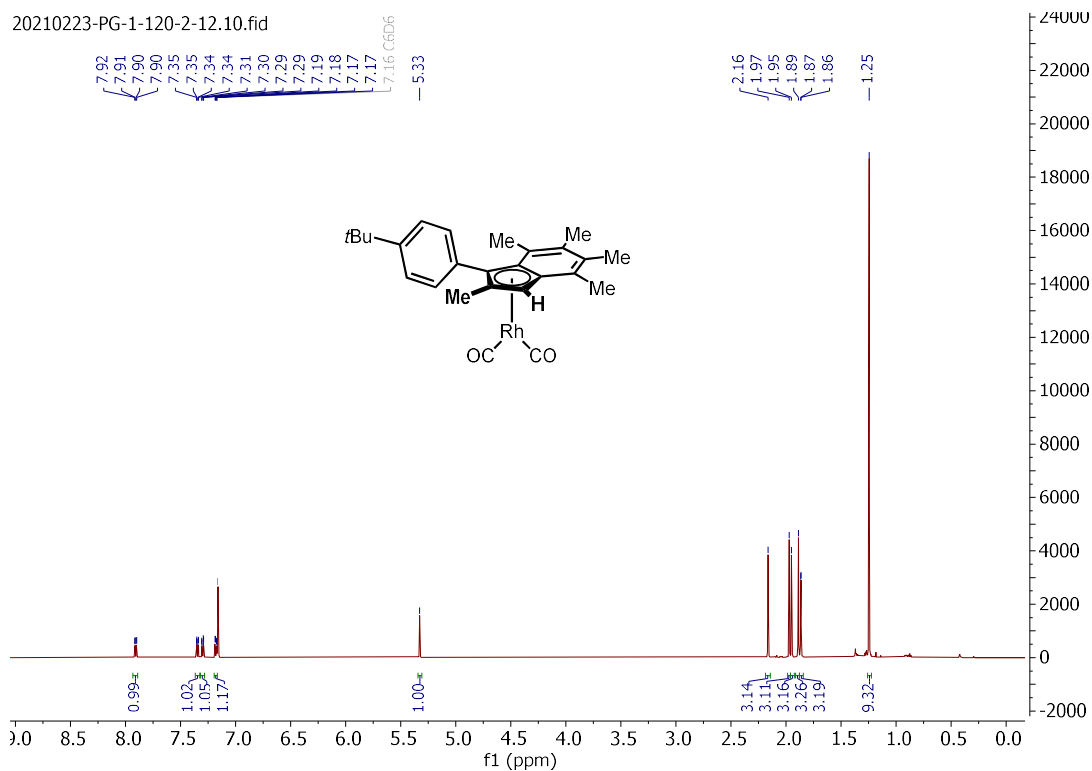
(±)-(η⁵-3-(3,5-di-tert-butylphenyl)-2,4,5,6,7-pentamethyl-1H-inden-1-yl)rhodium(III) diiodide dimer (2.81):



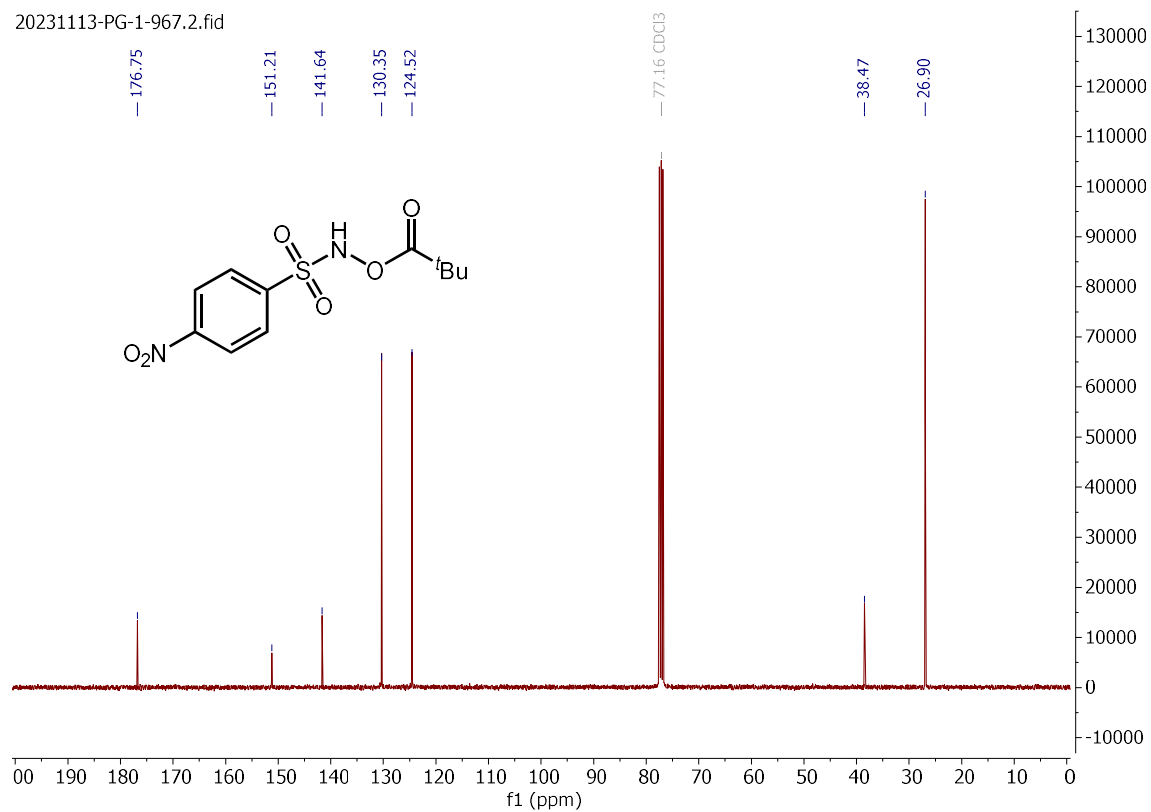
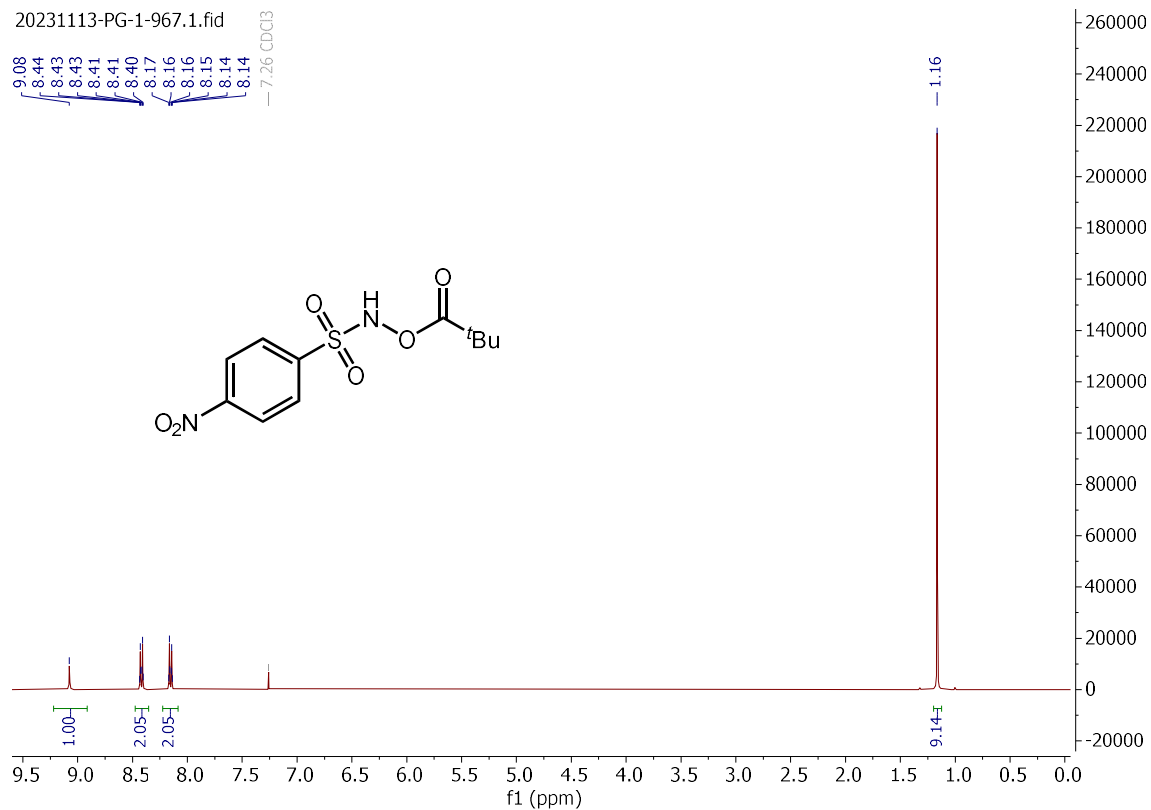
(±)-(η⁵-3-benzyl-2,4,5,6,7-pentamethyl-1H-inden-1-yl)rhodium(III) diiodide dimer (**2.82**):



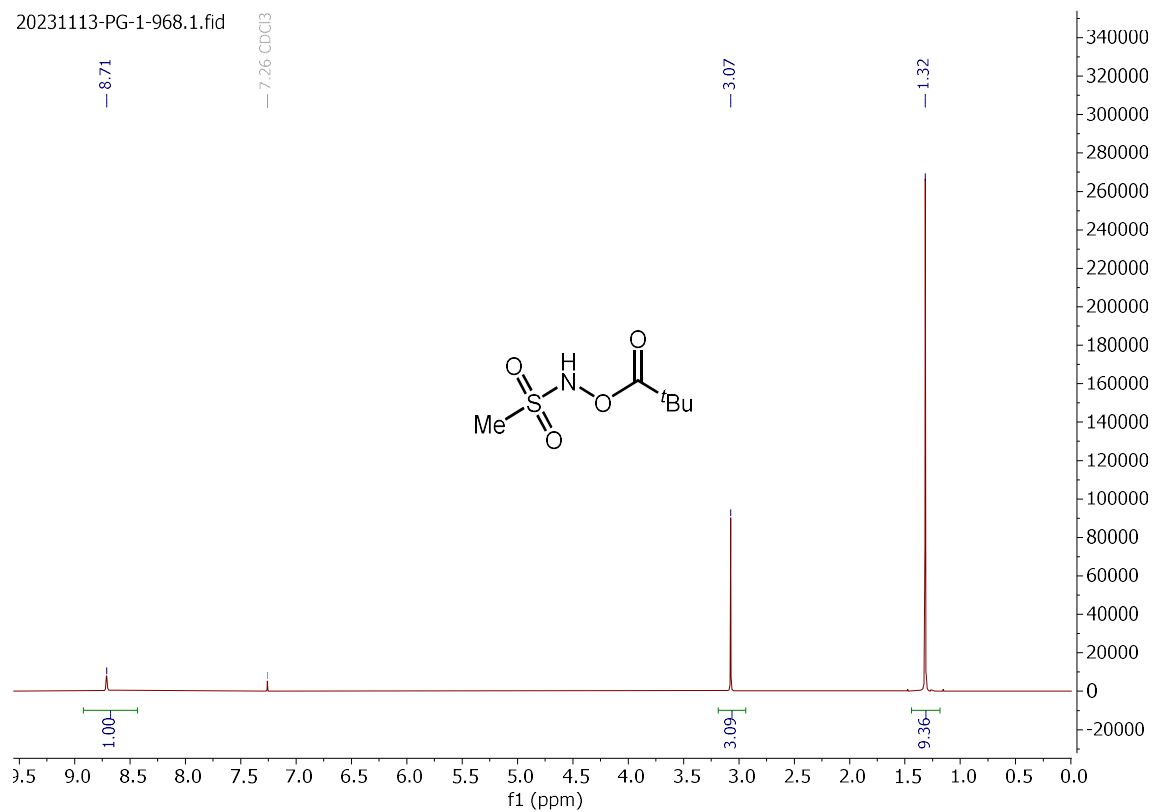
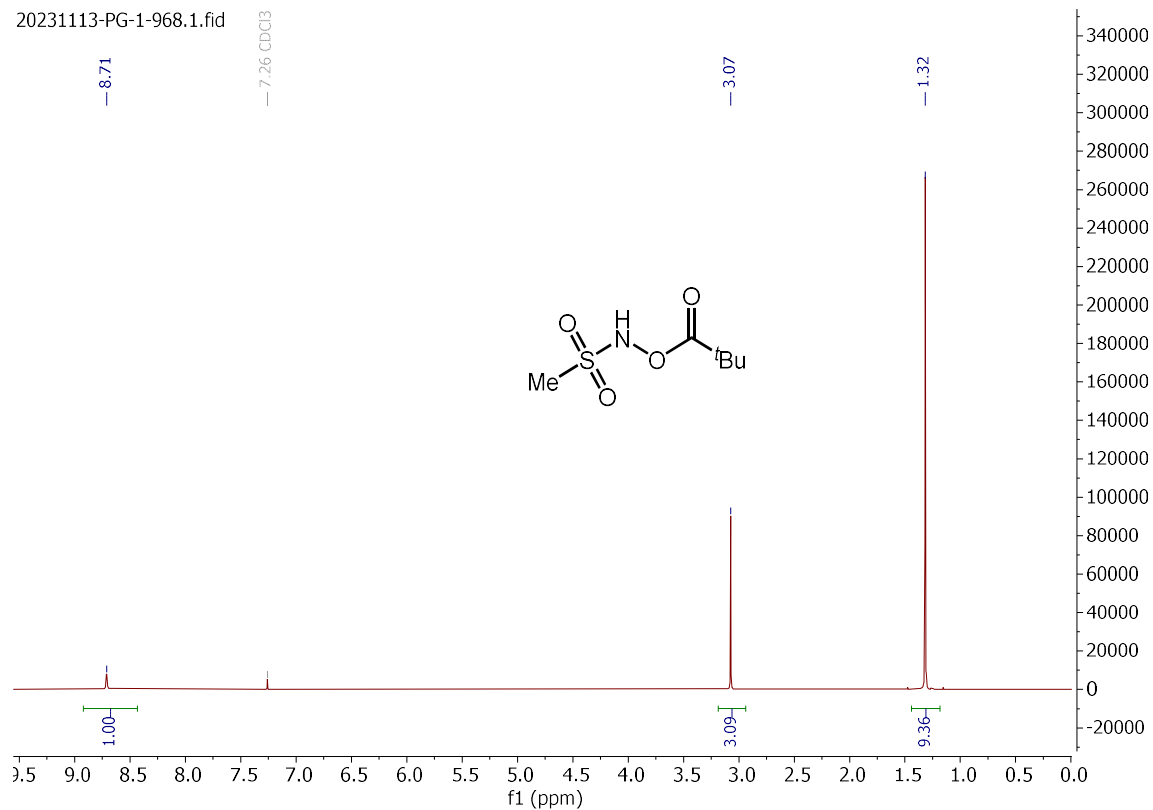
(±)-di-carbonyl-(η^5 -3-(4-(tert-butyl)phenyl)-2,4,5,6,7-pentamethylinden-1H-yl)rhodium(I) (**2.108**):



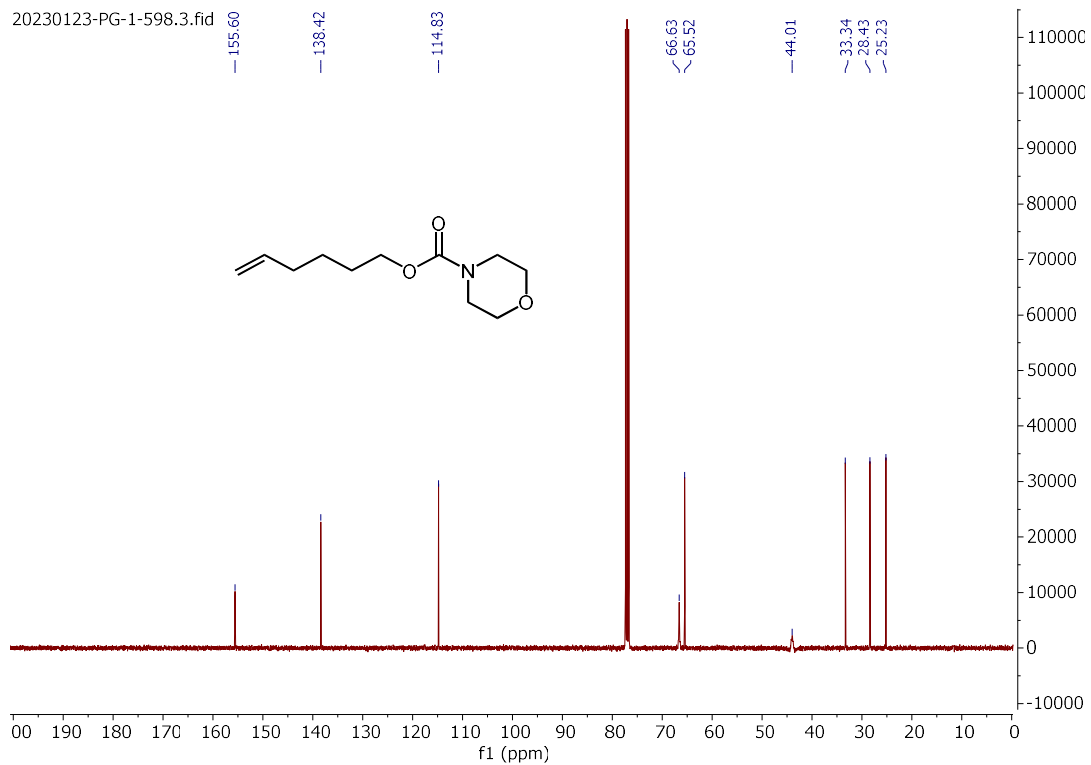
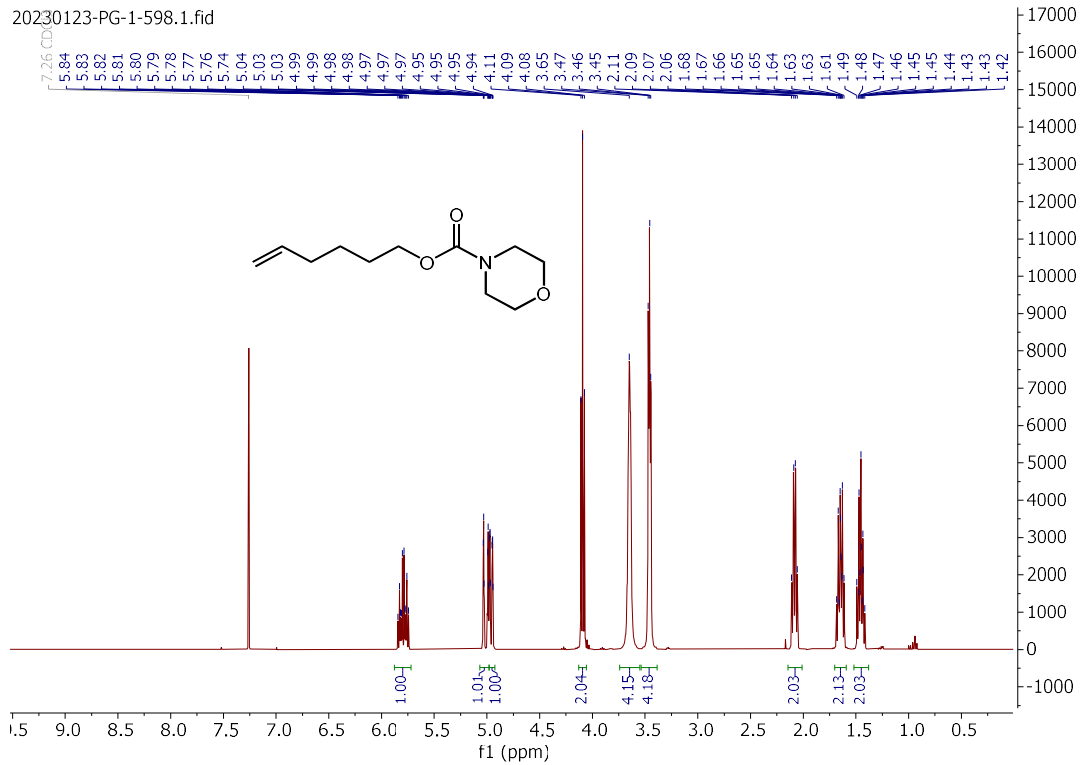
4-nitro-N-(pivaloyloxy)benzenesulfonamide (S31):



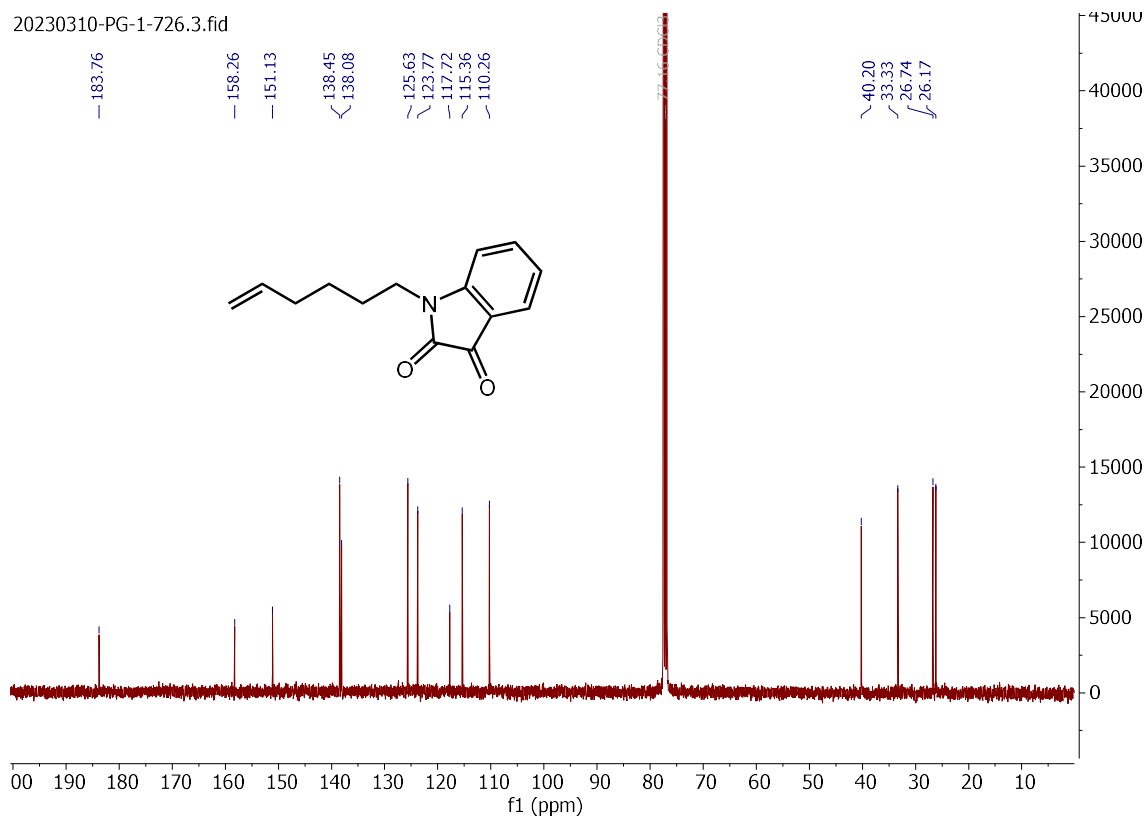
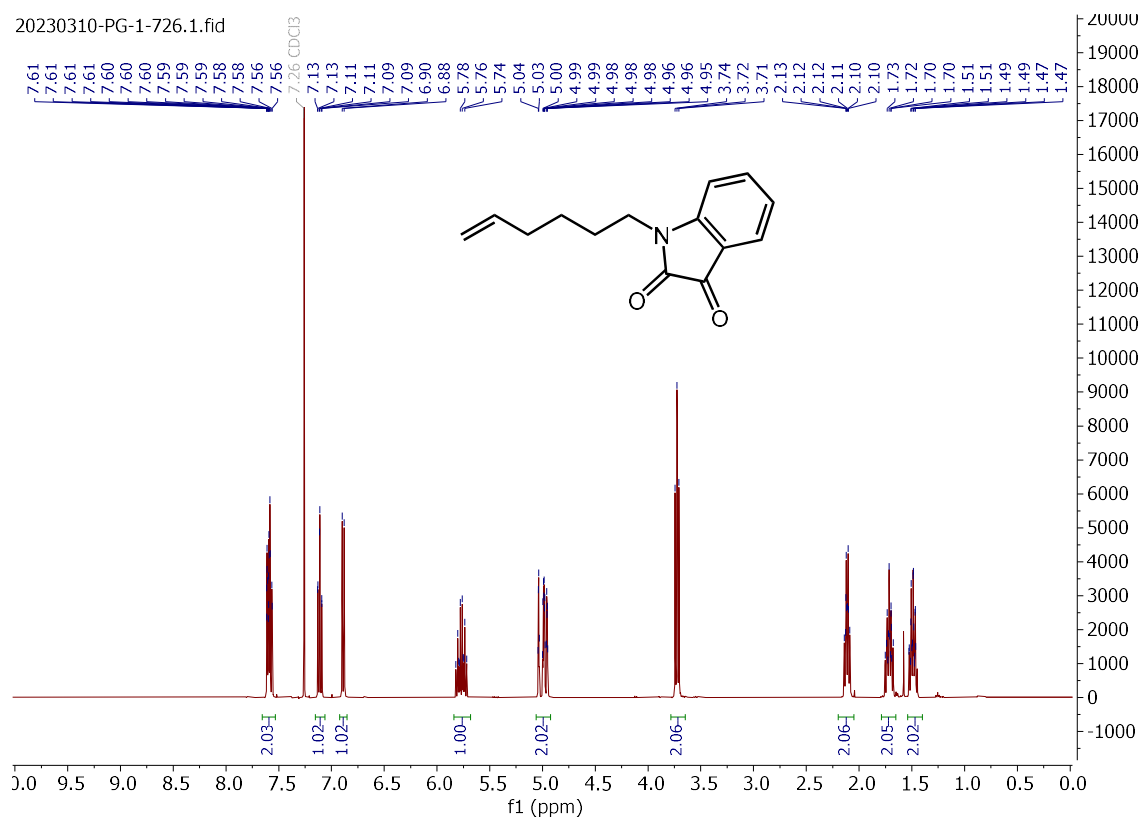
N-(pivaloyloxy)methanesulfonamide (**S32**):



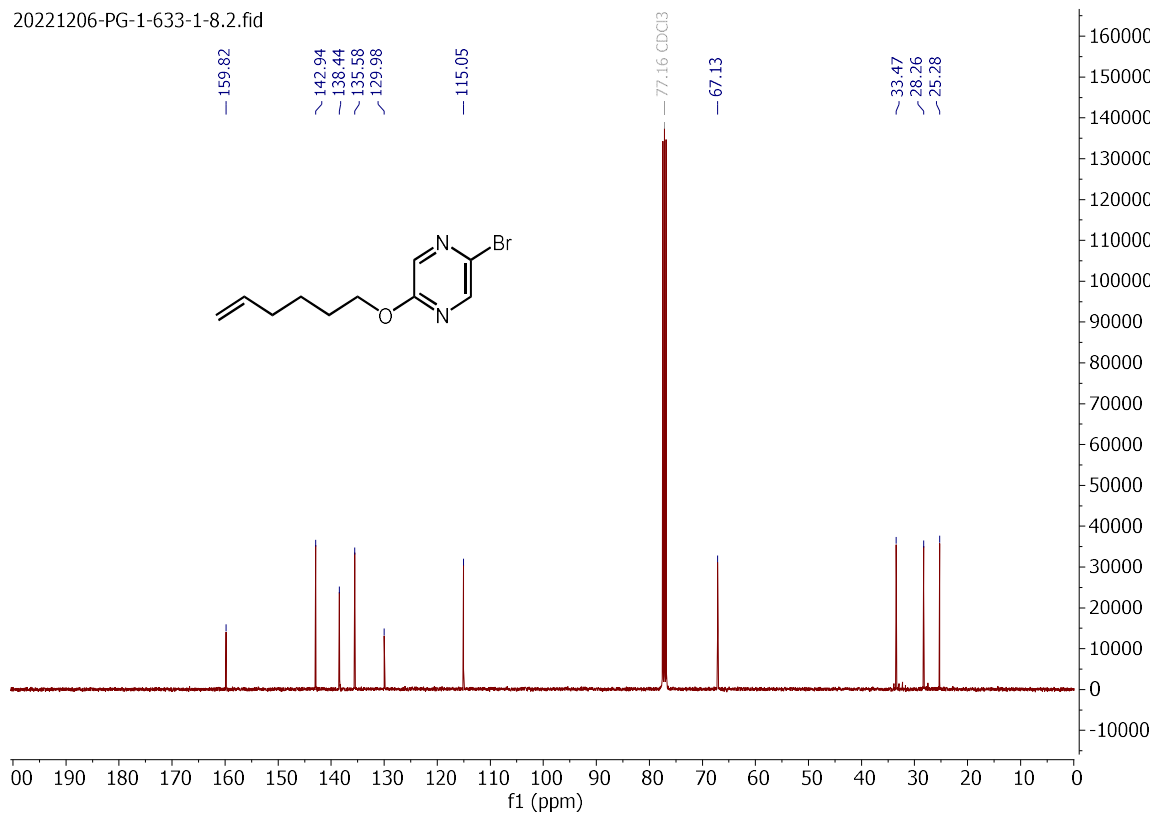
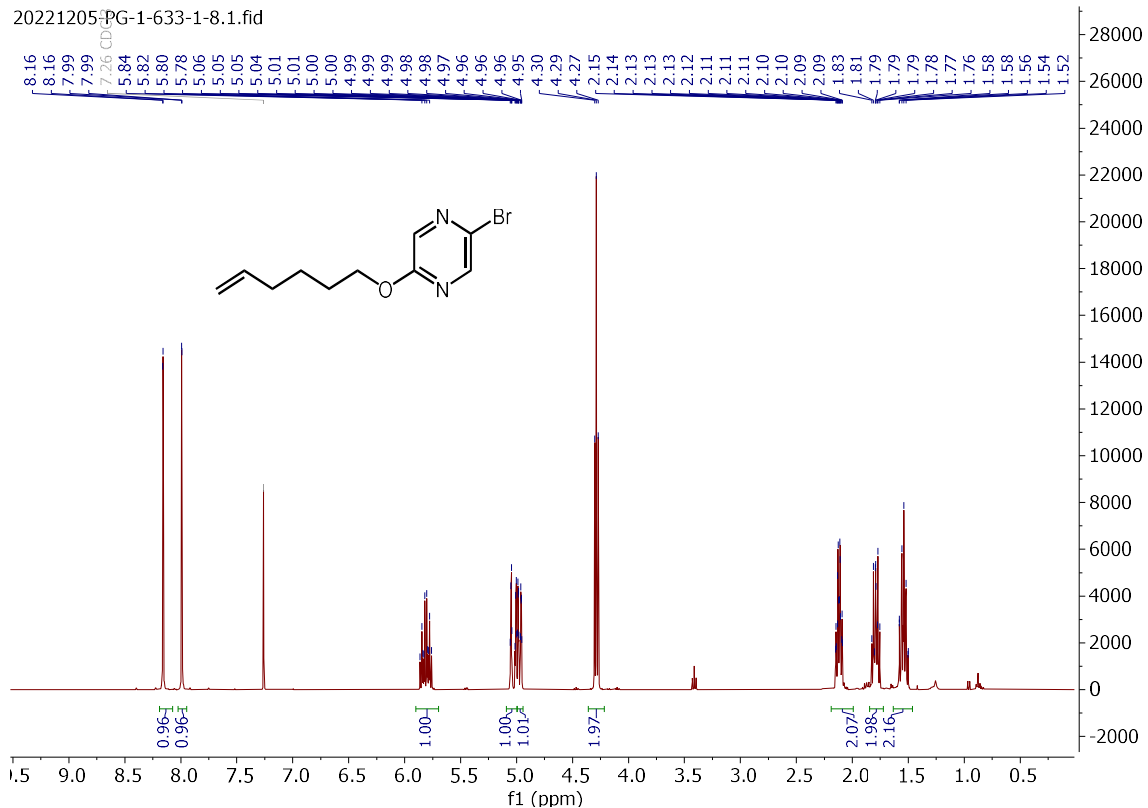
hex-5-en-1-yl morpholine-4-carboxylate (S33):



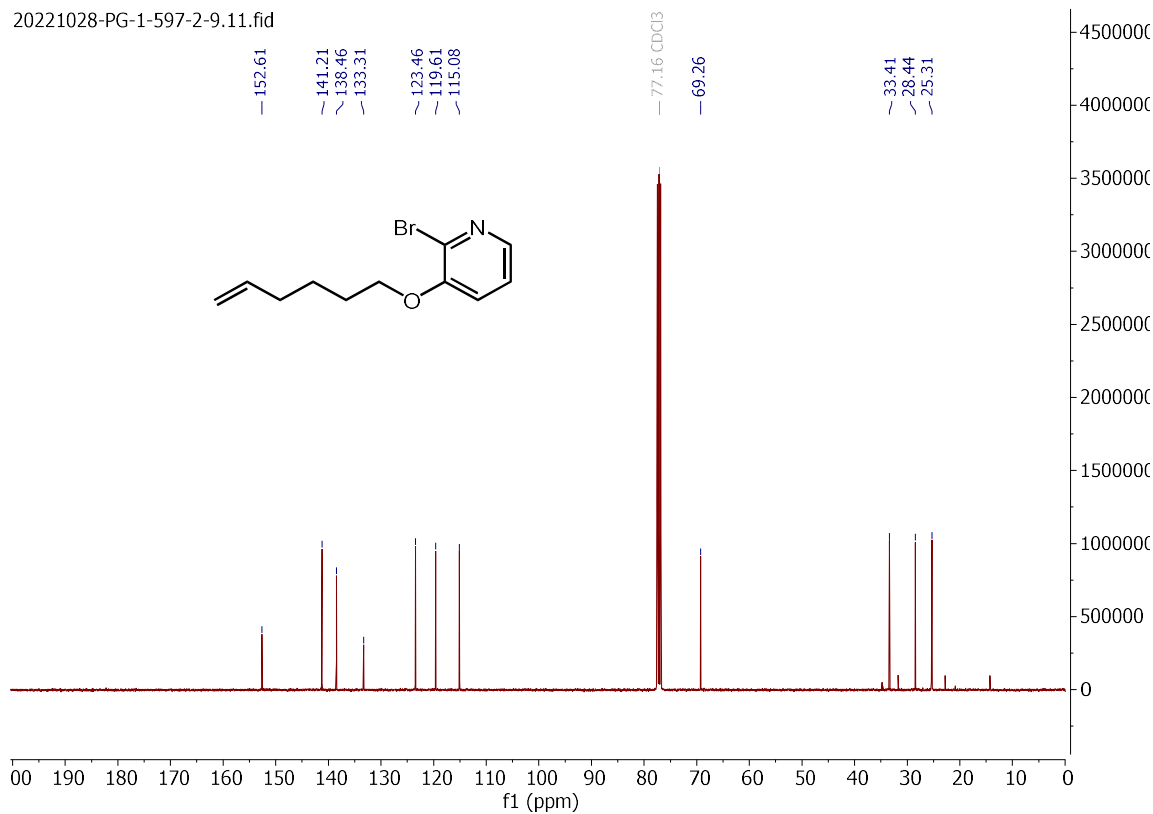
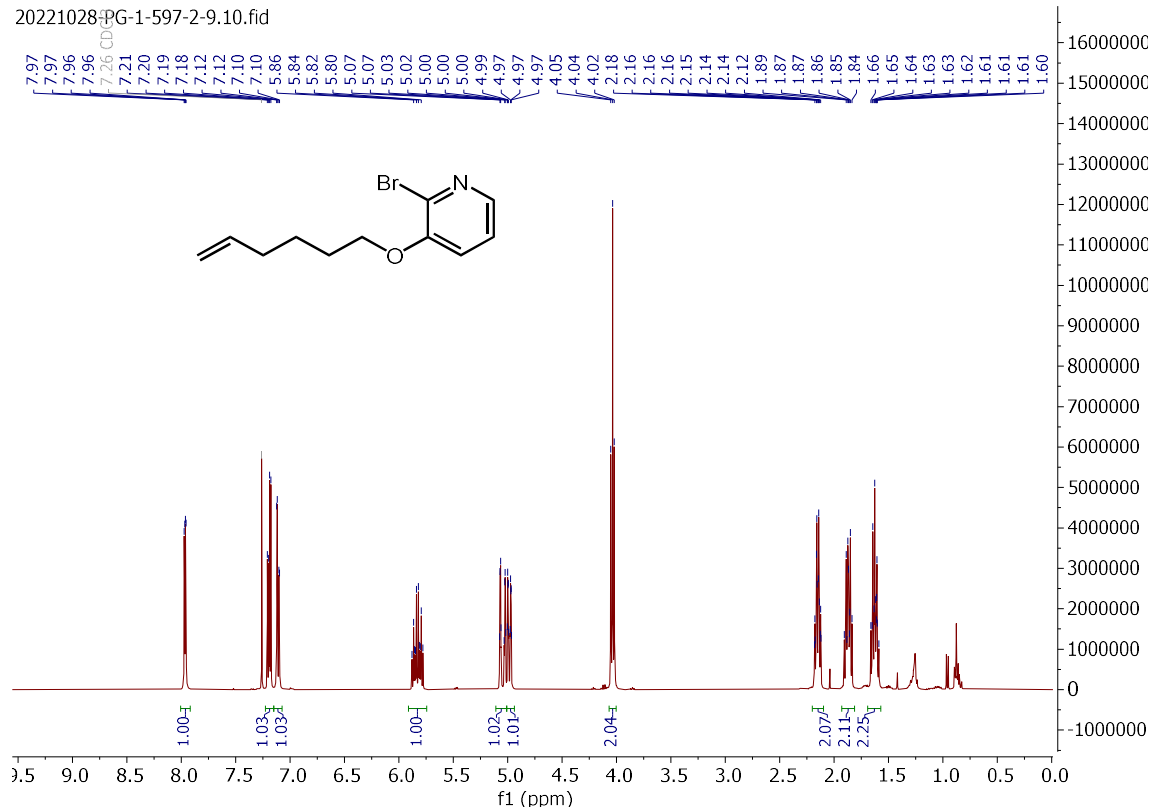
1-(hex-5-en-1-yl)indoline-2,3-dione (S34):



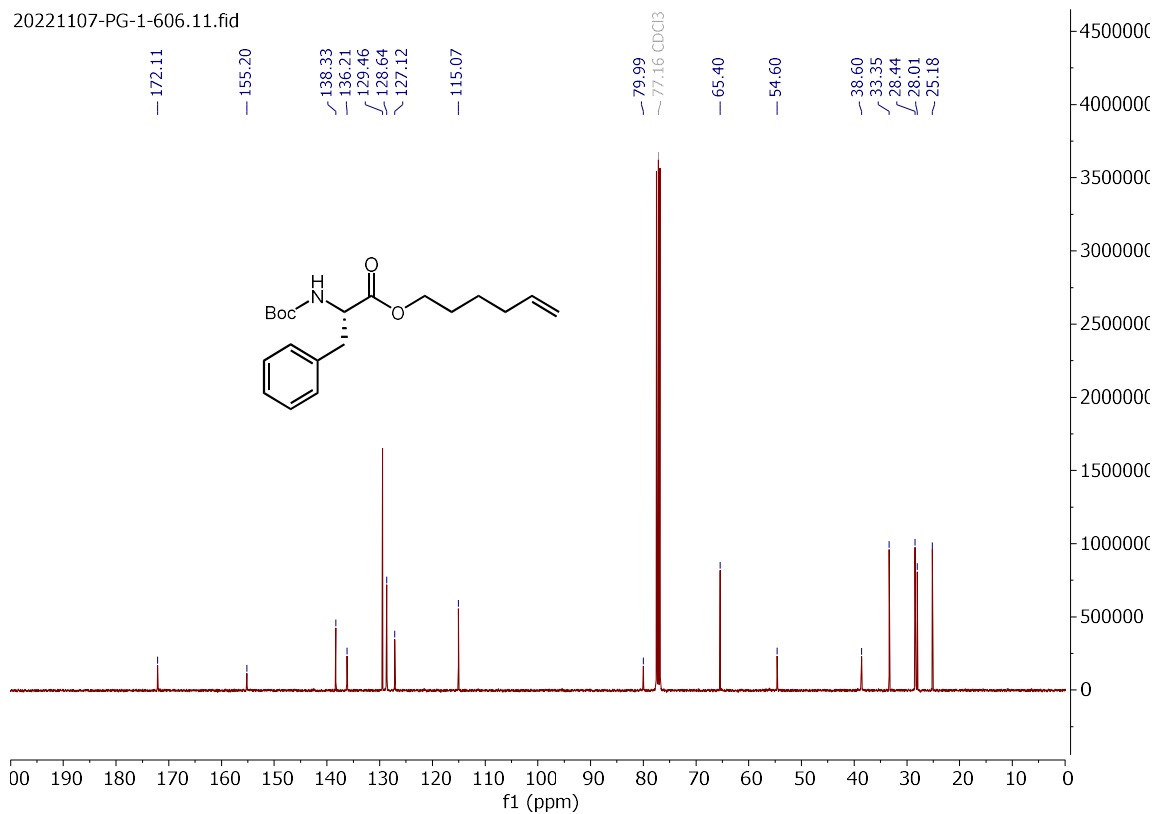
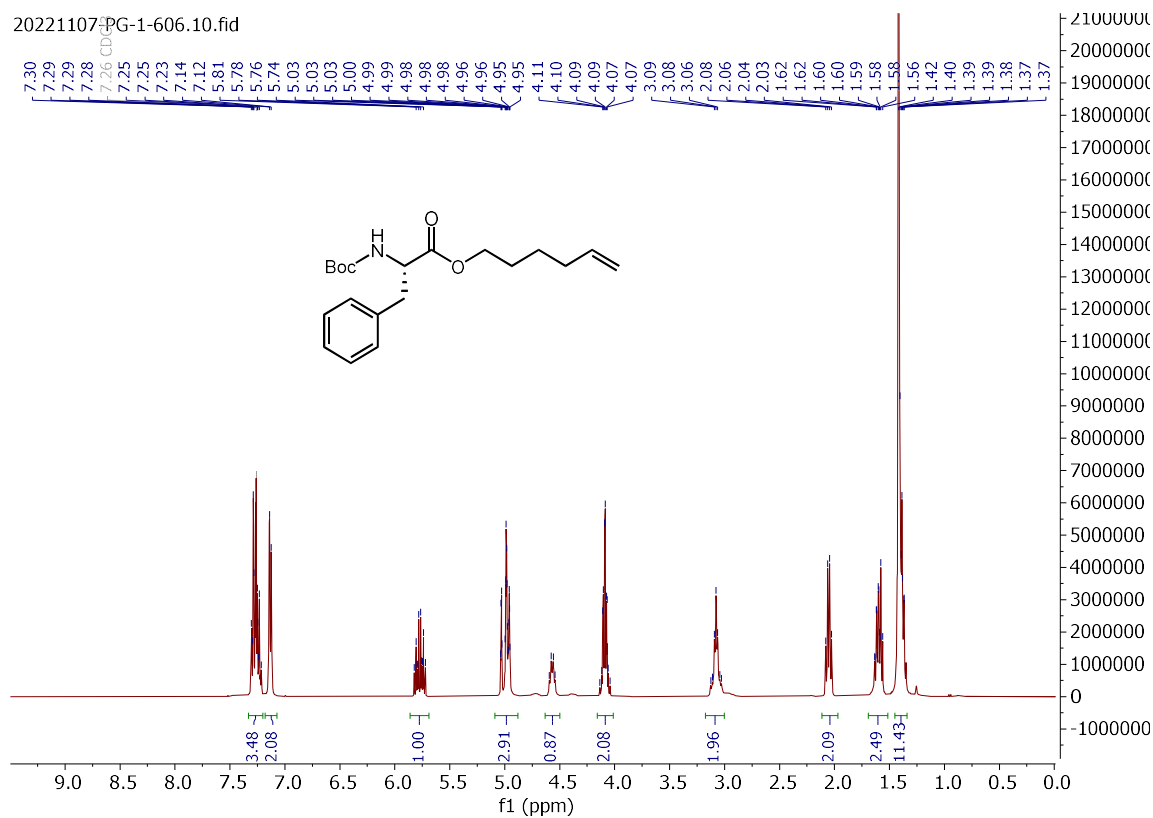
2-bromo-5-(hex-5-en-1-yloxy)pyrazine (S35):



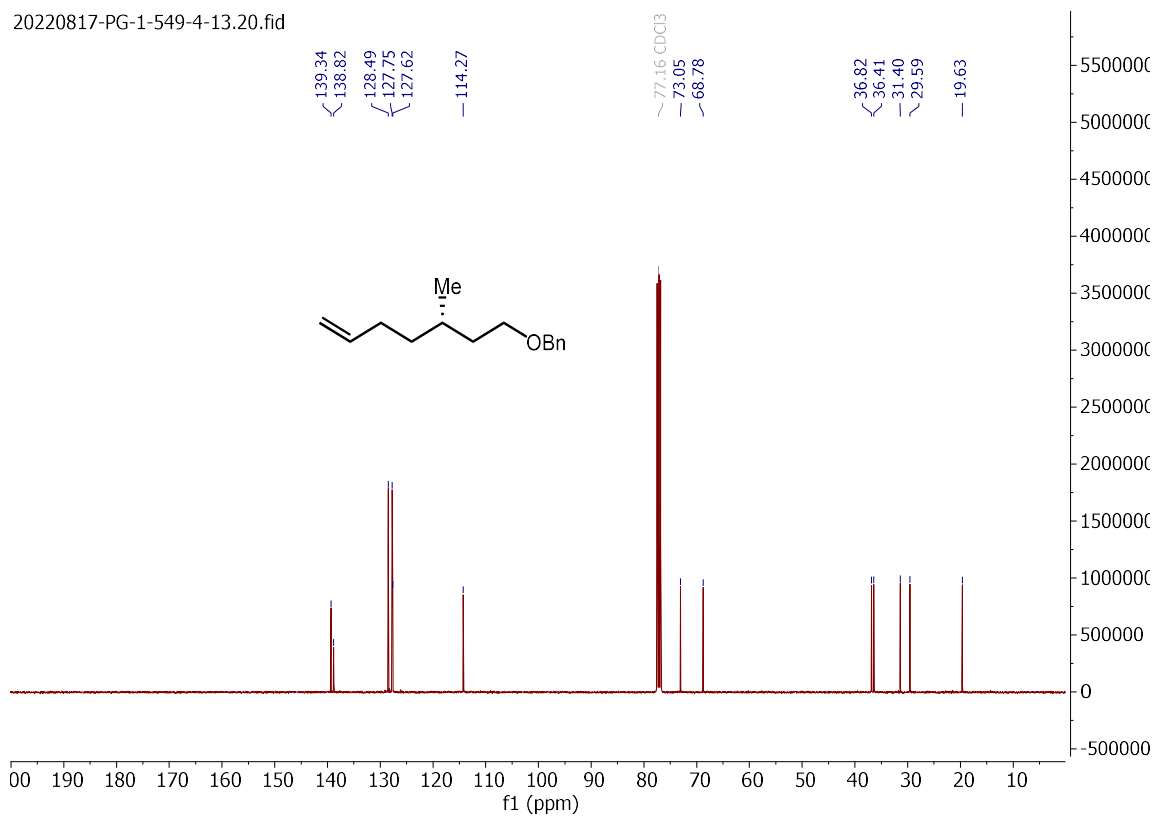
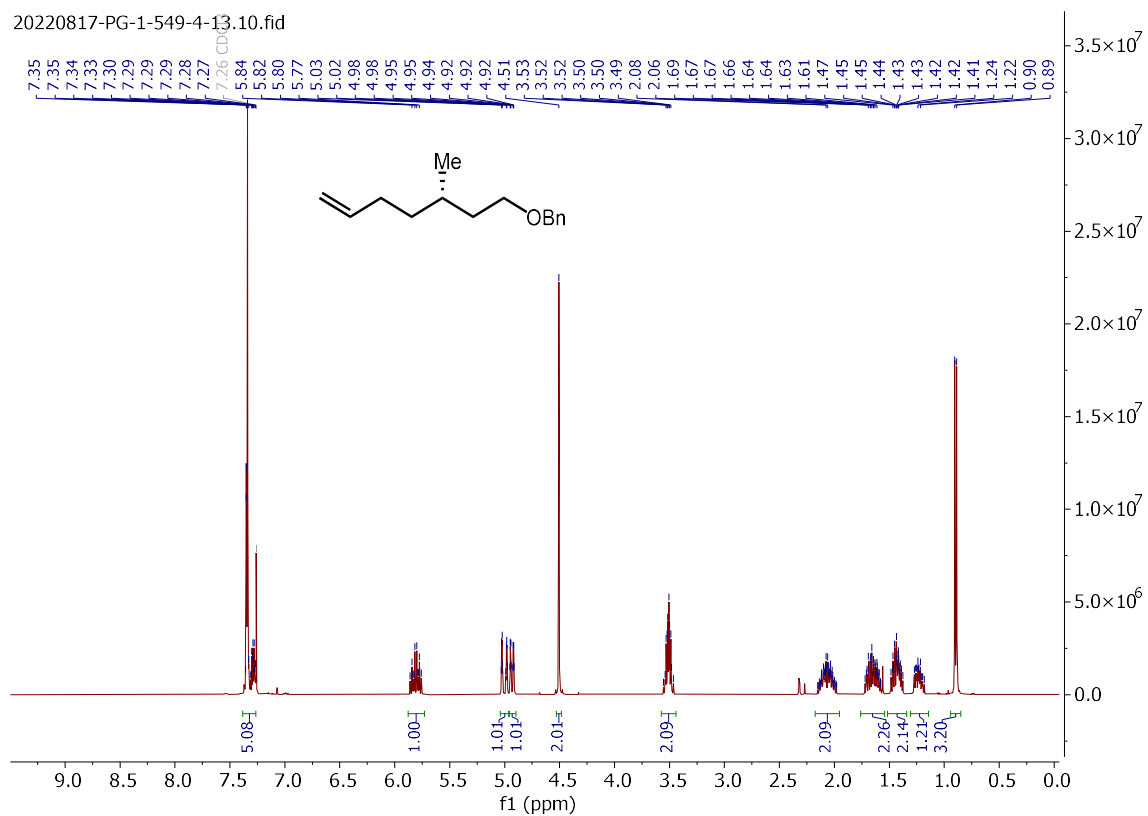
2-bromo-3-(hex-5-en-1-yloxy)pyridine (S36):



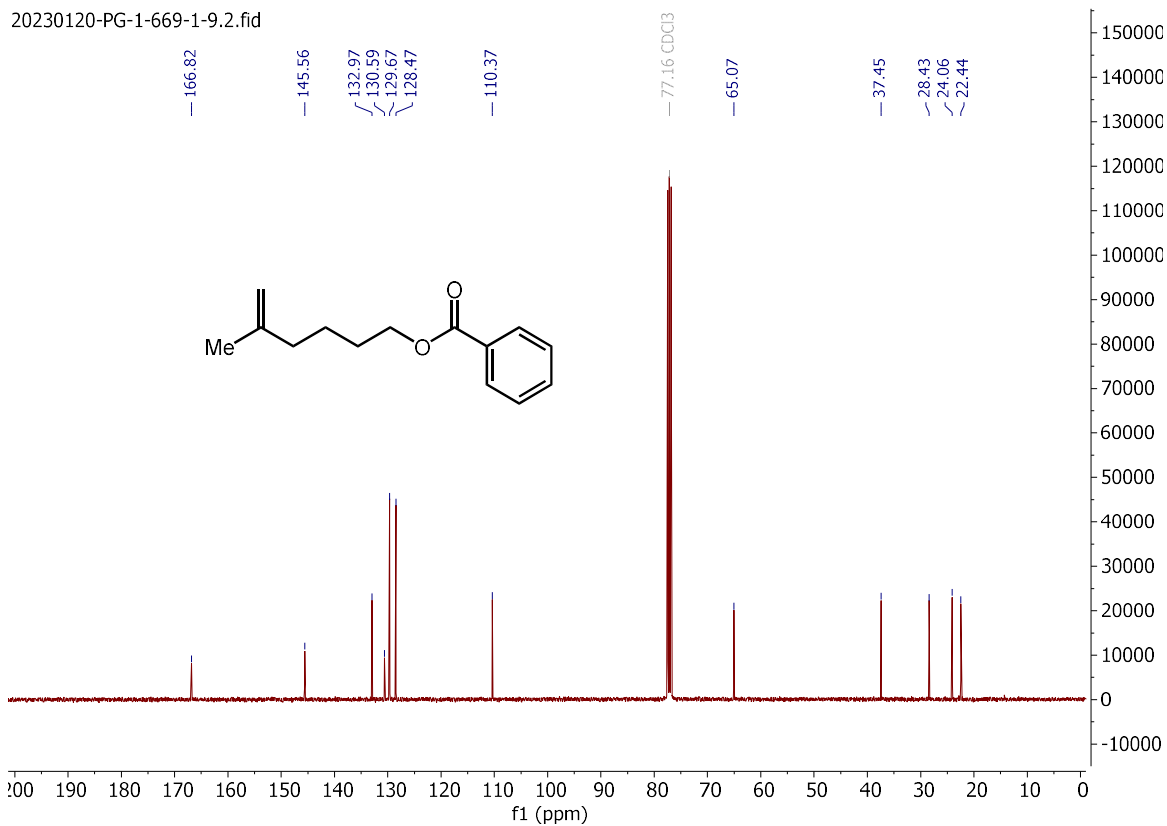
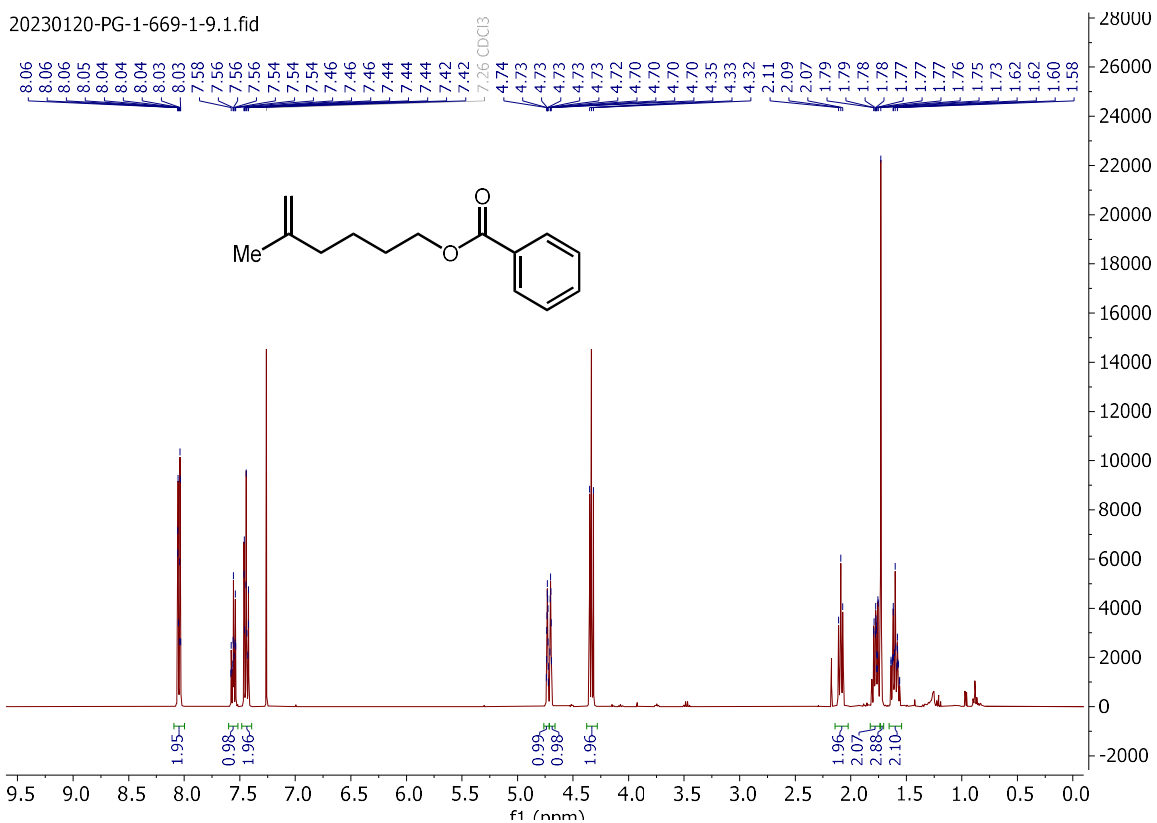
hex-5-en-1-yl (tert-butoxycarbonyl)-L-phenylalaninate (S37):



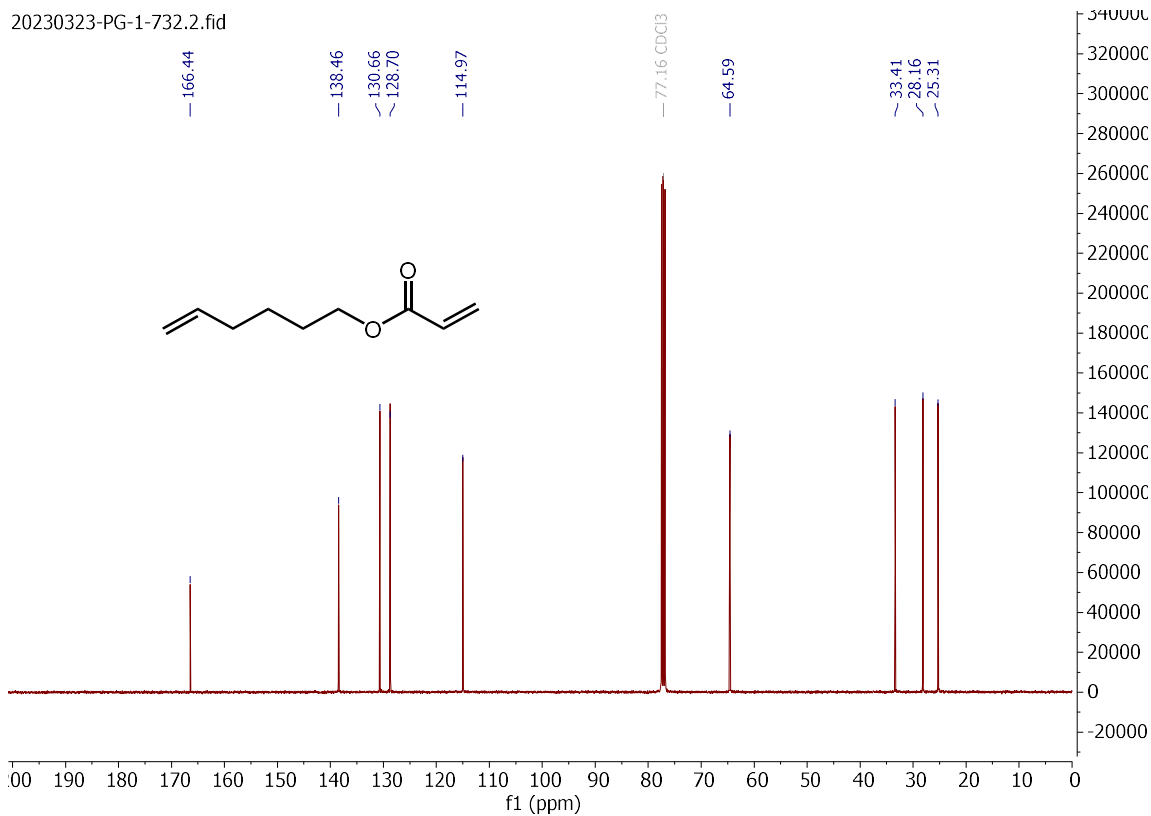
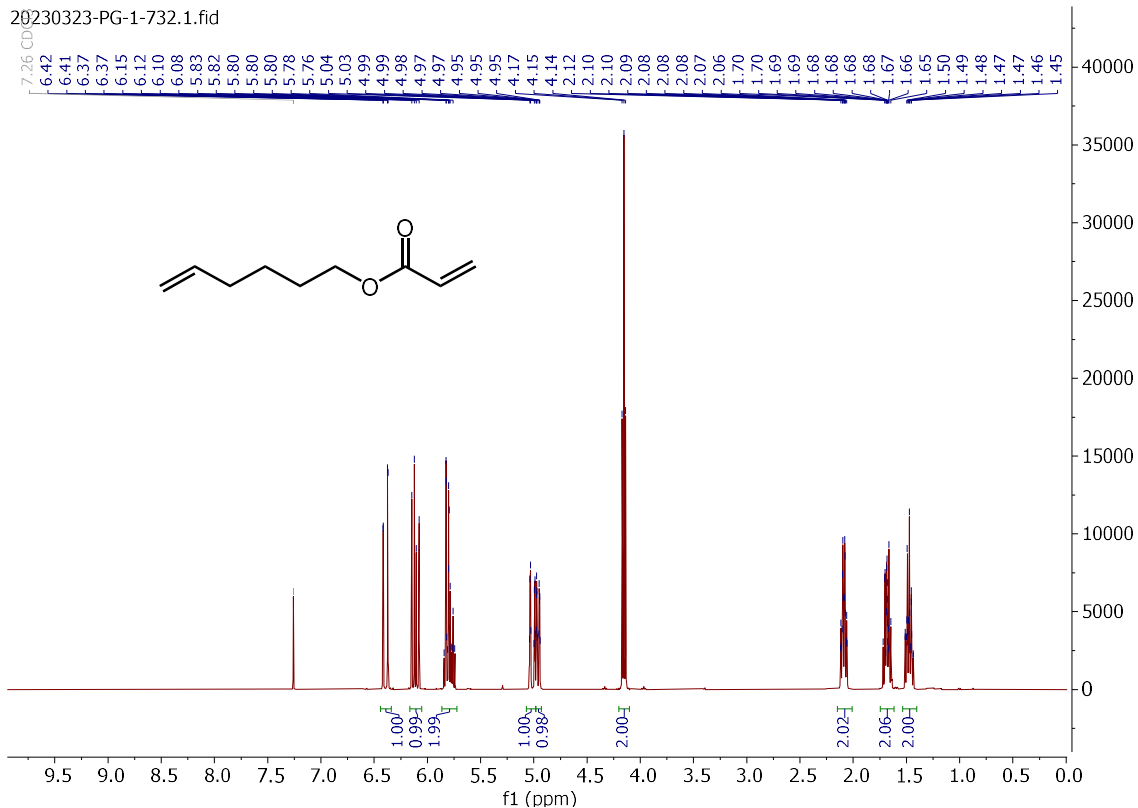
(S)-(((3-methylhept-6-en-1-yl)oxy)methyl)benzene (S41):



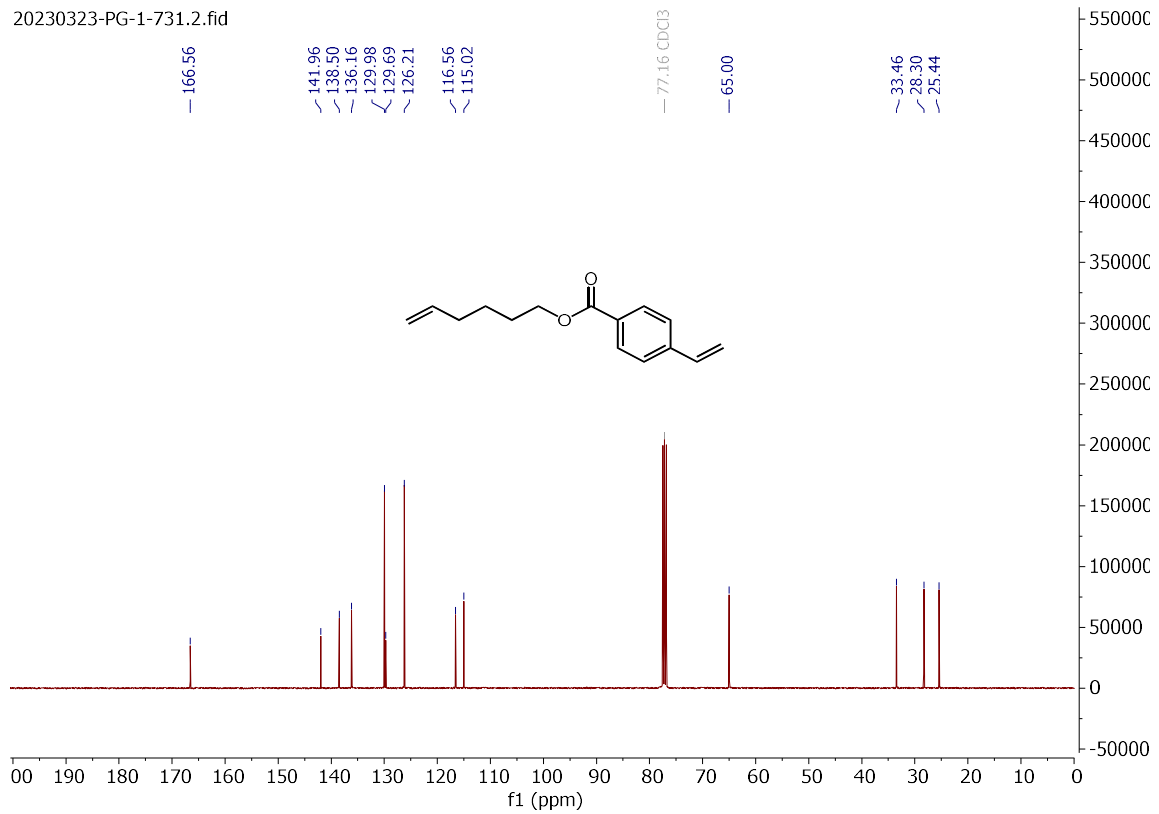
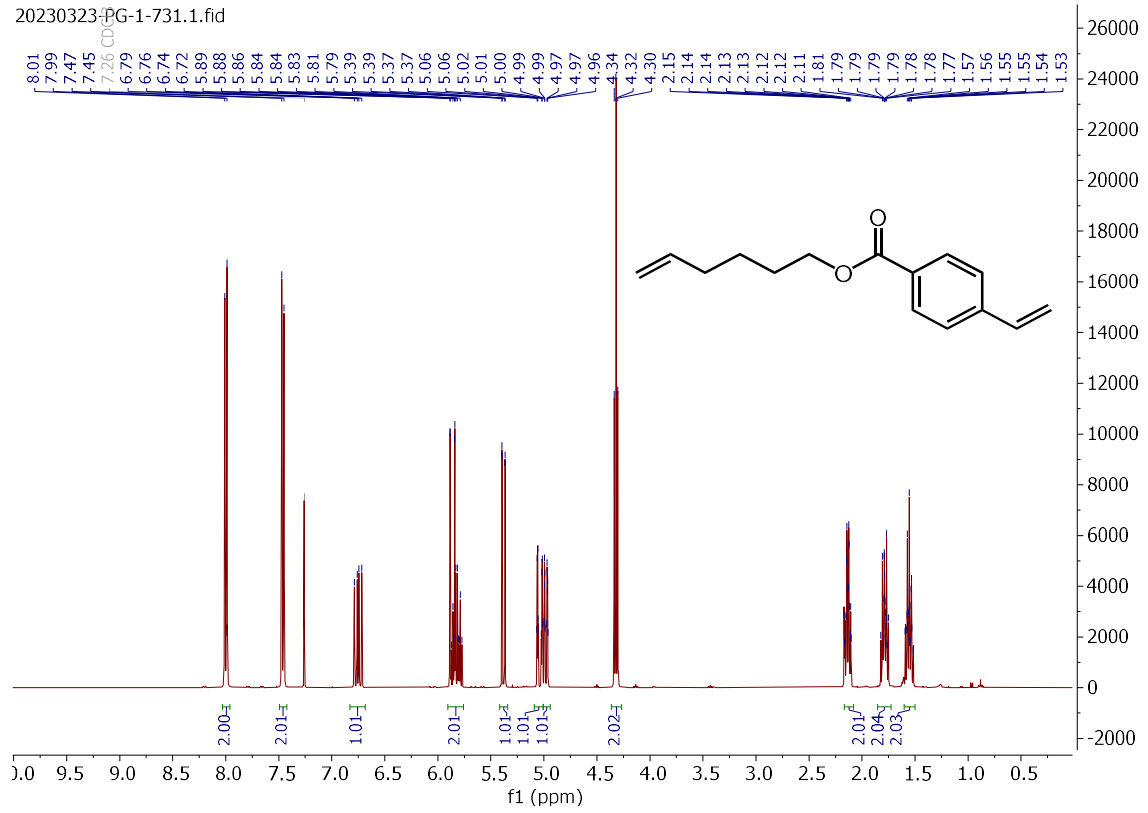
5-methylhex-5-en-1-yl benzoate (S48):



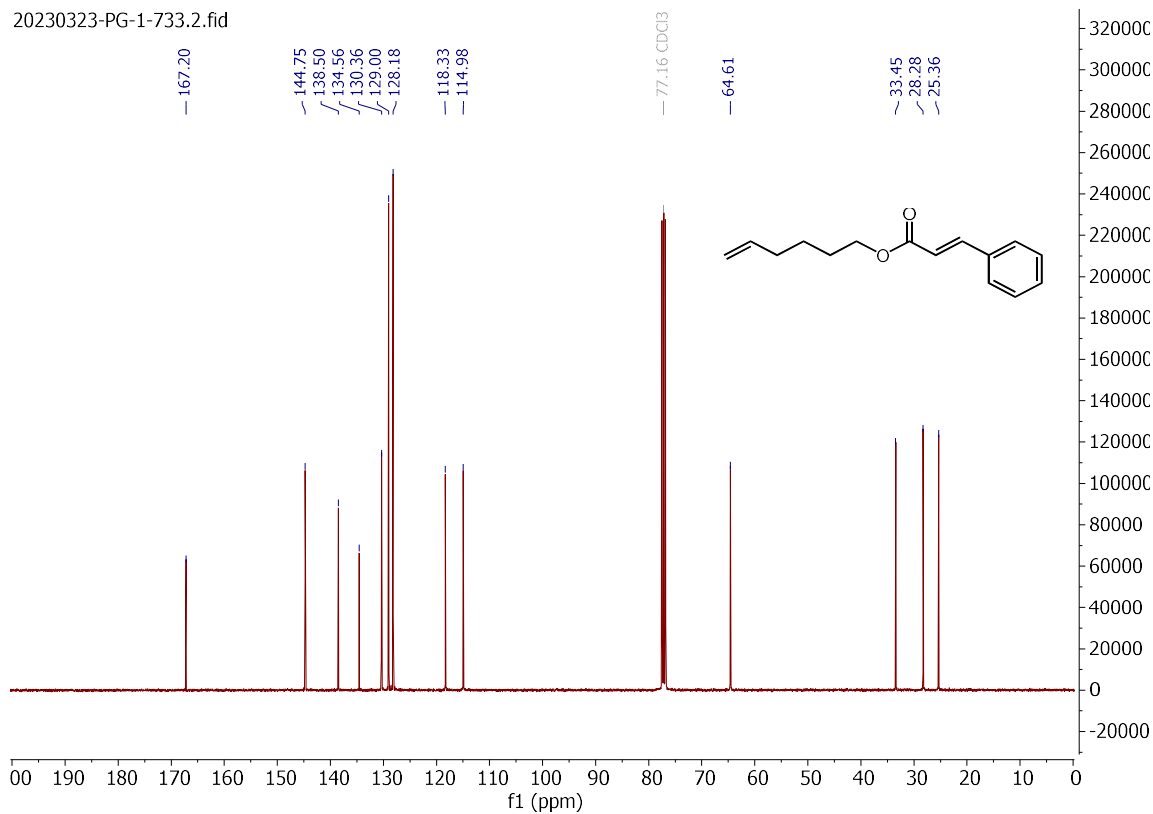
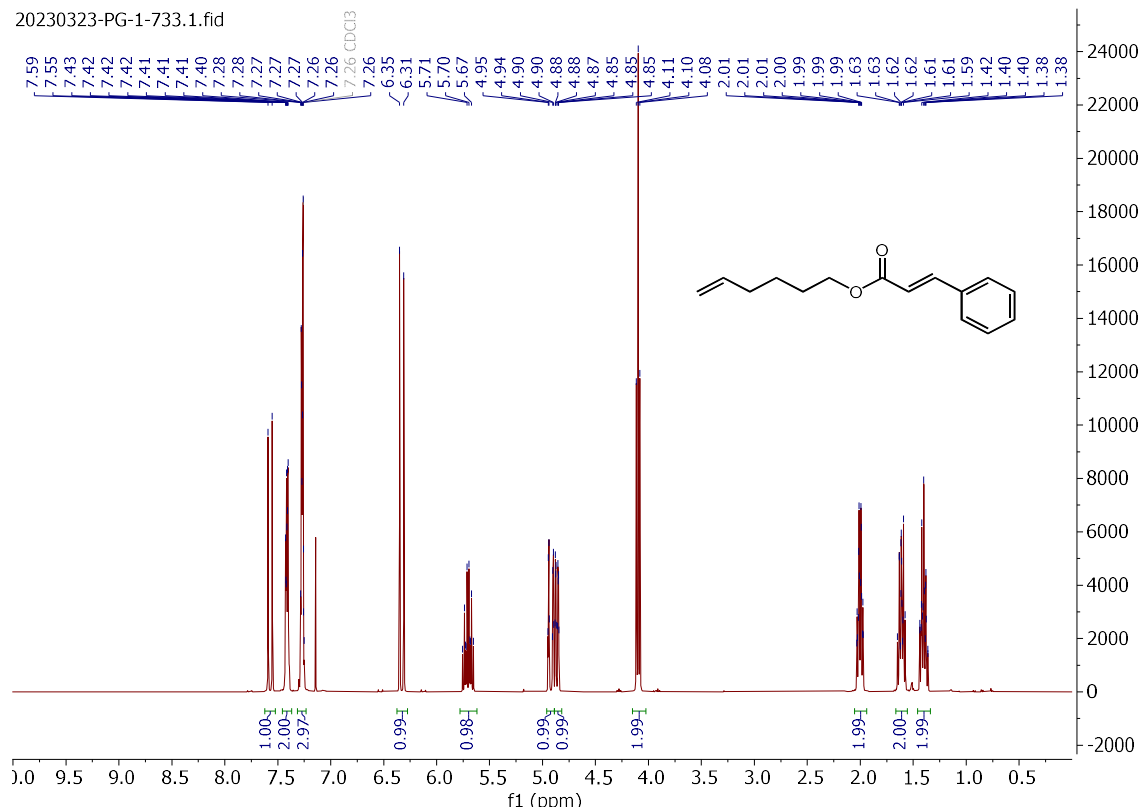
hex-5-en-1-yl acrylate (S49):



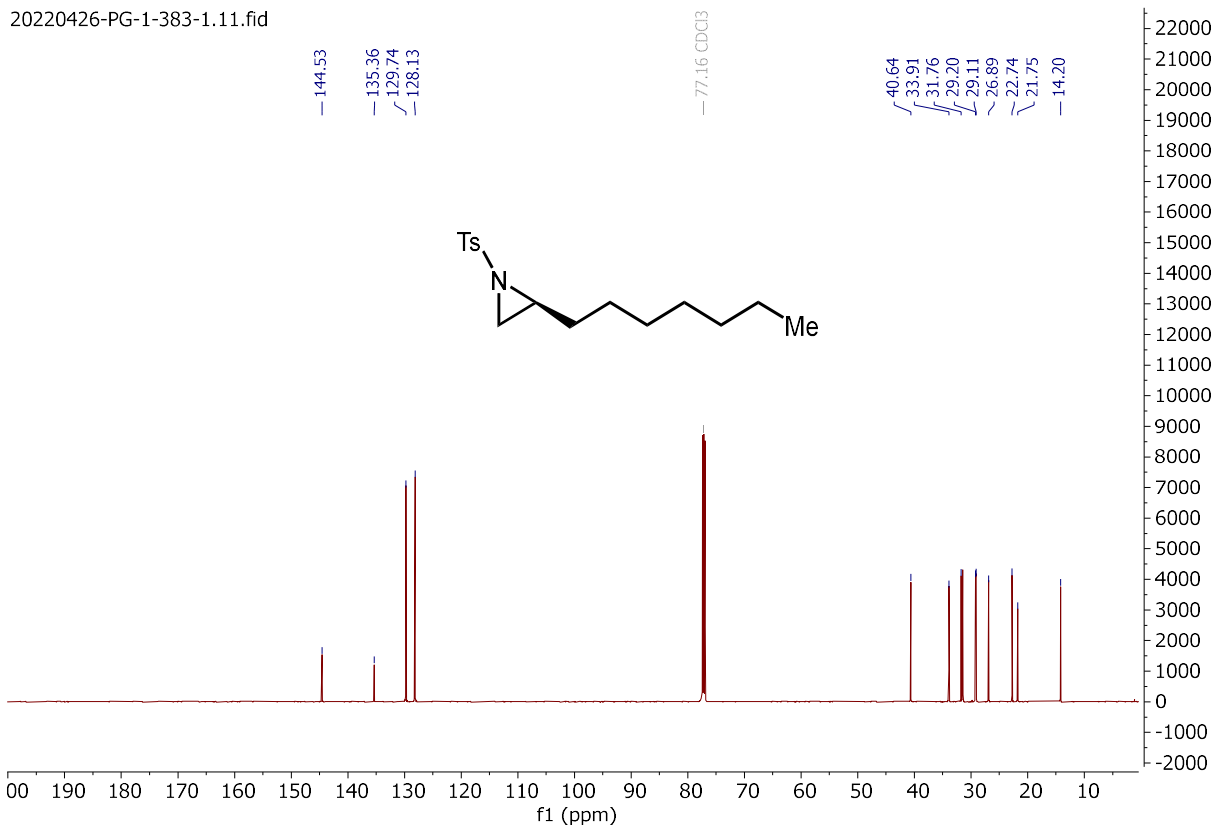
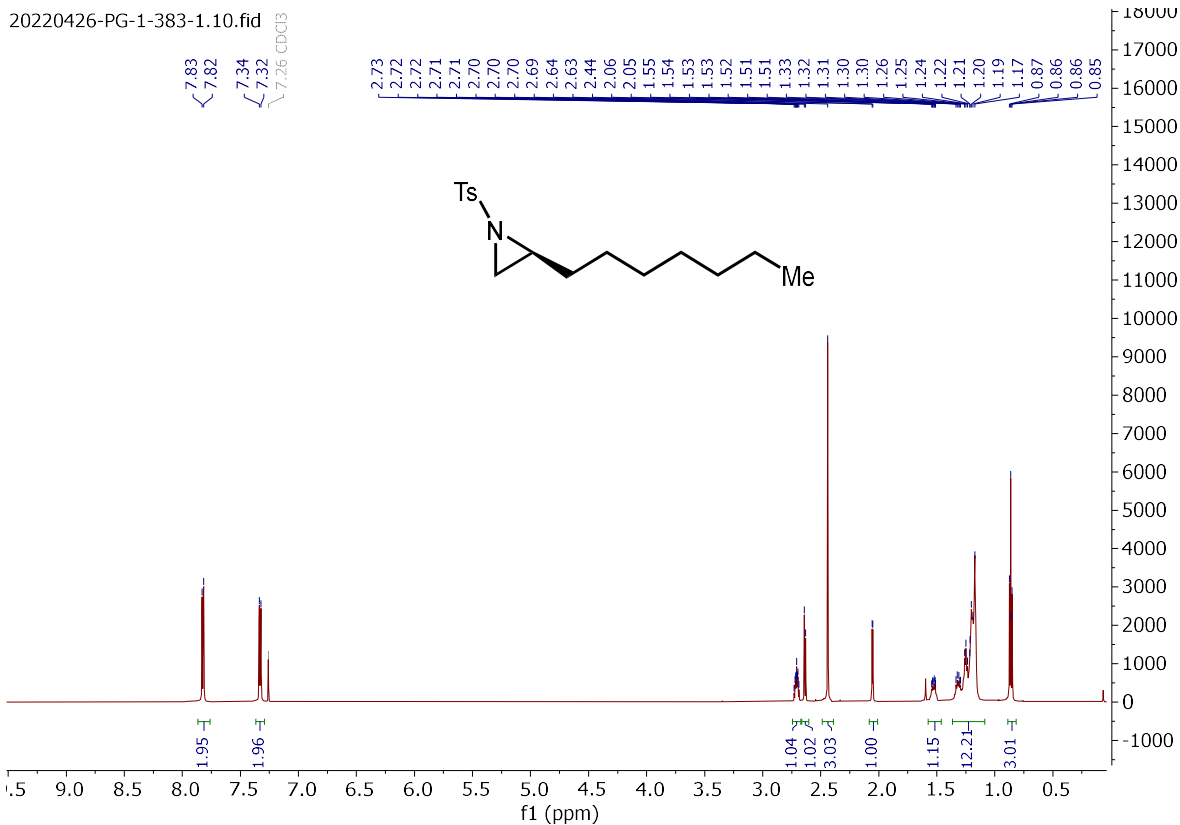
hex-5-en-1-yl 4-vinylbenzoate (S50):



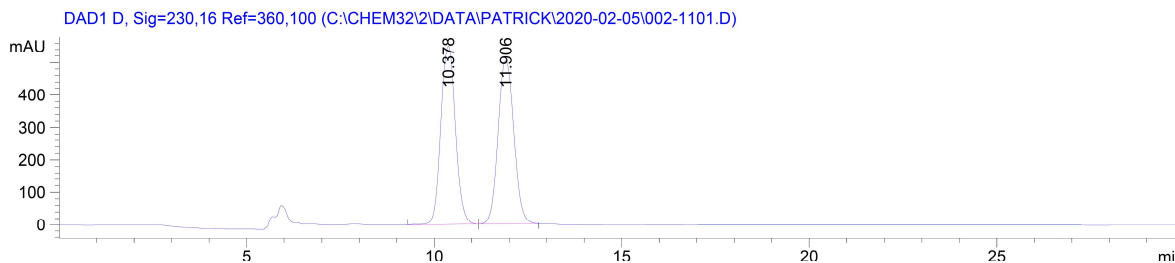
hex-5-en-1-yl cinnamate (S51):



(S)-2-heptyl-1-tosylaziridine (2.79)



(±)-2-heptyl-1-tosylaziridine (±-2.79)

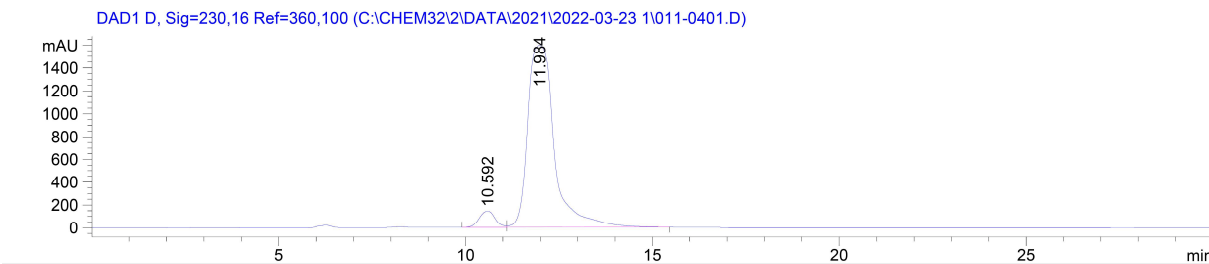


Signal 3: DAD1 D, Sig=230,16 Ref=360,100

| Peak # | RetTime [min] | Type | Width [min] | Area [mAU*s] | Height [mAU] | Area % |
|--------|---------------|------|-------------|--------------|--------------|---------|
| 1 | 10.378 | BV | 0.4221 | 1.47883e4 | 549.36700 | 49.9755 |
| 2 | 11.906 | VB | 0.4678 | 1.48028e4 | 502.37924 | 50.0245 |

Totals : 2.95912e4 1051.74625

(S)-2-heptyl-1-tosylaziridine (2.49)

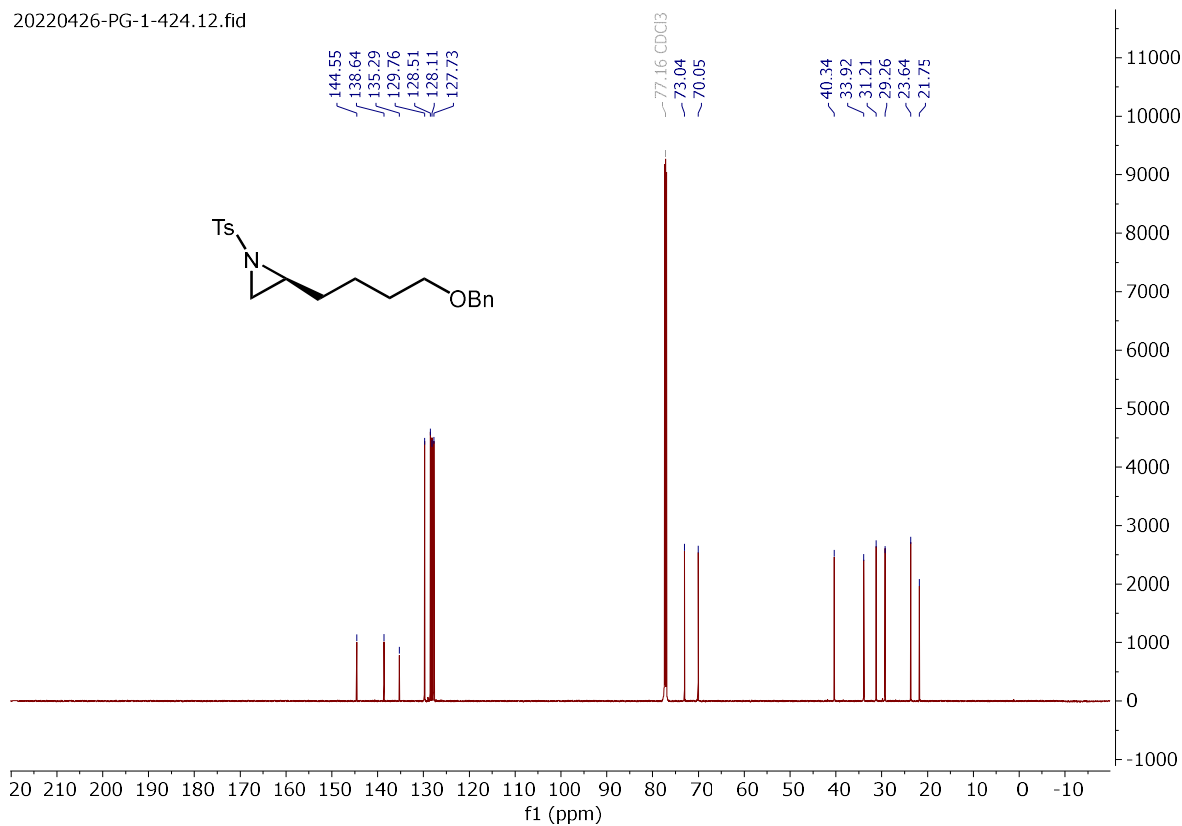
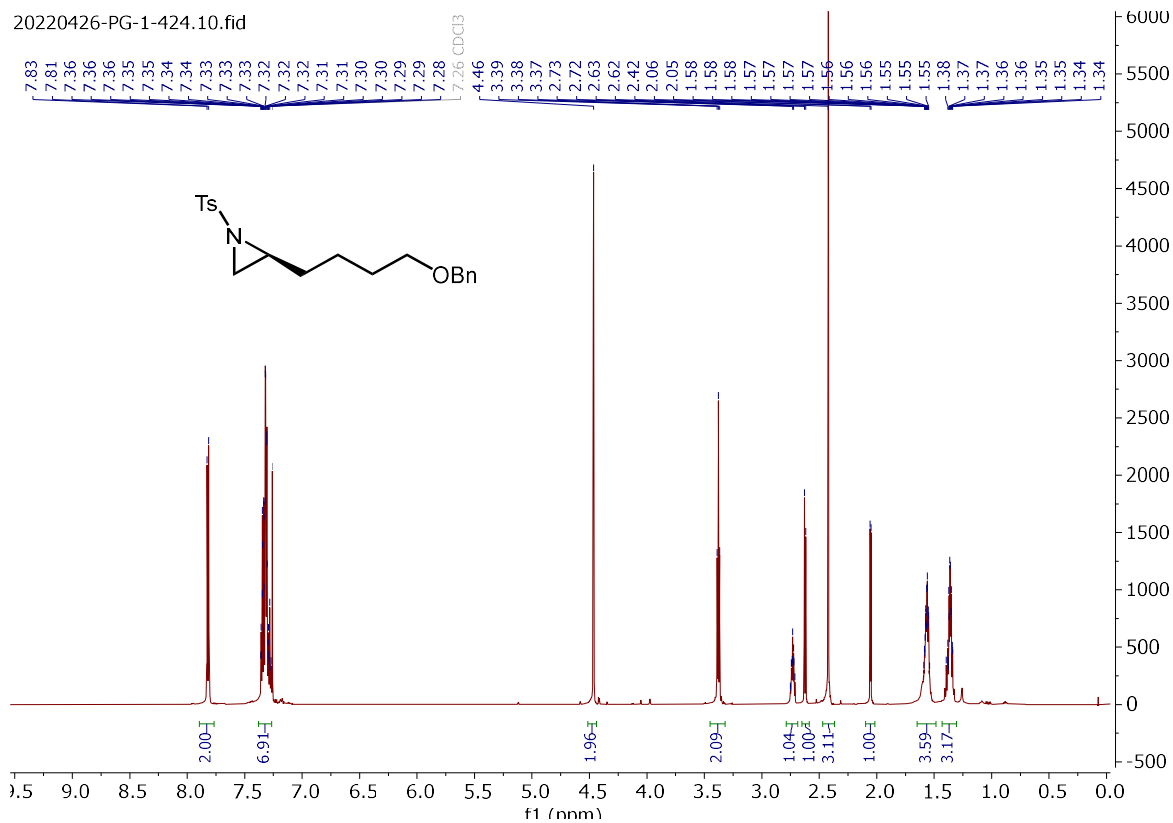


Signal 3: DAD1 D, Sig=230,16 Ref=360,100

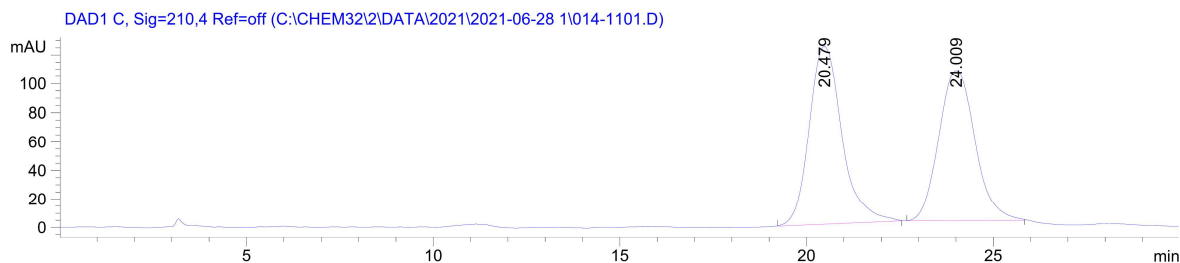
| Peak # | RetTime [min] | Type | Width [min] | Area [mAU*s] | Height [mAU] | Area % |
|--------|---------------|------|-------------|--------------|--------------|---------|
| 1 | 10.592 | BV | 0.4747 | 4295.61133 | 142.89545 | 5.1673 |
| 2 | 11.984 | VB | 0.7675 | 7.88350e4 | 1592.51965 | 94.8327 |

Totals : 8.31306e4 1735.41510

(S)-2-(4-(benzyloxy)butyl)-1-tosylaziridine (**2.109**)



(±)-2-(4-(benzyloxy)butyl)-1-tosylaziridine (±-2.109)

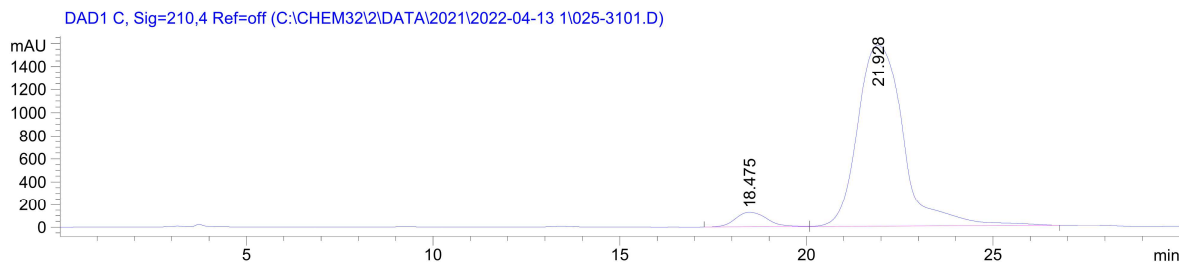


Signal 2: DAD1 C, Sig=210,4 Ref=off

| Peak # | RetTime [min] | Type | Width [min] | Area [mAU*s] | Height [mAU] | Area % |
|--------|---------------|------|-------------|--------------|--------------|---------|
| 1 | 20.479 | BB | 0.9443 | 7594.81641 | 123.70526 | 51.8482 |
| 2 | 24.009 | BB | 1.0605 | 7053.35010 | 104.35783 | 48.1518 |

Totals : 1.46482e4 228.06309

(S)-2-(4-(benzyloxy)butyl)-1-tosylaziridine (2.109)

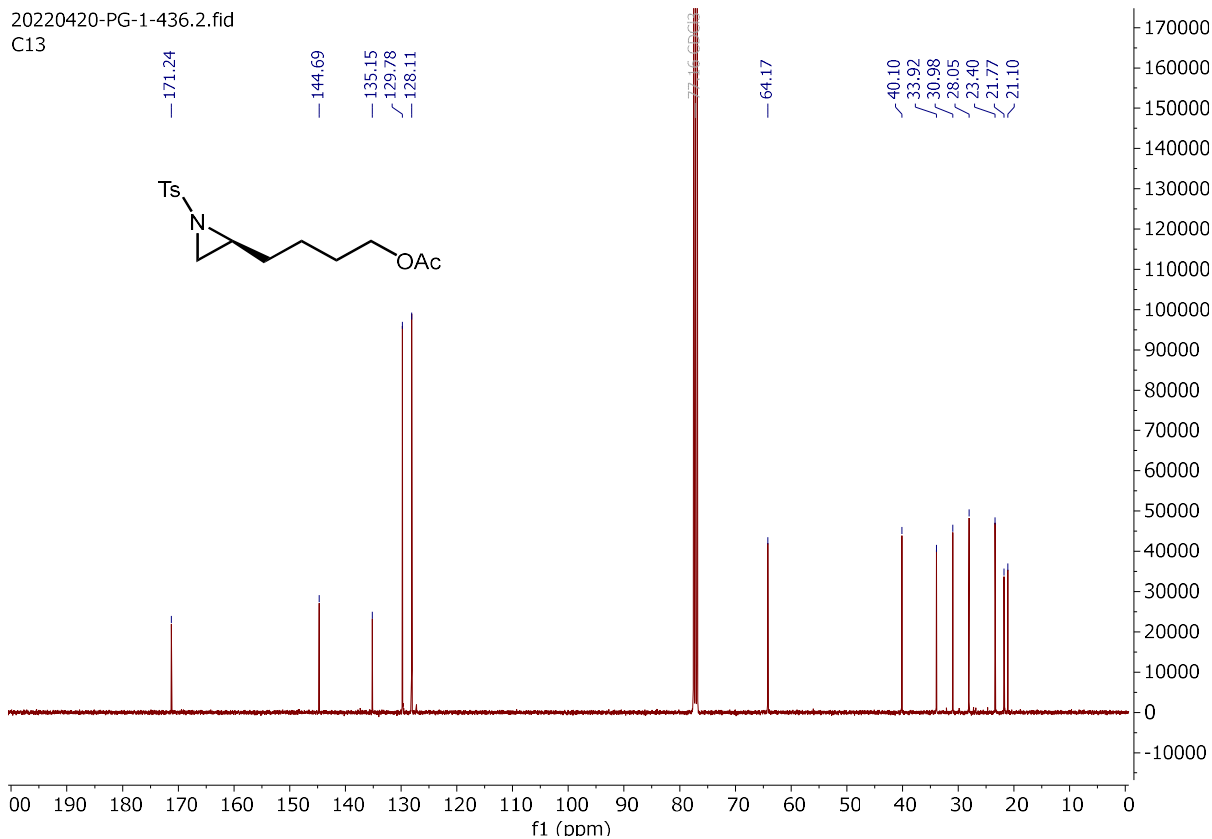
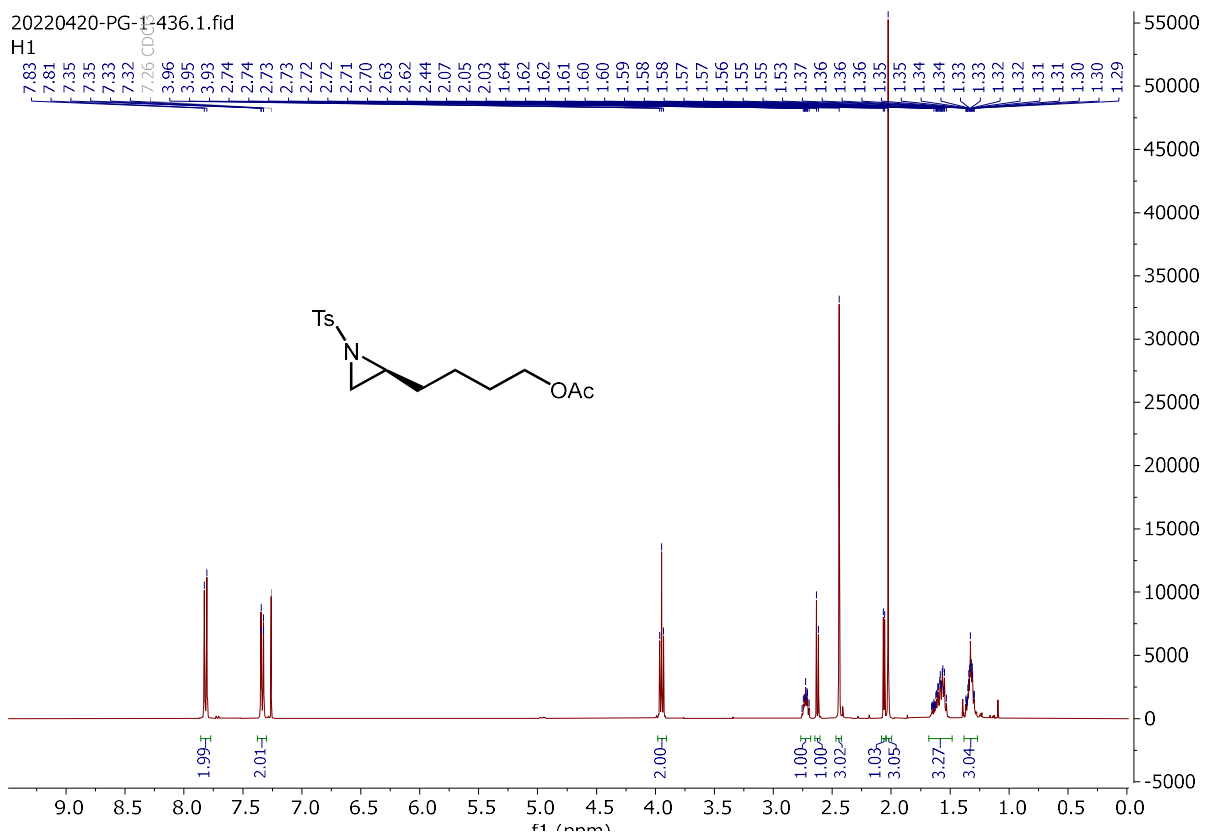


Signal 2: DAD1 C, Sig=210,4 Ref=off

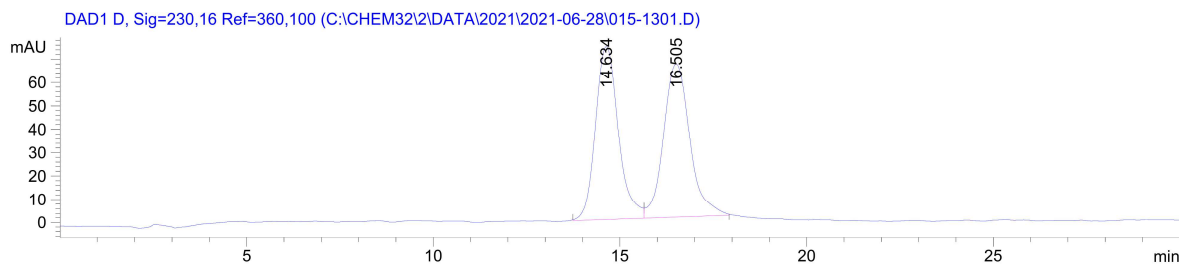
| Peak # | RetTime [min] | Type | Width [min] | Area [mAU*s] | Height [mAU] | Area % |
|--------|---------------|------|-------------|--------------|--------------|---------|
| 1 | 18.475 | BV | 0.9394 | 7518.84668 | 127.61226 | 5.2736 |
| 2 | 21.928 | VB | 1.0292 | 1.35056e5 | 1573.80371 | 94.7264 |

Totals : 1.42575e5 1701.41597

(S)-4-(1-tosylaziridin-2-yl)butyl acetate (**2.110**):



(±)-4-(1-tosylaziridin-2-yl)butyl acetate (±-2.110):

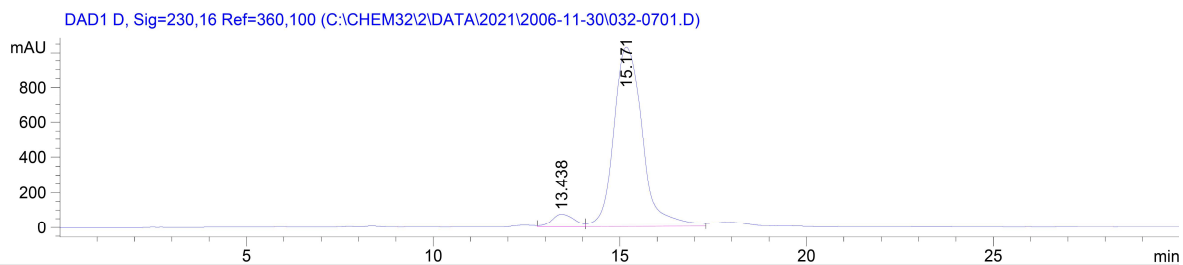


Signal 3: DAD1 D, Sig=230,16 Ref=360,100

| Peak # | RetTime [min] | Type | Width [min] | Area [mAU*s] | Height [mAU] | Area % |
|--------|---------------|------|-------------|--------------|--------------|---------|
| 1 | 14.634 | BV | 0.6631 | 3166.31494 | 74.01552 | 49.4688 |
| 2 | 16.505 | VB | 0.7644 | 3234.32153 | 65.69685 | 50.5312 |

Totals : 6400.63647 139.71237

(S)-4-(1-tosylaziridin-2-yl)butyl acetate (2.110):

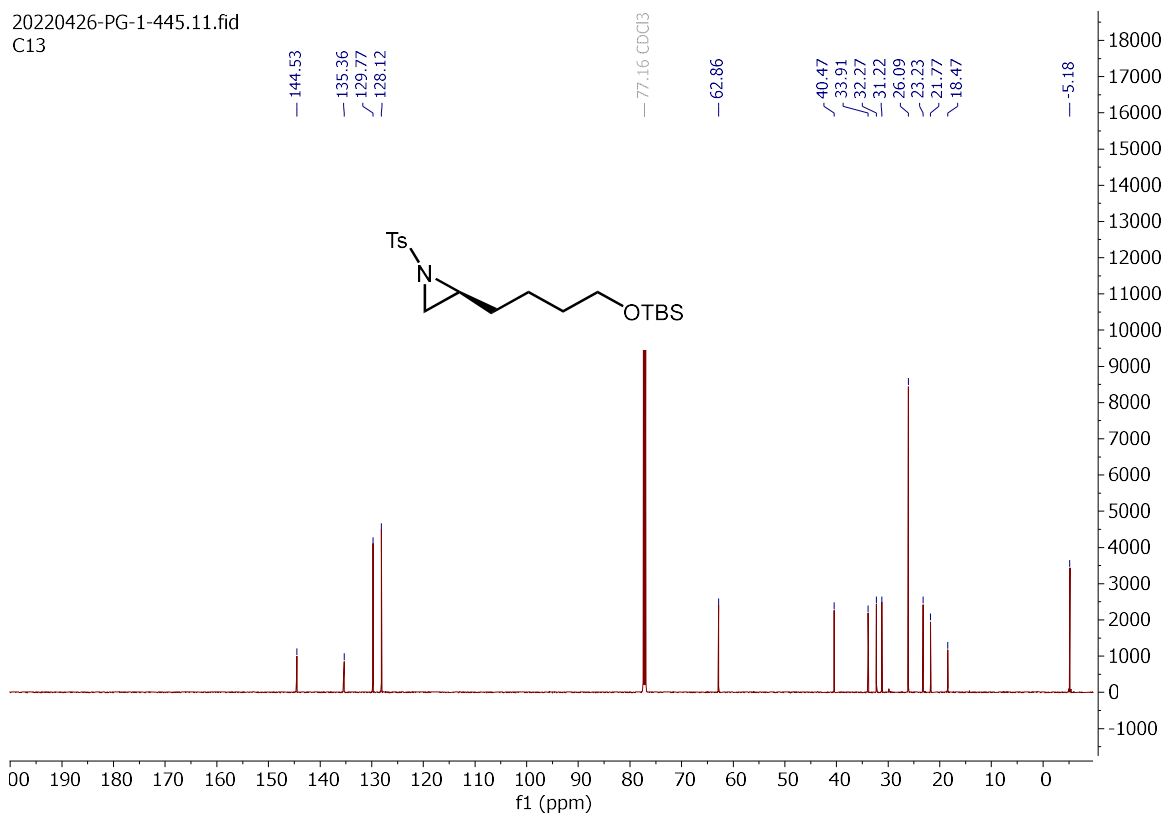
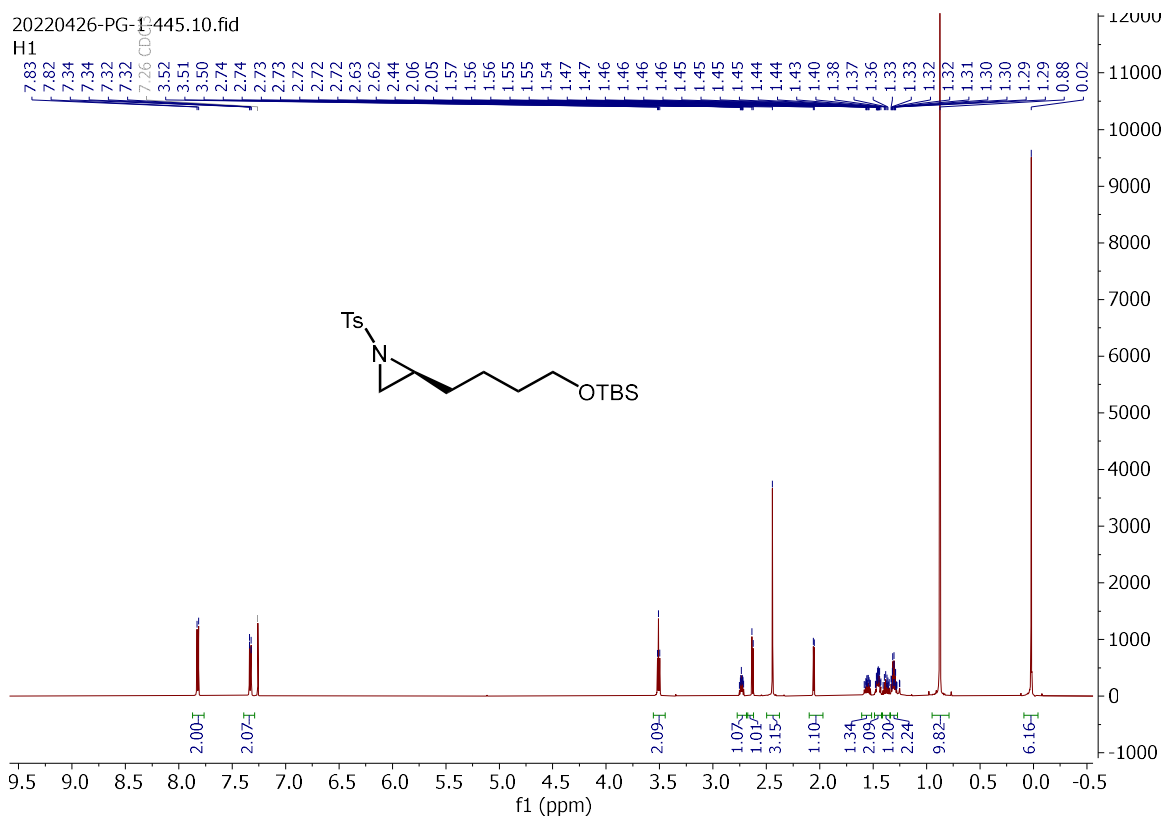


Signal 3: DAD1 D, Sig=230,16 Ref=360,100

| Peak # | RetTime [min] | Type | Width [min] | Area [mAU*s] | Height [mAU] | Area % |
|--------|---------------|------|-------------|--------------|--------------|---------|
| 1 | 13.438 | VV | 0.6679 | 3019.69897 | 72.20198 | 5.2439 |
| 2 | 15.171 | VB | 0.8474 | 5.45657e4 | 1027.76282 | 94.7561 |

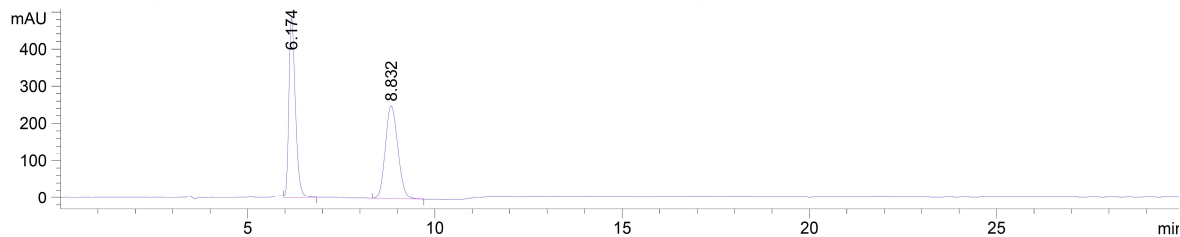
Totals : 5.75854e4 1099.96480

(S)-2-(4-((*tert*-butyldimethylsilyloxy)butyl)-1-tosylaziridine (**2.111**):



(±)-2-(4-((*tert*-butyldimethylsilyloxy)butyl)-1-tosylaziridine (±-2.111)

DAD1 D, Sig=230,16 Ref=360,100 (C:\CHEM32\DATA\2021\2021-06-29\013-1801.D)



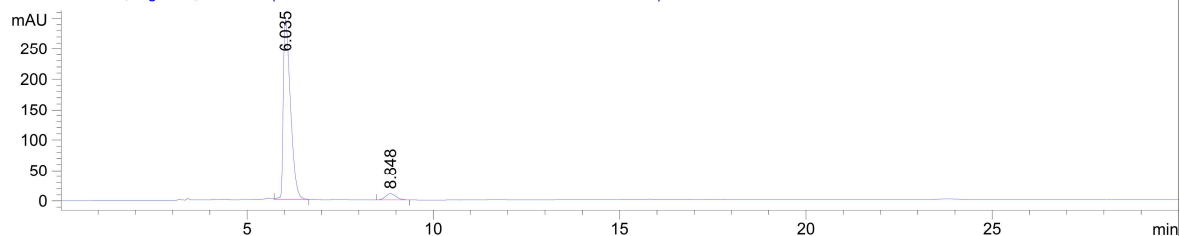
Signal 3: DAD1 D, Sig=230,16 Ref=360,100

| Peak # | RetTime [min] | Type | Width [min] | Area [mAU*s] | Height [mAU] | Area % |
|--------|---------------|------|-------------|--------------|--------------|---------|
| 1 | 6.174 | VB | 0.1861 | 5903.22070 | 484.65616 | 50.0539 |
| 2 | 8.832 | BB | 0.3657 | 5890.49951 | 251.13007 | 49.9461 |

Totals : 1.17937e4 735.78622

(S)-2-(4-((*tert*-butyldimethylsilyloxy)butyl)-1-tosylaziridine (2.111)

DAD1 A, Sig=254,4 Ref=off (C:\CHEM32\DATA\2021\2022-04-28 2\003-0301.D)

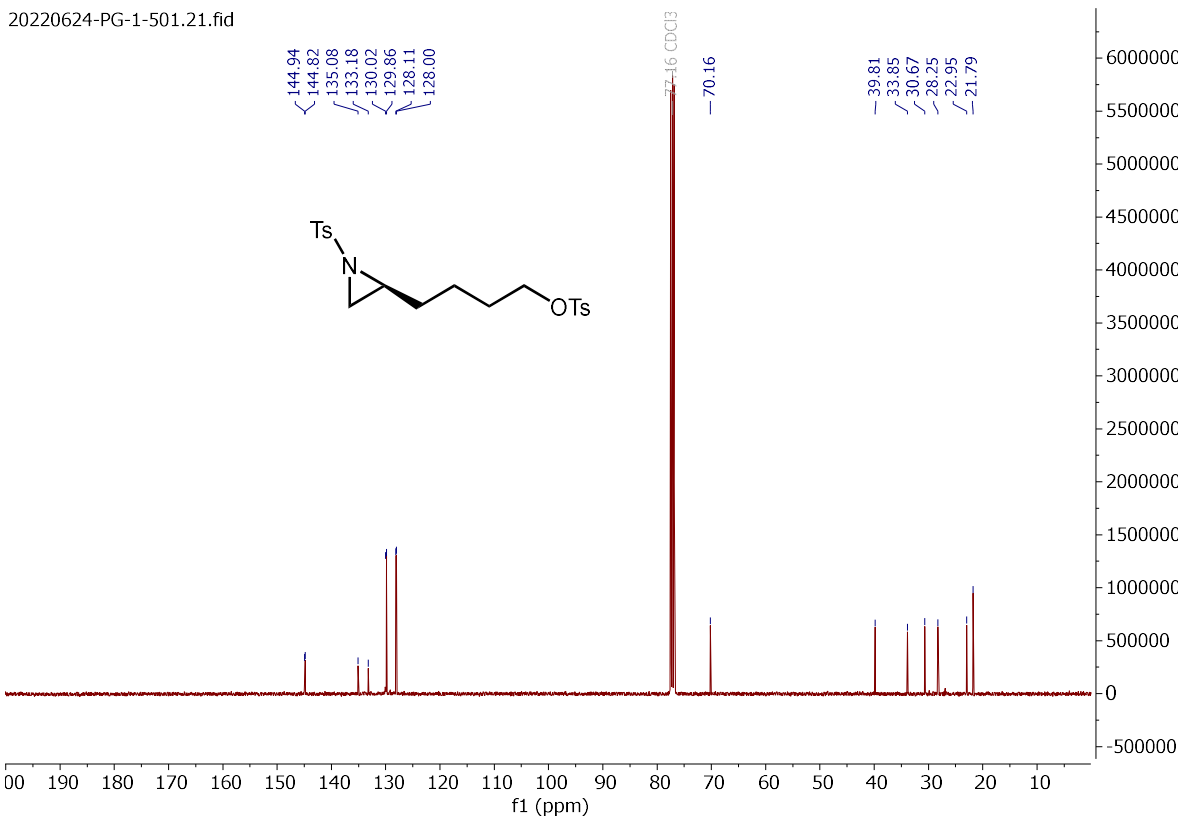
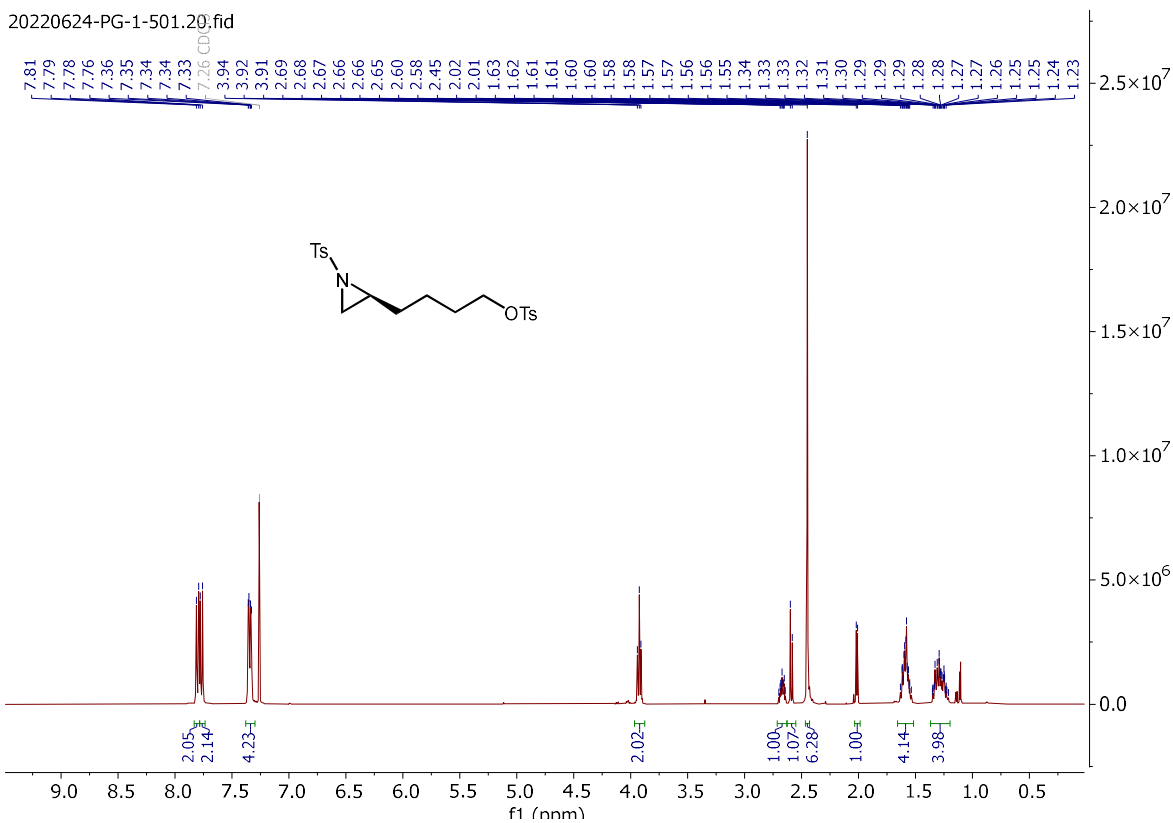


Signal 1: DAD1 A, Sig=254,4 Ref=off

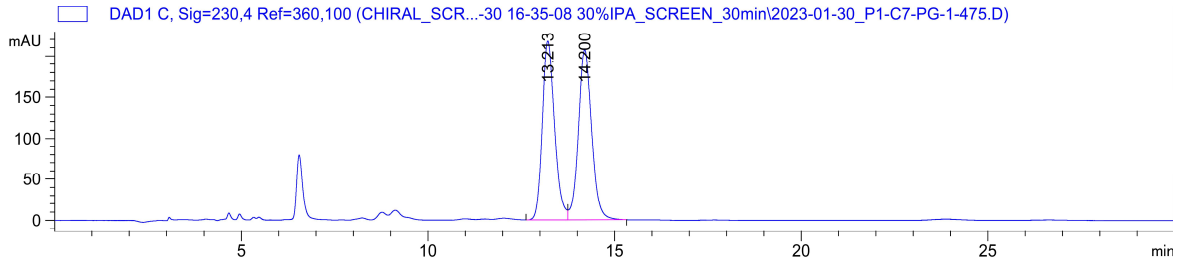
| Peak # | RetTime [min] | Type | Width [min] | Area [mAU*s] | Height [mAU] | Area % |
|--------|---------------|------|-------------|--------------|--------------|---------|
| 1 | 6.035 | VB | 0.2058 | 3994.16357 | 295.37958 | 95.2330 |
| 2 | 8.848 | BB | 0.3062 | 199.93347 | 10.04337 | 4.7670 |

Totals : 4194.09705 305.42295

(S)-4-(1-tosylaziridin-2-yl)butyl 4-methylbenzenesulfonate (**2.112**):



(±)-4-(1-tosylaziridin-2-yl)butyl 4-methylbenzenesulfonate (±-2.112):

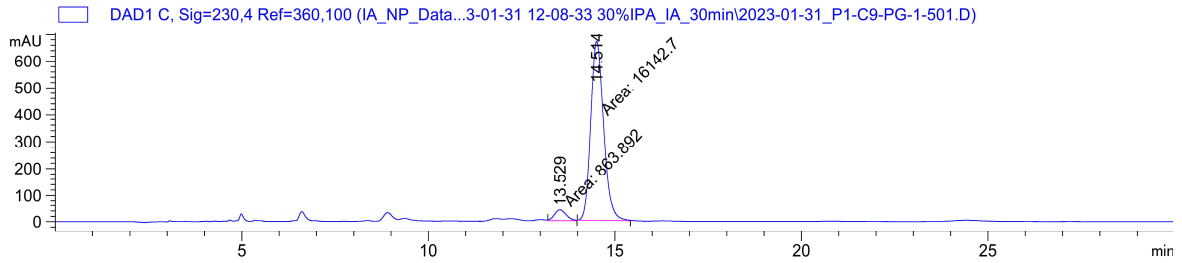


Signal 3: DAD1 C, Sig=230,4 Ref=360,100

| Peak # | RetTime [min] | Type | Width [min] | Area [mAU*s] | Height [mAU] | Area % |
|--------|---------------|------|-------------|--------------|--------------|---------|
| 1 | 13.213 | BV | 0.3481 | 4961.00391 | 217.13869 | 49.2370 |
| 2 | 14.200 | VB | 0.3607 | 5114.76611 | 206.68993 | 50.7630 |

Totals : 1.00758e4 423.82861

(S)-4-(1-tosylaziridin-2-yl)butyl 4-methylbenzenesulfonate (2.112):

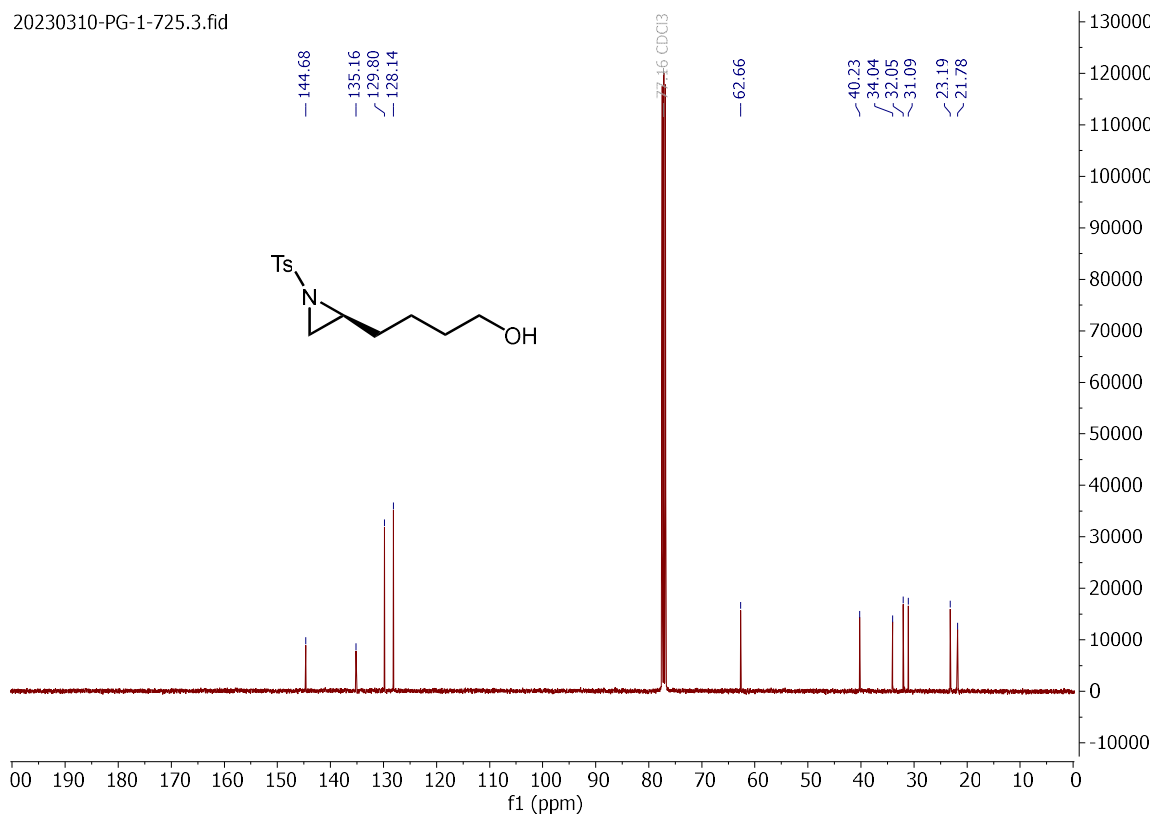
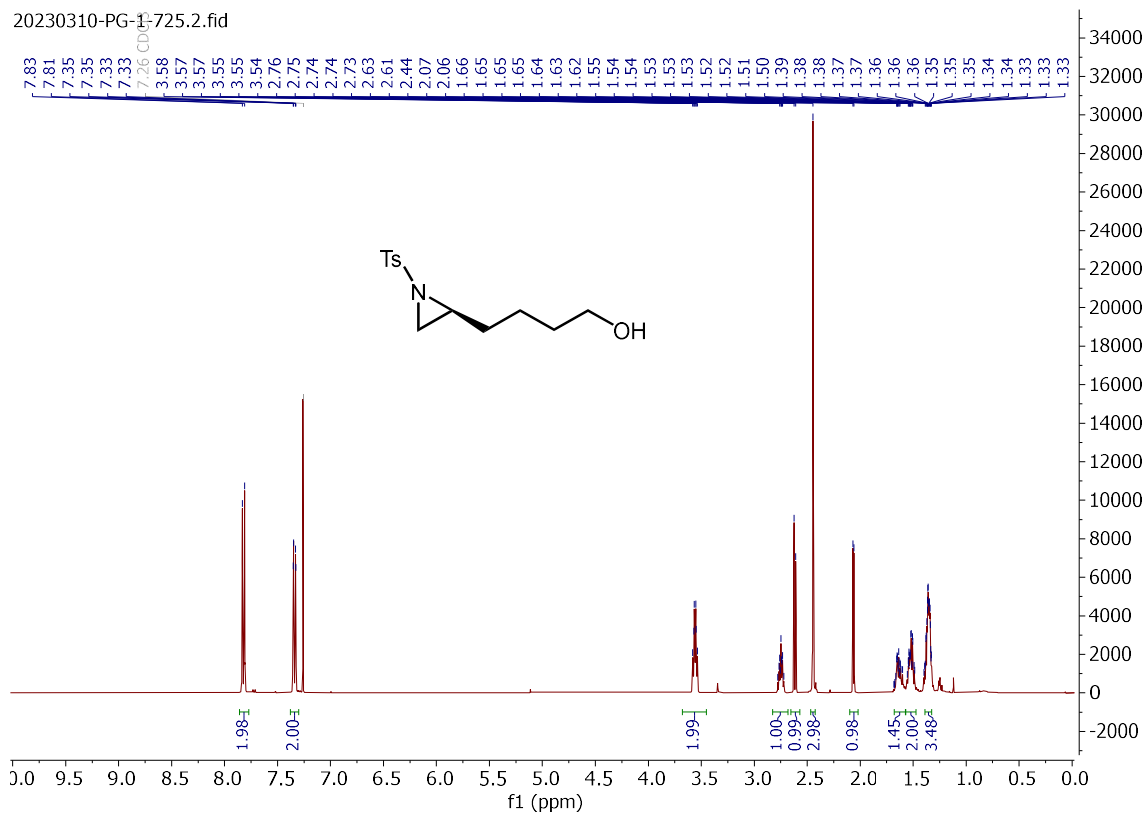


Signal 3: DAD1 C, Sig=230,4 Ref=360,100

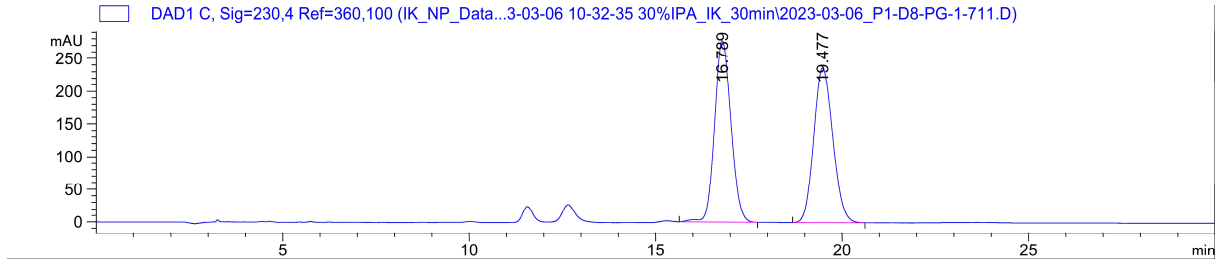
| Peak # | RetTime [min] | Type | Width [min] | Area [mAU*s] | Height [mAU] | Area % |
|--------|---------------|------|-------------|--------------|--------------|---------|
| 1 | 13.529 | MM | 0.3624 | 863.89215 | 39.72470 | 5.0797 |
| 2 | 14.514 | MM | 0.4019 | 1.61427e4 | 669.45471 | 94.9203 |

Totals : 1.70066e4 709.17942

(S)-4-(1-tosylaziridin-2-yl)butan-1-ol (**2.113**):



(±)-4-(1-tosylaziridin-2-yl)butan-1-ol (±-**2.113**):

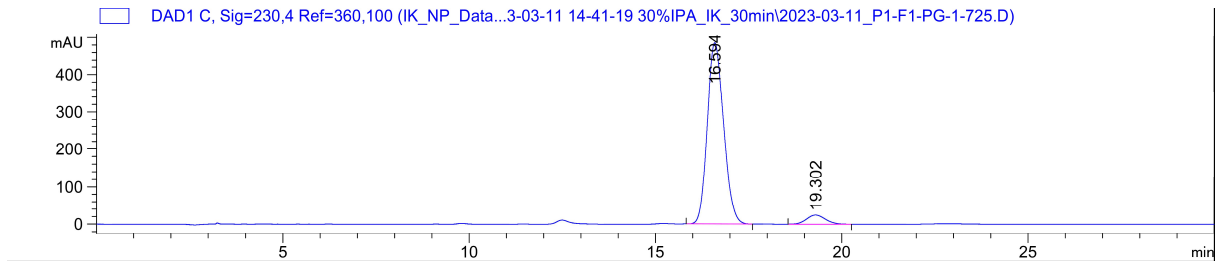


Signal 3: DAD1 C, Sig=230,4 Ref=360,100

| Peak # | RetTime [min] | Type | Width [min] | Area [mAU*s] | Height [mAU] | Area % |
|--------|---------------|------|-------------|--------------|--------------|---------|
| 1 | 16.789 | VB R | 0.4366 | 8467.90723 | 277.20874 | 50.1483 |
| 2 | 19.477 | BB | 0.4526 | 8417.83301 | 236.88470 | 49.8517 |

Totals : 1.68857e4 514.09344

(S)-4-(1-tosylaziridin-2-yl)butan-1-ol (**2.113**):

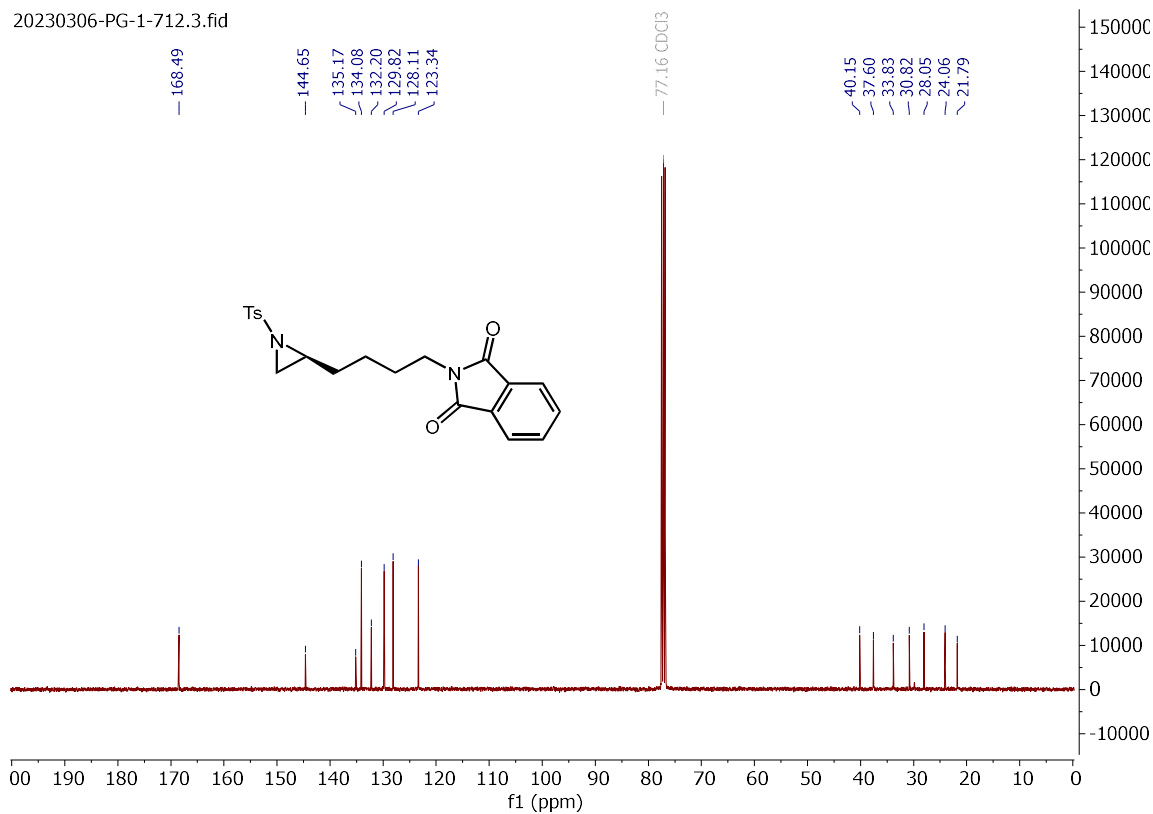
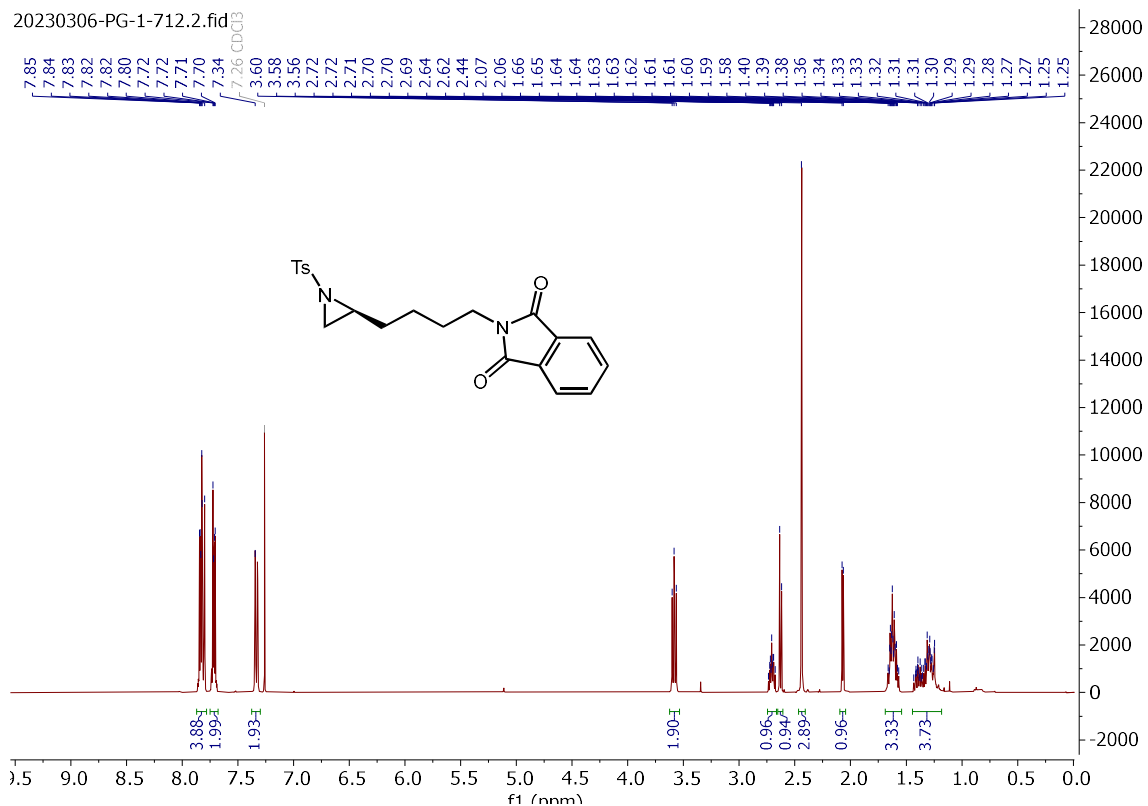


Signal 3: DAD1 C, Sig=230,4 Ref=360,100

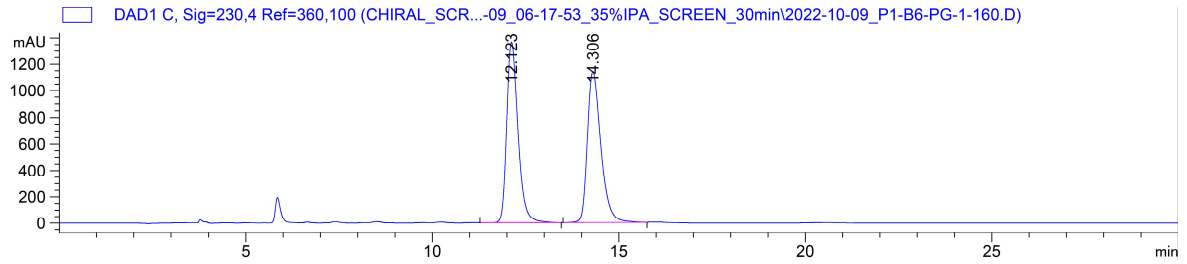
| Peak # | RetTime [min] | Type | Width [min] | Area [mAU*s] | Height [mAU] | Area % |
|--------|---------------|------|-------------|--------------|--------------|---------|
| 1 | 16.594 | BB | 0.4493 | 1.47459e4 | 485.49707 | 94.5369 |
| 2 | 19.302 | BB | 0.4127 | 852.13507 | 24.17467 | 5.4631 |

Totals : 1.55981e4 509.67174

(S)-2-(4-(1-tosylaziridin-2-yl)butyl)isoindoline-1,3-dione (2.114):



(±)-2-(4-(1-tosylaziridin-2-yl)butyl)isoindoline-1,3-dione (±-2.114):

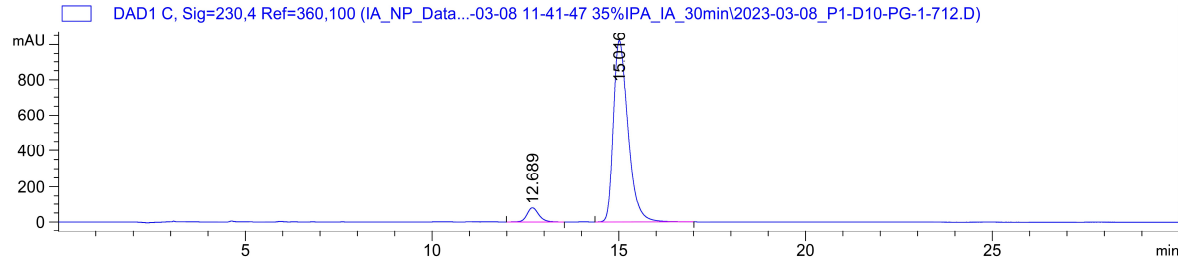


Signal 3: DAD1 C, Sig=230,4 Ref=360,100

| Peak # | RetTime [min] | Type | Width [min] | Area [mAU*s] | Height [mAU] | Area % |
|--------|---------------|------|-------------|--------------|--------------|---------|
| 1 | 12.123 | BB | 0.3200 | 2.87536e4 | 1366.31616 | 49.9879 |
| 2 | 14.306 | BB | 0.3813 | 2.87675e4 | 1138.56714 | 50.0121 |

Totals : 5.75211e4 2504.88330

(S)-2-(4-(1-tosylaziridin-2-yl)butyl)isoindoline-1,3-dione (2.114):



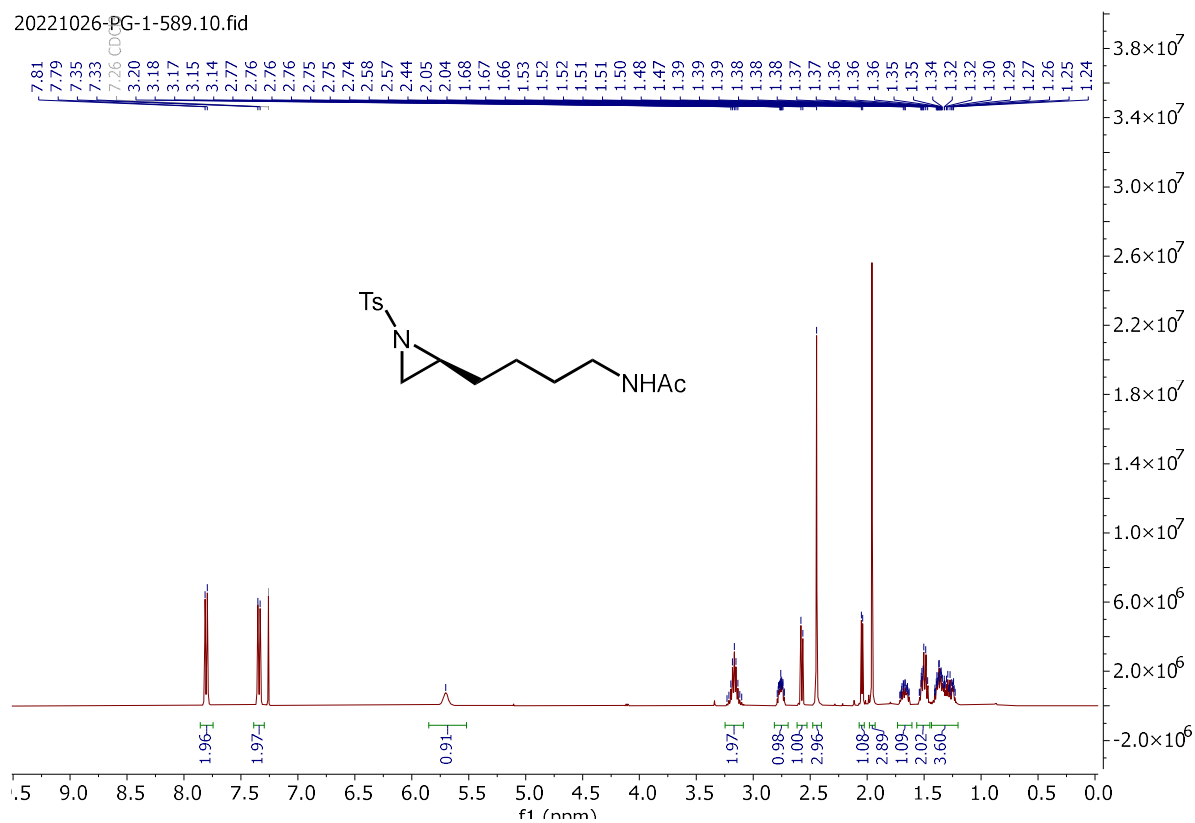
Signal 3: DAD1 C, Sig=230,4 Ref=360,100

| Peak # | RetTime [min] | Type | Width [min] | Area [mAU*s] | Height [mAU] | Area % |
|--------|---------------|------|-------------|--------------|--------------|---------|
| 1 | 12.689 | BB | 0.2821 | 1732.11353 | 78.28905 | 5.8859 |
| 2 | 15.016 | BB | 0.4030 | 2.76961e4 | 1020.82062 | 94.1141 |

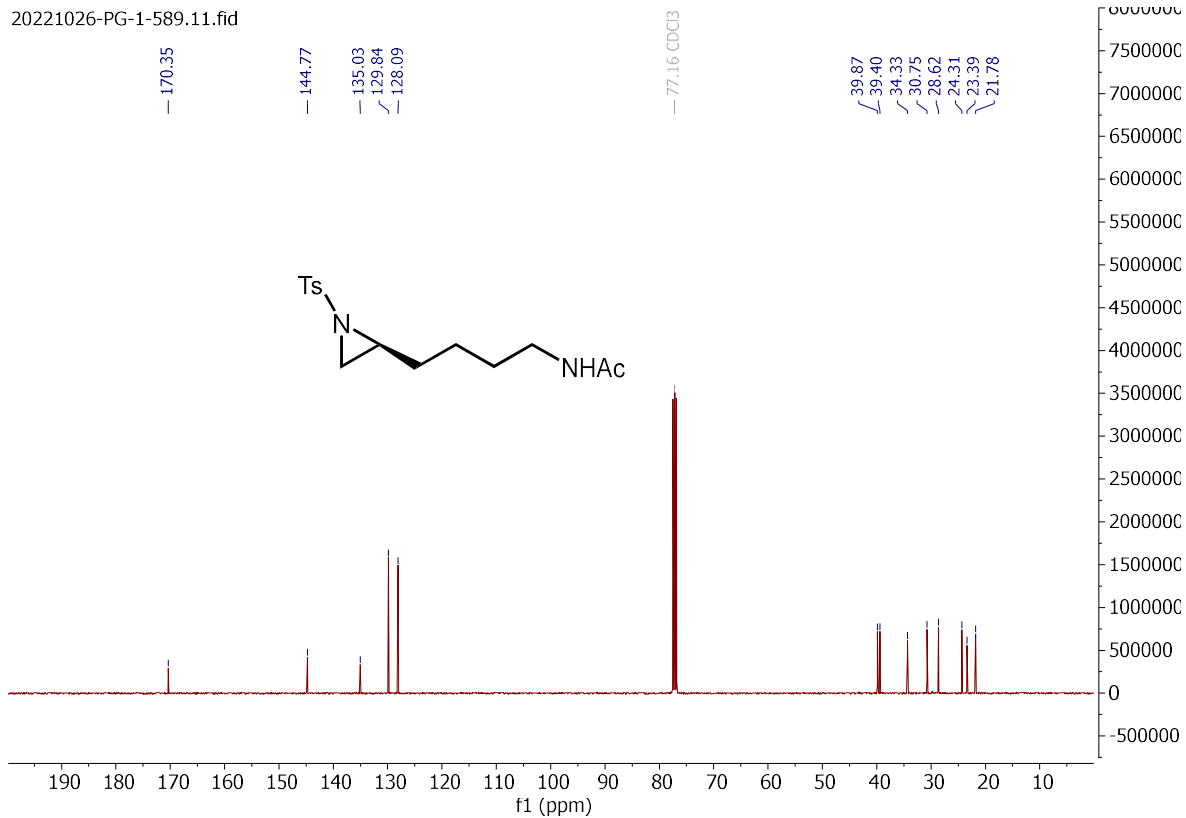
Totals : 2.94283e4 1099.10967

(S)-N-(4-(1-tosylaziridin-2-yl)butyl)acetamide (**2.115**):

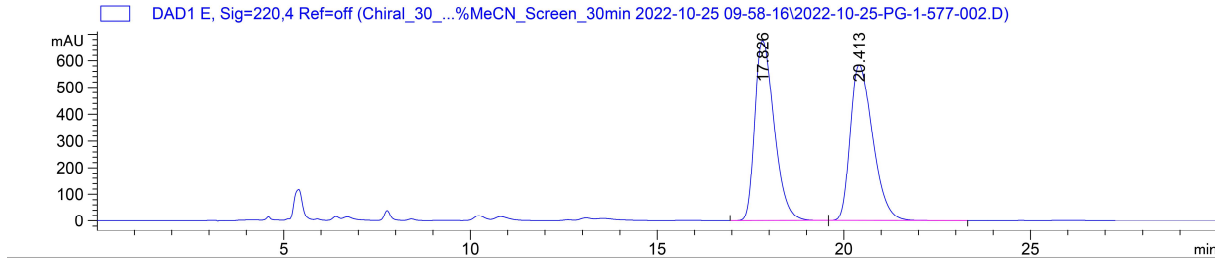
20221026-PG-1-589.10.fid



20221026-PG-1-589.11.fid



(±)-N-(4-(1-tosylaziridin-2-yl)butyl)acetamide (±-2.115):

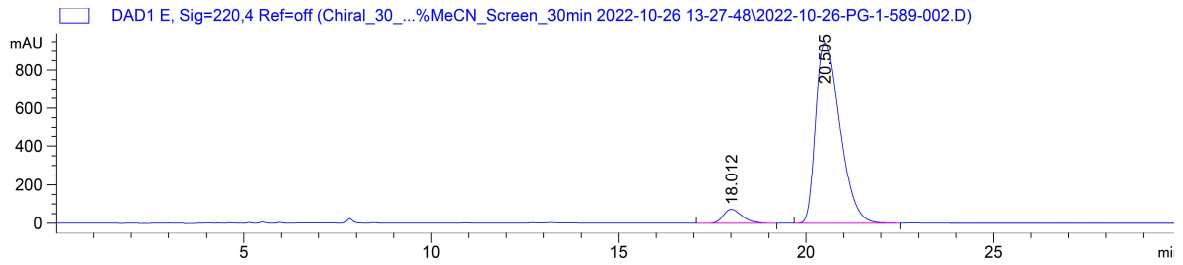


Signal 5: DAD1 E, Sig=220,4 Ref=off

| Peak # | RetTime [min] | Type | Width [min] | Area [mAU*s] | Height [mAU] | Area % |
|--------|---------------|------|-------------|--------------|--------------|---------|
| 1 | 17.826 | BB | 0.5576 | 2.44017e4 | 675.31604 | 49.9622 |
| 2 | 20.413 | BB | 0.6510 | 2.44386e4 | 583.09021 | 50.0378 |

Totals : 4.88403e4 1258.40625

(S)-N-(4-(1-tosylaziridin-2-yl)butyl)acetamide (2.115):

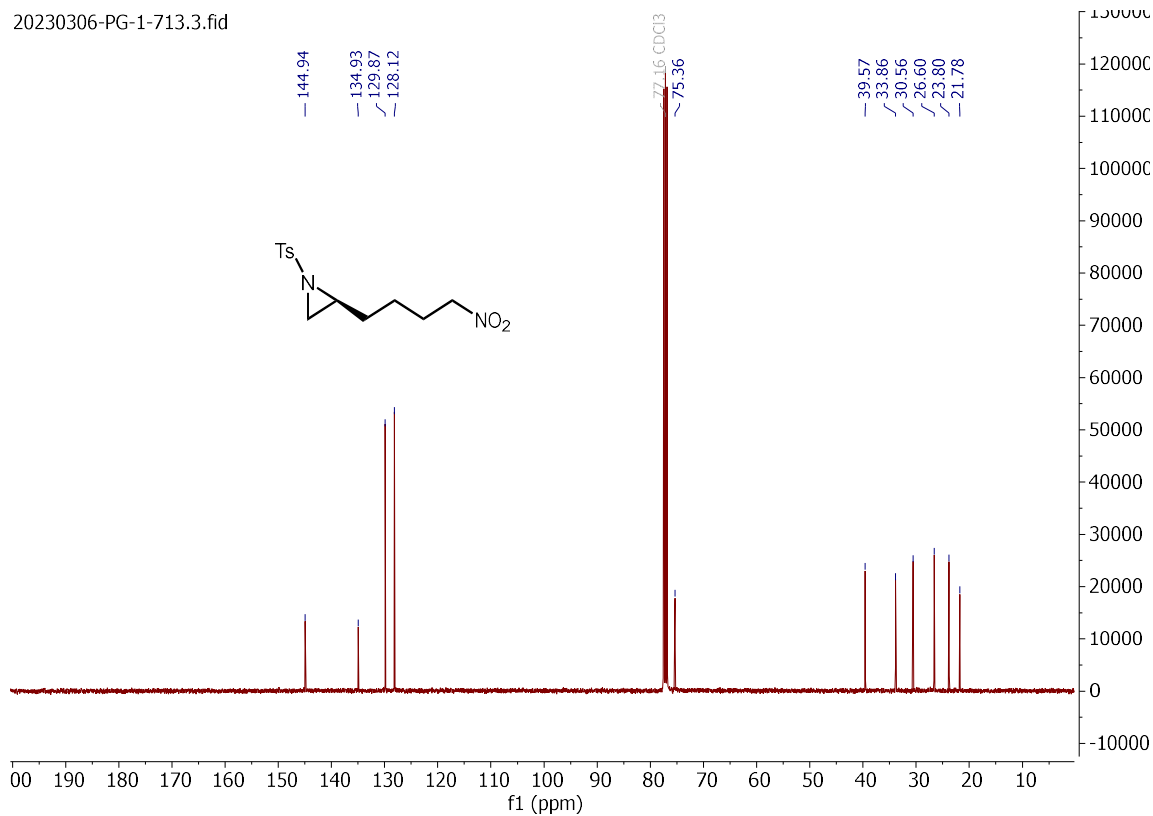
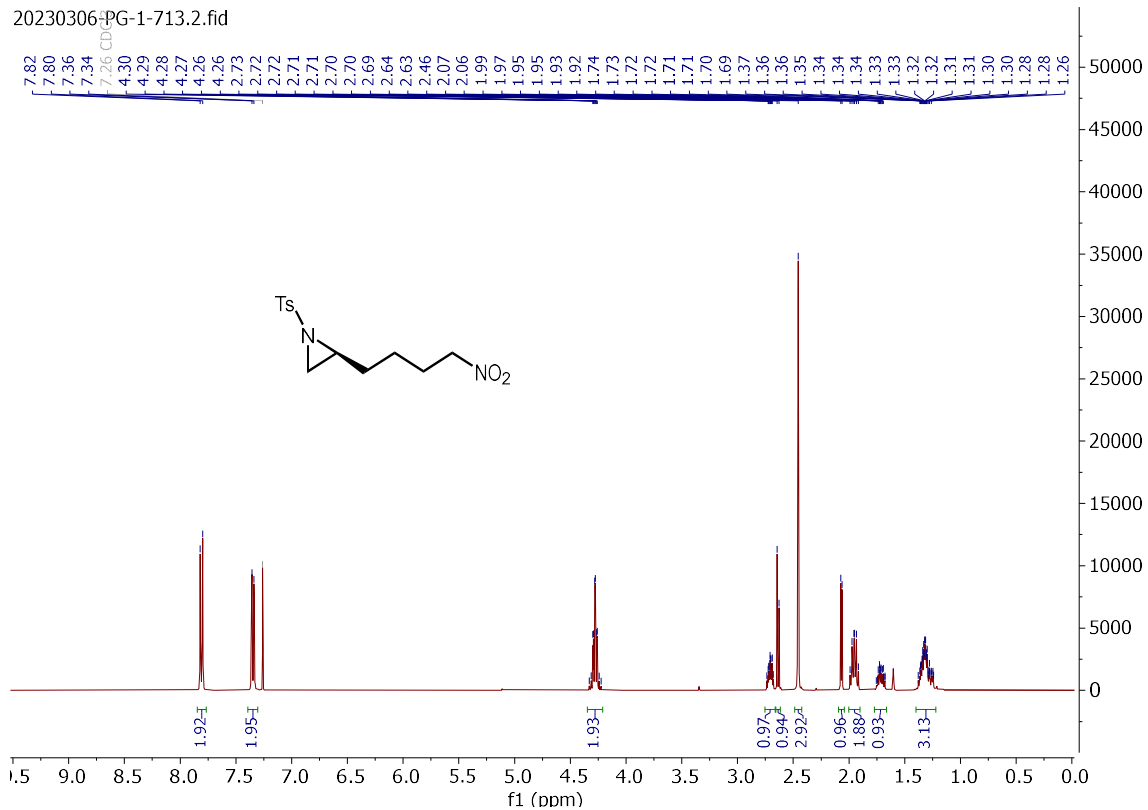


Signal 5: DAD1 E, Sig=220,4 Ref=off

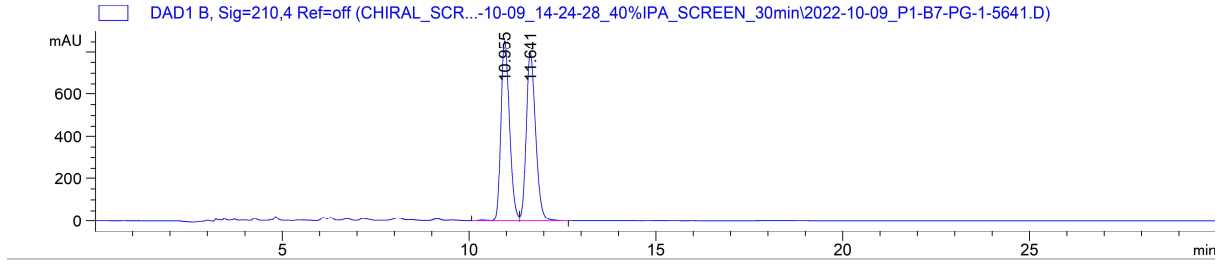
| Peak # | RetTime [min] | Type | Width [min] | Area [mAU*s] | Height [mAU] | Area % |
|--------|---------------|------|-------------|--------------|--------------|---------|
| 1 | 18.012 | BB | 0.5342 | 2510.60913 | 72.10947 | 5.7082 |
| 2 | 20.505 | BB | 0.6849 | 4.14717e4 | 943.26465 | 94.2918 |

Totals : 4.39823e4 1015.37411

(S)-2-(4-nitrobutyl)-1-tosylaziridine (2.116):



(±)-2-(4-nitrobutyl)-1-tosylaziridine (±-2.116):

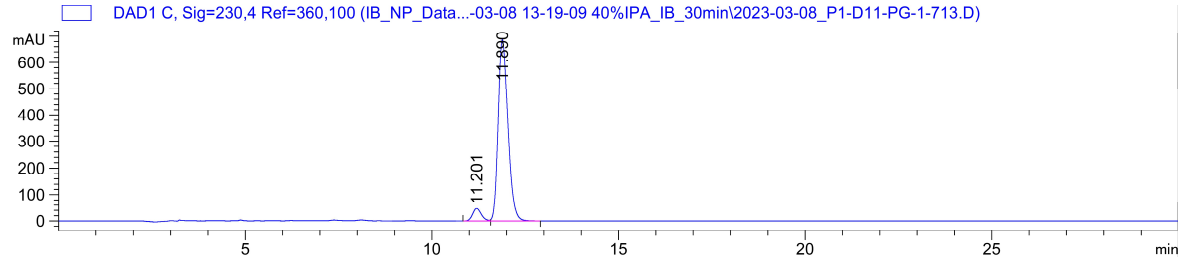


Signal 2: DAD1 B, Sig=210,4 Ref=off

| Peak # | RetTime [min] | Type | Width [min] | Area [mAU*s] | Height [mAU] | Area % |
|--------|---------------|------|-------------|--------------|--------------|---------|
| 1 | 10.955 | VV R | 0.2467 | 1.37106e4 | 855.09778 | 49.8023 |
| 2 | 11.641 | VB | 0.2678 | 1.38195e4 | 794.91217 | 50.1977 |

Totals : 2.75301e4 1650.00995

(S)-2-(4-nitrobutyl)-1-tosylaziridine (2.116):

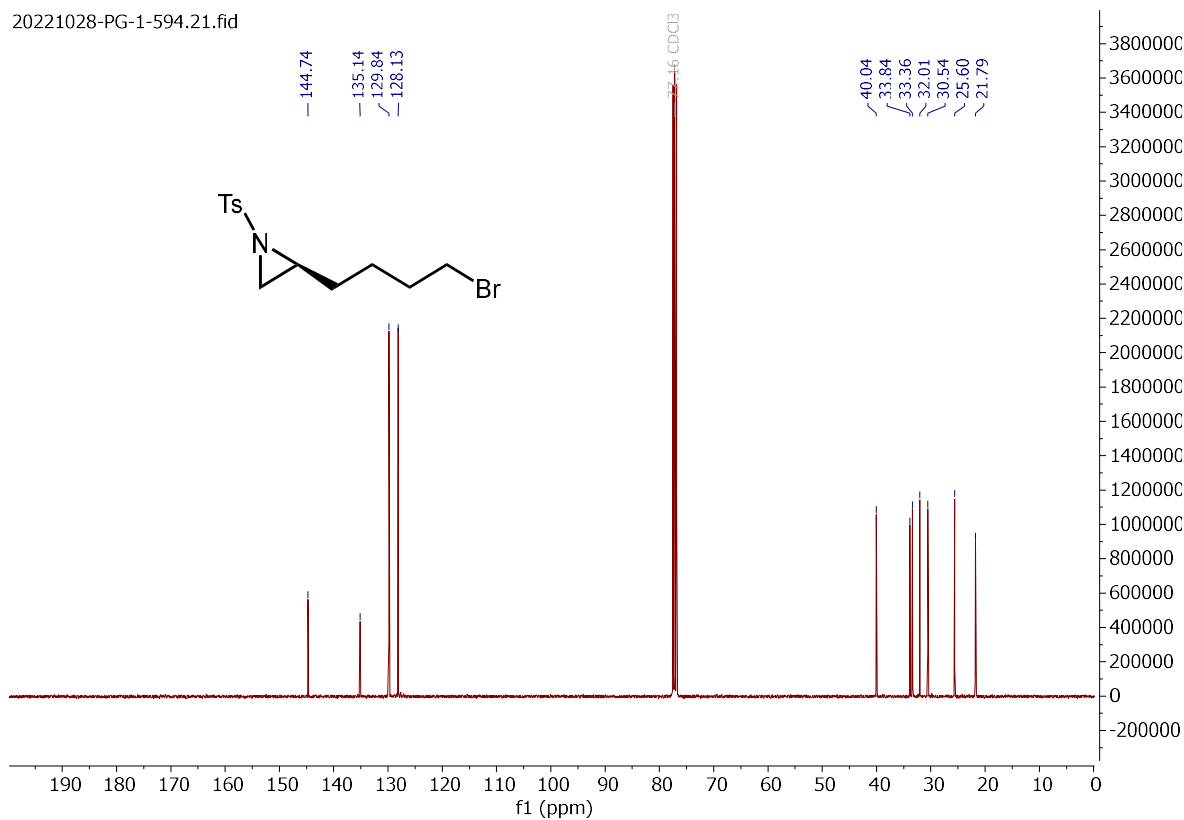
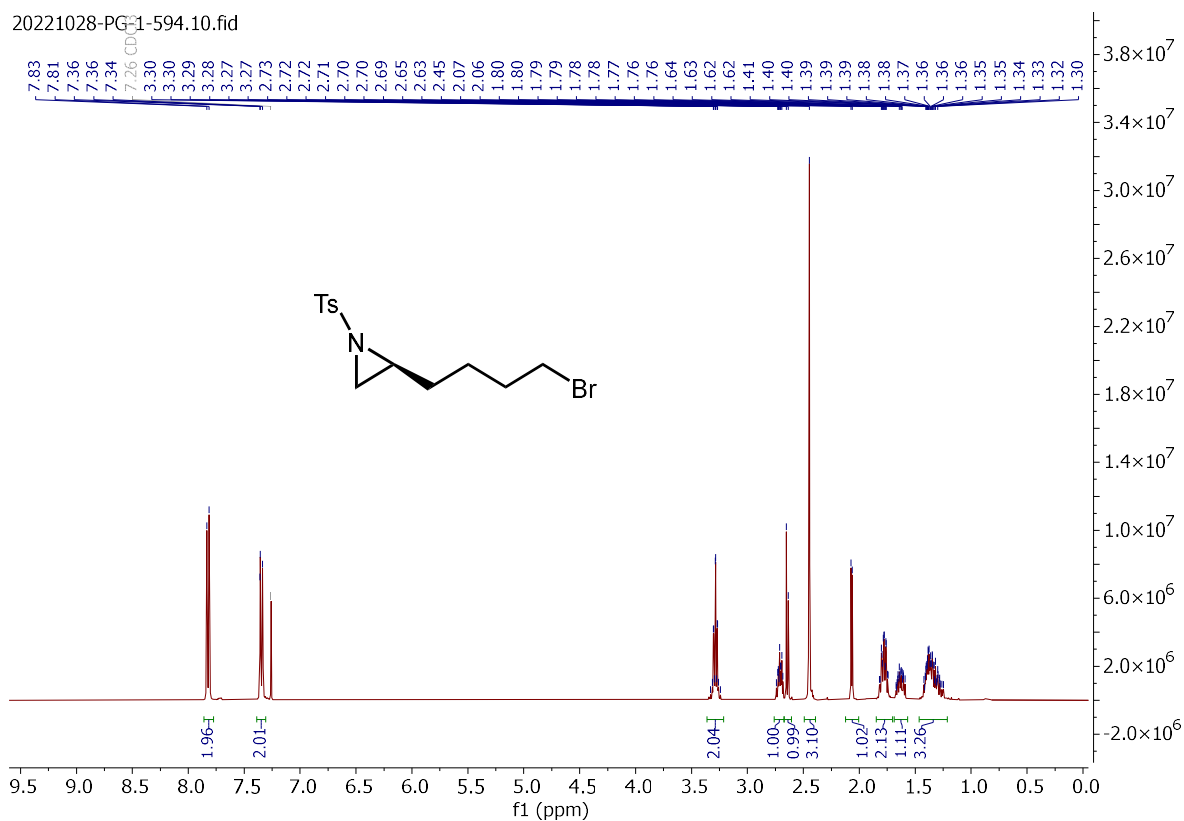


Signal 3: DAD1 C, Sig=230,4 Ref=360,100

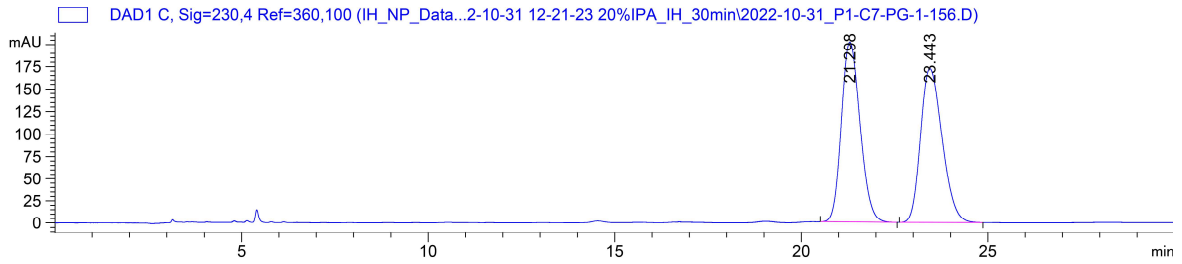
| Peak # | RetTime [min] | Type | Width [min] | Area [mAU*s] | Height [mAU] | Area % |
|--------|---------------|------|-------------|--------------|--------------|---------|
| 1 | 11.201 | BV E | 0.2231 | 758.55176 | 47.05001 | 5.7328 |
| 2 | 11.890 | VB R | 0.2792 | 1.24732e4 | 685.73492 | 94.2672 |

Totals : 1.32318e4 732.78493

(S)-2-(4-bromobutyl)-1-tosylaziridine (**2.117**):



(±)-2-(4-bromobutyl)-1-tosylaziridine (±-2.117):

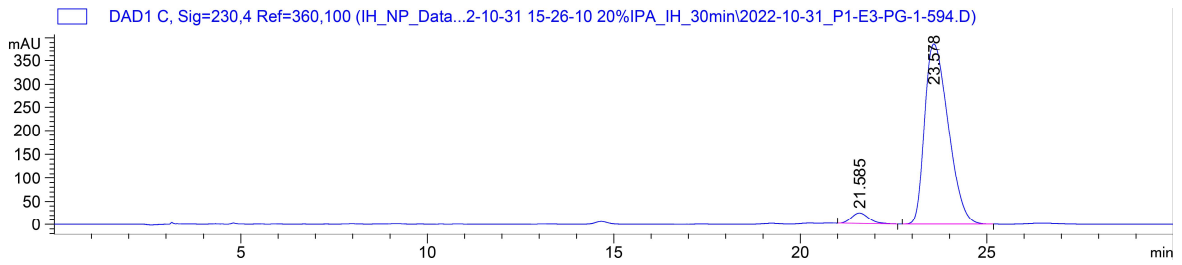


Signal 3: DAD1 C, Sig=230,4 Ref=360,100

| Peak # | RetTime [min] | Type | Width [min] | Area [mAU*s] | Height [mAU] | Area % |
|--------|---------------|------|-------------|--------------|--------------|---------|
| 1 | 21.298 | BB | 0.4907 | 7028.21191 | 201.85909 | 50.2308 |
| 2 | 23.443 | BB | 0.4848 | 6963.62256 | 172.38828 | 49.7692 |

Totals : 1.39918e4 374.24736

(S)-2-(4-bromobutyl)-1-tosylaziridine (2.117):

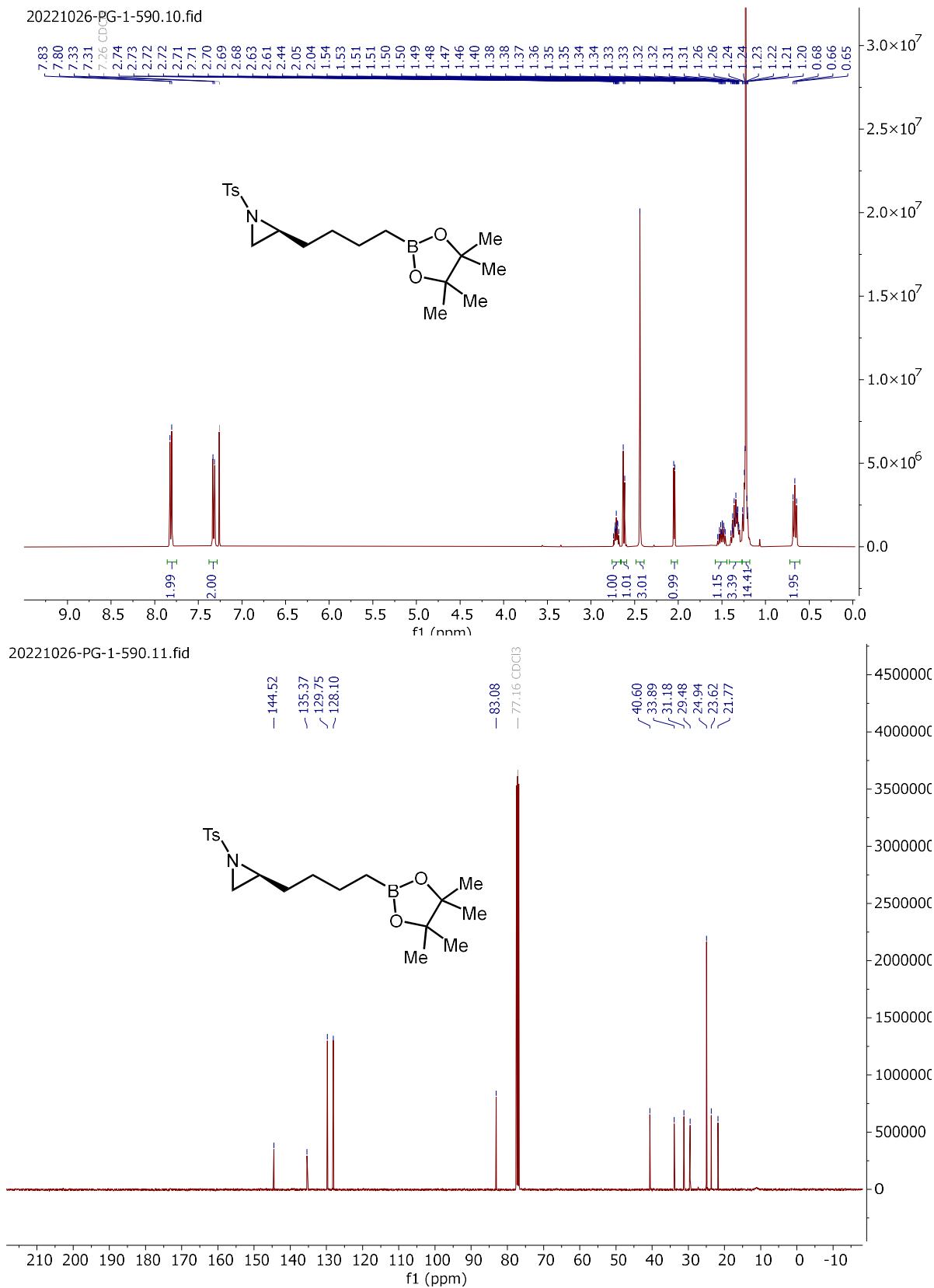


Signal 3: DAD1 C, Sig=230,4 Ref=360,100

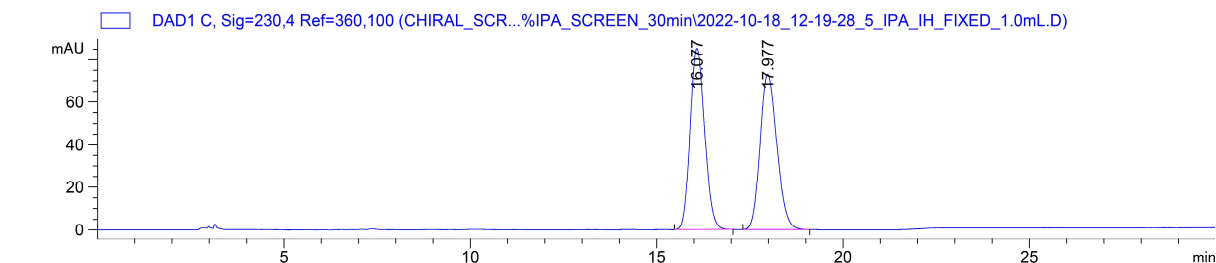
| Peak # | RetTime [min] | Type | Width [min] | Area [mAU*s] | Height [mAU] | Area % |
|--------|---------------|------|-------------|--------------|--------------|---------|
| 1 | 21.585 | BB | 0.3903 | 769.99579 | 23.46990 | 4.3422 |
| 2 | 23.578 | BB | 0.6332 | 1.69627e4 | 386.33487 | 95.6578 |

Totals : 1.77327e4 409.80477

(S)-2-(4-(4,4,5,5-tetramethyl-1,3,2-dioxaborolan-2-yl)butyl)-1-tosylaziridine (**2.118**):



(±)-2-(4-(4,4,5,5-tetramethyl-1,3,2-dioxaborolan-2-yl)butyl)-1-tosylaziridine (±-2.118):

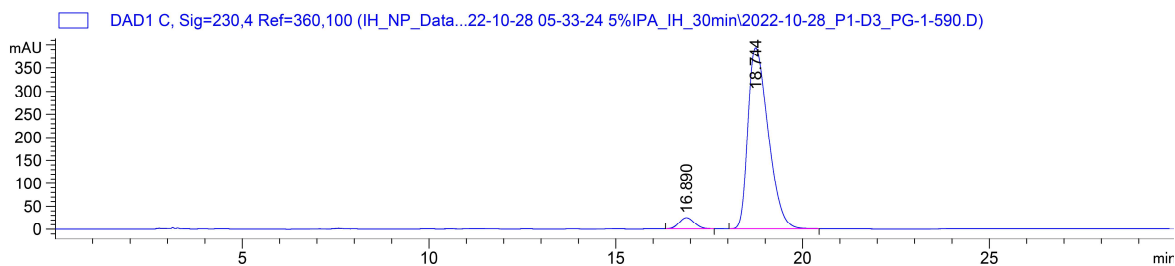


Signal 3: DAD1 C, Sig=230,4 Ref=360,100

| Peak # | RetTime [min] | Type | Width [min] | Area [mAU*s] | Height [mAU] | Area % |
|--------|---------------|------|-------------|--------------|--------------|---------|
| 1 | 16.077 | BB | 0.3867 | 2298.20679 | 85.32497 | 50.0368 |
| 2 | 17.977 | BB | 0.4201 | 2294.82422 | 72.93842 | 49.9632 |

Totals : 4593.03101 158.26340

(S)-2-(4-(4,4,5,5-tetramethyl-1,3,2-dioxaborolan-2-yl)butyl)-1-tosylaziridine (2.118):

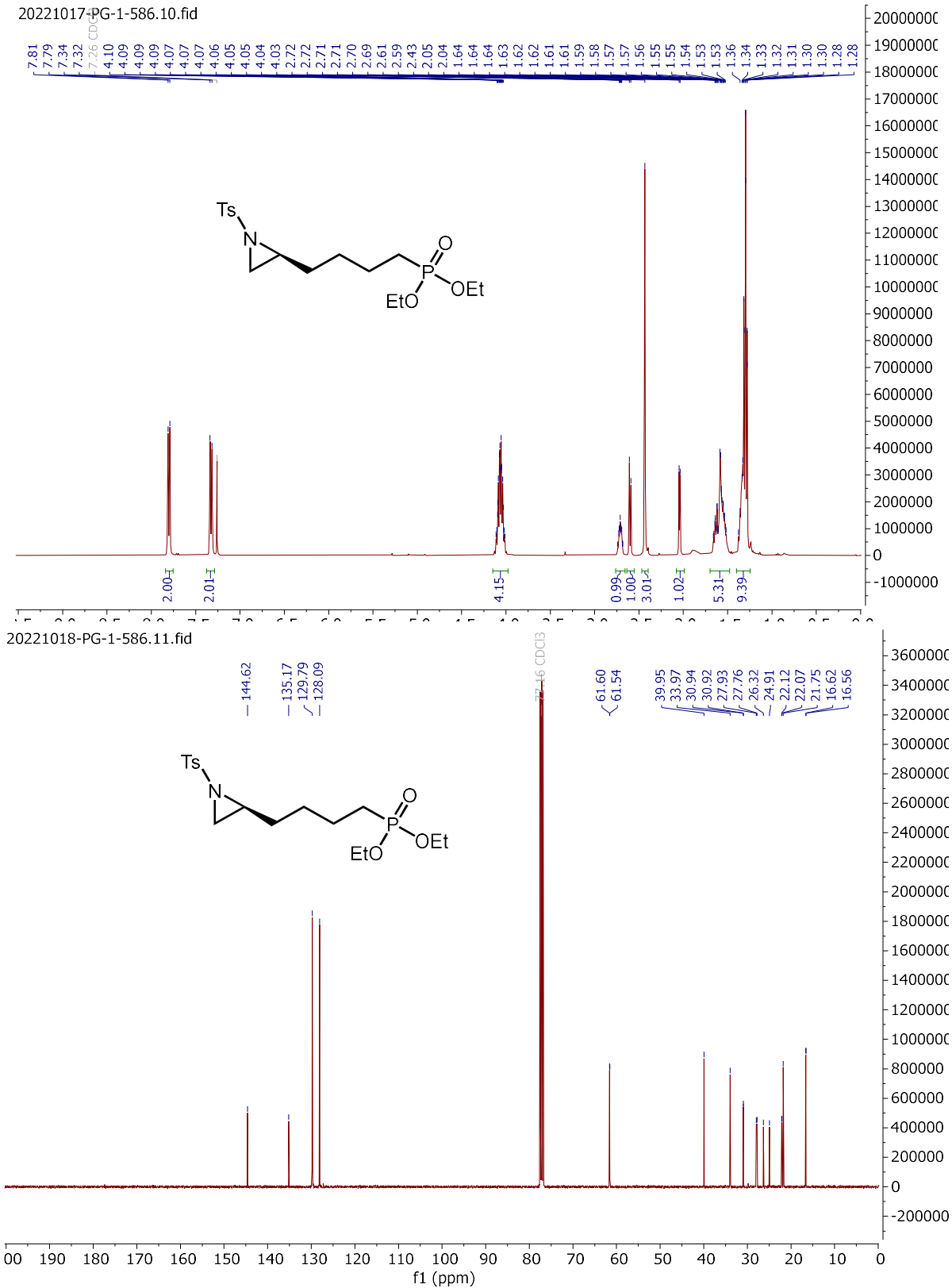


Signal 3: DAD1 C, Sig=230,4 Ref=360,100

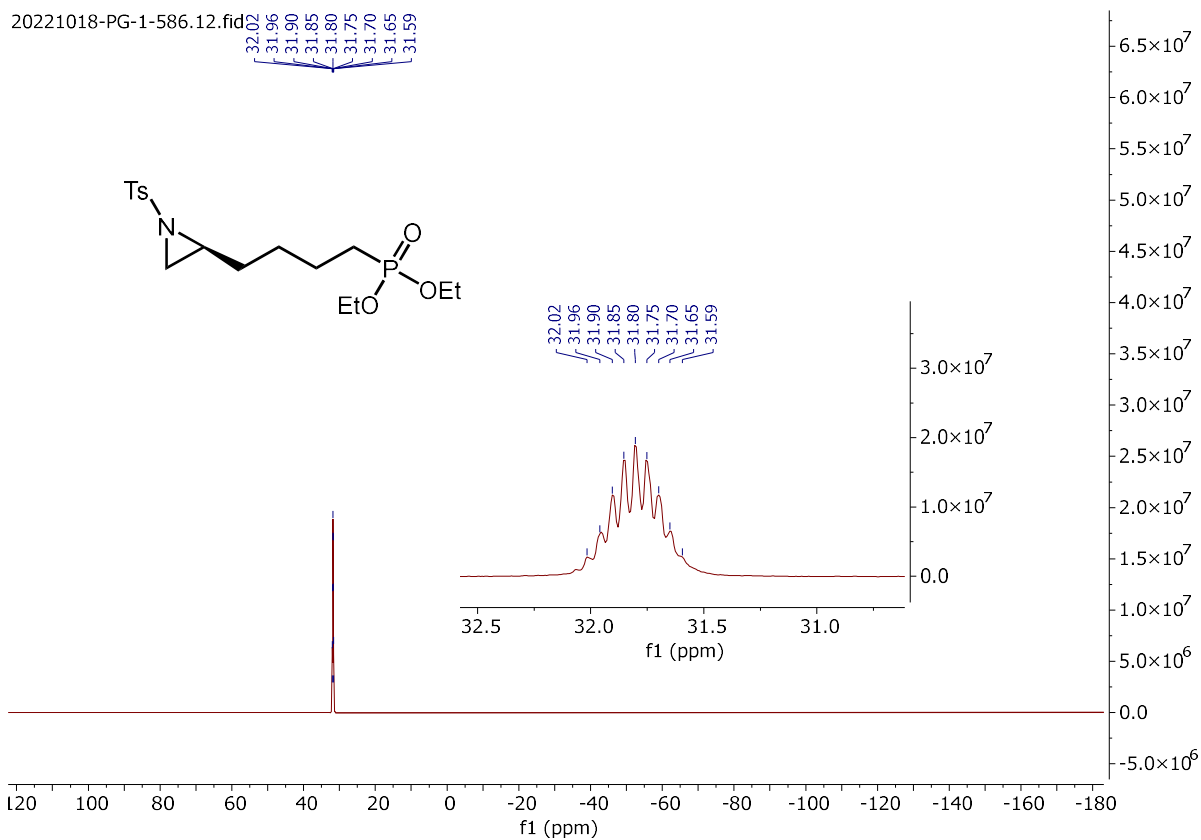
| Peak # | RetTime [min] | Type | Width [min] | Area [mAU*s] | Height [mAU] | Area % |
|--------|---------------|------|-------------|--------------|--------------|---------|
| 1 | 16.890 | BB | 0.3312 | 688.79572 | 24.48606 | 4.4435 |
| 2 | 18.744 | BB | 0.5245 | 1.48123e4 | 392.72430 | 95.5565 |

Totals : 1.55011e4 417.21036

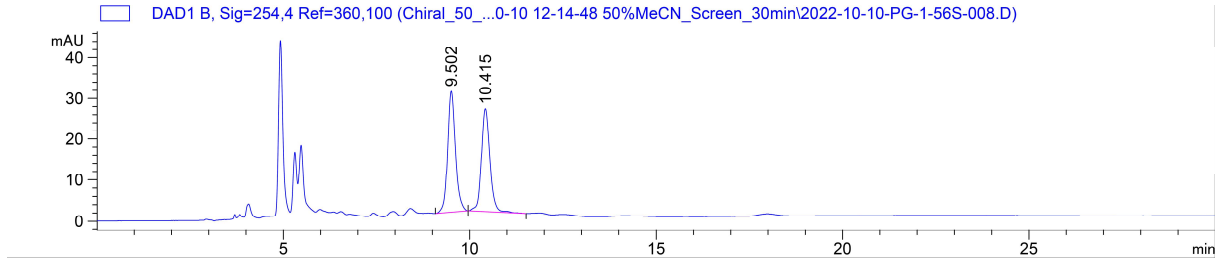
diethyl (*S*)-(4-(1-tosylaziridin-2-yl)butyl)phosphonate (**2.119**):



ethyl (*S*)-(4-(1-tosylaziridin-2-yl)butyl)phosphonate (**2.119**):



ethyl (±)-(4-(1-tosylaziridin-2-yl)butyl)phosphonate (±-**2.119**):

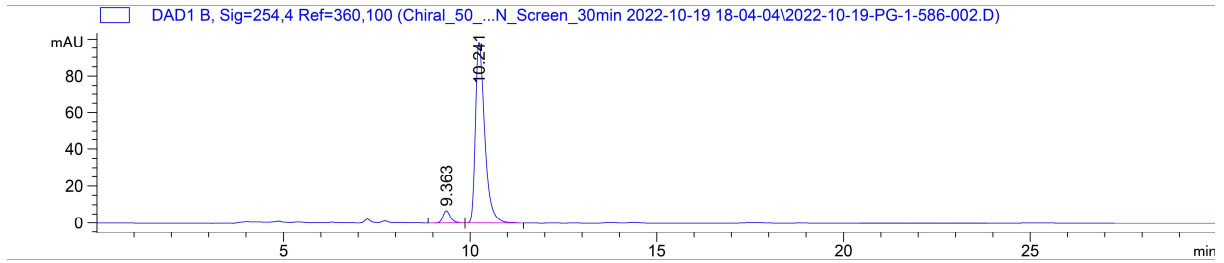


Signal 2: DAD1 B, Sig=254,4 Ref=360,100

| Peak # | RetTime [min] | Type | Width [min] | Area [mAU*s] | Height [mAU] | Area % |
|--------|---------------|------|-------------|--------------|--------------|---------|
| 1 | 9.502 | BB | 0.2194 | 429.23535 | 29.55379 | 51.9796 |
| 2 | 10.415 | BB | 0.2402 | 396.54083 | 25.11118 | 48.0204 |

Totals : 825.77618 54.66497

ethyl (*S*)-(4-(1-tosylaziridin-2-yl)butyl)phosphonate (**2.119**):

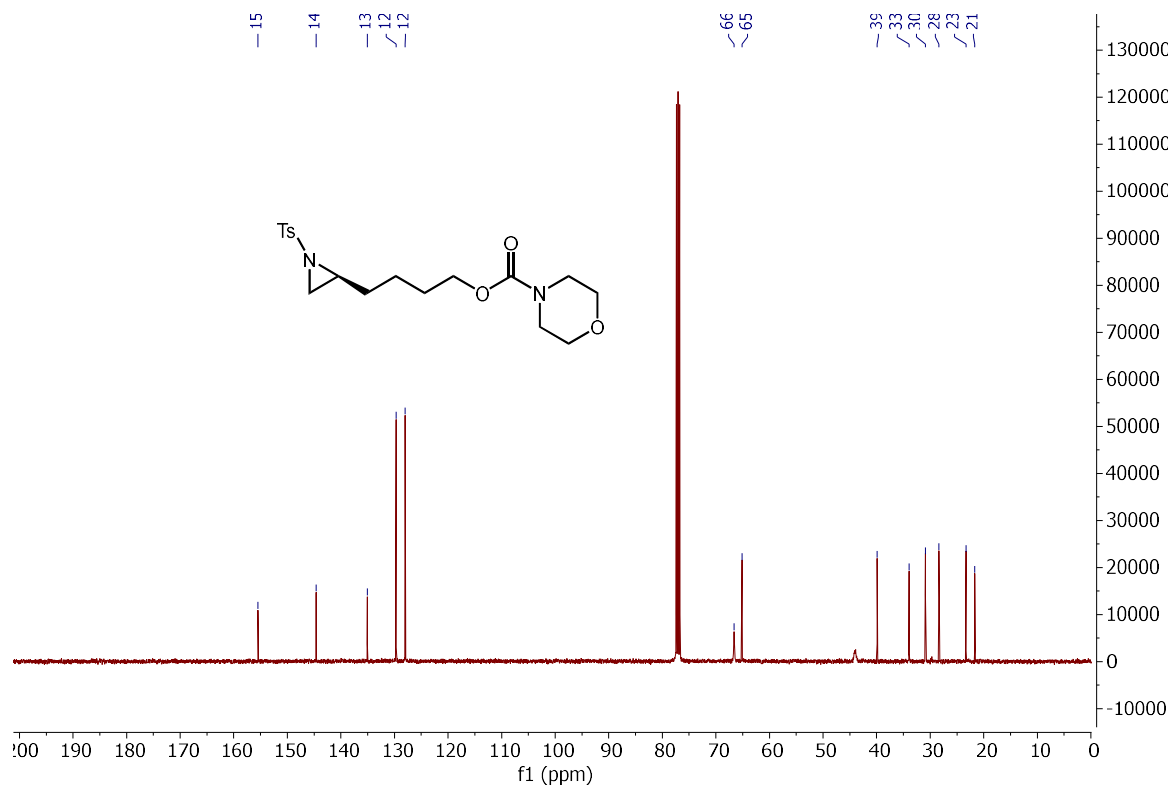
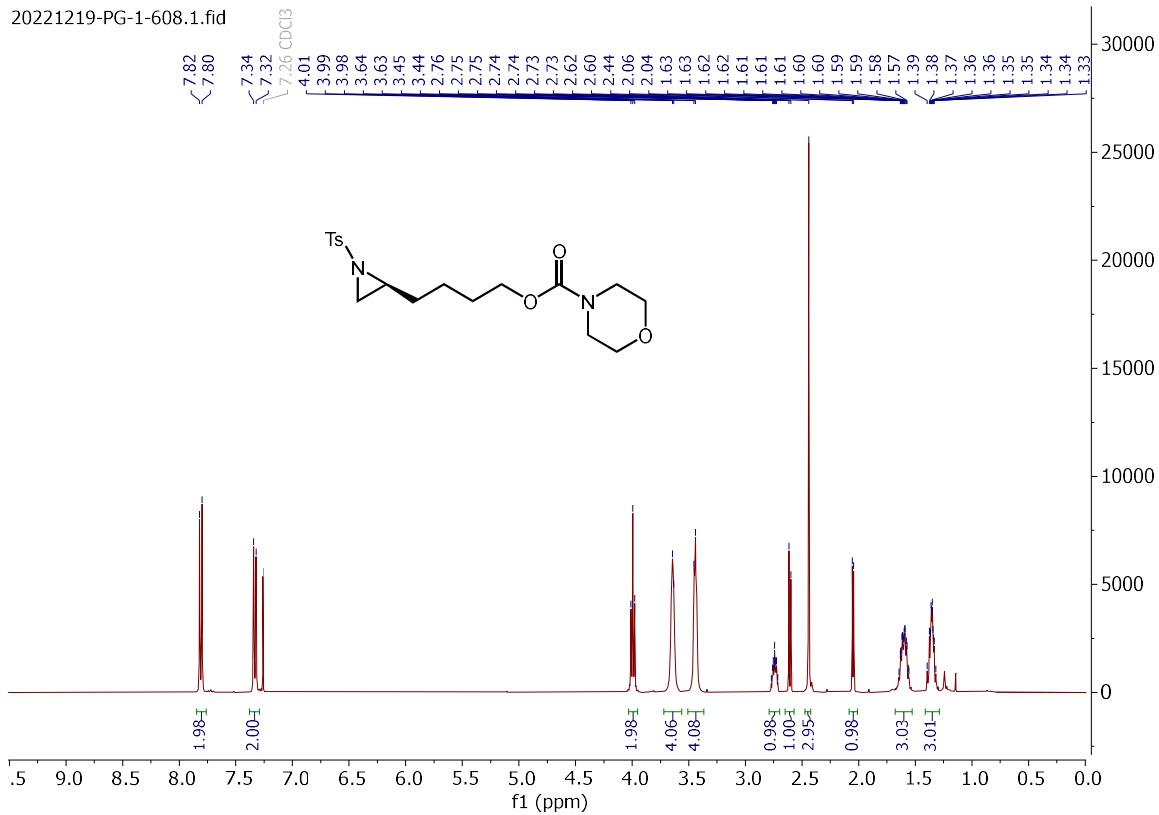


Signal 2: DAD1 B, Sig=254,4 Ref=360,100

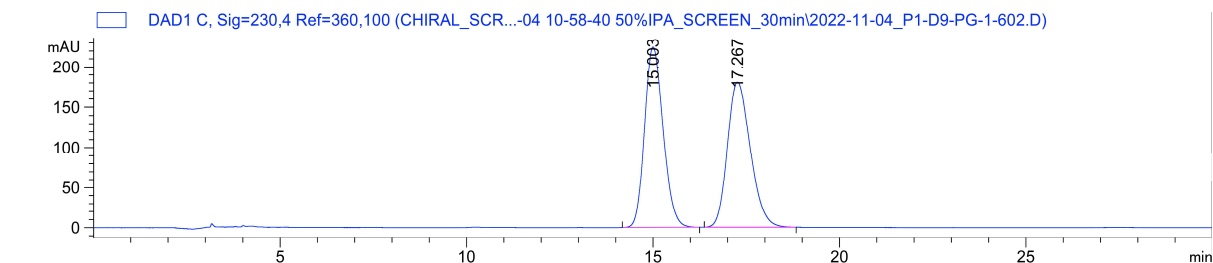
| Peak # | RetTime [min] | Type | Width [min] | Area [mAU*s] | Height [mAU] | Area % |
|--------|---------------|------|-------------|--------------|--------------|---------|
| 1 | 9.363 | BB | 0.2139 | 95.79315 | 6.81980 | 5.4138 |
| 2 | 10.241 | BB | 0.2585 | 1673.62292 | 98.38892 | 94.5862 |

Totals : 1769.41608 105.20871

(S)-4-(1-tosylaziridin-2-yl)butyl morpholine-4-carboxylate (**2.120**):



(±)-4-(1-tosylaziridin-2-yl)butyl morpholine-4-carboxylate (±-2.120):

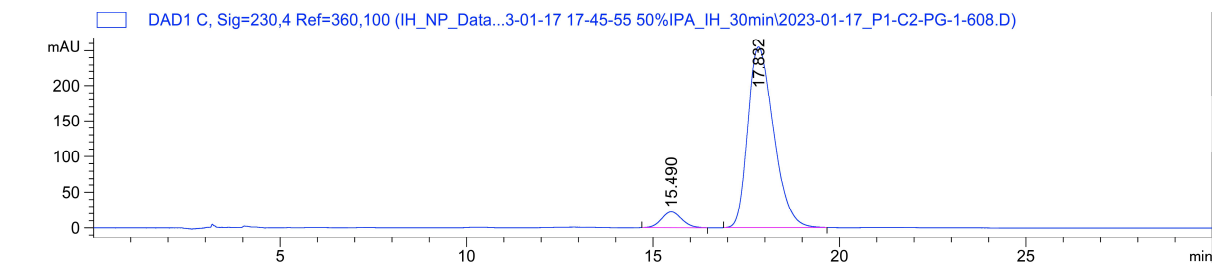


Signal 3: DAD1 C, Sig=230,4 Ref=360,100

| Peak # | RetTime [min] | Type | Width [min] | Area [mAU*s] | Height [mAU] | Area % |
|--------|---------------|------|-------------|--------------|--------------|---------|
| 1 | 15.003 | BB | 0.5036 | 7765.38818 | 224.21693 | 50.1402 |
| 2 | 17.267 | BB | 0.5204 | 7721.96191 | 180.19902 | 49.8598 |

Totals : 1.54874e4 404.41595

(S)-4-(1-tosylaziridin-2-yl)butyl morpholine-4-carboxylate (2.120):

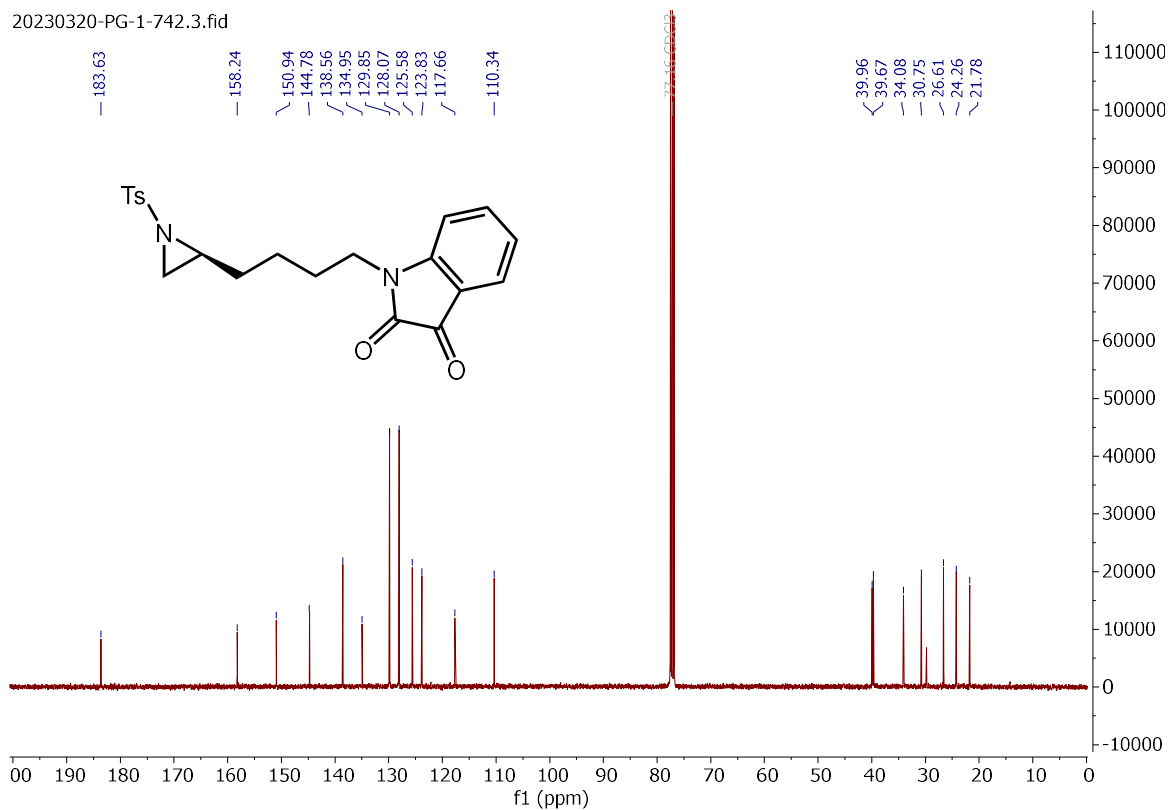
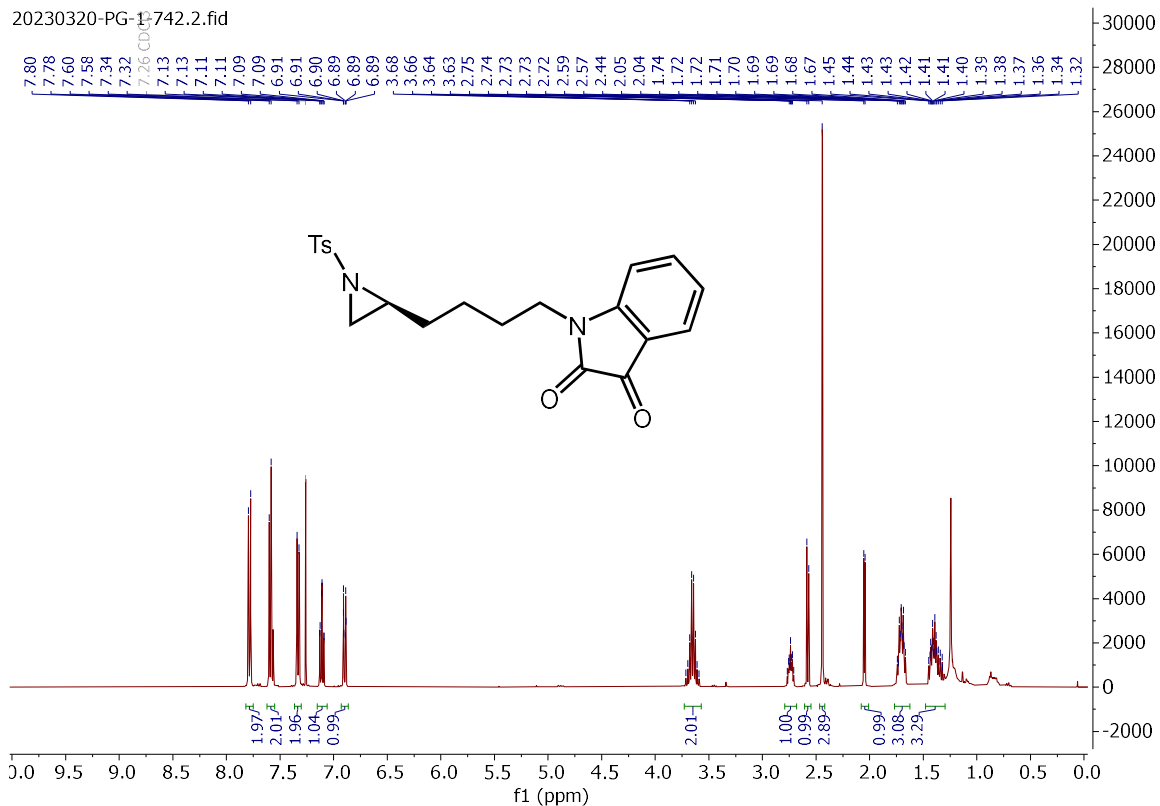


Signal 3: DAD1 C, Sig=230,4 Ref=360,100

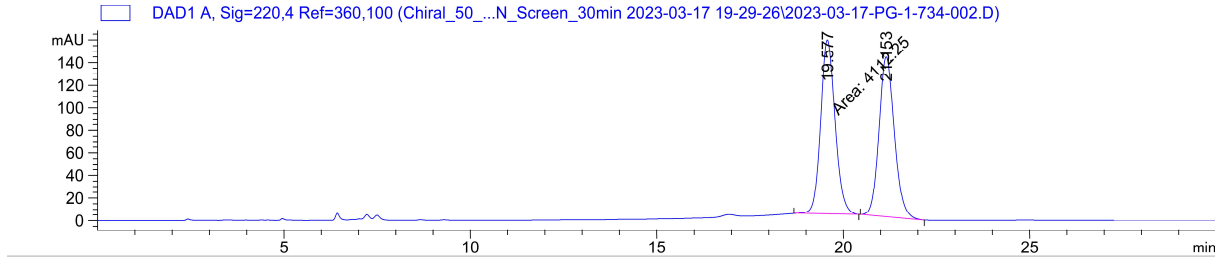
| Peak # | RetTime [min] | Type | Width [min] | Area [mAU*s] | Height [mAU] | Area % |
|--------|---------------|------|-------------|--------------|--------------|---------|
| 1 | 15.490 | BB | 0.4397 | 822.09857 | 21.96504 | 6.3195 |
| 2 | 17.832 | BB | 0.5734 | 1.21868e4 | 254.63814 | 93.6805 |

Totals : 1.30089e4 276.60318

(S)-1-(4-(1-tosylaziridin-2-yl)butyl)indoline-2,3-dione (**2.121**):



(±)-1-(4-(1-tosylaziridin-2-yl)butyl)indoline-2,3-dione (±-**2.121**):

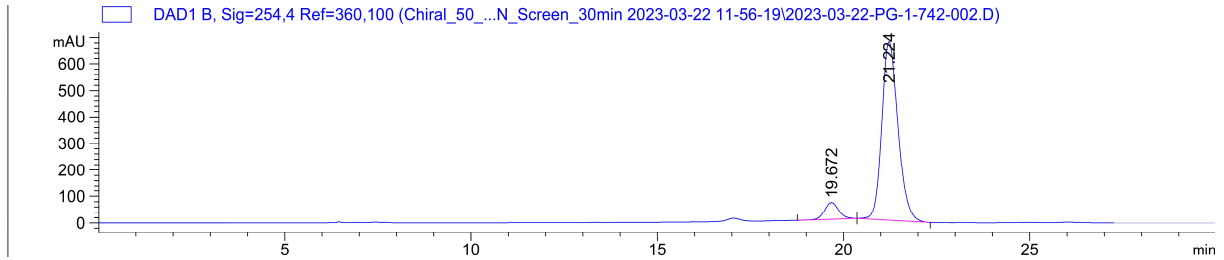


Signal 1: DAD1 A, Sig=220,4 Ref=360,100

| Peak # | RetTime [min] | Type | Width [min] | Area [mAU*s] | Height [mAU] | Area % |
|--------|---------------|------|-------------|--------------|--------------|---------|
| 1 | 19.577 | MM T | 0.4450 | 4112.25488 | 154.01982 | 50.2835 |
| 2 | 21.153 | BB | 0.4413 | 4065.88867 | 141.48030 | 49.7165 |

Totals : 8178.14355 295.50012

(S)-1-(4-(1-tosylaziridin-2-yl)butyl)indoline-2,3-dione (**2.121**):

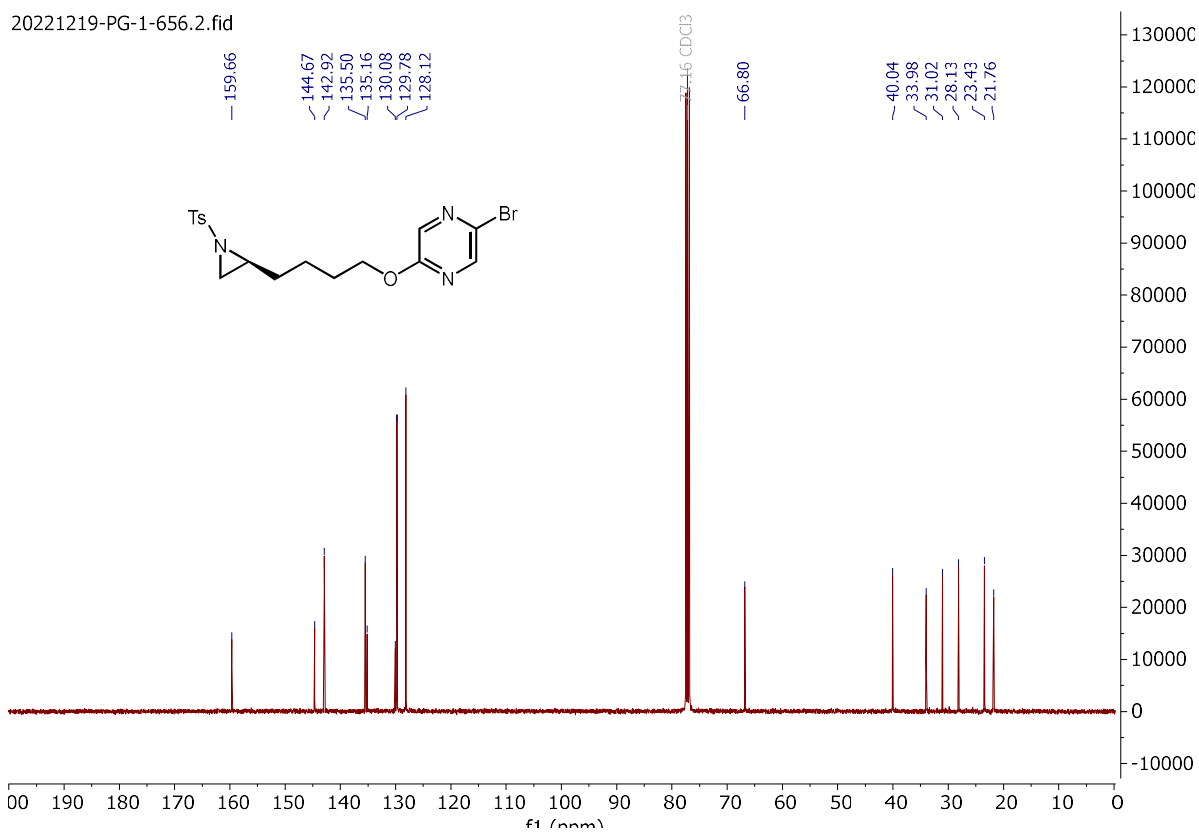
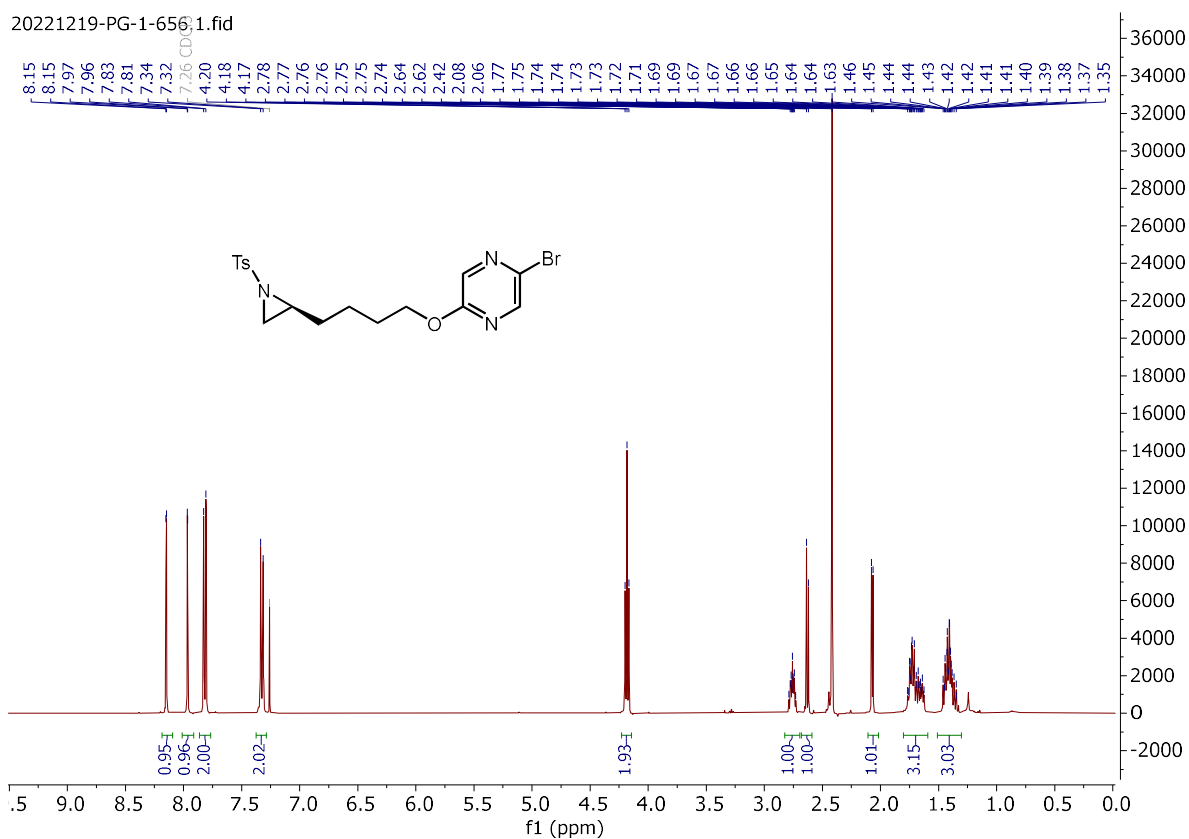


Signal 2: DAD1 B, Sig=254,4 Ref=360,100

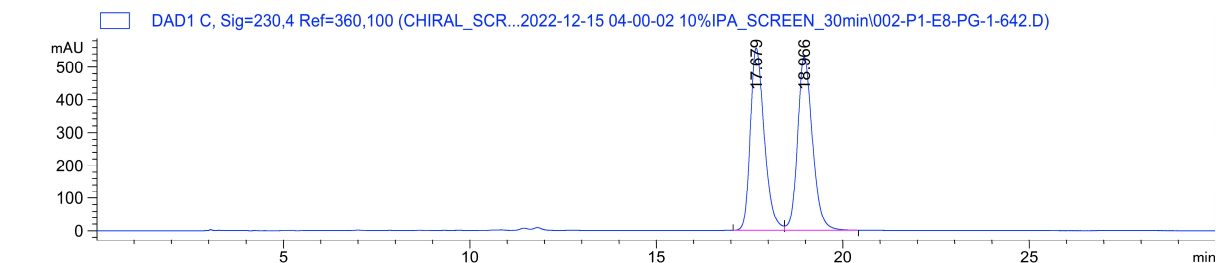
| Peak # | RetTime [min] | Type | Width [min] | Area [mAU*s] | Height [mAU] | Area % |
|--------|---------------|------|-------------|--------------|--------------|---------|
| 1 | 19.672 | BB | 0.4025 | 1629.29834 | 62.43285 | 7.4078 |
| 2 | 21.224 | BB | 0.4644 | 2.03651e4 | 674.12158 | 92.5922 |

Totals : 2.19944e4 736.55443

(S)-2-bromo-5-(4-(1-tosylaziridin-2-yl)butoxy)pyrazine (**2.122**):



(±)-2-bromo-5-(4-(1-tosylaziridin-2-yl)butoxy)pyrazine (**±-2.122**):

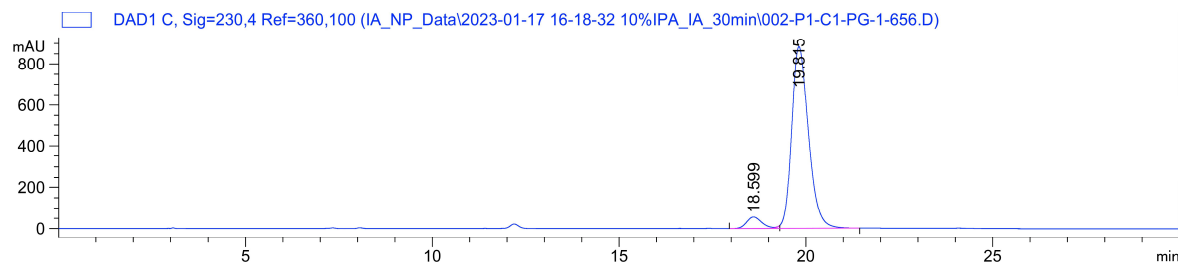


Signal 3: DAD1 C, Sig=230,4 Ref=360,100

| Peak # | RetTime [min] | Type | Width [min] | Area [mAU*s] | Height [mAU] | Area % |
|--------|---------------|------|-------------|--------------|--------------|---------|
| 1 | 17.679 | BV | 0.3918 | 1.44649e4 | 557.33893 | 49.6285 |
| 2 | 18.966 | VB | 0.4172 | 1.46814e4 | 529.94415 | 50.3715 |

Totals : 2.91463e4 1087.28308

(S)-2-bromo-5-(4-(1-tosylaziridin-2-yl)butoxy)pyrazine (**2.122**):

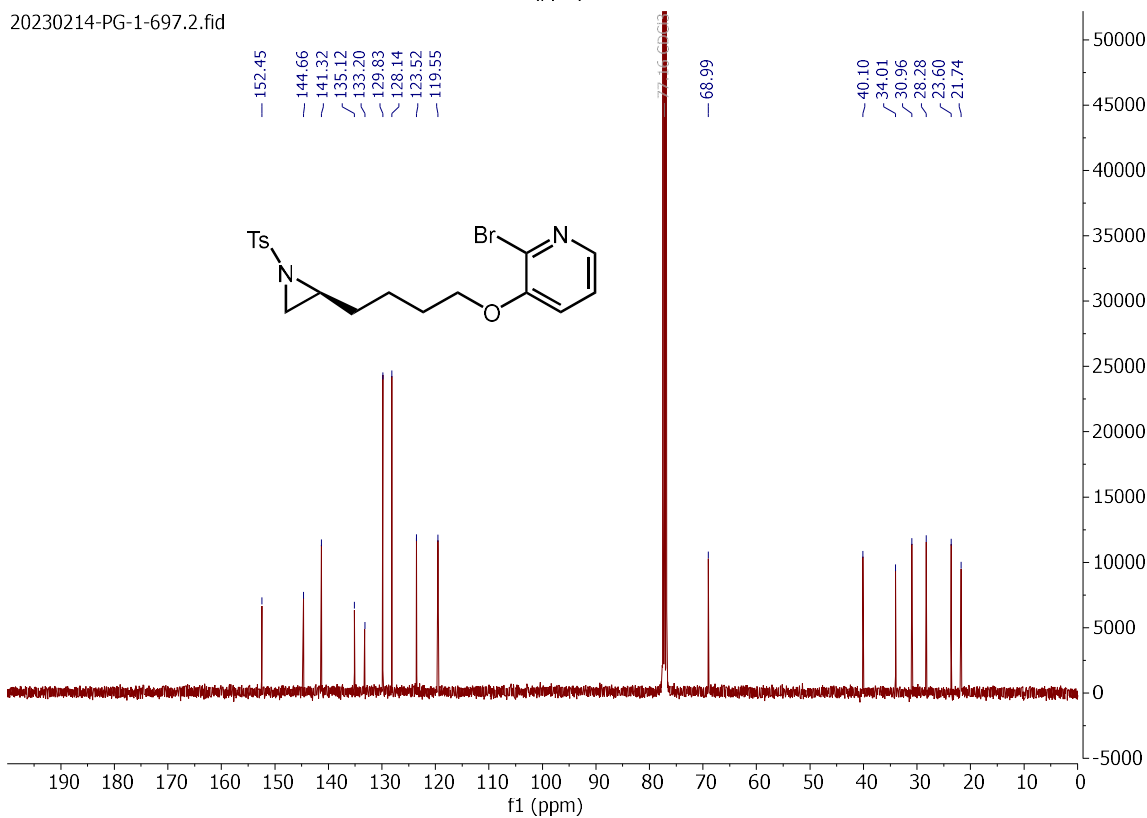
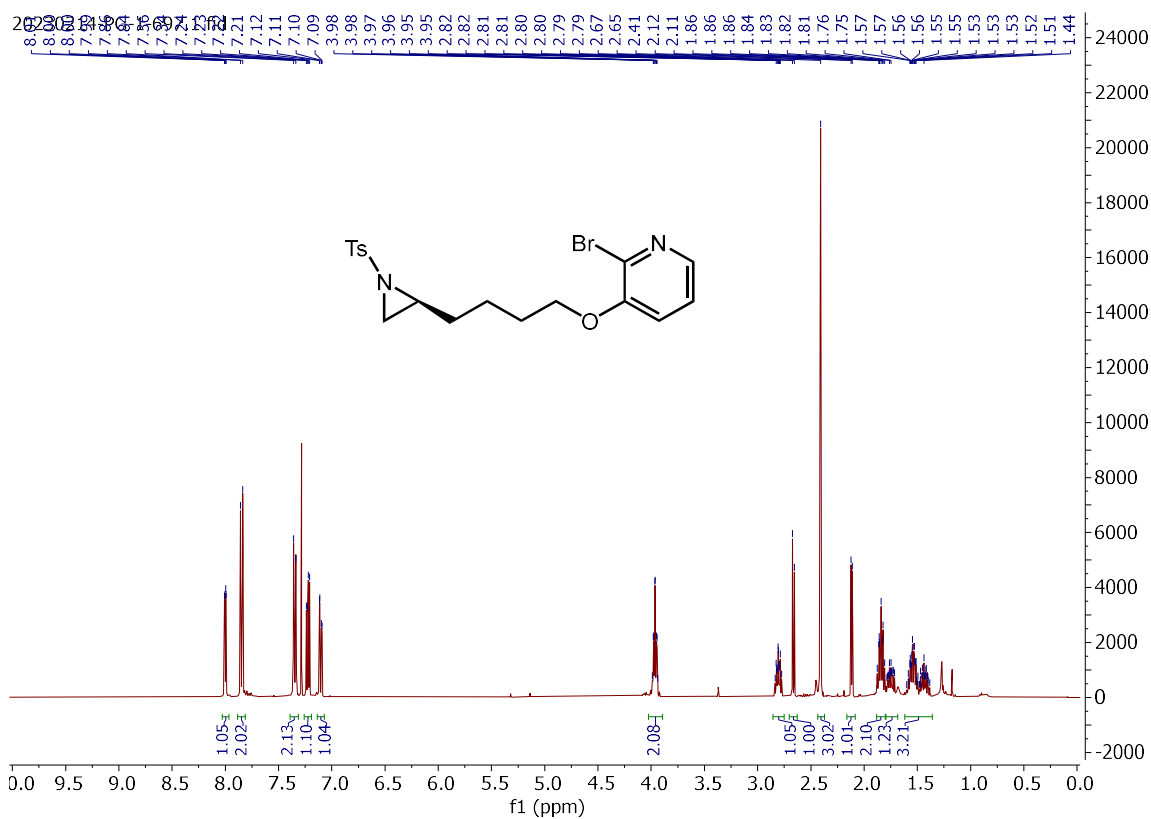


Signal 3: DAD1 C, Sig=230,4 Ref=360,100

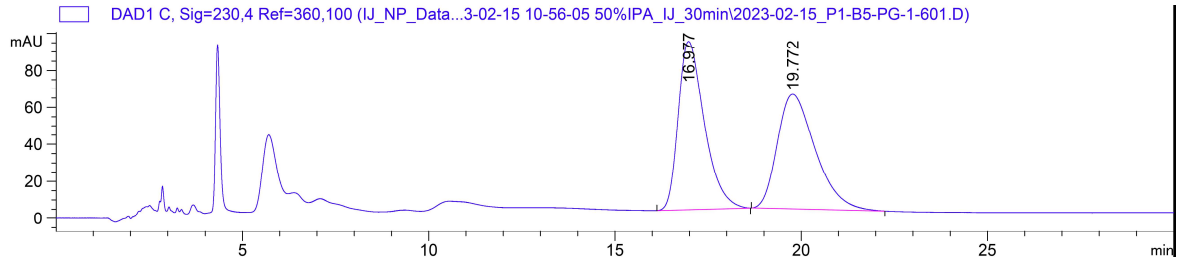
| Peak # | RetTime [min] | Type | Width [min] | Area [mAU*s] | Height [mAU] | Area % |
|--------|---------------|------|-------------|--------------|--------------|---------|
| 1 | 18.599 | BV E | 0.3382 | 1573.57642 | 55.60388 | 5.4165 |
| 2 | 19.815 | VB R | 0.4695 | 2.74781e4 | 883.12793 | 94.5835 |

Totals : 2.90517e4 938.73181

(S)-2-bromo-3-(4-(1-tosylaziridin-2-yl)butoxy)pyridine (**2.123**):



(±)-2-bromo-3-(4-(1-tosylaziridin-2-yl)butoxy)pyridine (±-2.123):

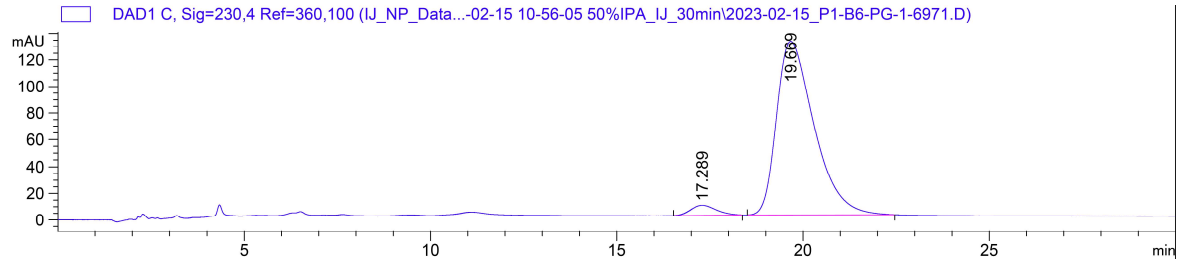


Signal 3: DAD1 C, Sig=230,4 Ref=360,100

| Peak # | RetTime [min] | Type | Width [min] | Area [mAU*s] | Height [mAU] | Area % |
|--------|---------------|------|-------------|--------------|--------------|---------|
| 1 | 16.977 | BB | 0.5678 | 4414.51611 | 90.95141 | 50.1847 |
| 2 | 19.772 | BB | 0.8302 | 4382.01660 | 61.83913 | 49.8153 |

Totals : 8796.53271 152.79054

(S)-2-bromo-3-(4-(1-tosylaziridin-2-yl)butoxy)pyridine (2.124):

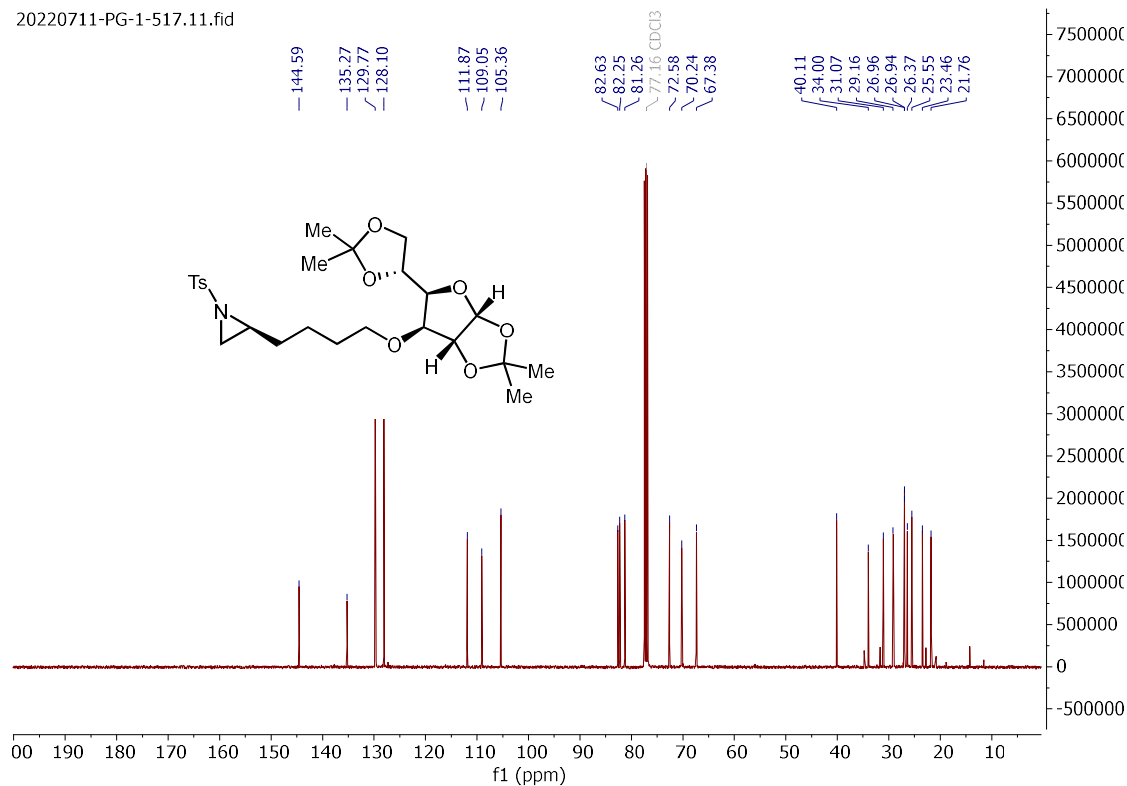
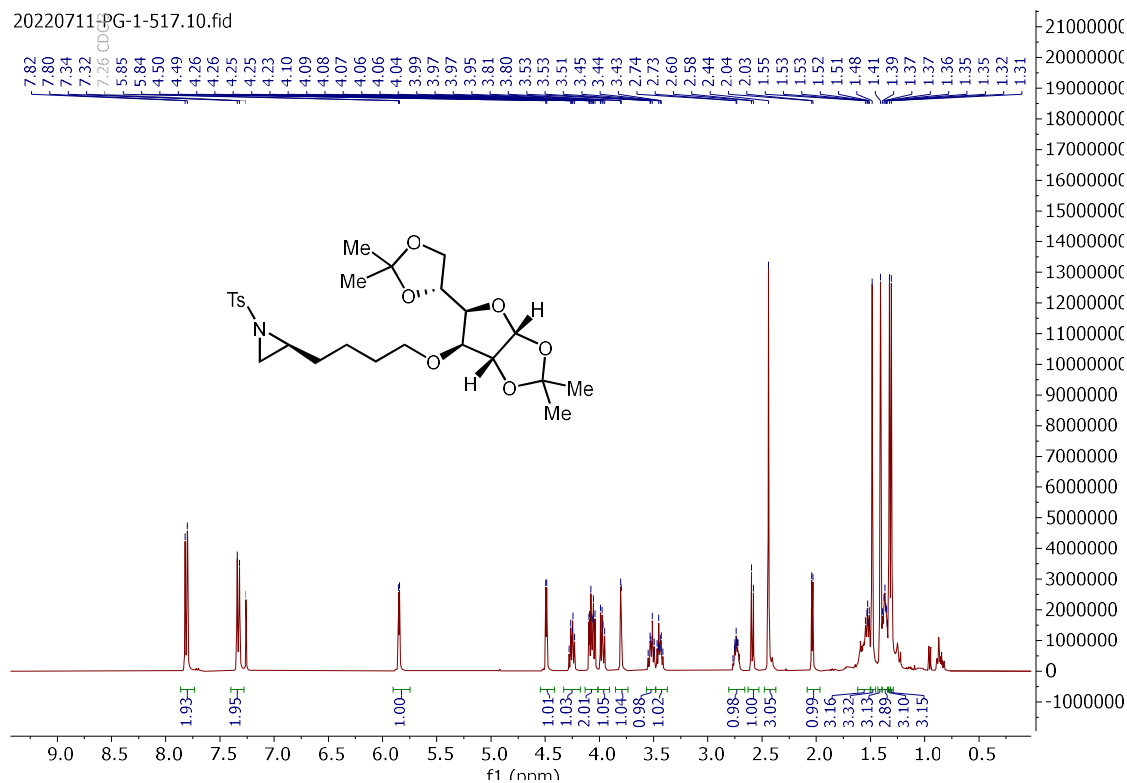


Signal 3: DAD1 C, Sig=230,4 Ref=360,100

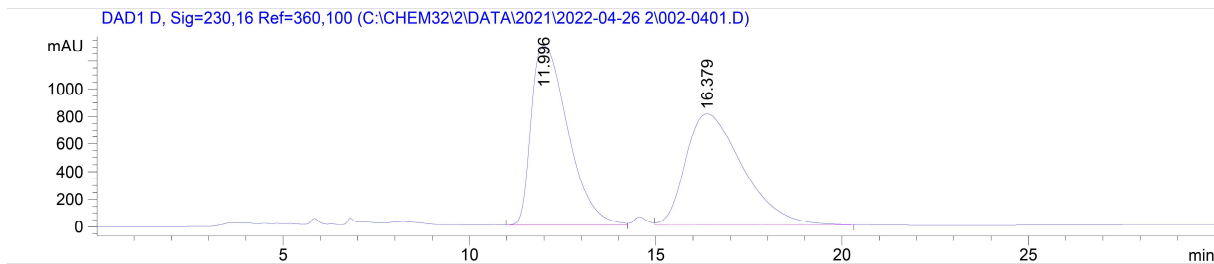
| Peak # | RetTime [min] | Type | Width [min] | Area [mAU*s] | Height [mAU] | Area % |
|--------|---------------|------|-------------|--------------|--------------|---------|
| 1 | 17.289 | BB | 0.5509 | 361.12485 | 7.66805 | 3.8178 |
| 2 | 19.669 | BB | 0.8194 | 9097.79199 | 130.40765 | 96.1822 |

Totals : 9458.91684 138.07571

(*S*)-2-(4-(((3*aR*,5*R*,6*S*,6*aR*)-5-((*R*)-2,2-dimethyl-1,3-dioxolan-4-yl)-2,2-dimethyltetrahydrofuro[2,3-*d*][1,3]dioxol-6-yl)oxy)butyl)-1-tosylaziridine (**2.124**):



2-(4-(((3aR,5R,6S,6aR)-5-((R)-2,2-dimethyl-1,3-dioxolan-4-yl)-2,2-dimethyltetrahydrofuro[2,3-d][1,3]dioxol-6-yl)oxy)butyl)-1-tosylaziridine (**2.124**):

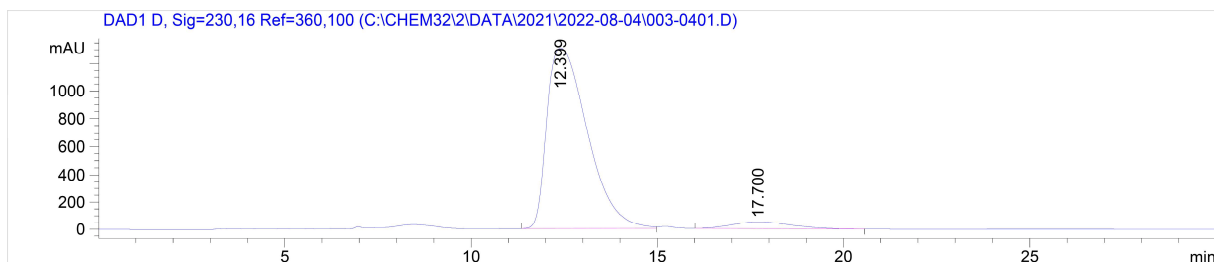


Signal 3: DAD1 D, Sig=230,16 Ref=360,100

| Peak # | RetTime [min] | Type | Width [min] | Area [mAU*s] | Height [mAU] | Area % |
|--------|---------------|------|-------------|--------------|--------------|---------|
| 1 | 11.996 | VV | 1.0645 | 8.88711e4 | 1301.70557 | 50.8187 |
| 2 | 16.379 | VB | 1.6105 | 8.60076e4 | 808.91321 | 49.1813 |

Totals : 1.74879e5 2110.61877

(S)-2-(4-(((3aR,5R,6S,6aR)-5-((R)-2,2-dimethyl-1,3-dioxolan-4-yl)-2,2-dimethyltetrahydrofuro[2,3-d][1,3]dioxol-6-yl)oxy)butyl)-1-tosylaziridine (**2.124**):

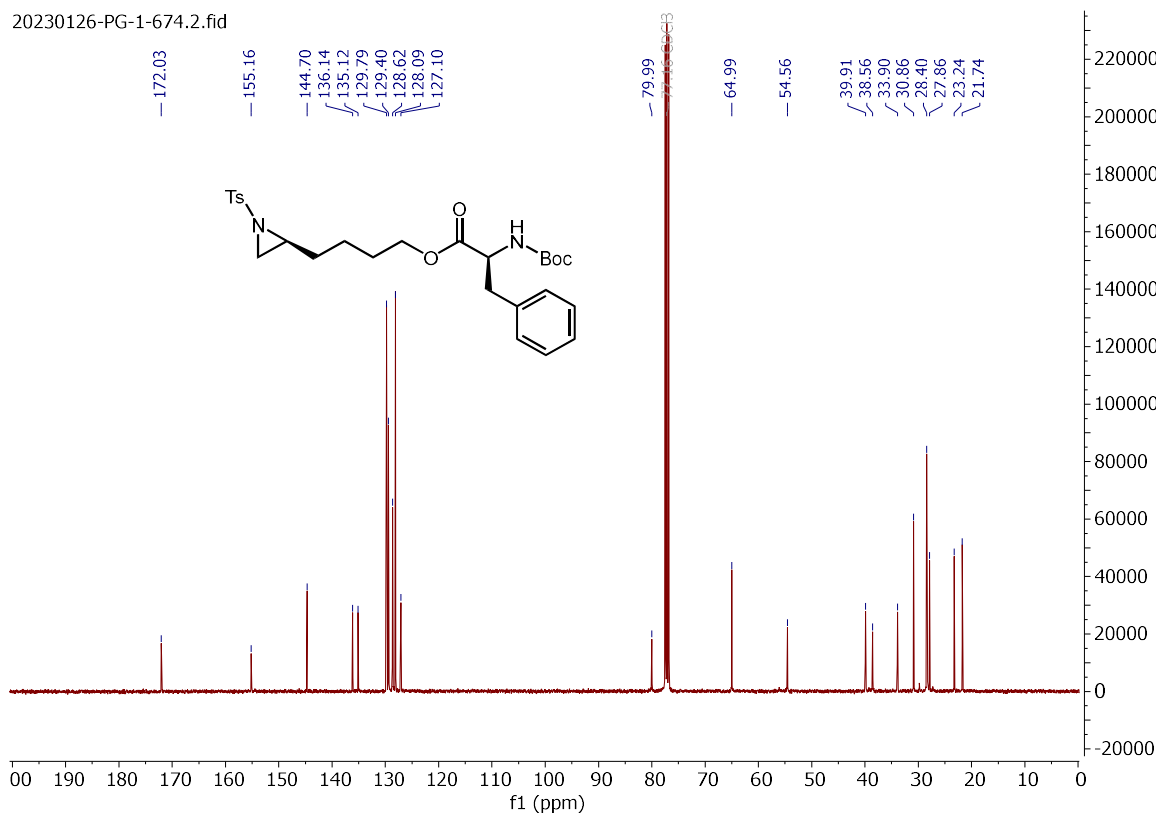
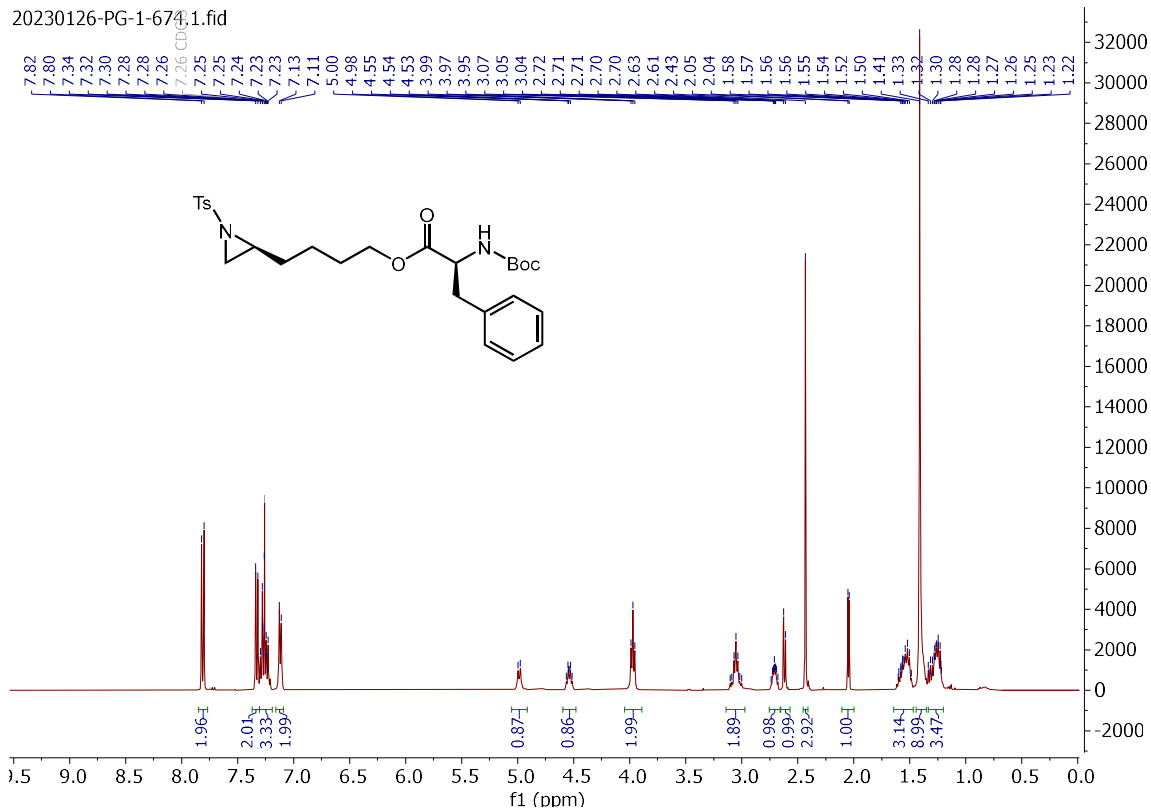


Signal 3: DAD1 D, Sig=230,16 Ref=360,100

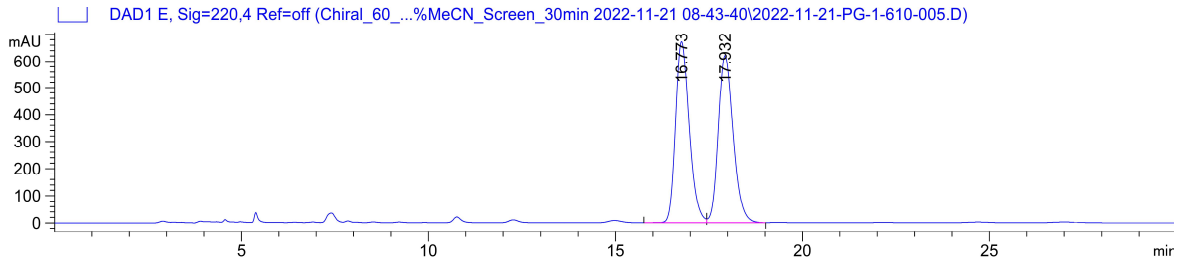
| Peak # | RetTime [min] | Type | Width [min] | Area [mAU*s] | Height [mAU] | Area % |
|--------|---------------|------|-------------|--------------|--------------|---------|
| 1 | 12.399 | BV | 1.1575 | 9.86357e4 | 1308.34302 | 94.7218 |
| 2 | 17.700 | BB | 1.5455 | 5496.31592 | 50.75129 | 5.2782 |

Totals : 1.04132e5 1359.09430

4-((S)-1-tosylaziridin-2-yl)butyl (tert-butoxycarbonyl)-L-phenylalaninate (**2.125**):



4-I-tosylaziridin-2-yl)butyl (tert-butoxycarbonyl)-L-phenylalaninate (2.125):

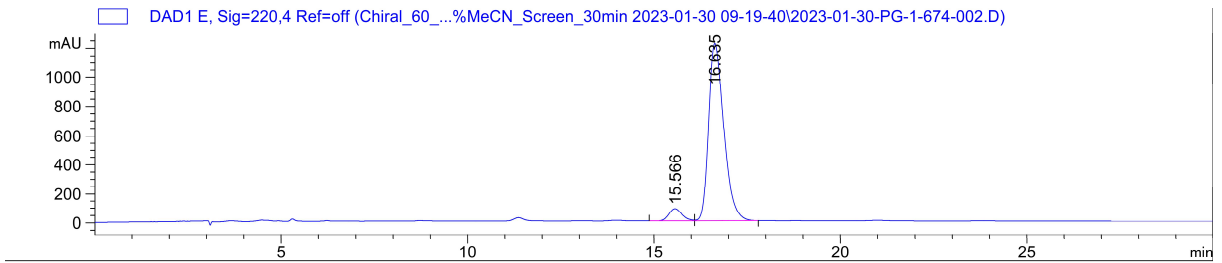


Signal 5: DAD1 E, Sig=220,4 Ref=off

| Peak # | RetTime [min] | Type | Width [min] | Area [mAU*s] | Height [mAU] | Area % |
|--------|---------------|------|-------------|--------------|--------------|---------|
| 1 | 16.773 | BV | 0.3897 | 1.70401e4 | 672.19922 | 49.9161 |
| 2 | 17.932 | VB | 0.4231 | 1.70974e4 | 621.28369 | 50.0839 |

Totals : 3.41375e4 1293.48291

4-((S)-1-tosylaziridin-2-yl)butyl (tert-butoxycarbonyl)-L-phenylalaninate (2.125):

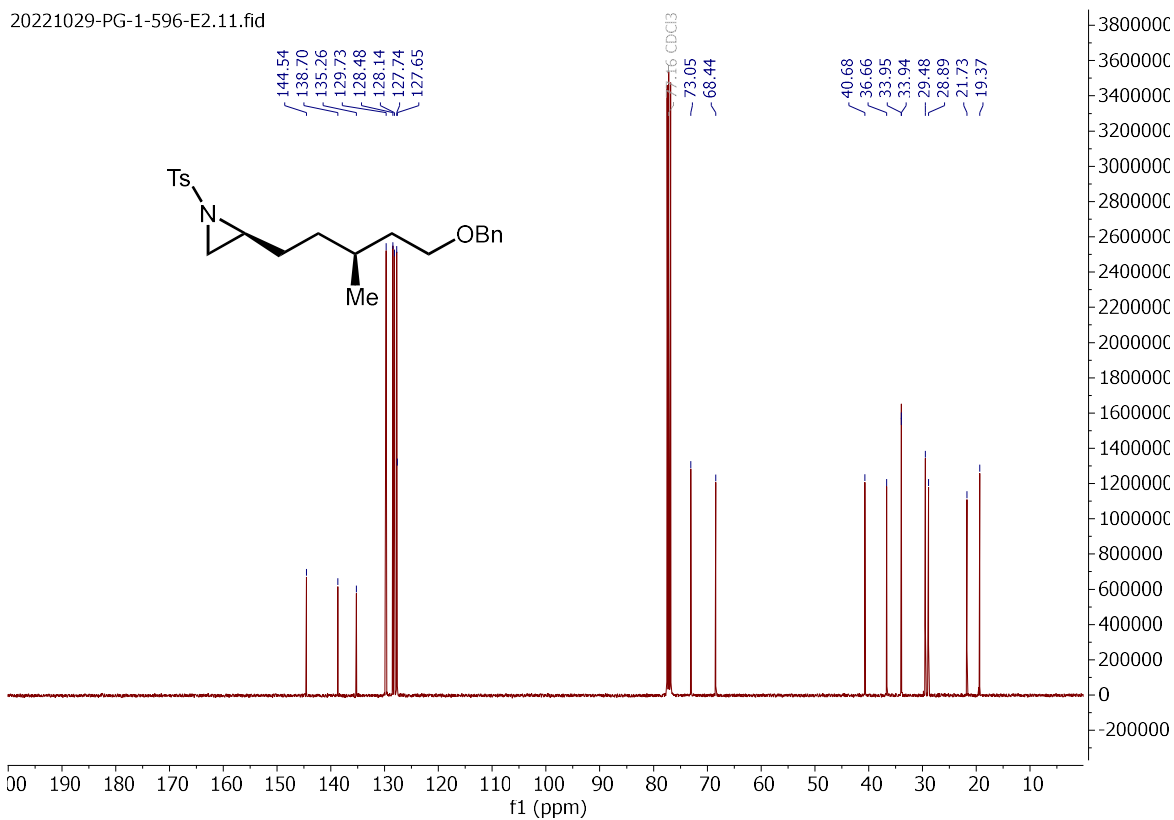
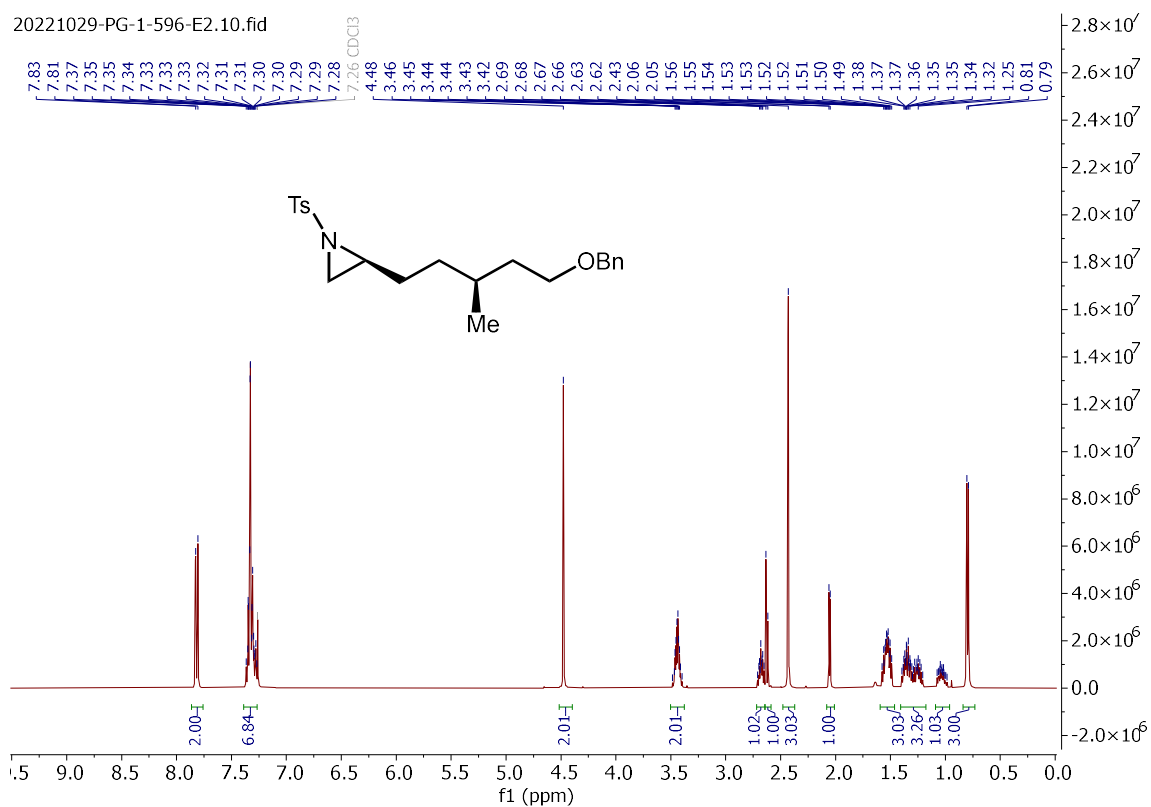


Signal 5: DAD1 E, Sig=220,4 Ref=off

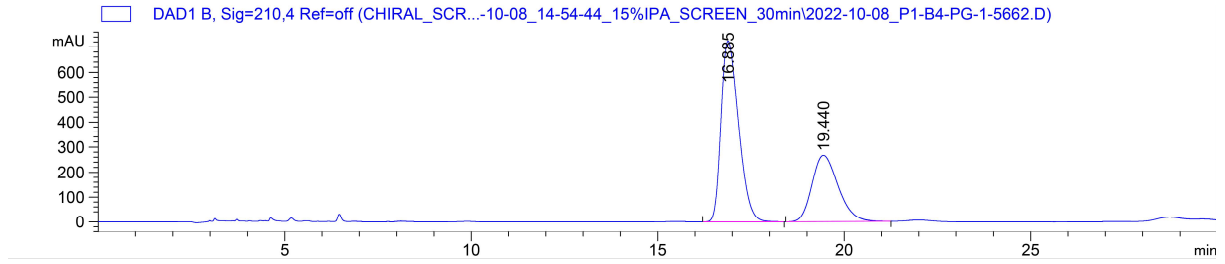
| Peak # | RetTime [min] | Type | Width [min] | Area [mAU*s] | Height [mAU] | Area % |
|--------|---------------|------|-------------|--------------|--------------|---------|
| 1 | 15.566 | BV | 0.3742 | 2028.79102 | 83.28348 | 5.5634 |
| 2 | 16.635 | VB | 0.4357 | 3.44380e4 | 1218.73645 | 94.4366 |

Totals : 3.64668e4 1302.01993

(S)-2-((S)-5-(benzyloxy)-3-methylpentyl)-1-tosylaziridine ((S,S)-2.126):



2-((S)-5-(benzyloxy)-3-methylpentyl)-1-tosylaziridine (**2.126**)

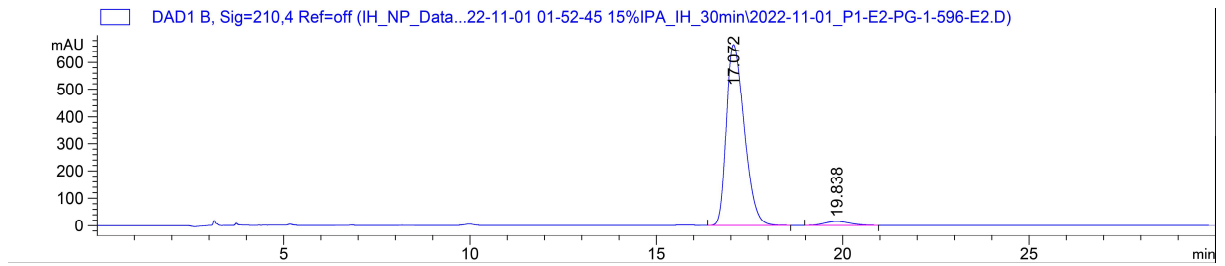


Signal 2: DAD1 B, Sig=210,4 Ref=off

| Peak # | RetTime [min] | Type | Width [min] | Area [mAU*s] | Height [mAU] | Area % |
|--------|---------------|------|-------------|--------------|--------------|---------|
| 1 | 16.885 | BB | 0.5058 | 2.36370e4 | 724.16583 | 64.3584 |
| 2 | 19.440 | BB | 0.6979 | 1.30901e4 | 266.55930 | 35.6416 |

Totals : 3.67271e4 990.72513

S)-2-((S)-5-(benzyloxy)-3-methylpentyl)-1-tosylaziridine ((S,S)-**2.216**):

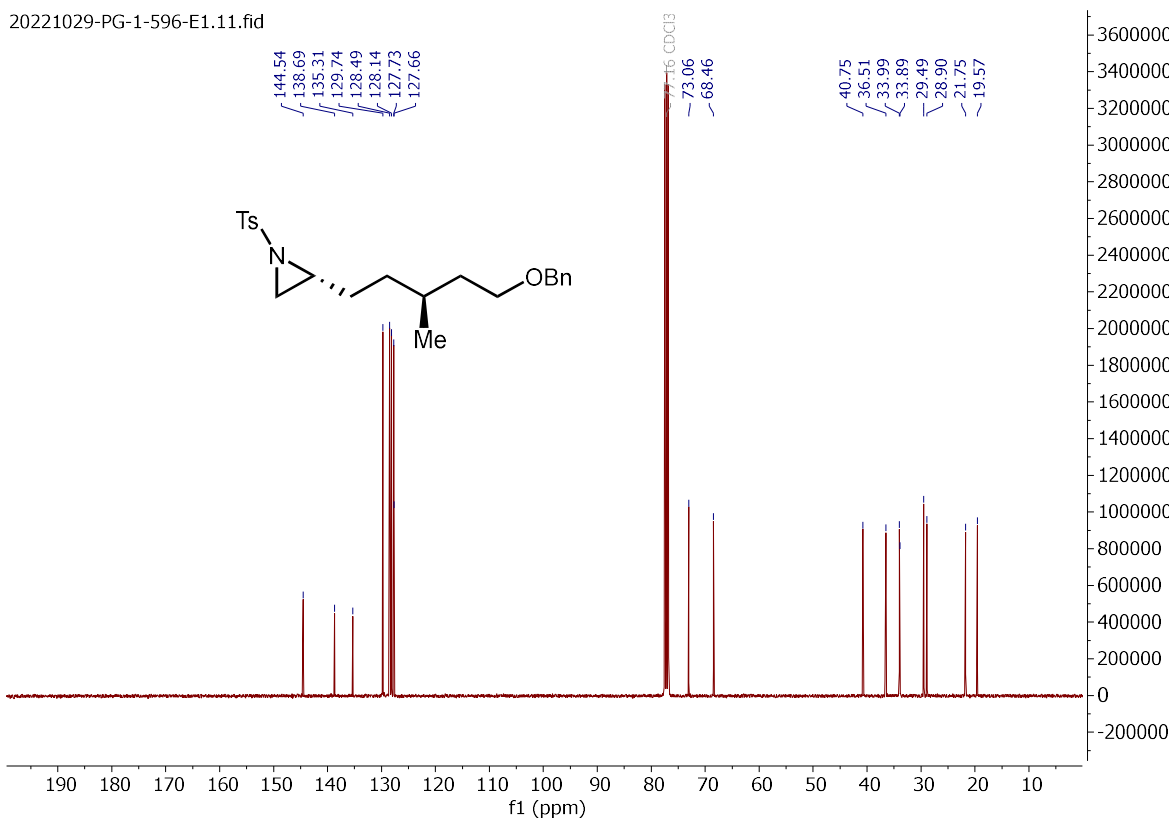
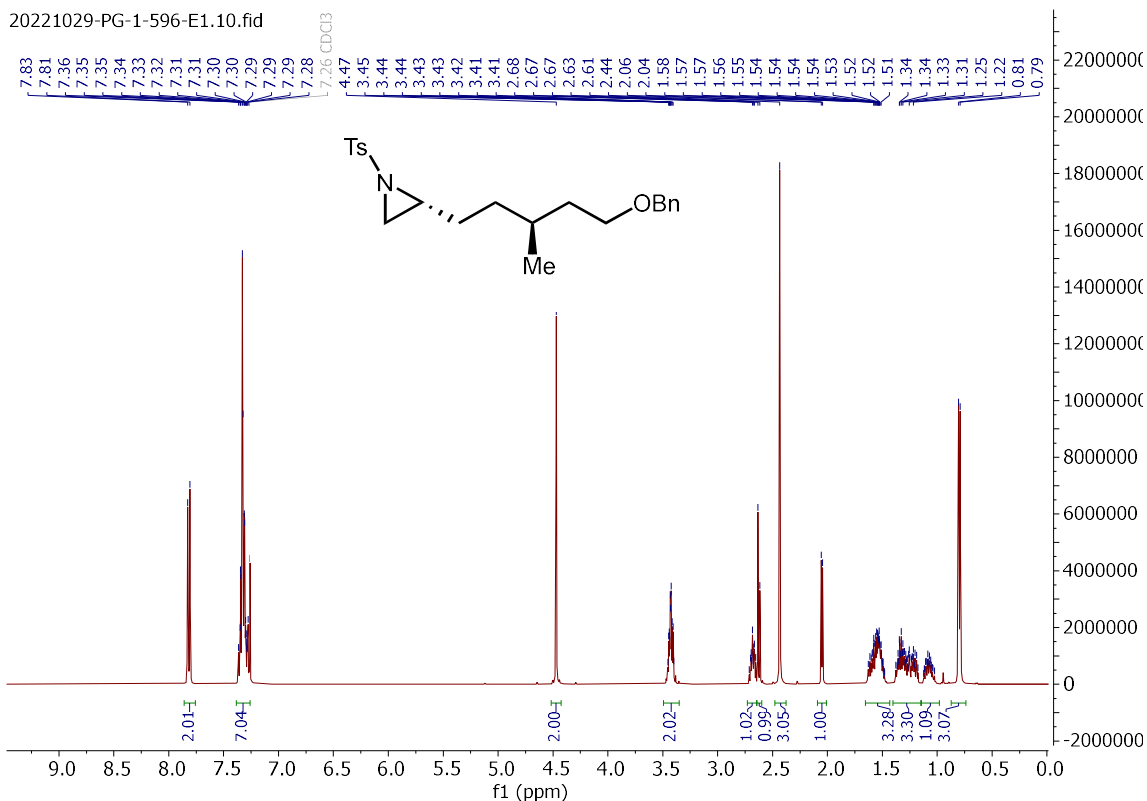


Signal 2: DAD1 B, Sig=210,4 Ref=off

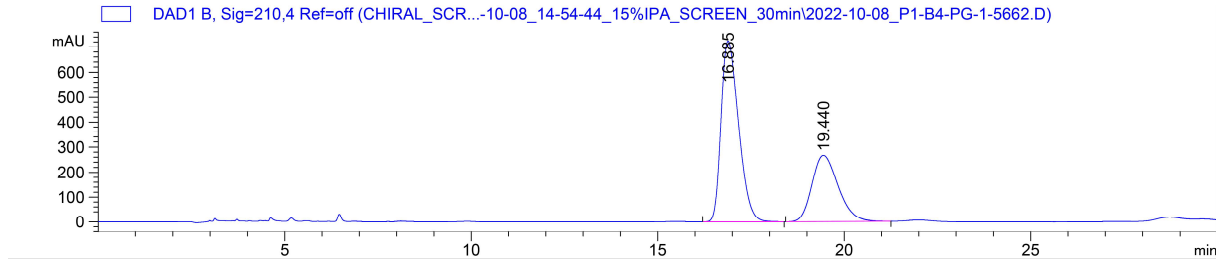
| Peak # | RetTime [min] | Type | Width [min] | Area [mAU*s] | Height [mAU] | Area % |
|--------|---------------|------|-------------|--------------|--------------|---------|
| 1 | 17.072 | BB | 0.4746 | 2.21371e4 | 664.59760 | 96.9773 |
| 2 | 19.838 | BB | 0.5469 | 689.98444 | 14.75927 | 3.0227 |

Totals : 2.28271e4 679.35686

(R)-2-((S)-5-(benzyloxy)-3-methylpentyl)-1-tosylaziridine ((R,S)-2.126):



2-((S)-5-(benzyloxy)-3-methylpentyl)-1-tosylaziridine (**2.126**)

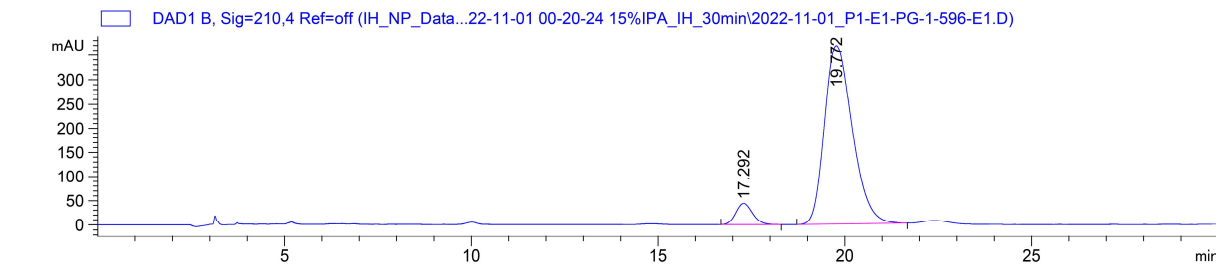


Signal 2: DAD1 B, Sig=210,4 Ref=off

| Peak # | RetTime [min] | Type | Width [min] | Area [mAU*s] | Height [mAU] | Area % |
|--------|---------------|------|-------------|--------------|--------------|---------|
| 1 | 16.885 | BB | 0.5058 | 2.36370e4 | 724.16583 | 64.3584 |
| 2 | 19.440 | BB | 0.6979 | 1.30901e4 | 266.55930 | 35.6416 |

Totals : 3.67271e4 990.72513

(R)-2-((S)-5-(benzyloxy)-3-methylpentyl)-1-tosylaziridine ((R,S)-**2.126**):

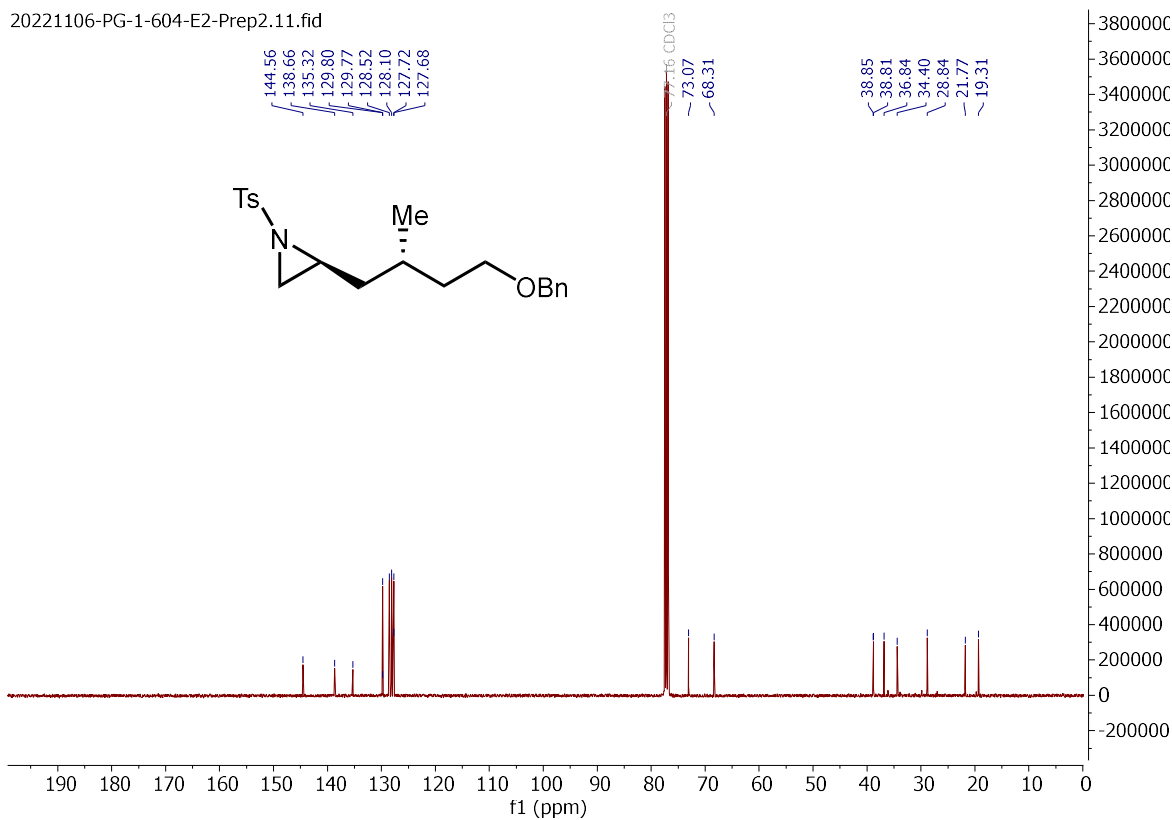
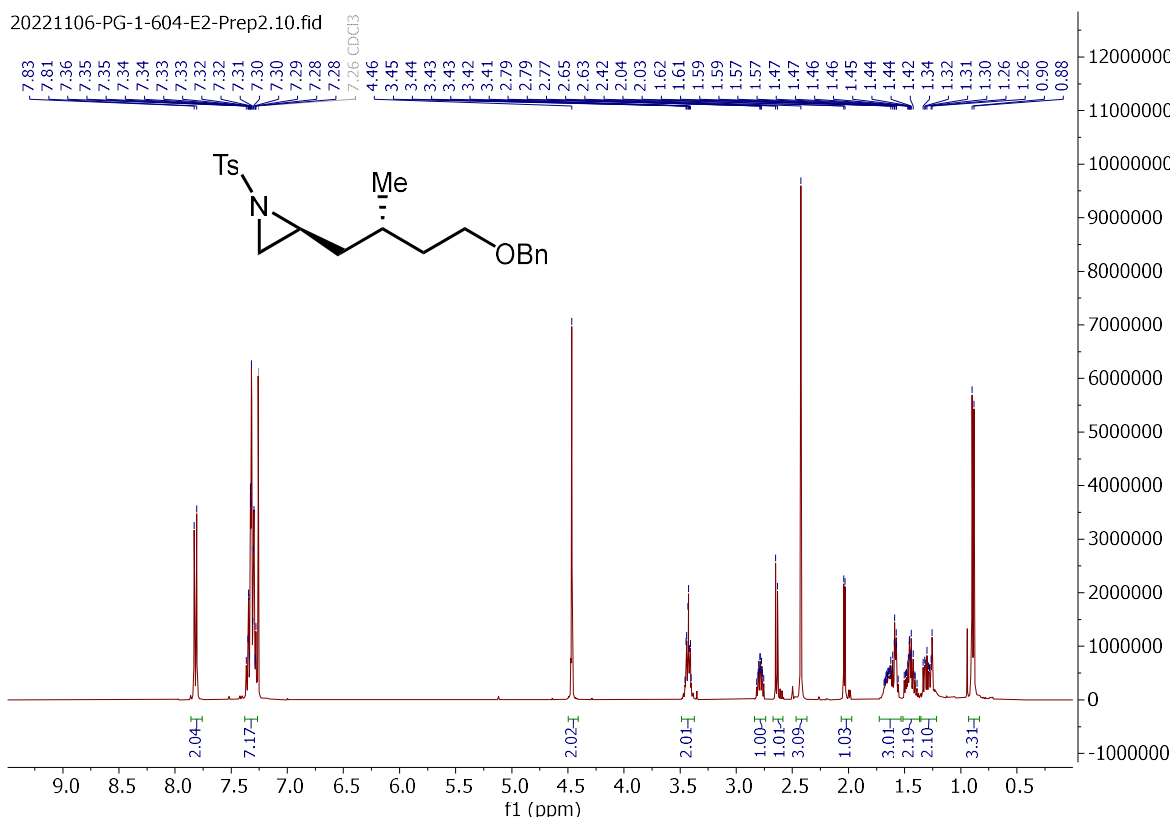


Signal 2: DAD1 B, Sig=210,4 Ref=off

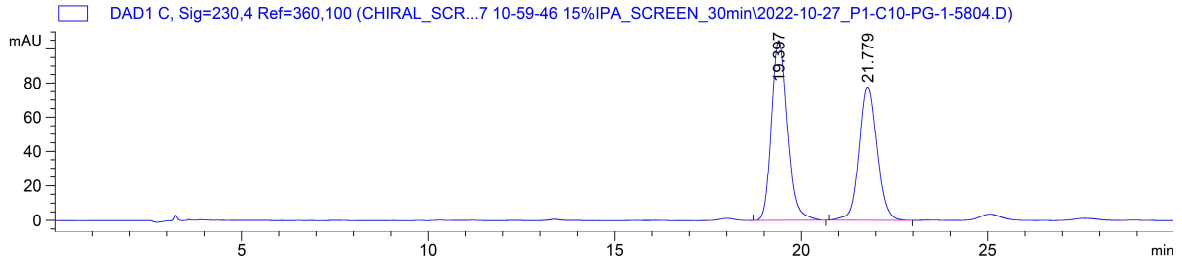
| Peak # | RetTime [min] | Type | Width [min] | Area [mAU*s] | Height [mAU] | Area % |
|--------|---------------|------|-------------|--------------|--------------|---------|
| 1 | 17.292 | BB | 0.3666 | 1346.15967 | 43.55563 | 6.5820 |
| 2 | 19.772 | BB | 0.6237 | 1.91061e4 | 368.32233 | 93.4180 |

Totals : 2.04522e4 411.87796

(S)-2-((S)-4-(benzyloxy)-2-methylbutyl)-1-tosylaziridine ((S,S)-2.127):



2-((S)-4-(benzyloxy)-2-methylbutyl)-1-tosylaziridine (**2.127**):

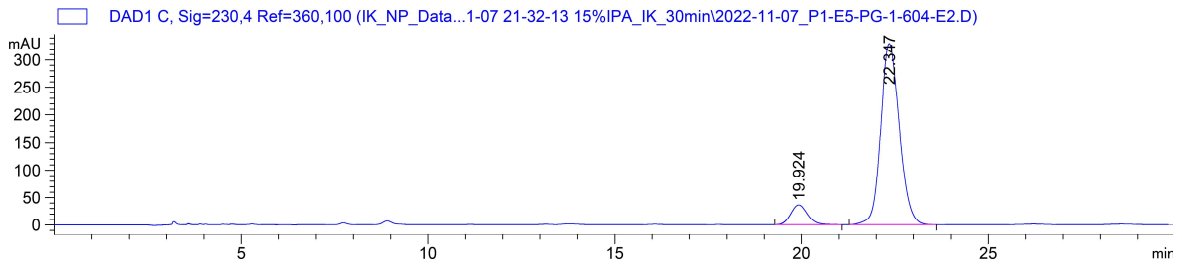


Signal 3: DAD1 C, Sig=230,4 Ref=360,100

| Peak # | RetTime [min] | Type | Width [min] | Area [mAU*s] | Height [mAU] | Area % |
|--------|---------------|------|-------------|--------------|--------------|---------|
| 1 | 19.397 | BB | 0.4214 | 3102.65259 | 104.80980 | 54.5842 |
| 2 | 21.779 | BB | 0.4107 | 2581.50830 | 77.57654 | 45.4158 |

Totals : 5684.16089 182.38634

(S)-2-((S)-4-(benzyloxy)-2-methylbutyl)-1-tosylaziridine ((S,S)-**2.127**):

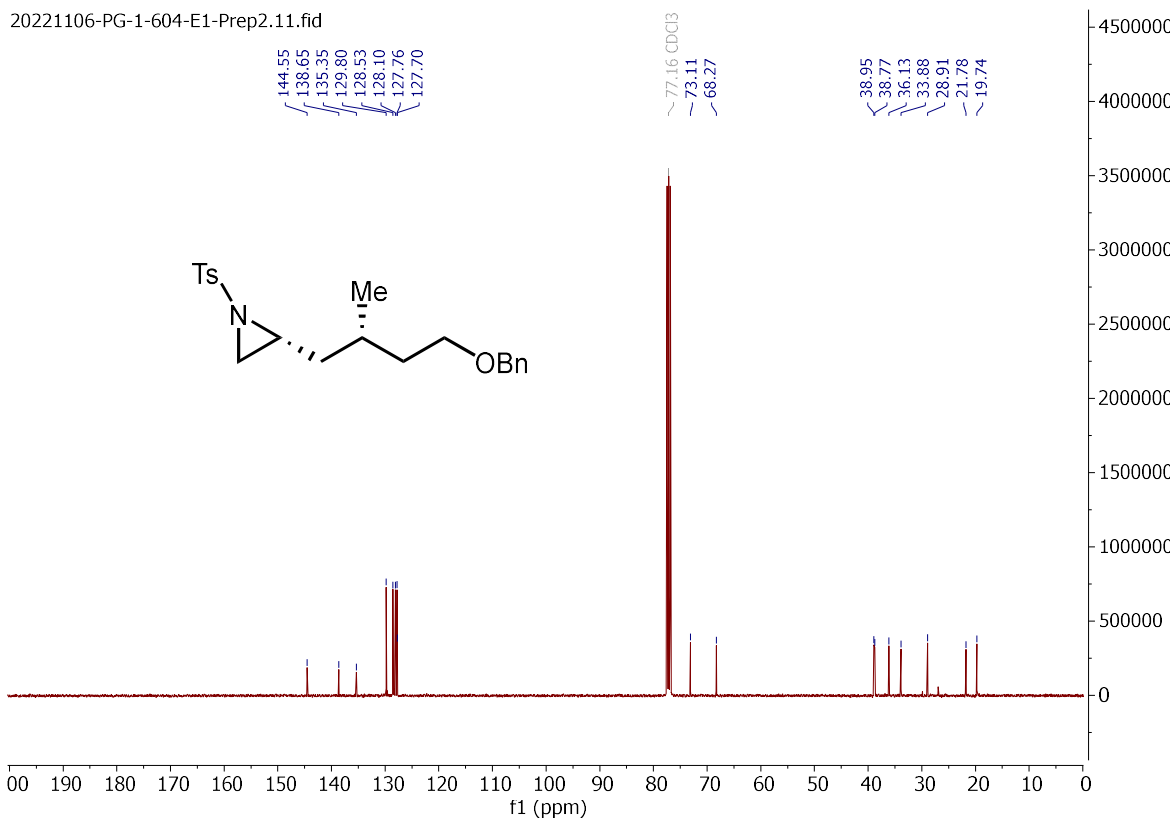
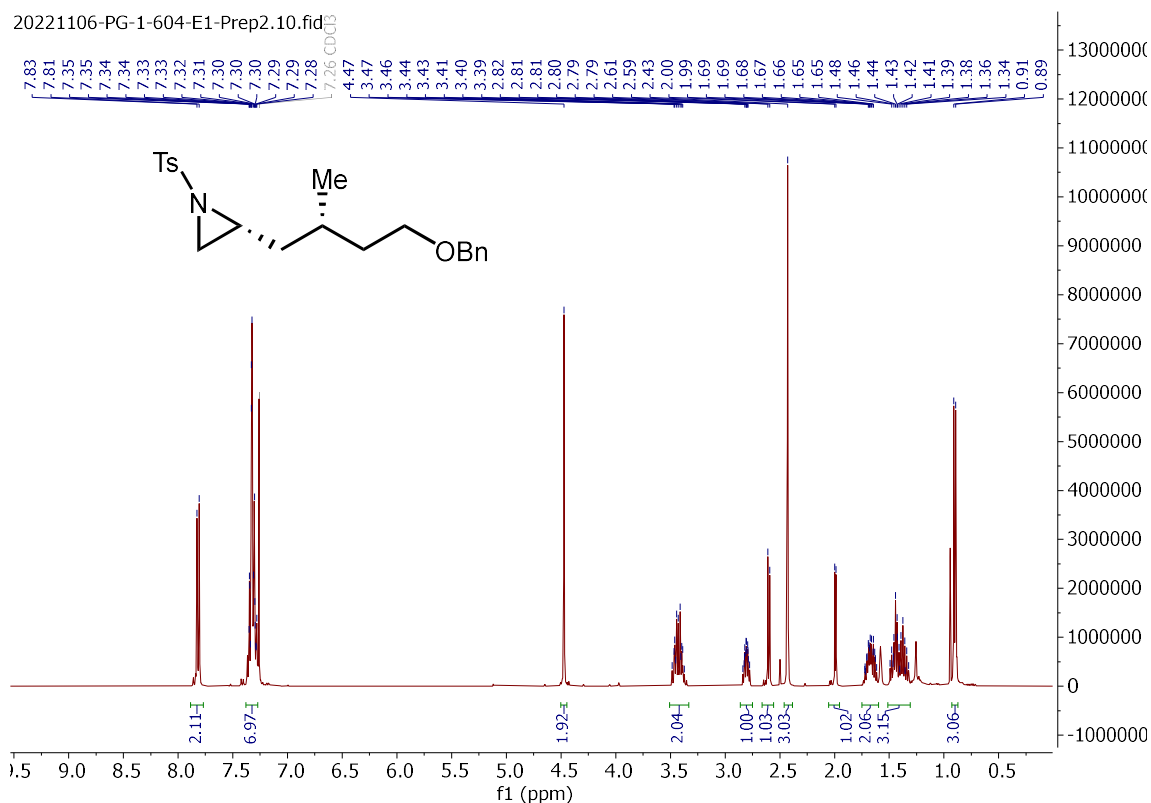


Signal 3: DAD1 C, Sig=230,4 Ref=360,100

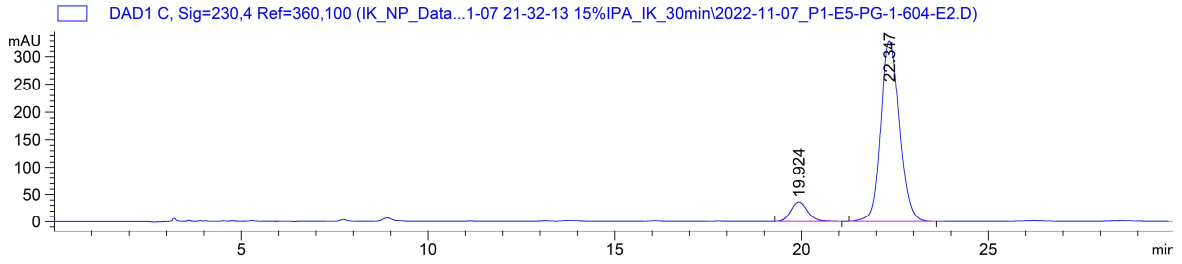
| Peak # | RetTime [min] | Type | Width [min] | Area [mAU*s] | Height [mAU] | Area % |
|--------|---------------|------|-------------|--------------|--------------|---------|
| 1 | 19.924 | BB | 0.3720 | 1128.92102 | 36.03534 | 8.9920 |
| 2 | 22.347 | BB | 0.5147 | 1.14257e4 | 329.39688 | 91.0080 |

Totals : 1.25547e4 365.43222

(R)-2-((S)-4-(benzyloxy)-2-methylbutyl)-1-tosylaziridine ((R,S)-2.127):



2-((S)-4-(benzyloxy)-2-methylbutyl)-1-tosylaziridine (**2.127**):

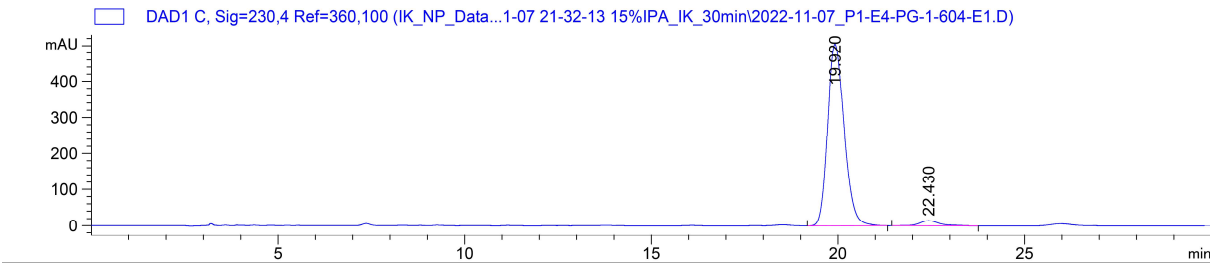


Signal 3: DAD1 C, Sig=230,4 Ref=360,100

| Peak # | RetTime [min] | Type | Width [min] | Area [mAU*s] | Height [mAU] | Area % |
|--------|---------------|------|-------------|--------------|--------------|---------|
| 1 | 19.397 | BB | 0.4214 | 3102.65259 | 104.80980 | 54.5842 |
| 2 | 21.779 | BB | 0.4107 | 2581.50830 | 77.57654 | 45.4158 |

Totals : 5684.16089 182.38634

(R)-2-((S)-4-(benzyloxy)-2-methylbutyl)-1-tosylaziridine ((*R,S*)-**2.127**):

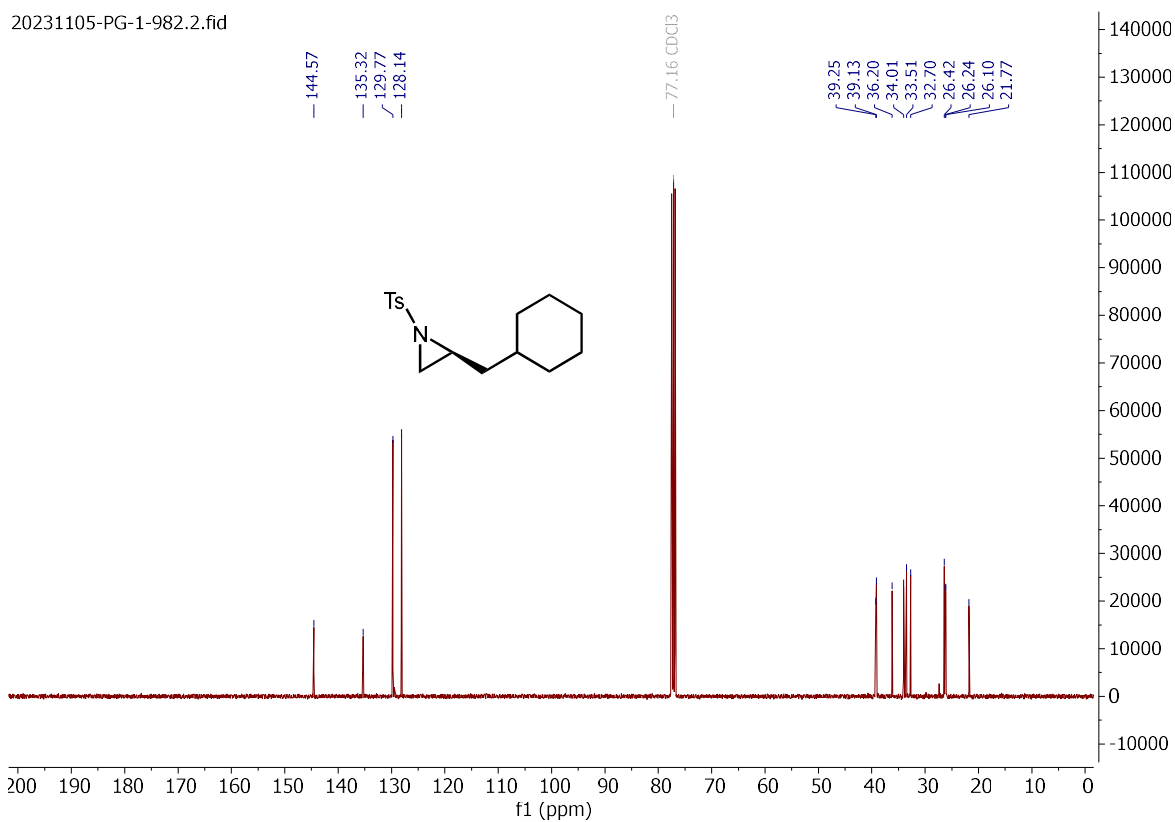
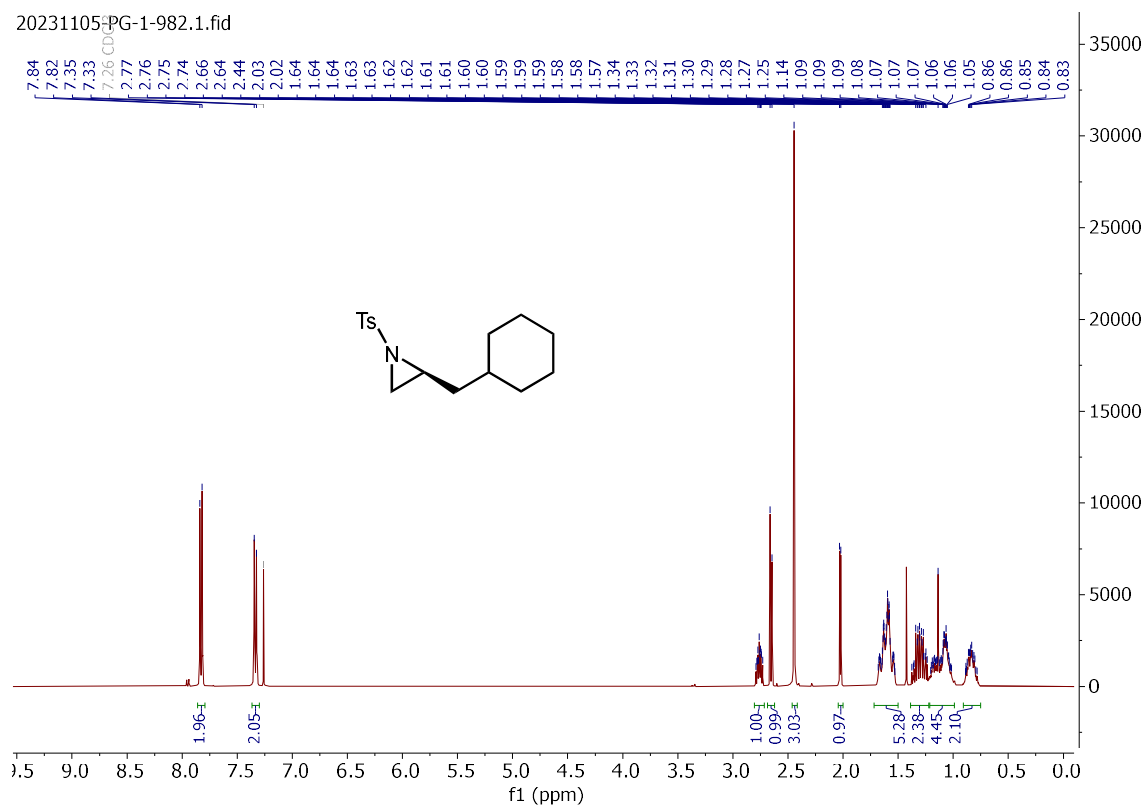


Signal 3: DAD1 C, Sig=230,4 Ref=360,100

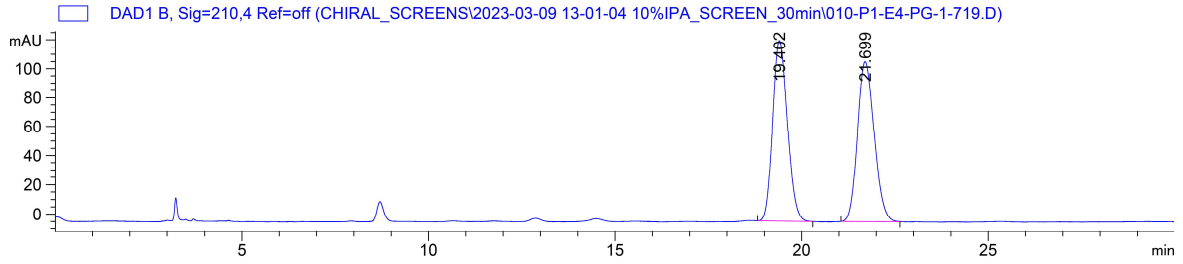
| Peak # | RetTime [min] | Type | Width [min] | Area [mAU*s] | Height [mAU] | Area % |
|--------|---------------|------|-------------|--------------|--------------|---------|
| 1 | 19.920 | BB | 0.4690 | 1.55667e4 | 504.50003 | 96.5241 |
| 2 | 22.430 | BB | 0.4532 | 560.57104 | 14.57487 | 3.4759 |

Totals : 1.61273e4 519.07491

(S)-2-(cyclohexylmethyl)-1-tosylaziridine (**2.128**):



(±)-2-(cyclohexylmethyl)-1-tosylaziridine (±-2.128):

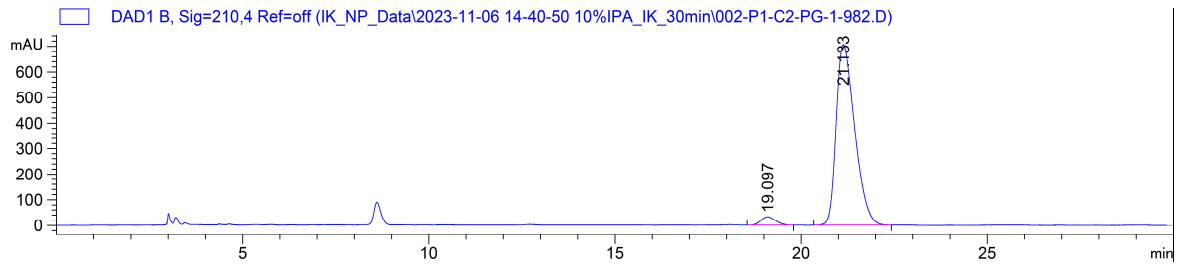


Signal 2: DAD1 B, Sig=210,4 Ref=off

| Peak # | RetTime [min] | Type | Width [min] | Area [mAU*s] | Height [mAU] | Area % |
|--------|---------------|------|-------------|--------------|--------------|---------|
| 1 | 19.402 | BV R | 0.3244 | 3395.34155 | 124.20193 | 49.8847 |
| 2 | 21.699 | BB | 0.3713 | 3411.03735 | 109.99075 | 50.1153 |

Totals : 6806.37891 234.19268

(S)-2-(cyclohexylmethyl)-1-tosylaziridine (2.128):

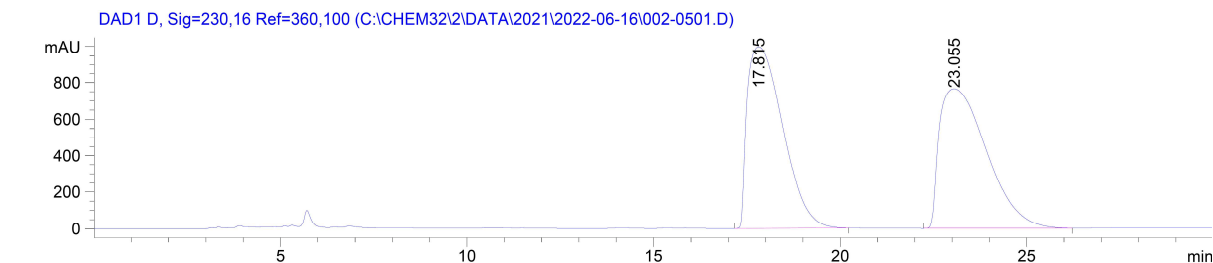


Signal 2: DAD1 B, Sig=210,4 Ref=off

| Peak # | RetTime [min] | Type | Width [min] | Area [mAU*s] | Height [mAU] | Area % |
|--------|---------------|------|-------------|--------------|--------------|---------|
| 1 | 19.097 | BV R | 0.3244 | 904.96912 | 32.84894 | 3.5732 |
| 2 | 21.133 | VB R | 0.4065 | 2.44217e4 | 706.94379 | 96.4268 |

Totals : 2.53267e4 739.79273

(±)-2-cyclohexyl-1-tosylaziridine (±-**2.129**):

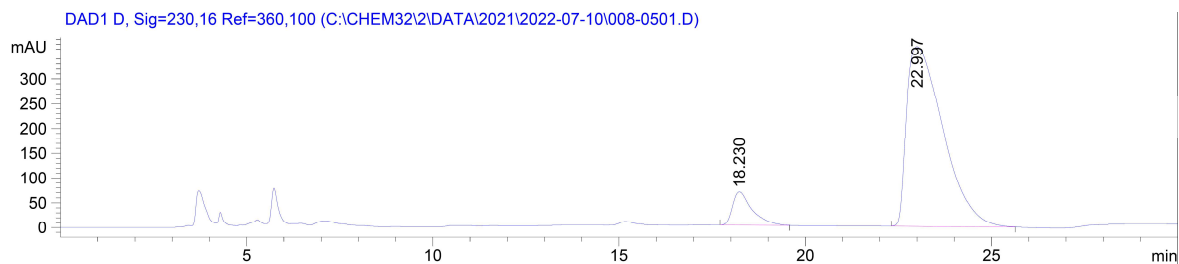


Signal 3: DAD1 D, Sig=230,16 Ref=360,100

| Peak # | RetTime [min] | Type | Width [min] | Area [mAU*s] | Height [mAU] | Area % |
|--------|---------------|------|-------------|--------------|--------------|---------|
| 1 | 17.815 | BB | 1.0732 | 6.60348e4 | 996.37714 | 49.4721 |
| 2 | 23.055 | BB | 1.4127 | 6.74440e4 | 764.86414 | 50.5279 |

Totals : 1.33479e5 1761.24127

(S)-2-cyclohexyl-1-tosylaziridine (**2.129**):

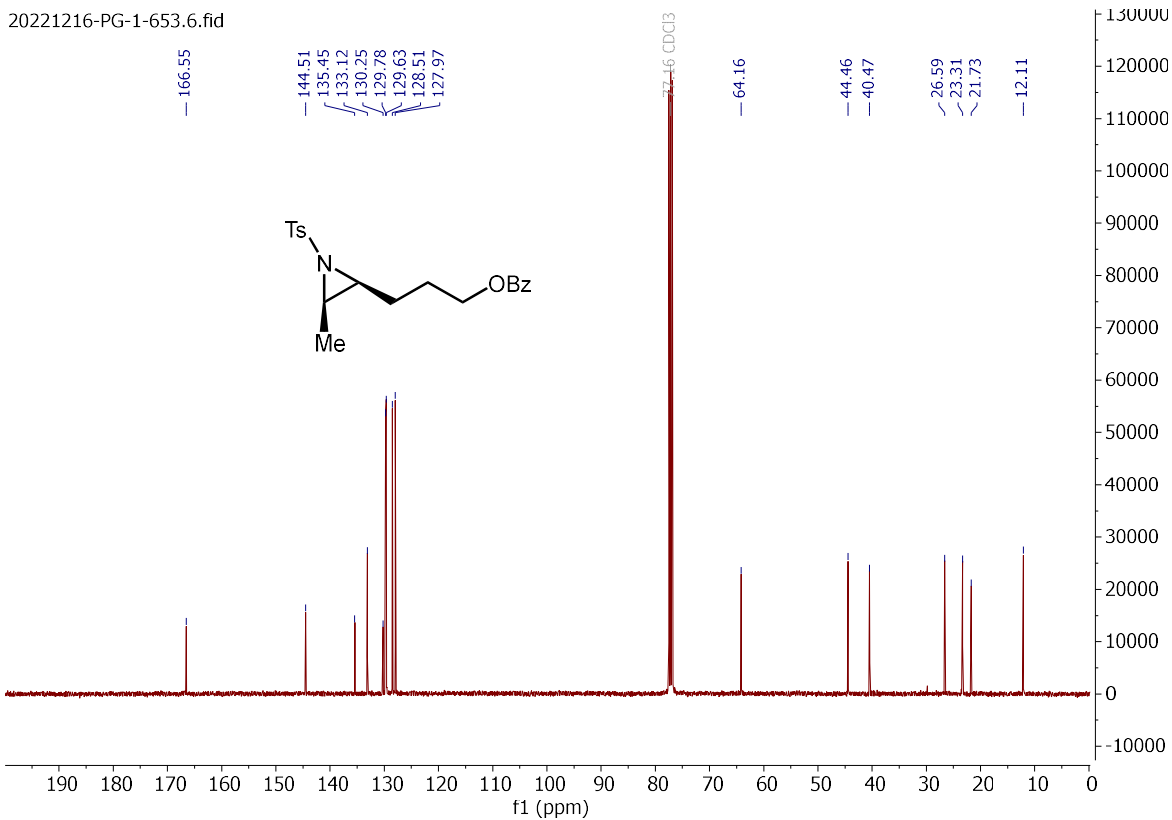
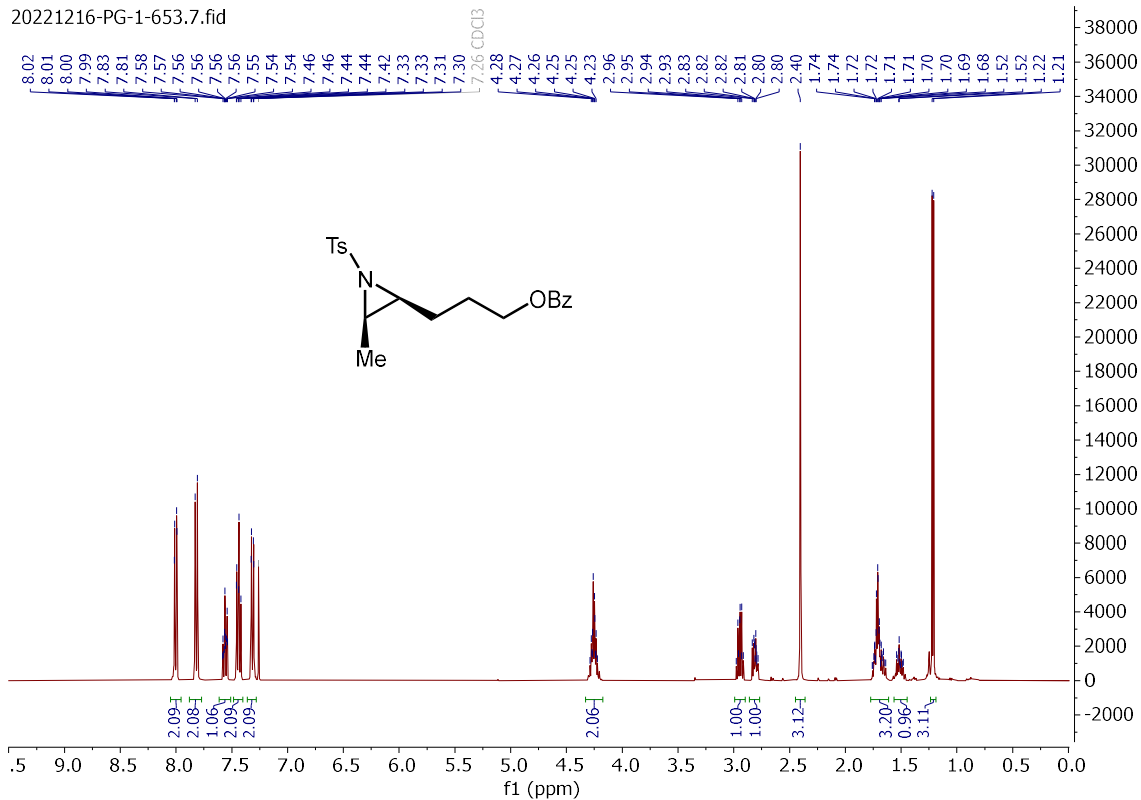


Signal 3: DAD1 D, Sig=230,16 Ref=360,100

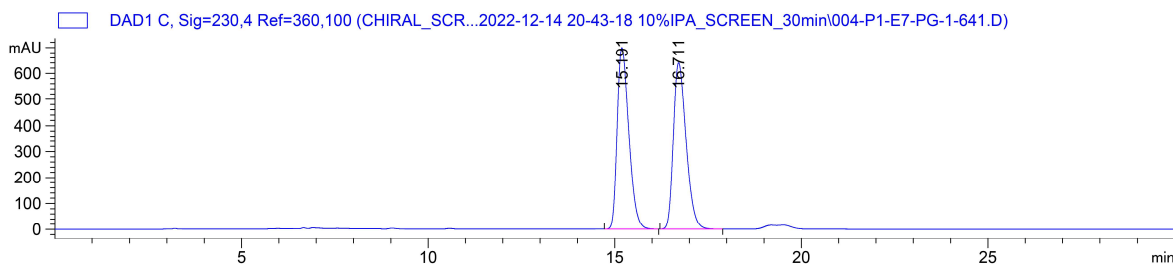
| Peak # | RetTime [min] | Type | Width [min] | Area [mAU*s] | Height [mAU] | Area % |
|--------|---------------|------|-------------|--------------|--------------|---------|
| 1 | 18.230 | BB | 0.5442 | 2477.47339 | 67.18789 | 9.0861 |
| 2 | 22.997 | BB | 1.0859 | 2.47891e4 | 363.38428 | 90.9139 |

Totals : 2.72666e4 430.57217

3-((2S,3R)-3-methyl-1-tosylaziridin-2-yl)propyl benzoate (**2.130**):



3-(3-methyl-1-tosylaziridin-2-yl)propyl benzoate (**2.130**):

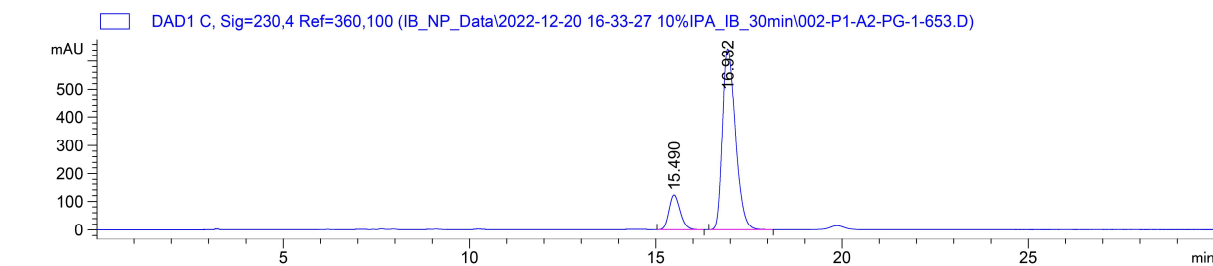


Signal 3: DAD1 C, Sig=230,4 Ref=360,100

| Peak # | RetTime [min] | Type | Width [min] | Area [mAU*s] | Height [mAU] | Area % |
|--------|---------------|------|-------------|--------------|--------------|---------|
| 1 | 15.191 | BB | 0.3271 | 1.51322e4 | 698.88940 | 49.9512 |
| 2 | 16.711 | BB | 0.3551 | 1.51618e4 | 639.47821 | 50.0488 |

Totals : 3.02939e4 1338.36761

3-((2S,3R)-3-methyl-1-tosylaziridin-2-yl)propyl benzoate (**2.130**):

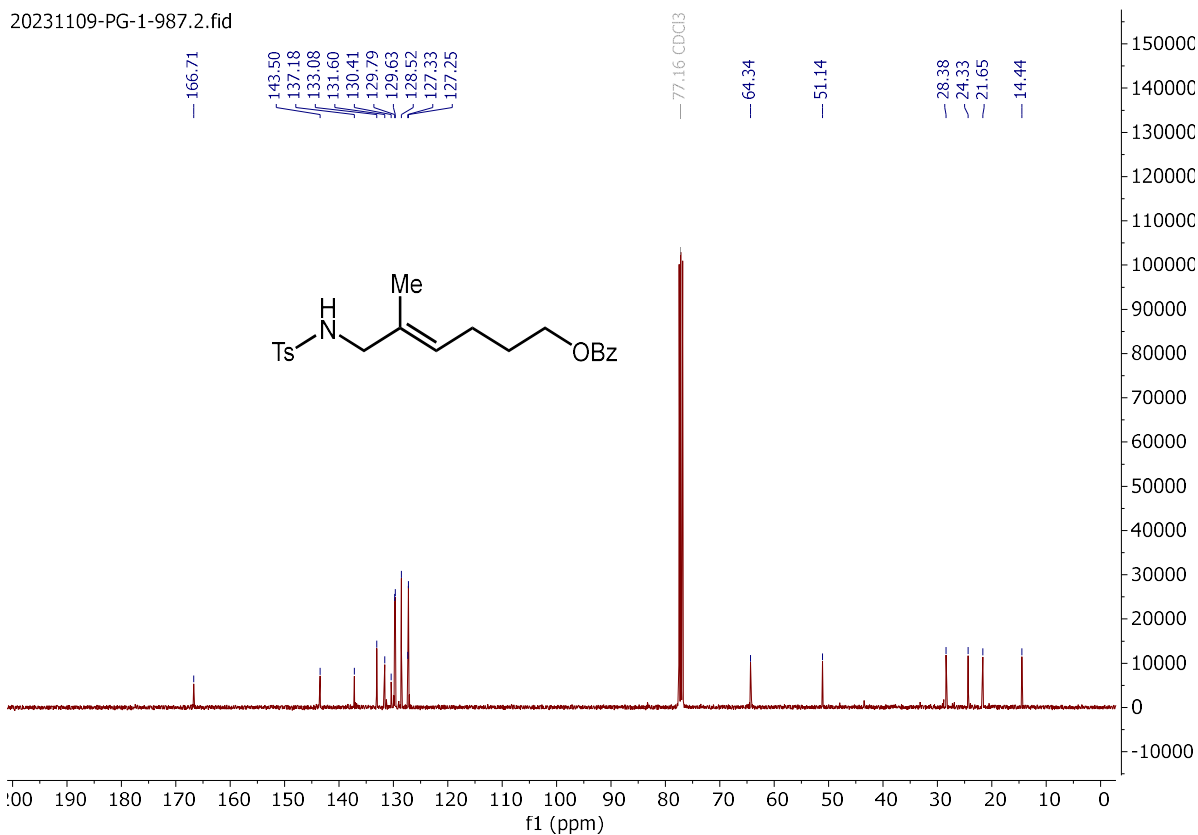
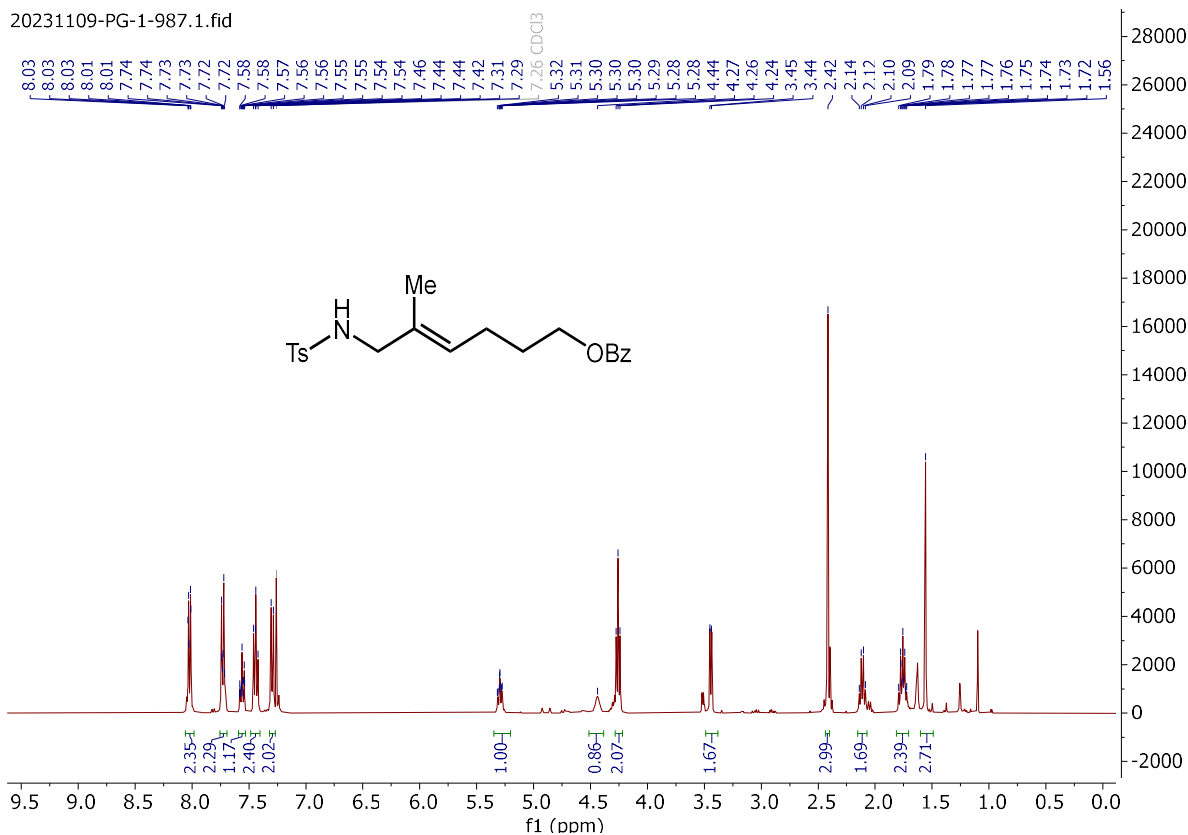


Signal 3: DAD1 C, Sig=230,4 Ref=360,100

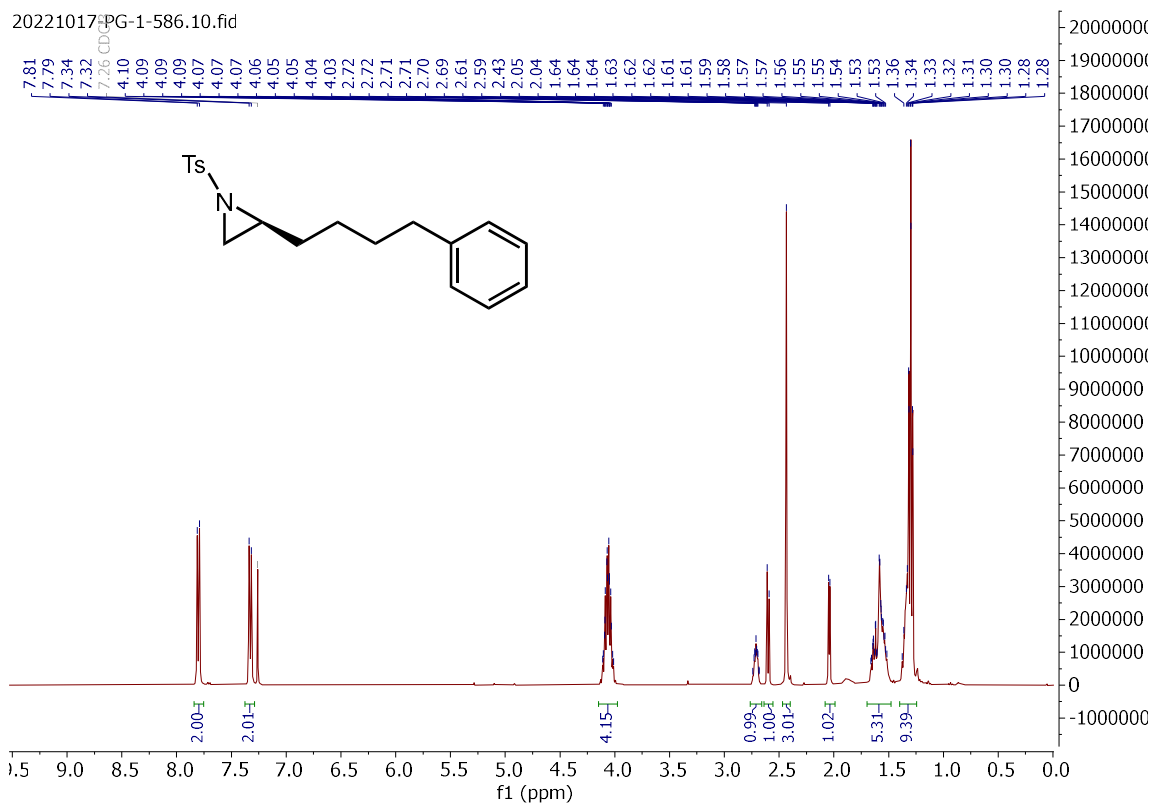
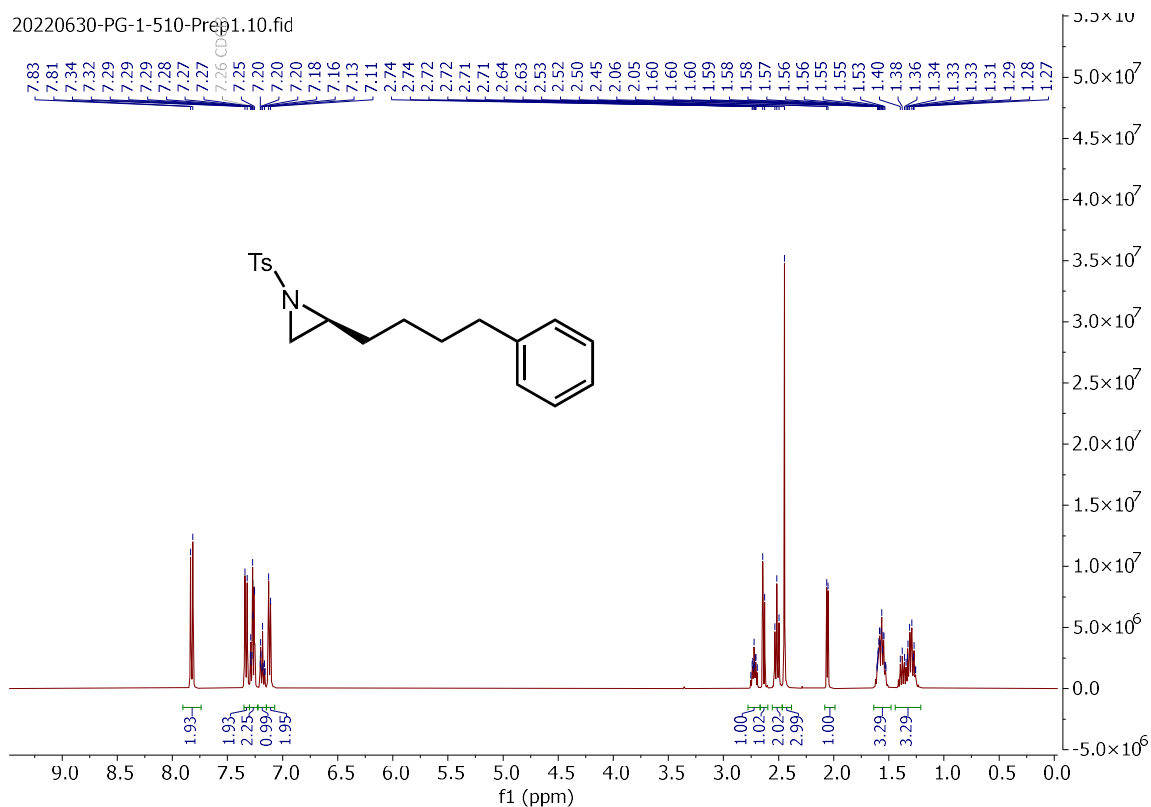
| Peak # | RetTime [min] | Type | Width [min] | Area [mAU*s] | Height [mAU] | Area % |
|--------|---------------|------|-------------|--------------|--------------|---------|
| 1 | 15.490 | BB | 0.3032 | 2553.55298 | 121.48096 | 14.1081 |
| 2 | 16.932 | BB | 0.3674 | 1.55464e4 | 643.39404 | 85.8919 |

Totals : 1.80999e4 764.87500

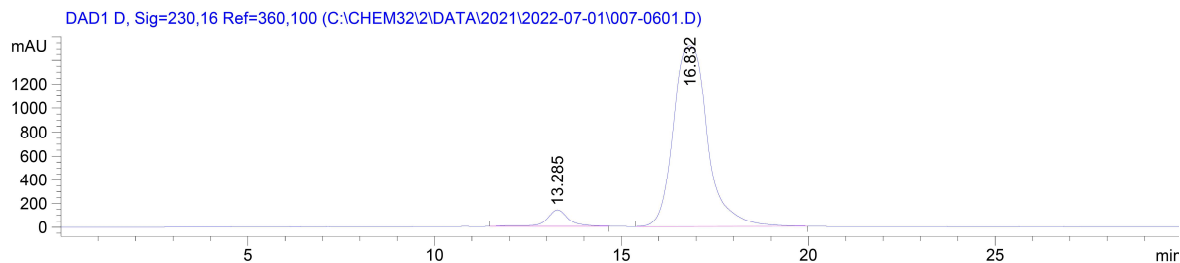
5-methyl-6-((4-methylphenyl)sulfonamido)hex-4-en-1-yl benzoate (2.132):



(S)-2-(4-phenylbutyl)-1-tosylaziridine (**2.133**):



(±)-2-(4-phenylbutyl)-1-tosylaziridine (±-2.133):

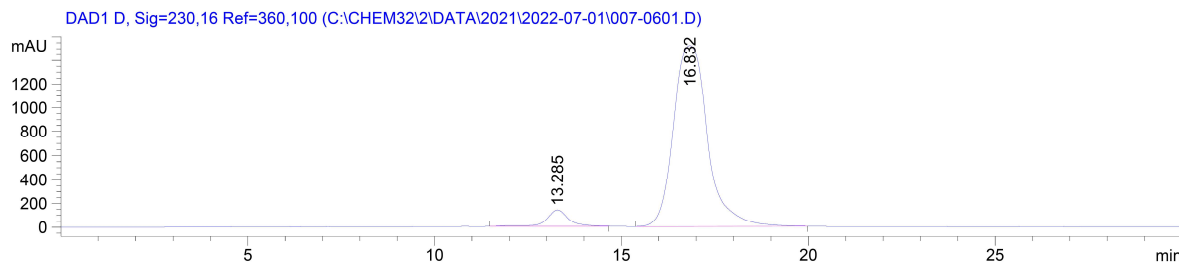


Signal 3: DAD1 D, Sig=230,16 Ref=360,100

| Peak # | RetTime [min] | Type | Width [min] | Area [mAU*s] | Height [mAU] | Area % |
|--------|---------------|------|-------------|--------------|--------------|---------|
| 1 | 12.921 | BB | 0.6441 | 4.17986e4 | 978.96667 | 50.1762 |
| 2 | 16.373 | BB | 0.7983 | 4.15050e4 | 793.39551 | 49.8238 |

Totals : 8.33036e4 1772.36218

(S)-2-(4-phenylbutyl)-1-tosylaziridine (2.133):

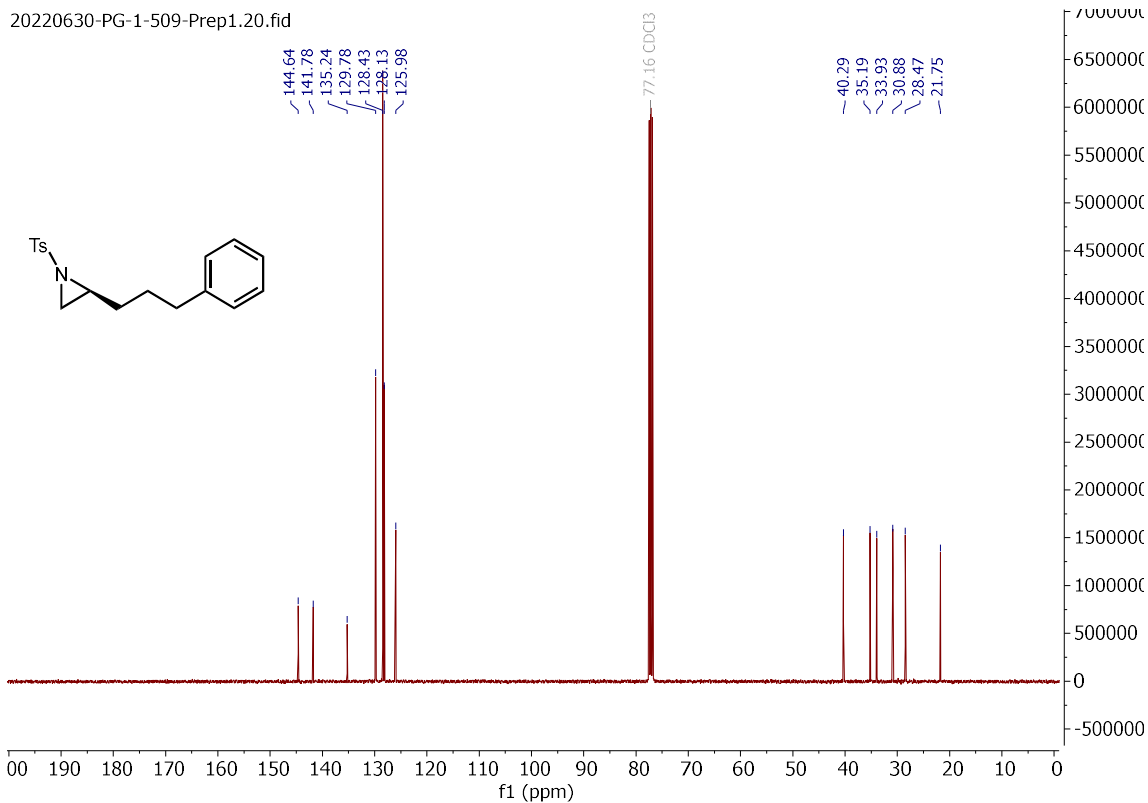
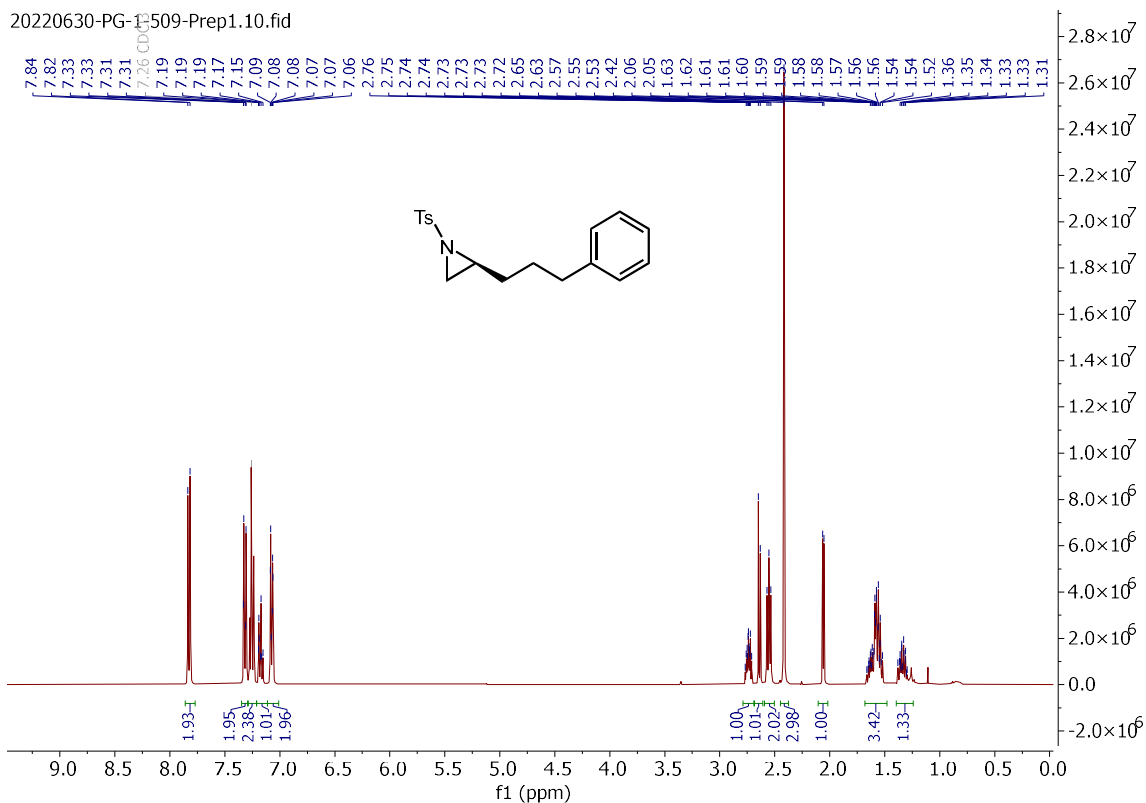


Signal 3: DAD1 D, Sig=230,16 Ref=360,100

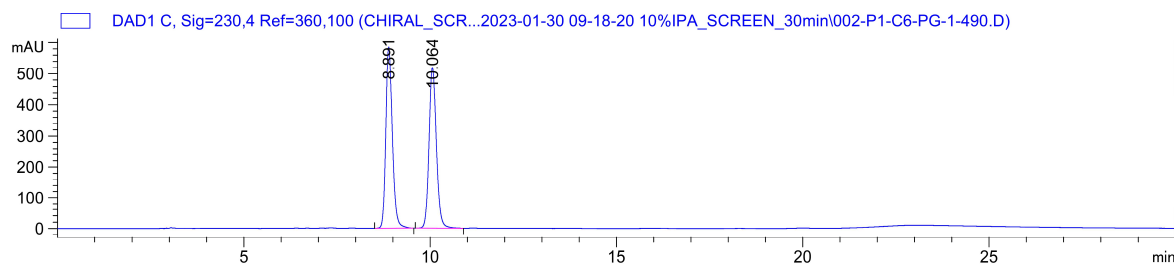
| Peak # | RetTime [min] | Type | Width [min] | Area [mAU*s] | Height [mAU] | Area % |
|--------|---------------|------|-------------|--------------|--------------|---------|
| 1 | 13.285 | BB | 0.6062 | 5664.38184 | 138.18881 | 5.5709 |
| 2 | 16.832 | BB | 0.9873 | 9.60131e4 | 1519.34229 | 94.4291 |

Totals : 1.01677e5 1657.53110

(S)-2-(3-phenylpropyl)-1-tosylaziridine (**2.134**):



(±)-2-(3-phenylpropyl)-1-tosylaziridine (**2.134**):

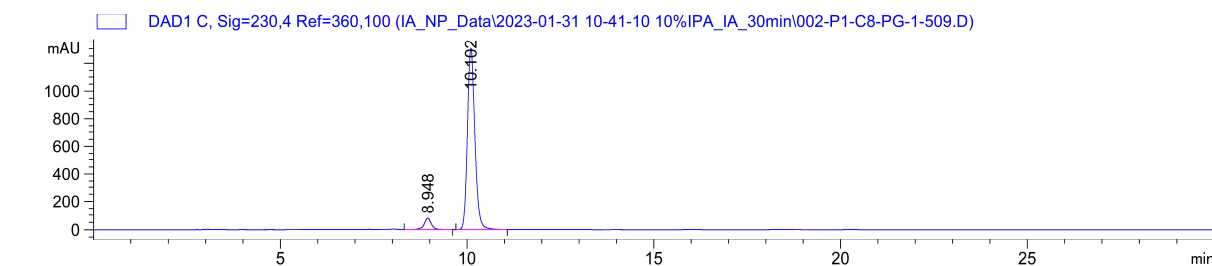


Signal 3: DAD1 C, Sig=230,4 Ref=360,100

| Peak # | RetTime [min] | Type | Width [min] | Area [mAU*s] | Height [mAU] | Area % |
|--------|---------------|------|-------------|--------------|--------------|---------|
| 1 | 8.891 | BB | 0.1872 | 7120.35449 | 584.38434 | 50.0245 |
| 2 | 10.064 | BB | 0.2102 | 7113.39063 | 519.70685 | 49.9755 |

Totals : 1.42337e4 1104.09119

(S)-2-(3-phenylpropyl)-1-tosylaziridine (**2.134**):

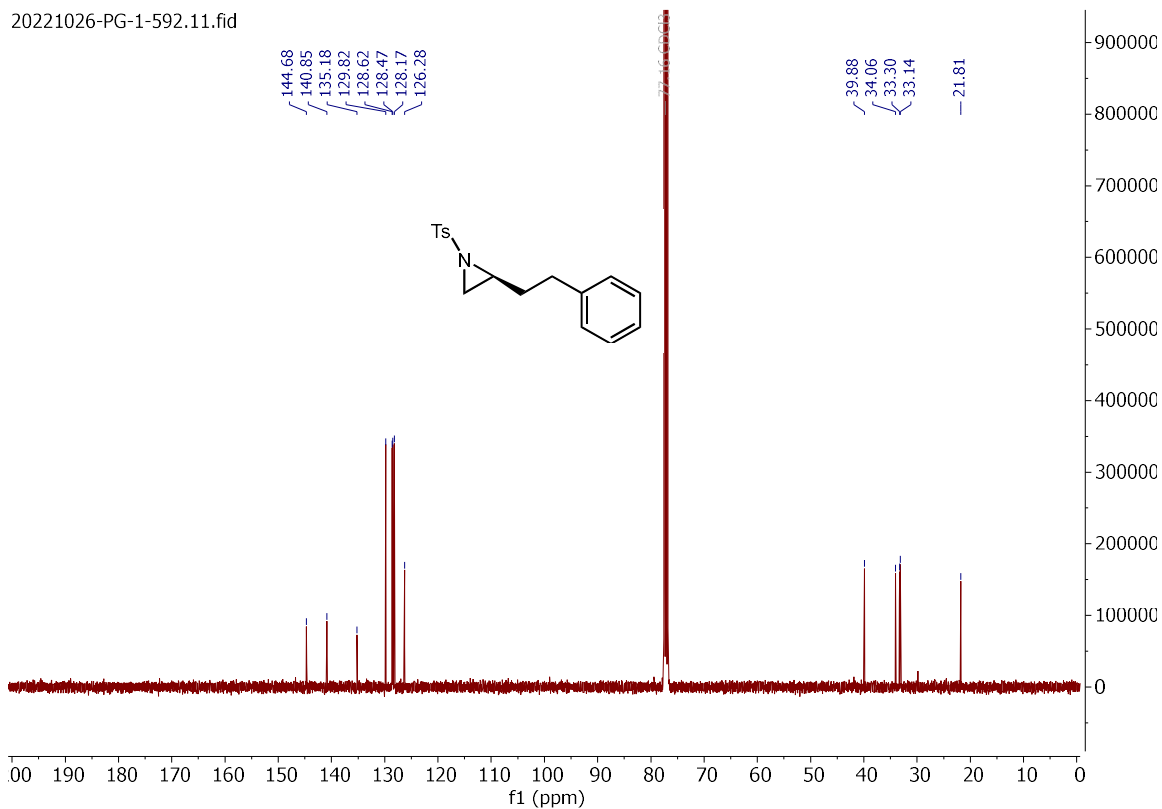
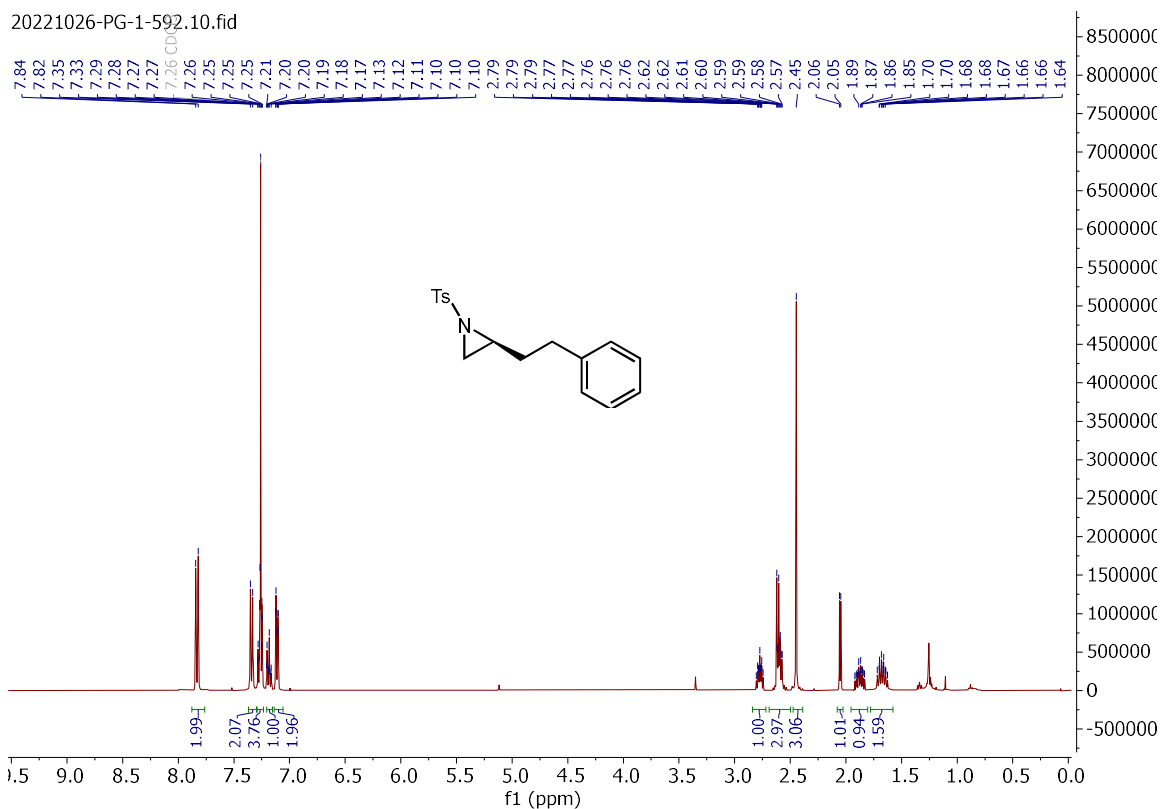


Signal 3: DAD1 C, Sig=230,4 Ref=360,100

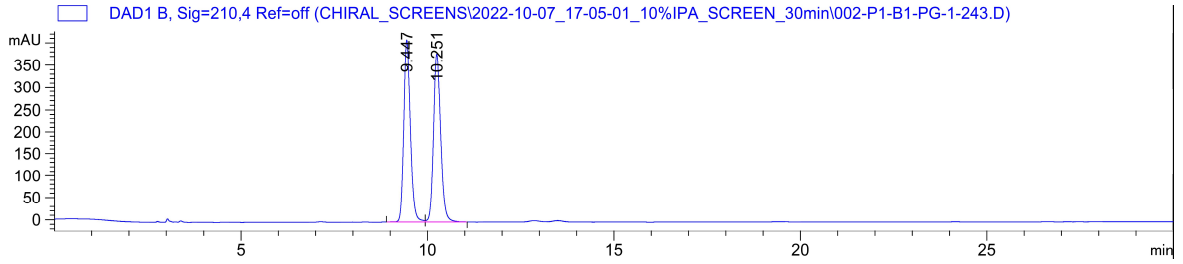
| Peak # | RetTime [min] | Type | Width [min] | Area [mAU*s] | Height [mAU] | Area % |
|--------|---------------|------|-------------|--------------|--------------|---------|
| 1 | 8.948 | BB | 0.2027 | 1072.08289 | 78.33858 | 5.6308 |
| 2 | 10.102 | BB | 0.2135 | 1.79675e4 | 1302.09705 | 94.3692 |

Totals : 1.90396e4 1380.43562

(S)-2-phenethyl-1-tosylaziridine (**2.135**):



2-phenethyl-1-tosylaziridine (\pm -2.135):

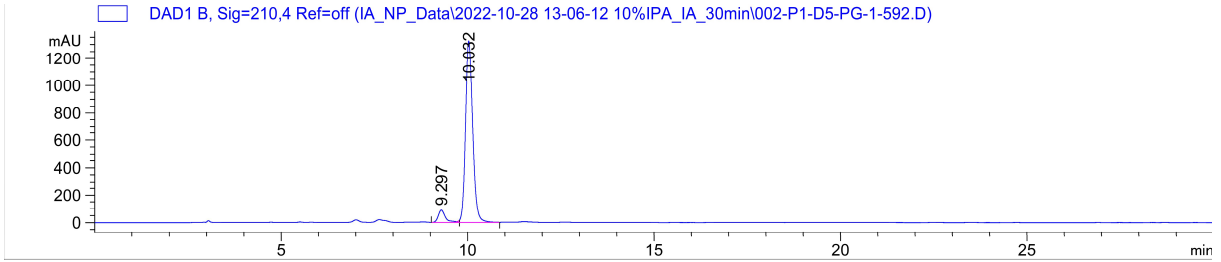


Signal 2: DAD1 B, Sig=210,4 Ref=off

| Peak # | RetTime [min] | Type | Width [min] | Area [mAU*s] | Height [mAU] | Area % |
|--------|---------------|------|-------------|--------------|--------------|---------|
| 1 | 9.447 | BV | 0.1882 | 5075.66797 | 411.93863 | 49.9091 |
| 2 | 10.251 | VB | 0.2043 | 5094.16162 | 380.34274 | 50.0909 |

Totals : 1.01698e4 792.28137

(S)-2-phenethyl-1-tosylaziridine ((S)-2.135):



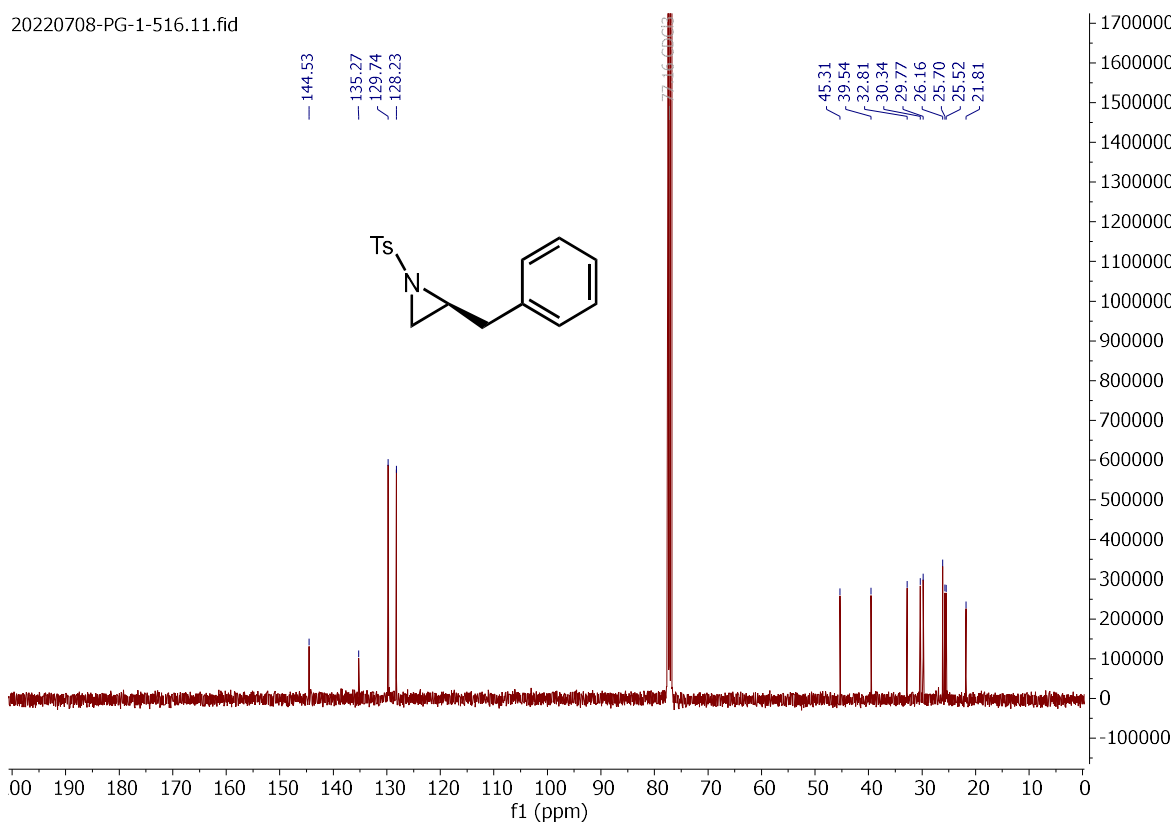
Signal 2: DAD1 B, Sig=210,4 Ref=off

| Peak # | RetTime [min] | Type | Width [min] | Area [mAU*s] | Height [mAU] | Area % |
|--------|---------------|------|-------------|--------------|--------------|---------|
| 1 | 9.297 | BV E | 0.1966 | 1147.87354 | 86.88118 | 6.1119 |
| 2 | 10.032 | VB R | 0.2040 | 1.76330e4 | 1323.14551 | 93.8881 |

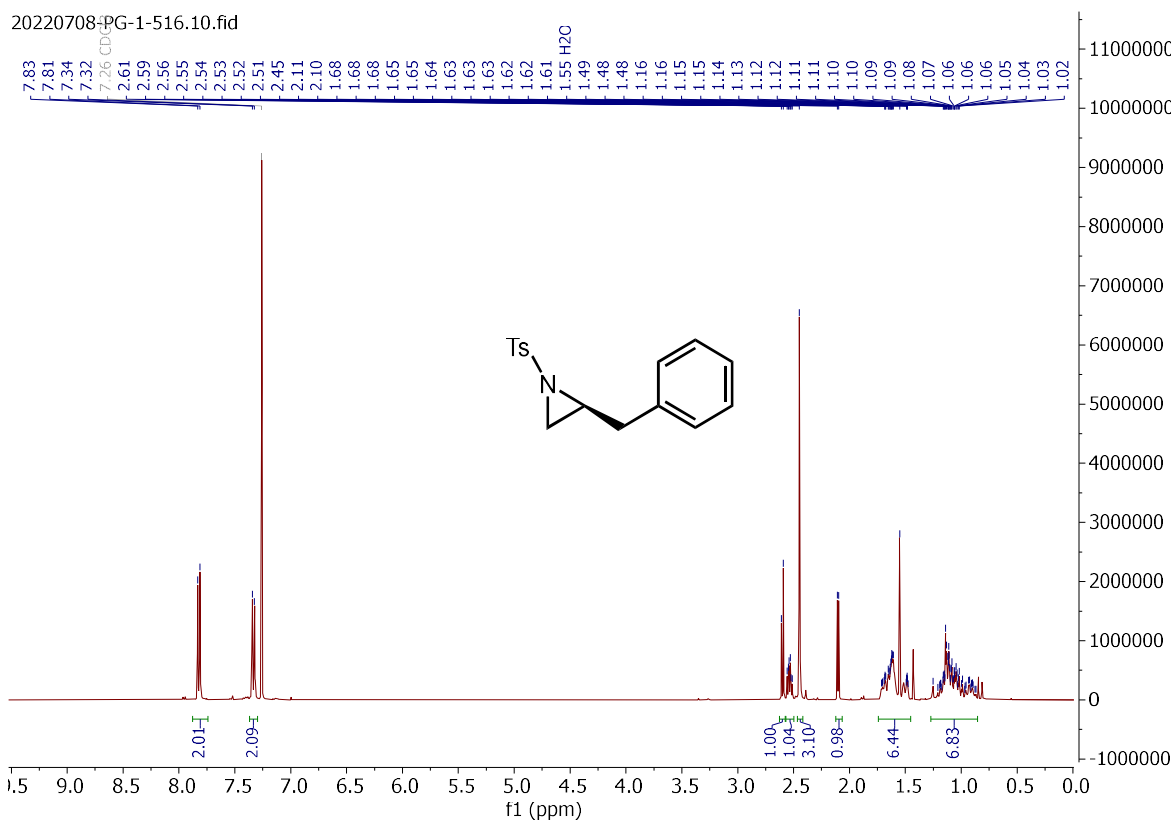
Totals : 1.87809e4 1410.02669

(S)-2-benzyl-1-tosylaziridine (**2.136**):

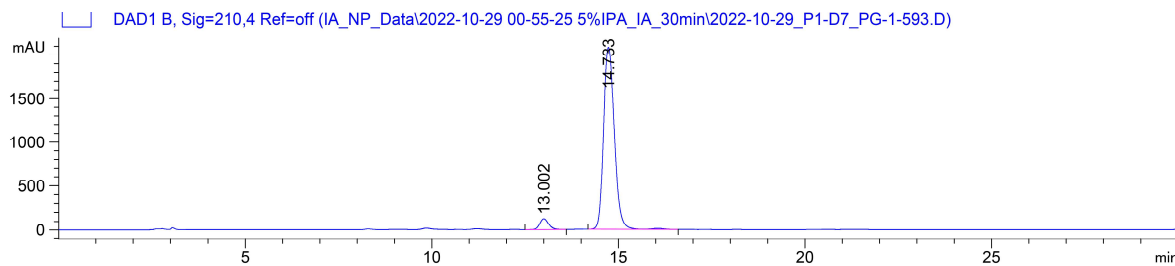
20220708-PG-1-516.11.fid



20220708-PG-1-516.10.fid



(±)-2-benzyl-1-tosylaziridine (±-2.136):

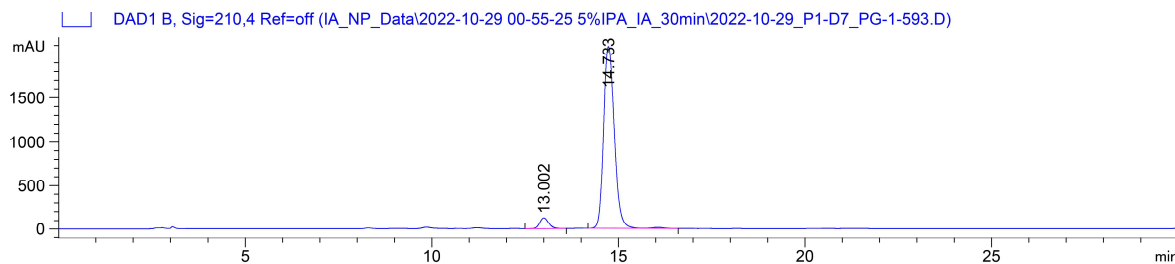


Signal 2: DAD1 B, Sig=210,4 Ref=off

| Peak # | RetTime [min] | Type | Width [min] | Area [mAU*s] | Height [mAU] | Area % |
|--------|---------------|------|-------------|--------------|--------------|---------|
| 1 | 13.002 | BB | 0.2471 | 2112.04272 | 127.29562 | 4.8152 |
| 2 | 14.733 | BV R | 0.2419 | 4.17496e4 | 2081.45728 | 95.1848 |

Totals : 4.38617e4 2208.75290

(S)-2-benzyl-1-tosylaziridine (2.136):

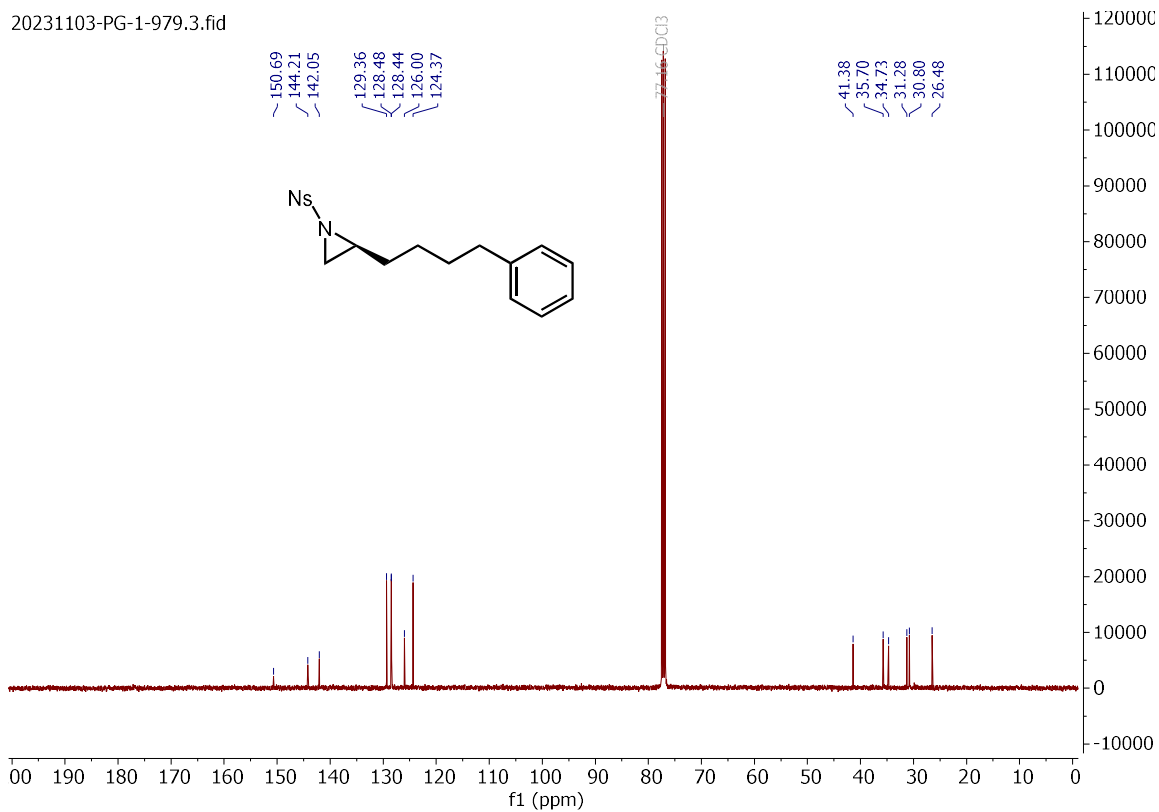
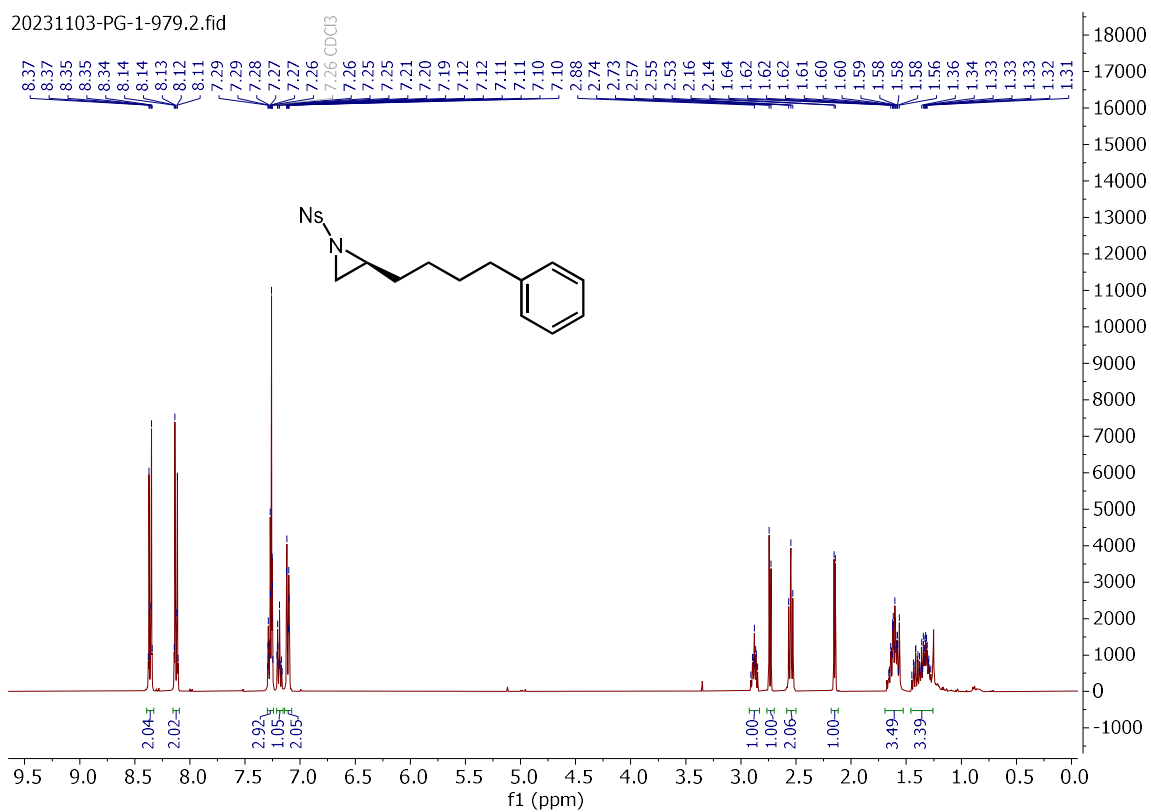


Signal 2: DAD1 B, Sig=210,4 Ref=off

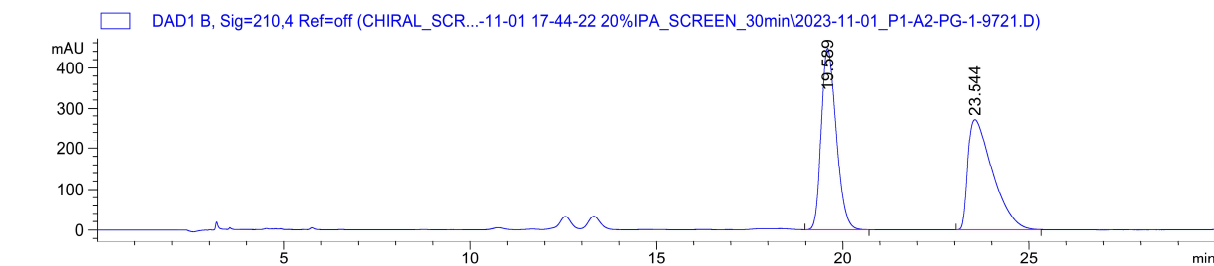
| Peak # | RetTime [min] | Type | Width [min] | Area [mAU*s] | Height [mAU] | Area % |
|--------|---------------|------|-------------|--------------|--------------|---------|
| 1 | 13.002 | BB | 0.2471 | 2112.04272 | 127.29562 | 4.8152 |
| 2 | 14.733 | BV R | 0.2419 | 4.17496e4 | 2081.45728 | 95.1848 |

Totals : 4.38617e4 2208.75290

(S)-1-((4-nitrophenyl)sulfonyl)-2-(4-phenylbutyl)aziridine (**2.137**):



(±)-1-((4-nitrophenyl)sulfonyl)-2-(4-phenylbutyl)aziridine (±-2.137):

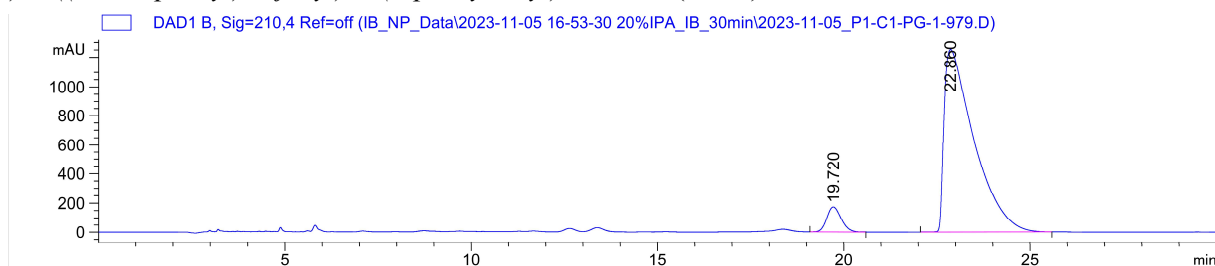


Signal 2: DAD1 B, Sig=210,4 Ref=off

| Peak # | RetTime [min] | Type | Width [min] | Area [mAU*s] | Height [mAU] | Area % |
|--------|---------------|------|-------------|--------------|--------------|---------|
| 1 | 19.589 | BB | 0.3499 | 1.24868e4 | 446.29572 | 49.9748 |
| 2 | 23.544 | BV R | 0.5451 | 1.24993e4 | 270.50516 | 50.0252 |

Totals : 2.49861e4 716.80087

(S)-1-((4-nitrophenyl)sulfonyl)-2-(4-phenylbutyl)aziridine (2.137):

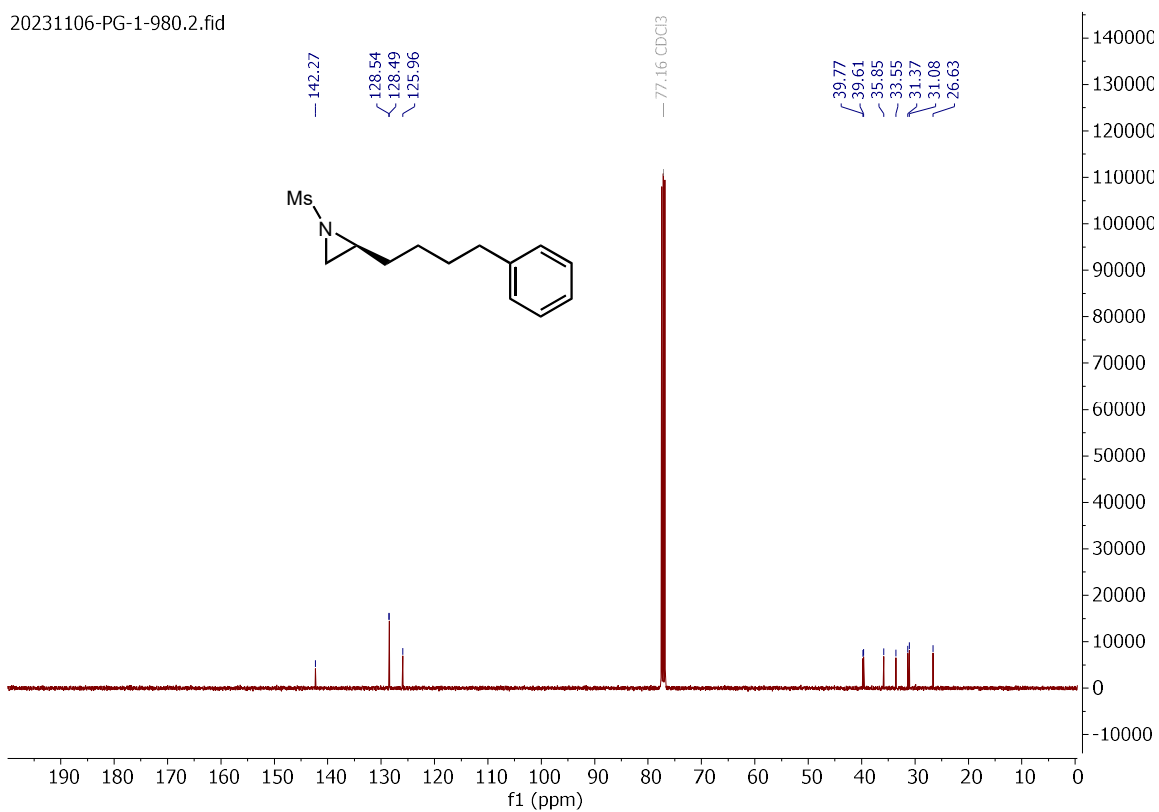
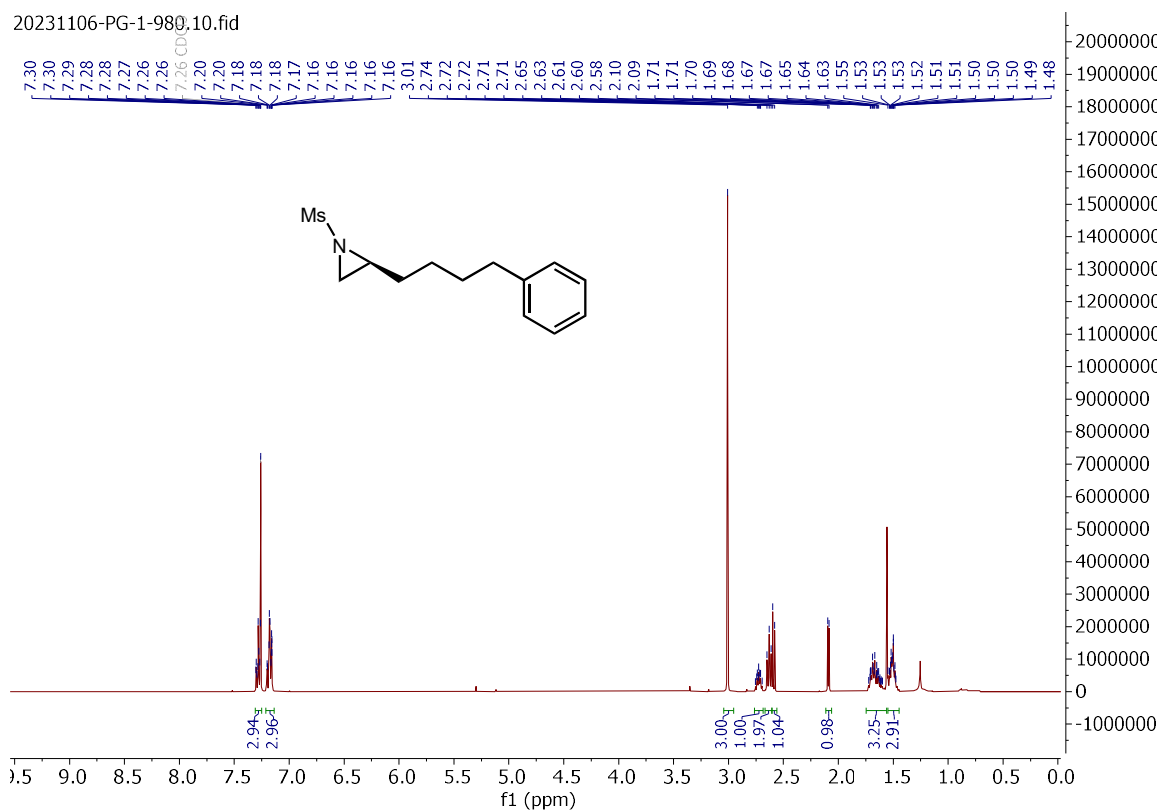


Signal 2: DAD1 B, Sig=210,4 Ref=off

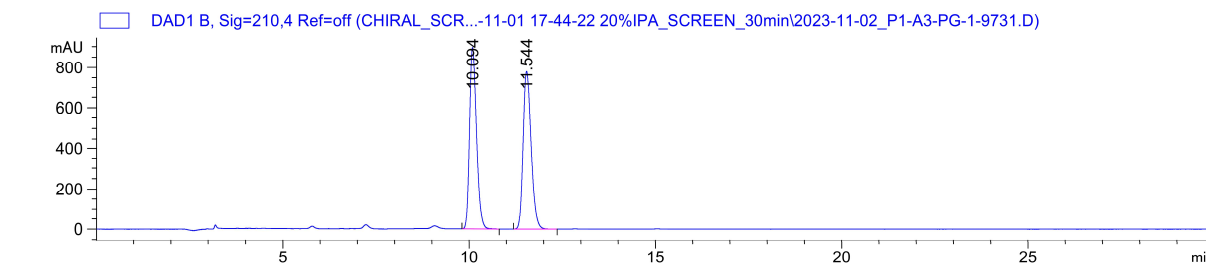
| Peak # | RetTime [min] | Type | Width [min] | Area [mAU*s] | Height [mAU] | Area % |
|--------|---------------|------|-------------|--------------|--------------|---------|
| 1 | 19.720 | VV R | 0.3241 | 4633.23389 | 171.83258 | 6.2234 |
| 2 | 22.860 | VV R | 0.6527 | 6.98153e4 | 1251.65906 | 93.7766 |

Totals : 7.44485e4 1423.49164

(S)-1-(methylsulfonyl)-2-(4-phenylbutyl)aziridine (**2.138**):



(±)-1-(methylsulfonyl)-2-(4-phenylbutyl)aziridine (±-2.138):

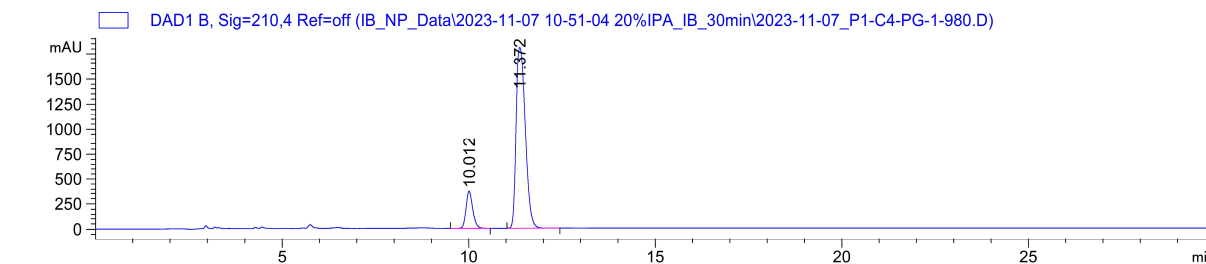


Signal 2: DAD1 B, Sig=210,4 Ref=off

| Peak # | RetTime [min] | Type | Width [min] | Area [mAU*s] | Height [mAU] | Area % |
|--------|---------------|------|-------------|--------------|--------------|---------|
| 1 | 10.094 | BB | 0.1957 | 1.16009e4 | 894.92395 | 49.9585 |
| 2 | 11.544 | VV R | 0.2199 | 1.16202e4 | 779.35724 | 50.0415 |

Totals : 2.32211e4 1674.28119

(S)-1-(methylsulfonyl)-2-(4-phenylbutyl)aziridine (2.138):

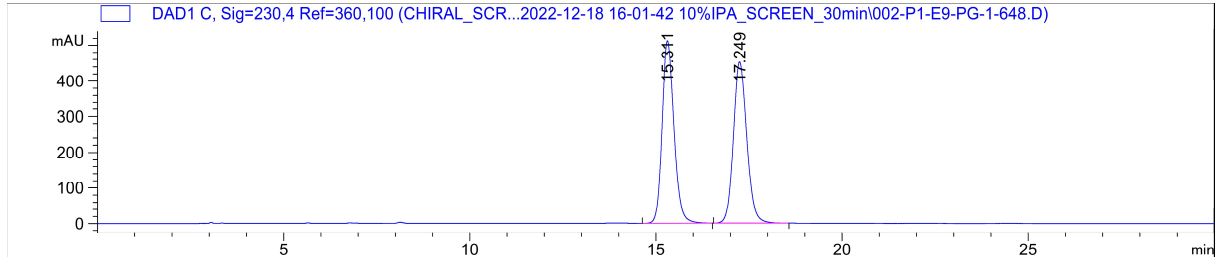


Signal 2: DAD1 B, Sig=210,4 Ref=off

| Peak # | RetTime [min] | Type | Width [min] | Area [mAU*s] | Height [mAU] | Area % |
|--------|---------------|------|-------------|--------------|--------------|---------|
| 1 | 10.012 | BB | 0.1892 | 4505.58838 | 361.92816 | 12.7795 |
| 2 | 11.372 | BB | 0.2437 | 3.07507e4 | 1805.56567 | 87.2205 |

Totals : 3.52563e4 2167.49384

(±)-4-(1-tosylaziridin-2-yl)butyl benzoate (±-2.139):

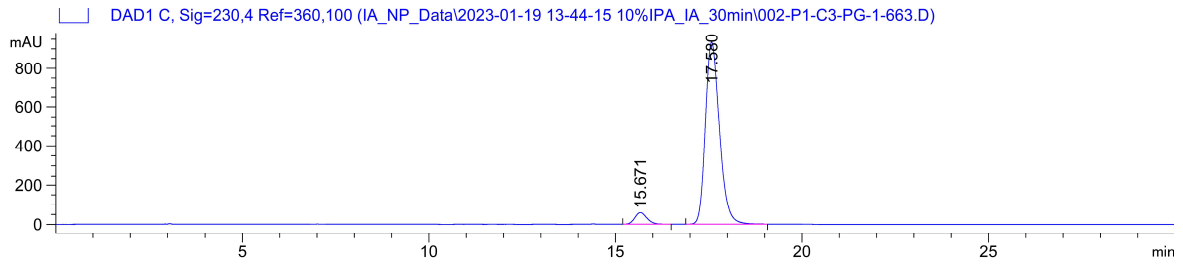


Signal 3: DAD1 C, Sig=230,4 Ref=360,100

| Peak # | RetTime [min] | Type | Width [min] | Area [mAU*s] | Height [mAU] | Area % |
|--------|---------------|------|-------------|--------------|--------------|---------|
| 1 | 15.311 | BB | 0.3338 | 1.13494e4 | 512.63116 | 50.0137 |
| 2 | 17.249 | BB | 0.3774 | 1.13432e4 | 452.59738 | 49.9863 |

Totals : 2.26926e4 965.22855

(S)-4-(1-tosylaziridin-2-yl)butyl benzoate (2.139):

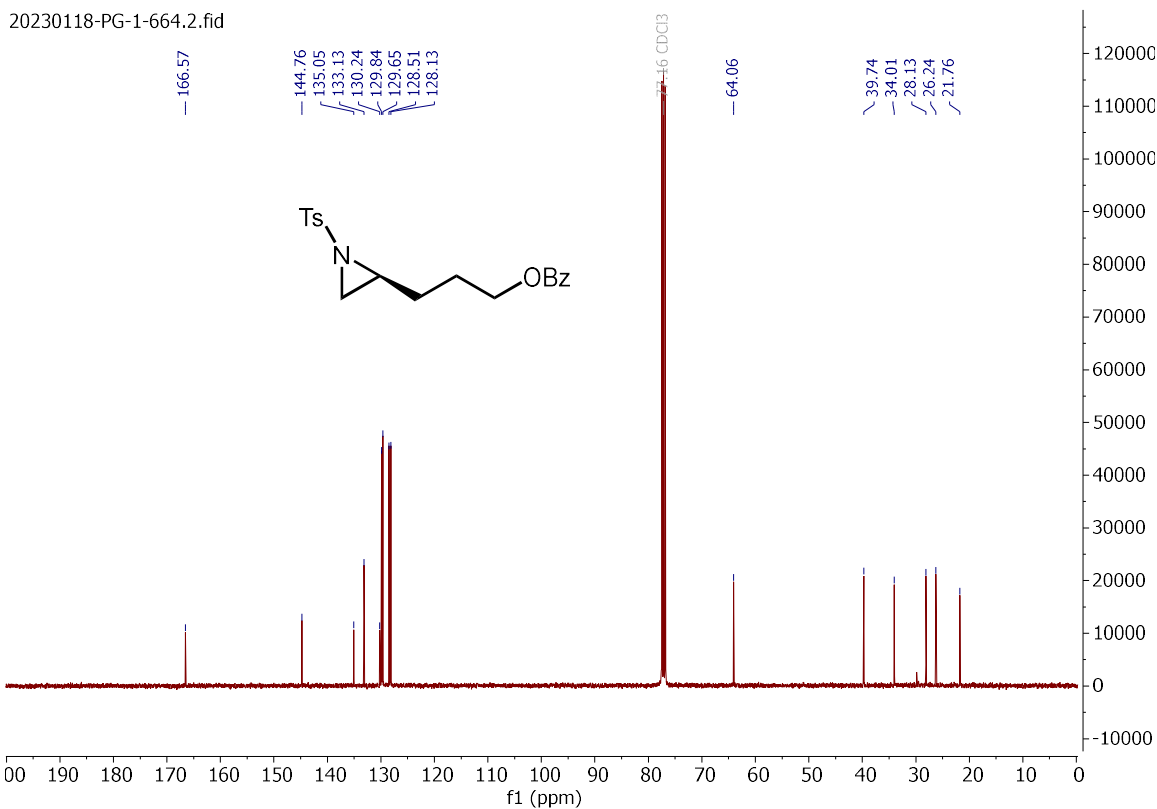
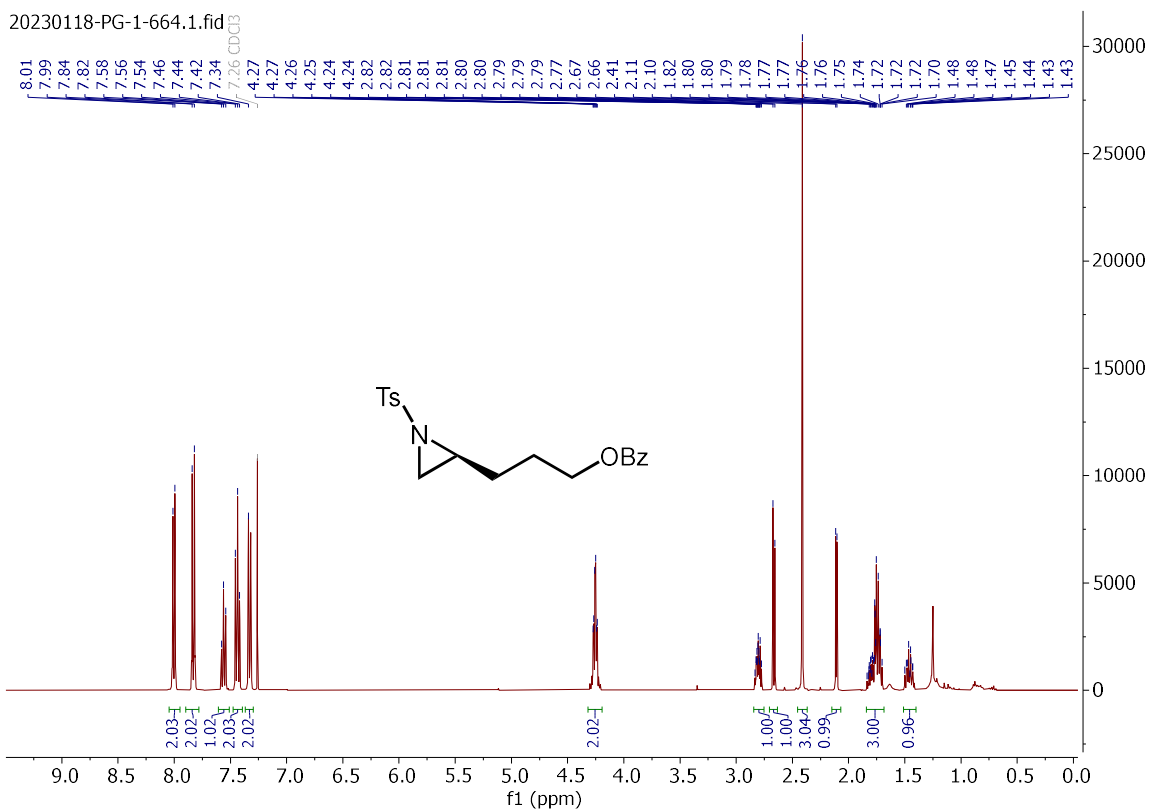


Signal 3: DAD1 C, Sig=230,4 Ref=360,100

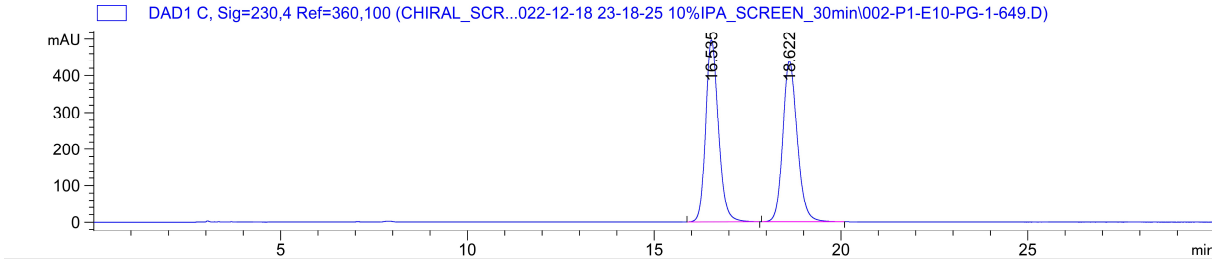
| Peak # | RetTime [min] | Type | Width [min] | Area [mAU*s] | Height [mAU] | Area % |
|--------|---------------|------|-------------|--------------|--------------|---------|
| 1 | 15.671 | BB | 0.2826 | 1345.70996 | 59.34549 | 5.2351 |
| 2 | 17.580 | BB | 0.3925 | 2.43598e4 | 933.29297 | 94.7649 |

Totals : 2.57055e4 992.63846

(S)-3-(1-tosylaziridin-2-yl)propyl benzoate (2.140):



3-(1-tosylaziridin-2-yl)propyl benzoate (\pm -**2.140**):

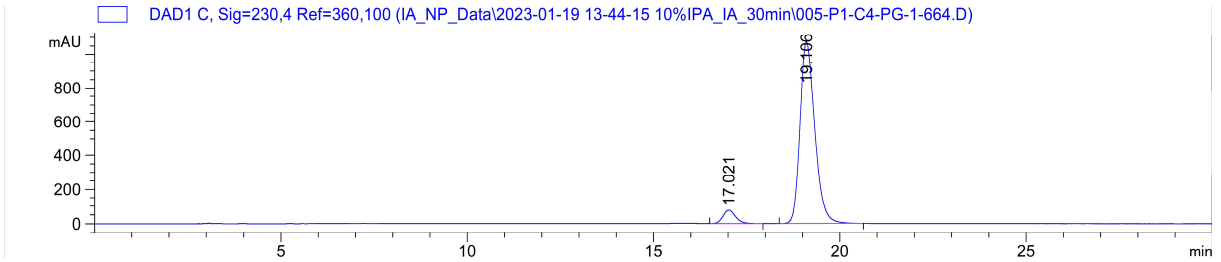


Signal 3: DAD1 C, Sig=230,4 Ref=360,100

| Peak # | RetTime [min] | Type | Width [min] | Area [mAU*s] | Height [mAU] | Area % |
|--------|---------------|------|-------------|--------------|--------------|---------|
| 1 | 16.535 | BB | 0.3573 | 1.17816e4 | 496.52261 | 50.0021 |
| 2 | 18.622 | BB | 0.4017 | 1.17807e4 | 438.11322 | 49.9979 |

Totals : 2.35623e4 934.63583

(S)-3-(1-tosylaziridin-2-yl)propyl benzoate (**(S)-2.140**):

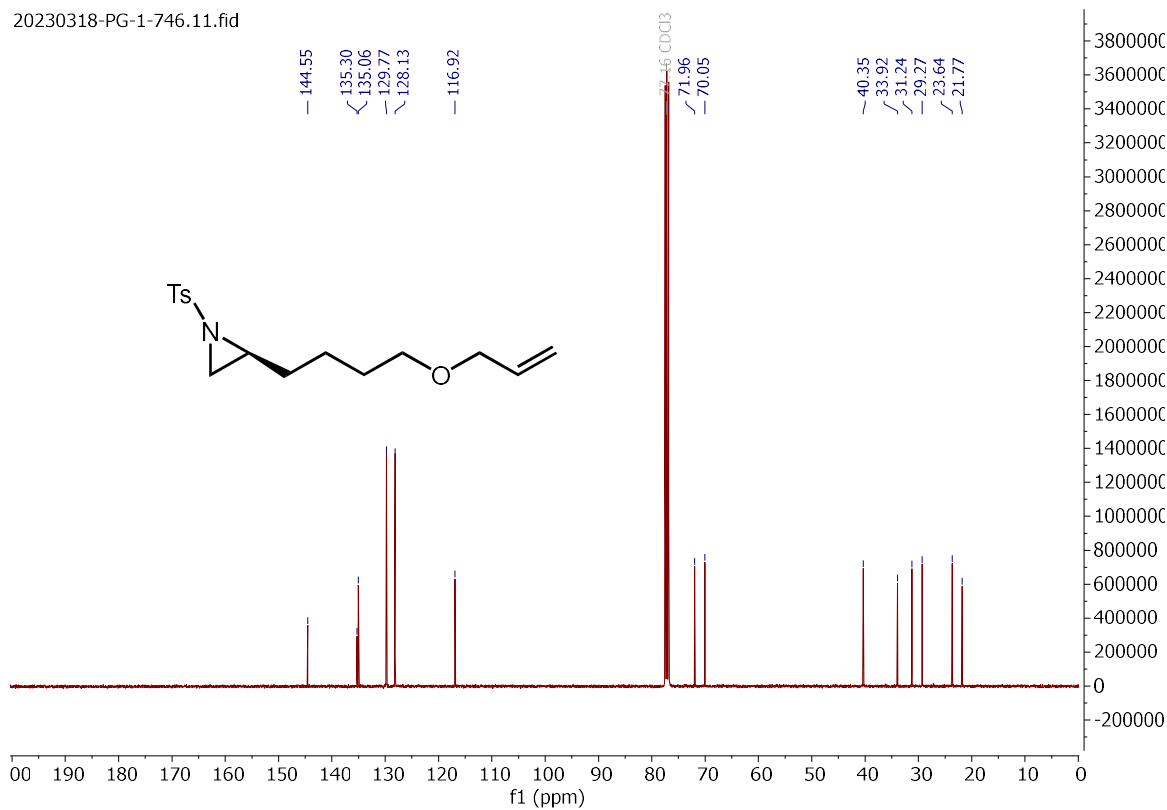
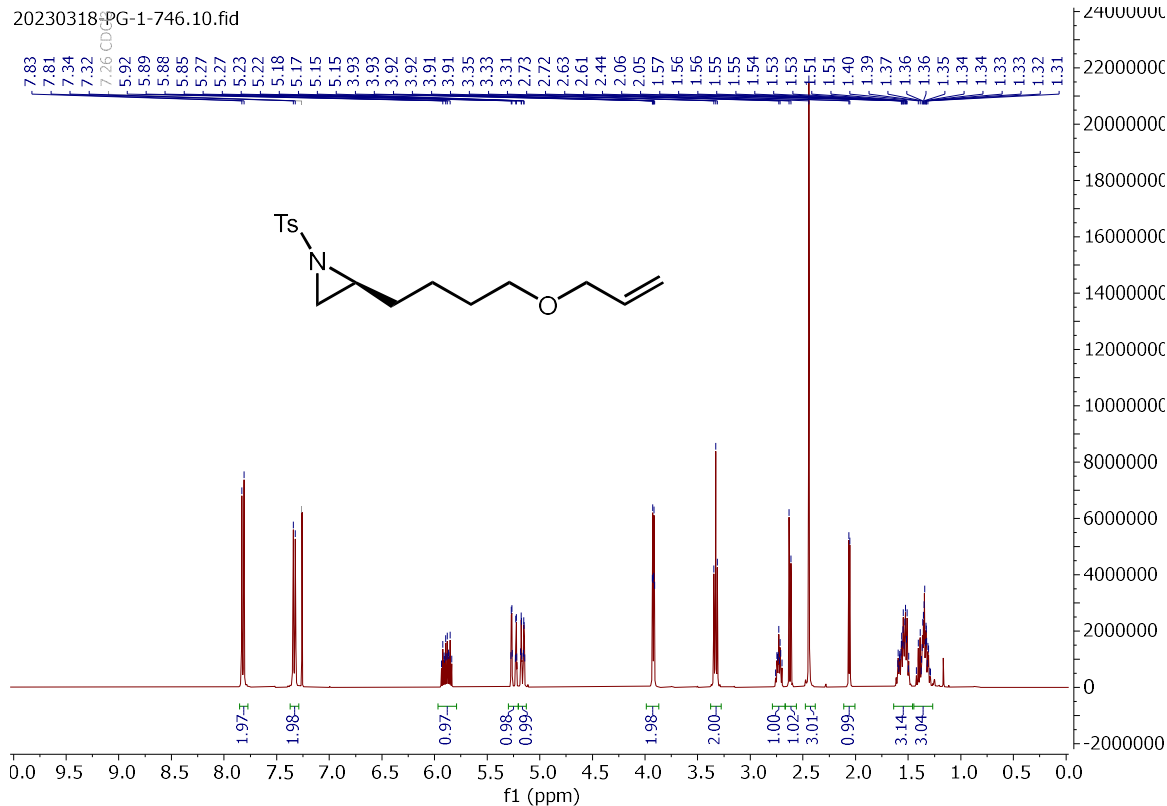


Signal 3: DAD1 C, Sig=230,4 Ref=360,100

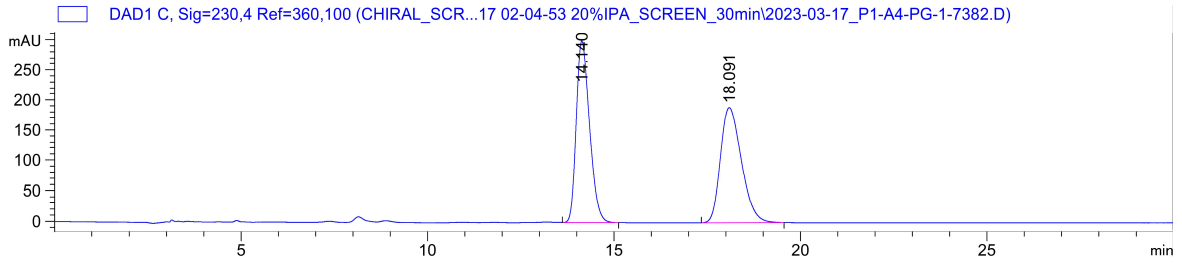
| Peak # | RetTime [min] | Type | Width [min] | Area [mAU*s] | Height [mAU] | Area % |
|--------|---------------|------|-------------|--------------|--------------|---------|
| 1 | 17.021 | BB | 0.3170 | 1784.06531 | 75.68227 | 5.7394 |
| 2 | 19.106 | BB | 0.4077 | 2.93004e4 | 1070.89087 | 94.2606 |

Totals : 3.10844e4 1146.57314

(S)-2-(4-(allyloxy)butyl)-1-tosylaziridine (**2.143**):



(±)-2-(4-(allyloxy)butyl)-1-tosylaziridine (±-2.143):

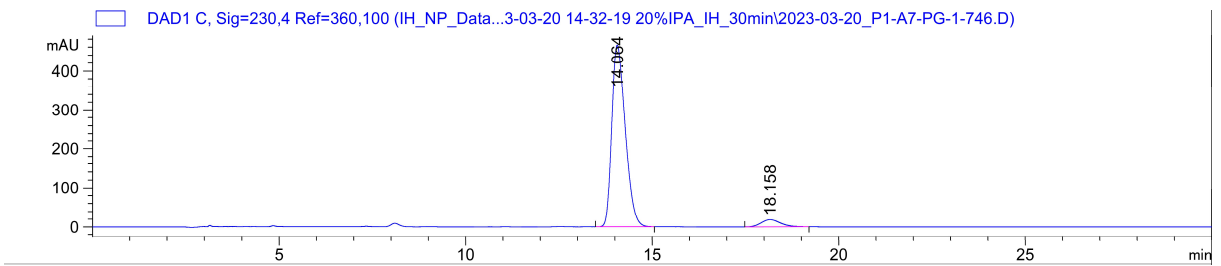


Signal 3: DAD1 C, Sig=230,4 Ref=360,100

| Peak # | RetTime [min] | Type | Width [min] | Area [mAU*s] | Height [mAU] | Area % |
|--------|---------------|------|-------------|--------------|--------------|---------|
| 1 | 14.140 | BB | 0.3654 | 7385.88965 | 299.78070 | 50.0015 |
| 2 | 18.091 | BB | 0.4703 | 7385.44824 | 189.85191 | 49.9985 |

Totals : 1.47713e4 489.63261

(S)-2-(4-(allyloxy)butyl)-1-tosylaziridine (2.143):

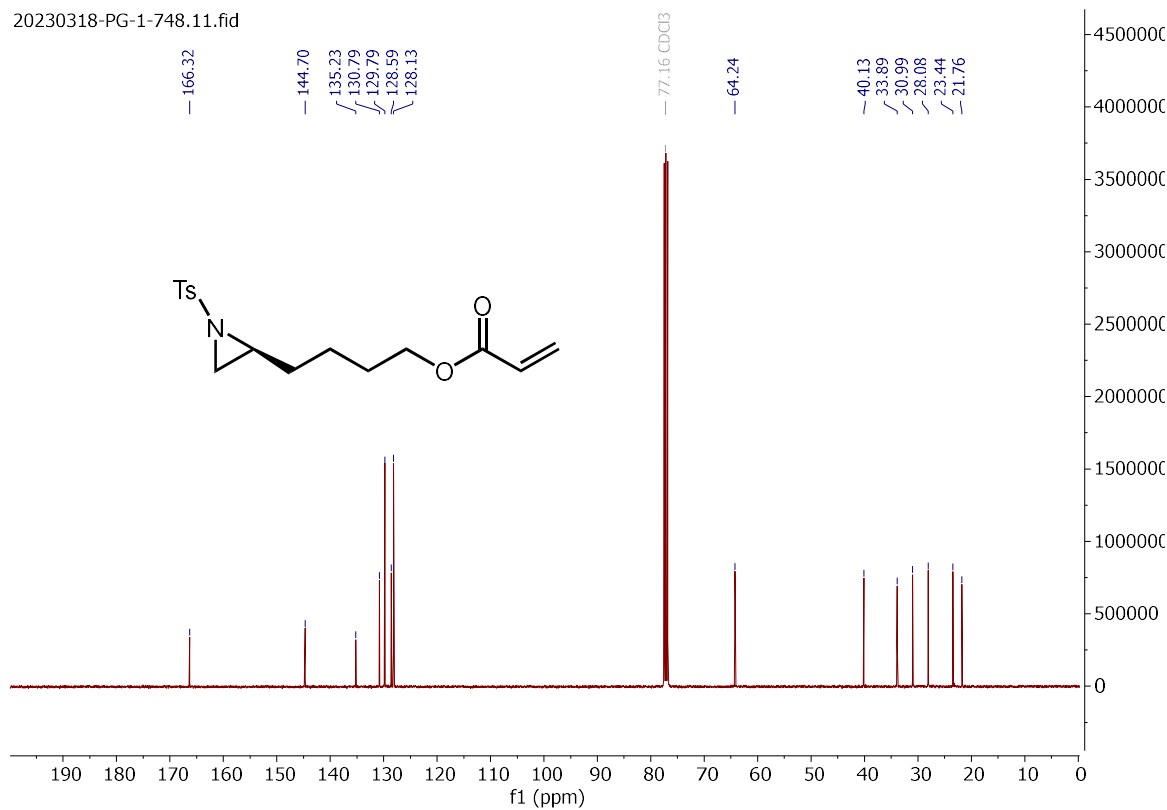
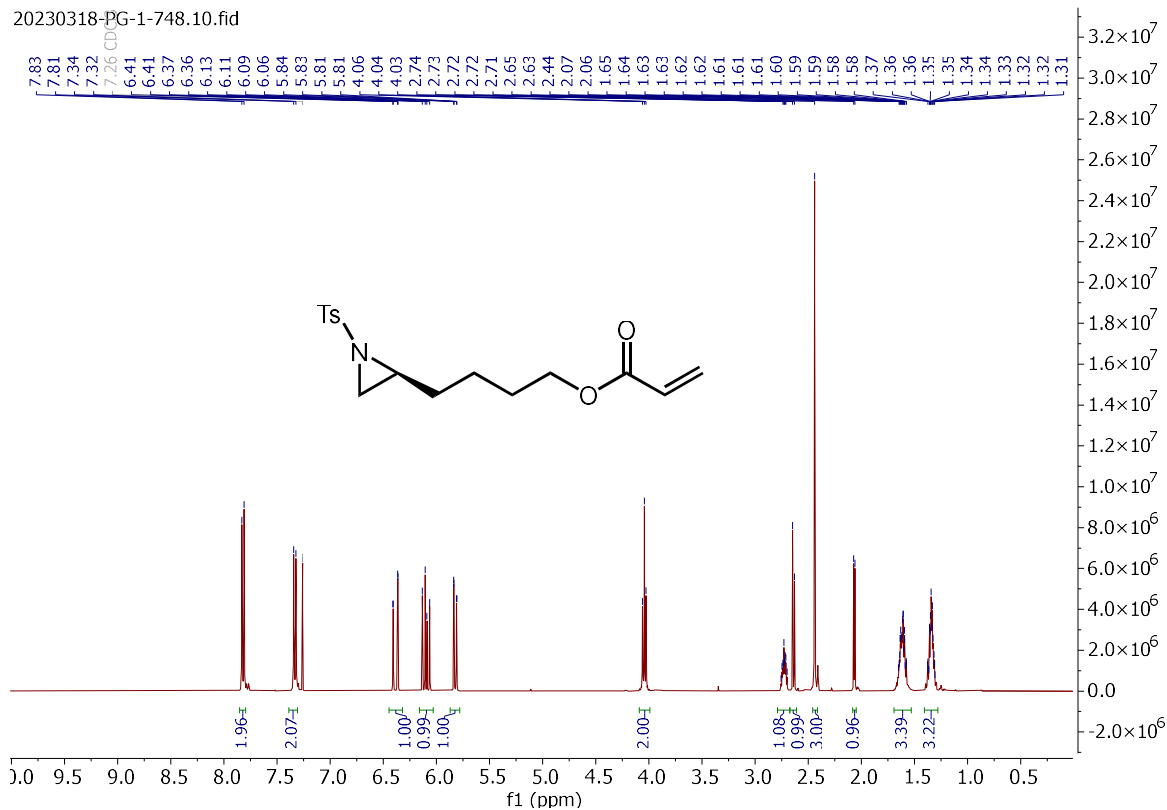


Signal 3: DAD1 C, Sig=230,4 Ref=360,100

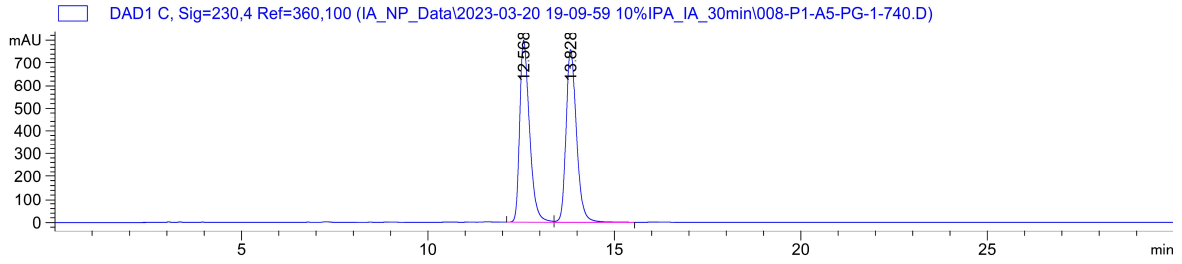
| Peak # | RetTime [min] | Type | Width [min] | Area [mAU*s] | Height [mAU] | Area % |
|--------|---------------|------|-------------|--------------|--------------|---------|
| 1 | 14.064 | BV R | 0.3724 | 1.16835e4 | 464.60098 | 94.5954 |
| 2 | 18.158 | BB | 0.4242 | 667.52789 | 18.50953 | 5.4046 |

Totals : 1.23511e4 483.11051

(S)-4-(1-tosylaziridin-2-yl)butyl acrylate (2.144):



(±)-4-(1-tosylaziridin-2-yl)butyl acrylate (±-2.144):

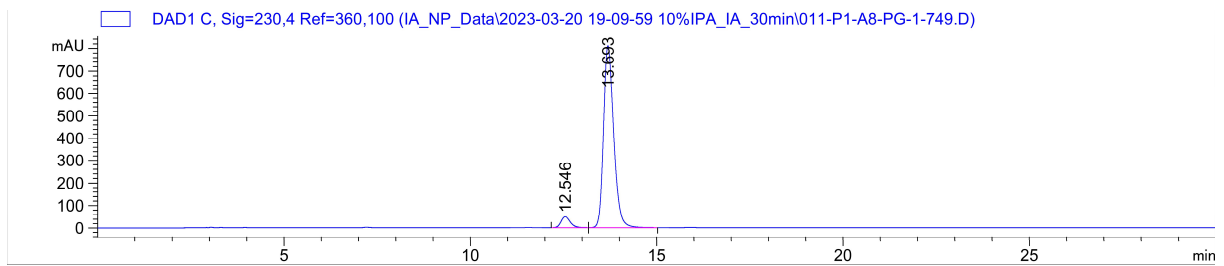


Signal 3: DAD1 C, Sig=230,4 Ref=360,100

| Peak # | RetTime [min] | Type | Width [min] | Area [mAU*s] | Height [mAU] | Area % |
|--------|---------------|------|-------------|--------------|--------------|---------|
| 1 | 12.568 | BV | 0.2773 | 1.45193e4 | 797.76776 | 49.7555 |
| 2 | 13.828 | VB | 0.2902 | 1.46620e4 | 757.92334 | 50.2445 |

Totals : 2.91812e4 1555.69110

(S)-4-(1-tosylaziridin-2-yl)butyl acrylate (2.144):

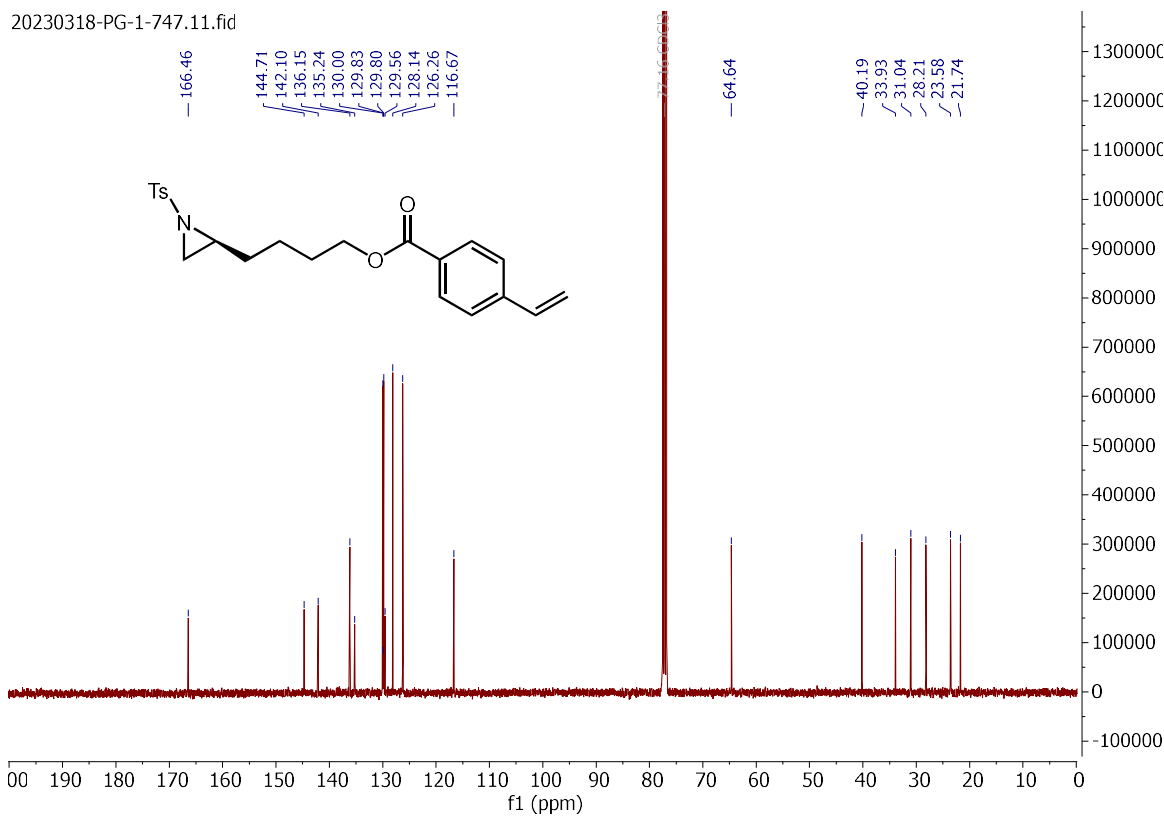
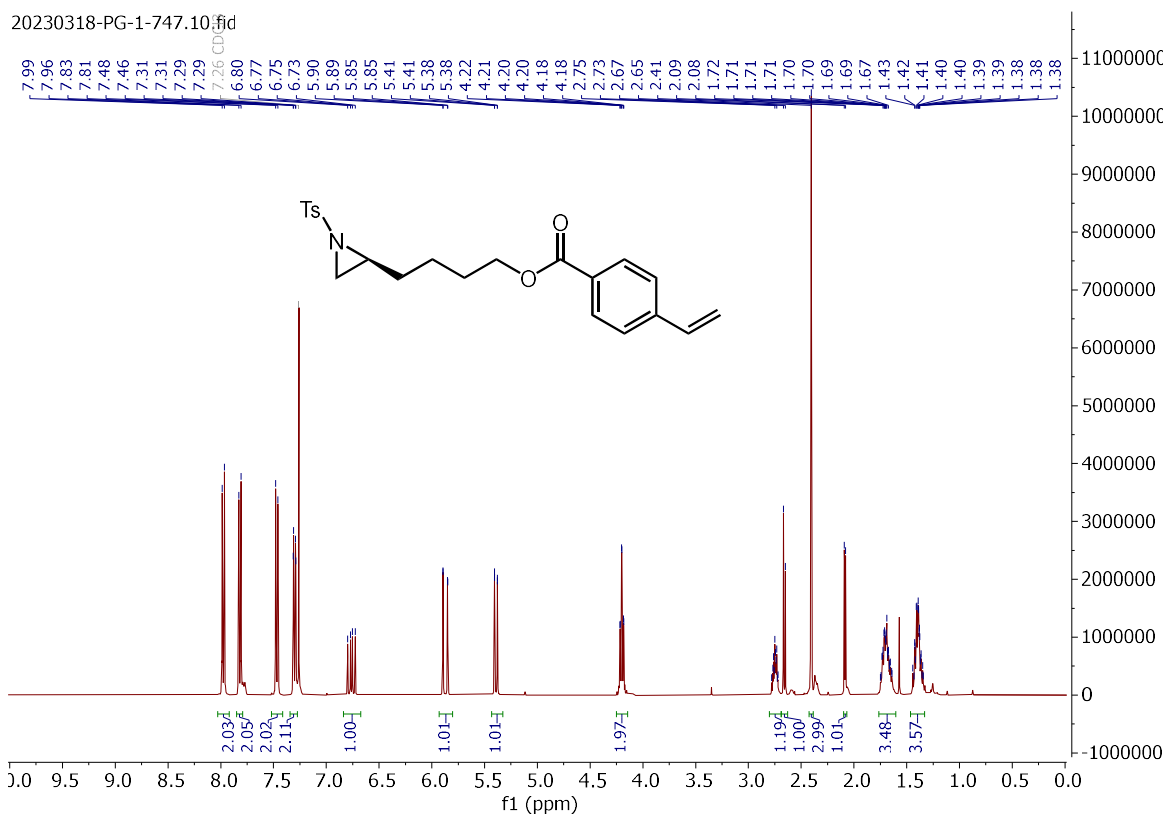


Signal 3: DAD1 C, Sig=230,4 Ref=360,100

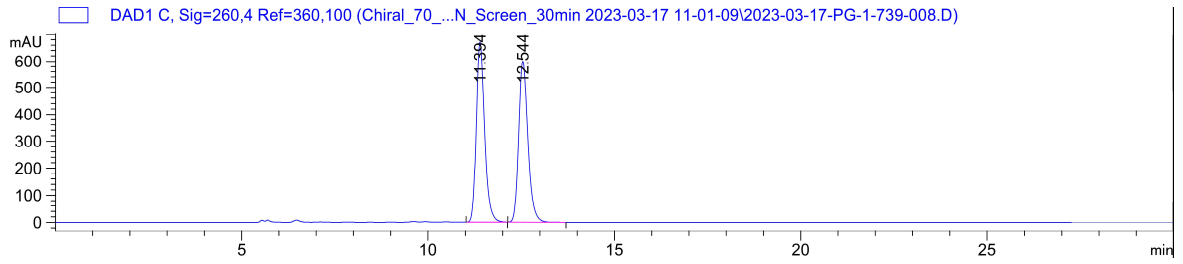
| Peak # | RetTime [min] | Type | Width [min] | Area [mAU*s] | Height [mAU] | Area % |
|--------|---------------|------|-------------|--------------|--------------|---------|
| 1 | 12.546 | BB | 0.2398 | 851.45819 | 49.72660 | 5.2585 |
| 2 | 13.693 | BB | 0.2864 | 1.53406e4 | 810.22791 | 94.7415 |

Totals : 1.61920e4 859.95450

(S)-4-(1-tosylaziridin-2-yl)butyl 4-vinylbenzoate (2.145):



(±)-4-(1-tosylaziridin-2-yl)butyl 4-vinylbenzoate (±-2.145):

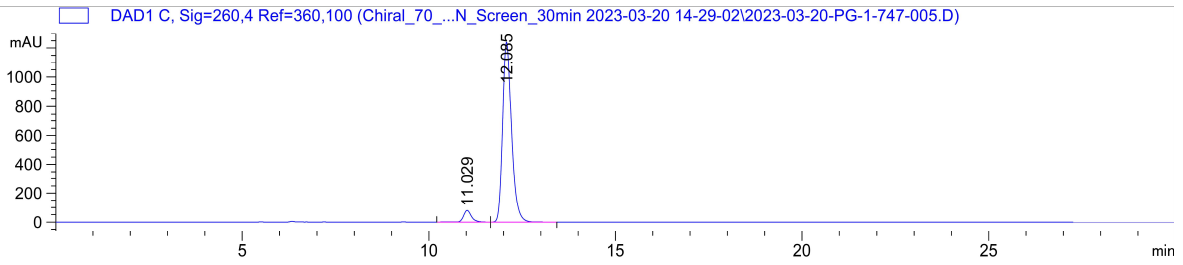


Signal 3: DAD1 C, Sig=260,4 Ref=360,100

| Peak # | RetTime [min] | Type | Width [min] | Area [mAU*s] | Height [mAU] | Area % |
|--------|---------------|------|-------------|--------------|--------------|---------|
| 1 | 11.394 | BB | 0.2361 | 1.03375e4 | 669.77283 | 50.0224 |
| 2 | 12.544 | BB | 0.2627 | 1.03282e4 | 600.28094 | 49.9776 |

Totals : 2.06657e4 1270.05377

(S)-4-(1-tosylaziridin-2-yl)butyl 4-vinylbenzoate (2.145):

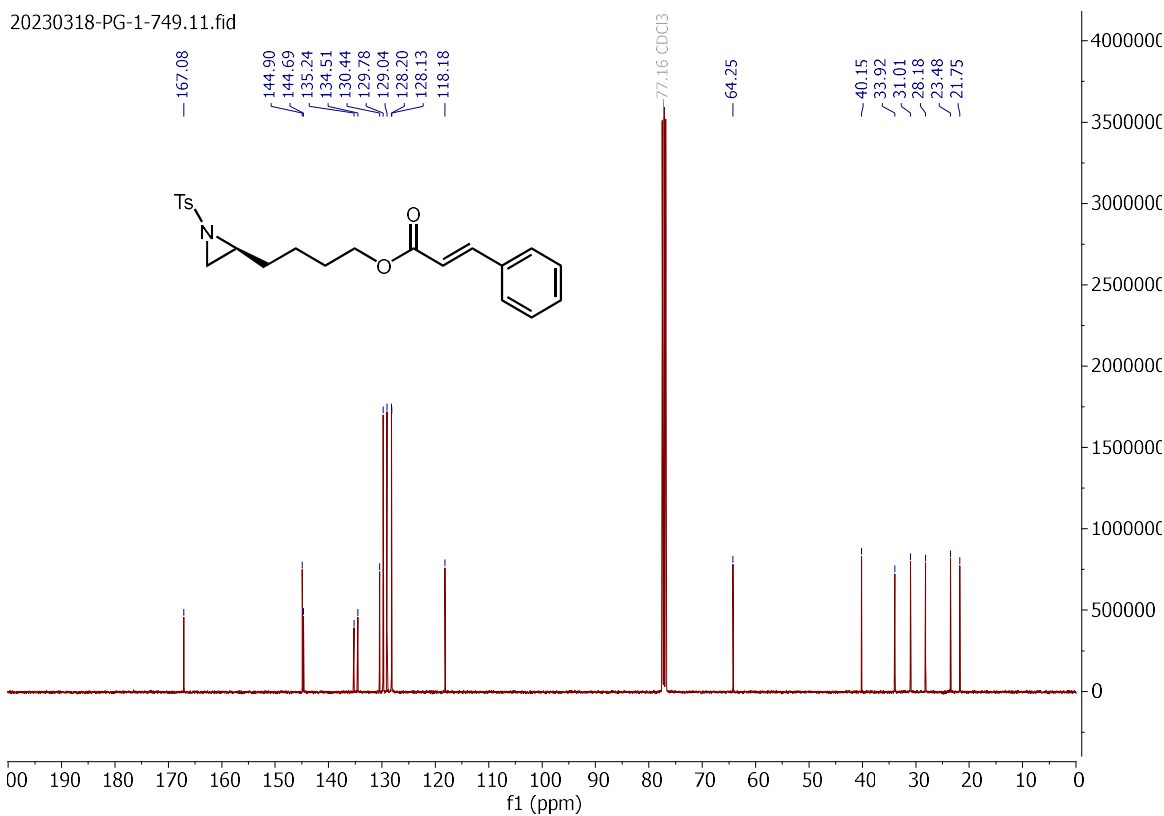
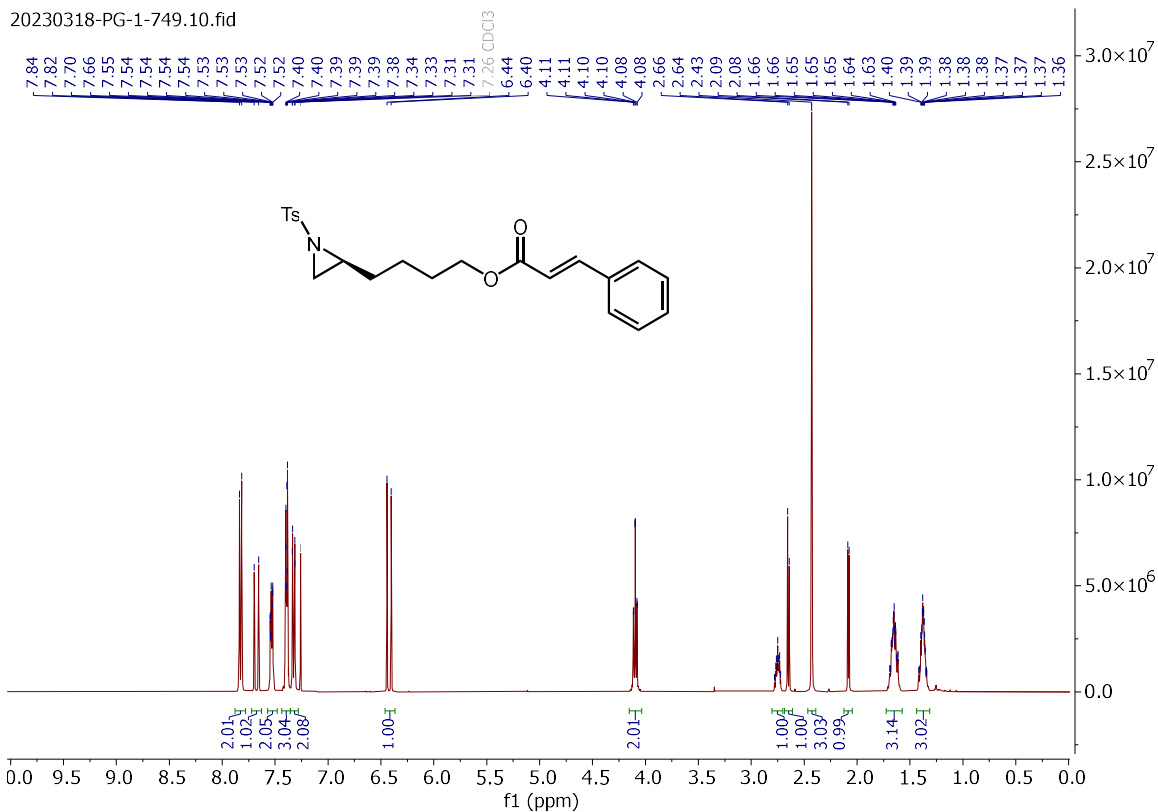


Signal 3: DAD1 C, Sig=260,4 Ref=360,100

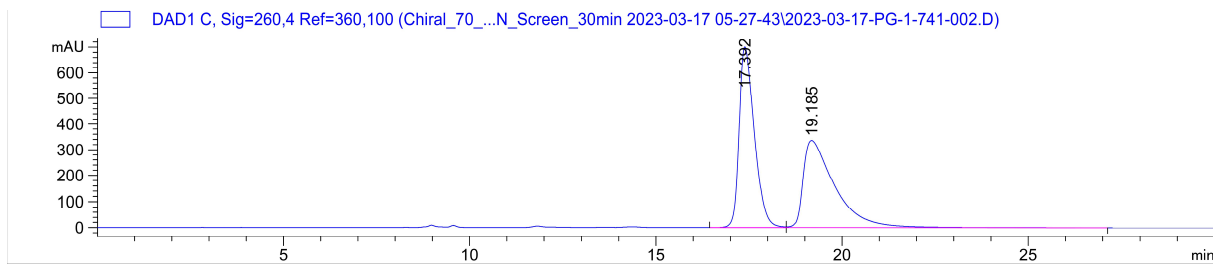
| Peak # | RetTime [min] | Type | Width [min] | Area [mAU*s] | Height [mAU] | Area % |
|--------|---------------|------|-------------|--------------|--------------|---------|
| 1 | 11.029 | VB R | 0.2222 | 1176.72290 | 78.86966 | 5.4314 |
| 2 | 12.085 | BB | 0.2528 | 2.04884e4 | 1239.53906 | 94.5686 |

Totals : 2.16651e4 1318.40872

(S)-4-(1-tosylaziridin-2-yl)butyl cinnamate (**2.146**):



(±)-4-(1-tosylaziridin-2-yl)butyl cinnamate (±-2.146):

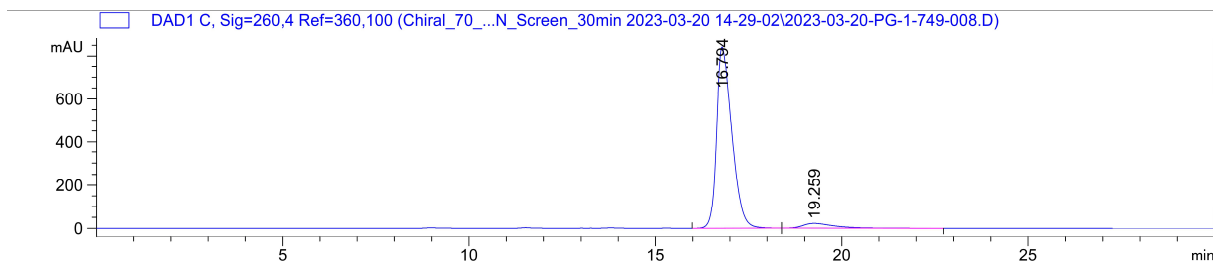


Signal 3: DAD1 C, Sig=260,4 Ref=360,100

| Peak # | RetTime [min] | Type | Width [min] | Area [mAU*s] | Height [mAU] | Area % |
|--------|---------------|------|-------------|--------------|--------------|---------|
| 1 | 17.392 | BV | 0.4308 | 1.98685e4 | 700.71686 | 49.9562 |
| 2 | 19.185 | VB | 0.8633 | 1.99033e4 | 335.88550 | 50.0438 |

Totals : 3.97718e4 1036.60236

(S)-4-(1-tosylaziridin-2-yl)butyl cinnamate (2.146):



Signal 3: DAD1 C, Sig=260,4 Ref=360,100

| Peak # | RetTime [min] | Type | Width [min] | Area [mAU*s] | Height [mAU] | Area % |
|--------|---------------|------|-------------|--------------|--------------|---------|
| 1 | 16.794 | BB | 0.4261 | 2.36567e4 | 841.26526 | 94.9186 |
| 2 | 19.259 | BB | 0.8441 | 1266.44214 | 21.78959 | 5.0814 |

Totals : 2.49231e4 863.05485

Chapter 3: Group IX Transition Metal-Catalyzed Activation of Electrophilic Nitrogen Reagents Towards Direct and Indirect Nucleophilic Attack

In this chapter we will discuss the reactivity of Group IX transition metal catalysts with electrophilic nitrogen reagents in the presence of nucleophiles. Particular focus will be placed on Co(III), Rh(III), and Ir(III) catalyzed reactions. The reactivity of these catalytic systems with electrophilic nitrogen reagents will be divided into direct nucleophilic attack onto an electrophilic nitrogen, or through indirect nucleophilic attack onto an electrophilic metal-substrate-nitrogen adduct. This chapter introduces relevant Group IX transition metal catalyzed reactivity as a foundation for the chemistry discussed in Chapter 4.

3.1 Introduction to Transition Metal-Catalyzed Activation of Electrophilic Nitrogen Reagents

The development of electrophilic amination strategies has been continually driven by the demand for the stereoselective and efficient formation of C–N bonds frequently encountered in pharmaceutical and agrochemical synthetic targets. Electrophilic amination allows for umpolung reactivity enabling the use of more common nucleophilic carbon sources to forge desired C–N bonds.¹ The development of modern electrophilic amination strategies has relied heavily on the development of electrophilic nitrogen reagents including *N*-halo-amines, hydroxylamines,^{2,3} azides, iminoiodinanes,⁴ and dioxazolones.⁵⁻⁷ Transition metal catalysts have extensively been used in combination with electrophilic nitrogen reagents as they are key in controlling the reactivity and the stereoselectivity in electrophilic aminations.⁸⁻¹⁰ Four major mechanistic pathways exist for the transition metal-mediated reaction with electrophilic nitrogen sources.^{11,12} The first mechanistic pathway begins with a directing group mediate C–H activation via a concerted metalation deprotonation (CMD) mechanism followed by an inner-sphere reductive elimination to form the C–N bond (**Figure 3.1a**).¹²⁻¹⁴ The second mechanistic pathway involves the formation of a metal nitrene followed by an outer-sphere concerted C–H insertion event to form the desired C–N bond (**Figure 3.1b**). The third mechanistic pathway involves the metal nitrene-mediated hydrogen atom transfer (HAT) leading to radical

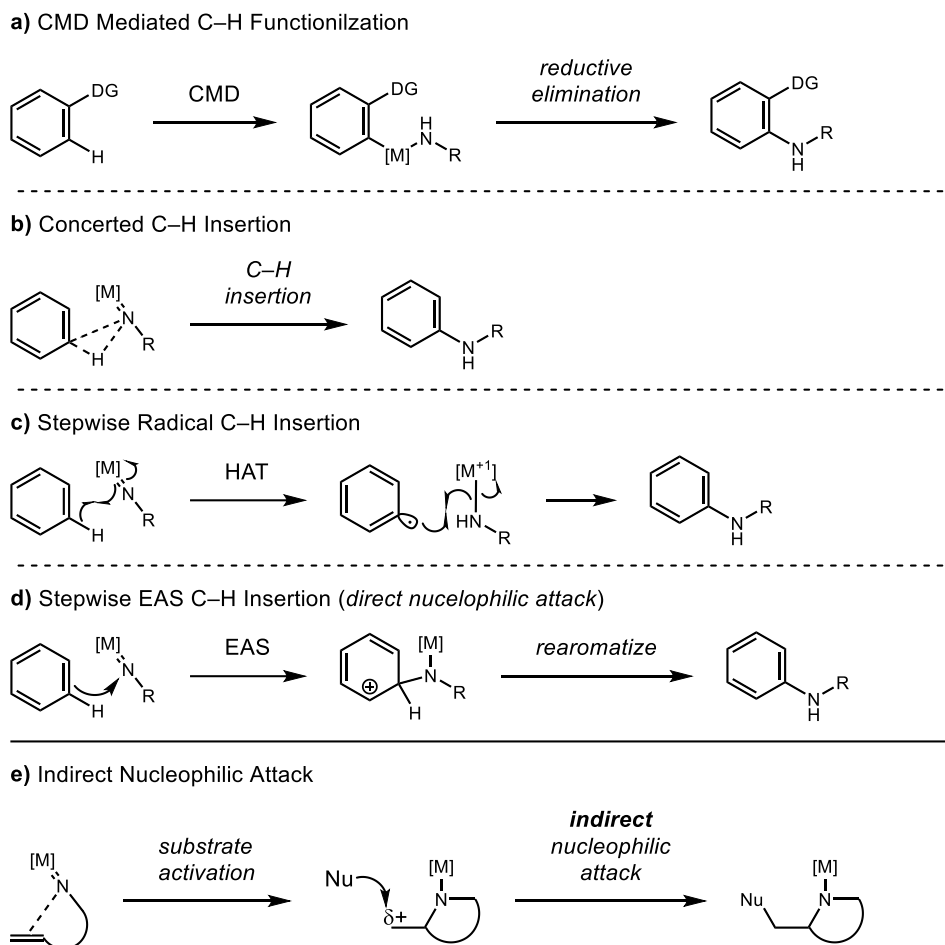


Figure 3.1 Overview of Mechanisms for Transition Metal Catalyzed C–N Bond Formations with Electrophilic Nitrogen Sources

C–H insertion pathway towards C–N bond formation(**Figure 3.1c**).¹⁵ This mechanistic pathway is frequently invoked with first-row transition metals.^{16–18} The fourth mechanistic pathway appears to be similar to the second and third outer-sphere metal mediated pathways, however the key C–N bond formation occurs via nucleophilic attack to the electrophilic nitrogen (**Figure 3.1d**). The increased electrophilic nature of the nitrogen upon metal nitrene formation enables nucleophilic attack which often occurs from electron rich π -nucleophiles and operates under electrophilic aromatic substitution (EAS) mechanisms.^{19–26}

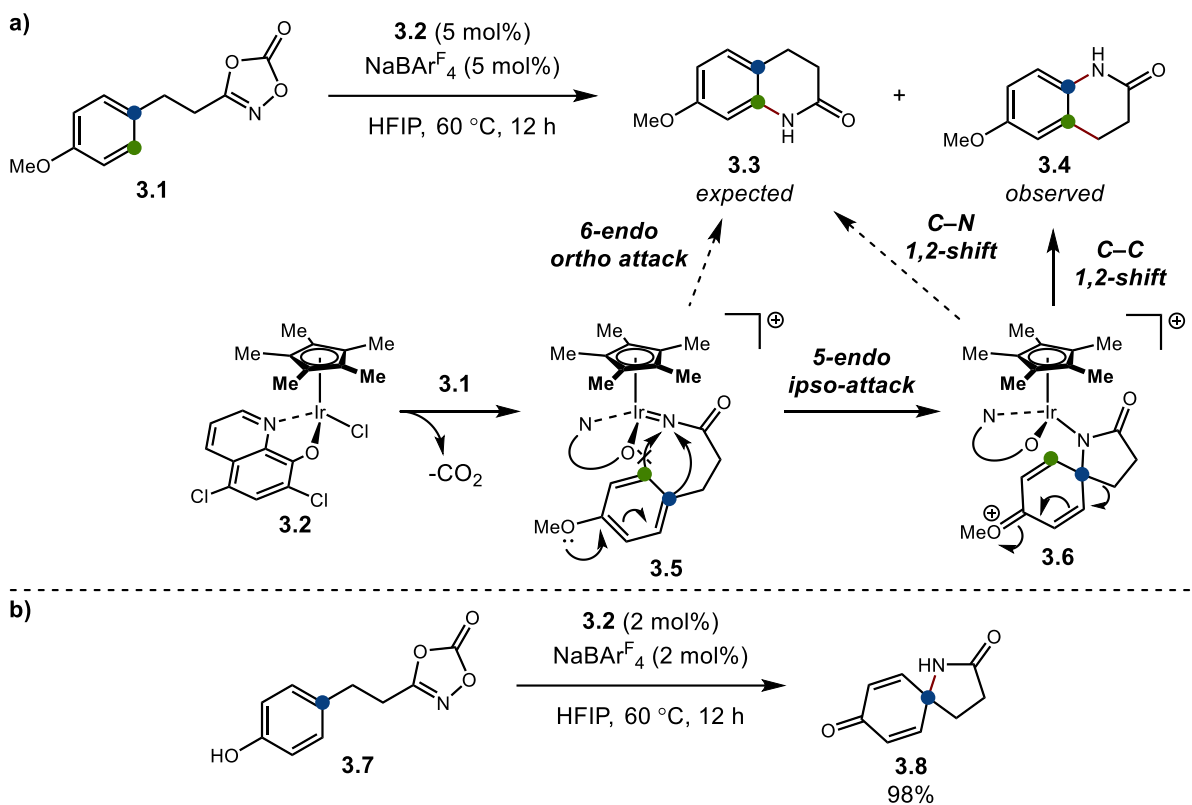
Group IX transition metal catalysis has particularly benefited from the development of electrophilic nitrogen reagents. A vast range of C–H functionalization strategies for the formation of C–N bonds have been developed utilizing the common M(III) cyclopentadienyl (Cp) piano stool catalyst platforms.

Mechanistically most of these transformations rely on the first three mechanistic pathways outlined above. Notably scarce from the vast array of CpM(III) reactions utilizing electrophilic nitrogen reagents are examples that operate via the fourth pathway of nucleophilic attack to the electrophilic nitrogen. For the few examples that exist two further mechanistic distinctions can be made. The first describes the typical *direct* nucleophilic attack on nitrogen following the formation of a highly electrophilic metal nitrene (**Figure 3.1d**). In the second mechanistic distinction, nucleophilic attack is described as *indirect* relative to electrophilic nitrogen. In this scenario the electrophilic nitrogen will first react with a substrate, typically an alkene, followed by the nucleophilic attack to a now activated carbon (**Figure 3.1e**).

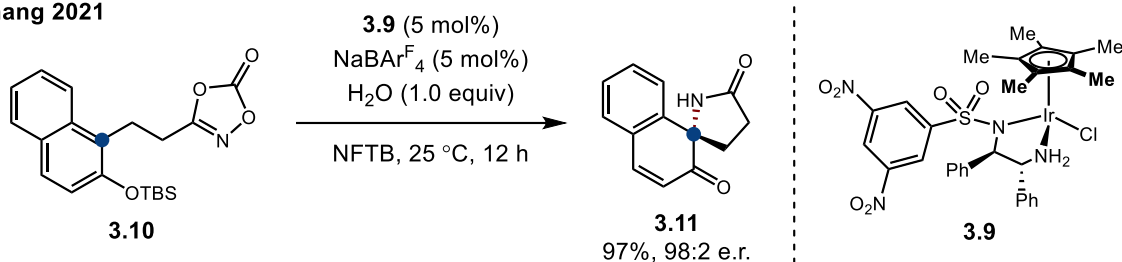
3.2 Direct Nucleophilic Attack

The first report of a nucleophilic attack occurring to an activated electrophilic nitrogen following Group IX piano stool catalyst activation was made by the Chang group in 2018.²⁷ This investigation sought to elucidate the detailed mechanism of an earlier publication in which the aromatic C–H functionalization appeared to operating under an EAS mechanism rather than the expected C–H insertion mechanism.²⁸ When the dioxazolone **3.1** was exposed to the iridium Cp* catalyst **3.2** the expected γ -lactam product **3.3** resulting from a 6-endo cyclization was not observed (**Scheme 3.1a**). Instead, the γ -lactam regioisomer **3.4** was isolated as the sole product of this transformation. The formation of this unexpected regioisomer was the result of the nucleophilic attack by the pendant aryl ring to the intermediate metal nitrene **3.5** in a 5-endo cyclization. The attack occurring from the ipso-position is a result of the increased nucleophilicity of the ipso-position over the ortho-position. Additionally, the resulting intermediate [4.5]-spirocycle **3.6** is stabilized through resonance onto the methoxy substituent. Spirocycle **3.6** then undergoes a selective skeletal rearrangement via a 1,2-carbon shift to form the observed product **3.4**. Formation of **3.3** via a 1,2-nitrogen shift was determined to be highly unfavorable. When utilizing the free phenol dioxazolone substrate **3.7** the selective ipso nucleophilic attack enabled the synthesis and isolation of the [4.5]-spirocycle **3.8**, along with a variety of substituted variants (**Scheme 3.1b**).

Chang 2018



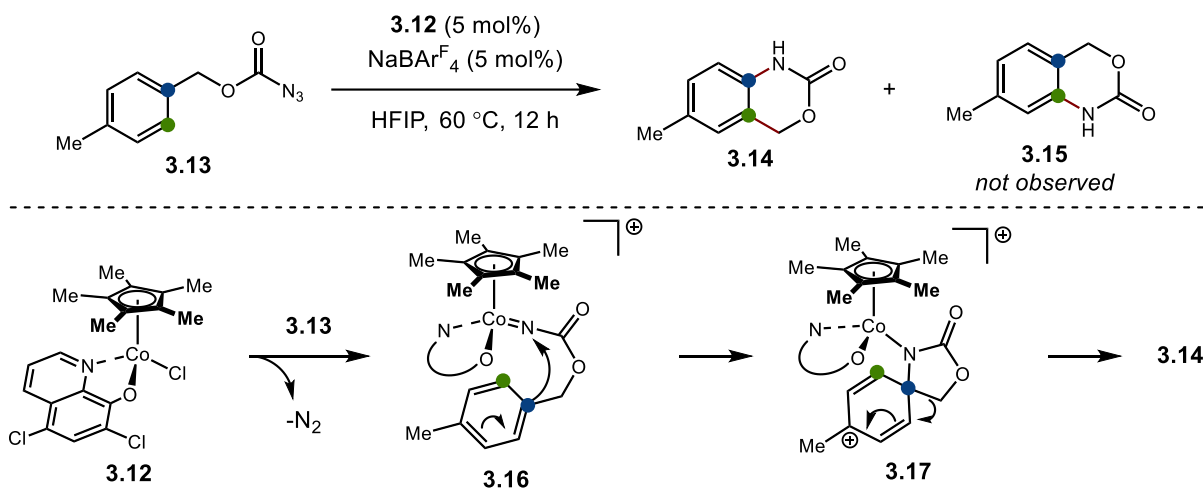
c)
Chang 2021



Scheme 3.1 Ir(III) Catalyzed Synthesis of Aryl γ -Lactams and Spirocyclic γ -Lactams

In 2021, the Chang group returned to these intermediate spirocycles to investigate their enantioselective synthesis.²⁹ Using the chiral iridium catalyst **3.9**, they were able to demonstrate the synthesis of a broad range of chiral [4.5]-spirocycle with high levels of enantioselectivity (**Scheme 3.1c**). Unlike their previous reports which showed the formation of spirocyclic products from unprotected phenols, the use of silyl protecting groups was crucial to providing high levels of enantiocontrol. This was especially true for ortho-substituted compounds such as **3.10** in which the bulky silyl group is orientated away from the Cp* ligand and would control the orientation of the subsequent nucleophilic attack of the aromatic ring leading to enantiocontrol over the new quaternary chiral center in **3.11**.

Chang 2020

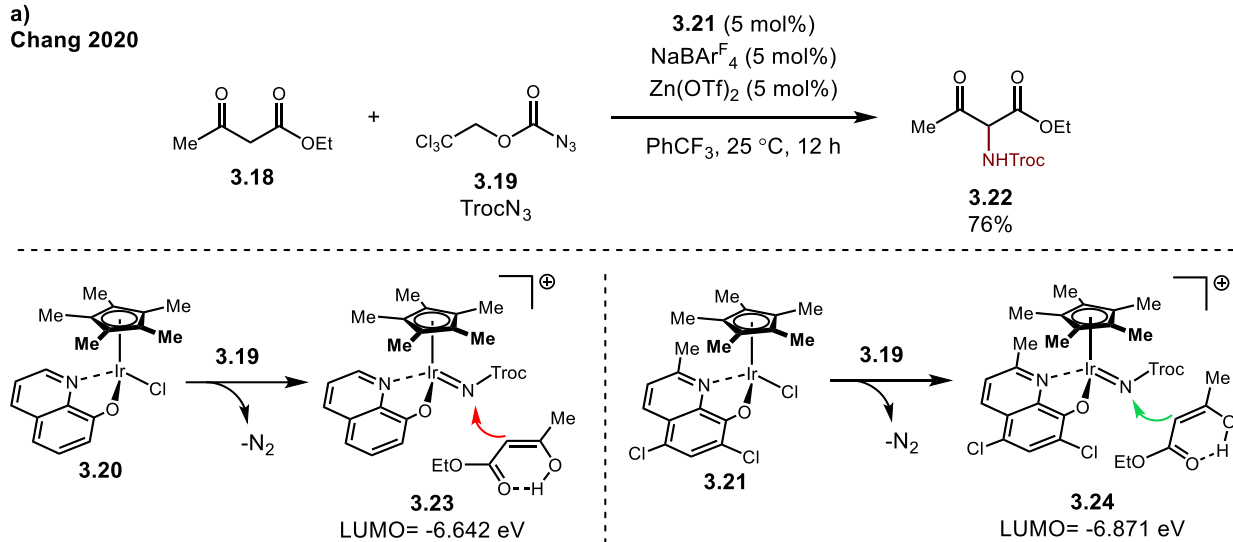


Scheme 3.2 Co(III) Catalyzed Synthesis of Cyclic Arylcarbamates via Nucleophilic Attack

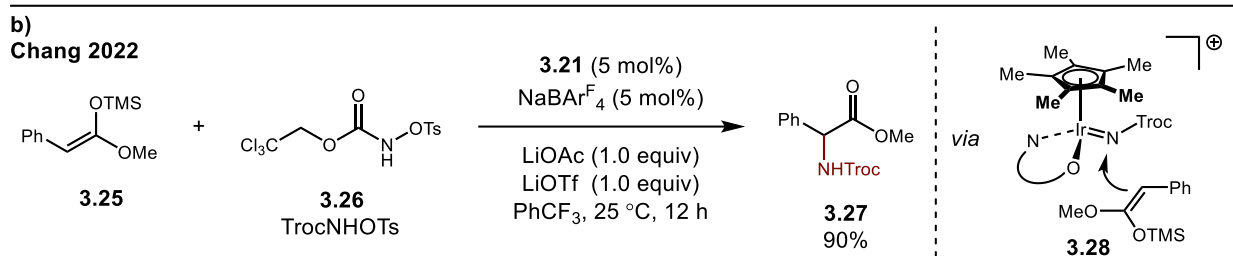
In 2020, the Chang group expanded upon their seminal 2018 report and disclosed the use of the cobalt Cp* catalyst **3.12** for the activation of metal nitrene intermediates formed from azide carbamates towards nucleophilic attack.³⁰ When utilizing the benzyl azidoformate **3.13** the rearranged carbamate **3.14** was formed as the sole product while the expected regioisomer **3.15** was not observed (**Scheme 3.2**). Once again, this is due to a selective nucleophilic attack occurring from the ipso-position to the metal nitrene **3.16**. The resulting spirocycle **3.17** undergoes a selective 1,2-carbon shift to form the carbamate product **3.14**.

Although the transition metal-catalyzed transfer of electrophilic nitrogen reagents via metal-nitrenes has achieved the functionalization of many C_{sp2}-H and simple C_{sp3}-H bonds, the functionalization of α -carbonyls was still considered to be a challenge, despite their increased reactivity due to polarization and resonance stabilization imparted by the carbonyl. Motivated by this gap in reactivity the Chang group set out to develop a C-H functionalization strategy of 1,3-dicarbonyls.³¹ These substrates were chosen as they readily tautomerize to their enol form for nucleophilic attack on to metal-nitrenes. As a result, in the presence of the iridium catalyst **3.21** the α -amination of β -keto-ester **3.18** to form **3.22** is achieved (**Scheme 3.3a**). Key to the success in developing this transformation was the computational

a)
Chang 2020



b)
Chang 2022

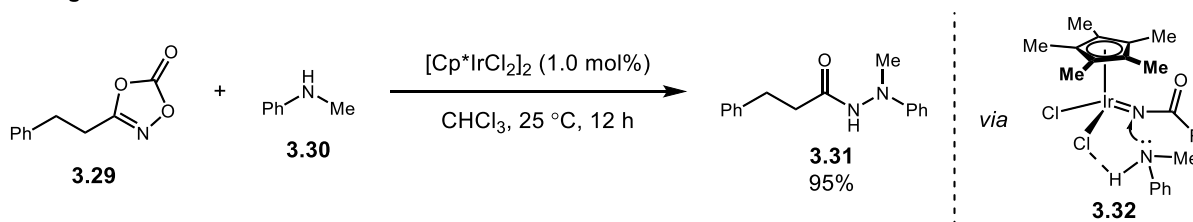


Scheme 3.3 Nucleophilic Attack of Enolates onto Co(V)-Nitrenes for the α -Amination of Carbonyl Compounds.

analysis of the initial metal nitrene intermediate **3.23** that was formed from the first catalyst **3.20** and electrophilic nitrogen source 2,2,2-trichloroethoxycarbonyl azide (TrocN₃) **3.19**. This revealed that under these initial conditions the HOMO-LUMO gap between the enol and metal nitrene were mismatched. The LUMO of the metal nitrene could be lowered by installing more electron withdrawing groups to form the more reactive catalyst **3.21**. Additionally, the use of a Lewis- or Brønsted acid was found to aid in the tautomerization of the of 1,3-dicarbonyls to their enol forms in solution. This allowed for a highly effective catalytic system for the α -amination of β -keto-esters and amides. Once again, computational analysis confirmed this transformation to occur via nucleophilic attack of the tautomerized enol to the metal nitrene. In 2022, the Chang group was able to extend this reactivity to the use of ester substrates to form α -amino esters (**Scheme 3.3b**).³² To achieve this reaction the isolable silyl enol ethers, such as **3.25**, had to be formed to enable the desired nucleophilic attack in order to form the α -amino products such as **3.27**. Once again, a more electron-withdrawing ligand scaffold was chosen to lower the LUMO of the metal nitrene

intermediate **3.28** formed from the nitrogen source TrocNHOTs **3.26** and enable nucleophilic attack from the silyl enol ether **3.25**.

Chang 2021



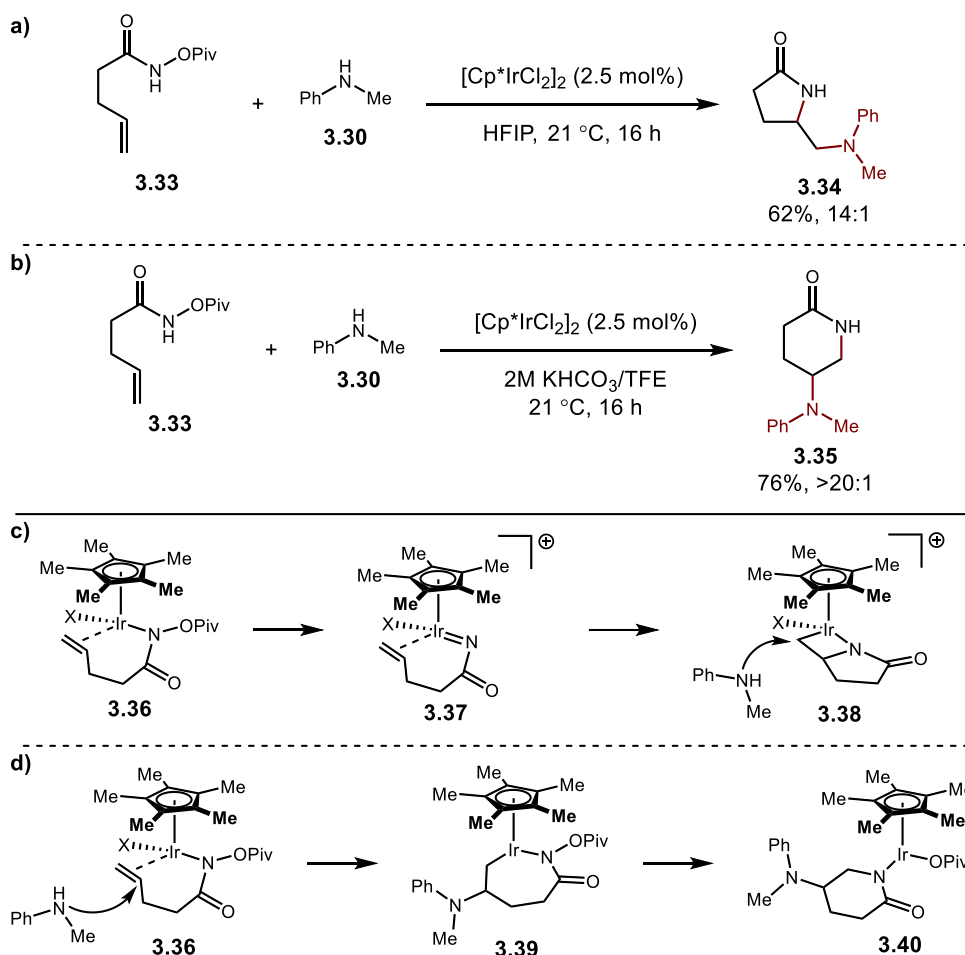
Scheme 3.4 Ir(III) Catalyzed Synthesis of Hydrazides via N–N Bond Formation

In 2021, the Chang group sought to leverage the highly electrophilic nature of the metal nitrene intermediates to further expand the scope of nucleophiles employed for direct nucleophilic attack. Carbon nucleophiles are most frequently employed in the direct nucleophilic attack to metal nitrenes, while the use of heteroatom nucleophiles, such as nitrogen or oxygen, have been notably absent from this area of research. This is due to the challenges in the direct coupling of heteroatoms to form N–N or N–O bonds. Using the $[\text{Cp}^*\text{IrCl}_2]_2$ catalyst, dioxazolone nitrene precursors, and secondary aryl amine nucleophiles, the Chang group was able to develop a N–N coupling strategy for the synthesis of hydrazides (**Scheme 3.4**).³³ This new synthetic disconnection enabled the preparation of an extensive scope of hydrazide products from dioxazolones and amines. Mechanistically this transformation was shown to undergo direct nucleophilic attack from the amine **3.30** to the metal nitrene **3.32**. Key to the success of this nucleophilic attack is the coordinated chloride ligand which guides the amine to the nitrene through hydrogen bonding.

3.3 Indirect Nucleophilic Attack

Nucleophilic attack onto substrate-metal-electrophilic nitrogen intermediates is not an uncommon form of catalytic activity and has been extensively used across the periodic table. This type of reactivity allows for the generation of more molecular complexity than the direct nucleophilic attack onto a electrophilic nitrogen, and frequently employed for the 1,2-functionalization of alkenes and alkynes. However, as with the direct nucleophilic attack strategies the examples employing Group IX piano stool catalysts have been rare.

Rovis 2018

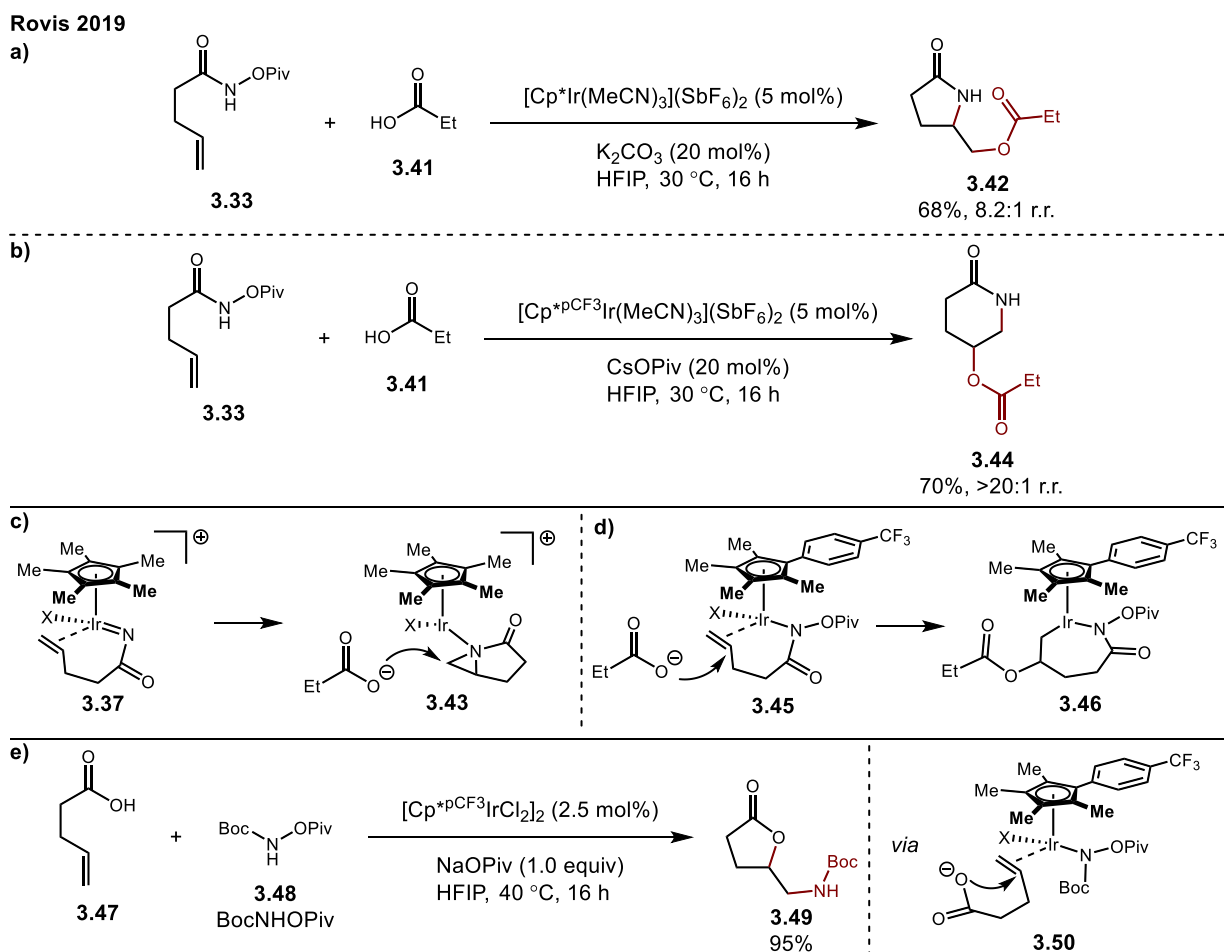


Scheme 3.5 Divergent Synthesis of Amine Substituted γ - and δ -Lactams via Indirect Amine Nucleophilic Attack onto Iridium Activated Electrophilic Nitrogen Reagents

The first example to report such reactivity was made in 2017 by Rovis who demonstrated the 1,2-di-functionalization of tethered hydroxamate alkenes with amine nucleophiles to form amine substituted γ - and δ -lactams.³⁴ This report was notable for the excellent levels of divergent regioselectivity that could be achieved depending upon the reaction conditions that were employed. When utilizing HFIP and no additives, $[\text{Cp}^*\text{IrCl}_2]_2$ catalyzes the formation of γ -lactam products in a 5-exo cyclization (**Scheme 3.5a**). However, the use of the less acidic solvent TFE and the addition of potassium bicarbonate led to formation of δ -lactam products in 6-endo cyclization (**Scheme 3.5b**). This divergence in reactivity was hypothesized to arise from the identity of the intermediate iridium-hydroxylamine adduct which would be subject to nucleophilic attack from **3.30**. Under the first conditions, the more acidic alcohol solvent HFIP

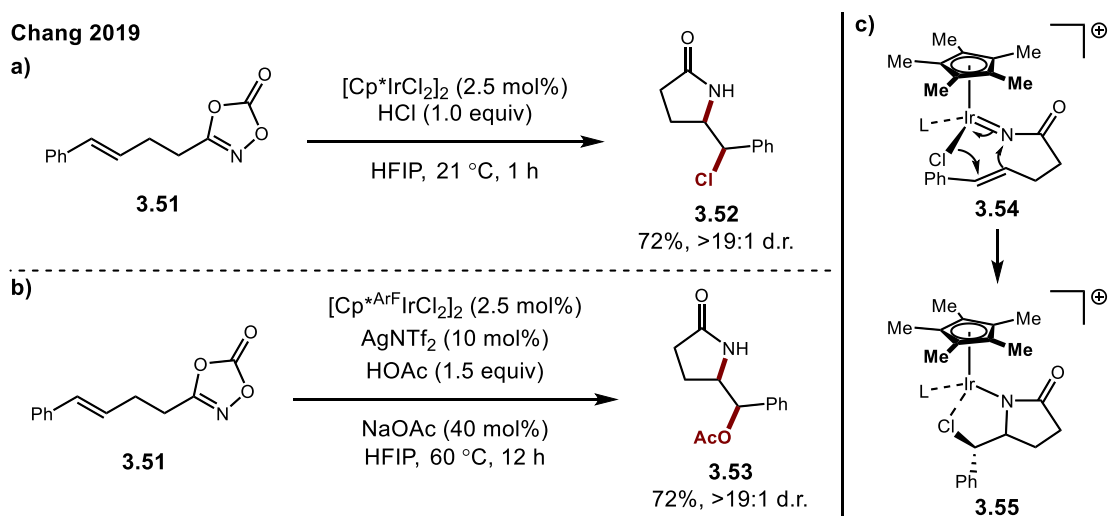
reduces the nucleophilicity of **3.30**, allowing for the formation of the metal nitrene **3.37** (Scheme 3.5c). This metal nitrene was hypothesized to undergo migratory insertion across the alkene to form the metallocycle **3.38** which would then be subjected to nucleophilic attack from **3.30** to form the γ -lactam **3.34**. Under the second reaction conditions, the less acidic TFE and the use of an inorganic base enables the nucleophilic attack to occur earlier on the Ir-hydroxylamine adduct **3.36** (Scheme 3.5d). The addition of the amine and iridium metal center across the alkenes leads to the formation of the seven membered metallocycle **3.39** which closes to the δ -lactam product **3.35**.

Following their initial report, the Rovis group continued to explore the use of nucleophiles with hydroxylamine-tethered alkenes to better understand the observed divergent regioselectivities. This resulted



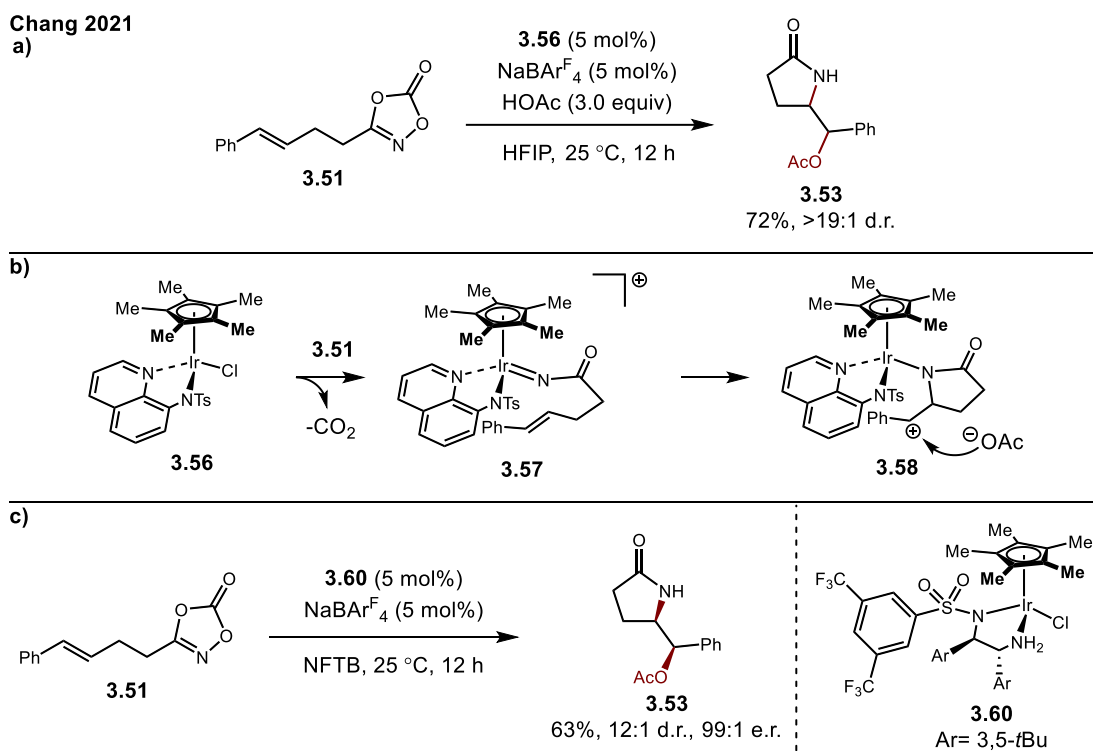
Scheme 3.6 Ligand Controlled Indirect Carboxylate Nucleophilic Attack on to Iridium Activated Hydroxylamines.

in their second report which extended this reactivity towards the 1,2-oxyamination of alkenes.³⁵ Once again excellent levels of divergent regioselectivity were observed for γ - and δ -lactams. However, unlike their seminal report, regioselectivity is controlled by the identity of the Cp ligand of the iridium catalyst rather than the reaction conditions. When using the Cp* iridium catalyst the hydroxylamine-tethered alkene **3.33** forms the γ -lactam product **3.42** (Scheme 3.6a). The selectivity could be reversed to form the δ -lactam product **3.44** when the more electron-withdrawing catalyst was used (Scheme 3.6b). In this report the electronics of the ligands dictated which iridium-hydroxylamine adduct would be subjected to nucleophilic attack from the carboxylate nucleophiles. The electron rich Cp* ligand enables formation of the metal nitrene **3.37**; however, in this proposed mechanism the concerted nitrene addition to the alkene lead to formation of aziridine adduct **3.43** rather than the previously proposed metallocycle **3.38** (Scheme 3.6c). Aziridine **3.43** is subjected to nucleophilic attack from the carboxylate to form the γ -lactams. The more electron-withdrawing catalyst directly activated the alkene to nucleophilic attack from the carboxylates forming the seven-membered metallocycle **3.46** which would then close to form the δ -lactams (Scheme 3.6d). The electron-withdrawing ligand also enabled the cyclization of **3.47** with the nitrogen reagent **3.48** to form the amine substituted γ -lactone **3.49** (Scheme 3.6e). In this role reversal, the nucleophilic attack occurs in an intramolecular fashion from the iridium-hydroxylamine adduct **3.50**.



Scheme 3.7 Synthesis of γ -Lactams via Iridium 1,3-Dipole Intermediates.

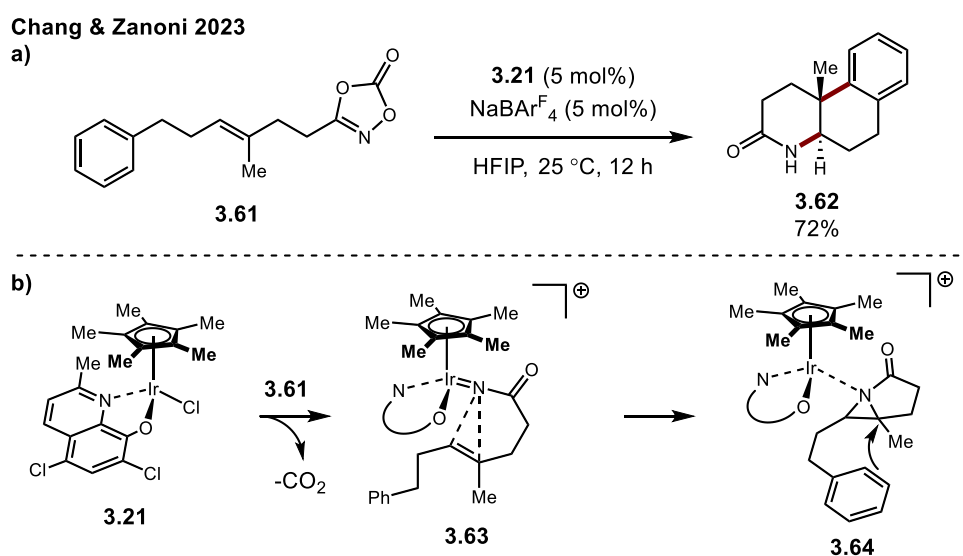
After two seminal reports from the Rovis group, the Chang group was the next to explore the activation of alkenes towards nucleophilic attack using electrophilic nitrogen metal intermediates. In their first report, the dioxazolone-tethered alkene **3.50** cyclized to form γ -lactam **3.51** with halo-nucleophiles when utilizing the Cp* iridium catalyst (**Scheme 3.7a**).³⁶ Similar to the Rovis report, the use of an electron-withdrawing catalyst enabled the use of carboxylate nucleophiles; however, unlike the Rovis report under these conditions the γ -lactam **3.53** was formed (**Scheme 3.7b**). Detailed stoichiometric and computational mechanistic investigations revealed an alternative mechanism to the one reported by Rovis. In this mechanism, the metal nitrene **3.54** that is formed from the dioxazolone acts as a 1,3-dipole and undergoes a [3+2] cycloaddition across the alkene. In this scenario, the nitrogen still acts as the electrophilic species, while the nucleophile is coordinated to the metal leading to metal mediated transfer of both the electrophile and nucleophile to the alkene (**Scheme 3.7c**).



Scheme 3.8 Synthesis of γ -Lactams via Indirect Carboxylates Nucleophilic Attack onto Iridium Activated of Dioxazolones.

In 2021, the Chang group published a follow-up study to their first report in which they once again sought to change the mechanism of the 1,2-difunctionalization.³⁷ Use of an ancillary ligand prevented

coordination of the carboxylate nucleophile, precluding the [3+2] cycloaddition mechanisms. Additionally, tuning of the ancillary ligand prevented nucleophilic attack from ancillary ligand itself to the alkene. As a result, the use of the dioxazolone substrate **3.50** once again allowed for the formation of the γ -lactam **3.53** (Scheme 3.8a). The new mechanism begins with the addition of the metal nitrene **3.57** to the alkene to form cationic γ -lactam intermediate **3.58** which is then subjected to an outer-sphere nucleophilic attack from the carboxylate (Scheme 3.8b). The change in mechanism also allowed for the use of a chiral ancillary ligand which rendered the synthesis of **3.53** enantioselective (Scheme 3.8c).



Scheme 3.9 Ir(III) Catalyzed Biomimetic Cascade Synthesis of Polycyclic δ -Lactams via Indirect Aryl Nucleophilic Attack.

The most recent example of an indirect nucleophilic attack onto an electrophilic nitrogen source catalyzed by a Group IX piano stool catalyst once again comes from the Chang group. In this 2023 publication, the dioxazolone nitrene precursor **3.61** tethered to an alkene with a pendant aryl moiety is subjected to catalyst **3.21** leading to a biomimetic cascade to form the polycyclic δ -lactam product **3.62** (Scheme 3.9a).³⁸ Based upon computational investigations this biomimetic cascade begins with the formation of the electrophilic metal nitrene **3.63** which then undergoes a concerted aziridination of the alkene to form **3.64** (Scheme 3.9b). While still coordinated to the iridium metal center, the aziridine **3.64** is subjected to a regioselective nucleophilic attack from the pendant aryl group in a 6-endo cyclization. This

indirect nucleophilic attack is a notable report, as it is the first outside of direct nucleophilic attack mechanisms to utilize an aryl nucleophile.

3.4 Conclusion

Electrophilic nitrogen reagents have expanded the toolbox for the synthesis of valuable C–N bonds. Transition metal Group IX piano stool-catalyzed C–H functionalizations have seen extensive use of these reagents, enabling the synthesis of a wide range of nitrogen scaffolds. Many transformations rely on the electrophilic nature of these reagents to enable reductive elimination or C–H insertion mechanisms in the key C–N bond forming step. Mechanisms which rely on the direct or indirect nucleophilic attack on electrophilic nitrogen intermediates are notably rare for Group IX piano stool-catalyzed transformations. Direct nucleophilic attacks occur on electrophilic metal nitrene intermediates and were first reported by the Chang group for intramolecular aryl nucleophiles. This reactivity was later expanded to include intermolecular nucleophilic attacks from enolates and even amines forming N–N bonds. Indirect nucleophilic attacks were first reported by the Rovis group harnessing the electrophilic nature of metal nitrene and aza-metallacycle intermediates to achieve the intramolecular 1,2-difunctionalization of alkenes to form substituted lactams and lactones with amine and carboxylate nucleophiles. The Chang group applied analogous intermediates for the formation of lactams, later extending this mechanism for a cascade synthesis of polycyclic lactams. In these mechanisms, achieving selectivity of the nucleophilic attack and ring-forming processes has depended upon the identity of intermediate electrophiles. While some divergent conditions have been developed to enable both inter- and intramolecular reactions, most transformations have relied on some form of intramolecular bond formation. Particularly for the indirect nucleophilic attack mechanisms, no reports have been made of intermolecular three-component reactions. Enantioselective versions of these transformations have also been limited, only two examples for the synthesis γ -lactams, have been reported. In Chapter 4 we will discuss our work towards the development of an enantioselective 1,2-arylamination for the synthesis of 2-aminotetralins and 2-amino-carbospirocycles.

3.5 References

- (1) Erdik, E.; Ay, M. Electrophilic amination of carbanions. *Chem. Rev.* **1989**, *89* (8), 1947.
- (2) Gasser, V. C. M.; Makai, S.; Morandi, B. The advent of electrophilic hydroxylamine-derived reagents for the direct preparation of unprotected amines. *Chem. Commun.* **2022**, *58* (72), 9991.
- (3) Gao, Y.; Li, H.; Zhao, Y.; Hu, X.-Q. Nitrene transfer reaction with hydroxylamine derivatives. *Chem. Commun.* **2023**, *59* (14), 1889.
- (4) Darses, B.; Rodrigues, R.; Neuville, L.; Mazurais, M.; Dauban, P. Transition metal-catalyzed iodine(III)-mediated nitrene transfer reactions: efficient tools for challenging syntheses. *Chem. Commun.* **2017**, *53* (3), 493.
- (5) van Vliet, K. M.; de Bruin, B. Dioxazolones: Stable Substrates for the Catalytic Transfer of Acyl Nitrenes. *ACS Catalysis* **2020**, *10* (8), 4751.
- (6) Wang, Y.-C.; Lai, X.-J.; Huang, K.; Yadav, S.; Qiu, G.; Zhang, L.; Zhou, H. Unravelling nitrene chemistry from acyclic precursors: recent advances and challenges. *Organic Chemistry Frontiers* **2021**, *8* (7), 1677.
- (7) Shimbayashi, T.; Sasakura, K.; Eguchi, A.; Okamoto, K.; Ohe, K. Recent Progress on Cyclic Nitrenoid Precursors in Transition-Metal-Catalyzed Nitrene-Transfer Reactions. *Chemistry – A European Journal* **2019**, *25* (13), 3156.
- (8) Barker, T. J.; Jarvo, E. R. Developments in Transition-Metal-Catalyzed Reactions Using Electrophilic Nitrogen Sources. *Synthesis* **2011**, *2011* (24), 3954.
- (9) Dong, X.; Liu, Q.; Dong, Y.; Liu, H. Transition-Metal-Catalyzed Electrophilic Amination: Application of O-Benzoylhydroxylamines in the Construction of the C–N Bond. *Chemistry – A European Journal* **2017**, *23* (11), 2481.
- (10) Park, Y.; Kim, Y.; Chang, S. Transition Metal-Catalyzed C–H Amination: Scope, Mechanism, and Applications. *Chem. Rev.* **2017**, *117* (13), 9247.

- (11) Muller, P.; Fruit, C. Enantioselective catalytic aziridinations and asymmetric nitrene insertions into CH bonds. *Chem. Rev.* **2003**, *103* (8), 2905.
- (12) Du, B.; Chan, C.-M.; Au, C.-M.; Yu, W.-Y. Transition Metal-Catalyzed Regioselective Direct C–H Amidation: Interplay between Inner- and Outer-Sphere Pathways for Nitrene Cross-Coupling Reactions. *Acc. Chem. Res.* **2022**, *55* (15), 2123.
- (13) Park, S. H.; Kwak, J.; Shin, K.; Ryu, J.; Park, Y.; Chang, S. Mechanistic Studies of the Rhodium-Catalyzed Direct C–H Amination Reaction Using Azides as the Nitrogen Source. *J. Am. Chem. Soc.* **2014**, *136* (6), 2492.
- (14) Sambiagio, C.; Schönbauer, D.; Blicke, R.; Dao-Huy, T.; Pototschnig, G.; Schaaf, P.; Wiesinger, T.; Zia, M. F.; Wencel-Delord, J.; Besset, T. et al. A comprehensive overview of directing groups applied in metal-catalysed C–H functionalisation chemistry. *Chem. Soc. Rev.* **2018**, *47* (17), 6603.
- (15) Kuijpers, P. F.; van der Vlugt, J. I.; Schneider, S.; de Bruin, B. Nitrene Radical Intermediates in Catalytic Synthesis. *Chemistry* **2017**, *23* (56), 13819.
- (16) Lee, J.; Jin, S.; Kim, D.; Hong, S. H.; Chang, S. Cobalt-Catalyzed Intermolecular C–H Amidation of Unactivated Alkanes. *J. Am. Chem. Soc.* **2021**, *143* (13), 5191.
- (17) Kweon, J.; Kim, D.; Kang, S.; Chang, S. Access to β -Lactams via Iron-Catalyzed Olefin Oxyamidation Enabled by the π -Accepting Phthalocyanine Ligand. *J. Am. Chem. Soc.* **2022**, *144* (4), 1872.
- (18) Kim, S.; Song, S. L.; Zhang, J.; Kim, D.; Hong, S.; Chang, S. Regio- and Enantioselective Catalytic δ -C–H Amidation of Dioxazolones Enabled by Open-Shell Copper-Nitrenoid Transfer. *J. Am. Chem. Soc.* **2023**, *145* (29), 16238.
- (19) Stokes, B. J.; Dong, H.; Leslie, B. E.; Pumphrey, A. L.; Driver, T. G. Intramolecular C–H Amination Reactions: Exploitation of the Rh₂(II)-Catalyzed Decomposition of Azidoacrylates. *J. Am. Chem. Soc.* **2007**, *129* (24), 7500.

- (20) Arai, K.; Ueda, Y.; Morisaki, K.; Furuta, T.; Sasamori, T.; Tokitoh, N.; Kawabata, T. Intermolecular chemo- and regioselective aromatic C–H amination of alkoxyarenes promoted by rhodium nitrenoids. *Chem. Commun.* **2018**, 54 (18), 2264.
- (21) Yu, J.-S.; Espinosa, M.; Noda, H.; Shibasaki, M. Traceless Electrophilic Amination for the Synthesis of Unprotected Cyclic β -Amino Acids. *J. Am. Chem. Soc.* **2019**, 141 (26), 10530.
- (22) Singh, R.; Nagesh, K.; Parameshwar, M. Rhodium(II)-Catalyzed Undirected and Selective C(sp²)–H Amination en Route to Benzoxazolones. *ACS Catalysis* **2016**, 6 (10), 6520.
- (23) Paudyal, M. P.; Adebessin, A. M.; Burt, S. R.; Ess, D. H.; Ma, Z.; Kürti, L.; Falck, J. R. Dirhodium-catalyzed C-H arene amination using hydroxylamines. *Science* **2016**, 353 (6304), 1144.
- (24) Ito, M.; Tanaka, A.; Higuchi, K.; Sugiyama, S. Rhodium(II)-Catalyzed Synthesis of N-Aryl-N'-tosyldiazenes from Primary Aromatic Amines Using (Tosylimino)aryliodinane: A Potent Stable Surrogate for Diazonium Salts. *Eur. J. Org. Chem.* **2017**, 2017 (9), 1272.
- (25) Donthoju, A.; Phanindrudu, M.; Ellandula, S.; Lal, M. R.; Nanubolu, J. B.; Chegondi, R. Rh₂(II)-Catalyzed Selective C(sp³)–H Bond Electrophilic Amination of Aryl Azide-Tethered 1,3-Dicarbonyl Compounds. *Org. Lett.* **2023**, 25 (41), 7589.
- (26) Sun, W.; Ling, C.-H.; Au, C.-M.; Yu, W.-Y. Ruthenium-Catalyzed Intramolecular Arene C(sp²)–H Amidation for Synthesis of 3,4-Dihydroquinolin-2(1H)-ones. *Org. Lett.* **2021**, 23 (9), 3310.
- (27) Hwang, Y.; Park, Y.; Kim, Y. B.; Kim, D.; Chang, S. Revisiting Arene C(sp²)–H Amidation by Intramolecular Transfer of Iridium Nitrenoids: Evidence for a Spirocyclization Pathway. *Angew. Chem. Int. Ed.* **2018**, 57 (41), 13565.
- (28) Hong, S. Y.; Park, Y.; Hwang, Y.; Kim, Y. B.; Baik, M.-H.; Chang, S. Selective formation of γ -lactams via C–H amidation enabled by tailored iridium catalysts. *Science* **2018**, 359 (6379), 1016.
- (29) Lee, E.; Hwang, Y.; Kim, Y. B.; Kim, D.; Chang, S. Enantioselective Access to Spirolactams via Nitrenoid Transfer Enabled by Enhanced Noncovalent Interactions. *J. Am. Chem. Soc.* **2021**, 143 (17), 6363.

- (30) Lee, J.; Lee, J.; Jung, H.; Kim, D.; Park, J.; Chang, S. Versatile Cp*Co(III)(LX) Catalyst System for Selective Intramolecular C-H Amidation Reactions. *J. Am. Chem. Soc.* **2020**, *142* (28), 12324.
- (31) Lee, M.; Jung, H.; Kim, D.; Park, J. W.; Chang, S. Modular Tuning of Electrophilic Reactivity of Iridium Nitrenoids for the Intermolecular Selective α -Amidation of β -Keto Esters. *J. Am. Chem. Soc.* **2020**, *142* (28), 11999.
- (32) Gwon, Y.; Lee, M.; Kim, D.; Chang, S. Iridium-Catalyzed Amidation of In Situ Prepared Silyl Ketene Acetals to Access α -Amino Esters. *Org. Lett.* **2022**, *24* (4), 1088.
- (33) Wang, H.; Jung, H.; Song, F.; Zhu, S.; Bai, Z.; Chen, D.; He, G.; Chang, S.; Chen, G. Nitrene-mediated intermolecular N–N coupling for efficient synthesis of hydrazides. *Nature Chemistry* **2021**, *13* (4), 378.
- (34) Conway, J. H., Jr.; Rovis, T. Regiodivergent Iridium(III)-Catalyzed Diamination of Alkenyl Amides with Secondary Amines: Complementary Access to γ - or δ -Lactams. *J. Am. Chem. Soc.* **2018**, *140* (1), 135.
- (35) Lei, H.; Conway, J. H., Jr.; Cook, C. C.; Rovis, T. Ligand Controlled Ir-Catalyzed Regiodivergent Oxyamination of Unactivated Alkenes. *J. Am. Chem. Soc.* **2019**, *141* (30), 11864.
- (36) Hong, S. Y.; Chang, S. Stereodefined Access to Lactams via Olefin Difunctionalization: Iridium Nitrenoids as a Motif of LUMO-Controlled Dipoles. *J. Am. Chem. Soc.* **2019**, *141* (26), 10399.
- (37) Kim, S.; Kim, D.; Hong, S. Y.; Chang, S. Tuning Orbital Symmetry of Iridium Nitrenoid Enables Catalytic Diastereo- and Enantioselective Alkene Difunctionalizations. *J. Am. Chem. Soc.* **2021**, *143* (10), 3993.
- (38) Tufano, E.; Lee, E.; Barilli, M.; Casali, E.; Oštrek, A.; Jung, H.; Morana, M.; Kang, J.; Kim, D.; Chang, S. et al. Iridium Acylnitrenoid-Initiated Biomimetic Cascade Cyclizations: Stereodefined Access to Polycyclic δ -Lactams. *J. Am. Chem. Soc.* **2023**, *145* (45), 24724.

Chapter 4: Enantioselective 1,2-Arylamination: Synthesis of 2-Aminotetralins and 2-Amino-Carbospirocycles

In this chapter, we discuss the development of an enantioselective 1,2-arylamination using planar chiral Rh(III) indenyl catalysts. The discovery and optimization of this reaction highlights the privileged role the indenyl scaffold plays in enabling this transformation. We report an extensive scope of the stereoselective synthesis of both chiral 2-aminotetralins and unique chiral 2-aminocarbospirocycles. Mechanistic investigations have led us to propose a unique catalytic cycle which differs from both our previous enantioselective aziridination and other reported Group-IX catalyzed nucleophilic attacks onto electrophilic nitrogen reagents. This chapter represents work in progress with outstanding substrates synthesized by Wesley Pullara and computational mechanistic investigations performed in collaboration with the Baik group at KAIST.

4.1 Introduction to 2-Aminotetralins

4.1.1 2-Aminotetralins in Medicinal Chemistry

Nitrogen is a key elemental building block in the development of biologically active molecules and as such most modern drug scaffolds contain a multitude of nitrogen atoms. The incorporation of nitrogen into a molecular scaffold can improve several physiochemical properties, such as enhancing oral bioavailability or increasing intra- and intermolecular interactions leading to higher drug potency.^{1,2} As a result, synthetic chemists are continually aiming to improve the synthetic toolbox for the construction of pharmaceutically relevant nitrogen-containing motifs. While the inclusion of relevant nitrogen-containing functional groups has been of longstanding interest, developments in elucidation, modeling, and testing of the active sites of drug targets has resulted in an increased focus on three-dimensional complex scaffolds which can have improved interactions within these active sites compared to their planar counterparts.^{3,4} As a result, research into the development of synthetic methods capable of building complex nitrogen scaffolds in a stereoselective fashion is of immense interest.⁵

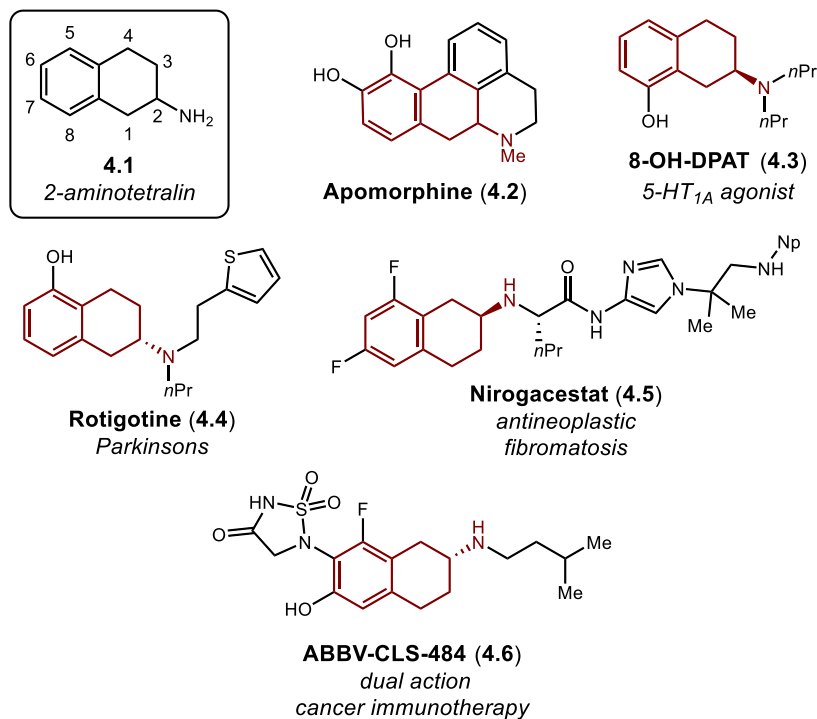
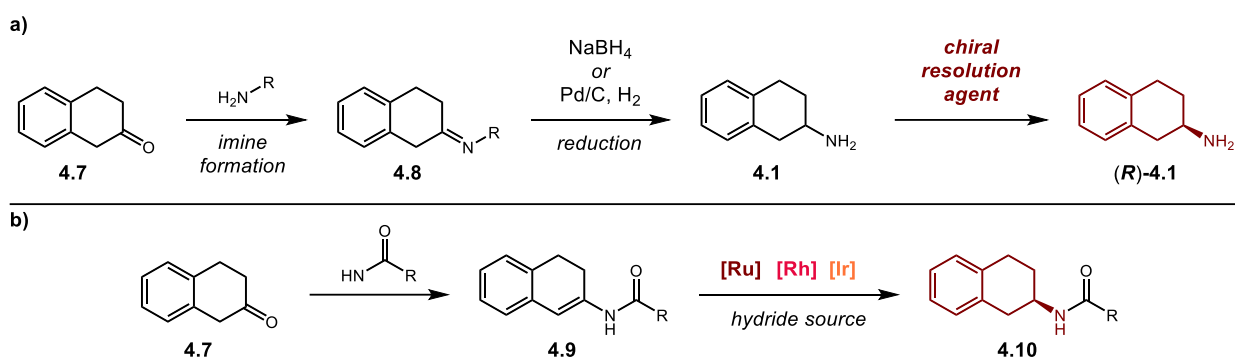


Figure 4.1 Examples of 2-Aminotetralin Motifs Found in Biologically Active Compounds.

One of the three-dimensional nitrogen-containing scaffolds that has received continued interest from medicinal chemists are 2-aminotetralins **4.1** (Figure 4.1). The first report of 2-aminotetralins exhibiting biological activity was disclosed by Bamberger and Filhene in 1889 although detailed understanding of their activity was limited.⁶ In 1969, Cannon and coworkers synthesized differentially substituted 2-aminotetralin scaffolds as simplified analogues of apomorphine **4.2** to better understand the biological activity of **4.2**.^{7,8} Further investigation into the biological activity of 2-aminotetralin led to the widespread recognition that this simple scaffold acts as a rigidified dopamine analogue and is a highly potent agonist for both dopamine and 5-hydroxytryptamine (5-HT) receptors.⁹⁻¹³ It has also been recognized that further research into the 2-aminotetralin scaffolds could lead to development of treatment options for a variety of neurological diseases such as Parkinson's disease,¹⁴ epilepsy,¹⁵ and addiction.¹⁶ Development of these scaffolds has successfully led to pharmaceuticals such as Rotigotine **4.4** which is used in the treatment of symptoms Parkinson's disease (Figure 4.1).¹⁷ The 2-aminotetralin scaffold has also been applied in the treatment of other disorders Nirogacestat **4.5**, for example, was first developed as an Alzheimer's disease treatment to reduce the formation of β -amyloid proteins, but ultimately found success as an anti-cancer

treatment for desmoid tumors, receiving a first-in-class designation from the FDA.^{18,19} Another recent example is ABBV-CLS-484 **4.6**, a dual action, immunotherapy anti-cancer agent which is designed to weaken cancerous cells and make them susceptible to attack from the body's immune system; this treatment is currently in Phase I clinical trials.²⁰ The success of the 2-aminotetralin framework over planar variants in these examples is due to the positioning of the chiral nitrogen center and the superior orientation this provides to attached functional groups necessary to bind within an active site.²¹

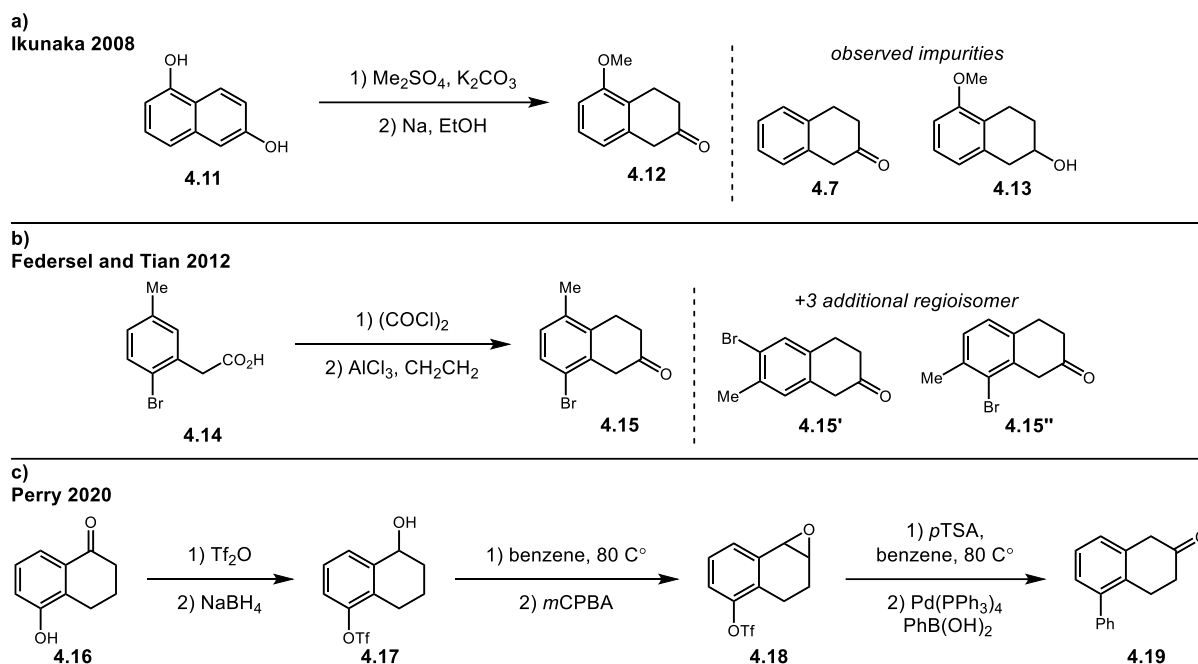
4.1.2 Enantioselective Synthesis of 2-Aminotetralins



Scheme 4.1 Enantioselective Synthesis of 2-Aminotetralins from β -Tetralones.

Although 2-aminotetralins have more than proven their worth in medicinal chemistry, the synthesis of this valuable scaffold, particularly the asymmetric synthesis, has been limited to a few approaches. The most prevalent synthetic strategy relies on the reductive amination of β -tetralones **4.7** via either imine or enamine intermediates (**Scheme 4.1a**). Early asymmetric synthetic routes relied on achiral reductions of imines followed by chiral resolution of the free amine **4.1** through the formation of diastereomeric salt pairs to obtain the desired chiral 2-aminotetralin (**Scheme 4.1a**).²²⁻²⁵ While this strategy has been successful and continues to be used, even on process scale, the formation of an unwanted enantiomer and the large amount of waste byproduct formed through the use of chiral resolution agents is inefficient and costly. Modern methods have sought to bypass these inefficiencies by applying advances in asymmetric hydrogenation chemistry to enable the enantioselective synthesis of 2-aminotetralins.²⁶ Transition metal-catalyzed asymmetric hydrogenations of enamides **4.9** have been the most frequently employed methods, commonly using Ru,²⁷⁻²⁹ Rh,³⁰⁻³² and Ir,³³⁻⁴⁰ with a variety of ligand scaffolds to provide high levels of enantioselectivity

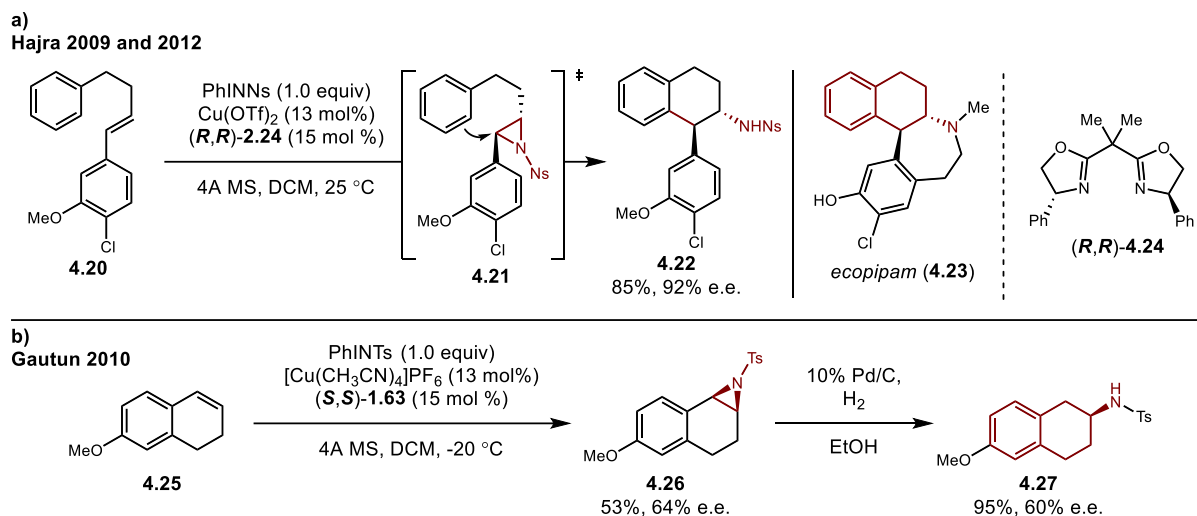
(Scheme 4.1b). An organocatalytic reductive amination was reported by Cheon in 2017; however, it does not exhibit the same excellent levels of enantiocontrol as transition metal-catalyzed methods.⁴¹



Scheme 4.2 Common Synthetic Routes Towards β -Tetralones.

Although both the achiral and asymmetric reductive amination of β -tetralones have become a reliable method to access chiral 2-aminotetralins, the synthesis of the required β -tetralones is a considerable bottleneck in this synthetic strategy. Most β -tetralones are commonly synthesized from the corresponding 2-naphthols **4.11** via Birch reduction (Scheme 4.2a).²² However, in some instances this process can lead to overreduction of the tetralin **4.7** and the formation of other inseparable byproducts **4.13**.²² Other routes have used phenylacetic acid derivatives **4.14** to conduct Friedel–Crafts alkylation in combination with ethylene (Scheme 4.2b).^{23,24} These, however, have been plagued by the formation of regioisomers (**4.15'**, **4.15''**) arising from the migration of substituents on cationic intermediates of the Friedel–Crafts alkylation. A more selective synthetic route has been employed by Perry beginning with the more accessible α -tetralone **4.16**; however, this route is significantly longer (Scheme 4.2c).¹³

Recognizing the challenges frequently encountered in the synthesis of 2-aminotetralins from β -tetralones, other synthetic routes have been explored. In 2009, Hajra reported the copper-catalyzed



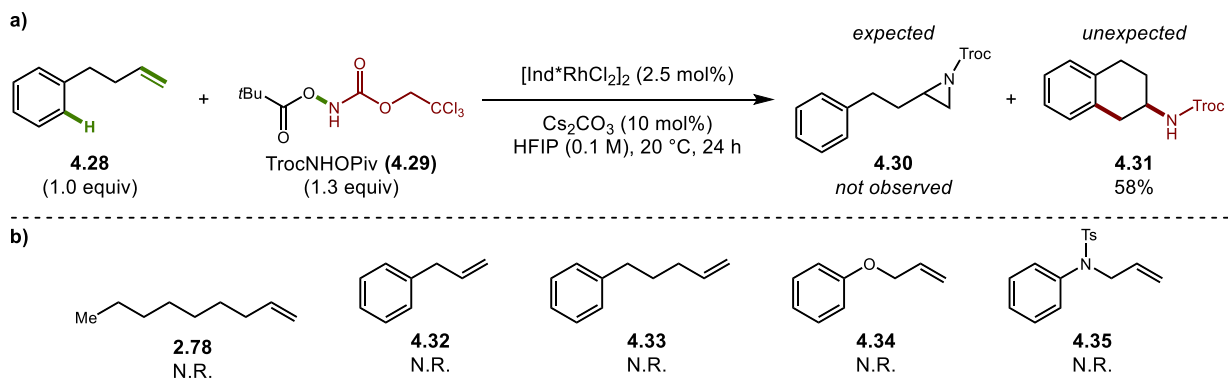
Scheme 4.3 Enantioselective Syntheses of 2-Aminotetralins Involving Aziridines Intermediates.

enantioselective synthesis of *trans*-aryl substituted 2-aminotetralins **4.22** via a tandem asymmetric aziridination of the linear precursor **4.20** followed by intramolecular ring opening of the aziridine **4.21** via an electrophilic aromatic substitution (**Scheme 4.3a**).⁴² This provided high levels of enantioselectivity enabling the synthesis of the dopamine agonist ecopipam **4.23**.⁴³ A similar strategy was reported by Gautun in 2010, which began with the enantioselective copper-catalyzed aziridination of the corresponding dihydronaphthalene **4.25**, followed by a regioselective palladium-catalyzed hydrogenolysis to provide the 2-aminotetralin **4.27** (**Scheme 4.3b**).⁴⁴ However, this method could only provide lower levels of enantioselectivity. Although strong precedent exists for the enantioselective synthesis of 2-aminotetralins, these can be plagued by significant side product formation. Given this limitation and the strong biological activity of the 2-aminotetralin scaffolds, the development of alternative synthetic methods is desirable.

4.2 Development of an Enantioselective 1,2-Arylamination

4.2.1 Reaction Discovery and Optimization

We became interested in 2-aminotetralin scaffolds following an unexpected discovery of new reactivity as we were exploring the breadth of our method for the enantioselective aziridination of unactivated alkenes.⁴⁵ We were interested in changing the *N*-substitution of the aziridines from the sulfonyl

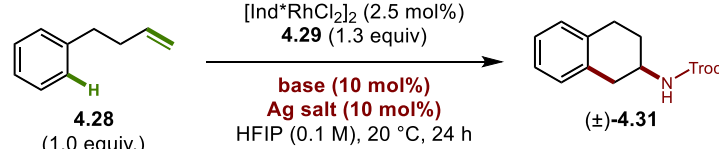


Scheme 4.4 Discovery of the 1,2-Arylamination of 4-phenylbutene.

group to a protecting group which would be more amenable towards mild deprotection. We investigated the use of carbamate protecting groups as these are commonly employed for the protection of amine functionalities and can be removed chemoselectively.⁴⁶ We selected the 2,2,2-trichloroethoxycarbonyl (Troc) protecting group as it has seen widespread success in electrophilic nitrogen reagents for the transfer of metal nitrenes to alkenes.⁴⁷ When we subjected 4-phenylbutene **4.28** and the electrophilic nitrogen reagent TrocNHOPiv **4.29** to our initial aziridination conditions utilizing $[\text{Ind}^*\text{RhCl}_2]_2$ we did not observe the formation of the desired aziridine **4.30** (Scheme 4.4a). Instead, the Troc-protected 2-aminotetralin **4.31** was formed in a 58% yield in a 6-*endo*-trig cyclization. Notably, **4.31** was the sole product formed with no allylic C–H amination products observed, and no products indicating a 5-*exo*-trig cyclization to form a substituted indane. We were further surprised to observe no reactivity when utilizing the alkene 1-nonene **2.78** which had proven to be an excellent substrate for aziridination under these conditions (Scheme 4.4b). Further investigation revealed this reaction to be highly selective, as the 5-*endo*-trig cyclization of allylbenzene **4.32** and the 7-*endo*-trig cyclization of 5-phenylpentene **4.33** were not observed. No reactivity was also observed for different oxygen and nitrogen linker substrates **4.34** and **4.35** hinting at similar selectivity for unactivated alkenes as in our aziridination work.

Having discovered this new reactivity, we next sought to optimize the racemic reaction conditions further. We began by investigating the addition of a silver halide scavenger as this had proven to be highly effective at improving the reactivity in our aziridination of unactivated alkenes. This was also found to be

Table 4.1 Optimization of Base and Silver Salt Additives in the Racemic 1,2-Arylamination



| entry | base | Ag salt | % yield ^a |
|-------|---------------------------------|--|----------------------|
| 1 | Cs ₂ CO ₃ | none | 58 |
| 2 | Cs ₂ CO ₃ | Ag ₂ CO ₃ ^b | 50 |
| 3 | Cs ₂ CO ₃ | AgSbF ₆ | 72 |
| 4 | Cs ₂ CO ₃ | AgNTf ₂ | 77 |
| 5 | CsOPiv | AgNTf ₂ | 74 |
| 6 | CsOAc | AgNTf ₂ | 83 |
| 7 | LiOAc | AgNTf ₂ | 76 |
| 8 | NaOAc | AgNTf ₂ | 78 |
| 9 | KOAc | AgNTf ₂ | 79 |
| 10 | none | none | 31 |
| 11 | none | AgNTf ₂ | 78 |
| 12 | CsOAc | none | 51 |

^aDetermined by ¹H-NMR using 1,3,5-trimethoxybenzene as an internal standard. ^b Ag₂CO₃ (5 mol%)

the case for this transformation as the addition of AgNTf₂ was found to be the most effective silver halide scavenger improving the yield of **4.31** to 77% (**Table 4.1, Entry 4**). Additional improvements could be achieved when changing the identity of the cesium base from carbonate to an acetate which provided **4.31** in an 83% yield (**Table 4.1, Entry 6**). Cesium was determined to be the best counteranion for the acetate base, with other base additives leading to reductions in yield (**Table 4.1, Entry 7-9**). Control reactions confirmed the importance of both additives as the absence of either or both was found to be detrimental to the reaction (**Table 4.1, Entry 10-12**).

We next sought to confirm the use of HFIP as the solvent and the use of an indenyl rhodium catalyst in the transformation as both can be considered exotic choices. Exploring several polar protic, polar aprotic, and nonpolar solvents confirmed the importance of HFIP in this transformation. Only TFE, often used interchangeably with HFIP, was able to produce **4.31** although in a significantly reduced yield of 37% (**Table 4.2, Entry 2**). All other solvents failed to provide the desired 2-aminotetrahydroindole **4.31** (**Table 4.1, Entry**

Table 4.2 Screening of Catalyst and Solvent in the Racemic 1,2-Arylamination.

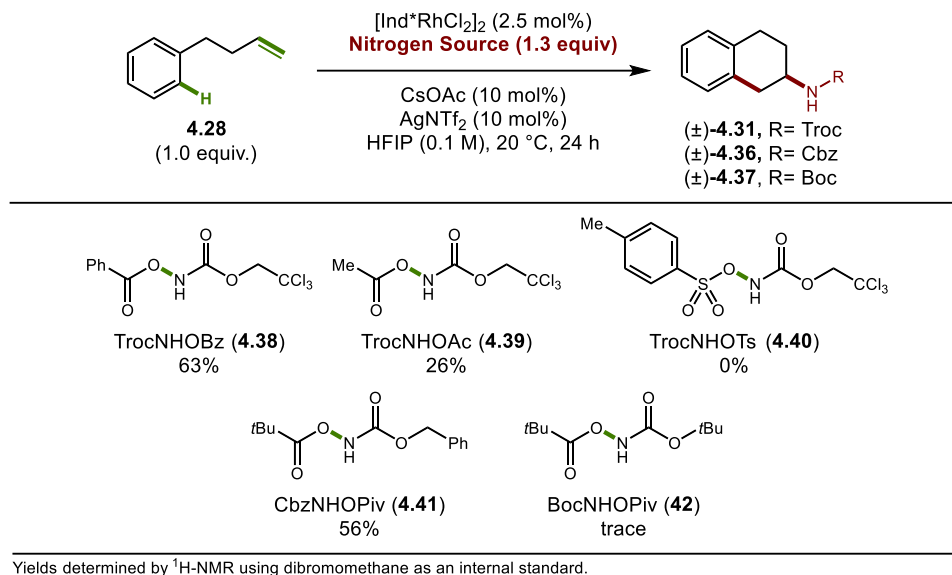
| entry | catalyst | Solvent | % yield ^a |
|-------|---------------------------------------|---------|----------------------|
| 1 | [Ind*RhCl ₂] ₂ | HFIP | 83 |
| 2 | [Ind*RhCl ₂] ₂ | TFE | 37 |
| 3 | [Ind*RhCl ₂] ₂ | MeOH | 0 |
| 4 | [Ind*RhCl ₂] ₂ | DCM | 0 |
| 5 | [Ind*RhCl ₂] ₂ | THF | 0 |
| 6 | [Ind*RhCl ₂] ₂ | toluene | 0 |
| 7 | [Ind*RhCl ₂] ₂ | DMF | 0 |
| 8 | Cp*Co(CO)I ₂ ^b | HFIP | 0 |
| 9 | [Cp*RhCl ₂] ₂ | HFIP | 0 |
| 10 | [Cp*IrCl ₂] ₂ | HFIP | 0 |

^aDetermined by ¹H-NMR using dibromomethane as an internal standard.

^b Cp*Co(CO)I₂ (5 mol%)

3-7). We propose the privileged nature of HFIP in this reaction is due to its observed ability to stabilize cationic intermediates.⁴⁸ To investigate the role of the indenyl ligand in this reaction, we tested the more common Cp* ligand on cobalt, rhodium and iridium catalysts. Surprisingly, no other catalyst examined was able to provide the 2-aminotetralin **4.31** confirming the importance of the indenyl ligand in this transformation (**Table 4.1, Entry 8-9**). Currently, computational investigations are being conducted by the Baik group to elucidate the origin in the vast difference in reactivity between the catalysts.

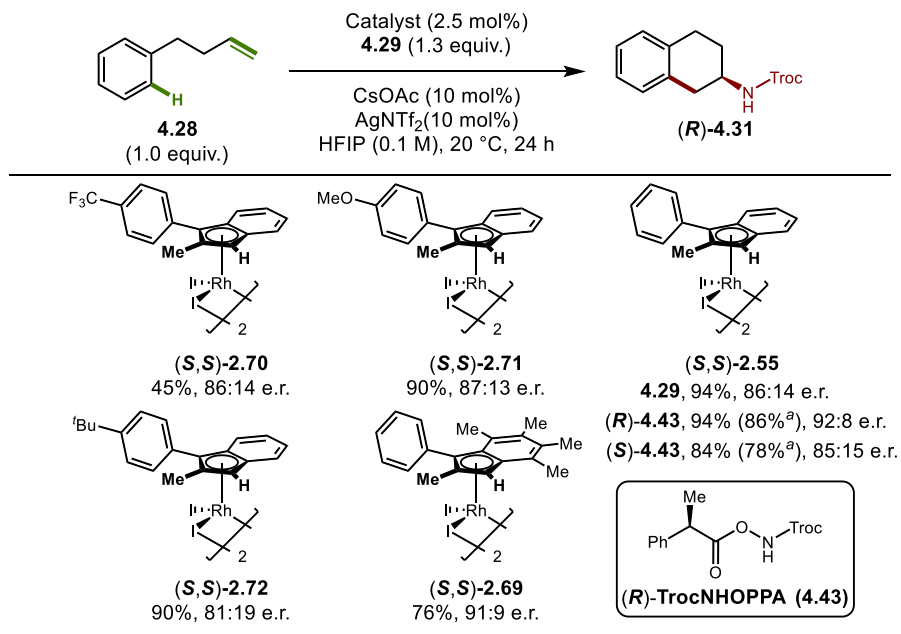
The last variable we sought to optimize in this racemic transformation was the identity of the nitrogen source itself, which was shown to be key to unlocking this new transformation. Changing the leaving group of the Troc nitrogen source from a pivalate on **4.29** to a benzoate **4.38** or acetate **4.39** was found to significantly reduce the reactivity only providing **4.31** in a 63% and 26% yield respectively (**Scheme 4.5**). Using a tosylate leaving group **4.40**—more commonly paired with a Troc-protected hydroxylamine electrophilic nitrogen reagent—we observed no reactivity, highlighting the importance the



Scheme 4.5 Examination of Hydroxylamine Carbamate Nitrogen Sources for the 1,2-Arylation.

carboxylate as the leaving group.⁴⁹⁻⁵¹ Finally, exchanging the Troc carbamate for either Cbz **4.41** or Boc **4.42** was found to be detrimental to the reaction providing the corresponding 2-aminotetralins **4.36** and **4.37** in a 56% and trace yields respectively (**Scheme 4.3b**). Once again, the importance of the Troc protecting group, and the divergent reactivity it provides compared to the Tosyl group of the aziridination is being investigated by the Baik group.

With optimized racemic reaction conditions in hand and results indicating a privileged role of the indenyl ligand we sought to render this transformation enantioselective using the planar chiral Rh(III) indenyl catalysts developed in our group. When utilizing the trifluoromethyl substituted catalyst (*S,S*)-**2.70**, the 2-aminotetralin (*R*)-**4.31** was formed in a 45% yield with a good enantioselectivity of 86:13 e.r. (**Scheme 4.5**). The methoxy substituted catalyst (*S,S*)-**2.71** was able to significantly improve the yield of (*R*)-**4.31** to 90% while maintaining good enantiocontrol (87:13 e.r.). Using the first-generation catalyst (*S,S*)-**2.55** further improved the yield to 94% (86:14 e.r.). The more electron-rich *tert*-butyl substituted catalyst (*S,S*)-**2.72** also provided (*R*)-**4.31** in an excellent yield of 90%, yet with reduced enantioselectivity (81:19 e.r.). Lastly, the highly electron-rich catalyst (*S,S*)-**2.69** could only provide (*R*)-**4.31** in a 76% yield yet with improved enantioselectivity of 91:9 e.r. due to the increased steric bulk of the methylated backbone.



Yields determined by ¹H-NMR using 1,3,5-trimethoxybenzene as an internal standard.

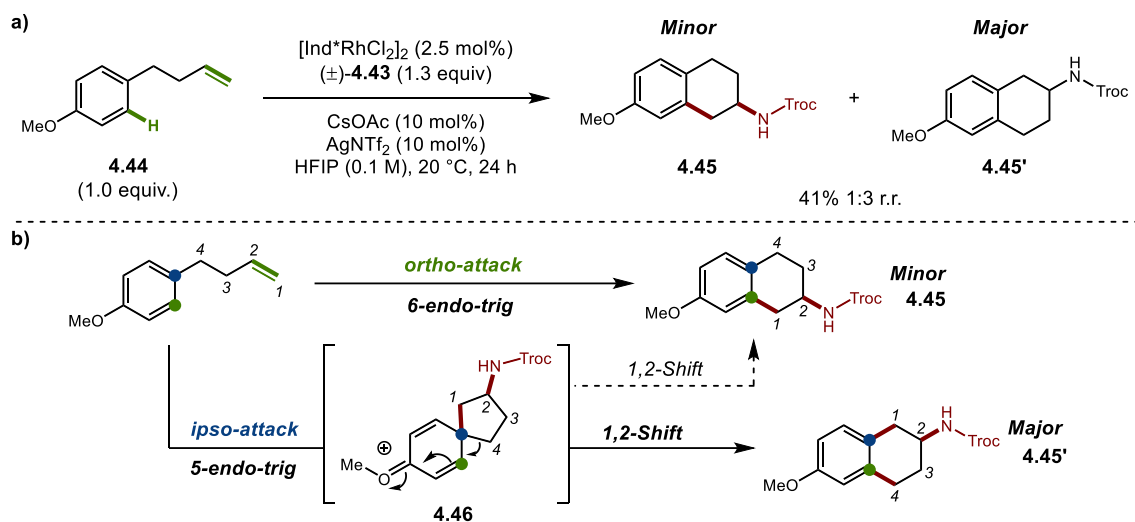
^a Isolated yield.

Scheme 4.6 Catalyst Optimization of the Enantioselective 1,2-Arylation.

While the yields provided by the first-generation catalyst were excellent, the enantiocontrol was not as strong. Furthermore, when attempting to isolate **(R)-4.31** from any of the reactions, we continually failed to remove excess of the nitrogen reagent **4.29**. This impurity could not be removed whether a basic workup was employed to wash out **4.29** or reductive methods were used to destroy the excess nitrogen source. The solution to the problem of low enantiocontrol and challenges in isolation was the use of the chiral nitrogen source TrocNHOPPA **4.43** (**Scheme 4.6**). This reagent exchanged the pivalate leaving group of **4.29** for a chiral 2-phenylpropionic acid leaving group. This leaving group retains some of the electronic and steric bulky characteristics of pivalate, while also enabling a cooperative effect with the chiral catalyst to improve the enantioselectivity of **(R)-4.31**. When the correct pairing of the chiral catalyst **(S,S)-2.55** was made with the new chiral nitrogen source **(R)-4.43**, the yield of **(R)-4.31** was maintained at 94%, with a now pure 86% isolated yield, and improved enantioselective to 92:8 e.r. The mismatched pairing of **(S)-4.43** with **(S,S)-2.55** led to a reduction in yield to 84% (78% isolated) and lower enantioselectivity (85:15 e.r.). The stereochemistry of **4.31** synthesized using catalyst **(S,S)-2.55** was assigned following comparison of the HPLC trace with a chiral standard of **(S)-4.31** which was synthesized via Troc-protection of the

commercially available unprotected chiral 2-aminotetralin (see SI for details). When this comparison was made the minor enantiomer formed was determined to be of the (*S*) configuration and the major enantiomer was assigned the (*R*) configuration. Therefore, **4.31** and all 1,2-arylamination products synthesized using the (*S,S*)-**2.55** catalyst were assigned the (*R*) configuration by analogy.

4.2.2 Regioselectivity and Scope of the Enantioselective 1,2-Arylamination

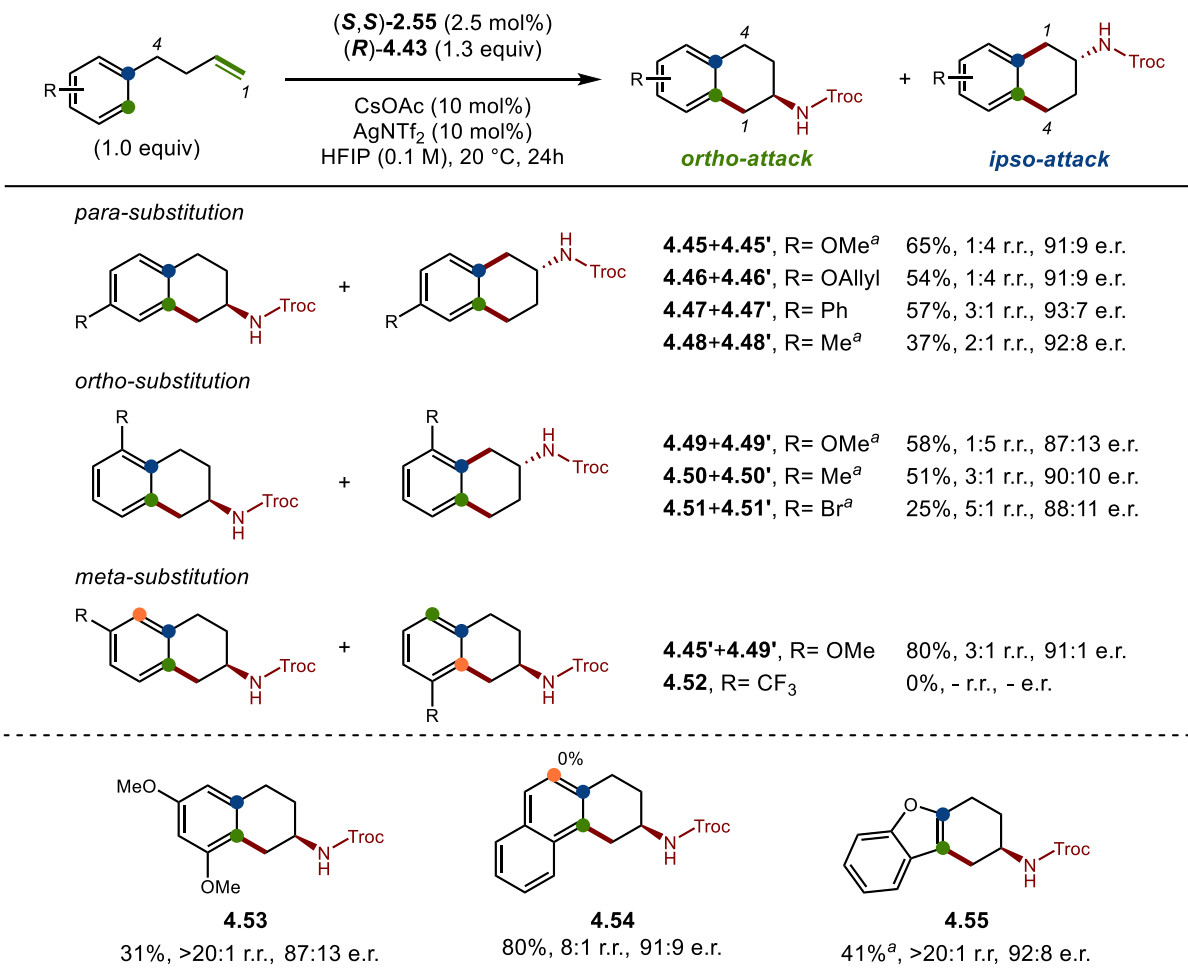


Scheme 4.7 Observation of 2-aminotetralin Regioisomers and Proposed Mechanisms Leading to the Formation of Both Regioisomers.

With optimized enantioselective conditions in hand, we set out to explore the scope of this 1,2-arylamination for the synthesis of 2-aminotetralins. As we began to explore a variety of substitutions on the aromatic ring of the 4-phenylbutene substrates we began to observe the formation of a new product. When subjecting the para-methoxy substrate **4.44** to racemic conditions using $[\text{Ind}^*\text{RhCl}_2]_2$ and (\pm)-**4.43**, we observed the formation of the expected 7-methoxy-2-aminotetralin **4.45** as the minor product while the 6-methoxy-2-aminotetralin **4.45'** was identified as the major (41%, 1:3 r.r.) (**Scheme 4.7a**). We hypothesize that the formation of the two regioisomers potentially arises due to two competing reaction pathways. The first is the 6-*endo*-trig cyclization to the *ortho* position, leading to the direct formation of the 7-substituted product **4.45** (**Scheme 4.7b**). The second pathway undergoes a 5-*endo*-trig cyclization to the *ipso* position, forming the intermediate hexadienone [4.5]-spirocycle **4.46**. This spirocycle can then undergo two potential

1,2-shifts. We hypothesize the shift of C4, leading to **4.45'**, is possibly preferred over the shift of C1, leading to formation of **4.45**, due to the proximity of the nitrogen at C2 deactivating C1 to rearrangement via inductive electron withdrawing effects. Although we do not have concrete evidence to preclude the 1,2-shift of C1, similar observations made by the Chang group regarding the skeletal rearrangement of γ -lactam spirocycles leads us to propose the 1,2-shift of C4 as the preferred skeletal rearrangement in this all-carbon spirocyclic intermediate (see **Chapter 3**).^{52,53} Despite this precedent from the Chang group, we acknowledge that we cannot preclude a 1,2-arylation mechanism which solely operates via a 5-*endo*-trig cyclization and at the time of completing this dissertation is an avenue which is being explored computationally in collaboration with the Baik group.

Having identified the formation of regioisomers in this cyclization we continued our investigation into the enantioselective scope of the 2-aminotetralins. The enantioselective synthesis of **4.45** could now be achieved in a 65% yield, a 91:9 e.r, and 1:4 r.r. favoring the formation of the 6-substituted product **4.45'** (**Scheme 4.8**). Similar reactivity was observed for the allyl-protected phenol which provided the 2-aminotetralin **4.46** in a 54% yield, 91:9 e.r, and 1:4 r.r. also favoring the 6-substituted **4.46'**. Para substitutions comprising of either phenyl and methyl were well tolerated, providing the 2-aminotetralins **4.47** and **4.48** in moderate to good yields (37-57%), and favoring the formation of 7-substituted 2-aminotetralins (2:1-3:1 r.r.), while maintaining high levels of enantioselectivity (92:8-93:7 e.r.). Placement of the methoxy group at the ortho-position provided **4.49** in a 58% yield, 1:5 r.r, and 87:13 e.r. favoring the formation of 8-methoxy-2-aminotetralin **4.49'** via the ipso-attack mechanism. The methyl and bromo ortho-substitution provided the 2-aminotetralins **4.50** and **4.51** in 51%, 90:10 e.r., and 25%, 88:11 e.r, respectively, both favoring the formation of the 5-substituted 2-aminotetralin (3:1-5:1 r.r.). Substitution at the meta-position was also tolerated providing the methoxy-substituted 2-aminotetralins **4.45'** and **4.49'** in a 80%, 3:1 r.r, and 91:1 e.r. The formation of both regioisomers in this example is likely not due to an intermediate spirocycle but due to the non-equivalent ortho-positions forming two different regioisomers via 6-*endo*-trig cyclization. Notably, trifluoromethyl meta-substitution does not allow for the formation of



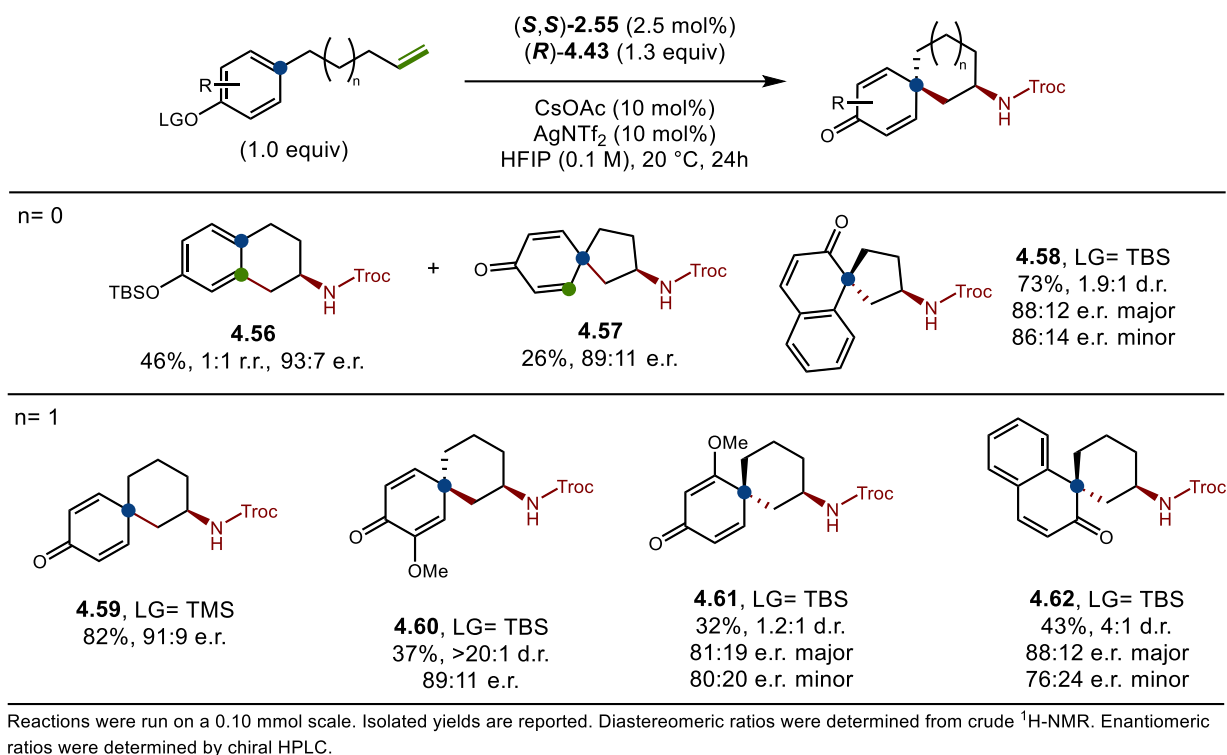
Reactions were run on a 0.10 mmol scale. Isolated yields are reported. Regioisomeric ratios were determined from crude NMR. Enantiomeric ratios of the major regioisomer were determined by chiral HPLC.^a 48 hr

Scheme 4.8 Scope of Chiral 2-Aminotetralins for the Enantioselective 1,2-Arylation.

4.52 and no reactivity is observed with this electron-poor substrate. This observation hints at a Friedel–Crafts type mechanism with electron-rich aromatic rings acting as nucleophiles.

Exploring other substitution patterns, the dimethoxy product **4.53** could be formed in a 31% yield and with excellent regioselectivity >20:1 r.r. (87:13 e.r.) (**Scheme 4.8**). The cyclization of a naphthyl substrate provided the bent product **4.54** in a 80% yield, 8:1 r.r., and 91:9 e.r., favoring cyclization at the nucleophilic 1-position of the naphthalene. It is important to note that while the minor regioisomer results from the formation of a spirocycle at the 2-position of the naphthalene, no linear products that would be formed from cyclization at the 3-position were observed. The benzofuran-derived product **4.55** was formed in a 41% yield, a single regioisomer (>20:1 r.r.), and in 92:8 e.r. Notably, this cyclization occurred at the

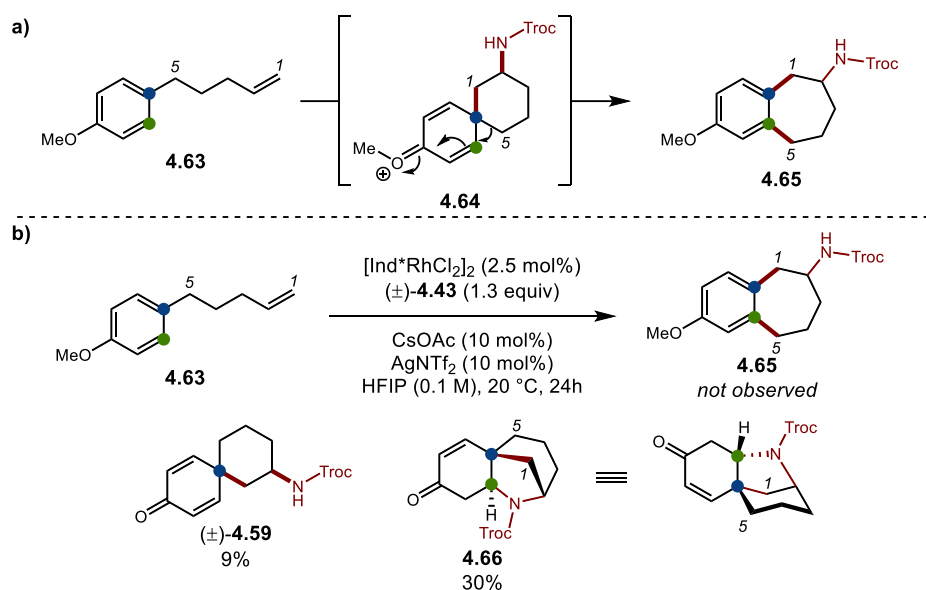
less nucleophilic 3-position of the benzofuran, with no products were observed indicating a 5-endo cyclization to the 2-position. This represents the current progress of the 2-aminotetralin scope which is being expanded upon by Wesley Pullara.



Scheme 4.9 Scope of Chiral 2-Aminospicycles for the Enantioselective 1,2-Arylamination.

We next turned our attention to investigating the formation of the intermediate hexadienone spirocycles, and whether these could be isolable products. Spirocyclic motifs are increasingly popular in drug design and provide an opportunity to impart significant three-dimensional complexity to a drug scaffold.⁵⁴ Subjecting the para-substituted silyl ether to the reaction conditions provided the 2-aminotetralin **4.56** in a 46% yield, 1:1 r.r., and 93:7 e.r., and the [4.5]-spirocycle **4.57** in a 26% yield and 89:11 e.r. (**Scheme 4.9**). When using a substrate which cannot undergo the 6-endo-trig cyclization pathway, the spirocycle can be formed as the sole product. Using a 2-naphthol derived substrate allowed for the isolation of the [4.5]-spirocycle **4.58** in a 73% yield, 1.9:1 d.r., and 88:12 e.r. Although 5-phenylpentene **4.33** did not react under the initial conditions, we hypothesized the formation of intermediate spirocycle would stabilize the dearomatization and enable the synthesis of [5.5]-spirocycles. This was proven to be true as the

[5.5]-spirocycle **4.59** could be formed in a 82% yield and 91:9 e.r. The 8-methoxy substituted [5.5]-spirocycle **4.60** could be formed in a 37% yield and as a single diastereomer (>20:1 d.r.), with a 89:11 e.r. The synthesis of 7-methoxy substituted [5.5]-spirocycle **4.61** could be achieved in a 32% yield and a reduced stereoselectivity of 1.2:1 d.r. and 81:19 e.r. for the major diastereomer. The 2-naphthol derived [5.5]-spirocycle **4.62** could be formed in a 43% yield with a 4:1 d.r. and 88:12 e.r. The lack of stereocontrol in the C–C bond formation likely indicates that the chiral catalyst is not directly involved in this step.

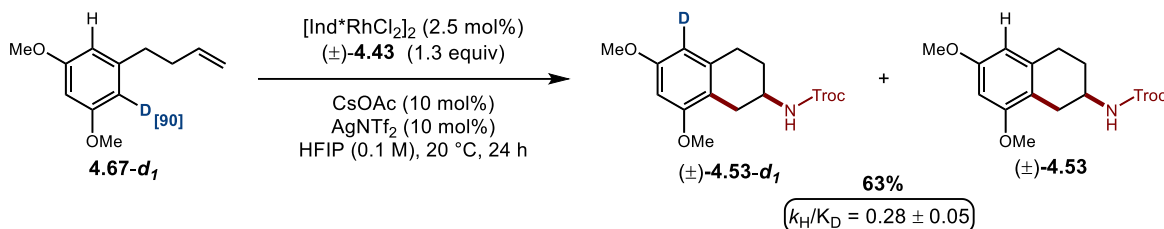


Scheme 4.10 Attempted Synthesis of a 2-Aminotetrahydroazulene Leading to the Formation of a Bridged Bicyclic Azepine.

Encouraged by the synthesis of the [5.5]-spirocycles, we sought to apply these as intermediates towards the synthesis of 2-aminotetrahydroazulenes **4.65** (Scheme 4.10a). We envisioned para-substituted 5-phenylpentene **4.63** undergoing the 6-endo-trig cyclization to the ipso-position to form the [5.5]-spirocycle intermediate **4.65**, which we then hypothesized would undergo the desired 1,2-shift forming the 2-aminotetrahydroazulene **4.65**. However, when **4.63** was subjected to the racemic conditions, we observed the formation of the spirocycle **4.59** in a 9% yield along with the formation of an unknown compound (Scheme 4.10b). After extensive 2D-NMR analysis the proposed structure for this compound is believed to be the bridged bicycle azepine **4.66** which was formed in a 30% yield (see SI for detailed NMR

analysis). We propose that this product is formed via nitrogen-directed C–H functionalization of the intermediate spirocycle **4.64**.

4.2.3 Mechanistic Investigations

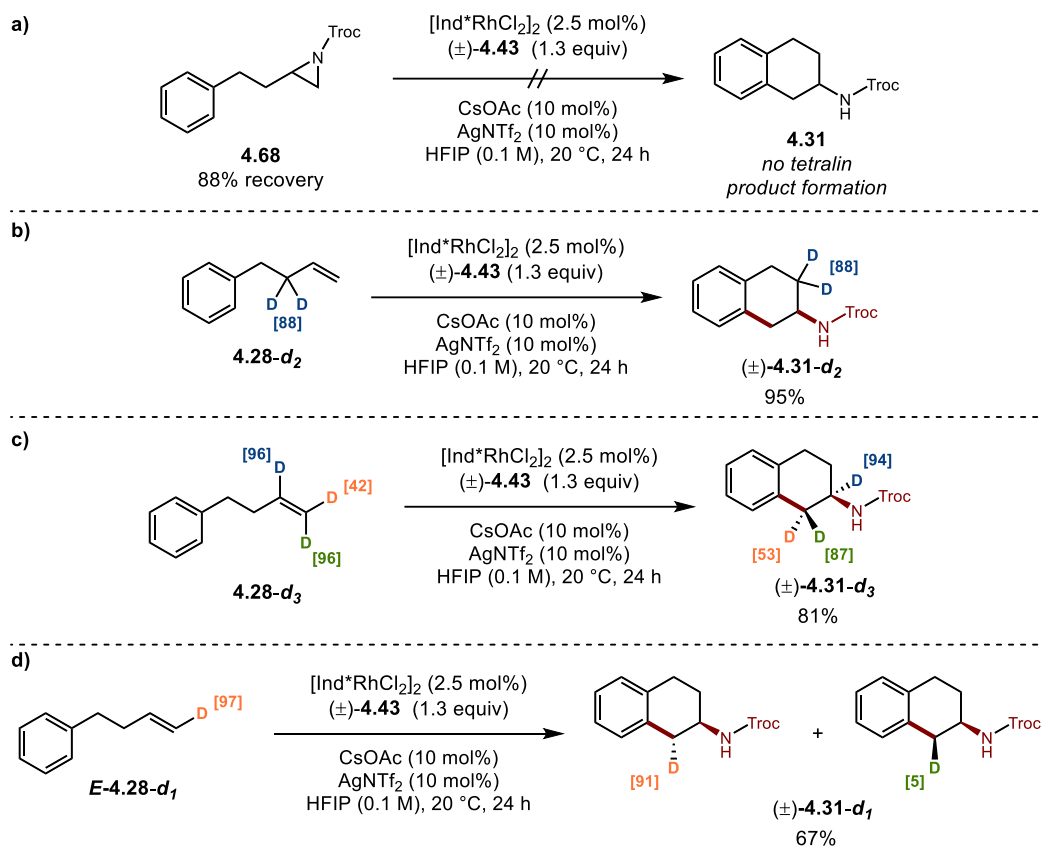


Scheme 4.11 Intramolecular Kinetic Isotope Effect Study

Within an extensive scope for the 1,2-arylamination nearly complete we sought to investigate the mechanism of this transformation. Based on several key observations made during the completion of the scope, namely the increased reactivity of electron-rich aryl rings, and the regioselectivity patterns of ortho- versus ipso-functionalization, we proposed that the key C–C bond formation occurs via an electrophilic aromatic substitution (EAS) mechanism. To further investigate the C–C bond formation we synthesized the monodeuterated substrate **4.67-d₁** and conducted an intramolecular kinetic isotope effect study (**Scheme 4.11**). When **4.67-d₁** was subjected to the reaction conditions the 2-aminotetralin **4.53-d₁** was formed in a 63% yield with an observed KIE of 0.28 ± 0.05 . While an inverse KIE is indicative of a secondary isotope effect associated with a sp^2 to sp^3 rehybridization observed during the C–C bond formation in an EAS mechanism, the magnitude of 0.28 is outside the anticipated range of 0.7-0.9 throwing the observed KIE into question.^{55,56} Ongoing experiments aim to clarify these results prior to publication of this research.

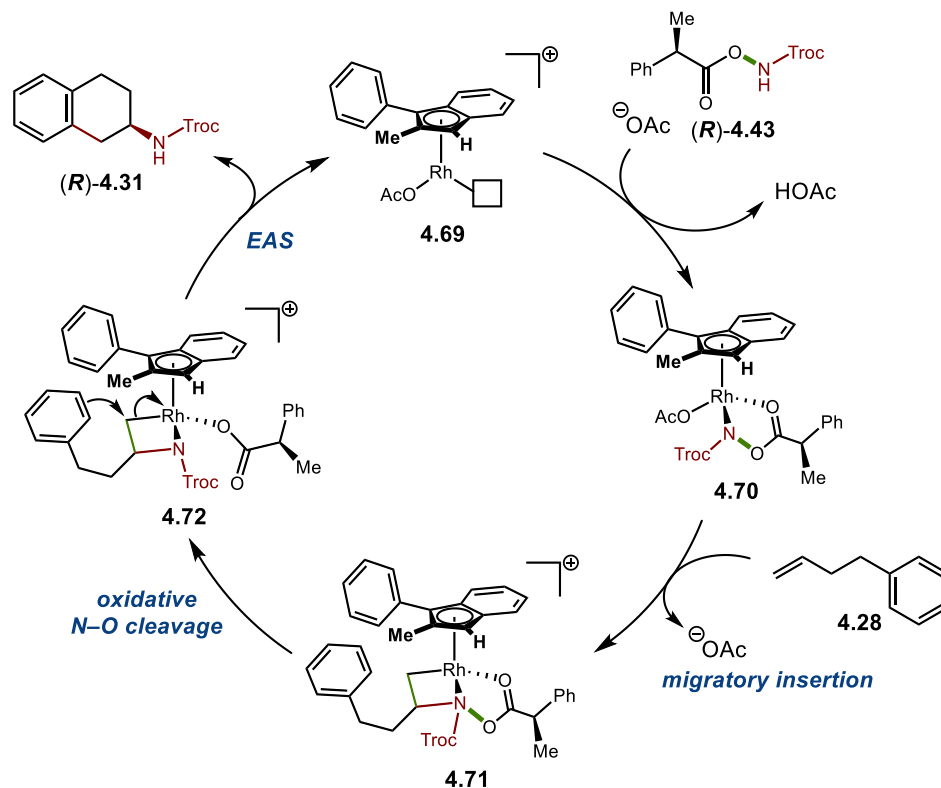
We next sought to identify the intermediate that is responsible for the C–N bond formation. An aziridine intermediate was initially considered as a candidate, since these have been proposed as key intermediates in Group IX catalyzed nucleophilic attacks involving electrophilic nitrogen reagents, as well as in the synthesis of 2-aminotetralins.^{42,57} However, the absence of any aziridine formation from reactions using either 4-phenylbutene **4.28** or 1-nonene **2.78** appeared to rule out this. To confirm this, we synthesized

Troc-protected aziridine **4.68** and subjected it to the reaction conditions which did not provide **4.31** and returned the unreacted aziridine **4.68** (88%) (**Scheme 4.12a**). Although we did not observe any allylic functionalization products, we next investigated whether a π -allyl intermediate could be involved in the C–N bond formation. When the allylic deuterated 4-phenylbutene **4.28-d₂** was subjected to the reaction



Scheme 4.12 Mechanistic Investigations to Identify the Electrophilic Intermediate in the 1,2-Arylamination.

conditions, the resulting 2-aminotetralin **4.31-d₂** (95%) did not show any deuterium scrambling at C3 which dispelled the intermediacy of a π -allyl (**Scheme 4.12b**). When subjecting the fully deuterated alkene **4.28-d₃** to the reaction conditions we observed no deuterium scrambling at C2 of the 2-aminotetralin **4.31-d₃** (81%) (**Scheme 4.12c**). The minimal deuterium scrambling observed at C1 (9%) is indicative of a mostly concerted mechanism. A second experiment using the monodeuterated *E*-**4.28-d₁** confirmed this as **4.31-d₁** (67% yield) also showed minimal deuterium scrambling (~5%) at C1 (**Scheme 4.12d**). These results indicate a concerted mechanism for the C–N bond formation in the 1,2-arylamination.



Scheme 4.13 Proposed Mechanism for the Enantioselective 1,2-Arylamination

At the time of the writing of this dissertation, our ongoing collaboration with the Baik group to elucidate the mechanism of this transformation computationally has not provided a conclusive answer to the identity of the electrophilic intermediate. However, based upon these experimental mechanistic investigations and the mechanistic investigations which were conducted for the enantioselective aziridination of unactivated alkenes, we propose the following catalytic cycle. The activation of the precatalyst (*S,S*)-2.55 by the silver halide scavenger provides the catalytic active species **4.69** (Scheme 4.13). The introduction of the nitrogen source **4.43** leads to the formation of intermediate **4.70**. Coordination and subsequent migratory insertion of the alkene **4.25** provides the four-membered aza-metallacycle **4.71** in a similar fashion to the enantioselective aziridination mechanism. Oxidative cleavage of the N–O bond forms the electrophilic Rh(V) aza-metallacycle **4.72** which is subjected to nucleophilic attack from the pendant aryl group. Subsequent rearomatization of the aromatic ring and protonation of the amine liberates the 2-aminotetralin **4.31** and closes the catalytic cycle. We propose the formation of the high valent Rh(V) intermediates **4.72** as the key step allowing the EAS mechanism to occur and is akin to the formation of

electrophilic metal nitrene intermediates and other electrophilic intermediates in precedent Group IX catalyzed nucleophilic attacks to electrophilic nitrogen species.

4.3 Conclusion

Following the development of our enantioselective unactivated alkene aziridination method, exploration into alternative aziridine *N*-substitution led to the discovery of a 1,2-arylamination of 4-phenylbutenes. This transformation provides an alternative synthetic route to pharmaceutically important 2-aminotetralin drug scaffold. During optimization studies, the Ind ligand was shown to be a privileged scaffold, over the more common Cp versions; this transformation could be rendered asymmetric using our planar chiral indenyl catalysts. Investigation of the scope of substituted 2-aminotetralins, revealed competing ortho- and ipso-cyclization mechanisms leading to the formation of regioisomers. Selective formation of the ipso-cyclization enabled the synthesis of unique 2-amino-carbospirocycles. Experimental mechanistic investigations indicate a nucleophilic attack of the aryl ring leads to the formation of the C–C bond. Aziridine and π -allyl intermediates have been ruled out for the formation of the C–N bond; our current proposed mechanism involves the formation of an aza-metallacycle as the key electrophilic intermediate. Ongoing computational mechanistic investigations conducted by the Baik group aim to identify the electrophilic intermediate and provide insight into how the divergent reactivity of the nitrogen sources results in either aziridination or 1,2 arylation.

4.4 References

- (1) Masand, V. H.; Al-Hussain, S.; Alzahrani, A. Y.; El-Sayed, N. N. E.; Yeo, C. I.; Tan, Y. S.; Zaki, M. E. A. Leveraging nitrogen occurrence in approved drugs to identify structural patterns. *Expert Opinion on Drug Discovery* **2024**, *19* (1), 111.
- (2) Pennington, L. D.; Moustakas, D. T. The Necessary Nitrogen Atom: A Versatile High-Impact Design Element for Multiparameter Optimization. *J. Med. Chem.* **2017**, *60* (9), 3552.
- (3) Lovering, F.; Bikker, J.; Humblet, C. Escape from Flatland: Increasing Saturation as an Approach to Improving Clinical Success. *J. Med. Chem.* **2009**, *52* (21), 6752.
- (4) Talele, T. T. Opportunities for Tapping into Three-Dimensional Chemical Space through a Quaternary Carbon. *J. Med. Chem.* **2020**, *63* (22), 13291.
- (5) Yang, H.; Yu, H.; Stolarzewicz, I. A.; Tang, W. Enantioselective Transformations in the Synthesis of Therapeutic Agents. *Chem. Rev.* **2023**, *123* (15), 9397.
- (6) Bamberger, E.; Filehne, W. Beziehungen zwischen physiologischen Eigenschaften und Constitution hydrirter Basen. *Berichte der deutschen chemischen Gesellschaft* **1889**, *22* (1), 777.
- (7) Sprenger, W.; Cannon, J.; Bahman, B.; Burkman, A. Centrally Acting Emetics. III. Derivatives of beta-Naphthylamine. *J. Med. Chem.* **1969**, *12* (3), 487.
- (8) Cannon, J. G.; Kim, J. C.; Aleem, M. A.; Long, J. P. Centrally acting emetics. 6. Derivatives of .beta.-naphthylamine and 2-indanamine. *J. Med. Chem.* **1972**, *15* (4), 348.
- (9) McDermed, J. D.; McKenzie, G. M.; Phillips, A. P. Synthesis and pharmacology of some 2-aminotetralins. Dopamine receptor agonists. *J. Med. Chem.* **1975**, *18* (4), 362.

- (10) Holmberg, P.; Sohn, D.; Leideborg, R.; Caldirola, P.; Zlatoidsky, P.; Hanson, S.; Mohell, N.; Rosqvist, S.; Nordvall, G.; Johansson, A. M. et al. Novel 2-Aminotetralin and 3-AminoChroman Derivatives as Selective Serotonin 5-HT₇ Receptor Agonists and Antagonists. *J. Med. Chem.* **2004**, *47* (16), 3927.
- (11) Canal, C. E.; Felsing, D. E.; Liu, Y.; Zhu, W.; Wood, J. T.; Perry, C. K.; Vemula, R.; Booth, R. G. An Orally Active Phenylaminotetralin-Chemotype Serotonin 5-HT₇ and 5-HT_{1A} Receptor Partial Agonist That Corrects Motor Stereotypy in Mouse Models. *ACS Chemical Neuroscience* **2015**, *6* (7), 1259.
- (12) Saraf, T. S.; McGlynn, R. P.; Bhatavdekar, O. M.; Booth, R. G.; Canal, C. E. FPT, a 2-Aminotetralin, Is a Potent Serotonin 5-HT_{1A}, 5-HT_{1B}, and 5-HT_{1D} Receptor Agonist That Modulates Cortical Electroencephalogram Activity in Adult Fmr1 Knockout Mice. *ACS Chemical Neuroscience* **2022**, *13* (24), 3629.
- (13) Perry, C. K.; Casey, A. B.; Felsing, D. E.; Vemula, R.; Zaka, M.; Herrington, N. B.; Cui, M.; Kellogg, G. E.; Canal, C. E.; Booth, R. G. Synthesis of novel 5-substituted-2-aminotetralin analogs: 5-HT_{1A} and 5-HT₇ G protein-coupled receptor affinity, 3D-QSAR and molecular modeling. *Bioorg. Med. Chem.* **2020**, *28* (3), 115262.
- (14) Meiring, L.; Petzer, J. P.; Legoabe, L. J.; Petzer, A. The evaluation of N-propargylamine-2-aminotetralin as an inhibitor of monoamine oxidase. *Bioorg. Med. Chem. Lett.* **2022**, *67*, 128746.
- (15) Armstrong, J. L.; Casey, A. B.; Saraf, T. S.; Mukherjee, M.; Booth, R. G.; Canal, C. E. (S)-5-(2'-Fluorophenyl)-N,N-dimethyl-1,2,3,4-tetrahydronaphthalen-2-amine, a Serotonin Receptor Modulator, Possesses Anticonvulsant, Prosocial, and Anxiolytic-like Properties

- in an Fmr1 Knockout Mouse Model of Fragile X Syndrome and Autism Spectrum Disorder. *ACS Pharmacology & Translational Science* **2020**, *3* (3), 509.
- (16) Fragola, N. R.; Brems, B. M.; Mukherjee, M.; Cui, M.; Booth, R. G. Conformationally Selective 2-Aminotetralin Ligands Targeting the α_2A - and α_2C -Adrenergic Receptors. *ACS Chemical Neuroscience* **2023**, *14* (10), 1884.
- (17) Horn, A. S.; Tepper, P.; Van Der Weide, J.; Watanabe, M.; Grigoriadis, D.; Seeman, P. Synthesis and radioreceptor binding activity of N-0437, a new, extremely potent and selective D2 dopamine receptor agonist. *Pharmaceutisch Weekblad* **1985**, *7* (5), 208.
- (18) Kummar, S.; Coyne, G. O. S.; Do, K. T.; Turkbey, B.; Meltzer, P. S.; Polley, E.; Choyke, P. L.; Meehan, R.; Vilimas, R.; Horneffer, Y. et al. Clinical Activity of the γ -Secretase Inhibitor PF-03084014 in Adults With Desmoid Tumors (Aggressive Fibromatosis). *Journal of Clinical Oncology* **2017**, *35* (14), 1561.
- (19) Brodney, M. A.; Auperin, D. D.; Becker, S. L.; Bronk, B. S.; Brown, T. M.; Coffman, K. J.; Finley, J. E.; Hicks, C. D.; Karmilowicz, M. J.; Lanz, T. A. et al. Design, synthesis, and in vivo characterization of a novel series of tetralin amino imidazoles as γ -secretase inhibitors: Discovery of PF-3084014. *Bioorg. Med. Chem. Lett.* **2011**, *21* (9), 2637.
- (20) Baumgartner, C. K.; Ebrahimi-Nik, H.; Iracheta-Vellve, A.; Hamel, K. M.; Olander, K. E.; Davis, T. G. R.; McGuire, K. A.; Halvorsen, G. T.; Avila, O. I.; Patel, C. H. et al. The PTPN2/PTPN1 inhibitor ABBV-CLS-484 unleashes potent anti-tumour immunity. *Nature* **2023**, *622* (7984), 850.
- (21) Karlen, A.; Johansson, A. M.; Kenne, L.; Arvidsson, L. E.; Hacksell, U. Conformational analysis of the dopamine-receptor agonist 5-hydroxy-2-(dipropylamino)tetralin and its C(2)-methyl-substituted derivative. *J. Med. Chem.* **1986**, *29* (6), 917.

- (22) Hirayama, Y.; Ikunaka, M.; Matsumoto, J. An Expeditious Scalable Synthesis of (S)-2-Amino-5-methoxytetralin via Resolution. *Organic Process Research & Development* **2005**, *9* (1), 30.
- (23) Federsel, H.-J.; Hedberg, M.; Qvarnström, F. R.; Tian, W. Optimization and Scale-up of a Pd-Catalyzed Aromatic C–N Bond Formation: A Key Step in the Synthesis of a Novel 5-HT1B Receptor Antagonist. *Organic Process Research & Development* **2008**, *12* (3), 512.
- (24) Schuisky, P.; Federsel, H.-J.; Tian, W. Regioisomerism in the Synthesis of a Chiral Aminotetralin Drug Compound: Unraveling Mechanistic Details and Diastereomer-Specific In-Depth NMR Investigations. *The Journal of Organic Chemistry* **2012**, *77* (13), 5503.
- (25) Akıncıoğlu, A.; Akbaba, Y.; Köse, L. P.; Akyüz, L. D.; Göksu, S. Synthesis and asymmetric resolution of substituted 2-aminoindane and 2-aminotetralin derivatives. *Tetrahedron* **2023**, *133*, 133277.
- (26) Cabré, A.; Verdager, X.; Riera, A. Recent Advances in the Enantioselective Synthesis of Chiral Amines via Transition Metal-Catalyzed Asymmetric Hydrogenation. *Chem. Rev.* **2022**, *122* (1), 269.
- (27) Imanishi, M.; Nakajima, Y.; Tomishima, Y.; Hamashima, H.; Washizuka, K.; Sakurai, M.; Matsui, S.; Imamura, E.; Ueshima, K.; Yamamoto, T. et al. Discovery of a Novel Series of Benzoic Acid Derivatives as Potent and Selective Human β_3 Adrenergic Receptor Agonists with Good Oral Bioavailability. 3. Phenylethanolaminotetraline (PEAT) Skeleton Containing Biphenyl or Biphenyl Ether Moiety. *J. Med. Chem.* **2008**, *51* (15), 4804.
- (28) Pautigny, C.; Debout, C.; Vayron, P.; Ayad, T.; Ratovelomanana-Vidal, V. Asymmetric hydrogenation of trisubstituted N-acetyl enamides derived from 2-tetralones using

- ruthenium-SYNPHOS catalysts: a practical synthetic approach to the preparation of β 3-adrenergic agonist SR58611A. *Tetrahedron: Asymmetry* **2010**, *21* (11), 1382.
- (29) Dupau, P.; Hay, A.-E.; Bruneau, C.; Dixneuf, P. H. Synthesis of optically active 2-aminotetraline derivatives via enantioselective ruthenium-catalyzed hydrogenation of ene carbamates. *Tetrahedron: Asymmetry* **2001**, *12* (6), 863.
- (30) Arribas, I.; Rubio, M.; Kleman, P.; Pizzano, A. Rhodium Phosphine–Phosphite Catalysts in the Hydrogenation of Challenging N-(3,4-dihydronaphthalen-2-yl) Amide Derivatives. *The Journal of Organic Chemistry* **2013**, *78* (8), 3997.
- (31) Jiang, X.-B.; Lefort, L.; Goudriaan, P. E.; de Vries, A. H. M.; van Leeuwen, P. W. N. M.; de Vries, J. G.; Reek, J. N. H. Screening of a Supramolecular Catalyst Library in the Search for Selective Catalysts for the Asymmetric Hydrogenation of a Difficult Enamide Substrate. *Angew. Chem. Int. Ed.* **2006**, *45* (8), 1223.
- (32) Liu, G.; Liu, X.; Cai, Z.; Jiao, G.; Xu, G.; Tang, W. Design of Phosphorus Ligands with Deep Chiral Pockets: Practical Synthesis of Chiral β -Arylamines by Asymmetric Hydrogenation. *Angew. Chem. Int. Ed.* **2013**, *52* (15), 4235.
- (33) Margalef, J.; Biosca, M.; de la Cruz-Sánchez, P.; Caldentey, X.; Rodríguez-Escrich, C.; Pàmies, O.; Pericàs, M. A.; Diéguez, M. Indene Derived Phosphorus-Thioether Ligands for the Ir-Catalyzed Asymmetric Hydrogenation of Olefins with Diverse Substitution Patterns and Different Functional Groups. *Adv. Synth. Catal.* **2021**, *363* (19), 4561.
- (34) Kawada, T.; Yabushita, K.; Yasuda, T.; Ohta, T.; Yajima, T.; Tanaka, K.; Utsumi, N.; Watanabe, M.; Murata, K.; Kayaki, Y. et al. Asymmetric Transfer Hydrogenative Amination of Benzylic Ketones Catalyzed by Cp*Ir(III) Complexes Bearing a Chiral N-(2-Picolyl)sulfonamidato Ligand. *The Journal of Organic Chemistry* **2022**, *87* (13), 8458.

- (35) Magre, M.; Pàmies, O.; Diéguez, M. PHOX-Based Phosphite-Oxazoline Ligands for the Enantioselective Ir-Catalyzed Hydrogenation of Cyclic β -Enamides. *ACS Catalysis* **2016**, *6* (8), 5186.
- (36) Biosca, M.; Magre, M.; Pàmies, O.; Diéguez, M. Asymmetric Hydrogenation of Disubstituted, Trisubstituted, and Tetrasubstituted Minimally Functionalized Olefins and Cyclic β -Enamides with Easily Accessible Ir-P,Oxazoline Catalysts. *ACS Catalysis* **2018**, *8* (11), 10316.
- (37) Renaud, J. L.; Dupau, P.; Hay, A.-E.; Guingouain, M.; Dixneuf, P. H.; Bruneau, C. Ruthenium-Catalysed Enantioselective Hydrogenation of Trisubstituted Enamides Derived from 2-Tetralone and 3-Chromanone: Influence of Substitution on the Amide Arm and the Aromatic Ring. *Adv. Synth. Catal.* **2003**, *345* (1-2), 230.
- (38) Patureau, F. W.; Worch, C.; Siegler, M. A.; Spek, A. L.; Bolm, C.; Reek, J. N. H. SIAPhos: Phosphorylated Sulfonimidamides and their Use in Iridium-Catalyzed Asymmetric Hydrogenations of Sterically Hindered Cyclic Enamides. *Adv. Synth. Catal.* **2012**, *354* (1), 59.
- (39) Salomó, E.; Orgué, S.; Riera, A.; Verdaguer, X. Highly Enantioselective Iridium-Catalyzed Hydrogenation of Cyclic Enamides. *Angew. Chem. Int. Ed.* **2016**, *55* (28), 7988.
- (40) Álvarez-Yebra, R.; Rojo, P.; Riera, A.; Verdaguer, X. Iridium complexes with P-stereogenic phosphino imidazole ligands: Synthesis, structure and catalysis. *Tetrahedron* **2019**, *75* (32), 4358.
- (41) Park, D. Y.; Kim, K.-H.; Cheon, C.-H. Enantioselective Synthesis of β -Aminotetralins via Chiral Phosphoric Acid-catalyzed Reductive Amination of β -Tetralones. *Adv. Synth. Catal.* **2018**, *360* (3), 462.

- (42) Hajra, S.; Maji, B.; Mal, D. A Catalytic and Enantioselective Synthesis of trans-2-Amino-1-aryltetralins. *Adv. Synth. Catal.* **2009**, *351* (6), 859.
- (43) Hajra, S.; Bar, S. Catalytic enantioselective synthesis of the dopamine D1 antagonist ecopipam. *Tetrahedron-Asymmetry* **2012**, *23* (2), 151.
- (44) Aaseng, J. E.; Melnes, S.; Reian, G.; Gautun, O. R. Asymmetric catalytic aziridination of dihydronaphthalenes for the preparation of substituted 2-aminotetralins. *Tetrahedron* **2010**, *66* (52), 9790.
- (45) Gross, P.; Im, H.; Laws, D., III; Park, B.; Baik, M.-H.; Blakey, S. B. Enantioselective Aziridination of Unactivated Terminal Alkenes Using a Planar Chiral Rh(III) Indenyl Catalyst. *J. Am. Chem. Soc.* **2024**, *146* (2), 1447.
- (46) Wuts, P. G. M.; Greene, T. W. *Greene's Protective Groups in Organic Synthesis*, 2006.
- (47) Luo, Y.; Zhang, X.; Xia, Y. Recent advances in transition-metal catalyzed nitrene transfer reactions with carbamates. *Chin. Chem. Lett.* **2024**, *35* (3), 108778.
- (48) Motiwala, H. F.; Armaly, A. M.; Cacioppo, J. G.; Coombs, T. C.; Koehn, K. R. K.; Norwood, V. M. I. V.; Aubé, J. HFIP in Organic Synthesis. *Chem. Rev.* **2022**, *122* (15), 12544.
- (49) Lebel, H.; Huard, K. De Novo Synthesis of Troc-Protected Amines: Intermolecular Rhodium-Catalyzed C–H Amination with N-Tosylloxycarbamates. *Org. Lett.* **2007**, *9* (4), 639.
- (50) Huard, K.; Lebel, H. N-Tosylloxycarbamates as Reagents in Rhodium-Catalyzed C–H Amination Reactions. *Chemistry – A European Journal* **2008**, *14* (20), 6222.
- (51) Lebel, H.; Lectard, S.; Parmentier, M. Copper-Catalyzed Alkene Aziridination with N-Tosylloxycarbamates. *Org. Lett.* **2007**, *9* (23), 4797.

- (52) Lee, E.; Hwang, Y.; Kim, Y. B.; Kim, D.; Chang, S. Enantioselective Access to Spirolactams via Nitrenoid Transfer Enabled by Enhanced Noncovalent Interactions. *J. Am. Chem. Soc.* **2021**, *143* (17), 6363.
- (53) Lee, J.; Lee, J.; Jung, H.; Kim, D.; Park, J.; Chang, S. Versatile Cp*Co(III)(LX) Catalyst System for Selective Intramolecular C-H Amidation Reactions. *J. Am. Chem. Soc.* **2020**, *142* (28), 12324.
- (54) Hiesinger, K.; Dar'ın, D.; Proschak, E.; Krasavin, M. Spirocyclic Scaffolds in Medicinal Chemistry. *J. Med. Chem.* **2021**, *64* (1), 150.
- (55) Gómez-Gallego, M.; Sierra, M. A. Kinetic Isotope Effects in the Study of Organometallic Reaction Mechanisms. *Chem. Rev.* **2011**, *111* (8), 4857.
- (56) Shi, S.-L.; Buchwald, S. L. Palladium-Catalyzed Intramolecular C-H Difluoroalkylation: Synthesis of Substituted 3,3-Difluoro-2-oxindoles. *Angew. Chem. Int. Ed.* **2015**, *54* (5), 1646.
- (57) Bergmeier, S. C.; Katz, S. J.; Huang, J.; McPherson, H.; Donoghue, P. J.; Reed, D. D. Intramolecular cyclization reactions of aziridines with π -nucleophiles. *Tetrahedron Lett.* **2004**, *45* (26), 5011.

4.5 Supporting Information

4.5.1 General Information

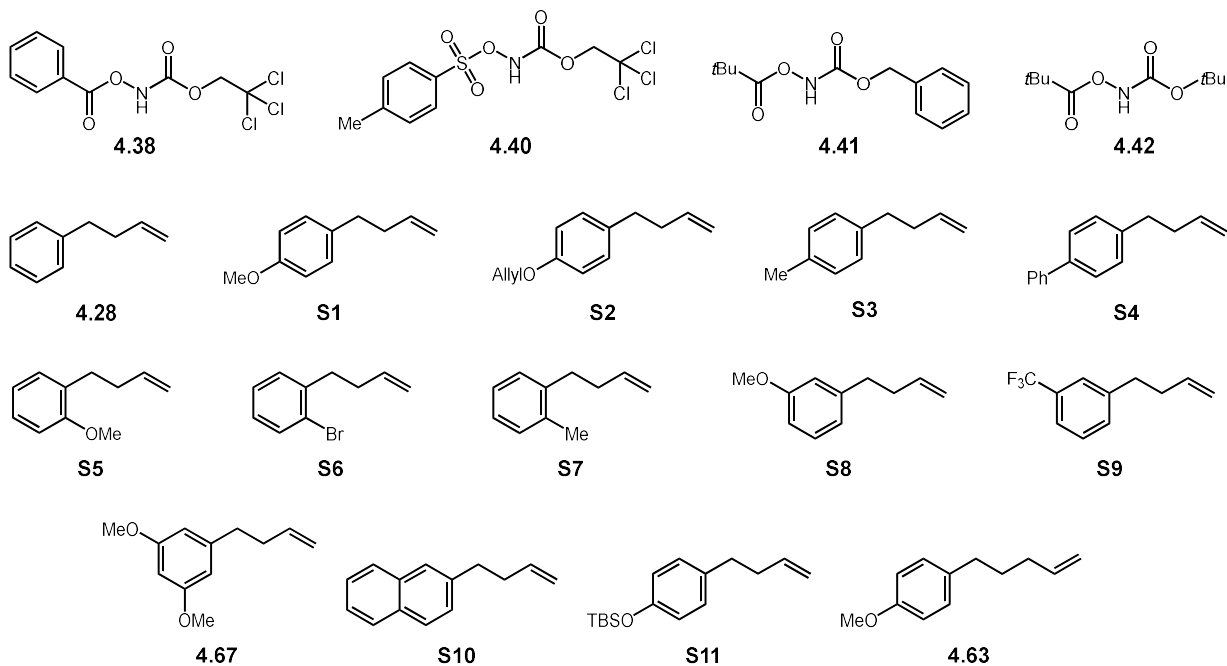
All reactions were conducted under nitrogen atmosphere with anhydrous solvents in oven- or flame-dried glassware using standard Schlenk technique, unless otherwise stated. Anhydrous dichloromethane (DCM), diethyl ether (Et₂O), tetrahydrofuran (THF), and were obtained by passage through activated alumina using a *Glass Contours* solvent purification system. 1,1,1,3,3,3-hexafluoroisopropanol (HFIP) was distilled over activated 4Å molecular sieves and stored over activated 4Å molecular sieves. Solvents for workup, extraction, and column chromatography were used as received from commercial suppliers without further purification. All catalysts were stored and weighed in a nitrogen-filled glovebox. All other chemicals were purchased from Millipore Sigma, Strem Chemicals, Oakwood Chemicals, Alfa Aesar, TCI, Combi Blocks, or Ambeed and used as received without further purification, unless otherwise stated.

¹H and ¹³C nuclear magnetic resonance (NMR) spectra were recorded on a Varian Inova 600 spectrometer (600 MHz ¹H, 151 MHz ¹³C), a Varian Inova 500 spectrometer (500 MHz ¹H, 126 MHz ¹³C), a Bruker 400 spectrometer (400 MHz ¹H, 126 MHz), a Varian Inova 400 spectrometer (400 MHz ¹H, 126 MHz ¹³C), and a. Chemical shifts δ values were reported in parts per million (ppm) relative to CHCl₃ (7.26 ppm for ¹H, 77.16 ppm for ¹³C) for CDCl₃, relative to C₆H₆ ((7.16 ppm for ¹H, 128.06 ppm for ¹³C) for C₆D₆, relative to DMSO (2.50 ppm for ¹H, 39.52 ppm for ¹³C) for DMSO-*d*₆. Coupling constants (*J* values) were reported in Hz and multiplicities were indicated using the following abbreviations: s = singlet, d = doublet, t = triplet, q = quartet, qn = quintet, m = multiplet, br = broad. High resolution mass spectra (HRMS) were obtained using a Thermo Electron Corporation Finigan LTQFTMS (at the Mass Spectrometry Facility, Emory University). High Pressure Liquid Chromatography (HPLC) was performed on an Agilent 1260 Infinity II series HPLC utilizing CHIRALPAK[®] IA, IB, IH, IJ, and IK 4.6 x 150 mm analytical columns. Semi preparative HPLC was performed on an Agilent 1260 Infinity II series preparative HPLC using a CHIRALCEL[®] OD-H 20 x 250 mm column. Supercritical Fluid Chromatography (SFC) was performed on

a Waters Acquity UPC2 system using methanol/isopropanol with 0.2% formic acid in supercritical carbon dioxide utilizing CHIRALCEL[®] OJ3 3 μm particle size, 150 mm x 3 mm analytical columns. Optical rotations were measured on a PerkinElmer 341 polarimeter. Analytical thin layer chromatography (TLC) was performed on precoated glass-backed Silicycle SiliaPureR 0.25 mm silica gel 60 plates and visualized with UV light or ethanolic *p*-anisaldehyde. Silica gel column chromatography was performed using Silicycle SiliaFlashR F60 silica gel (40- 63 μm). Flash column chromatography was performed using Silicycle SiliaFlashR F60 silica gel (40- 63 μm) on a Biotage Isolera One system. Preparatory TLC was performed on precoated glass backed Silicycle SiliaPureR 1.0 mm silica gel 60 plates.

4.5.2 Experimental Procedures and Tabulated Data

Preparation of Starting Materials



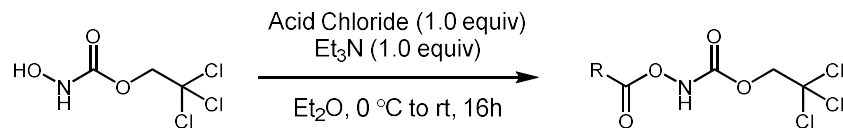
4.28 was obtained commercially and used without further purification.

4.38,¹ 4.40,² 4.41,³ 4.42,⁴ S1,⁵ S2,⁶ S3,⁵ S4,⁷ S5,⁸ S6,⁹ S7,¹⁰ S8,⁵ S9,⁷ 4.67,¹¹ S10,¹² S11,¹³ and 4.63¹⁴ were synthesized following reported literature procedures.

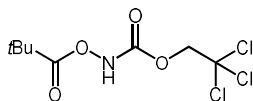
[Ind*RhCl₂]₂ catalyst was synthesized following a reported literature procedure.¹⁵

Catalysts (*S,S*)-2.55, (*S,S*)-2.69, (*S,S*)-2.70, (*S,S*)-2.71, and (*S,S*)-2.72 were all synthesized using a method previously reported by us.¹⁶

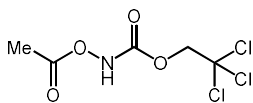
General Procedure A: Nitrogen Source Synthesis



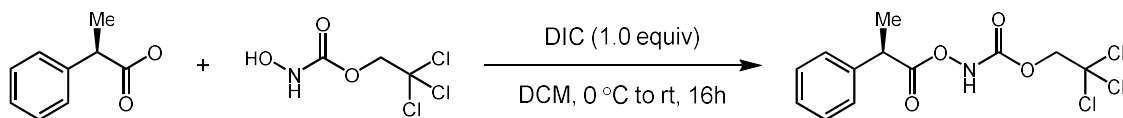
Under a N₂ atmosphere, Et₃N (1.0 equiv) was slowly added to a solution of 2,2,2-trichloroethyl hydroxycarbamate¹⁷ (1.0 equiv) in Et₂O (60mL) at 0 °C. Afterwards, acid chloride (1.0 equiv) was added dropwise leading to the formation of a white precipitate which was left to stir at room temperature overnight. The reaction was filtered through a Celite plug flushing with extra Et₂O. The solvent was removed under reduced pressure to provide the nitrogen source as an oil.



2,2,2-trichloroethyl (pivaloyloxy)carbamate (4.29): Prepared using General Procedure A, using 2,2,2-trichloroethyl hydroxycarbamate¹⁷ (8.0 g, 39 mmol) and pivaloyl chloride (4.7mL, 39 mmol) to provide **4.29** which was used without further purification (11.3 g, quant.) ¹H NMR (400 MHz, CDCl₃) δ 8.22 (s, 1H), 4.80 (s, 2H), 1.32 (s, 9H). ¹³C NMR (101 MHz, CDCl₃) δ 177.35, 154.88, 94.51, 75.27, 38.40, 27.05. HRMS (+APCI) calculated for C₈H₁₁O₄NC₃ [M-H]⁻ 289.97591, found 289.97671.

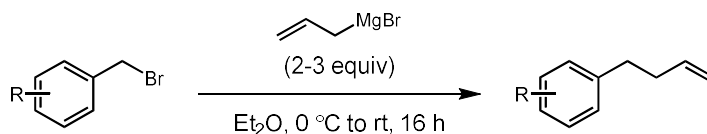


2,2,2-trichloroethyl acetoxycarbamate (4.39): Prepared using General Procedure A, using 2,2,2-trichloroethyl hydroxycarbamate¹⁷ (2.1 g, 10 mmol) and acetyl chloride (0.7 mL, 10 mmol) to provide **4.39** which was used without further purification (2.51 g, quant.) ¹H NMR (400 MHz, CDCl₃) δ 8.41 (s, 1H), 4.80 (s, 2H), 2.24 (s, 3H). ¹³C NMR (101 MHz, CDCl₃) δ 169.60, 154.67, 94.49, 75.23, 18.33. HRMS (+APCI) calculated for C₅H₅O₄NC₃ [M-H]⁻ 247.92896, found 247.92879.



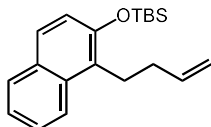
2,2,2-trichloroethyl (R)-((2-phenylpropanoyl)oxy)carbamate ((R)-4.43): Using an adapted procedure by Meggers.¹⁷ Under an N₂ atmosphere, in a 250 mL RBF equipped with a stir bar, 2,2,2-trichloroethyl hydroxycarbamate¹⁷ (4.17 g, 20.0 mmol, 1.0 equiv) was dissolved in DCM (124 mL) and the reaction vessel placed in an ice bath. Once cool, (*R*)-2-phenylpropanoic acid (2.7 mL, 20.0 mmol, 1.0 equiv) was added followed by the addition of a DIC (3.1 mL, 200 mmol 1.0 equiv). The reaction was stirred at room temperature overnight. Once complete, the solvent was removed under reduced pressure and the crude residue was immediately columned using flash column chromatography (5% EtOAc in Hexanes) to afford (*R*)-4.43 as a slow crystallizing colorless solid. (4.84 g, 72%) ¹H NMR (400 MHz, CDCl₃) δ 8.15 (s, 1H), 7.38 – 7.27 (m, 5H), 4.80 (d, *J* = 11.9 Hz, 1H), 4.76 (d, *J* = 11.9 Hz, 1H), 3.93 (q, *J* = 7.2 Hz, 1H), 1.61 (d, *J* = 7.2 Hz, 3H). ¹³C NMR (101 MHz, CDCl₃) δ 173.44, 154.59, 138.50, 129.04, 127.96, 127.71, 94.45, 75.27, 43.38, 18.57. Spectroscopic data for (*R*)-4.43 matches those previously reported in the literature.¹⁷ (±)-4.43 and (*S*)-4.43 were synthesized in the same manner.

General Procedure B: Allyl Magnesium Bromide Addition to Benzylbromides



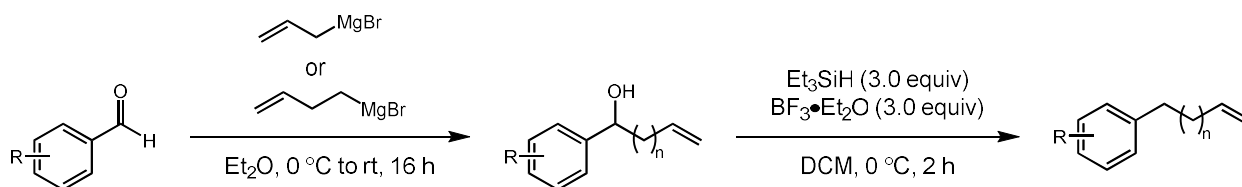
Under an N₂ atmosphere and at 0 °C, allyl magnesium bromide (1.0M in Et₂O, 2-3 equiv) was slowly added to a solution of the benzyl bromide substrate (1.0 equiv) in Et₂O (0.25M). Once the addition was completed the reaction was left to stir at room temperature overnight. The reaction was placed in an ice bath and slowly quenched with sat. NH₄Cl. The resulting biphasic solution was extracted with Et₂O (3x) and the combined organic layers washed with brine 1x. The organic layers were dried over MgSO₄ and the solvent removed

under reduced pressure. The crude product was purified on silica gel column chromatography (100% Hexanes) to provide the final product.



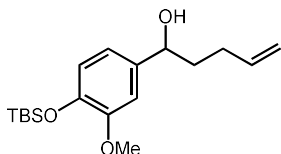
((1-(but-3-en-1-yl)naphthalen-2-yl)oxy)(tert-butyl)dimethylsilane (S12): Prepared using General Procedure B and *((1-(bromomethyl)naphthalen-2-yl)oxy)(tert-butyl)dimethylsilane*¹⁸ (1.76g, 5.0 mmol). **S12** colorless oil (0.968 g, 62% yield). ¹H NMR (400 MHz, CDCl₃) δ 7.95 (dd, *J* = 8.6, 1.0 Hz, 1H), 7.78 (dd, *J* = 8.2, 1.5 Hz, 1H), 7.62 (d, *J* = 8.8 Hz, 1H), 7.48 (ddd, *J* = 8.4, 6.8, 1.4 Hz, 1H), 7.34 (ddd, *J* = 8.0, 6.7, 1.1 Hz, 1H), 7.10 (d, *J* = 8.8 Hz, 1H), 5.99 (ddt, *J* = 16.9, 10.2, 6.6 Hz, 1H), 5.12 (dq, *J* = 17.1, 1.7 Hz, 1H), 5.02 (ddd, *J* = 10.1, 2.1, 1.1 Hz, 1H), 3.20 – 3.10 (m, 2H), 2.43 – 2.32 (m, 2H), 1.08 (s, 9H), 0.28 (s, 6H). ¹³C NMR (101 MHz, CDCl₃) δ 150.62, 138.83, 133.44, 129.61, 128.61, 127.32, 126.19, 125.17, 123.43, 123.31, 120.43, 114.64, 34.15, 25.99, 25.30, 18.46, -3.75. HRMS (+APCI) calculated for C₂₀H₂₉OSi [M+H]⁺ 313.19822, found 313.19797.

General Procedure C: Grignard Addition to Benzaldehydes

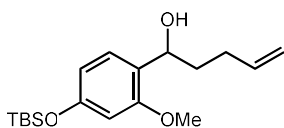


Under an N₂ atmosphere and at 0 °C, either allyl magnesium bromide or freshly prepared 3-butenylmagnesium bromide (1.0M in Et₂O, 2-3 equiv) was slowly added to a solution of the benzaldehyde substrate (1.0 equiv) in THF (0.25M). Once the addition was completed the reaction was left to stir at room temperature overnight. The reaction was placed in an ice bath and slowly quenched with sat. NH₄Cl. The resulting biphasic solution was extracted with Et₂O (3x) and the combined organic layers washed with brine 1x. The organic layers were dried over MgSO₄ and the solvent removed under reduced pressure. The crude

product was purified on silica gel column chromatography (0-10% EtOAc in Hexanes) to provide the benzyl alcohol product.

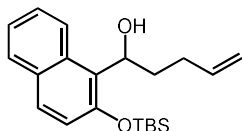


1-(4-((tert-butyldimethylsilyl)oxy)-3-methoxyphenyl)pent-4-en-1-ol (**S13**): Prepared using General Procedure C, 4-((tert-butyldimethylsilyl)oxy)-3-methoxybenzaldehyde¹³ (2.04g, 7.67 mmol) and 3-butenylmagnesium bromide (20 mL, 1.0M in Et₂O, 2.6 equiv). **S13** colorless oil (1.951 g, 79% yield). ¹H NMR (400 MHz, CDCl₃) δ 6.86 (d, *J* = 2.0 Hz, 1H), 6.80 (d, *J* = 8.0 Hz, 1H), 6.76 (dd, *J* = 8.2, 2.0 Hz, 1H), 5.83 (ddt, *J* = 16.9, 10.2, 6.6 Hz, 1H), 5.03 (dq, *J* = 17.1, 1.7 Hz, 1H), 4.97 (ddt, *J* = 10.2, 2.2, 1.3 Hz, 1H), 4.61 (t, *J* = 6.7 Hz, 1H), 3.81 (s, 3H), 2.21 – 1.99 (m, 2H), 1.95 – 1.71 (m, 3H), 0.99 (s, 9H), 0.15 (s, 6H). ¹³C NMR (101 MHz, CDCl₃) δ 150.99, 144.42, 138.31, 138.15, 120.64, 118.28, 114.91, 109.68, 74.03, 55.47, 38.02, 30.22, 25.74, 18.47, -4.61. HRMS (+APCI) calculated for C₁₈H₃₁O₃Si [M+H]⁺ 323.2037, found 323.2040



1-(4-((tert-butyldimethylsilyl)oxy)-2-methoxyphenyl)pent-4-en-1-ol (**S14**): Prepared using General Procedure C, 4-((tert-butyldimethylsilyl)oxy)-2-methoxybenzaldehyde¹⁹ (2.04 g, 7.67 mmol), and 3-butenylmagnesium bromide (20 mL, 1.0M in Et₂O, 2.6 equiv). **S14** colorless oil (1.651 g, 67% yield). ¹H NMR (400 MHz, CDCl₃) δ 7.10 (d, *J* = 8.2 Hz, 1H), 6.41 (dd, *J* = 8.1, 2.2 Hz, 1H), 6.38 (d, *J* = 2.2 Hz, 1H), 5.85 (ddt, *J* = 16.9, 10.2, 6.5 Hz, 1H), 5.04 (ddt, *J* = 17.2, 2.1, 1.6 Hz, 1H), 4.96 (ddt, *J* = 10.2, 2.2, 1.3 Hz, 1H), 4.80 (dt, *J* = 7.9, 5.9 Hz, 1H), 3.80 (s, 3H), 2.47 (d, *J* = 6.3 Hz, 1H), 2.27 – 2.15 (m, 1H), 2.15 – 2.04 (m, 1H), 1.98 – 1.75 (m, 2H), 0.98 (s, 9H), 0.20 (s, 6H). ¹³C NMR (101 MHz, CDCl₃) δ 157.60,

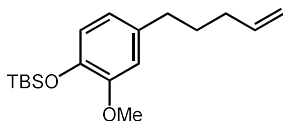
156.01, 138.66, 127.50, 125.22, 114.57, 111.57, 103.56, 70.40, 55.26, 36.33, 30.42, 25.71, 18.23, -
4.36. **HRMS** (+APCI) calculated for C₁₈H₃₁O₃Si [M+H]⁺ 323.2037, found 323.20416



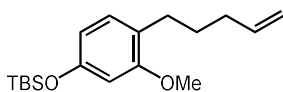
1-(2-((tert-butyl dimethylsilyl)oxy)naphthalen-1-yl)pent-4-en-1-ol (S15): Prepared using General Procedure C, 2-((tert-butyl dimethylsilyl)oxy)-1-naphthaldehyde²⁰ (3.10 g, 10.8 mmol), and 3-butenylmagnesium bromide (22 mL, 1.0M in Et₂O, 2.0 equiv). **S15** colorless oil (2.16 g, 58% yield). **¹H NMR** (400 MHz, CDCl₃) δ 8.27 (d, *J* = 8.7 Hz, 1H), 7.77 (d, *J* = 7.9 Hz, 1H), 7.67 (d, *J* = 8.9 Hz, 1H), 7.47 (ddd, *J* = 8.5, 6.8, 1.5 Hz, 1H), 7.36 (ddd, *J* = 8.0, 6.8, 1.1 Hz, 1H), 7.09 (d, *J* = 8.9 Hz, 1H), 5.90 (ddt, *J* = 16.6, 10.1, 6.4 Hz, 1H), 5.61 (dd, *J* = 8.9, 5.1 Hz, 1H), 5.07 (dq, *J* = 17.0, 1.3 Hz, 1H), 4.99 (ddt, *J* = 10.1, 2.2, 1.1 Hz, 1H), 3.39 (s, 1H), 2.50 – 2.32 (m, 1H), 2.33 – 2.11 (m, 2H), 2.03 – 1.85 (m, 1H), 1.08 (s, 9H), 0.38 (s, 3H), 0.33 (s, 3H). **¹³C NMR** (101 MHz, CDCl₃) δ 150.58, 138.55, 132.31, 129.82, 129.00, 128.66, 126.37, 126.10, 124.00, 123.75, 120.05, 114.91, 69.38, 36.55, 30.79, 26.09, 18.51, -3.29, -3.78. **HRMS** (+APCI) calculated for C₂₁H₂₉O₂Si [M-H]⁻ 341.19423, found 341.19365

General Procedure D: Deoxygenation

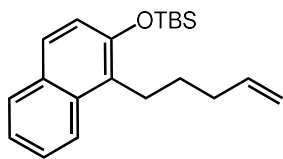
Under an N₂ atmosphere, the benzyl alcohol (1.0 equiv) was dissolved in a DCM (0.1M) and placed in an ice bath to cool to 0 °C. Once cool, Et₃SiH (3.0 equiv) was added followed by the dropwise addition of BF₃•Et₂O (3.0 equiv). The reaction was left to stir at 0 °C and product formation was monitored by TLC. Once consumption of starting material was observed (~2 h) sat. NaHCO₃ was slowly added, and the reaction was stirred for an additional 20 min at 0 °C. The reaction was extracted with DCM (3X) and the combined organic washed with brine (1x). The organic layers were dried over Na₂SO₄ and solvent removed under reduced pressure. The crude product was purified on silica gel column chromatography (0-5% EtOAc in Hexanes) to provide the final product.



tert-butyl(2-methoxy-4-(pent-4-en-1-yl)phenoxy)dimethylsilane (S16): Prepared using General Procedure D and **S13** (0.847 g, 2.63 mmol). **S16** colorless oil (0.535 g, 66% yield). **¹H NMR** (400 MHz, CDCl₃) δ 6.76 (d, *J* = 8.0 Hz, 1H), 6.67 (d, *J* = 2.0 Hz, 1H), 6.62 (dd, *J* = 8.0, 2.1 Hz, 1H), 5.84 (ddt, *J* = 16.9, 10.2, 6.6 Hz, 1H), 5.09 – 4.93 (m, 2H), 3.79 (s, 3H), 2.60 – 2.49 (m, 2H), 2.14 – 2.03 (m, 2H), 1.76 – 1.64 (m, 2H), 1.00 (s, 9H), 0.15 (s, 5H). **¹³C NMR** (101 MHz, CDCl₃) δ 150.63, 142.91, 138.77, 135.95, 120.60, 120.47, 114.65, 112.51, 55.48, 35.02, 33.34, 30.79, 25.78, 18.47, -4.61. **HRMS** (+APCI) calculated for C₁₈H₃₁O₂Si [M+H]⁺ 307.20878, found 307.20899

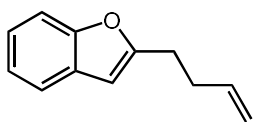


tert-butyl(3-methoxy-4-(pent-4-en-1-yl)phenoxy)dimethylsilane (S17): Prepared using General Procedure D and **S14** (0.837 g, 2.60 mmol). **S17** colorless oil (0.3474 g, 43% yield). **¹H NMR** (400 MHz, CDCl₃) δ 6.93 (d, *J* = 8.6 Hz, 1H), 6.38 – 6.33 (m, 2H), 5.85 (ddt, *J* = 16.9, 10.2, 6.6 Hz, 1H), 5.02 (ddd, *J* = 17.1, 3.8, 1.6 Hz, 1H), 4.95 (ddt, *J* = 10.2, 2.4, 1.2 Hz, 1H), 3.77 (s, 2H), 2.58 – 2.49 (m, 2H), 2.12 – 2.03 (m, 2H), 1.69 – 1.58 (m, 2H), 0.99 (s, 8H), 0.20 (s, 5H). **¹³C NMR** (101 MHz, CDCl₃) **HRMS** (+APCI) calculated for C₁₈H₃₁O₂Si [M+H]⁺ 307.20878, found 307.20901

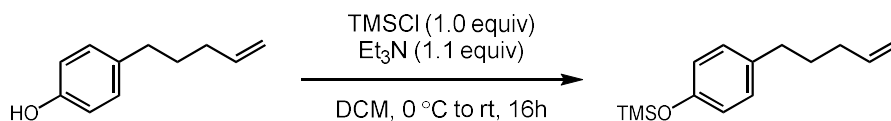


tert-butyl dimethyl((1-(pent-4-en-1-yl)naphthalen-2-yl)oxy)silane (S18): Prepared using General Procedure D and **S15** (2.163 g, 6.31 mmol). **S18** colorless oil (1.72 g, 66% yield). **¹H NMR** (400 MHz, CDCl₃) δ 7.94 (d, *J* = 8.6 Hz, 1H), 7.78 (d, *J* = 8.3 Hz, 1H), 7.61 (d, *J* = 8.8 Hz, 1H), 7.47 (ddd, *J* = 8.4, 6.7, 1.4 Hz, 1H), 7.33 (ddd, *J* = 8.0, 6.7, 1.1 Hz, 1H), 7.09 (d, *J* = 8.8 Hz, 1H), 5.91 (ddt, *J* = 16.9, 10.1, 6.7 Hz, 1H), 5.07

(dq, $J = 17.1, 1.7$ Hz, 1H), 4.99 (ddd, $J = 10.2, 2.3, 1.1$ Hz, 1H), 3.13 – 2.99 (m, 2H), 2.23 (q, $J = 7.4$ Hz, 2H), 1.79 – 1.63 (m, 2H), 1.08 (s, 9H), 0.28 (s, 6H). ^{13}C NMR (101 MHz, CDCl_3) δ 150.56, 138.96, 133.50, 129.63, 128.58, 127.15, 126.10, 125.81, 123.53, 123.27, 120.49, 114.75, 34.42, 29.35, 26.01, 25.42, 18.48, -3.73. HRMS (+APCI) calculated for $\text{C}_{21}\text{H}_{31}\text{OSi}$ $[\text{M}+\text{H}]^+$ 327.21387, found 327.21411



2-(but-3-en-1-yl)benzofuran (**S19**): Prepared using General Procedure D and 1-(benzofuran-2-yl)but-3-en-1-ol²¹ (0.941 g, 5.00 mmol). **S19** colorless oil (0.179 g, 21% yield). Spectroscopic data for **S19** matches those previously reported in the literature.²²



trimethyl(4-(pent-4-en-1-yl)phenoxy)silane (**S20**): Under an N_2 atmosphere, in a 24 mL reaction vial equipped with a stir bar, 4-(pent-4-en-1-yl)phenol (0.36 g, 2.2 mmol, 1.0 equiv) was dissolved in DCM (8 mL) and the reaction vial placed in an ice bath. Once cool, Et_3N (0.33 mL, 2.4 mmol, 1.1 equiv) was added followed by the addition of a TMSCl (0.29 mL, 2.2 mmol 1.0 equiv). The reaction was stirred at room temperature overnight. Once complete, the solvent was removed under reduced pressure and pentane was added to precipitate the amine chloride salt which was removed by filtration over Celite. Removal of the pentane filtrate provided **S20** as an oil which did not require further purification (0.51 g, 97%). ^1H NMR (400 MHz, CDCl_3) δ 7.04 (d, $J = 8.4$ Hz, 2H), 6.76 (d, $J = 8.5$ Hz, 2H), 5.84 (ddt, $J = 16.9, 10.2, 6.6$ Hz, 1H), 5.02 (dq, $J = 17.2, 1.6$ Hz, 1H), 4.97 (ddt, $J = 10.1, 2.3, 1.2$ Hz, 1H), 2.56 (t, $J = 7.6$ Hz, 2H), 2.09 (qt, $J = 7.8, 7.0, 1.3$ Hz, 2H), 1.69 (p, $J = 7.6$ Hz, 2H), 0.26 (s, 9H). ^{13}C NMR (101 MHz, CDCl_3) δ 153.20, 138.87, 135.43, 129.42, 119.92, 114.75, 34.63, 33.44, 30.90, 0.37. HRMS (+APCI) calculated for $\text{C}_{14}\text{H}_{23}\text{OSi}$ $[\text{M}+\text{H}]^+$ 235.15127, found 235.15111.

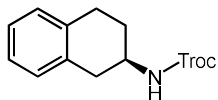
General Procedure E: Optimization of Enantioselective 1,2-Arylamination using 4-phenylbutene (4.28)

In an oven-dried 4 dram reaction vial, with Teflon tape wrapped threads, and equipped with an oven dried stir bar was brought into the glovebox. Base (10 mol%), silver salt additive, and catalyst (2.5 mol%) were added to the reaction vial. The vial was sealed with a Teflon septum screw cap and brought out of the box to complete the reaction. Under an N₂ atmosphere, HFIP (0.5 mL) was added directly to the reaction vial followed by the nitrogen source as a stock solution in HFIP (0.5 mL, 0.26 mmol, 1.3 equiv) and 4-phenylbutene **4.28** (15.0 μL, 0.10 mmol, 1.0 equiv.) using a micro syringe. The reaction was left to stir at room temperature under a N₂ balloon for 24 hours. After which, the crude reaction was filtered through a Celite pipette plug using DCM. The solvent was removed under reduced pressure and a crude NMR sample was prepared using dibromomethane as an internal standard. The crude material purified via preparative TLC (5% EtOAc in hexanes) to yield the corresponding 2-aminotetralin product **4.31** which was analyzed via chiral HPLC (AD-H column 3% 2-propanol in hexanes, 1.0 mL/min) to determine the enantiomeric ratio.

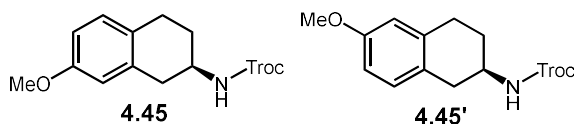
General Procedure F: Enantioselective 1,2-Arylamination Procedure

In an oven-dried 4 dram reaction vial, with Teflon tape wrapped threads, and equipped with an oven dried stir bar was brought into the glovebox. To the vial, CsOAc (0.01 mmol, 0.1 equiv.), AgNTf₂ (0.30 mmol, 0.3 equiv.), and **2** (2.5 mol%) were added to the reaction vial. The vial was sealed with a Teflon septum screw cap and brought out of the box to complete the reaction. Under an N₂ atmosphere outside of the glovebox, the nitrogen source was transferred to the reaction as stock solution in HFIP (0.5 mL, 0.26 mmol, 1.3 equiv). The olefin substrate (0.10 mmol 1.0 equiv.) was added to the reaction vial using HFIP washing the vial three times (0.2 mL + 0.2 mL + 0.1 mL) to ensure complete transfer of the olefin. The reaction was left to stir at room temperature under an N₂ balloon for 24 hours. After 24 hours, the crude reaction was filtered through a Celite pipette plug using DCM to flush. The solvent was removed under reduced pressure

and the crude material purified via preparative TLC using the indicated eluent to yield the corresponding 2-aminotetralin or spirocycle product.



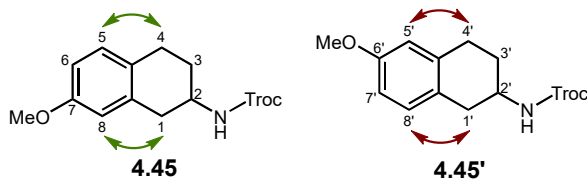
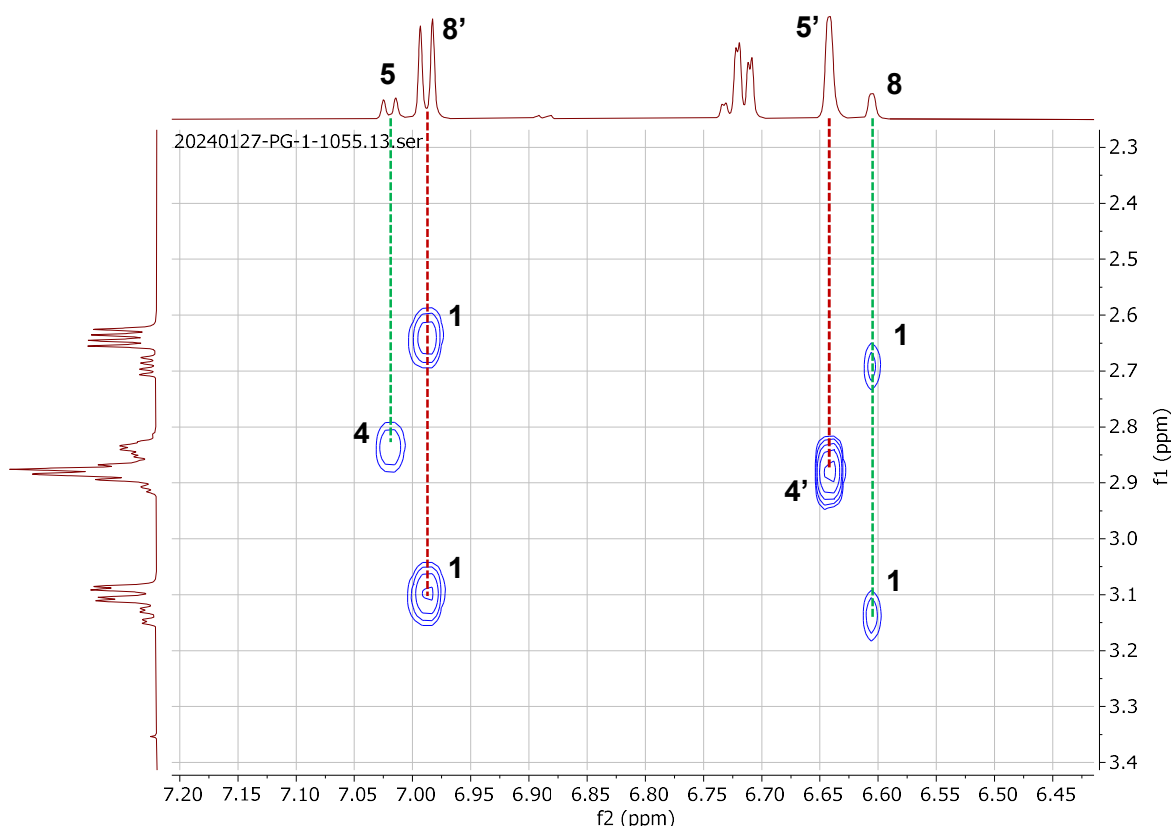
2,2,2-trichloroethyl (*R*)-(1,2,3,4-tetrahydronaphthalen-2-yl)carbamate (**4.31**): Prepared using **General Procedure E** using 4-phenylbutene **4.28**, (*R*)-**4.43**, and (*S,S*)-**2.55**. Purified via preparative TLC using (20% Acetone in Hexanes) to provide **4.31** (0.0277 g, 86% yield, 92:8 e.r.) as a colorless oil. $^1\text{H NMR}$ (400 MHz, CDCl_3) δ 7.19 – 7.04 (m, 4H), 5.06 (d, $J = 7.4$ Hz, 1H), 4.76 (d, $J = 12.0$ Hz, 2H), 4.72 (d, $J = 12.0$ Hz, 2H), 4.09 (qdd, $J = 8.2, 5.1, 3.1$ Hz, 1H), 3.18 (dd, $J = 16.3, 5.2$ Hz, 1H), 2.91 (t, $J = 6.1$ Hz, 2H), 2.72 (dd, $J = 16.3, 8.1$ Hz, 1H), 2.20 – 2.04 (m, 1H), 1.92 – 1.76 (m, 1H). $^{13}\text{C NMR}$ (101 MHz, CDCl_3) δ 154.02, 135.41, 133.76, 129.62, 129.01, 126.44, 126.17, 95.74, 74.58, 47.28, 35.84, 28.80, 27.04. **HRMS** (+APCI) calculated for $\text{C}_{13}\text{H}_{15}\text{O}_2\text{NCl}_3$ $[\text{M}+\text{H}]^+$ 322.01629, found 322.01679. **HPLC** (IJ column 5% 2-propanol in hexanes, 1.0 mL/min) $t_{\text{M}} = 13.7$ min $t_{\text{m}} = 16.1$ min, 92:8 e.r.



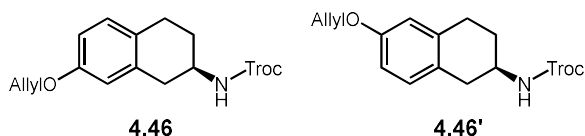
2,2,2-trichloroethyl (*R*)-(7-methoxy-1,2,3,4-tetrahydronaphthalen-2-yl)carbamate (**4.45**) and 2,2,2-trichloroethyl (*R*)-(6-methoxy-1,2,3,4-tetrahydronaphthalen-2-yl)carbamate (**4.45'**): Prepared using **General Procedure F** using **S1**, (*R*)-**4.43**, and (*S,S*)-**2.55**. Purified via preparative TLC using (20% Acetone in Hexanes) to provide **4.45** and **4.45'** as a colorless oil and mixture of inseparable regioisomers (0.0235 g, 65% yield, 1:4 r.r., 91:9 e.r.). $^1\text{H NMR}$ (800 MHz, CDCl_3) δ 7.02 (d, $J = 8.4$ Hz, 1H, minor regioisomer), 6.99 (d, $J = 8.4$ Hz, 1H), 6.72 (td, $J = 8.9, 8.5, 2.7$ Hz, 1H), 6.64 (d, $J = 2.7$ Hz, 1H), 6.61 (d, $J = 2.7$ Hz, 1H, minor regioisomer), 5.05 (d, $J = 8.1$ Hz, 1H), 4.75 (d, $J = 12.1$ Hz, 1H), 4.72 (d, $J = 12.0$ Hz, 1H), 4.10 – 4.01 (m, 1H), 3.78 (d, $J = 4.0$ Hz, 3H), 3.14 (dd, $J = 16.4, 5.0$ Hz, 1H, minor regioisomer), 3.10 (dd, $J = 15.9, 5.1$ Hz, 1H), 2.94 – 2.80 (m, 2H), 2.69 (dd, $J = 16.3, 7.9$ Hz, 1H, minor regioisomer),

2.64 (dd, $J = 15.9, 8.0$ Hz, 1H), 2.13 – 2.01 (m, 1H), 1.87 – 1.74 (m, 1H). ^{13}C NMR (201 MHz, CDCl_3) δ 158.18, 157.95, 154.03, 136.53, 134.87, 130.49, 129.91, 127.44, 125.75, 114.06, 113.50, 112.87, 112.62, 95.77, 74.59, 55.41, 55.40, 47.48, 47.24, 36.11, 35.08, 28.97, 28.73, 27.31, 26.14. HRMS (+APCI) calculated for $\text{C}_{14}\text{H}_{17}\text{O}_3\text{NCl}_3$ $[\text{M}+\text{H}]^+$ 352.02685, found 352.02703. SFC (ChiralCel OJ-3 5% MeOH/IPA with 0.2% Formic Acid, 2.5 mL/min) (**4.45**): $t_{\text{M}} = 6.05$ min $t_{\text{m}} = 4.43$ min, 92:8 e.r. (**4.45'**): $t_{\text{M}} = 4.84$ min $t_{\text{m}} = 3.82$ min, 91:9 e.r.

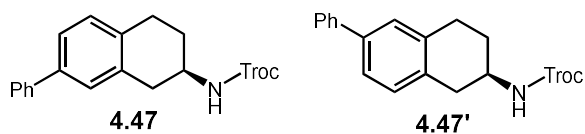
Structural Assignment of 2-aminotetralins via NOESY Correlations



The identity of the major and minor regioisomers for all 2-aminotetralins was determined via the NOESY correlations between C1-C8 and between C4-C5.

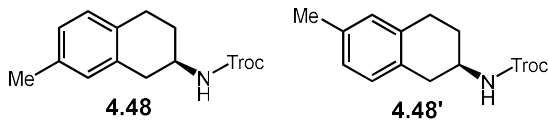


2,2,2-trichloroethyl (*R*)-(7-(allyloxy)-1,2,3,4-tetrahydronaphthalen-2-yl)carbamate (**4.46**) and 2,2,2-trichloroethyl (*R*)-(6-(allyloxy)-1,2,3,4-tetrahydronaphthalen-2-yl)carbamate (**4.46'**): Prepared using **General Procedure F** using **S2**, (*R*)-**4.43**, and (*S,S*)-**2.55**. Purified via preparative TLC using (20% Acetone in Hexanes) to provide **4.46** and **4.46'** as a colorless oil and mixture of inseparable regioisomers (0.0227 g, 54% yield, 1:4 r.r., 91:9 e.r.). ¹H NMR (800 MHz, CDCl₃) δ 7.01 (d, *J* = 8.4 Hz, 1H, minor regioisomer), 6.98 (d, *J* = 8.4 Hz, 1H), 6.76 – 6.71 (m, 1H), 6.66 (d, *J* = 2.7 Hz, 1H), 6.62 (d, *J* = 2.7 Hz, 1H, minor regioisomer), 6.05 (ddtd, *J* = 18.8, 10.5, 5.3, 3.0 Hz, 1H), 5.40 (dp, *J* = 17.2, 1.5 Hz, 1H), 5.28 (dq, *J* = 10.5, 1.4 Hz, 1H), 5.03 (d, *J* = 8.0 Hz, 1H), 4.75 (d, *J* = 12.0 Hz, 1H), 4.72 (d, *J* = 12.0 Hz, 1H), 4.56 – 4.48 (m, 2H), 4.11 – 4.00 (m, 1H), 3.18 – 3.04 (m, 1H), 2.93 – 2.80 (m, 2H), 2.68 (dd, *J* = 16.2, 8.0 Hz, 1H, minor regioisomer), 2.64 (dd, *J* = 15.9, 8.0 Hz, 1H), 2.17 – 2.00 (m, 1H), 1.82 (dtd, *J* = 12.7, 8.7, 6.3 Hz, 1H). ¹³C NMR (201 MHz, CDCl₃) δ 157.19, 156.96, 154.02, 136.52, 134.87, 133.52, 130.47, 129.89, 127.64, 125.96, 117.71, 115.06, 114.50, 113.61, 113.34, 95.77, 74.59, 68.97, 47.47, 47.24, 36.11, 35.10, 28.97, 28.72, 27.30, 26.16. HRMS (+APCI) calculated for C₁₆H₁₉O₃NCl₃ [M+H]⁺ 378.0425, found 378.04273. SFC (ChiralCel OJ-3 5% MeOH/IPA with 0.2% Formic Acid, 2.5 mL/min) (**4.46**): *t*_M = 8.70 min *t*_m = 5.44 min, 92:8 e.r. (**4.46'**): *t*_M = 6.02 min *t*_m = 5.05 min, 91:9 e.r.

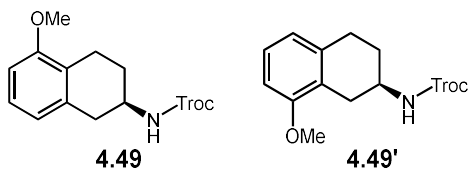


2,2,2-trichloroethyl (*R*)-(7-phenyl-1,2,3,4-tetrahydronaphthalen-2-yl)carbamate (**4.47**) and 2,2,2-trichloroethyl (*R*)-(6-phenyl-1,2,3,4-tetrahydronaphthalen-2-yl)carbamate (**4.47'**): Prepared using **General Procedure F** using **S3**, (*R*)-**4.43**, and (*S,S*)-**2.55**. Purified via preparative TLC using (20% Acetone in Hexanes) to provide **4.47** and **4.47'** as a colorless oil and mixture of inseparable regioisomers (0.0238 g, 57% yield, 3:1 r.r., 93:7 e.r.). ¹H NMR (800 MHz, CDCl₃) δ 7.57 (d, *J* = 7.4 Hz, 2H), 7.43 (t, *J*

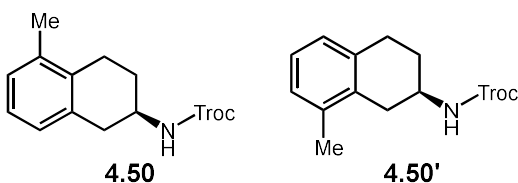
= 7.6 Hz, 2H), 7.41 – 7.36 (m, 1H), 7.34 (t, $J = 7.2$ Hz, 1H), 7.31 (s, 1H), 7.19 (d, $J = 7.9$ Hz, 1H), 7.16 (d, $J = 7.9$ Hz, 1H, minor regioisomer), 5.08 (d, $J = 6.9$ Hz, 1H), 4.77 (d, $J = 12.1$ Hz, 1H), 4.74 (d, $J = 12.0$ Hz, 1H), 4.13 (dp, $J = 12.6, 4.3$ Hz, 1H), 3.28 – 3.18 (m, 1H), 3.01 – 2.90 (m, 2H), 2.83 – 2.72 (m, 1H), 2.21 – 2.10 (m, 1H), 1.89 (dq, $J = 14.9, 7.9$ Hz, 1H). ^{13}C NMR (201 MHz, CDCl_3) δ 154.30, 154.04, 141.04, 141.01, 139.56, 139.30, 135.78, 134.57, 134.17, 132.90, 130.06, 129.47, 128.89, 128.24, 127.66, 127.32, 127.30, 127.14, 127.11, 125.35, 125.08, 95.76, 74.91, 74.62, 47.97, 47.35, 47.33, 35.99, 35.60, 29.50, 28.85, 28.84, 27.21, 26.76. **HRMS** (+APCI) calculated for $\text{C}_{19}\text{H}_{19}\text{O}_2\text{NCl}_3$ $[\text{M}+\text{H}]^+$ 398.04759, found 398.04798. **HPLC** (IJ column 20% 2-propanol in hexanes, 1.0 mL/min) (**4.47**): $t_{\text{M}} = 24.9$ min $t_{\text{m}} = 37.0$ min, 93:7 e.r. (**4.47'**): $t_{\text{M}} = 20.0$ min $t_{\text{m}} = 17.9$ min, 89:11 e.r.



2,2,2-trichloroethyl (*R*)-(7-methyl-1,2,3,4-tetrahydronaphthalen-2-yl)carbamate (**4.48**) and 2,2,2-trichloroethyl (*R*)-(6-methyl-1,2,3,4-tetrahydronaphthalen-2-yl)carbamate (**4.48'**): Prepared using **General Procedure F** using **S4**, (*R*)-**4.43**, and (*S,S*)-**2.55**. Purified via preparative TLC using (15% Acetone in Hexanes) to provide **4.48** and **4.48'** as a colorless oil and mixture of inseparable regioisomers (0.0123 g, 37% yield, 2:1 r.r., 92:8 e.r.). ^1H NMR (800 MHz, CDCl_3) δ 7.00 (d, $J = 7.7$ Hz, 1H), 6.99 – 6.94 (m, 1H), 6.93 (s, 1H, minor regioisomer), 6.90 (s, 1H), 5.03 (d, $J = 8.0$ Hz, 1H), 4.75 (d, $J = 12.0$ Hz, 1H), 4.72 (d, $J = 12.0$ Hz, 1H), 4.12 – 4.02 (m, 1H), 3.13 (dd, $J = 16.2, 5.2$ Hz, 1H), 2.91 – 2.82 (m, 2H), 2.68 (dd, $J = 16.2, 7.8$ Hz, 1H), 2.29 (s, 3H), 2.14 – 2.05 (m, 1H), 1.83 (dq, $J = 14.6, 8.6, 8.2$ Hz, 1H). ^{13}C NMR (201 MHz, CDCl_3) δ 154.04, 136.01, 135.71, 135.22, 133.55, 132.32, 130.61, 130.13, 129.56, 129.52, 128.91, 127.33, 127.06, 95.78, 74.60, 47.40, 47.34, 35.81, 35.48, 28.91, 28.83, 26.92, 26.55, 21.10, 21.07. **HRMS** (+APCI) calculated for $\text{C}_{14}\text{H}_{17}\text{O}_2\text{NCl}_3$ $[\text{M}+\text{H}]^+$ 336.03194, found 336.03206. **SFC** (ChiralCel OJ-3 5% MeOH/IPA with 0.2% Formic Acid, 2.5 mL/min) (**4.48**): $t_{\text{M}} = 7.77$ min $t_{\text{m}} = 4.42$ min, 92:8 e.r. (**4.48'**): $t_{\text{M}} = 5.48$ min $t_{\text{m}} = 4.08$ min, 87:13 e.r. *This data was collected by Wesley Pullara*

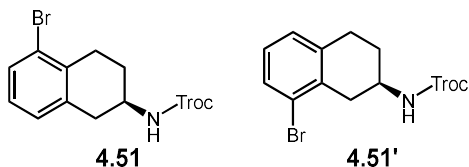


2,2,2-trichloroethyl (*R*)-(5-methoxy-1,2,3,4-tetrahydronaphthalen-2-yl)carbamate (**4.49**) and 2,2,2-trichloroethyl (*R*)-(8-methoxy-1,2,3,4-tetrahydronaphthalen-2-yl)carbamate (**4.49'**): Prepared using **General Procedure F** using **S5**, (*R*)-**4.43**, and (*S,S*)-**2.55**. Purified via preparative TLC using (15% Acetone in Hexanes) to provide **4.49** and **4.49'** as a colorless oil and mixture of inseparable regioisomers (0.0203 g, 58% yield, 1:5 r.r., 86:13 e.r.). $^1\text{H NMR}$ (600 MHz, CDCl_3) δ 7.12 (t, $J = 7.9$ Hz, 1H), 6.73 (d, $J = 7.7$ Hz, 1H), 6.72 – 6.65 (m, 1H), 5.04 (d, $J = 7.9$ Hz, 1H), 4.78 – 4.67 (m, 2H), 4.06 (ddt, $J = 10.9, 8.3, 4.3$ Hz, 1H), 3.82 (s, 3H, minor regioisomer), 3.81 (s, 3H), 3.18 – 3.08 (m, 1H), 2.95 – 2.66 (m, 2H), 2.52 (dd, $J = 17.2, 8.0$ Hz, 1H), 2.17 – 2.03 (m, 1H), 1.89 – 1.74 (m, 1H). $^{13}\text{C NMR}$ (151 MHz, CDCl_3) δ 157.62, 157.35, 154.06, 154.03, 136.82, 135.04, 126.75, 126.71, 124.35, 122.78, 121.69, 121.08, 107.56, 107.22, 95.80, 74.60, 55.38, 47.24, 46.87, 35.84, 29.93, 28.45, 28.20, 27.25, 20.99. **HRMS** (+APCI) calculated for $\text{C}_{14}\text{H}_{17}\text{O}_3\text{NCl}_3$ $[\text{M}+\text{H}]^+$ 352.02685, found 352.02703. **HPLC** (IB column 10% 2-propanol in hexanes, 1.0 mL/min) (**4.49**): $t_{\text{M}} = 10.7$ min $t_{\text{m}} = 8.7$ min, 88:12 e.r. (**4.49'**): $t_{\text{M}} = 9.38$ min $t_{\text{m}} = 11.8$ min, 86:13 e.r. *This data was collected by Wesley Pullara*

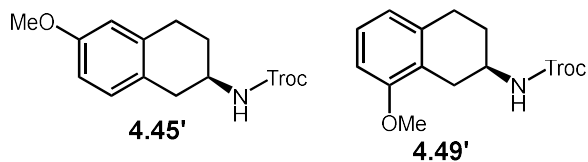


2,2,2-trichloroethyl (*R*)-(5-methyl-1,2,3,4-tetrahydronaphthalen-2-yl)carbamate (**4.50**) and 2,2,2-trichloroethyl (*R*)-(8-methyl-1,2,3,4-tetrahydronaphthalen-2-yl)carbamate (**4.50'**): Prepared using **General Procedure F** using **S7**, (*R*)-**4.43**, and (*S,S*)-**2.55**. Purified via preparative TLC using (20% Acetone in Hexanes) to provide **4.50** and **4.50'** as a colorless oil and mixture of inseparable regioisomers (0.0178 g, 60% yield, 3:1 r.r., 90:10 e.r.). $^1\text{H NMR}$ (800 MHz, CDCl_3) δ 7.09 – 7.05 (m, 1H), 7.05 – 7.00

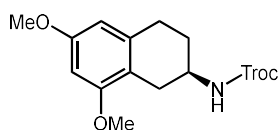
(m, 1H), 6.98 (d, $J = 7.4$ Hz, 1H, minor regioisomer), 6.94 (d, $J = 7.4$ Hz, 1H), 5.08 (d, $J = 8.0$ Hz, 1H, minor regioisomer), 5.04 (d, $J = 8.0$ Hz, 1H), 4.79 – 4.69 (m, 2H), 4.14 – 4.02 (m, 1H), 3.16 (dd, $J = 16.0$, 4.9 Hz, 1H), 3.08 (dd, $J = 16.6$, 5.5 Hz, 1H, minor regioisomer), 2.96 – 2.87 (m, 1H), 2.82 – 2.70 (m, 2H), 2.51 (dd, $J = 16.6$, 8.2 Hz, 1H, minor regioisomer), 2.24 (s, 2H), 2.22 (s, 1H), 2.18 – 2.07 (m, 1H), 1.93 – 1.84 (m, 1H), 1.84 – 1.76 (m, 1H, minor regioisomer). ^{13}C NMR (201 MHz, CDCl_3) δ 154.05, 137.01, 136.70, 135.37, 133.94, 133.61, 132.51, 127.98, 127.67, 127.47, 126.75, 126.06, 126.00, 95.77, 74.63, 74.60, 47.74, 46.91, 36.27, 33.51, 28.76, 28.62, 27.73, 24.55, 19.70. **HRMS** (+APCI) calculated for $\text{C}_{14}\text{H}_{17}\text{O}_2\text{NCl}_3$ $[\text{M}+\text{H}]^+$ 336.03194, found 336.03208. **SFC** (ChiralCel OJ-3 1% MeOH/IPA with 0.2% Formic Acid, 2.5 mL/min) (**4.50**): $t_{\text{M}} = 4.64$ min $t_{\text{m}} = 7.03$ min, 90:10 e.r. (**4.50'**): inseparable



2,2,2-trichloroethyl (R)-(5-bromo-1,2,3,4-tetrahydronaphthalen-2-yl)carbamate (**4.51**) and 2,2,2-trichloroethyl (R)-(8-bromo-1,2,3,4-tetrahydronaphthalen-2-yl)carbamate (**4.51'**): Prepared using **General Procedure F** using **S6**, (**R**)-**4.43**, and (**S,S**)-**2.55**. Purified via preparative TLC using (15% Acetone in Hexanes) to provide **4.51** and **4.51'** as a colorless oil and mixture of inseparable regioisomers (0.0100 g, 25% yield, 5:1 r.r., 88:11 e.r.). ^1H NMR (800 MHz, CDCl_3) δ 7.44 – 7.39 (m, 1H), 7.07 (d, $J = 7.5$ Hz, 1H, minor regioisomer), 7.05 – 6.98 (m, 2H), 5.01 (d, $J = 7.9$ Hz, 1H), 4.73 (s, 2H), 4.13 – 3.99 (m, 1H), 3.22 (dd, $J = 17.1$, 5.6 Hz, 1H, minor regioisomer), 3.17 (dd, $J = 16.3$, 4.9 Hz, 1H), 2.98 – 2.89 (m, 1H), 2.88 – 2.80 (m, 1H), 2.75 (dd, $J = 16.3$, 8.0 Hz, 1H), 2.62 (dd, $J = 17.1$, 8.3 Hz, 1H, minor regioisomer), 2.21 – 2.06 (m, 1H), 1.88 (td, $J = 14.6$, 8.5 Hz, 1H). ^{13}C NMR (201 MHz, CDCl_3) δ 154.02, 136.24, 134.96, 130.75, 130.41, 128.84, 128.15, 127.59, 127.48, 125.87, 125.67, 95.70, 74.68, 74.65, 47.68, 46.80, 36.69, 36.25, 29.85, 28.78, 28.17, 27.98. **HRMS** (+APCI) calculated for $\text{C}_{14}\text{H}_{17}\text{O}_3\text{NCl}_3$ $[\text{M}+\text{H}]^+$ 352.02685, found 352.02703. **SFC** (ChiralCel OJ-3 5% MeOH/IPA with 0.2% Formic Acid, 2.5 mL/min) (**4.51**): $t_{\text{M}} = 16.9$ min $t_{\text{m}} = 11.6$ min, 88:11 e.r. (**4.51'**): inseparable *This data was collected by Wesley Pullara*

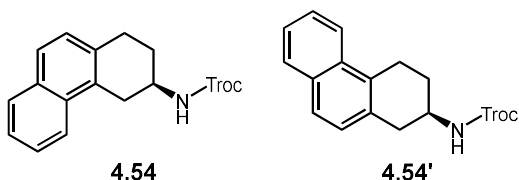


2,2,2-trichloroethyl (*R*)-(6-methoxy-1,2,3,4-tetrahydronaphthalen-2-yl)carbamate (**4.45'**) and 2,2,2-trichloroethyl (*R*)-(8-methoxy-1,2,3,4-tetrahydronaphthalen-2-yl)carbamate (**4.49'**): Prepared using **General Procedure F** using **S8**, (*R*)-**4.43**, and (*S,S*)-**2.55**. Purified via preparative TLC using (20% Acetone in Hexanes) to provide **4.45'** and **4.49'** as a colorless oil and mixture of inseparable regioisomers (0.0297 g, 80% yield, 3:1 r.r., 91:9 e.r.). $^1\text{H NMR}$ (800 MHz, CDCl_3) δ 7.12 (t, $J = 7.9$ Hz, 1H, minor regioisomer), 6.99 (d, $J = 8.4$ Hz, 1H), 6.75 – 6.69 (m, 1H), 6.68 (d, $J = 8.1$ Hz, 1H, minor regioisomer), 6.64 (d, $J = 2.7$ Hz, 1H), 5.05 (d, $J = 7.6$ Hz, 1H), 4.76 – 4.73 (m, 1H), 4.72 (d, $J = 12.1$ Hz, 1H), 4.06 (tq, $J = 8.3, 4.2, 3.3$ Hz, 1H), 3.81 (s, 3H, minor regioisomer), 3.78 (s, 3H), 3.16 – 3.06 (m, 1H), 2.94 – 2.83 (m, 2H), 2.64 (dd, $J = 15.9, 8.0$ Hz, 1H), 2.52 (dd, $J = 17.1, 8.1$ Hz, 1H, minor regioisomer), 2.14 – 2.01 (m, 1H), 1.89 – 1.75 (m, 1H). $^{13}\text{C NMR}$ (201 MHz, CDCl_3) δ 158.18, 157.61, 154.03, 136.81, 136.53, 130.49, 126.73, 125.75, 122.78, 121.07, 113.50, 112.62, 107.21, 95.78, 74.59, 55.40, 47.48, 47.24, 35.54, 35.08, 29.92, 28.73, 28.45, 27.31, 27.25. **HRMS** (+APCI) calculated for $\text{C}_{14}\text{H}_{17}\text{O}_3\text{NCl}_3$ $[\text{M}+\text{H}]^+$ 352.02685, found 352.02703. **HPLC** (IA column 5% 2-propanol in hexanes, 1.0 mL/min) (**4.45'**): $t_{\text{M}} = 10.8$ min $t_{\text{m}} = 11.7$ min, 91:9 e.r. (**4.49'**): $t_{\text{M}} = 9.1$ min $t_{\text{m}} = 17.5$ min, 92:8 e.r.

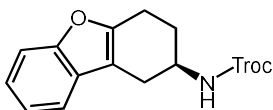


2,2,2-trichloroethyl (*R*)-(6,8-dimethoxy-1,2,3,4-tetrahydronaphthalen-2-yl)carbamate (**4.53**): Prepared using **General Procedure F** using **4.67**, (*R*)-**4.43**, and (*S,S*)-**2.55**. Purified via preparative TLC using (20% Et_2O in Pentane) to provide **4.53** (0.0120 g, 31% yield, 87:13 e.r.) as a colorless oil. $^1\text{H NMR}$ (400 MHz, CDCl_3) δ 6.29 (d, $J = 2.4$ Hz, 1H), 6.24 (d, $J = 2.4$ Hz, 1H), 5.03 (d, $J = 7.9$ Hz, 1H), 4.75 (d, $J = 11.9$ Hz, 2H), 4.71 (d, $J = 12.0$ Hz, 2H), 4.03 (dddd, $J = 16.7, 8.3, 5.7, 2.9$ Hz, 1H), 3.78 (s, 6H), 3.03 (dd, $J = 16.8, 5.5$ Hz, 1H), 2.85 (td, $J = 6.7, 3.0$ Hz, 2H), 2.44 (dd, $J = 16.8, 7.9$ Hz, 1H), 2.15 – 1.98 (m, 1H), 1.88 – 1.72

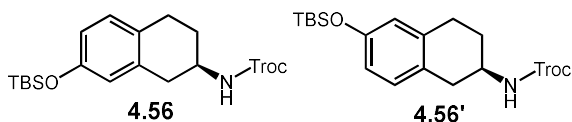
(m, 1H). ^{13}C NMR (201 MHz, CDCl_3) δ 158.97, 158.60, 154.04, 137.27, 115.14, 104.06, 96.25, 95.81, 74.59, 55.47, 55.41, 47.30, 29.47, 28.54, 27.64. HRMS (+APCI) calculated for $\text{C}_{15}\text{H}_{19}\text{O}_4\text{NCl}_3$ $[\text{M}+\text{H}]^+$ 382.03742, found 382.03794. HPLC (IA column 10% 2-propanol in hexanes, 1.0 mL/min) $t_{\text{M}} = 8.5$ min $t_{\text{m}} = 13.0$ min, 87:13 e.r.



2,2,2-trichloroethyl (*R*)-(1,2,3,4-tetrahydrophenanthren-3-yl)carbamate (**4.54**) and 2,2,2-trichloroethyl (*R*)-(1,2,3,4-tetrahydrophenanthren-2-yl)carbamate (**4.54'**): Prepared using **General Procedure F** using **S10**, (*R*)-**4.43**, and (*S,S*)-**2.55**. Purified via preparative TLC using (20% Acetone in Hexanes) to provide **4.54** and **4.54'** as an off white solid and mixture of inseparable regioisomers (0.0309 g, 80% yield, 8:1 r.r., 91:9 e.r.). ^1H NMR (400 MHz, CDCl_3) δ 7.96 (d, $J = 8.4$ Hz, 1H, minor regioisomer), 7.91 (d, $J = 8.4$ Hz, 1H), 7.82 (dd, $J = 8.0, 1.5$ Hz, 1H), 7.67 (d, $J = 8.4$ Hz, 1H), 7.52 (ddd, $J = 8.4, 6.7, 1.6$ Hz, 1H), 7.47 (ddd, $J = 8.0, 6.7, 1.3$ Hz, 1H), 7.23 (d, $J = 8.4$ Hz, 1H), 7.18 (d, $J = 8.4$ Hz, 1H, minor regioisomer), 5.17 (d, $J = 8.0$ Hz, 1H), 4.79 (d, $J = 12.0$ Hz, 1H), 4.74 (d, $J = 12.0$ Hz, 1H), 4.32 – 4.07 (m, 1H), 3.57 (dd, $J = 16.6, 5.5$ Hz, 1H), 3.15 – 2.93 (m, 3H), 2.87 (dd, $J = 16.5, 7.7$ Hz, 1H, minor regioisomer), 2.30 – 2.12 (m, 1H), 2.07 – 1.84 (m, 1H). ^{13}C NMR (201 MHz, CDCl_3) δ 154.11, 132.85, 132.43, 132.30, 128.66, 128.43, 127.66, 126.72, 126.39, 125.42, 125.32, 123.01, 122.68, 95.76, 74.65, 74.61, 47.53, 46.94, 32.46, 28.47, 28.05. HRMS (+APCI) calculated for $\text{C}_{17}\text{H}_{17}\text{O}_2\text{NCl}_3$ $[\text{M}+\text{H}]^+$ 372.03194, found 372.03218. SFC (ChiralCel OJ-3 5% MeOH/IPA with 0.2% Formic Acid, 2.5 mL/min) (**4.54**): $t_{\text{M}} = 8.77$ min $t_{\text{m}} = 10.35$ min, 91:9 e.r. (**4.54'**): $t_{\text{M}} = 5.22$ min $t_{\text{m}} = 7.76$ min, 95:5 e.r.

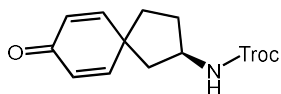


2,2,2-trichloroethyl (*R*)-(1,2,3,4-tetrahydrodibenzo[*b,d*]furan-2-yl)carbamate (**4.55**): Prepared using **General Procedure F** using **S19**, (*R*)-**4.43**, and (*S,S*)-**2.55**. Purified via preparative TLC using (20% Acetone in Hexanes) to provide **4.55** (0.0154 g, 41% yield, 92:8 e.r.) as a colorless oil. **¹H NMR** (800 MHz, CDCl₃) δ 7.42 (d, *J* = 8.0 Hz, 1H), 7.39 (d, *J* = 7.5 Hz, 1H), 7.24 (t, *J* = 7.5 Hz, 1H), 7.21 (d, *J* = 14.4 Hz, 1H), 5.12 (d, *J* = 8.2 Hz, 1H), 4.76 (d, *J* = 12.1 Hz, 1H), 4.73 (d, *J* = 12.0 Hz, 1H), 4.25 – 4.16 (m, 1H), 3.09 (dd, *J* = 15.6, 5.1 Hz, 1H), 2.94 – 2.81 (m, 2H), 2.65 – 2.58 (m, 1H), 2.21 – 2.14 (m, 1H), 2.09 (dq, *J* = 13.5, 7.0 Hz, 1H). **¹³C NMR** (201 MHz, CDCl₃) δ 155.00, 154.12, 152.50, 128.38, 123.77, 122.63, 118.53, 111.16, 110.47, 95.70, 74.66, 46.86, 28.20, 27.47, 20.97. **HRMS** (+APCI) calculated for C₁₅H₁₅O₃N³⁵Cl₃ [M+H]⁺ 362.0112, found 362.01163. **HPLC** (IH column 5% 2-propanol in hexanes, 1.0 mL/min) *t*_M = 17.9 min *t*_m = 16.6 min, 92:8 e.r.

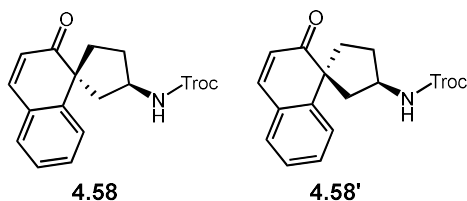


2,2,2-trichloroethyl (*R*)-(7-((*tert*-butyldimethylsilyl)oxy)-1,2,3,4-tetrahydronaphthalen-2-yl)carbamate (**4.56**) and 2,2,2-trichloroethyl (*R*)-(6-((*tert*-butyldimethylsilyl)oxy)-1,2,3,4-tetrahydronaphthalen-2-yl)carbamate (**4.56'**): Prepared using **General Procedure F** using **S11**, (*R*)-**4.43**, and (*S,S*)-**2.55**. Purified via preparative TLC using (20% Acetone in Hexanes) to provide **4.56** and **4.56'** as a colorless oil and mixture of inseparable regioisomers (0.0221 g, 46% yield, 1:1 r.r., 90:10 e.r.). **¹H NMR** (800 MHz, CDCl₃) δ 6.95 (d, *J* = 8.2 Hz, 1H), 6.91 (d, *J* = 8.3 Hz, 1H), 6.63 (ddd, *J* = 9.5, 8.3, 2.6 Hz, 2H), 6.58 (d, *J* = 2.5 Hz, 1H), 6.55 (d, *J* = 2.5 Hz, 1H), 5.02 (d, *J* = 7.9 Hz, 2H), 4.77 – 4.70 (m, 4H), 4.05 (dddd, *J* = 12.1, 6.0, 4.5, 2.6 Hz, 2H), 3.09 (ddd, *J* = 15.9, 11.0, 5.1 Hz, 2H), 2.83 (qd, *J* = 8.8, 4.6 Hz, 4H), 2.64 (td, *J* = 17.0, 8.0 Hz, 2H), 2.14 – 2.01 (m, 2H), 1.81 (dddd, *J* = 14.8, 12.8, 8.5, 6.3 Hz, 2H), 0.98 (s, 9H), 0.98 (s, 9H), 0.19 (s, 6H), 0.18 (s, 6H). **¹³C NMR** (201 MHz, CDCl₃) δ 154.08, 154.04, 154.02, 153.85, 136.47, 134.82,

130.35, 129.78, 127.98, 126.31, 120.49, 119.95, 118.51, 118.22, 95.79, 74.60, 47.52, 47.26, 35.97, 35.18, 29.00, 28.73, 27.15, 26.26, 25.84, 18.32, -4.26. **HRMS** (+APCI) calculated for $C_{19}H_{29}O_3NCl_3Si$ $[M+H]^+$ 452.09768, found 452.09821. **SFC** (ChiralCel OJ-3 1% MeOH/IPA with 0.2% Formic Acid, 2.5 mL/min) **(4.56)**: $t_M = 4.84$ min $t_m = 5.72$ min, 93:7 e.r. **(4.56')**: *Inseparable*



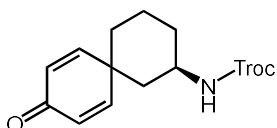
2,2,2-trichloroethyl (R)-(8-oxospiro[4.5]deca-6,9-dien-2-yl)carbamate (4.57): Prepared using **General Procedure F** using **S11**, **(R)-4.43**, and **(S,S)-2.55**. Purified via preparative TLC using (20% Acetone in Hexanes) to provide **4.57** (0.0089 g, 26% yield, 89:11 e.r.) as a colorless oil. **1H NMR** (800 MHz, $CDCl_3$) δ 6.88 (t, $J = 8.3$ Hz, 2H), 6.22 (dd, $J = 9.7, 8.0$ Hz, 2H), 5.15 (d, $J = 17.1$ Hz, 1H), 4.73 (s, 2H), 4.36 (h, $J = 7.4$ Hz, 1H), 2.40 (q, $J = 11.9, 9.5$ Hz, 1H), 2.27 (dd, $J = 13.8, 7.6$ Hz, 1H), 2.04 – 1.95 (m, 1H), 1.86 (td, $J = 12.8, 7.8$ Hz, 2H), 1.80 (dd, $J = 13.8, 7.8$ Hz, 1H). **^{13}C NMR** (201 MHz, $CDCl_3$) δ 185.88, 154.31, 154.08, 153.24, 127.82, 127.55, 95.59, 74.70, 52.81, 47.06, 43.81, 35.86, 32.62. **HRMS** (+APCI) calculated for $C_{13}H_{15}O_3NCl_3$ $[M+H]^+$ 338.0112, found 338.0118. **HPLC** (IA column 10% 2-propanol in hexanes, 1.0 mL/min) $t_M = 15.4$ min $t_m = 19.8$ min, 89:11 e.r.



2,2,2-trichloroethyl ((1R,3R)-2'-oxo-2'H-spiro[cyclopentane-1,1'-naphthalen]-3-yl)carbamate (4.58) and **2,2,2-trichloroethyl ((1S,3R)-2'-oxo-2'H-spiro[cyclopentane-1,1'-naphthalen]-3-yl)carbamate (4.58')**: Prepared using **General Procedure F** using **S12**, **(R)-4.43**, and **(S,S)-2.55**. Purified via preparative TLC using (20% EtOAc in Hexanes) to provide **4.58** and **4.58'** separable diastereomers (0.0293g, 73% yield, 1.9:1 d.r.).

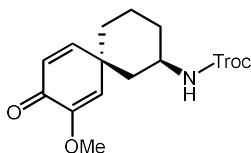
4.58: Colorless oil (0.0187 g, 46% yield, 89:11 e.r.). $^1\text{H NMR}$ (800 MHz, CDCl_3) δ 7.48 (d, $J = 7.8$ Hz, 1H), 7.46 – 7.39 (m, 2H), 7.33 – 7.26 (m, 2H), 6.15 (d, $J = 9.7$ Hz, 1H), 5.13 (s, 1H), 4.78 (d, $J = 11.8$ Hz, 1H), 4.70 (d, $J = 12.1$ Hz, 1H), 4.43 (q, $J = 7.4$ Hz, 1H), 2.74 (dd, $J = 13.8, 7.2$ Hz, 1H), 2.46 – 2.34 (m, 2H), 2.09 – 1.99 (m, 1H), 1.97 (dd, $J = 13.7, 8.1$ Hz, 1H), 1.94 – 1.85 (m, 1H). $^{13}\text{C NMR}$ (201 MHz, CDCl_3) δ 204.13, 153.97, 147.49, 145.10, 130.59, 129.55, 129.30, 127.01, 126.51, 124.33, 95.80, 74.57, 57.53, 53.58, 45.61, 39.10, 33.08. **HRMS** (+APCI) calculated for $\text{C}_{17}\text{H}_{17}\text{O}_3\text{NCl}_3$ $[\text{M}+\text{H}]^+$ 388.02685, found 388.02715. **HPLC** (IH column 20% 2-propanol in hexanes, 1.0 mL/min) (**4.58**): $t_{\text{M}} = 13.4$ min $t_{\text{m}} = 15.5$ min, 89:11 e.r.

4.58': Colorless oil (0.0106 g, 26% yield, 86:14 e.r.). $^1\text{H NMR}$ (800 MHz, CDCl_3) δ 7.49 (d, $J = 9.8$ Hz, 1H), 7.44 (t, $J = 7.5$ Hz, 1H), 7.39 (d, $J = 7.9$ Hz, 1H), 7.33 (d, $J = 7.4$ Hz, 1H), 7.30 (t, $J = 7.3$ Hz, 1H), 6.43 (d, $J = 8.6$ Hz, 1H), 6.21 (dd, $J = 9.7, 1.2$ Hz, 1H), 4.75 (s, 2H), 4.59 (dh, $J = 9.0, 4.9$ Hz, 1H), 2.49 (dd, $J = 14.6, 7.8$ Hz, 1H), 2.36 (dt, $J = 14.1, 7.4$ Hz, 1H), 2.33 – 2.23 (m, 2H), 2.02 (dq, $J = 12.7, 6.4$ Hz, 1H), 1.89 (dt, $J = 13.7, 6.8$ Hz, 1H). $^{13}\text{C NMR}$ (201 MHz, CDCl_3) δ 205.91, 154.25, 147.89, 146.21, 130.90, 129.73, 128.91, 127.12, 126.18, 124.26, 95.91, 74.60, 57.93, 54.39, 45.36, 42.28, 34.63. **HRMS** (+APCI) calculated for $\text{C}_{17}\text{H}_{17}\text{O}_3\text{NCl}_3$ $[\text{M}+\text{H}]^+$ 388.02685, found 388.02722. **HPLC** (IK column 20% 2-propanol in hexanes, 1.0 mL/min) (**4.58'**): $t_{\text{M}} = 10.0$ min $t_{\text{m}} = 8.6$ min, 86:14 e.r.



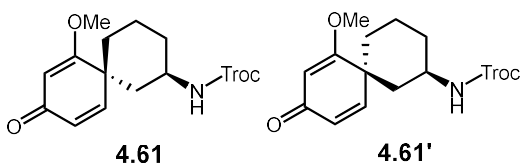
2,2,2-trichloroethyl (R)-(9-oxospiro[5.5]undeca-7,10-dien-2-yl)carbamate (4.59): Prepared using **General Procedure F** using **S20**, (**R**)-**4.43**, and (**S,S**)-**2.55**. Purified via preparative TLC using (20% Acetone in Hexanes) to provide **4.59** (0.0299 g, 82% yield, 91:9 e.r.) as a colorless oil. $^1\text{H NMR}$ (800 MHz, CDCl_3) δ 7.31 (dd, $J = 10.4, 3.0$ Hz, 1H), 6.67 (dd, $J = 10.0, 3.0$ Hz, 1H), 6.31 (d, $J = 10.3$ Hz, 1H), 6.23 (d, $J = 9.9$ Hz, 1H), 4.96 (s, 1H), 4.69 (s, 2H), 3.87 (tdt, $J = 12.1, 8.1, 4.0$ Hz, 1H), 2.20 (d, $J = 12.4$ Hz, 1H), 1.88 (dt, $J = 14.0, 3.6$ Hz, 1H), 1.83 (d, $J = 12.4$ Hz, 1H), 1.74 (qt, $J = 13.5, 4.1$ Hz, 1H), 1.59 – 1.50 (m, 2H), 1.44 (t, $J = 12.4$ Hz, 1H), 1.27 (qd, $J = 12.7, 4.0$ Hz, 1H). $^{13}\text{C NMR}$ (201 MHz, CDCl_3) δ 185.79, 156.24, 153.75,

150.53, 129.22, 128.43, 95.64, 74.59, 46.77, 41.77, 41.23, 34.63, 32.57, 21.19. **HRMS** (+APCI) calculated for $C_{14}H_{17}O_3NCl_3$ $[M+H]^+$ 352.02685, found 352.02722. **HPLC** (IB column 20% 2-propanol in hexanes, 1.0 mL/min) $t_M = 9.1$ min $t_m = 10.4$ min, 91:9 e.r.



2,2,2-trichloroethyl ((2*R*,6*R*)-8-methoxy-9-oxospiro[5.5]undeca-7,10-dien-2-yl)carbamate (**4.60**):

Prepared using **General Procedure F** using **S16**, (*R*)-**4.43**, and (*S,S*)-**2.55**. Purified via preparative TLC using (50% EtOAc in Hexanes) to provide **4.60** as a colorless oil (0.0142 g, 37% yield, >20:1 d.r., 89:11 e.r.). **¹H NMR** (800 MHz, $CDCl_3$) δ 6.69 (dd, $J = 9.9, 2.6$ Hz, 1H), 6.28 (d, $J = 9.9$ Hz, 1H), 6.15 (d, $J = 2.7$ Hz, 1H), 4.87 (s, 1H), 4.75 – 4.65 (m, 2H), 3.88 (tdt, $J = 12.1, 8.1, 4.0$ Hz, 1H), 3.71 (s, 3H), 2.23 (d, $J = 13.0$ Hz, 1H), 1.90 (dt, $J = 14.2, 3.8$ Hz, 1H), 1.80 (d, $J = 12.3$ Hz, 1H), 1.74 (qt, $J = 13.7, 3.7$ Hz, 1H), 1.59 (td, $J = 13.4, 4.0$ Hz, 1H), 1.53 – 1.40 (m, 2H), 1.29 – 1.21 (m, 2H). **¹³C NMR** (201 MHz, $CDCl_3$) δ 180.85, 156.50, 153.80, 151.30, 127.70, 116.40, 95.63, 74.62, 55.07, 47.13, 42.29, 42.00, 35.42, 32.66, 21.46. **HRMS** (+APCI) calculated for $C_{15}H_{19}O_4NCl_3$ $[M+H]^+$ 382.03742, found 382.03765. **HPLC** (IB column 20% 2-propanol in hexanes, 1.0 mL/min) (**4.60**): $t_M = 8.6$ min $t_m = 10.0$ min, 89:11 e.r.

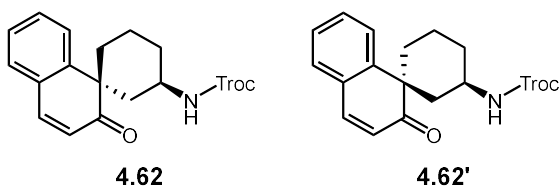


2,2,2-trichloroethyl ((2*R*,6*R*)-7-methoxy-9-oxospiro[5.5]undeca-7,10-dien-2-yl)carbamate (**4.61**) and

2,2,2-trichloroethyl ((2*R*,6*S*)-7-methoxy-9-oxospiro[5.5]undeca-7,10-dien-2-yl)carbamate (**4.61'**):

Prepared using **General Procedure F** using **S17**, (*R*)-**4.43**, and (*S,S*)-**2.55**. Purified via preparative TLC using (20% Acetone in Hexanes) to provide **4.61** and **4.61'** as a colorless oil and mixture of inseparable diastereomers (0.0182 g, 47% yield, 1.2:1 d.r., 81:19 e.r.). **¹H NMR** (800 MHz, $CDCl_3$) δ 7.10 (d, $J = 10.2$ Hz, 1H), 6.44 (d, $J = 9.9$ Hz, 1H, minor), 6.23 (dd, $J = 10.2, 1.6$ Hz, 1H), 6.09 (dd, $J = 9.9, 1.6$ Hz, 1H,

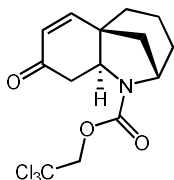
minor), 5.58 (d, $J = 1.6$ Hz, 1H), 5.49 (d, $J = 1.7$ Hz, 1H, minor), 4.87 (dd, $J = 16.5, 8.1$ Hz, 1H), 4.71 – 4.66 (m, 2H), 4.21 (ddp, $J = 10.9, 6.9, 4.1$ Hz, 1H, minor), 3.91 (tdt, $J = 12.4, 8.5, 4.2$ Hz, 1H), 3.77 (s, 3H, minor), 3.73 (s, 4H), 2.21 – 2.14 (m, 1H), 2.11 – 2.05 (m, 2H), 2.04 – 1.94 (m, 2H), 1.91 – 1.82 (m, 2H), 1.76 (dq, $J = 17.6, 6.6, 5.3, 2.2$ Hz, 3H), 1.52 (ddd, $J = 14.7, 12.1, 4.8$ Hz, 1H, minor), 1.47 – 1.43 (m, 1H), 1.41 (dd, $J = 13.7, 10.6$ Hz, 1H, minor), 1.31 – 1.19 (m, 3H). ^{13}C NMR (201 MHz, CDCl_3) δ 187.75, 187.03, 180.83, 178.44, 153.81, 153.72, 152.05, 146.77, 127.83, 126.70, 102.43, 101.09, 95.72, 95.67, 74.60, 74.54, 55.90, 55.75, 46.65, 46.58, 44.09, 43.39, 39.85, 39.41, 34.02, 32.92, 32.56, 31.60, 20.92, 20.84. **HRMS** (+APCI) calculated for $\text{C}_{15}\text{H}_{19}\text{O}_4\text{NCl}_3$ $[\text{M}+\text{H}]^+$ 382.03742, found 382.03797. **HPLC** (IK column 30% 2-propanol in hexanes, 1.0 mL/min) (**4.61**): $t_M = 18.5$ min $t_m = 12.4$ min, 81:19 e.r. (**4.61'**): $t_M = 8.7$ min $t_m = 10.9$ min, 80:20 e.r.



2,2,2-trichloroethyl ((1S,3R)-2'-oxo-2'H-spiro[cyclohexane-1,1'-naphthalen]-3-yl)carbamate (**4.62**) and *2,2,2-trichloroethyl ((1R,3R)-2'-oxo-2'H-spiro[cyclohexane-1,1'-naphthalen]-3-yl)carbamate* (**4.62'**):

Prepared using **General Procedure F** using **S18**, (*R*)-**4.43**, and (*S,S*)-**2.55**. Purified via preparative TLC using (20% EtOAc in Hexanes) to provide **4.62** and **4.62'** as a colorless oil and mixture of inseparable diastereomers (0.0177 g, 43% yield, 4:1 d.r., 88:12 e.r.). ^1H NMR (800 MHz, CDCl_3) δ 7.59 (d, $J = 8.0$ Hz, 1H), 7.49 (d, $J = 8.0$ Hz, 1H, minor), 7.43 (t, $J = 7.3$ Hz, 1H), 7.38 (d, $J = 9.8$ Hz, 1H), 7.33 – 7.27 (m, 3H), 6.86 (d, $J = 8.5$ Hz, 1H), 6.12 (d, $J = 9.7$ Hz, 1H), 6.06 (d, $J = 9.8$ Hz, 1H, minor), 4.75 (d, $J = 12.0$ Hz, 2H), 4.73 (d, $J = 12.0$ Hz, 2H), 4.69 (d, $J = 4.4$ Hz, 2H, minor), 4.49 (tdt, $J = 11.8, 8.3, 4.3$ Hz, 1H, minor), 4.26 (dq, $J = 11.0, 5.5$ Hz, 1H), 2.32 (dd, $J = 14.9, 5.9$ Hz, 1H), 2.19 – 2.14 (m, 1H, minor), 2.09 (dd, $J = 14.9, 5.9$ Hz, 1H), 1.94 (ddd, $J = 14.1, 7.4, 3.5$ Hz, 1H), 1.89 – 1.81 (m, 1H), 1.76 (tdd, $J = 12.6, 9.4, 3.2$ Hz, 1H), 1.74 – 1.67 (m, 2H), 1.66 – 1.58 (m, 1H, minor), 1.55 (dtt, $J = 13.6, 6.8, 3.3$ Hz, 1H). ^{13}C NMR (201 MHz, CDCl_3) δ 206.13, 154.15, 146.74, 144.93, 130.27, 130.22, 129.74, 127.23, 126.94,

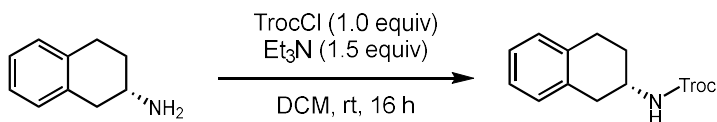
124.21, 96.01, 74.51, 52.45, 46.08, 37.31, 35.27, 31.16, 17.88. **HRMS** (+APCI) calculated for $C_{18}H_{19}O_3NCl_3$ $[M+H]^+$ 402.0425, found 402.04321. **HPLC** (IK column 5% 2-propanol in hexanes, 1.0 mL/min) (**4.62**): $t_M = 38.5$ min $t_m = 29.8$ min, 88:12 e.r. (**4.62'**): $t_M = 52.9$ min $t_m = 42.6$ min, 76:24 e.r.



2,2,2-trichloroethyl-8-oxo-2,3,4,5,9,9a-hexahydro-2,5a-methanobenzo[b]azepine-1(8H)-carboxylate

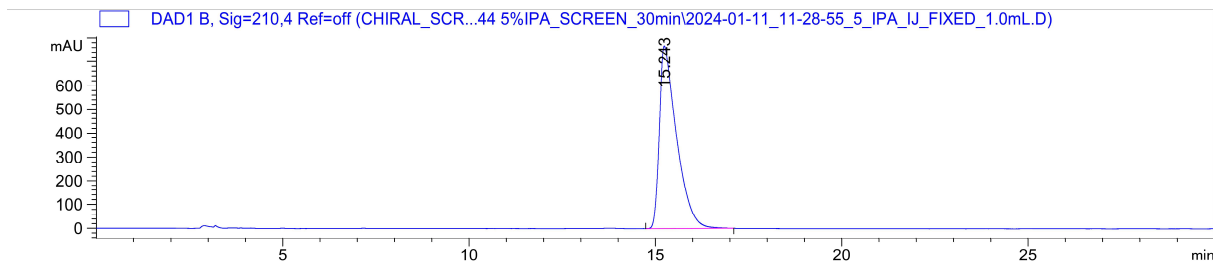
(4.66): Prepared using **General Procedure F** using **4.63**, **(R)-4.43**, and $[Ind^*RhCl_2]_2$. Purified via preparative TLC using (40% EtOAc in Hexanes) to provide **4.66** as a colorless oil and mixture of two conformers (0.0105 g, 30% yield.). **1H NMR** (800 MHz, $CDCl_3$) δ 6.58 (t, $J = 10.2$ Hz, 2H), 5.97 (d, $J = 5.5$ Hz, 1H), 5.95 (d, $J = 5.5$ Hz, 1H), 4.97 (d, $J = 12.0$ Hz, 1H), 4.82 (d, $J = 12.0$ Hz, 1H), 4.76 (d, $J = 11.9$ Hz, 1H), 4.56 (d, $J = 12.0$ Hz, 1H), 4.38 (t, $J = 5.3$ Hz, 1H), 4.35 (t, $J = 5.3$ Hz, 1H), 4.13 (d, $J = 6.3$ Hz, 1H), 4.11 (d, $J = 6.4$ Hz, 1H), 3.28 (ddd, $J = 23.6, 16.4, 6.3$ Hz, 2H), 2.41 (dd, $J = 16.4, 11.6$ Hz, 1H), 2.34 (dd, $J = 16.3, 11.7$ Hz, 1H), 2.28 – 2.24 (m, 1H), 2.24 – 2.20 (m, 1H), 2.17 (ddd, $J = 13.5, 9.1, 5.1$ Hz, 2H), 1.76 (dt, $J = 13.7, 5.3$ Hz, 2H), 1.73 – 1.58 (m, 8H), 1.44 (td, $J = 13.0, 5.5$ Hz, 1H), 1.40 (td, $J = 13.0, 5.5$ Hz, 1H). **^{13}C NMR** (201 MHz, $CDCl_3$) δ 197.11, 197.02, 152.31, 152.17, 151.79, 151.51, 127.90, 127.70, 95.81, 95.72, 74.80, 74.74, 61.07, 60.60, 56.96, 56.85, 43.82, 43.03, 42.04, 40.90, 40.19, 39.52, 37.08, 29.21, 27.66, 18.48, 18.40.

Confirmation of Product Stereochemistry



2,2,2-trichloroethyl (S)-(1,2,3,4-tetrahydronaphthalen-2-yl)carbamate ((S)-4.31): Under an N₂ atmosphere in a 8 dram vial equipped with stir bar, (S)-2-aminotetralin (0.075 g, 0.50 mmol, 1.0 equiv) and triethylamine (0.11 mL, 0.75 mmol, 1.5 equiv) were dissolved in DCM (2.5 mL). To this solution 2,2,2-trichloroethyl carbonochloridate (TrocCl) (0.08 mL, 0.50 mmol, 1.0 equiv) was added and the reaction was stirred at room temperature overnight. The reaction was quenched by the addition of 1M HCl followed by extraction with DCM (3x). The combined organic layers were washed with brine (1x) and dried over Na₂SO₄ before removing the solvent under reduced pressure. The crude product was purified using flash column chromatography with 10% EtOAc in hexanes to provide (S)-4.31 as a colorless oil (0.097 g, 59% yield). ¹H NMR (400 MHz, CDCl₃) δ 7.23 – 6.99 (m, 4H), 5.08 (d, *J* = 7.6 Hz, 1H), 4.76 (d, *J* = 12.1 Hz, 1H), 4.72 (d, *J* = 12.0 Hz, 1H), 4.09 (ddtd, *J* = 13.1, 8.2, 5.1, 3.1 Hz, 1H), 3.18 (dd, *J* = 16.3, 5.1 Hz, 1H), 2.99 – 2.83 (m, 2H), 2.72 (dd, *J* = 16.3, 8.1 Hz, 1H), 2.18 – 2.05 (m, 1H), 1.91 – 1.78 (m, 1H). ¹³C NMR (101 MHz, CDCl₃) δ 154.01, 135.40, 133.76, 129.60, 129.00, 126.42, 126.16, 95.74, 74.56, 47.28, 35.82, 28.79, 27.04. HRMS (+APCI) calculated for C₁₃H₁₅O₂NC₃ [M+H]⁺ 322.01629, found 322.01679. HPLC (IJ column 5% 2-propanol in hexanes, 1.0 mL/min) *t*_M = 15.2min

2,2,2-trichloroethyl (*S*)-(1,2,3,4-tetrahydronaphthalen-2-yl)carbamate ((*S*)-4.31):

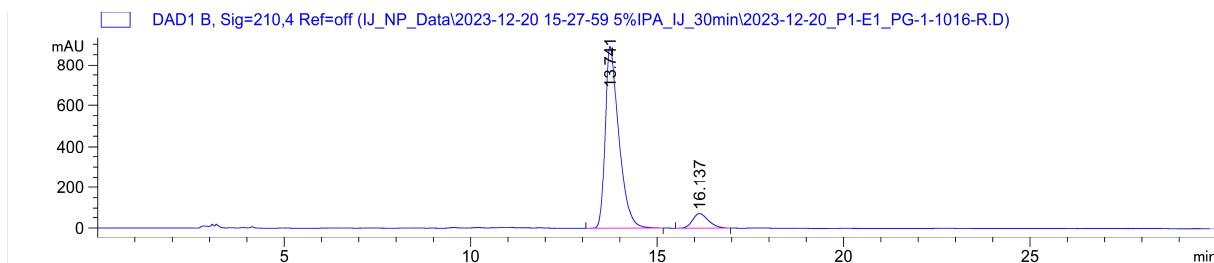


Signal 2: DAD1 B, Sig=210,4 Ref=off

| Peak # | RetTime [min] | Type | Width [min] | Area [mAU*s] | Height [mAU] | Area % |
|--------|---------------|------|-------------|--------------|--------------|----------|
| 1 | 15.243 | BV R | 0.3815 | 2.45226e4 | 767.96552 | 100.0000 |

Totals : 2.45226e4 767.96552

2,2,2-trichloroethyl (*R*)-(1,2,3,4-tetrahydronaphthalen-2-yl)carbamate ((*R*)-4.31):



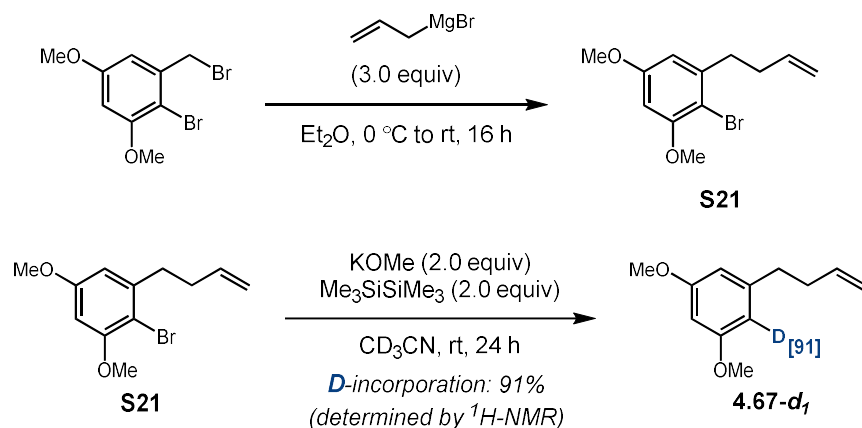
Signal 2: DAD1 B, Sig=210,4 Ref=off

| Peak # | RetTime [min] | Type | Width [min] | Area [mAU*s] | Height [mAU] | Area % |
|--------|---------------|------|-------------|--------------|--------------|---------|
| 1 | 13.741 | VV R | 0.3316 | 2.25000e4 | 891.12781 | 91.6616 |
| 2 | 16.137 | VV R | 0.3432 | 2046.81458 | 69.97881 | 8.3384 |

Totals : 2.45468e4 961.10662

Based on the comparison of the HPLC traces of (*S*)-4.31 with the sample of 4.31 prepared by using (*R*)-4.43, and (*S,S*)-2.55 the product stereochemistry of the 2-aminotetralins and the spirocycles has been assigned to be (*R*)

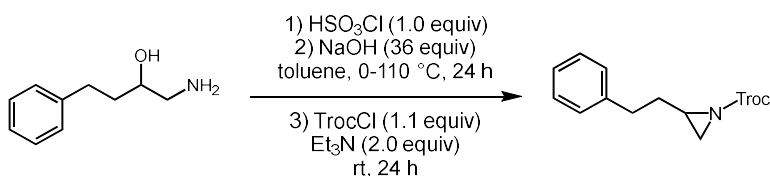
Synthesis of Substrates for Mechanistic Studies



2-bromo-1-(but-3-en-1-yl)-3,5-dimethoxybenzene (**S21**): Under an N₂ atmosphere and at 0 °C, allyl magnesium bromide (30 mL, 1.0M in Et₂O, 3.0 equiv) was slowly added to a solution of 2-bromo-1-(bromomethyl)-3,5-dimethoxybenzene substrate²³ (3.10 g, 10.0 mmol, 1.0 equiv) in Et₂O (40 mL, 0.25M). Once the addition was completed the reaction was left to stir at room temperature overnight. The reaction was placed in an ice bath and slowly quenched with sat. NH₄Cl. The resulting biphasic solution was extracted with Et₂O (3x) and the combined organic layers washed with brine 1x. The organic layers were dried over MgSO₄ and the solvent removed under reduced pressure and the crude product was purified using silica gel column chromatography using 5% EtOAc in Pentane to provide **S21** as a colorless oil (1.964 g, 72%). ¹H NMR (400 MHz, CDCl₃) δ 6.41 (d, *J* = 2.7 Hz, 1H), 6.36 (d, *J* = 2.7 Hz, 1H), 5.89 (ddt, *J* = 16.9, 10.2, 6.6 Hz, 1H), 5.07 (dq, *J* = 17.1, 1.7 Hz, 1H), 5.00 (ddt, *J* = 10.2, 2.1, 1.2 Hz, 1H), 3.86 (s, 3H), 3.80 (s, 3H), 2.86–2.78 (m, 2H), 2.37 (dt, *J* = 9.4, 6.6, 1.4 Hz, 2H). ¹³C NMR (101 MHz, CDCl₃) δ 159.55, 156.81, 143.23, 137.89, 115.23, 106.85, 104.80, 97.55, 56.41, 55.61, 36.31, 33.92. HRMS (+APCI) calculated for C₁₂H₁₆O₂Br [M+H]⁺ 271.03282, found 271.03291.

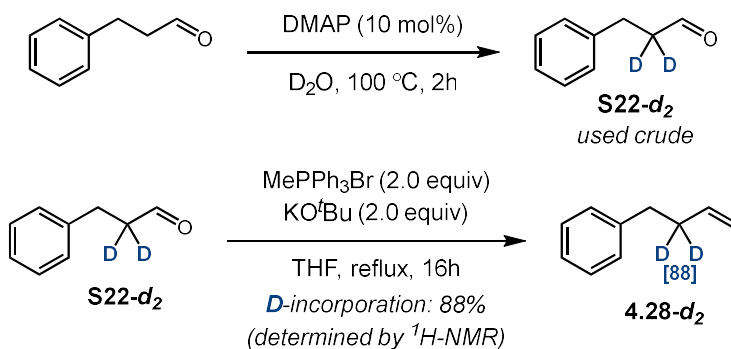
1-(but-3-en-1-yl)-3,5-dimethoxybenzene-2-d (**4.67-d₁**): Using an adapted procedure by Liu.²⁴ In a dry 24 mL reaction vial equipped with a stir bar and under a N₂ atmosphere, **S21** (0.538 g, 2.0 mmol, 1.0 equiv), potassium methoxide (0.284 g, 4.0 mmol, 2.0 equiv), and hexamethyl disilane (0.82 mL, 4.0 mmol, 2.0 equiv) were dissolved in a CD₃CN (5mL) and left to stir at room temperature for 24 hours. The reaction

was quenched with DI H₂O (6 mL) and extracted with Et₂O (3x10mL). The combined organic layers were washed with brine (1x) and dried over MgSO₄. The solvent was removed under reduced pressure and the crude product was purified using silica gel column chromatography 5% EtOAc in Hexanes to provide **4.67-d₁** as a colorless oil (0.3145 g, 82%). ¹H NMR (400 MHz, CDCl₃) δ 6.36 (d, *J* = 2.3 Hz, 1H), 6.31 (d, *J* = 2.3 Hz, 1H), 5.87 (ddt, *J* = 16.9, 10.2, 6.6 Hz, 1H), 5.06 (dt, *J* = 17.2, 1.8 Hz, 1H), 4.99 (ddt, *J* = 10.2, 2.2, 1.3 Hz, 1H), 3.79 (s, 6H), 2.66 (dd, *J* = 9.0, 6.7 Hz, 2H), 2.37 (tdt, *J* = 7.8, 6.5, 1.4 Hz, 2H). ¹³C NMR (101 MHz, CDCl₃) δ 160.81, 160.79, 144.36, 138.18, 115.06, 106.60, 106.29 (t, *J* = 23.9 Hz), 97.89, 55.37, 35.75, 35.42. HRMS (+APCI) calculated for C₁₂H₁₆DO₂ [M+H]⁺ 194.12858, found 194.12871.



2,2,2-trichloroethyl 2-phenethylaziridine-1-carboxylate (**4.68**): Using an adapted procedure by Doyle.²⁵ Under an N₂ atmosphere, in a 100 mL RBF equipped with a stir bar, 1-amino-4-phenylbutan-2-ol²⁶ (0.500 g, 3.0 mmol, 1.0 equiv) was dissolved in Toluene (20 mL) and the reaction vessel placed in an ice bath. Once cool, chlorosulfonic acid (0.20 mL, 3.0 mmol, 1.0 equiv) was added and the reaction stirred at room temperature. After two hours NaOH (18mL, 6M, 36 equiv) was added, a condenser attached, and the reaction was refluxed overnight. The reaction was cooled to room temperature and extracted with Et₂O (3x) and washed with brine (1x). The combined organic layers were dried over MgSO₄ and the Et₂O removed under reduced pressure. The remaining toluene solution containing the crude unprotected aziridine was placed in a 100mL RBF and the reaction vessel was placed in an ice bath. Once cool, Et₃N (0.85 mL, 6.0 mmol, 2.0 equiv) was added followed by TrocCl (0.46 mL, 0.33 mmol, 1.1 equiv) and the reaction was stirred at room temperature overnight. The reaction was quenched by adding sat. NaHCO₃ and then extracting with DCM (3X). The combined organic layers were dried over MgSO₄ and the solvent removed under reduced pressure. The crude product was first purified by silica silica gel column chromatography using 10% EtOAc in Hexanes followed by Kugelrohr distillation to provide **4.68** as a colorless oil (0.412

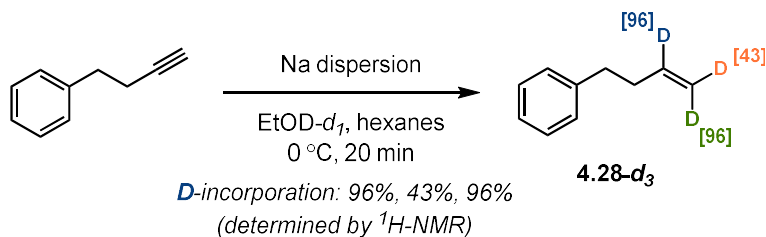
g, 42%). $^1\text{H NMR}$ (400 MHz, CDCl_3) δ 7.34 – 7.27 (m, 2H), 7.25 – 7.16 (m, 3H), 4.79 (d, $J = 12.0$ Hz, 1H), 4.75 (d, $J = 12.0$ Hz, 1H), 2.97 – 2.76 (m, 2H), 2.61 (dddd, $J = 7.2, 6.1, 5.2, 3.8$ Hz, 1H), 2.45 (d, $J = 6.1$ Hz, 1H), 2.10 (d, $J = 3.8$ Hz, 1H), 1.94 – 1.76 (m, 2H). $^{13}\text{C NMR}$ (101 MHz, CDCl_3) δ 161.83, 141.20, 128.61, 128.59, 126.23, 95.15, 75.52, 38.59, 34.19, 33.29, 32.42. **HRMS** (+APCI) calculated for $\text{C}_{13}\text{H}_{15}\text{O}_2\text{NCl}_3$ $[\text{M}+\text{H}]^+$ 322.01629, found 322.01673.



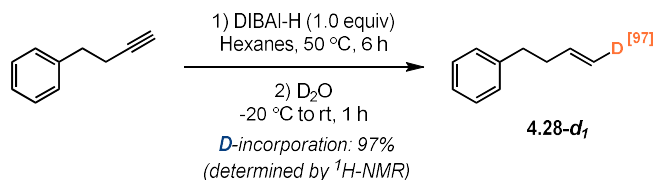
3-phenylpropanal-2,2-d₂ (**S22-d₂**): Using an adapted procedure by Zhang.⁷ In a 24 mL reaction equipped with a stir bar, 3-phenylpropanal (3.30 mL, 25.0 mmol, 1.0 equiv) and DMAP (0.31 g, 2.5 mmol, 0.1 equiv) were dissolved in D_2O (5.0 mL). The reaction vessel was sealed, placed in an aluminum heating block and heated at 100 C. After two hours, the reaction vessel was cooled to room temperature and the reaction was extracted with DCM (3x10mL). The combined organic layers were washed with 1M HCl (10 mL), sat. NaHCO_3 (10mL) and brine (10 mL) before drying over Na_2SO_4 . The solvent was removed, and the crude material was used directly in the next step.

(but-3-en-1-yl-2,2-d₂)benzene (**4.28-d₂**): Under an N_2 atmosphere, in a 250 RBF equipped with a stir bar and condenser methyltriphenylphosphonium bromide was dissolved in THF (125 mL) and the reaction vessel placed in an ice bath. Once cool, the vessel was quickly opened and potassium tert-butoxide (5.66 g, 50 mmol, 2.0 equiv) was added quickly. The reaction was sealed, and the yellow solution was stirred for one hour. Crude **S22-d₂** was dissolved in THF (10 mL) and added to the reaction before placing in heating block and refluxed overnight. The reaction was cooled to room temperature and placed in an ice bath before quenching with sat. NH_4Cl . The reaction was extracted with Et_2O (3x) and washed with brine (1x). The

combined organic layers were dried over MgSO₄ and the solvent removed under reduced pressure. The crude reaction mixture was purified using on silica gel column chromatography using Pentane to provide **4.28-d₂** as colorless oil (2.25 g, 67%) ¹H NMR (400 MHz, CDCl₃) δ 7.36 – 7.27 (m, 2H), 7.21 (dd, *J* = 7.1, 1.8 Hz, 3H), 5.88 (dd, *J* = 17.1, 10.3 Hz, 1H), 5.07 (dt, *J* = 17.2, 1.9 Hz, 1H), 5.00 (dt, *J* = 10.2, 1.8 Hz, 1H), 2.72 (s, 2H). Spectroscopic data for **4.28-d₂** matches those previously reported in the literature.²⁷



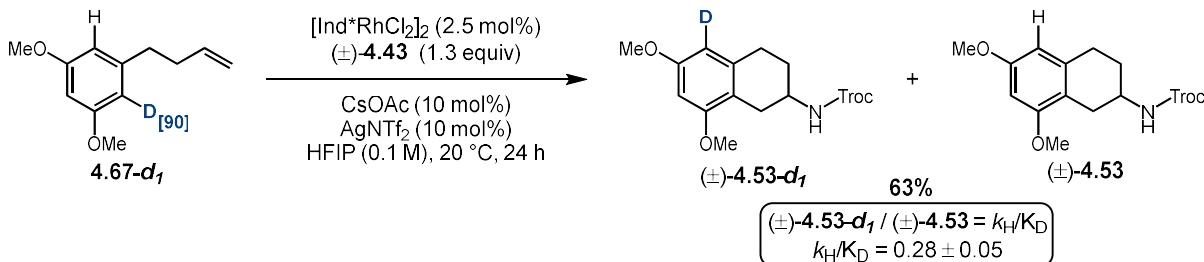
(*but-3-en-1-yl-3,4,4-d₃*)benzene (**4.28-d₃**): Using an adapted procedure by An.²⁸ Under an N₂ atmosphere, in a 250 mL RBF equipped with a stir bar, 3-butenylbenzene (0.70 mL, 5.00mmol, 1.0 equiv) was dissolved in Hexanes (60 mL) and the reaction vessel placed in an ice bath. Once cool, EtOD (3.5 mL, 60 mmol, 12 equiv) was added followed by the addition of a sodium dispersion in mineral oil (4.5 g, 25% wt, 10 equiv). The reaction was stirred very vigorously for two hours. The reaction was quenched through the addition of sat. NaHCO₃ and stirred for an additional 20min. The reaction was extracted with Et₂O (3x) and washed with brine (1x). The combined organic layers were dried over MgSO₄, and the solvent was removed under reduced pressure. The crude product was first purified by silica gel column chromatography using 100% Pentane followed by Kugelrohr distillation to provide **4.28-d₃** as a colorless oil (0.5373 g, 80%) ¹H NMR (400 MHz, CDCl₃) δ 7.34 – 7.27 (m, 2H), 7.25 – 7.17 (m, 3H), 2.80 – 2.65 (m, 2H), 2.39 (t, *J* = 7.9 Hz, 2H). Spectroscopic data for **4.28-d₃** matches those previously reported in the literature.²⁸



(E)-(but-3-en-1-yl-4-*d*)benzene (*E*-4.28-*d*₁): Using an adapted procedure by Hirino and Murana.²⁹ Under an N₂ atmosphere, 3-butenylbenzene (0.70 mL, 5.00mmol, 1.0 equiv) was dissolved in Hexanes (27 mL) followed by the dropwise addition of DIBAL-H (14.4 mL, 1.0M in toluene) at room temperature. The reaction was placed in an alumina heating block and stirred at 50 °C for 6 hours. Afterwards, the reaction was cooled to -20 °C and D₂O (0.70 mL, 5.00mmol, 1.0 equiv) was added and the reaction was stirred for an additional hour at room temperature. To the reaction sat. NH₄Cl was added and the resulting suspension was filtered through alumina. The filtrate was dried over Na₂SO₄ and the solvent removed under reduced pressure to afford the crude product which was purified via flash column chromatography (100% Pentane) to afford *E*-4.28-*d*₁ as a colorless oil (1.0 g, 60%). ¹H NMR (800 MHz, CDCl₃) δ 7.32 – 7.27 (m, 2H), 7.23 – 7.17 (m, 3H), 5.92 – 5.81 (m, 1H), 5.08 – 5.01 (m, 1H), 2.72 (t, *J* = 7.8 Hz, 2H), 2.42 – 2.35 (m, 2H). ¹³C NMR (201 MHz, CDCl₃) δ 142.02, 138.13, 128.58, 128.43, 125.95, 114.78 (t, *J* = 24.2 Hz), 35.62, 35.53. HRMS (+APCI) calculated for C₁₀H₁₂D [M+H]⁺ 134.10745, found 134.10758. *This data was collected by Wesley Pullara*

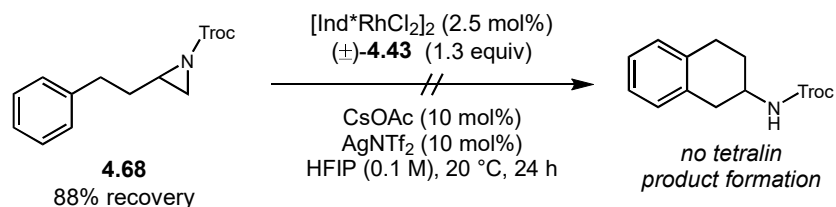
Mechanistic Studies

Kinetic Isotope Effect (KIE) Study



In an oven-dried 4 dram reaction vial, with Teflon tape wrapped threads, and equipped with an oven dried stir bar was brought into the glovebox. To the vial, CsOAc (0.01 mmol, 0.1 equiv.), AgNTf₂ (0.30 mmol, 0.3 equiv.), and $[\text{Ind}^*\text{RhCl}_2]_2$ (2.5 mol%) were added to the reaction vial. The vial was sealed with a Teflon septum screw cap and brought out of the box to complete the reaction. Under an N₂ atmosphere outside of the glovebox, $(\pm)\text{-4.43}$ was transferred to the reaction as stock solution in HFIP (0.5 mL, 0.26 mmol, 1.3 equiv). The deuterated substrate **4.67-*d*₁** (0.10 mmol 1.0 equiv.) was added to the reaction vial using HFIP washing the vial three times (0.2 mL + 0.2 mL + 0.1 mL) to ensure complete transfer of the olefin. The reaction was left to stir at room temperature under an N₂ balloon for 24 hours. After 24 hours, the crude reaction was filtered through a Celite pipette plug using DCM to flush. The solvent was removed under reduced pressure and the crude material purified via preparative TLC using the indicated eluent to yield the corresponding deuterated 2-aminotetralin **(±)-4.53-*d*₁**. The yield was determined to be 65% from the isolated product. The kinetic isotope effect was determined to be $k_{\text{H}}/k_{\text{D}} = 0.28 \pm 0.05$ based on ¹H-NMR analysis of the isolated product.

Intermediate Aziridine



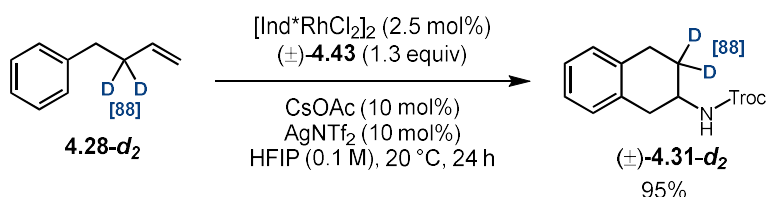
In an oven-dried 4 dram reaction vial, with Teflon tape wrapped threads, and equipped with an oven dried stir bar was brought into the glovebox. To the vial, CsOAc (0.01 mmol, 0.1 equiv.), AgNTf₂ (0.30 mmol, 0.3 equiv.), and $[\text{Ind}^*\text{RhCl}_2]_2$ (2.5 mol%) were added to the reaction vial. The vial was sealed with a Teflon septum screw cap and brought out of the box to complete the reaction. Under an N₂ atmosphere outside of the glovebox, $(\pm)\text{-4.43}$ was transferred to the reaction as stock solution in HFIP (0.5 mL, 0.26 mmol, 1.3 equiv). The aziridine **4.68** (0.10 mmol 1.0 equiv.) was added to the reaction vial using HFIP washing the vial three times (0.2 mL + 0.2 mL + 0.1 mL) to ensure complete transfer of the olefin. The reaction was left to stir at room temperature under an N₂ balloon for 24 hours. After 24 hours, the crude reaction was filtered through a Celite pipette plug using DCM to flush. The solvent was removed under reduced pressure and the crude reaction was analyzed by ¹H-NMR using dibromomethane as an internal standard. No 2-aminotetralin product formation was observed and the aziridine **4.68** was recovered in a 88% yield.

Deuterium Labeling Studies

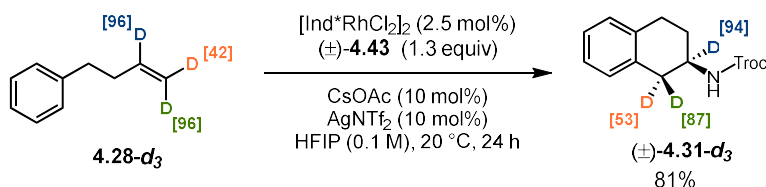
General Procedure G: 1,2-Arylamination Procedure for Deuterium Labeling Studies

In an oven-dried 4 dram reaction vial, with Teflon tape wrapped threads, and equipped with an oven dried stir bar was brought into the glovebox. To the vial, CsOAc (0.01 mmol, 0.1 equiv.), AgNTf₂ (0.30 mmol, 0.3 equiv.), and $[\text{Ind}^*\text{RhCl}_2]_2$ (2.5 mol%) were added to the reaction vial. The vial was sealed with a Teflon septum screw cap and brought out of the box to complete the reaction. Under an N₂ atmosphere outside of the glovebox, $(\pm)\text{-4.43}$ was transferred to the reaction as stock solution in HFIP (0.5 mL, 0.26 mmol, 1.3 equiv). The deuterated olefin substrate (0.10 mmol 1.0 equiv.) was added to the reaction vial using HFIP

washing the vial three times (0.2 mL + 0.2 mL + 0.1 mL) to ensure complete transfer of the olefin. The reaction was left to stir at room temperature under an N₂ balloon for 24 hours. After 24 hours, the crude reaction was filtered through a Celite pipette plug using DCM to flush. The solvent was removed under reduced pressure and the crude material purified via preparative TLC using the indicated eluent to yield the corresponding deuterated 2-aminotetralin or spirocycle product. Deuterium incorporation was determined by analysis of the ¹H-NMR.

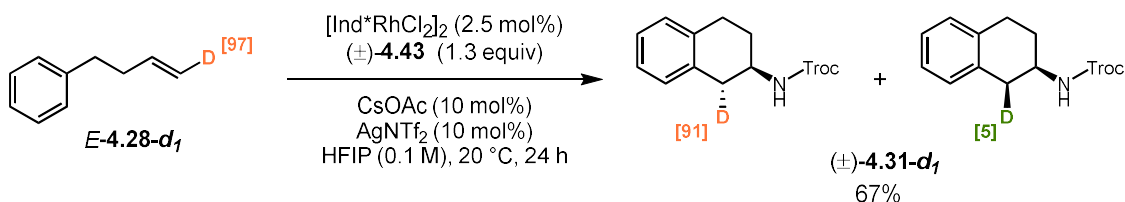


2,2,2-trichloroethyl (1,2,3,4-tetrahydronaphthalen-2-yl-3,3-d₂)carbamate ((±)-**4.31-d₂**): Prepared using **General Procedure G** using **4.28-d₂**. Purified via preparative TLC using (20% Acetone in Hexanes) to provide ((±)-**4.31-d₂** as a colorless oil (0.0355 g, 95% yield). ¹H NMR (400 MHz, CDCl₃) δ 7.20 – 7.04 (m, 4H), 5.04 (d, *J* = 6.9 Hz, 1H), 4.76 (d, *J* = 12.1 Hz, 1H), 4.72 (d, *J* = 12.1 Hz, 1H), 4.08 (td, *J* = 8.0, 5.0 Hz, 1H), 3.17 (dd, *J* = 16.3, 5.1 Hz, 1H), 2.90 (s, 2H), 2.72 (dd, *J* = 16.3, 8.0 Hz, 1H). ¹³C NMR (201 MHz, CDCl₃) δ 154.04, 135.42, 133.77, 129.62, 129.03, 126.45, 126.17, 95.76, 74.60, 47.16, 35.80, 28.59 – 27.78 (m), 26.83. HRMS (+APCI) calculated for C₁₃H₁₃D₂O₂NCl₃ [M+H]⁺ 324.02884, found 324.02926.



2,2,2-trichloroethyl (1,2,3,4-tetrahydronaphthalen-2-yl-1,1,2-d₃)carbamate ((±)-**4.31-d₃**): Prepared using **General Procedure G** using **4.28-d₃**. Purified via preparative TLC using (20% Acetone in Hexanes) to provide ((±)-**4.31-d₃** as a colorless oil (0.0283 g, 81% yield). ¹H NMR (400 MHz, CDCl₃) δ 7.19 – 7.03 (m, 4H), 5.05 (s, 1H), 4.76 (d, *J* = 12.0 Hz, 1H), 4.72 (d, *J* = 12.2 Hz, 1H), 2.98 – 2.84 (m, 2H), 2.10 (dt, *J* =

12.4, 6.0 Hz, 1H), 1.84 (dt, $J = 13.4, 7.1$ Hz, 1H). ^{13}C NMR (201 MHz, CDCl_3) δ 153.92, 135.35 (d, $J = 4.4$ Hz), 133.57 (d, $J = 8.5$ Hz), 129.52, 128.89, 126.34, 95.65, 74.48, 46.89 – 46.52 (m), 35.51 – 34.92 (m), 28.53, 26.88 (d, $J = 6.2$ Hz). HRMS (+APCI) calculated for $\text{C}_{13}\text{H}_{12}\text{D}_3\text{O}_2\text{NCl}_3$ $[\text{M}+\text{H}]^+$ 325.03512, found 325.03546.



2,2,2-trichloroethyl (1,2,3,4-tetrahydronaphthalen-2-yl-1-d)carbamate ((±)-**4.31-d₁**): Prepared using **General Procedure G** using *E-4.28-d₁*. Purified via preparative TLC using (20% Acetone in Hexanes) to provide ((±)-**4.31-d₁** as a colorless oil (0.0227 g, 67% yield). ^1H NMR (400 MHz, CDCl_3) δ 7.23 – 7.06 (m, 4H), 5.08 (d, $J = 7.8$ Hz, 1H), 4.78 (d, $J = 12.1$ Hz, 1H), 4.74 (d, $J = 12.0$ Hz, 1H), 4.10 (qd, $J = 8.2, 3.1$ Hz, 1H), 2.94 (t, $J = 6.1$ Hz, 2H), 2.72 (d, $J = 8.2$ Hz, 1H), 2.14 (dtd, $J = 12.2, 6.0, 3.1$ Hz, 1H), 1.86 (ddd, $J = 15.8, 12.8, 8.1$ Hz, 1H). ^{13}C NMR (201 MHz, CDCl_3) δ 154.04, 135.44, 133.73, 129.61, 129.00, 126.45, 126.17, 95.77, 74.60, 47.26, 35.52 (t, $J = 19.9$ Hz), 28.82, 27.08. HRMS (+APCI) calculated for $\text{C}_{13}\text{H}_{14}\text{DO}_2\text{NCl}_3$ $[\text{M}+\text{H}]^+$ 323.02257, found 323.02184. *This data was collected by Wesley Pullara*

4.5.3 Supplementary Information References

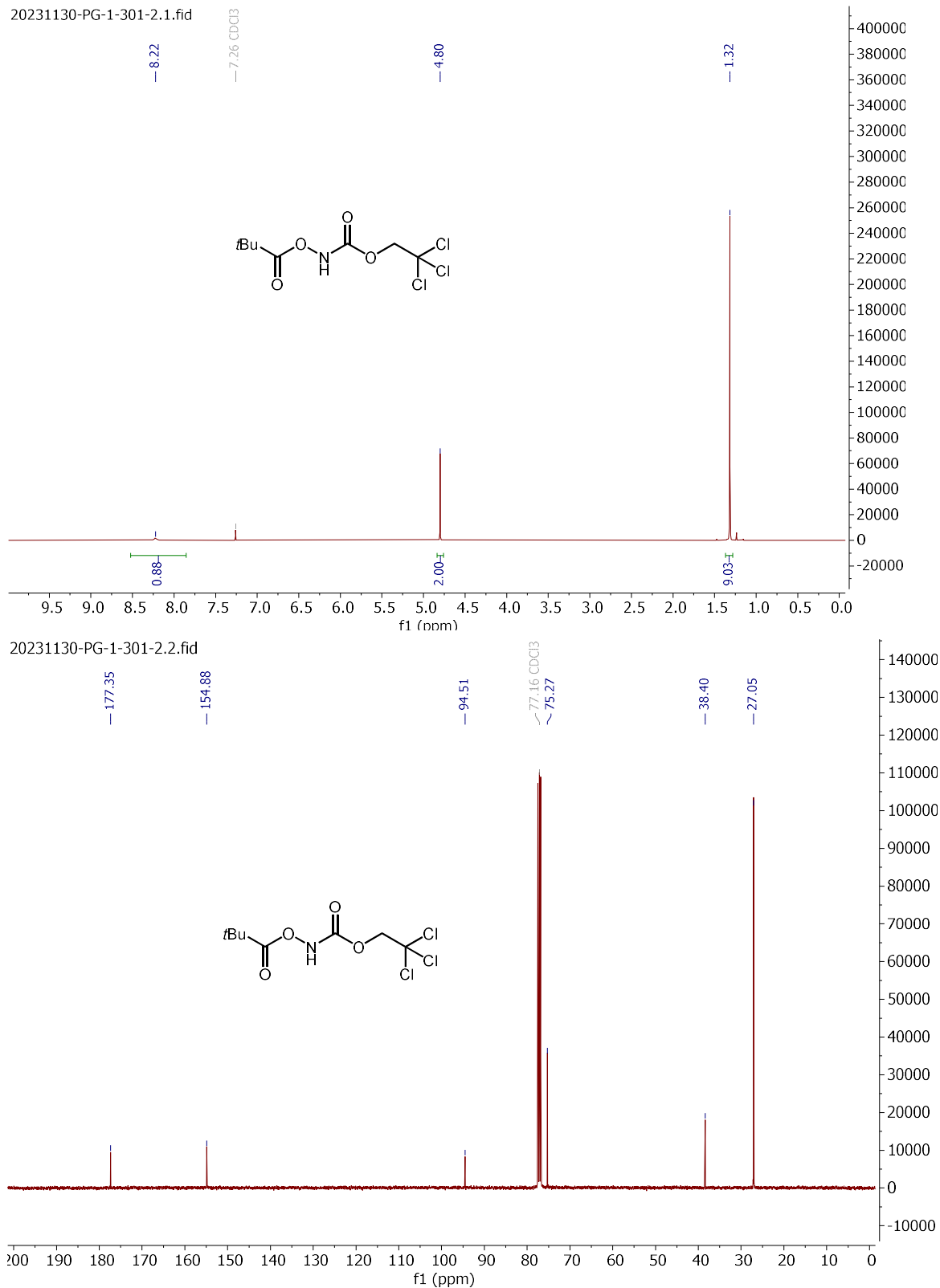
- (1) Lu, D.-F.; Zhu, C.-L.; Sears, J. D.; Xu, H. Iron(II)-Catalyzed Intermolecular Aminofluorination of Unfunctionalized Olefins Using Fluoride Ion. *J. Am. Chem. Soc.* **2016**, *138* (35), 11360.
- (2) Masruri; Willis, A. C.; McLeod, M. D. Osmium-Catalyzed Vicinal Oxyamination of Alkenes by N-(4-Toluenesulfonyloxy)carbamates. *The Journal of Organic Chemistry* **2012**, *77* (19), 8480.
- (3) Jing, C.; Jones, B. T.; Adams, R. J.; Bower, J. F. Cyclopropane-Fused N-Heterocycles via Aza-Heck-Triggered C(sp³)-H Functionalization Cascades. *J. Am. Chem. Soc.* **2022**, *144* (37), 16749.
- (4) Falk, E.; Makai, S.; Delcaillau, T.; Gürtler, L.; Morandi, B. Design and Scalable Synthesis of N-Alkylhydroxylamine Reagents for the Direct Iron-Catalyzed Installation of Medicinally Relevant Amines**. *Angew. Chem. Int. Ed.* **2020**, *59* (47), 21064.
- (5) Wang, Y.-F.; Gao, Y.-R.; Mao, S.; Zhang, Y.-L.; Guo, D.-D.; Yan, Z.-L.; Guo, S.-H.; Wang, Y.-Q. Wacker-Type Oxidation and Dehydrogenation of Terminal Olefins Using Molecular Oxygen as the Sole Oxidant without Adding Ligand. *Org. Lett.* **2014**, *16* (6), 1610.
- (6) Ranu, B. C.; Banerjee, S.; Adak, L. Regioselective cross-coupling of allylindium reagents with activated benzylic bromides—a simple and efficient procedure for the synthesis of terminal alkenes. *Tetrahedron Lett.* **2007**, *48* (41), 7374.
- (7) Zhang, Q.; Wang, S.; Zhang, Q.; Xiong, T.; Zhang, Q. Radical Addition-Triggered Remote Migratory Isomerization of Unactivated Alkenes to Difluoromethylene-Containing Alkenes Enabled by Bimetallic Catalysis. *ACS Catalysis* **2022**, *12* (1), 527.
- (8) Lu, Y.; Nakatsuji, H.; Okumura, Y.; Yao, L.; Ishihara, K. Enantioselective Halo-oxy- and Halo-azacyclizations Induced by Chiral Amidophosphate Catalysts and Halo-Lewis Acids. *J. Am. Chem. Soc.* **2018**, *140* (19), 6039.
- (9) Lin, S.; Song, C.-X.; Cai, G.-X.; Wang, W.-H.; Shi, Z.-J. Intra/Intermolecular Direct Allylic Alkylation via Pd(II)-Catalyzed Allylic C-H Activation. *J. Am. Chem. Soc.* **2008**, *130* (39), 12901.

- (10) Liu, R.; Lu, Z.-H.; Hu, X.-H.; Li, J.-L.; Yang, X.-J. Monocarboxylation and Intramolecular Coupling of Butenylated Arenes via Palladium-Catalyzed C–H Activation Process. *Org. Lett.* **2015**, *17* (6), 1489.
- (11) Smith, M. J. S.; Tu, W.; Robertson, C. M.; Bower, J. F. Stereospecific Aminative Cyclizations Triggered by Intermolecular Aza-Prilezhaev Alkene Aziridination. *Angew. Chem. Int. Ed.* **2023**, *62* (48), e202312797.
- (12) Meng, Q.-Y.; Schirmer, T. E.; Katou, K.; König, B. Controllable Isomerization of Alkenes by Dual Visible-Light-Cobalt Catalysis. *Angew. Chem. Int. Ed.* **2019**, *58* (17), 5723.
- (13) Trost, B. M.; Yeh, V. S. C.; Ito, H.; Bremeyer, N. Effect of Ligand Structure on the Zinc-Catalyzed Henry Reaction. Asymmetric Syntheses of (–)-Denopamine and (–)-Arbutamine. *Org. Lett.* **2002**, *4* (16), 2621.
- (14) Murai, M.; Nishimura, K.; Takai, K. Palladium-catalyzed double-bond migration of unsaturated hydrocarbons accelerated by tantalum chloride. *Chem. Commun.* **2019**, *55* (19), 2769.
- (15) Semakul, N.; Jackson, K. E.; Paton, R. S.; Rovis, T. Heptamethylindenyl (Ind*) enables diastereoselective benzamidation of cyclopropenes via Rh(iii)-catalyzed C-H activation. *Chem Sci* **2017**, *8* (2), 1015.
- (16) Gross, P.; Im, H.; Laws, D., III; Park, B.; Baik, M.-H.; Blakey, S. B. Enantioselective Aziridination of Unactivated Terminal Alkenes Using a Planar Chiral Rh(III) Indenyl Catalyst. *J. Am. Chem. Soc.* **2024**, *146* (2), 1447.
- (17) Ye, C.-X.; Shen, X.; Chen, S.; Meggers, E. Stereocontrolled 1,3-nitrogen migration to access chiral α -amino acids. *Nature Chemistry* **2022**, *14* (5), 566.
- (18) Hilby, K. M.; Denmark, S. E. Lewis Base Catalyzed, Sulfenium Ion Initiated Enantioselective, Spiroketalization Cascade. *The Journal of Organic Chemistry* **2021**, *86* (21), 14250.
- (19) Muranaka, K.; Ichikawa, S.; Matsuda, A. Development of the Carboxamide Protecting Group, 4-(tert-Butyldimethylsiloxy)-2-methoxybenzyl. *The Journal of Organic Chemistry* **2011**, *76* (22), 9278.

- (20) Song, Z.; Jia, Y.; Zhang, D.; Wang, D. DMAP Mediated Efficient Construction of Functionalized Chromenes through One-Pot Reaction of para-Quinone Methides with Allenates. *Eur. J. Org. Chem.* **2021**, *2021* (12), 1942.
- (21) Büyükdalı, N. N.; Aslan, N.; Gümüş, S.; Gümüş, A. Stereoselective synthesis of benzofuran and benzothiophene substituted dihydropyran derivatives via ring closing metathesis. *Tetrahedron: Asymmetry* **2016**, *27* (19), 954.
- (22) Wang, H.; Liu, C.-F.; Martin, R. T.; Gutierrez, O.; Koh, M. J. Directing-group-free catalytic dicarbofunctionalization of unactivated alkenes. *Nature Chemistry* **2022**, *14* (2), 188.
- (23) Snyder, S. A.; Zografos, A. L.; Lin, Y. Total Synthesis of Resveratrol-Based Natural Products: A Chemoselective Solution. *Angew. Chem. Int. Ed.* **2007**, *46* (43), 8186.
- (24) Wang, X.; Zhu, M.-H.; Schuman, D. P.; Zhong, D.; Wang, W.-Y.; Wu, L.-Y.; Liu, W.; Stoltz, B. M.; Liu, W.-B. General and Practical Potassium Methoxide/Disilane-Mediated Dehalogenative Deuteration of (Hetero)Arylhalides. *J. Am. Chem. Soc.* **2018**, *140* (35), 10970.
- (25) Williams, W. L.; Gutiérrez-Valencia, N. E.; Doyle, A. G. Branched-Selective Cross-Electrophile Coupling of 2-Alkyl Aziridines and (Hetero)aryl Iodides Using Ti/Ni Catalysis. *J. Am. Chem. Soc.* **2023**, *145* (44), 24175.
- (26) Seefeld, M. A.; Rouse, M. B.; Heerding, D. A.; Peace, S.; Yamashita, D. S.; McNulty, K. C., 2008; Vol. WO2008098104.
- (27) Kohler, D. G.; Gockel, S. N.; Kennemur, J. L.; Waller, P. J.; Hull, K. L. Palladium-catalysed anti-Markovnikov selective oxidative amination. *Nature Chemistry* **2018**, *10* (3), 333.
- (28) Han, M.; Ding, Y.; Yan, Y.; Li, H.; Luo, S.; Adijiang, A.; Ling, Y.; An, J. Transition-Metal-Free, Selective Reductive Deuteration of Terminal Alkynes with Sodium Dispersions and EtOD-d1. *Org. Lett.* **2018**, *20* (10), 3010.
- (29) Xu, S.; Hirano, K.; Miura, M. Nickel-Catalyzed Regio- and Stereospecific C–H Coupling of Benzamides with Aziridines. *Org. Lett.* **2021**, *23* (14), 5471.

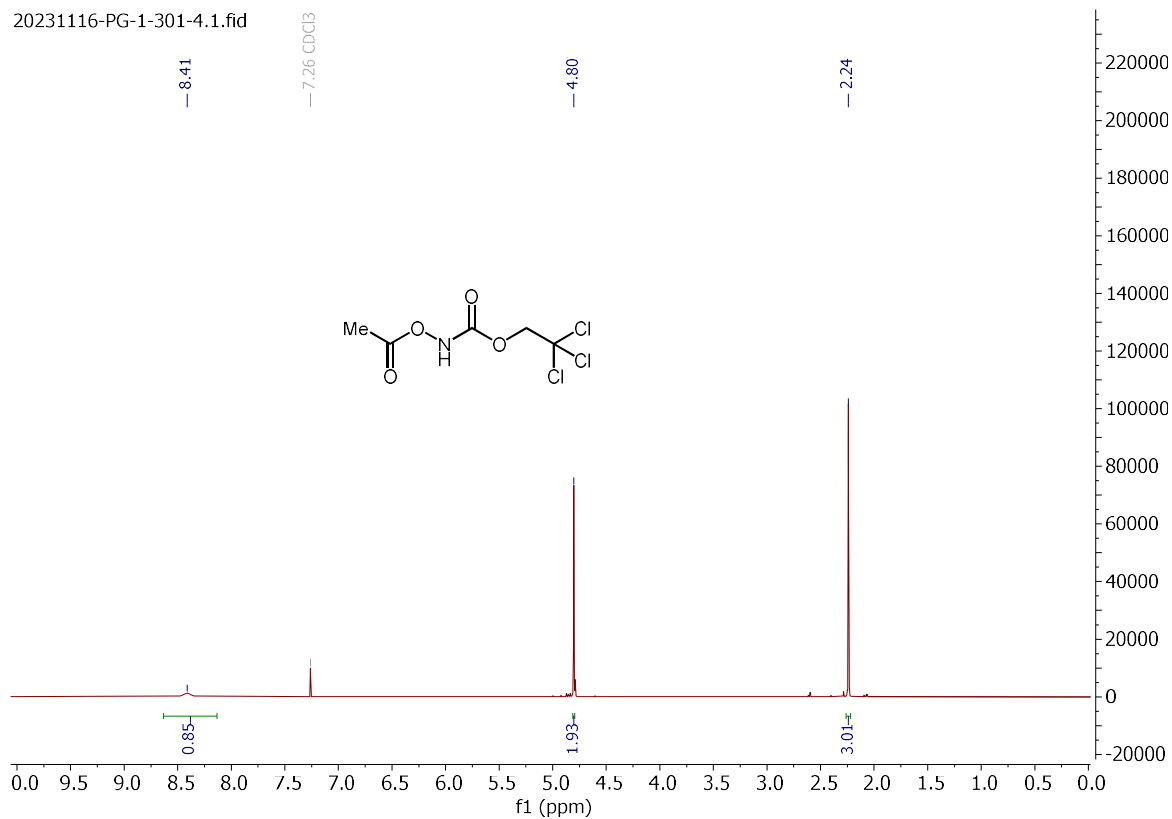
4.5.4 NMR, HPLC and SFC Data

2,2,2-trichloroethyl (pivaloyloxy)carbamate (**4.29**):

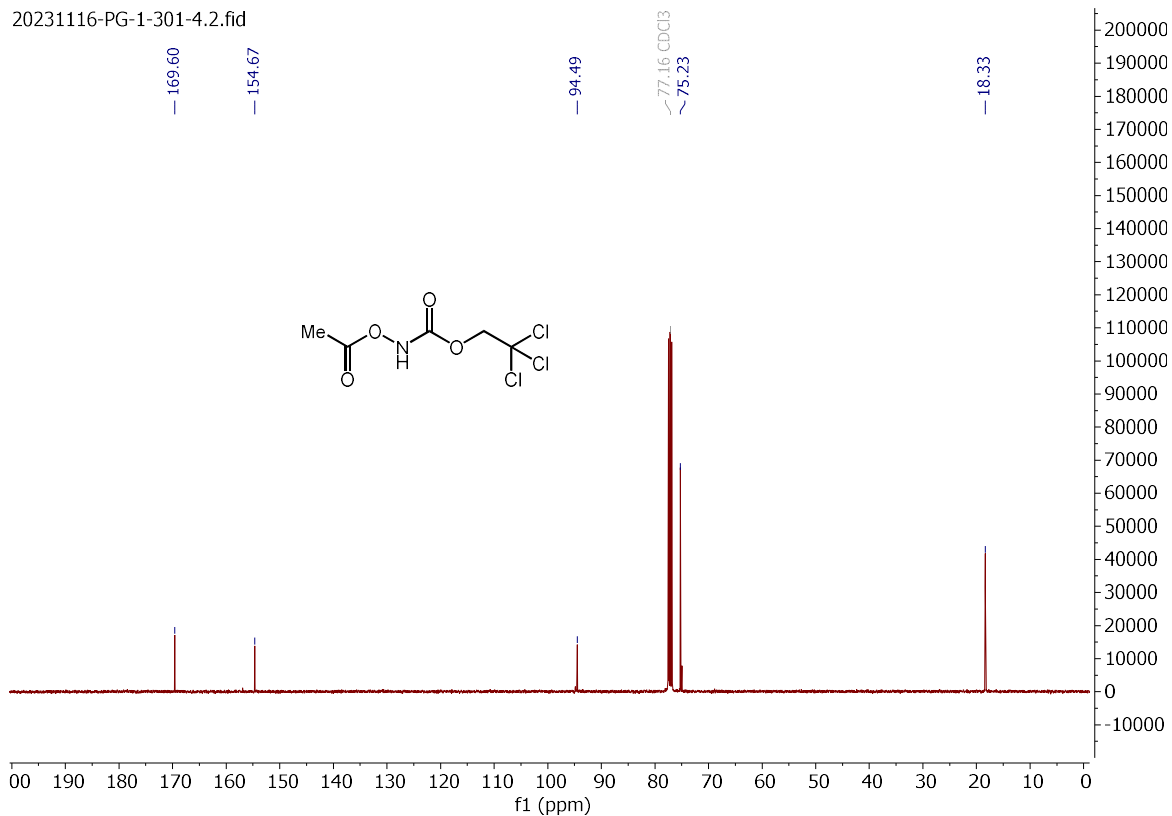


2,2,2-trichloroethyl acetoxycarbamate (4.39):

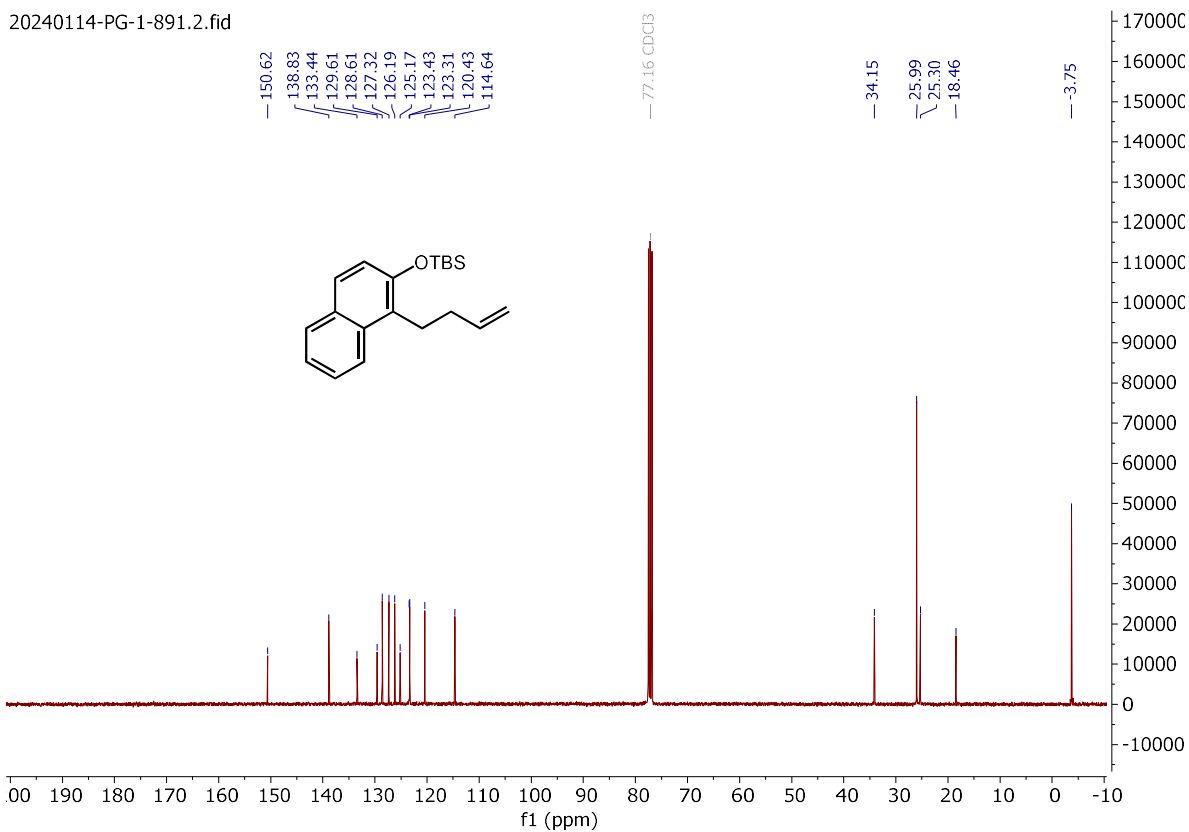
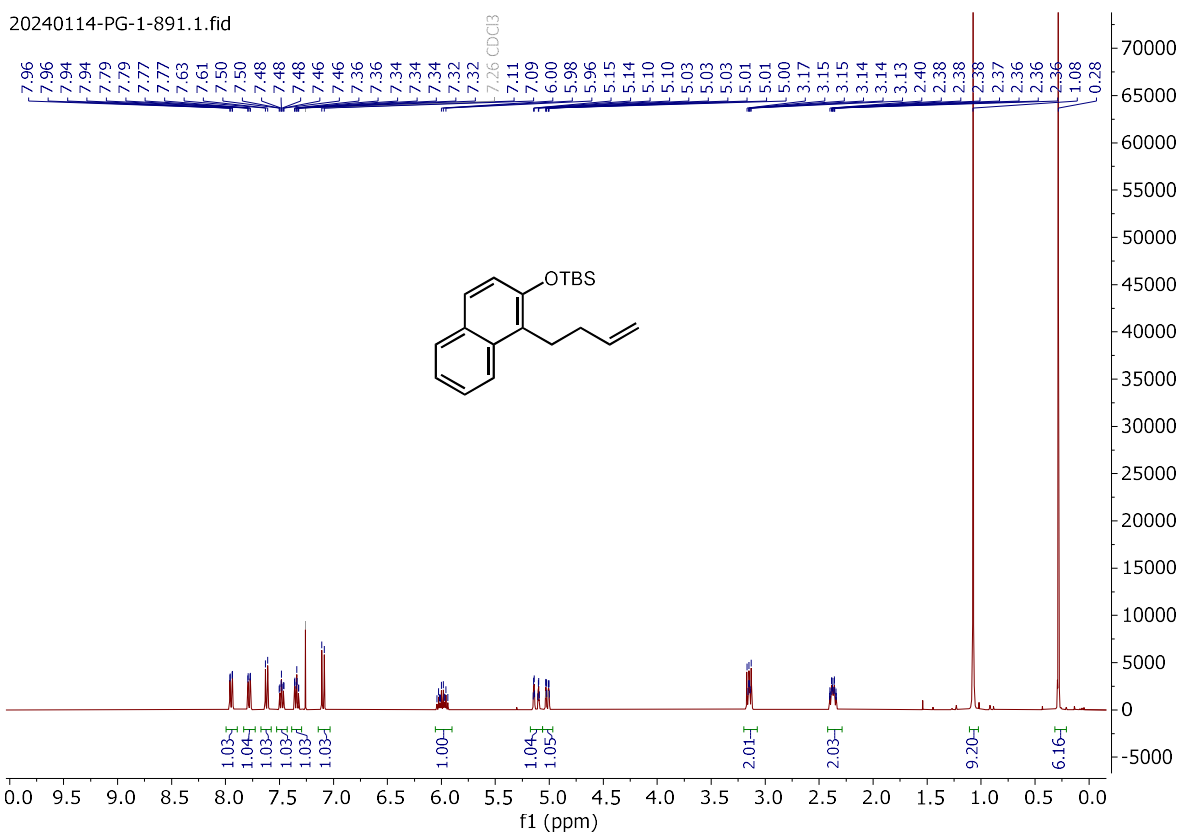
20231116-PG-1-301-4.1.fid



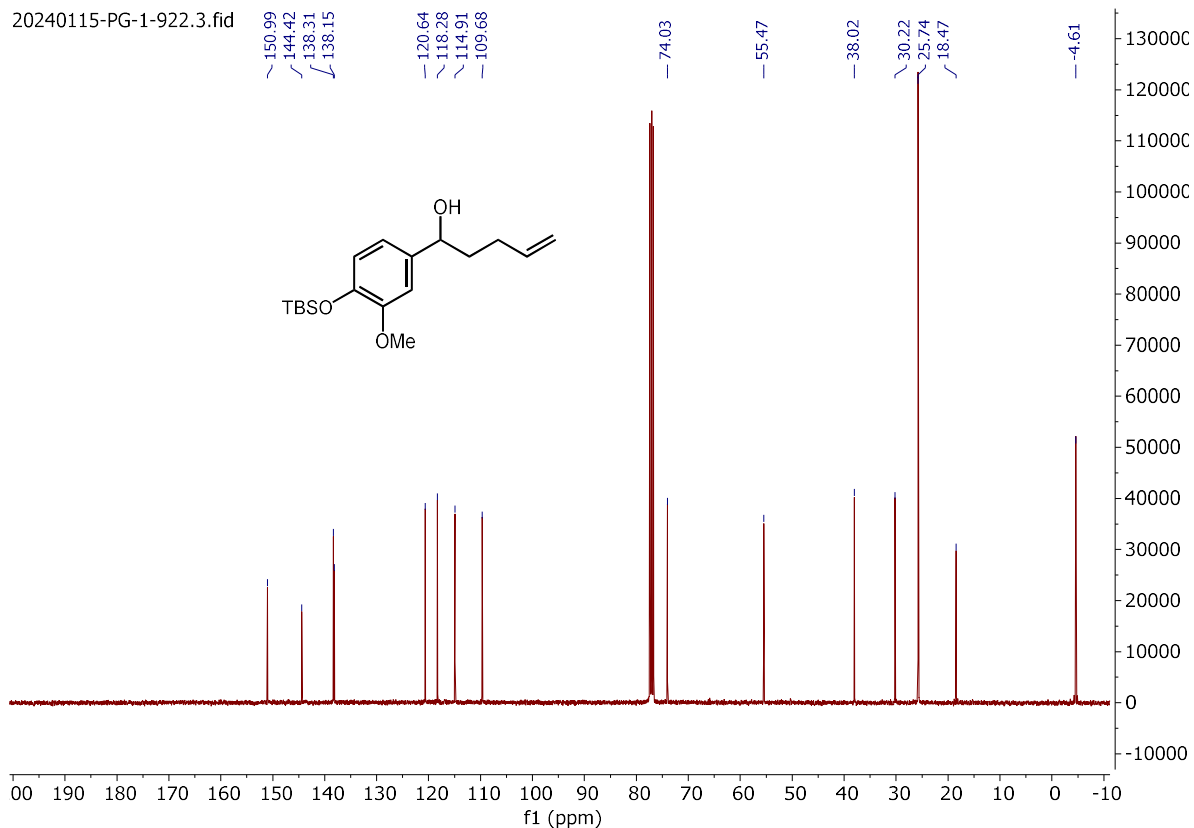
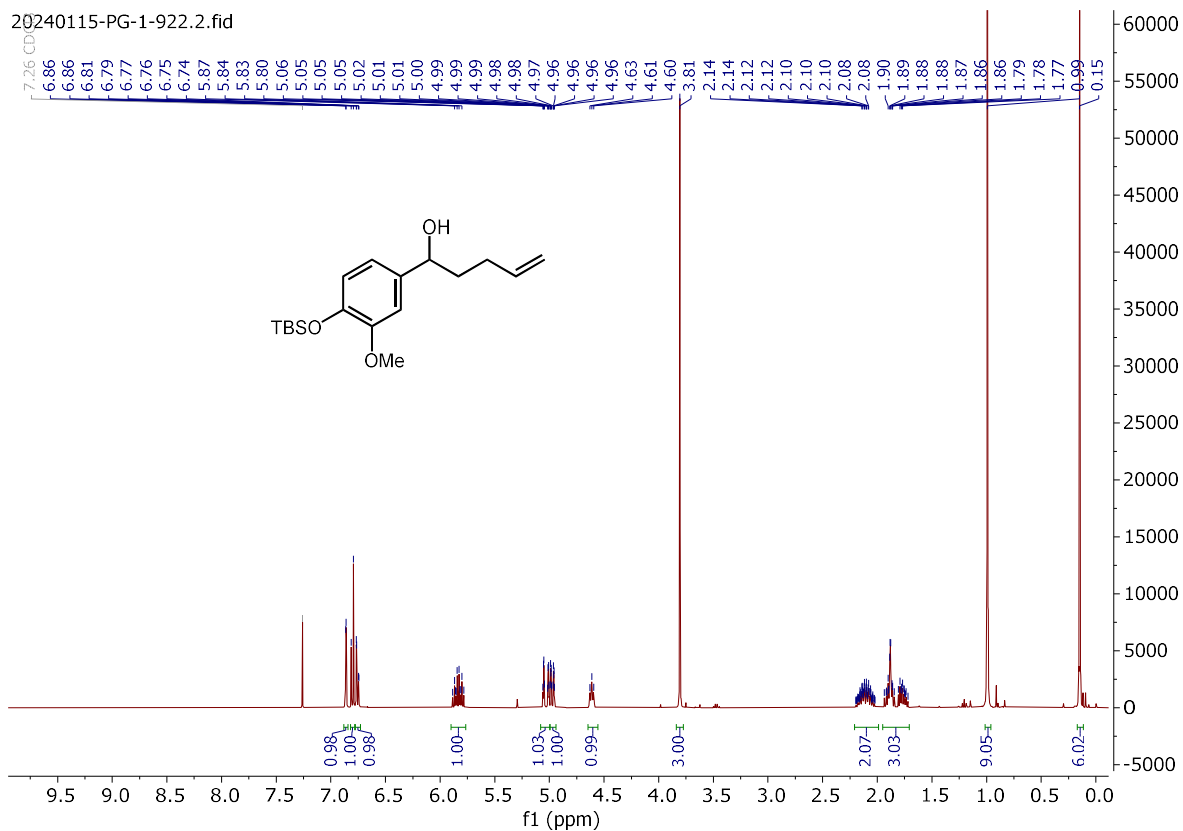
20231116-PG-1-301-4.2.fid



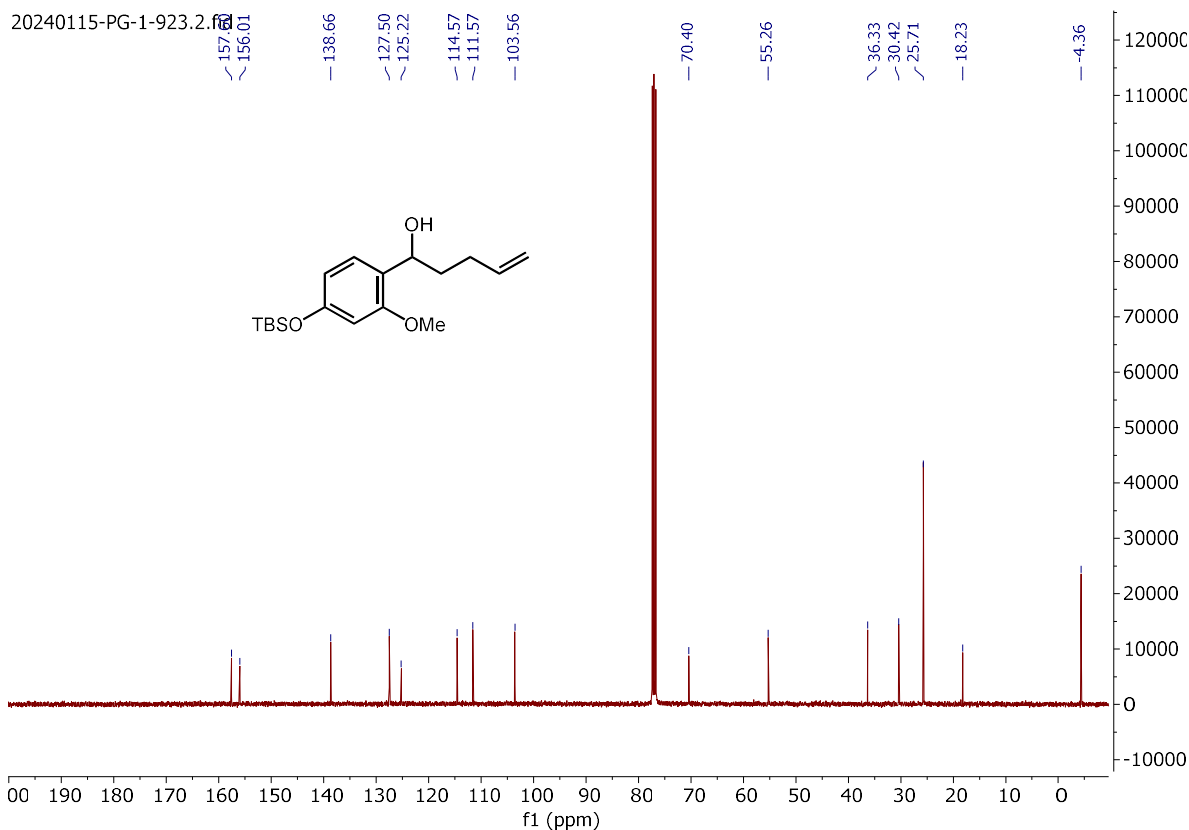
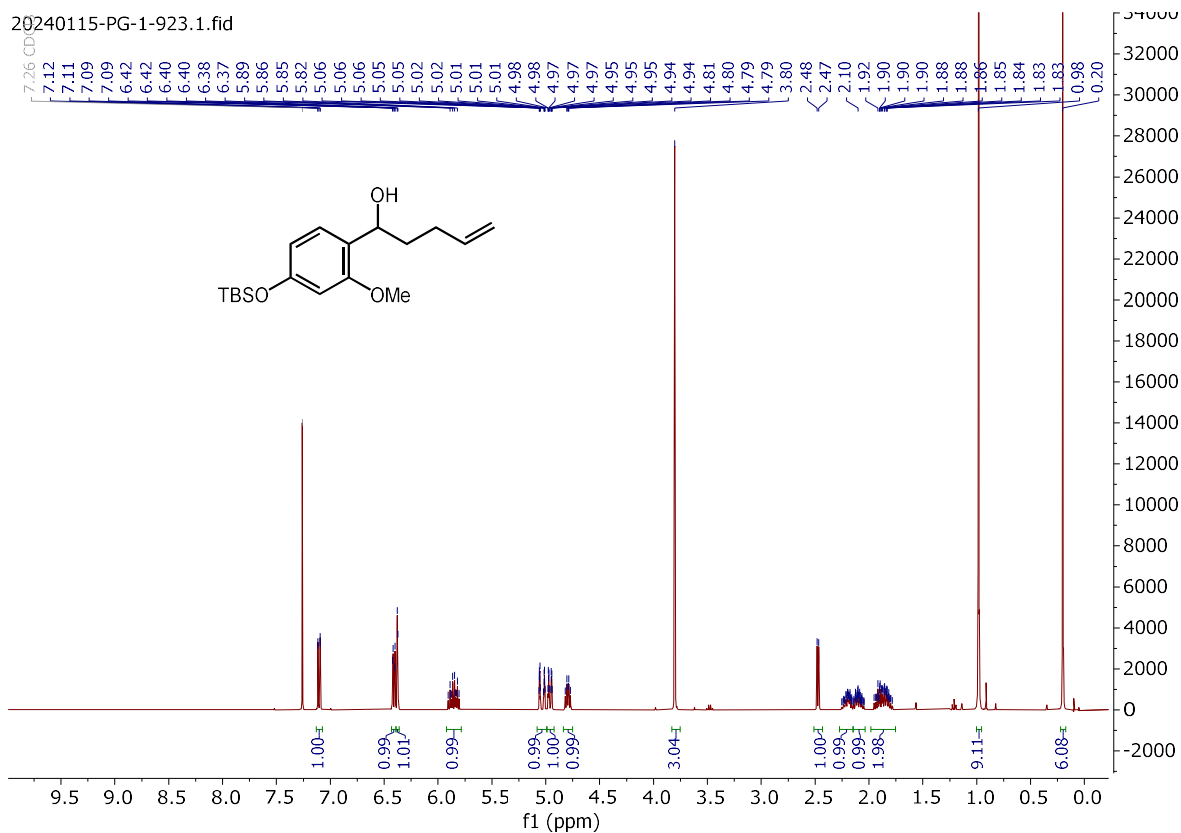
((1-(but-3-en-1-yl)naphthalen-2-yl)oxy)(tert-butyl)dimethylsilane (S12):



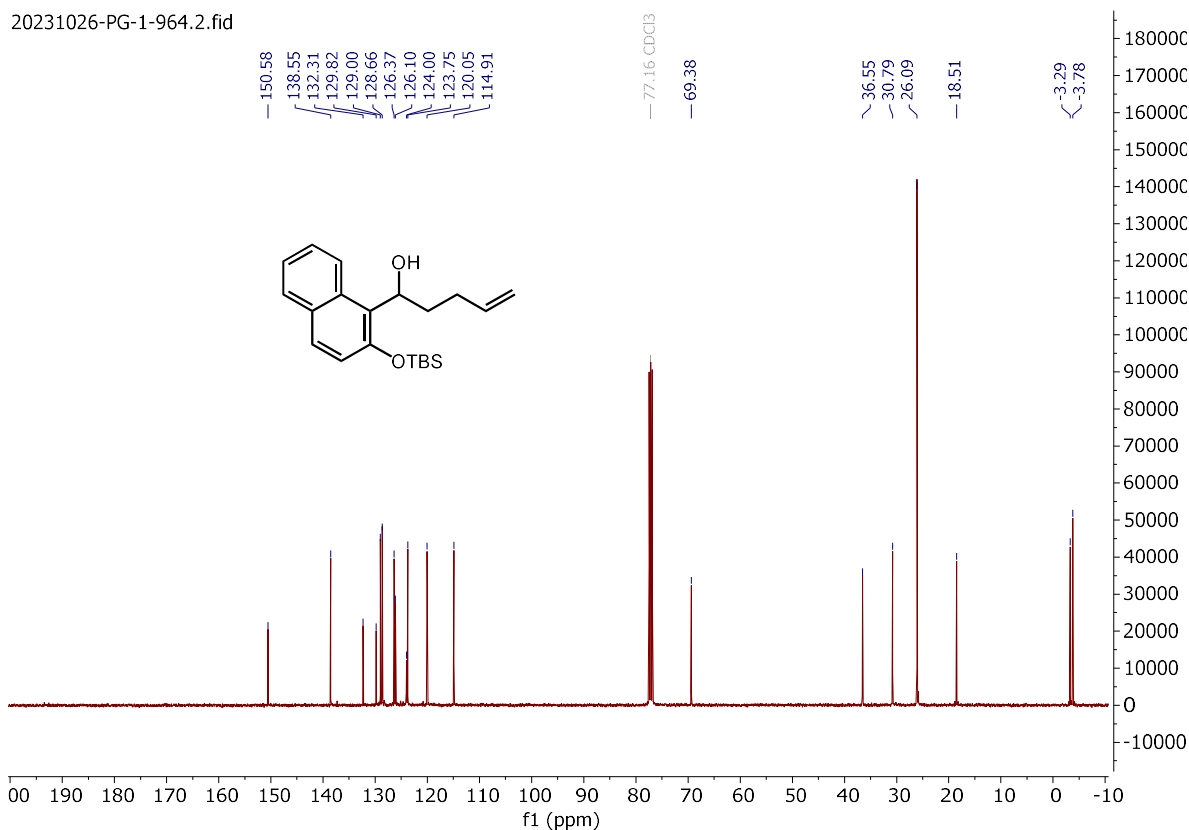
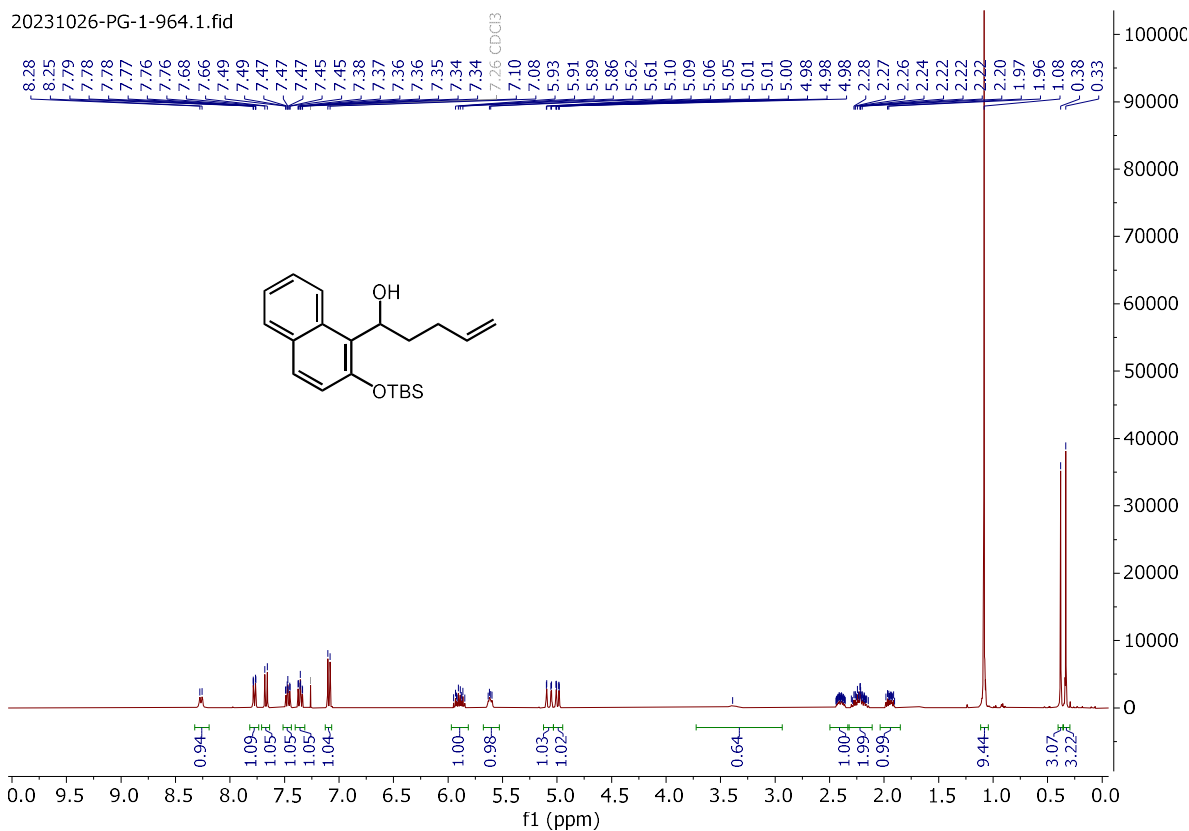
1-(4-((tert-butyl dimethylsilyl)oxy)-3-methoxyphenyl)pent-4-en-1-ol (S13):



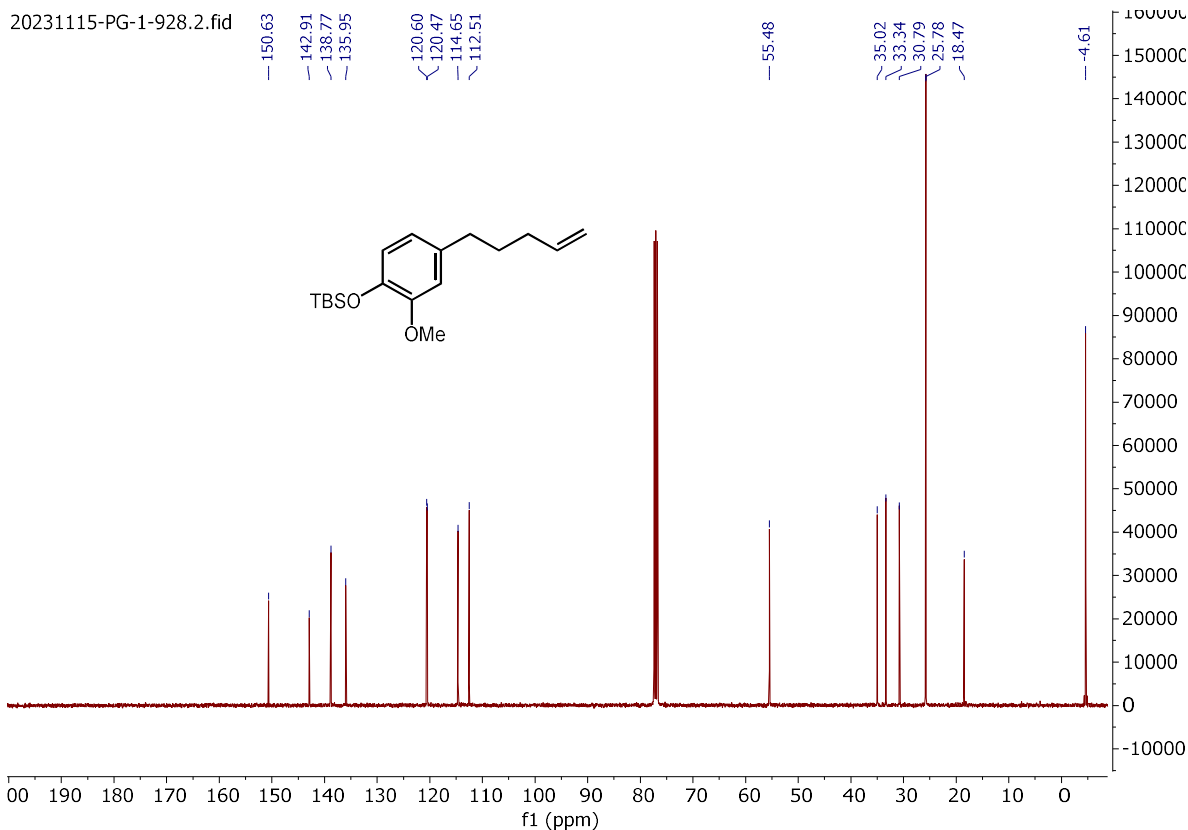
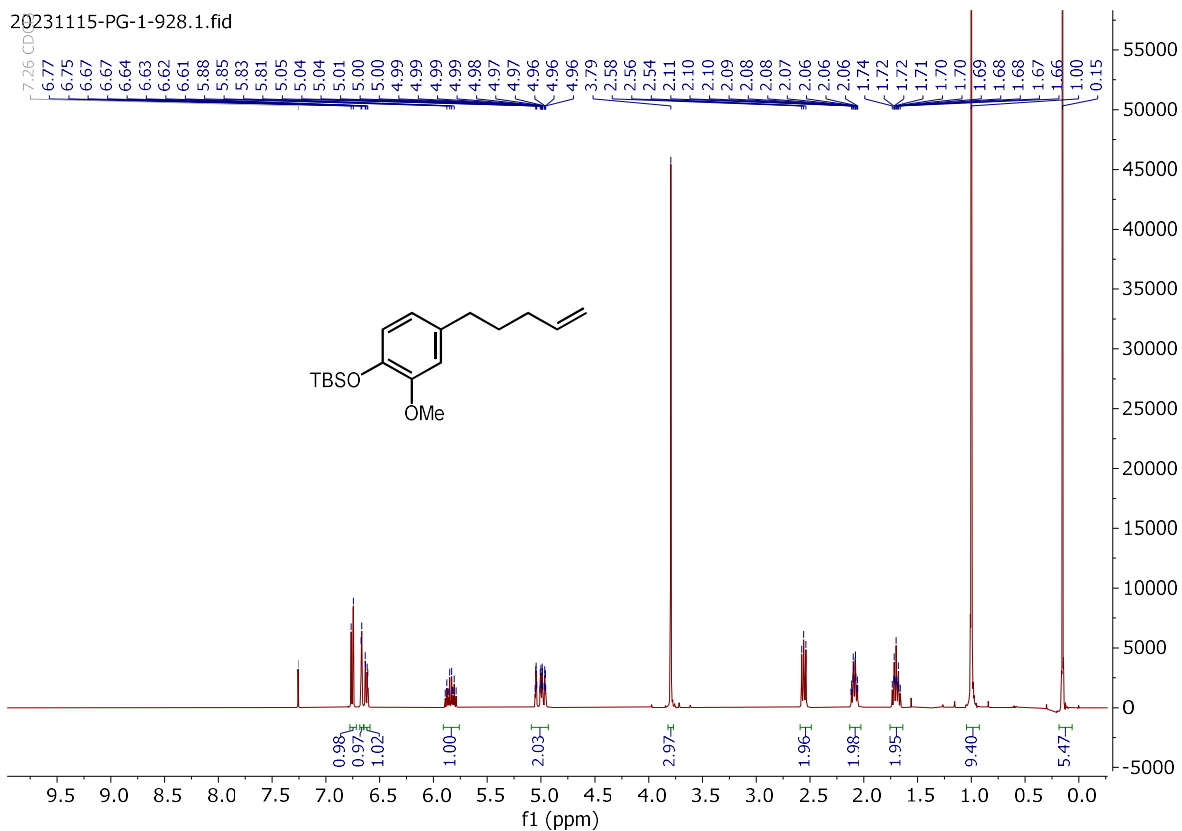
1-(4-((tert-butyl dimethylsilyl)oxy)-2-methoxyphenyl)pent-4-en-1-ol (S14):



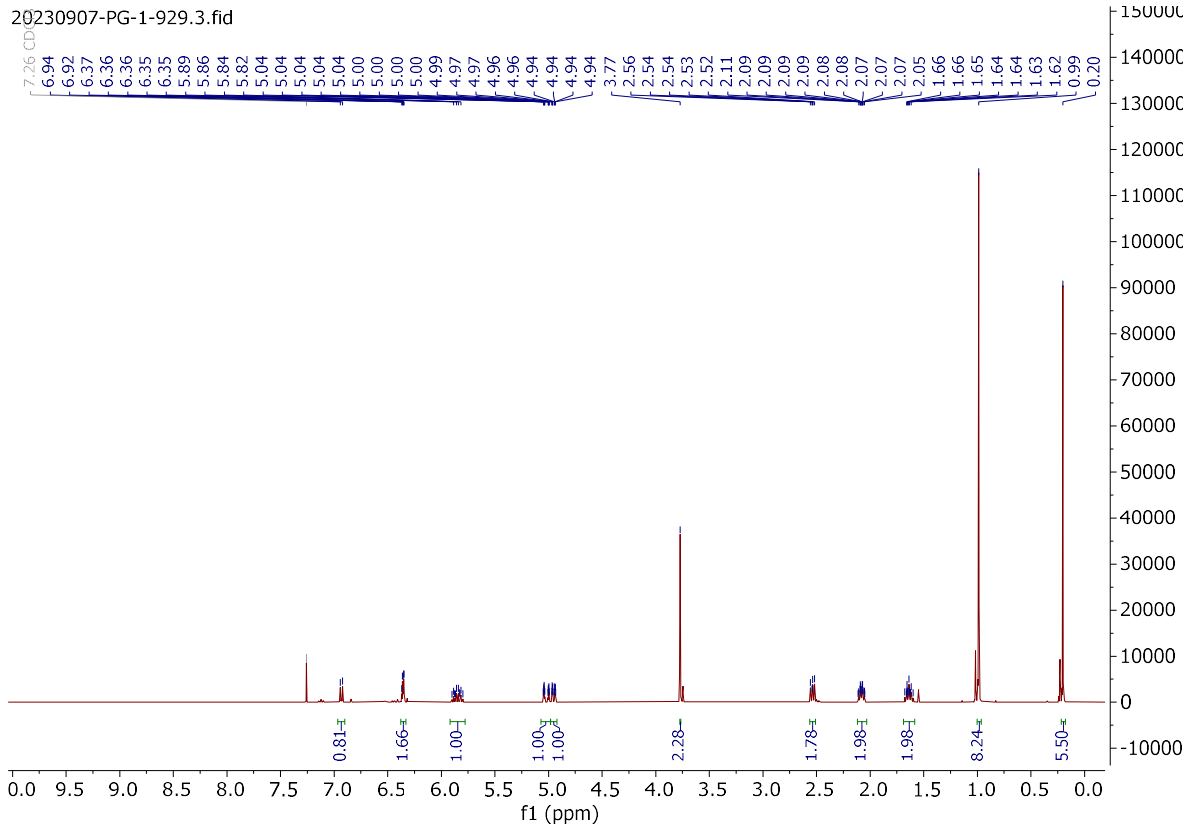
1-(2-((tert-butyl dimethylsilyl)oxy)naphthalen-1-yl)pent-4-en-1-ol (S15):



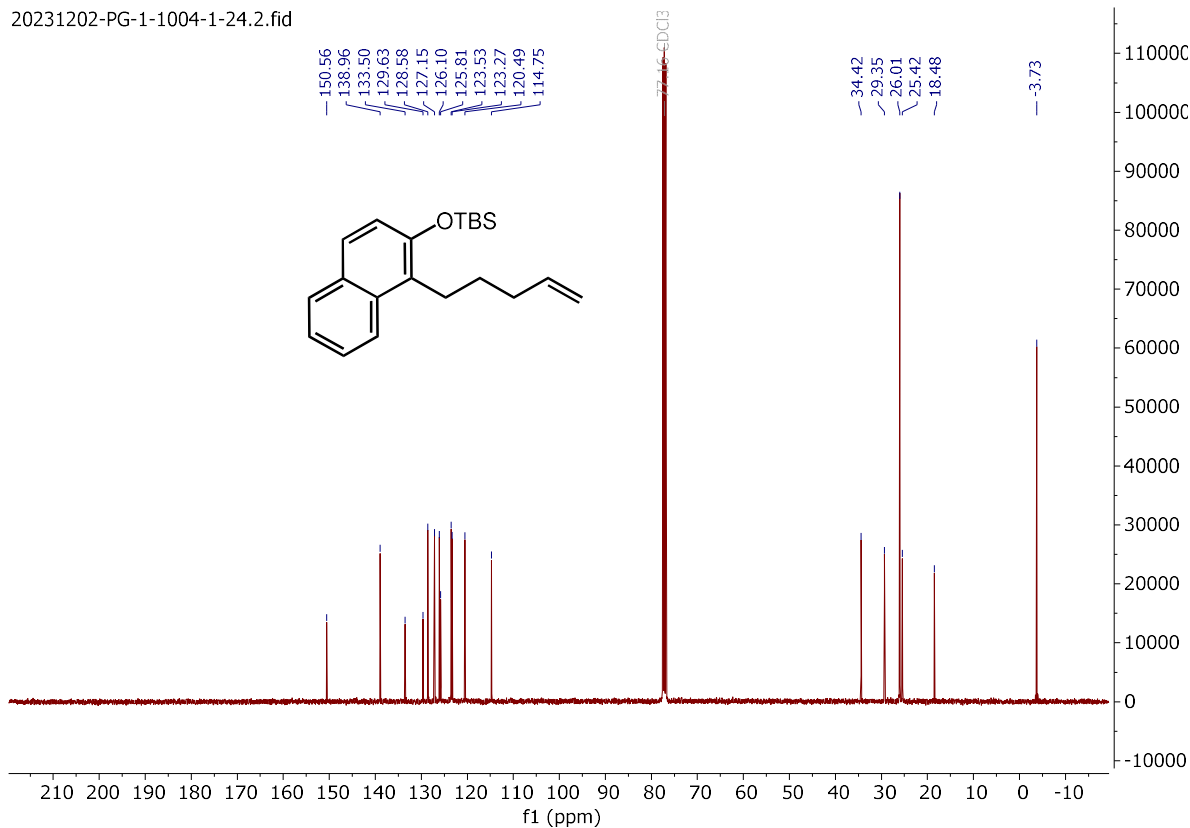
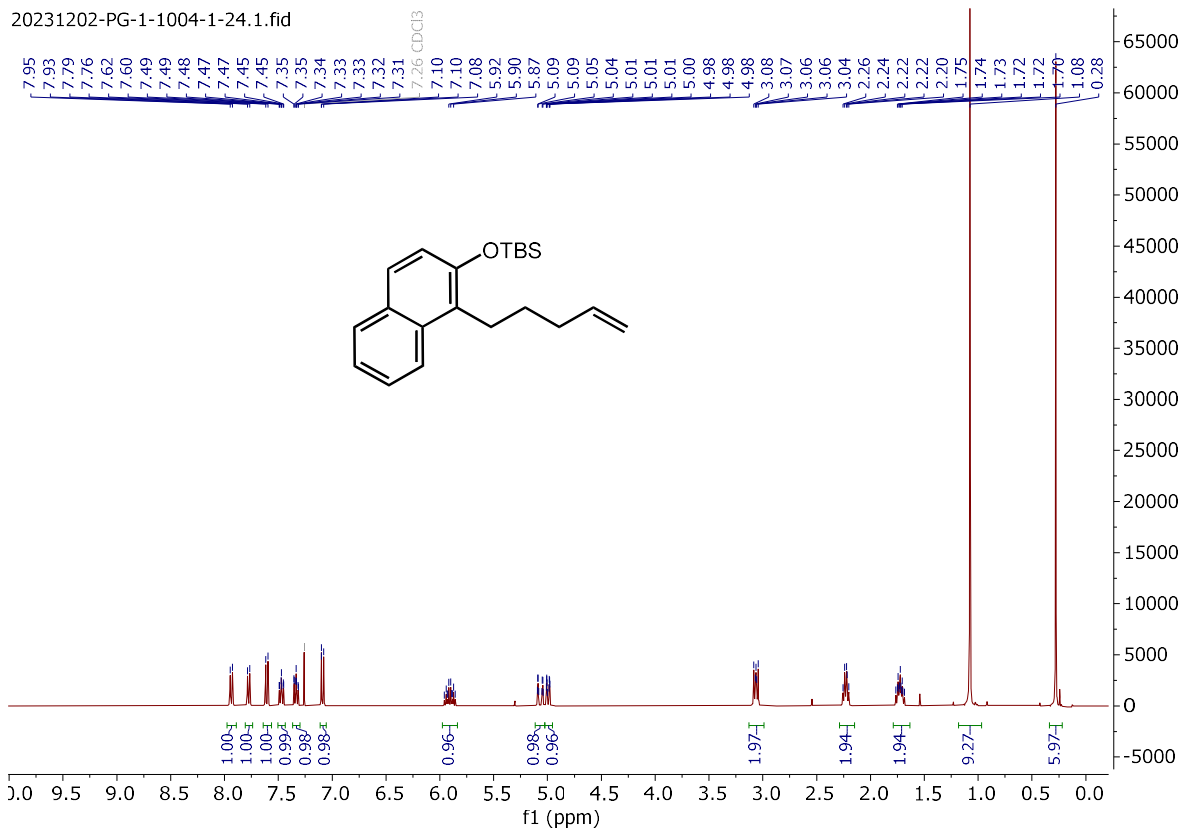
tert-butyl(2-methoxy-4-(pent-4-en-1-yl)phenoxy)dimethylsilane (**S16**):



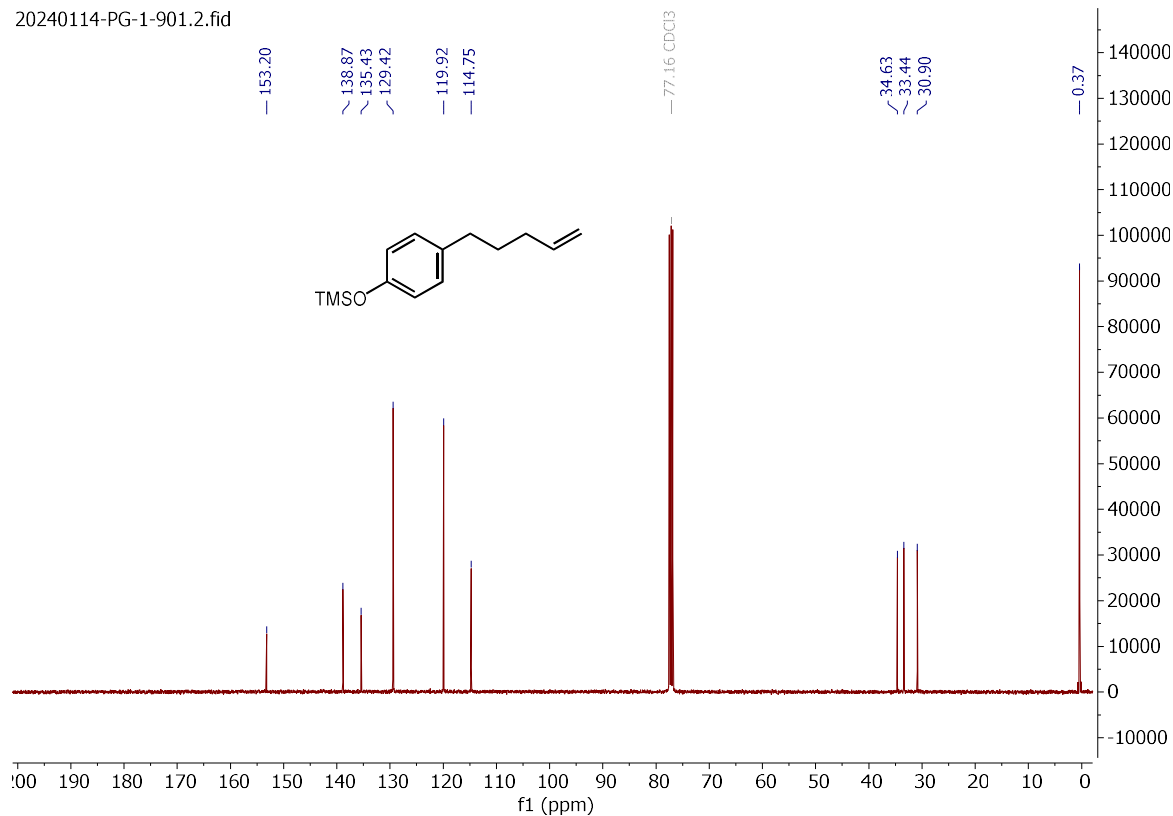
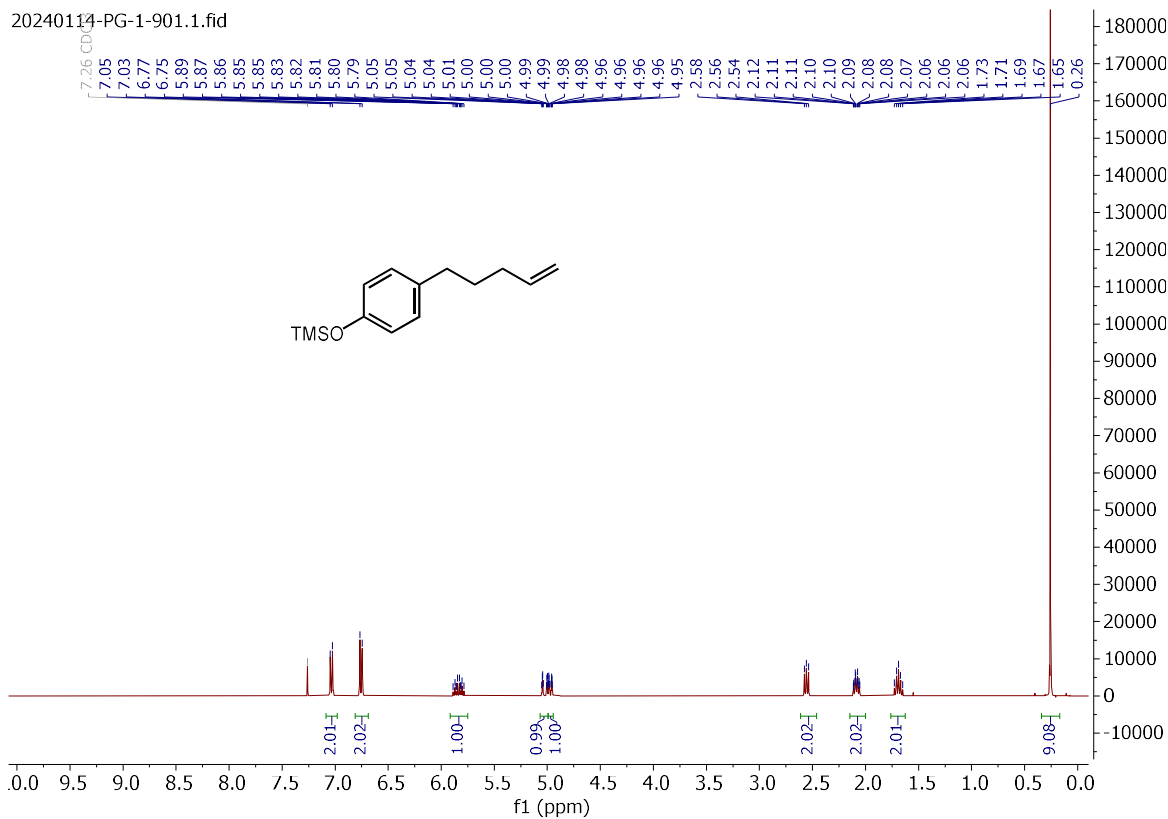
tert-butyl(3-methoxy-4-(pent-4-en-1-yl)phenoxy)dimethylsilane (S17):



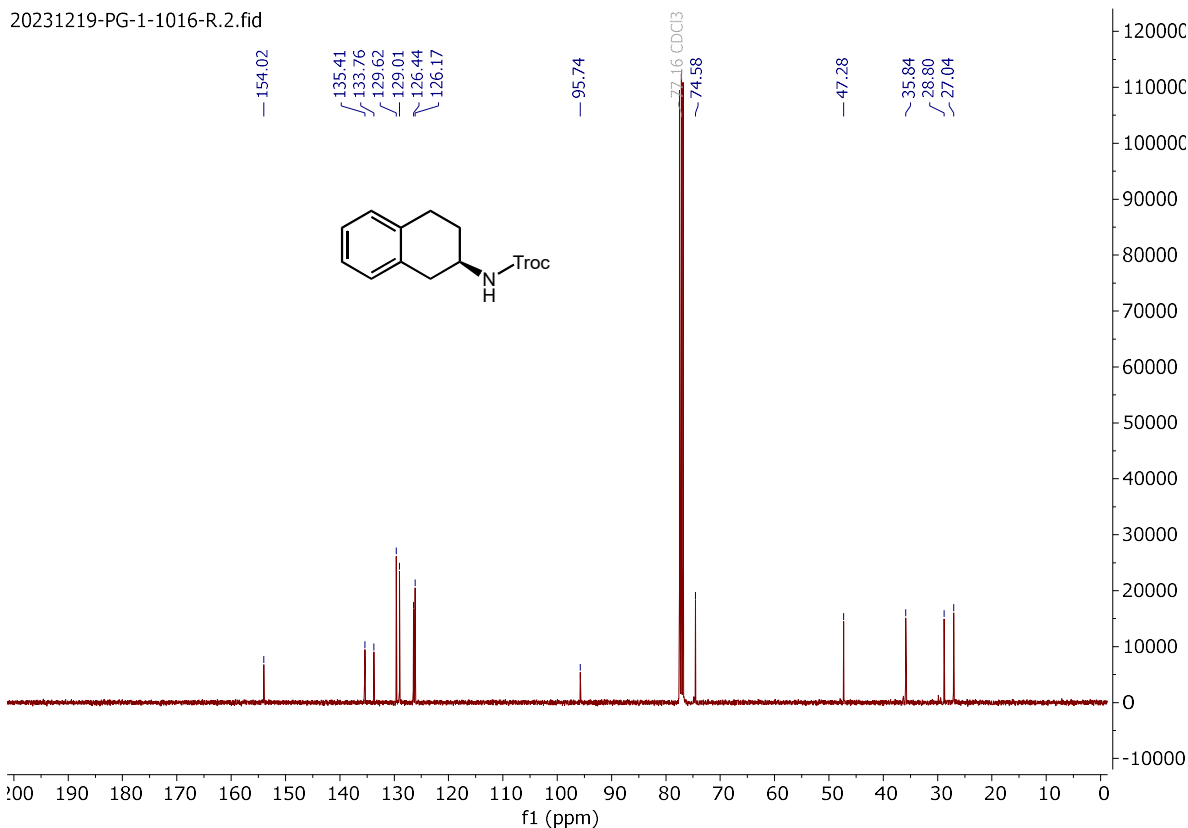
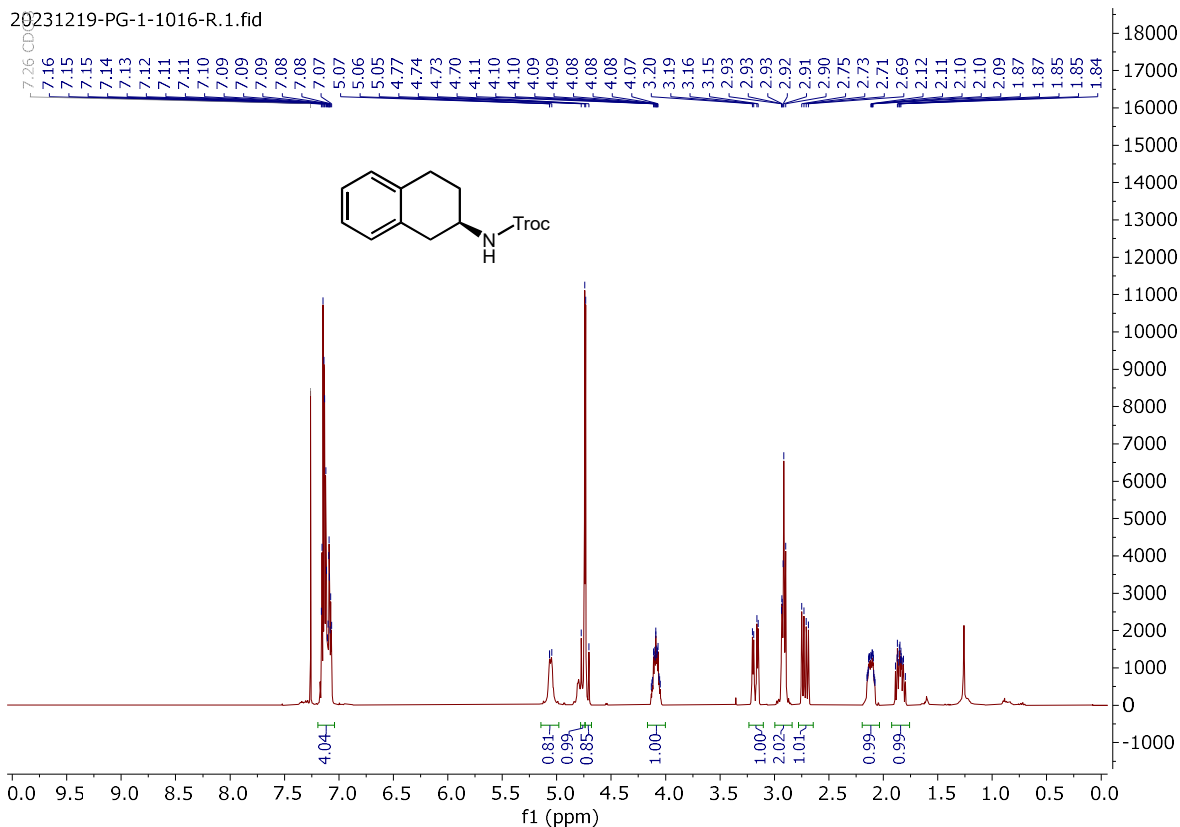
tert-butyldimethyl((1-(pent-4-en-1-yl)naphthalen-2-yl)oxy)silane (**S18**):



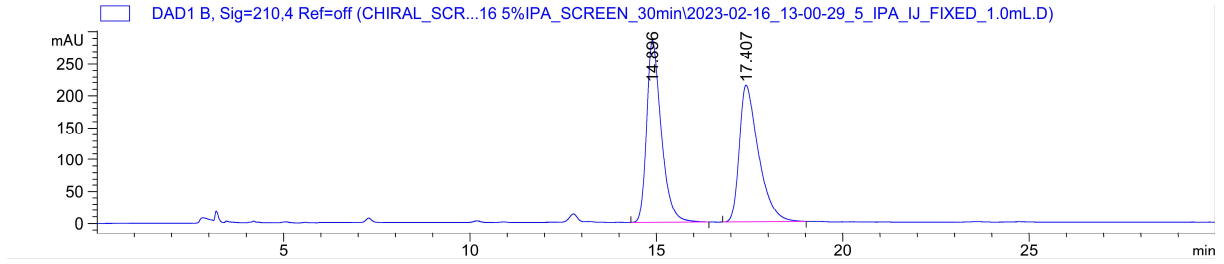
trimethyl(4-(pent-4-en-1-yl)phenoxy)silane (S20):



2,2,2-trichloroethyl (R)-(1,2,3,4-tetrahydronaphthalen-2-yl)carbamate ((R)-4.31):



2,2,2-trichloroethyl (1,2,3,4-tetrahydronaphthalen-2-yl)carbamate (\pm -4.31):

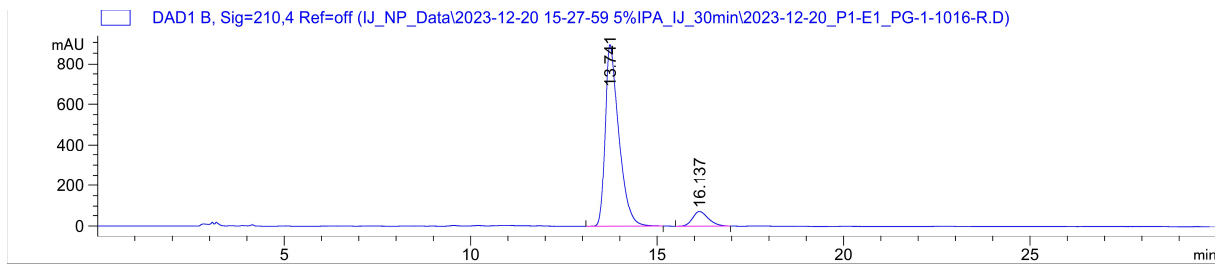


Signal 2: DAD1 B, Sig=210,4 Ref=off

| Peak # | RetTime [min] | Type | Width [min] | Area [mAU*s] | Height [mAU] | Area % |
|--------|---------------|------|-------------|--------------|--------------|---------|
| 1 | 14.896 | BB | 0.3731 | 7745.97803 | 285.46552 | 50.3063 |
| 2 | 17.407 | BB | 0.4476 | 7651.66211 | 214.02701 | 49.6937 |

Totals : 1.53976e4 499.49252

2,2,2-trichloroethyl (R)-(1,2,3,4-tetrahydronaphthalen-2-yl)carbamate (4.31):

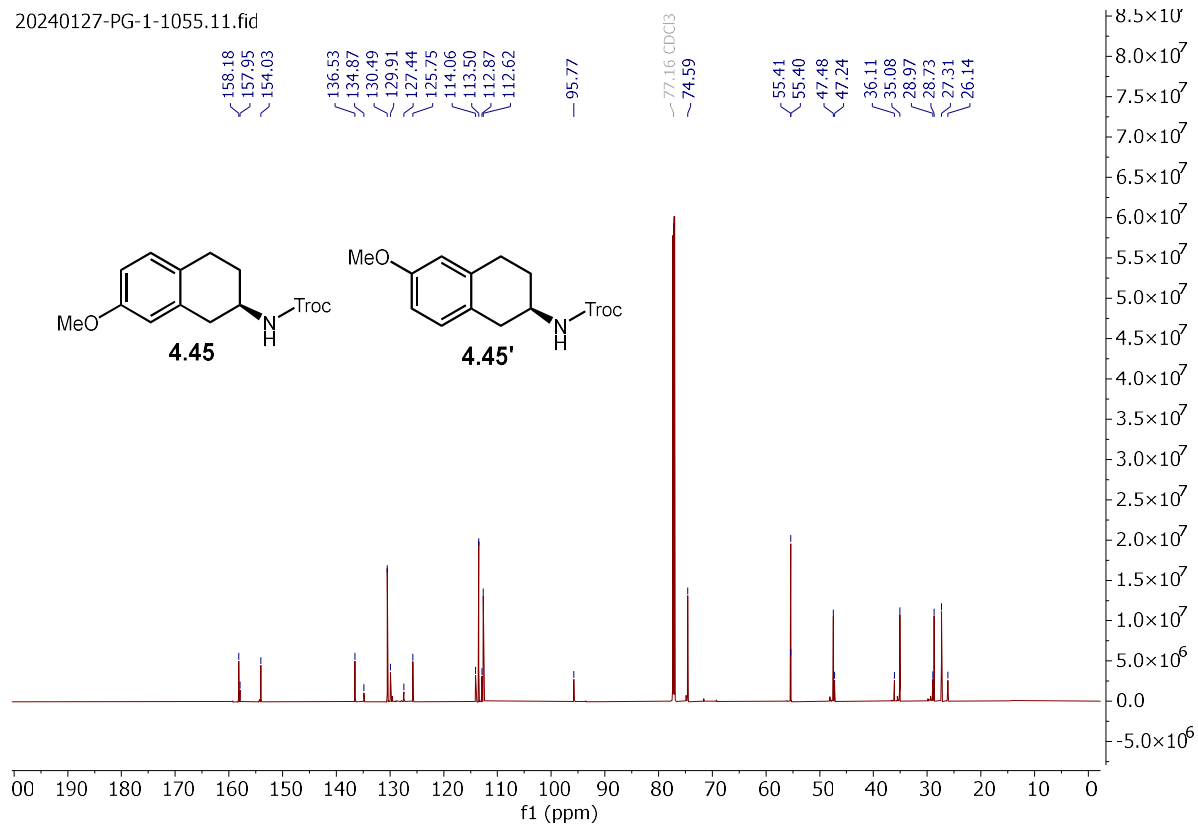
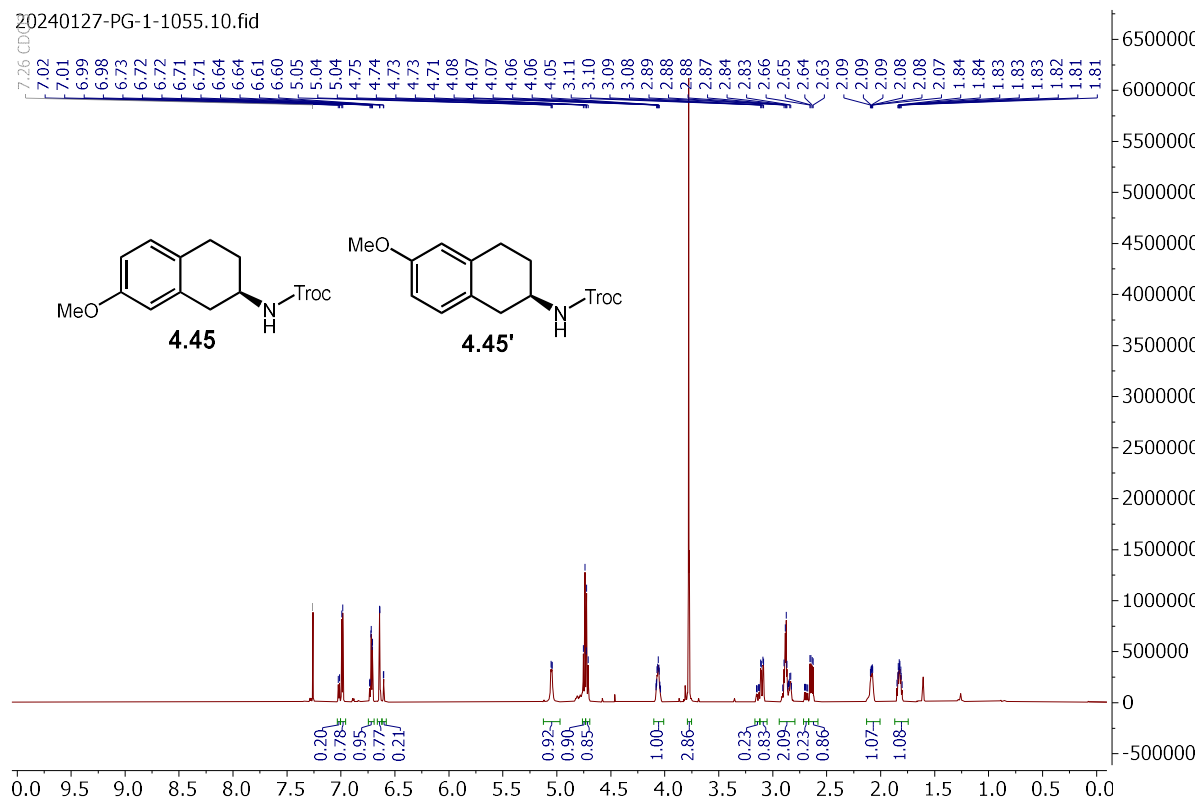


Signal 2: DAD1 B, Sig=210,4 Ref=off

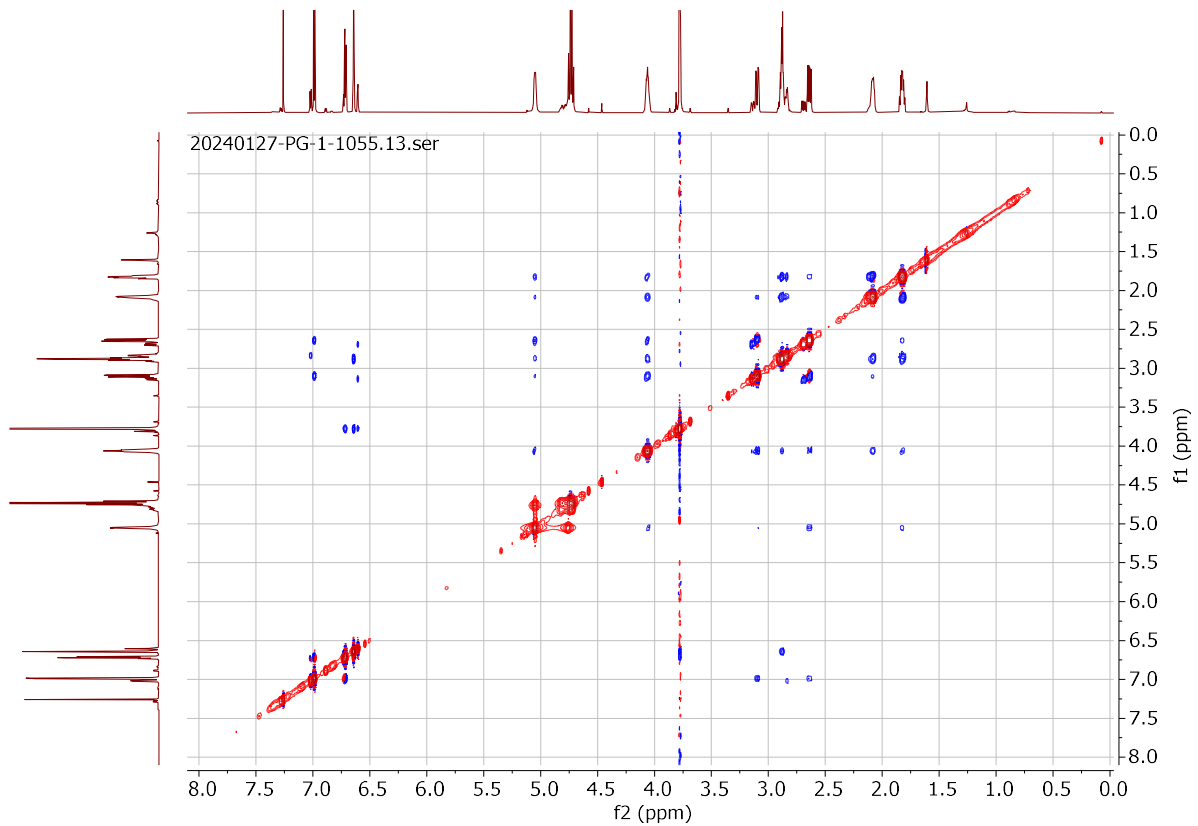
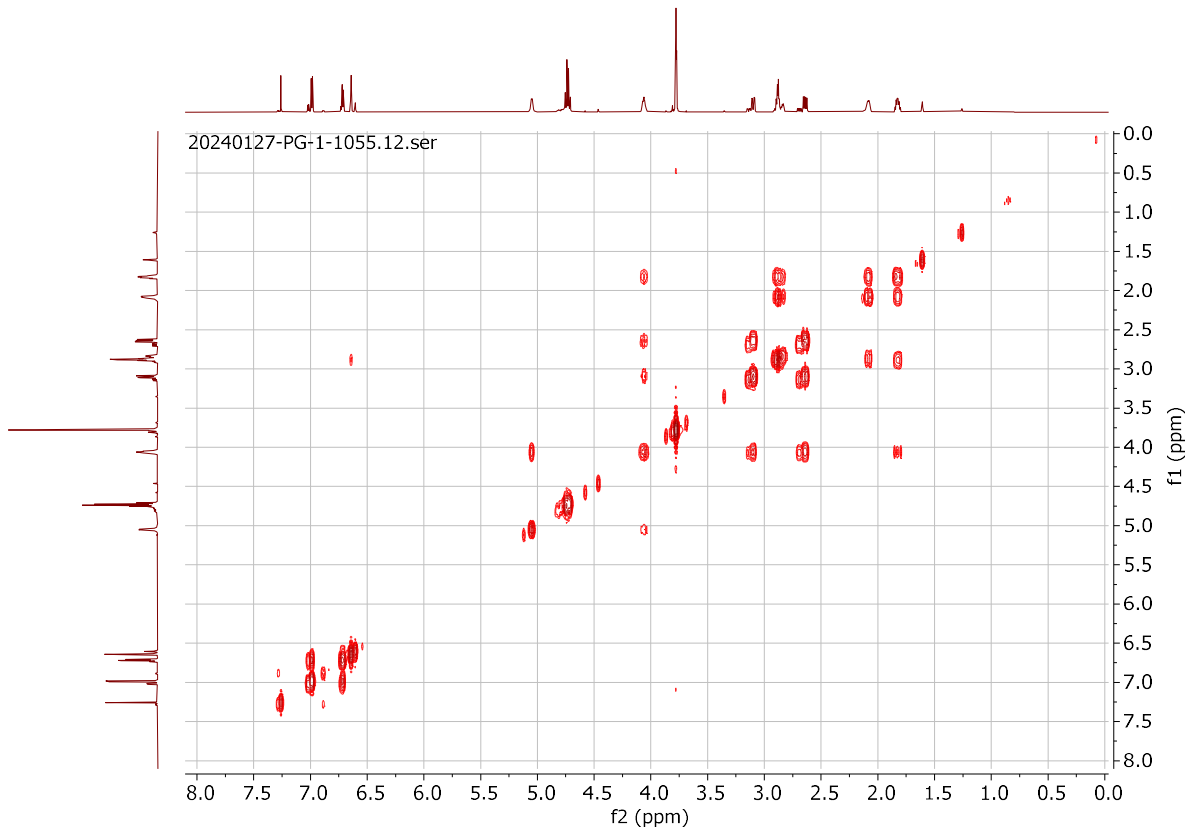
| Peak # | RetTime [min] | Type | Width [min] | Area [mAU*s] | Height [mAU] | Area % |
|--------|---------------|------|-------------|--------------|--------------|---------|
| 1 | 13.741 | VV R | 0.3316 | 2.25000e4 | 891.12781 | 91.6616 |
| 2 | 16.137 | VV R | 0.3432 | 2046.81458 | 69.97881 | 8.3384 |

Totals : 2.45468e4 961.10662

2,2,2-trichloroethyl (R)-(7-methoxy-1,2,3,4-tetrahydronaphthalen-2-yl)carbamate (**4.45**) and 2,2,2-trichloroethyl (R)-(6-methoxy-1,2,3,4-tetrahydronaphthalen-2-yl)carbamate (**4.45'**):

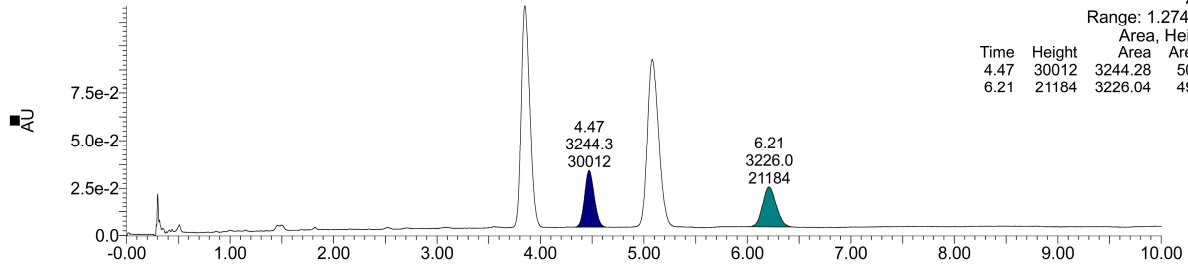


(4.45) and (4.45'):



2,2,2-trichloroethyl (7-methoxy-1,2,3,4-tetrahydronaphthalen-2-yl)carbamate (±-4.45):

HU_2_11_OJ3_3_B1_4 Sm (Mn, 2x3)

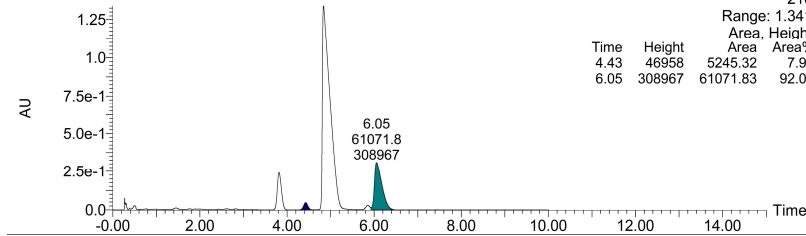


Diode Array
230
Range: 1.274e-1

| Time | Height | Area | Area% |
|------|--------|---------|-------|
| 4.47 | 30012 | 3244.28 | 50.14 |
| 6.21 | 21184 | 3226.04 | 49.86 |

2,2,2-trichloroethyl (R)-(7-methoxy-1,2,3,4-tetrahydronaphthalen-2-yl)carbamate (4.45):

PG1_1055_chir_f_P7B1b Sm (Mn, 2x3)

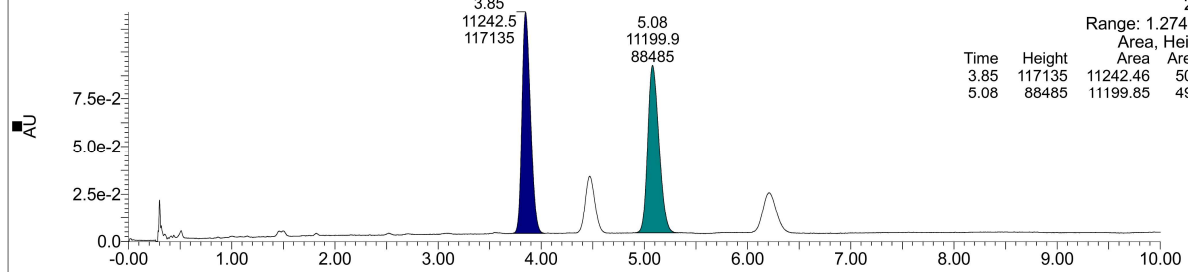


Diode Array
210
Range: 1.341

| Time | Height | Area | Area% |
|------|--------|----------|-------|
| 4.43 | 46958 | 5245.32 | 7.91 |
| 6.05 | 308967 | 61071.83 | 92.09 |

2,2,2-trichloroethyl (6-methoxy-1,2,3,4-tetrahydronaphthalen-2-yl)carbamate (±-4.45'):

HU_2_11_OJ3_3_B1_4 Sm (Mn, 2x3)

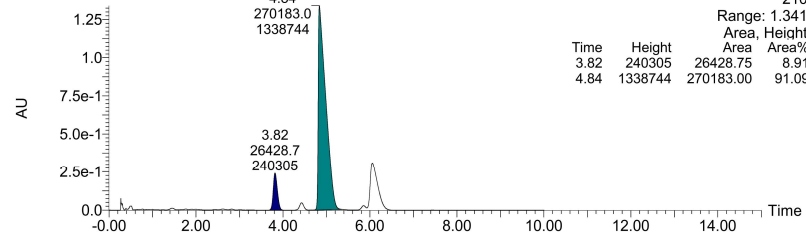


Diode Array
230
Range: 1.274e-1

| Time | Height | Area | Area% |
|------|--------|----------|-------|
| 3.85 | 117135 | 11242.46 | 50.09 |
| 5.08 | 88485 | 11199.85 | 49.91 |

2,2,2-trichloroethyl (R)-(6-methoxy-1,2,3,4-tetrahydronaphthalen-2-yl)carbamate (4.45'):

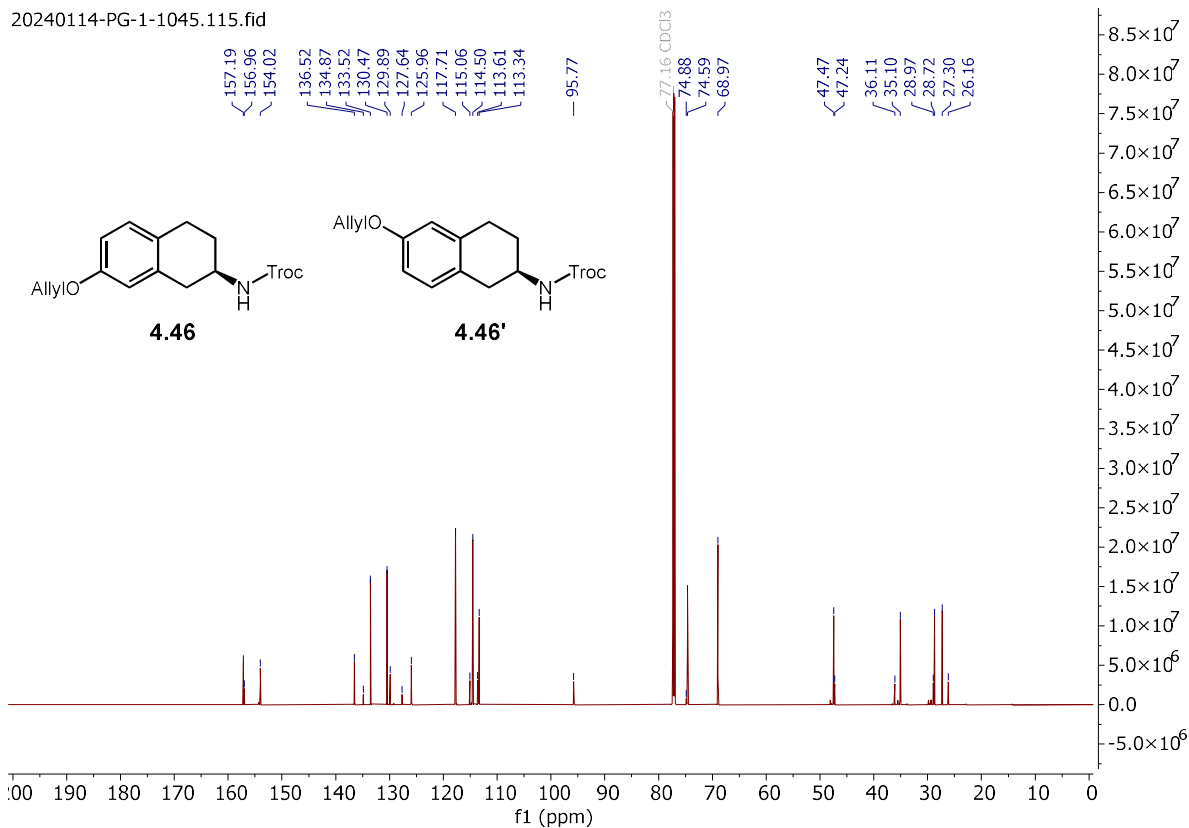
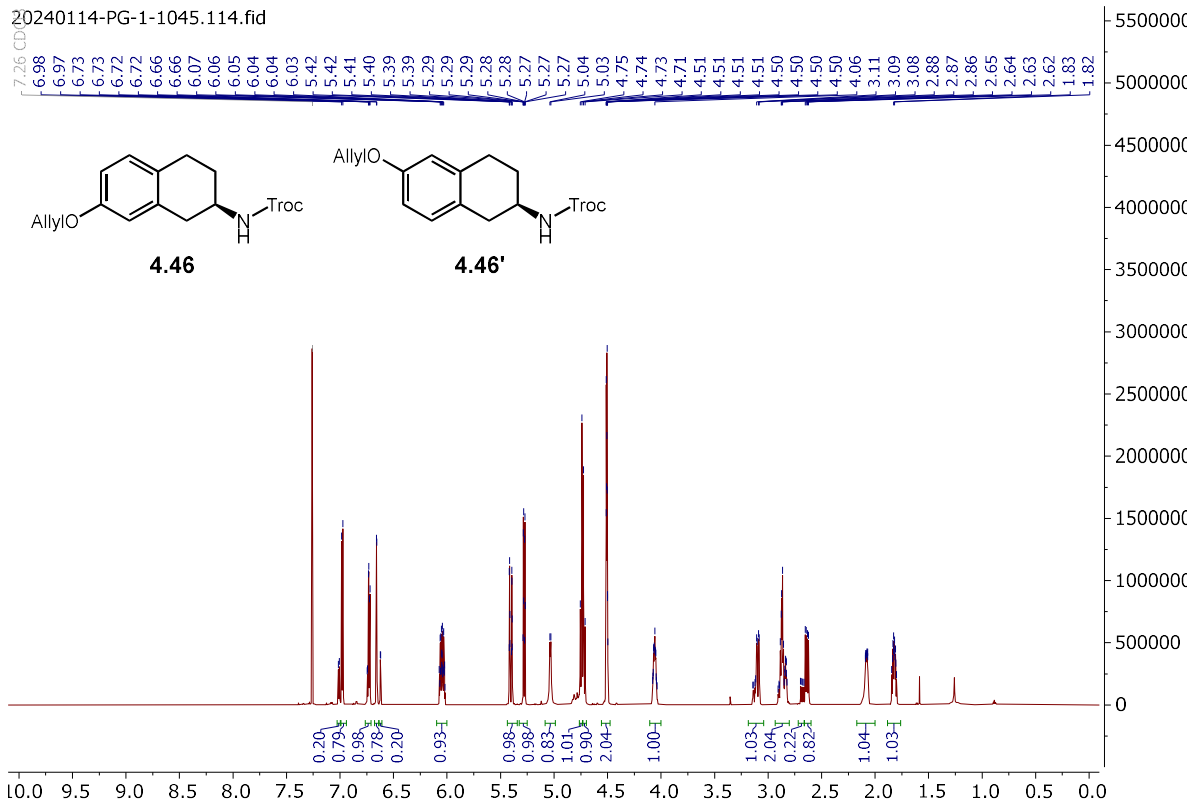
PG1_1055_chir_f_P7B1b Sm (Mn, 2x3)



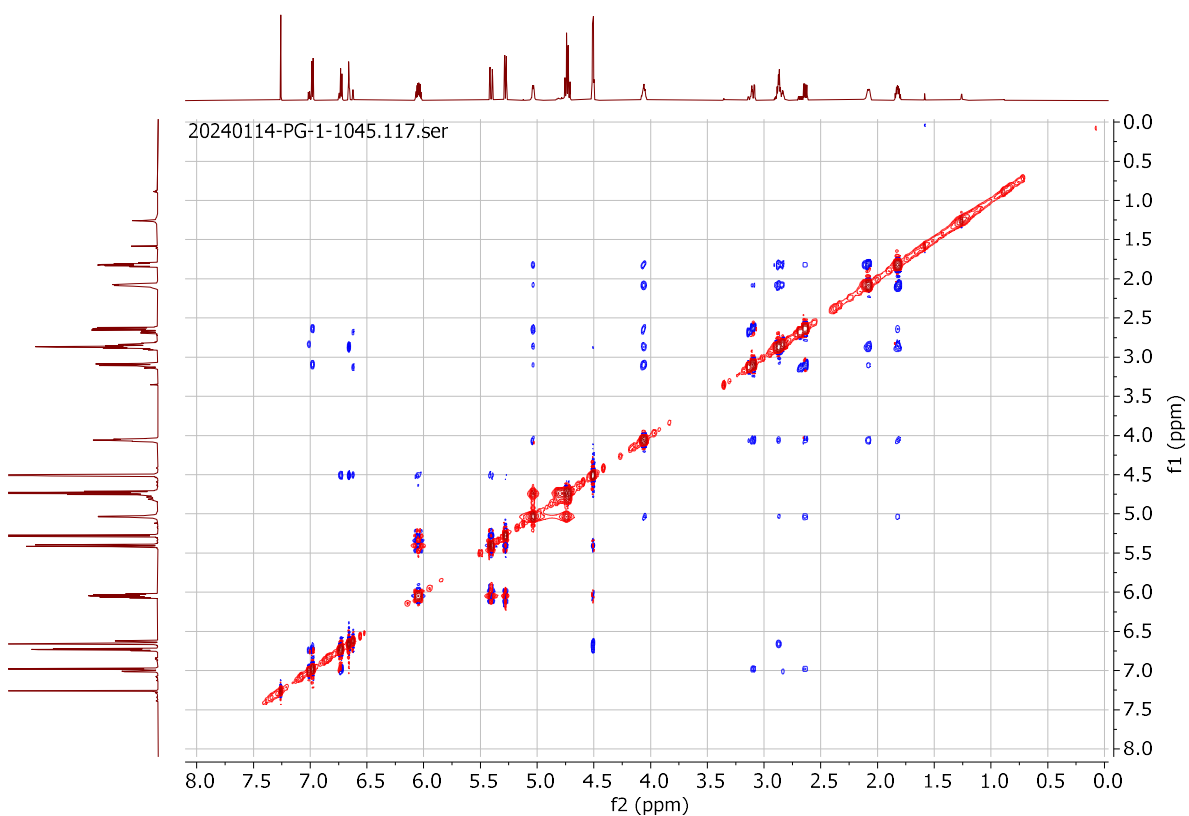
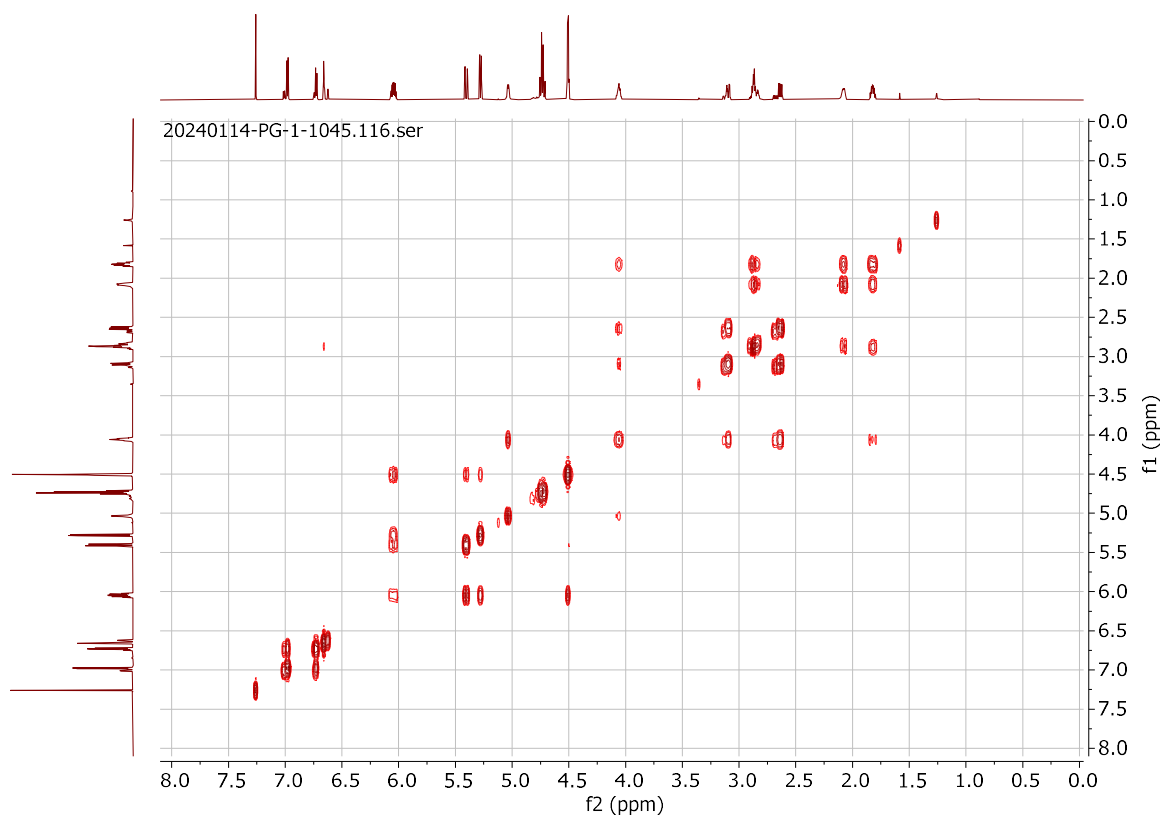
Diode Array
210
Range: 1.341

| Time | Height | Area | Area% |
|------|---------|-----------|-------|
| 3.82 | 240305 | 26428.75 | 8.91 |
| 4.84 | 1338744 | 270183.00 | 91.09 |

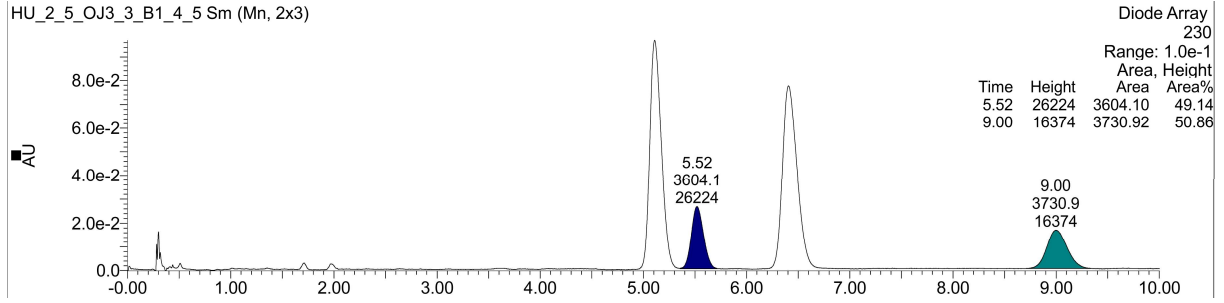
2,2,2-trichloroethyl (R)-(7-(allyloxy)-1,2,3,4-tetrahydronaphthalen-2-yl)carbamate (**4.46**) and 2,2,2-trichloroethyl (R)-(6-(allyloxy)-1,2,3,4-tetrahydronaphthalen-2-yl)carbamate (**4.46'**):



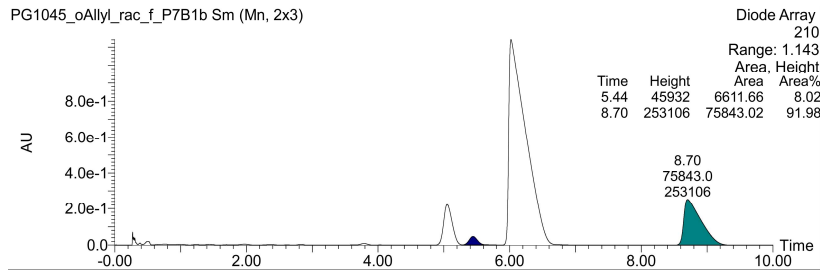
(4.46) and (4.46')



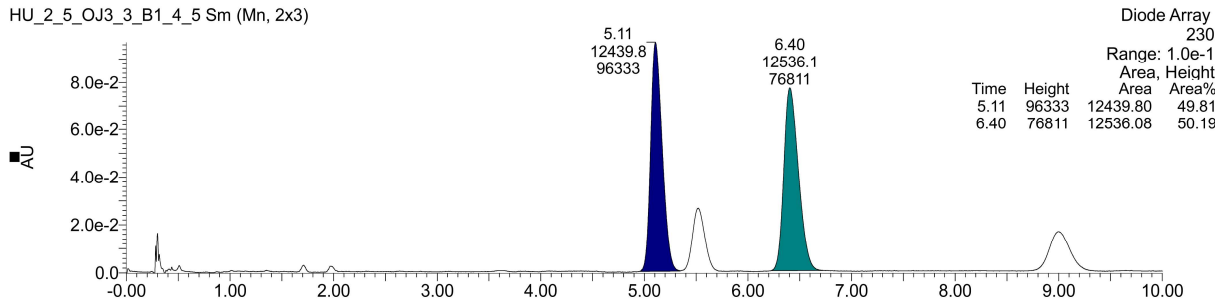
2,2,2-trichloroethyl (7-(allyloxy)-1,2,3,4-tetrahydronaphthalen-2-yl)carbamate (±-4.46):



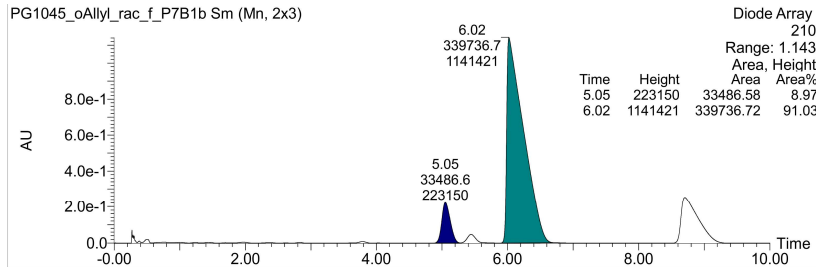
2,2,2-trichloroethyl (R)-(7-(allyloxy)-1,2,3,4-tetrahydronaphthalen-2-yl)carbamate (4.46):



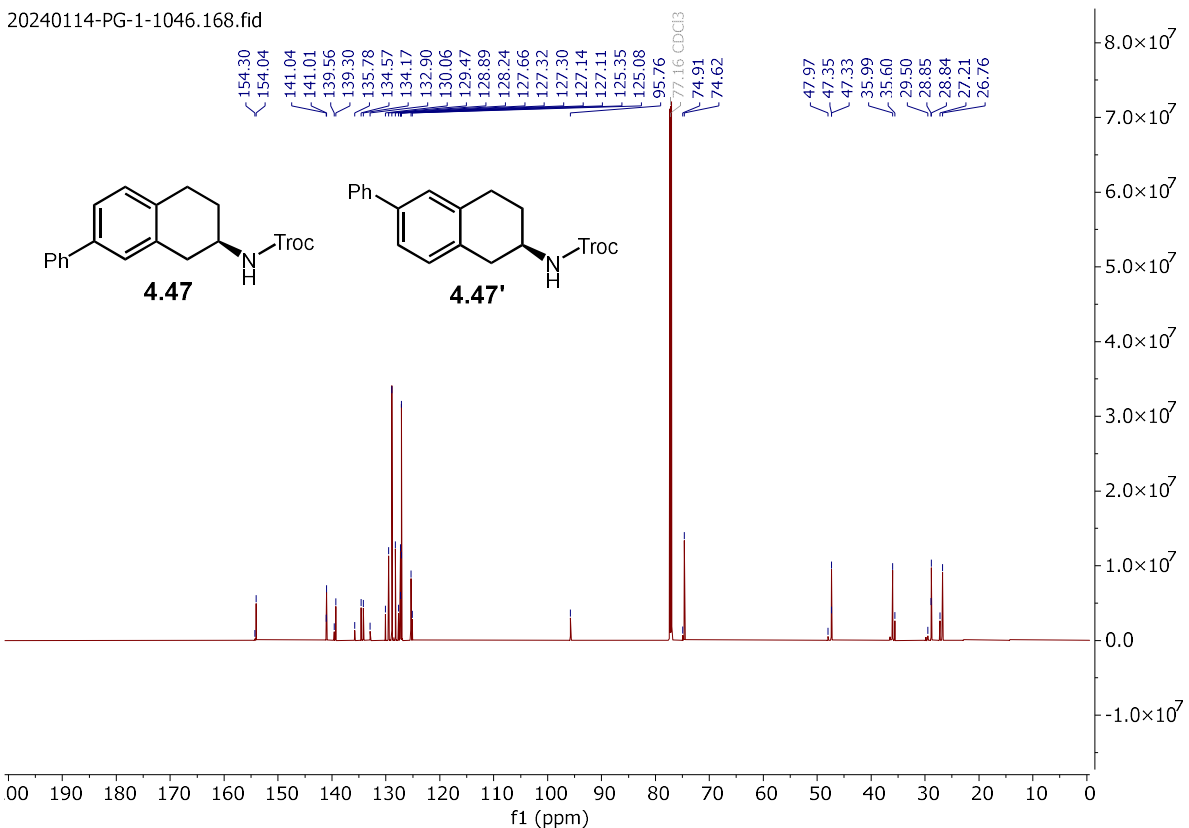
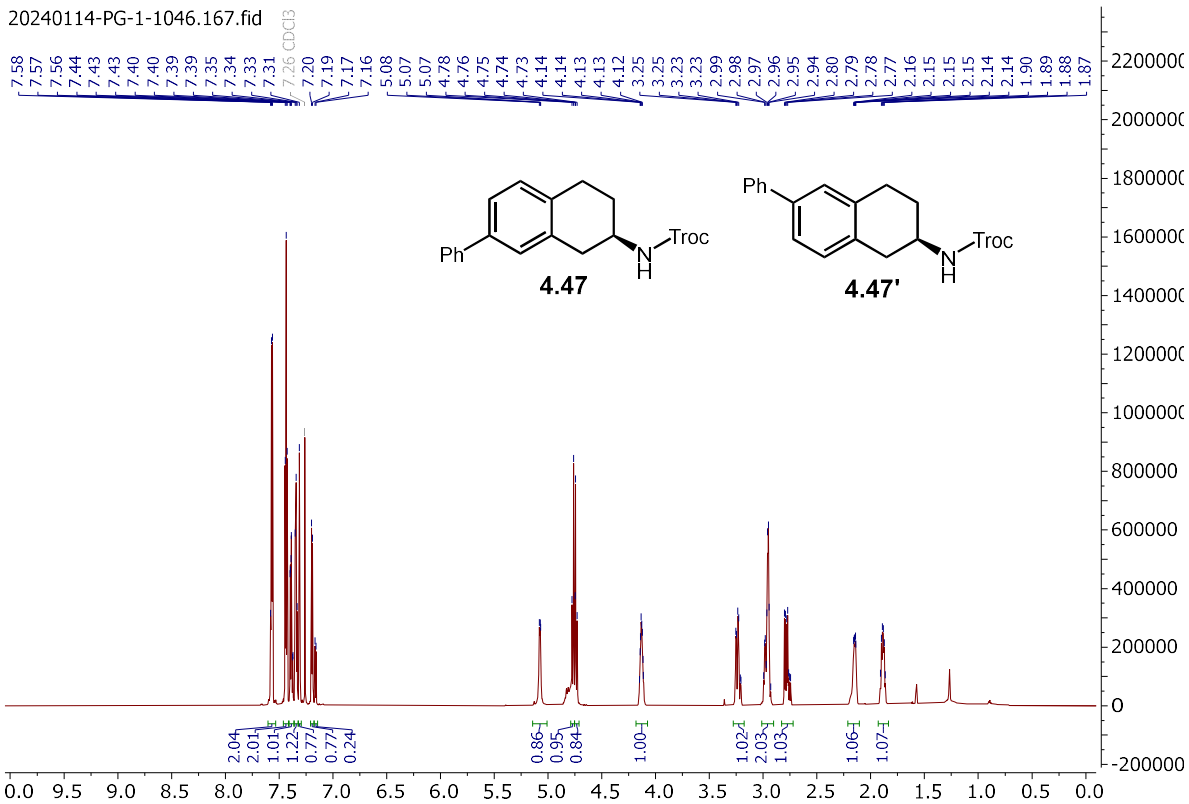
2,2,2-trichloroethyl (6-(allyloxy)-1,2,3,4-tetrahydronaphthalen-2-yl)carbamate (±-4.46'):



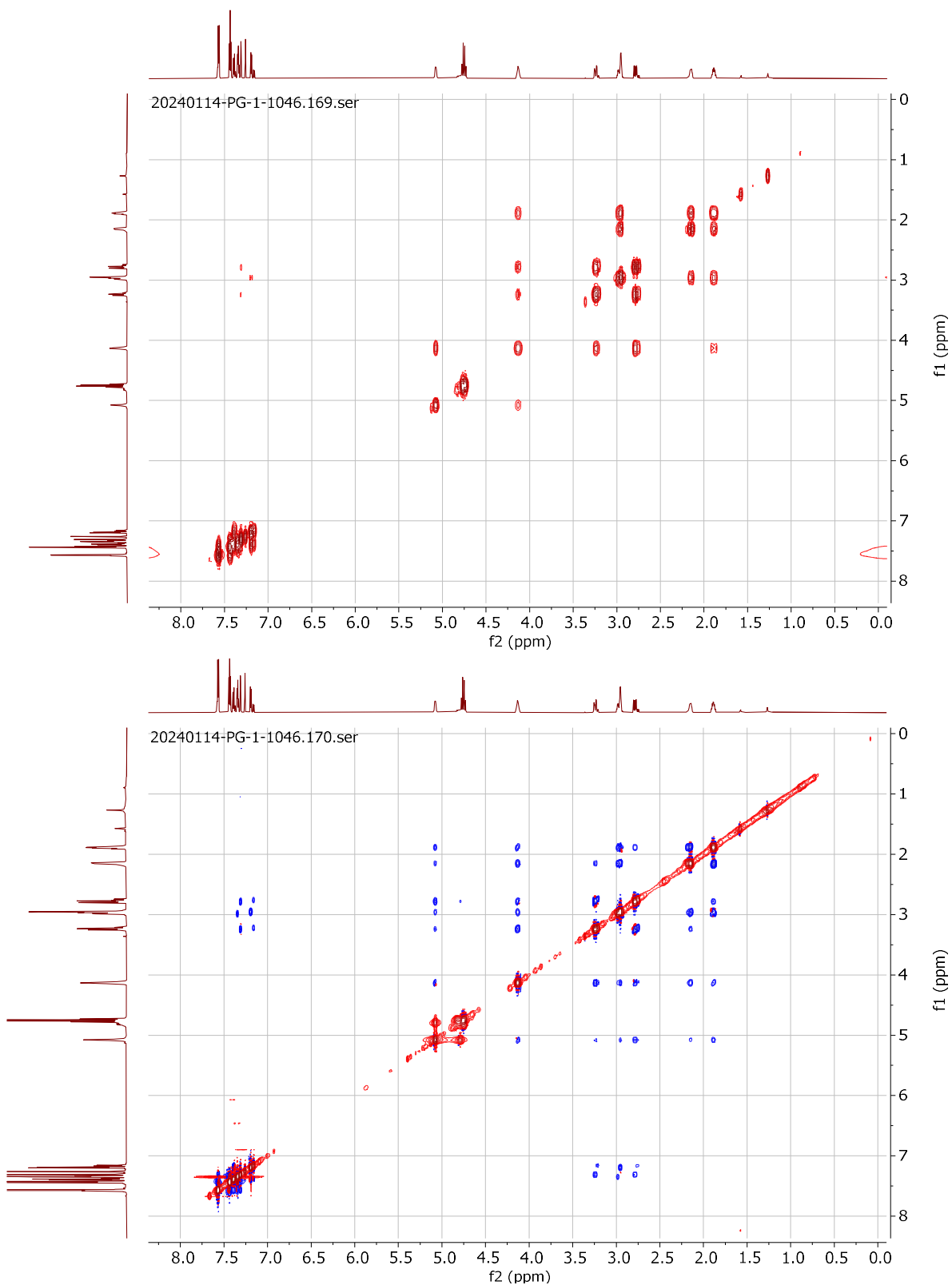
2,2,2-trichloroethyl (R)-(6-(allyloxy)-1,2,3,4-tetrahydronaphthalen-2-yl)carbamate (4.46'):



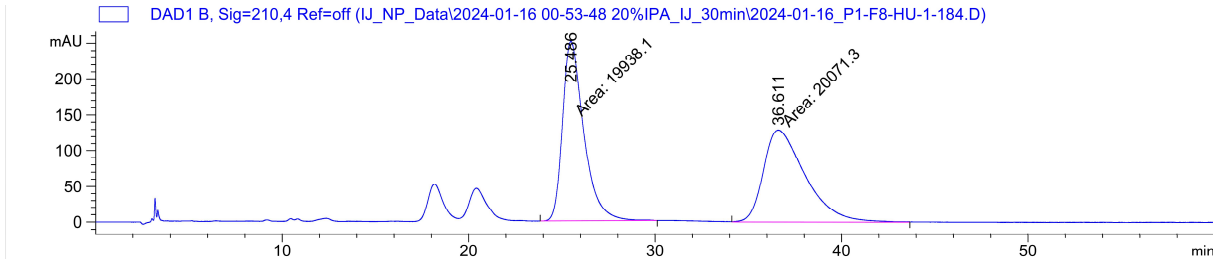
2,2,2-trichloroethyl (R)-(7-phenyl-1,2,3,4-tetrahydronaphthalen-2-yl)carbamate (**4.47**) and 2,2,2-trichloroethyl (R)-(6-phenyl-1,2,3,4-tetrahydronaphthalen-2-yl)carbamate (**4.47'**):



(4.47) and (4.47'):



2,2,2-trichloroethyl (7-phenyl-1,2,3,4-tetrahydronaphthalen-2-yl)carbamate (\pm -4.47)

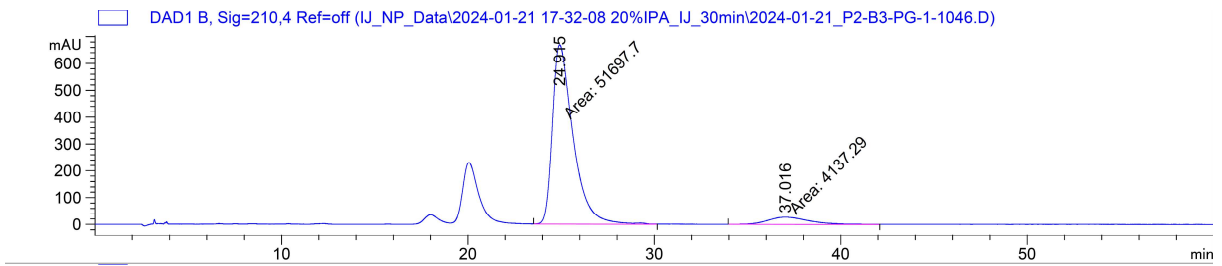


Signal 2: DAD1 B, Sig=210,4 Ref=off

| Peak # | RetTime [min] | Type | Width [min] | Area [mAU*s] | Height [mAU] | Area % |
|--------|---------------|------|-------------|--------------|--------------|---------|
| 1 | 25.486 | MM T | 1.3228 | 1.99381e4 | 251.21323 | 49.8335 |
| 2 | 36.611 | MM T | 2.5864 | 2.00713e4 | 129.33791 | 50.1665 |

Totals : 4.00095e4 380.55113

2,2,2-trichloroethyl (R)- (7-phenyl-1,2,3,4-tetrahydronaphthalen-2-yl)carbamate (4.47):

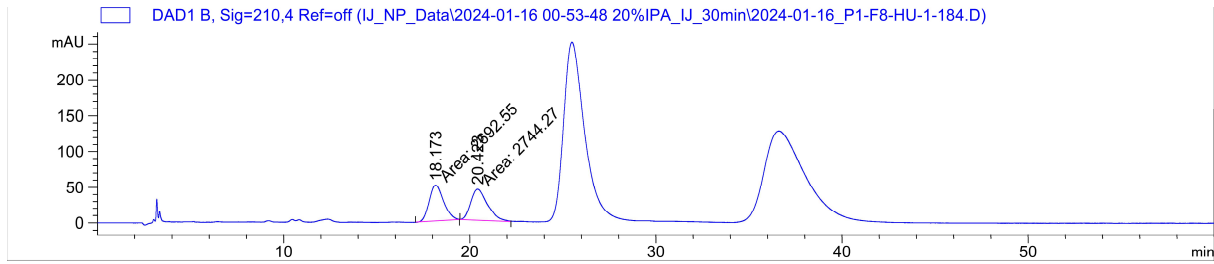


Signal 2: DAD1 B, Sig=210,4 Ref=off

| Peak # | RetTime [min] | Type | Width [min] | Area [mAU*s] | Height [mAU] | Area % |
|--------|---------------|------|-------------|--------------|--------------|---------|
| 1 | 24.915 | MM T | 1.2889 | 5.16977e4 | 668.48682 | 92.5901 |
| 2 | 37.016 | MM T | 2.5634 | 4137.29492 | 26.90002 | 7.4099 |

Totals : 5.58349e4 695.38684

2,2,2-trichloroethyl (6-phenyl-1,2,3,4-tetrahydronaphthalen-2-yl)carbamate (\pm -4.47'):

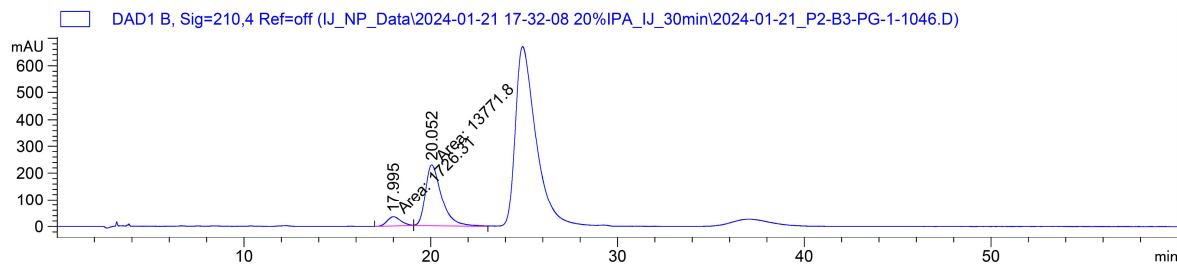


Signal 2: DAD1 B, Sig=210,4 Ref=off

| Peak # | RetTime [min] | Type | Width [min] | Area [mAU*s] | Height [mAU] | Area % |
|--------|---------------|------|-------------|--------------|--------------|---------|
| 1 | 18.173 | MM | 0.8862 | 2692.54590 | 50.63799 | 49.5243 |
| 2 | 20.423 | MM T | 1.0138 | 2744.27246 | 43.92320 | 50.4757 |

Totals : 5436.81836 94.56119

2,2,2-trichloroethyl (R)-(6-phenyl-1,2,3,4-tetrahydronaphthalen-2-yl)carbamate (4.47):

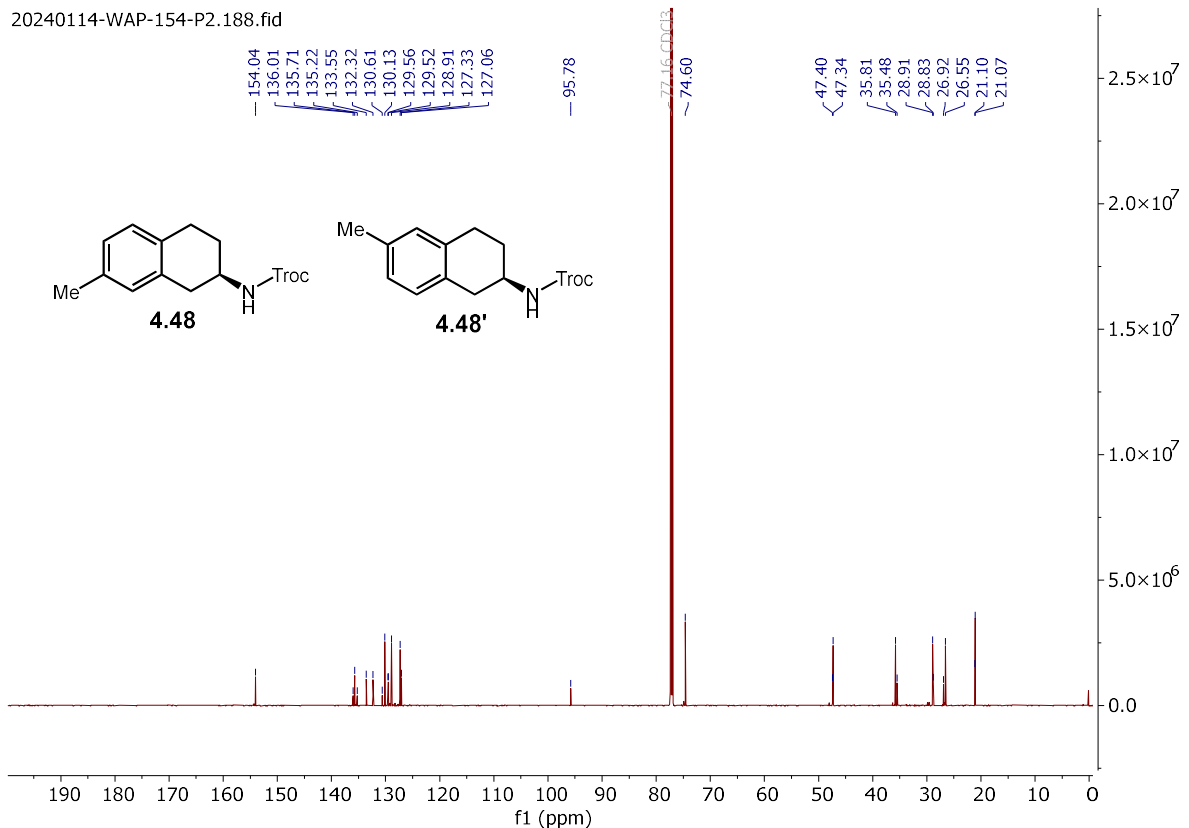
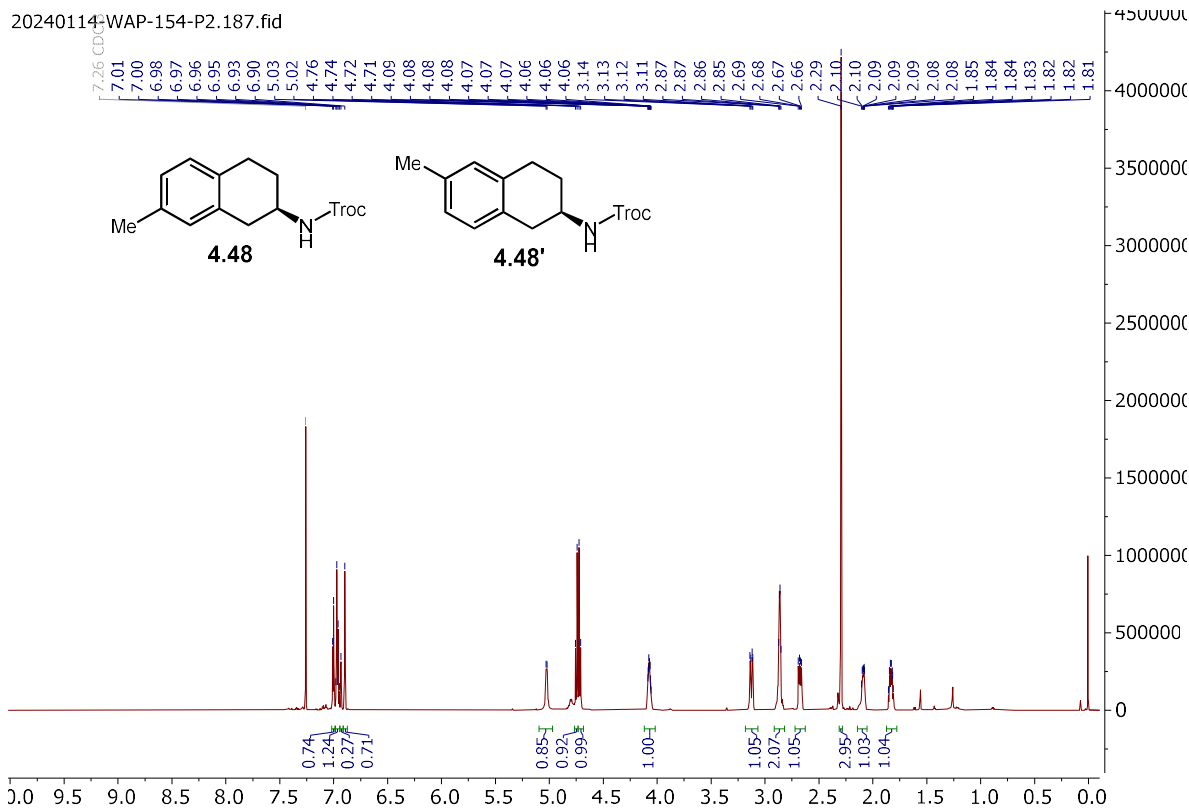


Signal 2: DAD1 B, Sig=210,4 Ref=off

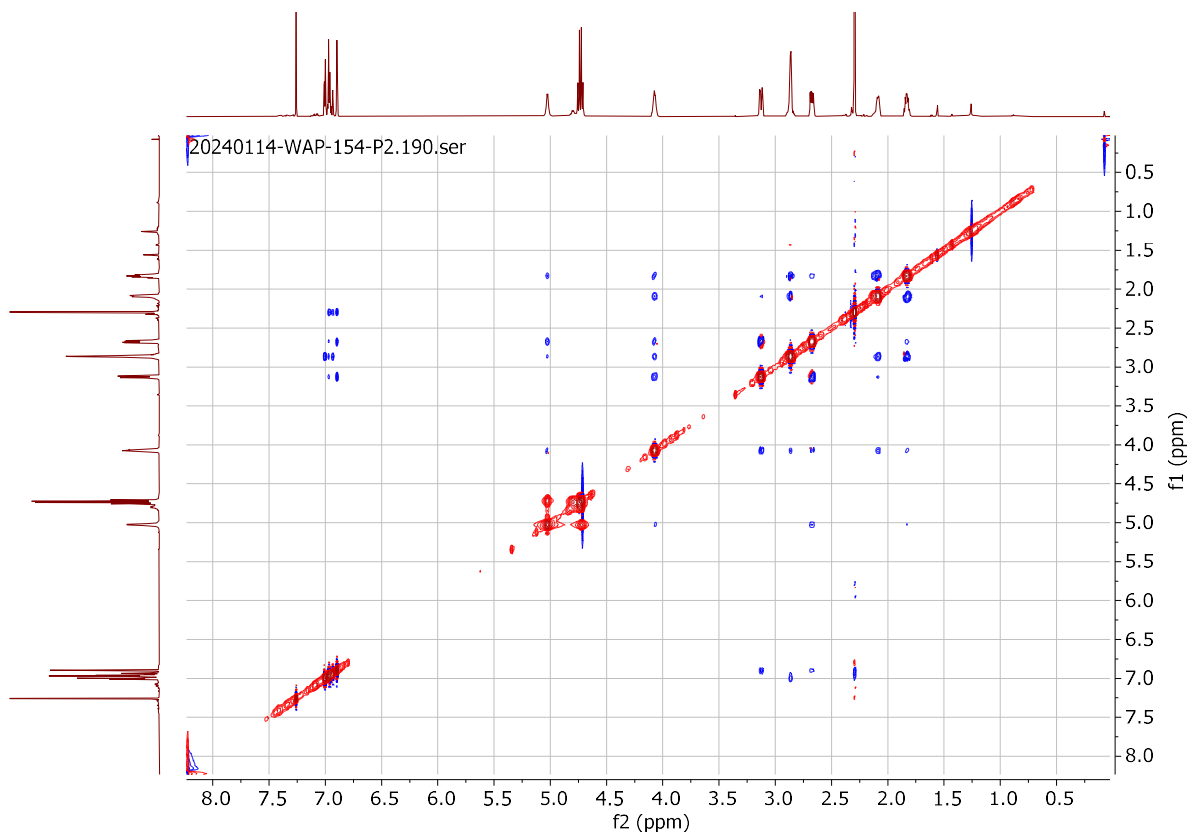
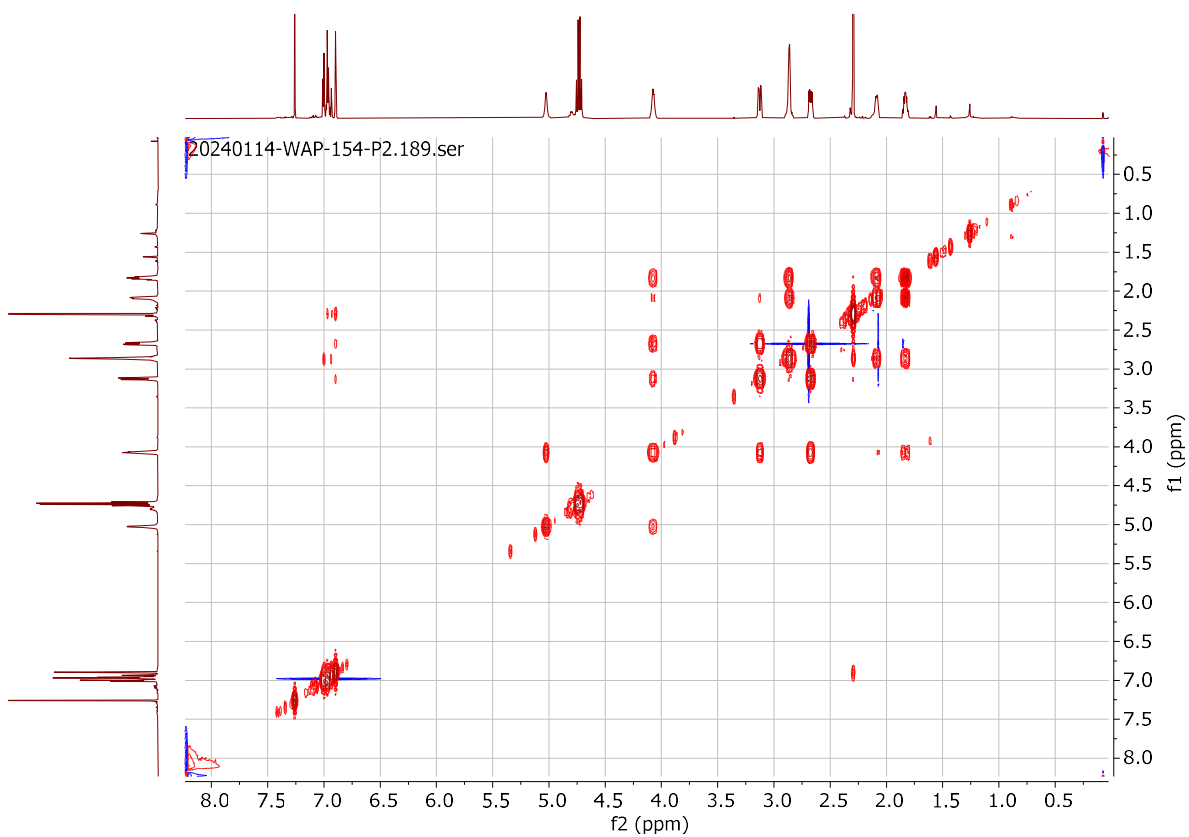
| Peak # | RetTime [min] | Type | Width [min] | Area [mAU*s] | Height [mAU] | Area % |
|--------|---------------|------|-------------|--------------|--------------|---------|
| 1 | 17.995 | MM T | 0.8437 | 1726.30750 | 34.10238 | 11.1388 |
| 2 | 20.052 | MM T | 1.0072 | 1.37718e4 | 227.89500 | 88.8612 |

Totals : 1.54981e4 261.99738

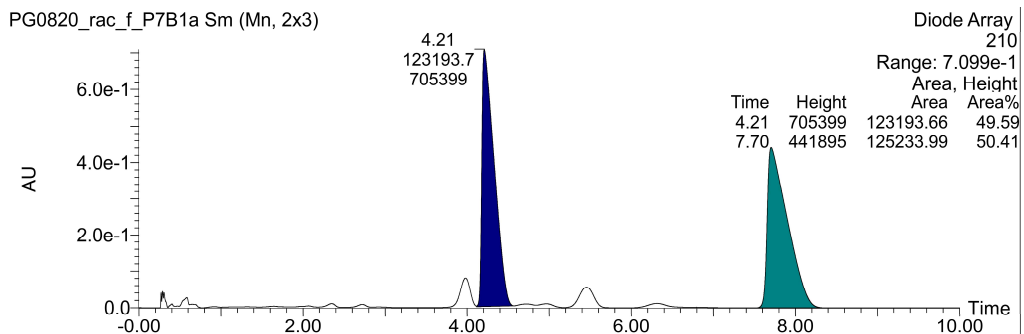
2,2,2-trichloroethyl (R)-(7-methyl-1,2,3,4-tetrahydronaphthalen-2-yl)carbamate (**4.48**) and 2,2,2-trichloroethyl (R)-(6-methyl-1,2,3,4-tetrahydronaphthalen-2-yl)carbamate (**4.48'**):



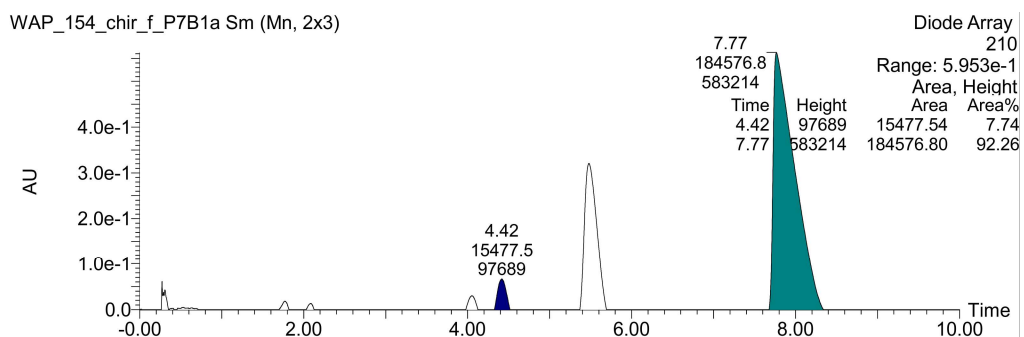
(4.48) and (4.48'):



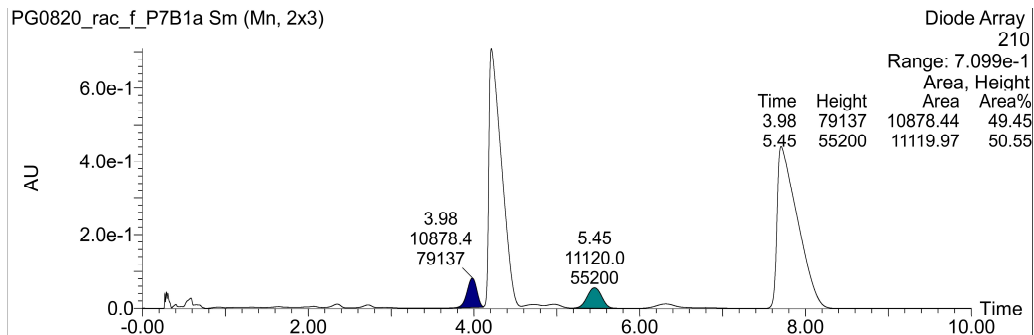
2,2,2-trichloroethyl (7-methyl-1,2,3,4-tetrahydronaphthalen-2-yl)carbamate (\pm -4.48):



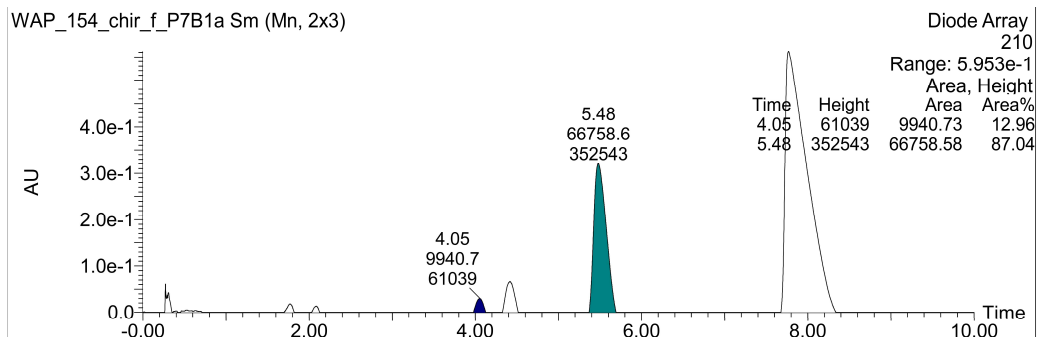
2,2,2-trichloroethyl (R)-(7-methyl-1,2,3,4-tetrahydronaphthalen-2-yl)carbamate (4.48):



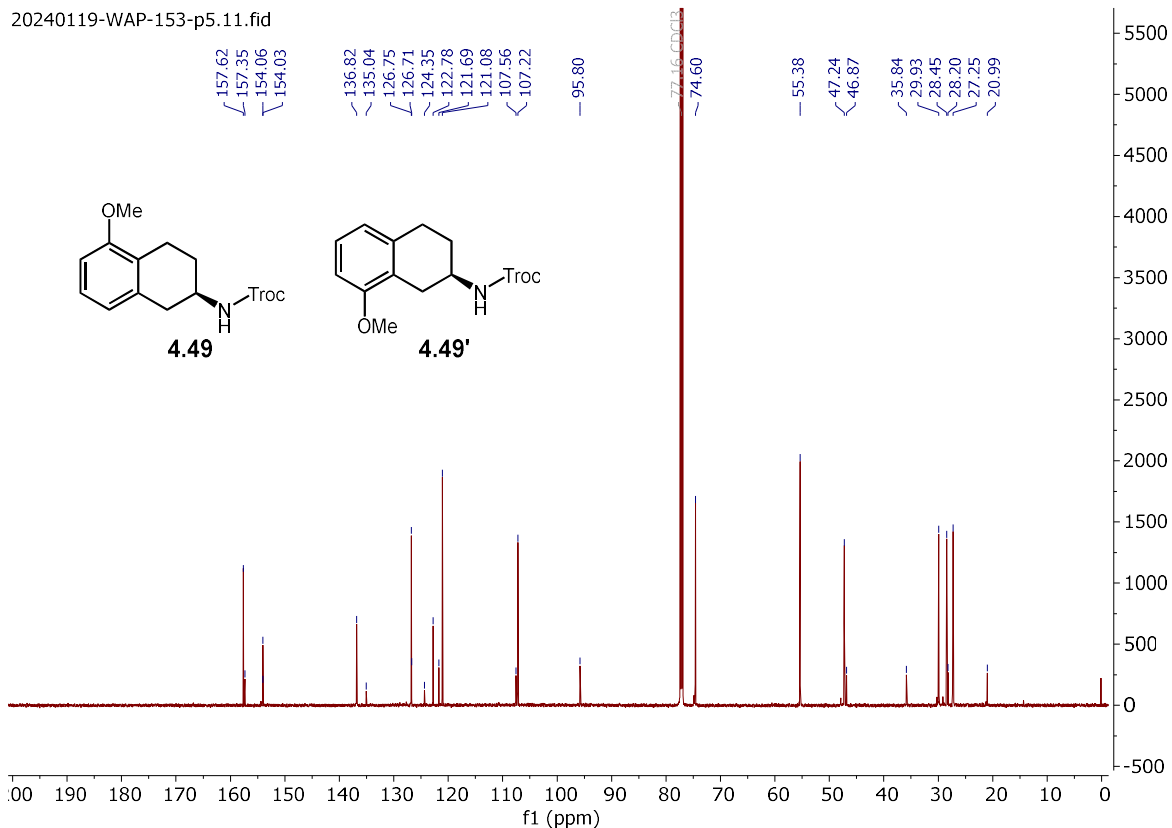
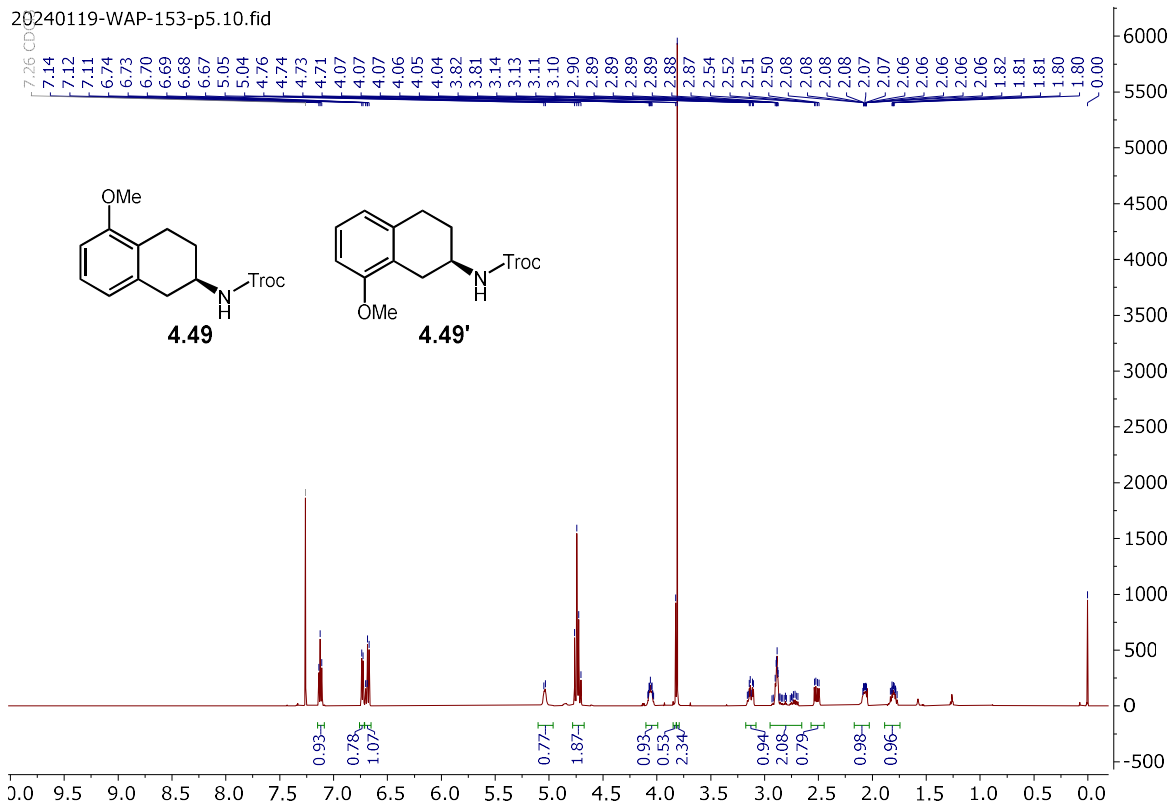
2,2,2-trichloroethyl (6-methyl-1,2,3,4-tetrahydronaphthalen-2-yl)carbamate (\pm -4.48'):



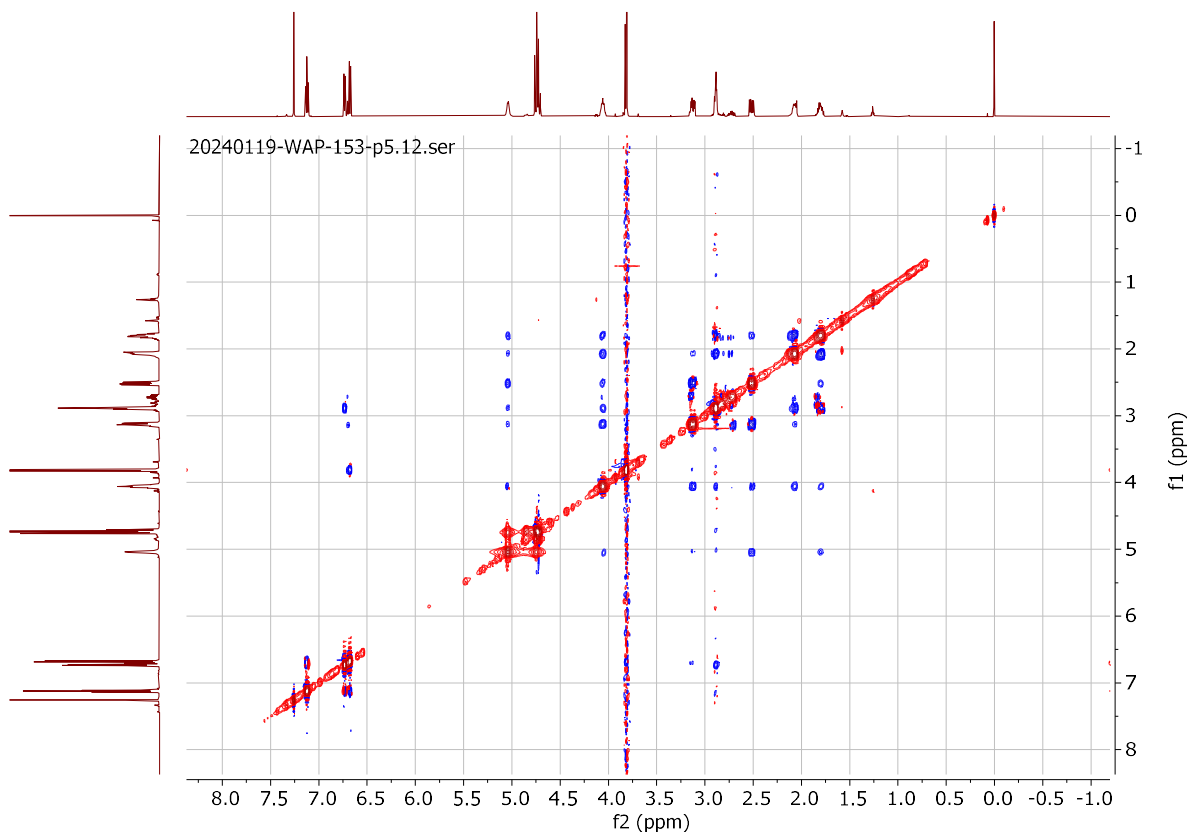
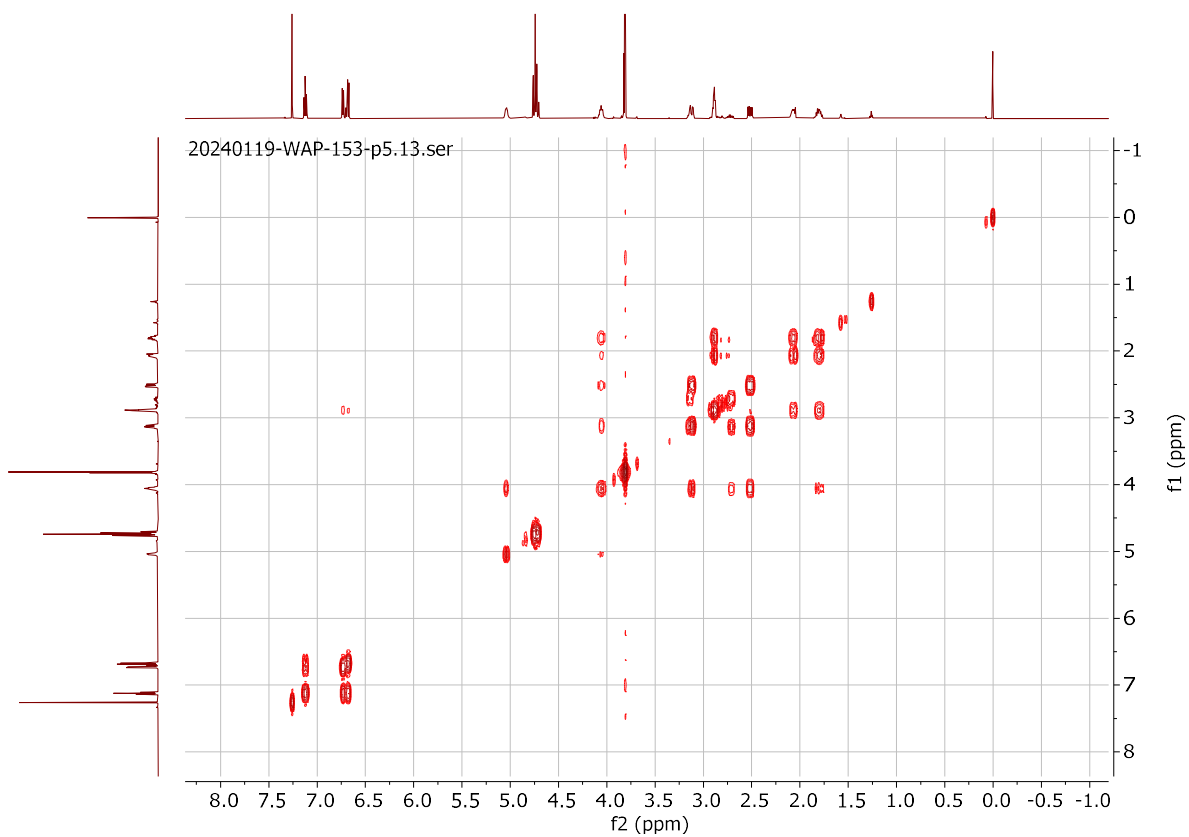
2,2,2-trichloroethyl (R)-(6-methyl-1,2,3,4-tetrahydronaphthalen-2-yl)carbamate (4.48'):



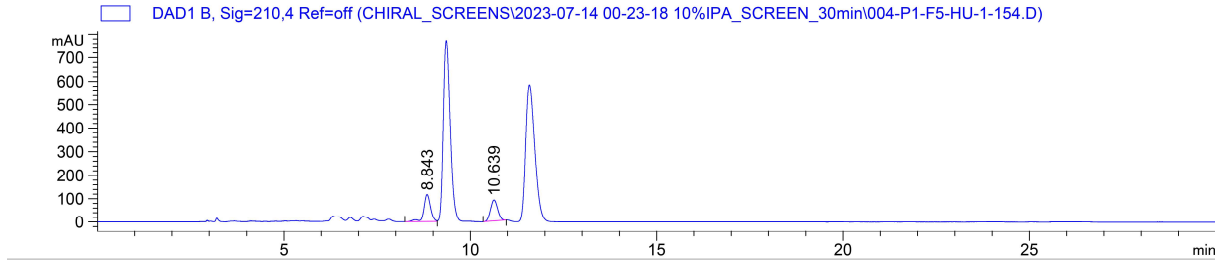
2,2,2-trichloroethyl (R)-(5-methoxy-1,2,3,4-tetrahydronaphthalen-2-yl)carbamate (**4.49**) and 2,2,2-trichloroethyl (R)-(8-methoxy-1,2,3,4-tetrahydronaphthalen-2-yl)carbamate (**4.49'**):



(4.49) and (4.49'):



2,2,2-trichloroethyl (5-methoxy-1,2,3,4-tetrahydronaphthalen-2-yl)carbamate (4.49):

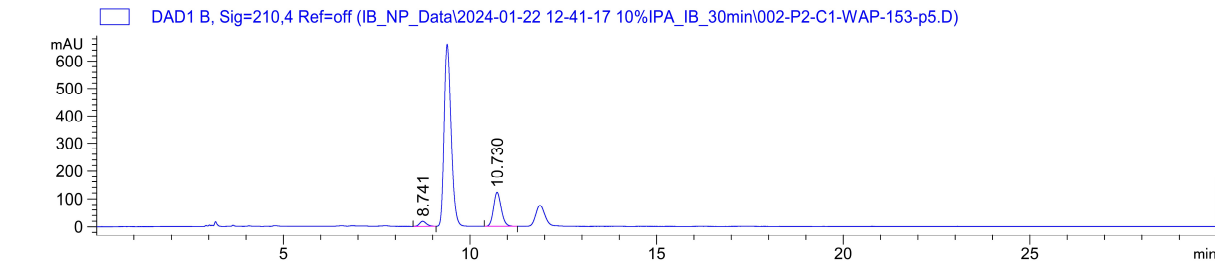


Signal 2: DAD1 B, Sig=210,4 Ref=off

| Peak # | RetTime [min] | Type | Width [min] | Area [mAU*s] | Height [mAU] | Area % |
|--------|---------------|------|-------------|--------------|--------------|---------|
| 1 | 8.843 | VV R | 0.1734 | 1462.58716 | 116.43881 | 54.5366 |
| 2 | 10.639 | BV R | 0.1864 | 1219.25684 | 90.63749 | 45.4634 |

Totals : 2681.84399 207.07630

2,2,2-trichloroethyl (R)-(5-methoxy-1,2,3,4-tetrahydronaphthalen-2-yl)carbamate (4.49):

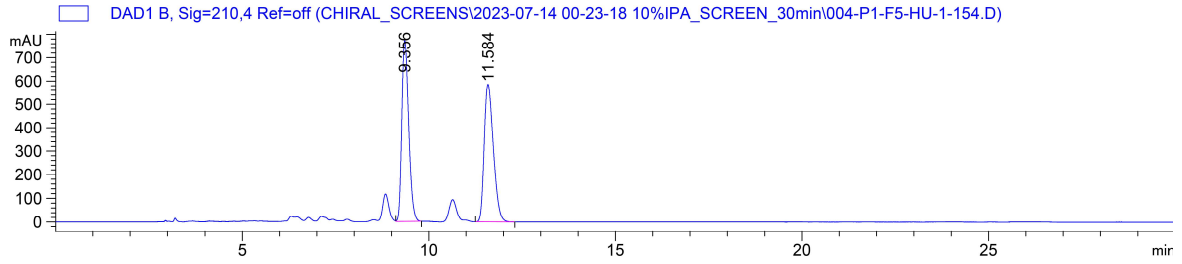


Signal 2: DAD1 B, Sig=210,4 Ref=off

| Peak # | RetTime [min] | Type | Width [min] | Area [mAU*s] | Height [mAU] | Area % |
|--------|---------------|------|-------------|--------------|--------------|---------|
| 1 | 8.741 | BV R | 0.1511 | 230.56030 | 18.10416 | 11.6884 |
| 2 | 10.730 | VV R | 0.1908 | 1741.99695 | 121.47370 | 88.3116 |

Totals : 1972.55725 139.57786

2,2,2-trichloroethyl (8-methoxy-1,2,3,4-tetrahydronaphthalen-2-yl)carbamate (±-4.49'):

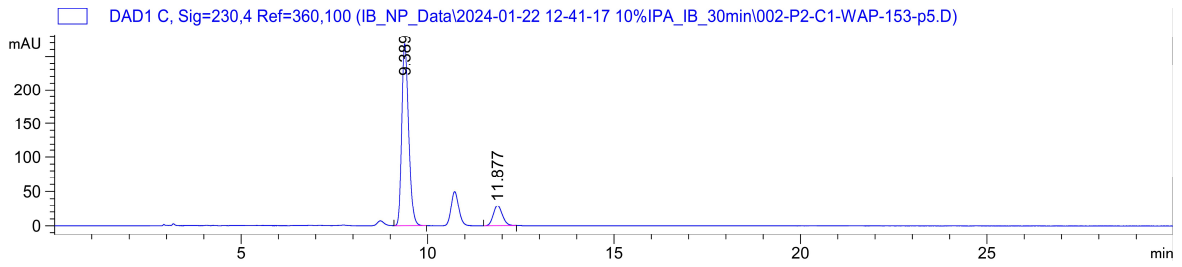


Signal 2: DAD1 B, Sig=210,4 Ref=off

| Peak # | RetTime [min] | Type | Width [min] | Area [mAU*s] | Height [mAU] | Area % |
|--------|---------------|------|-------------|--------------|--------------|---------|
| 1 | 9.356 | VB | 0.1939 | 9832.21582 | 770.42181 | 49.5640 |
| 2 | 11.584 | BV R | 0.2432 | 1.00052e4 | 586.10193 | 50.4360 |

Totals : 1.98374e4 1356.52374

2,2,2-trichloroethyl (R)-(8-methoxy-1,2,3,4-tetrahydronaphthalen-2-yl)carbamate (4.49'):

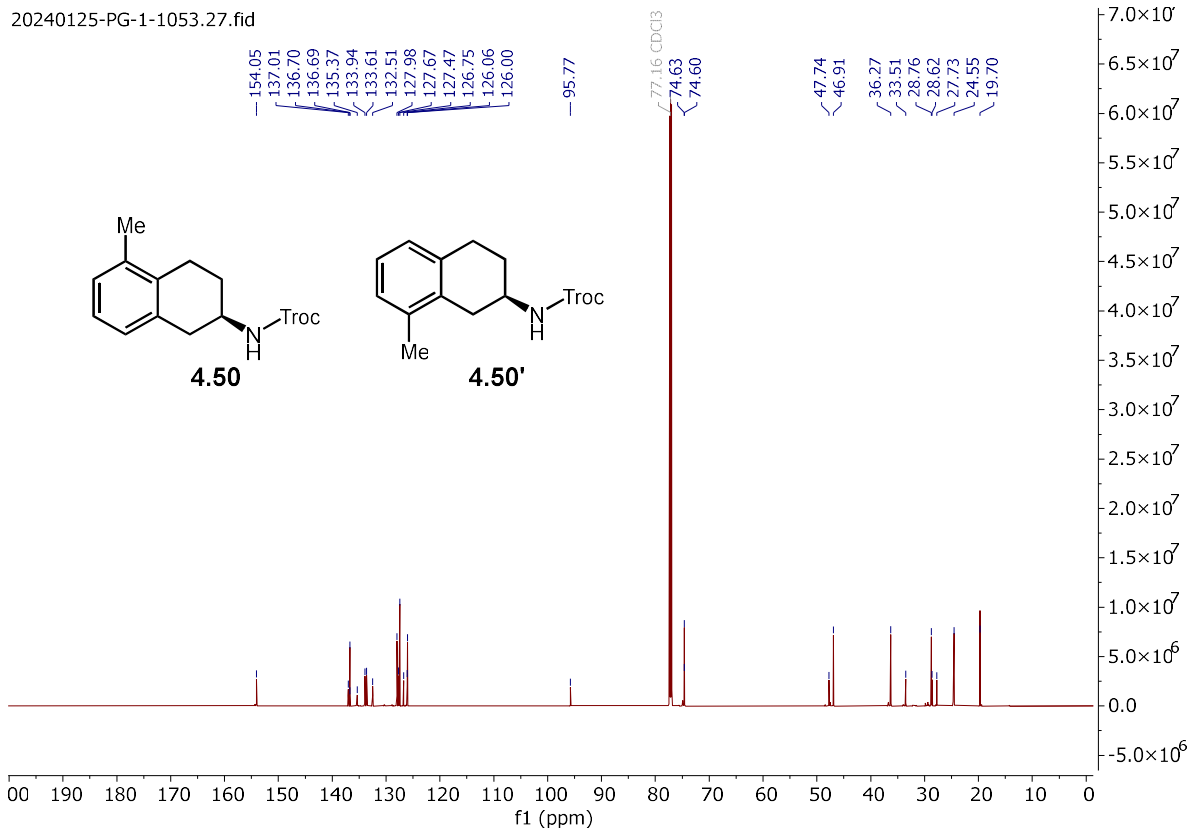
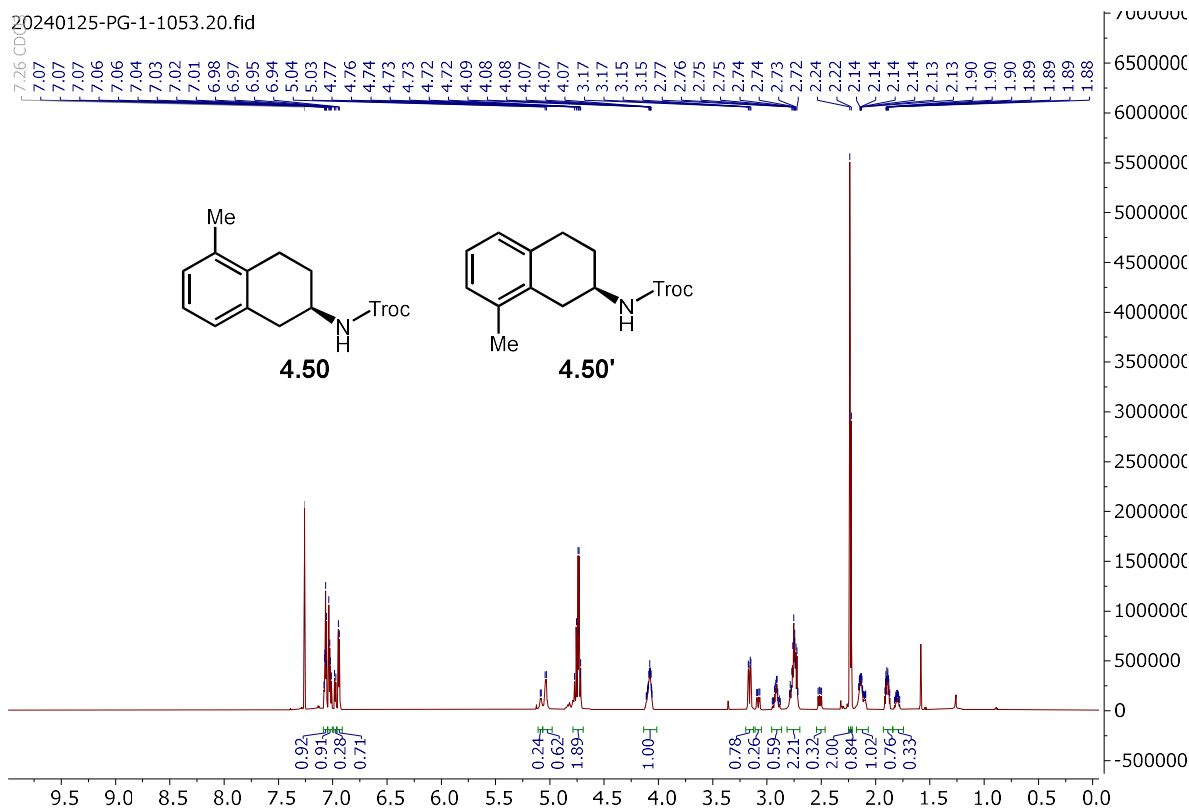


Signal 2: DAD1 B, Sig=210,4 Ref=off

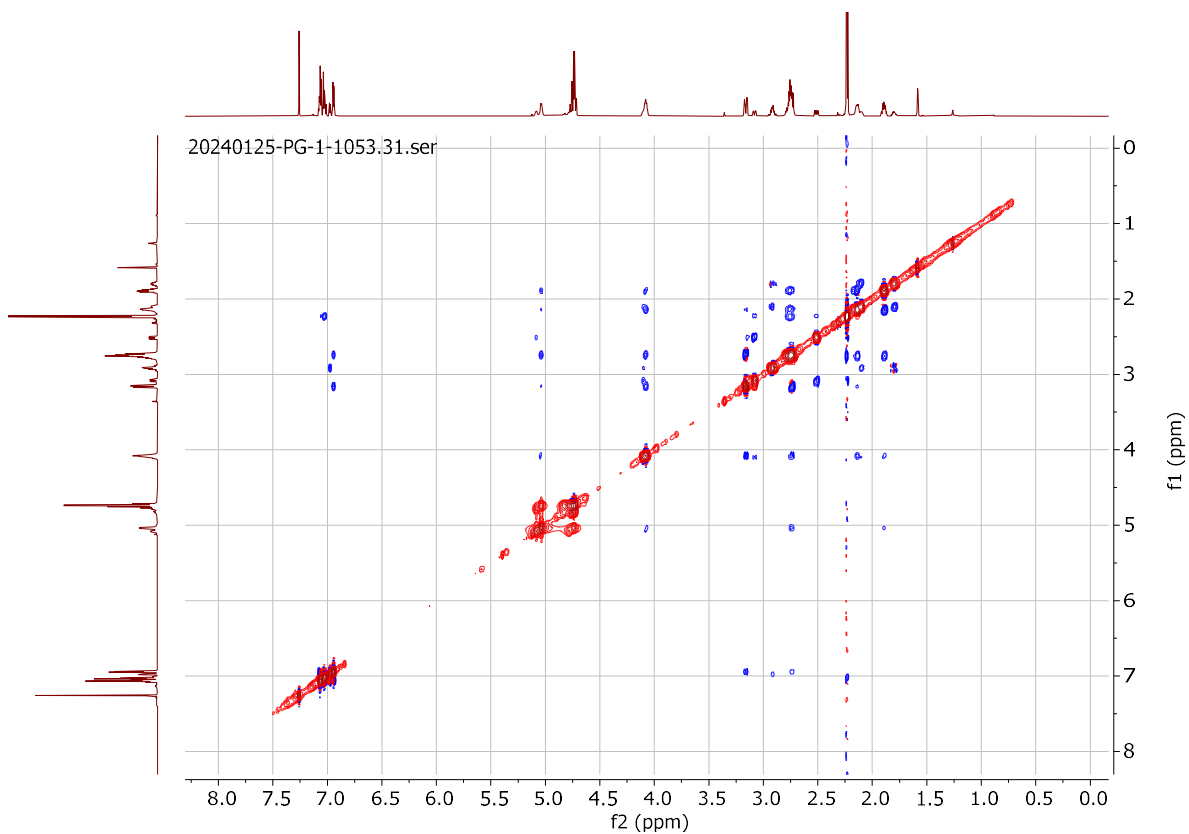
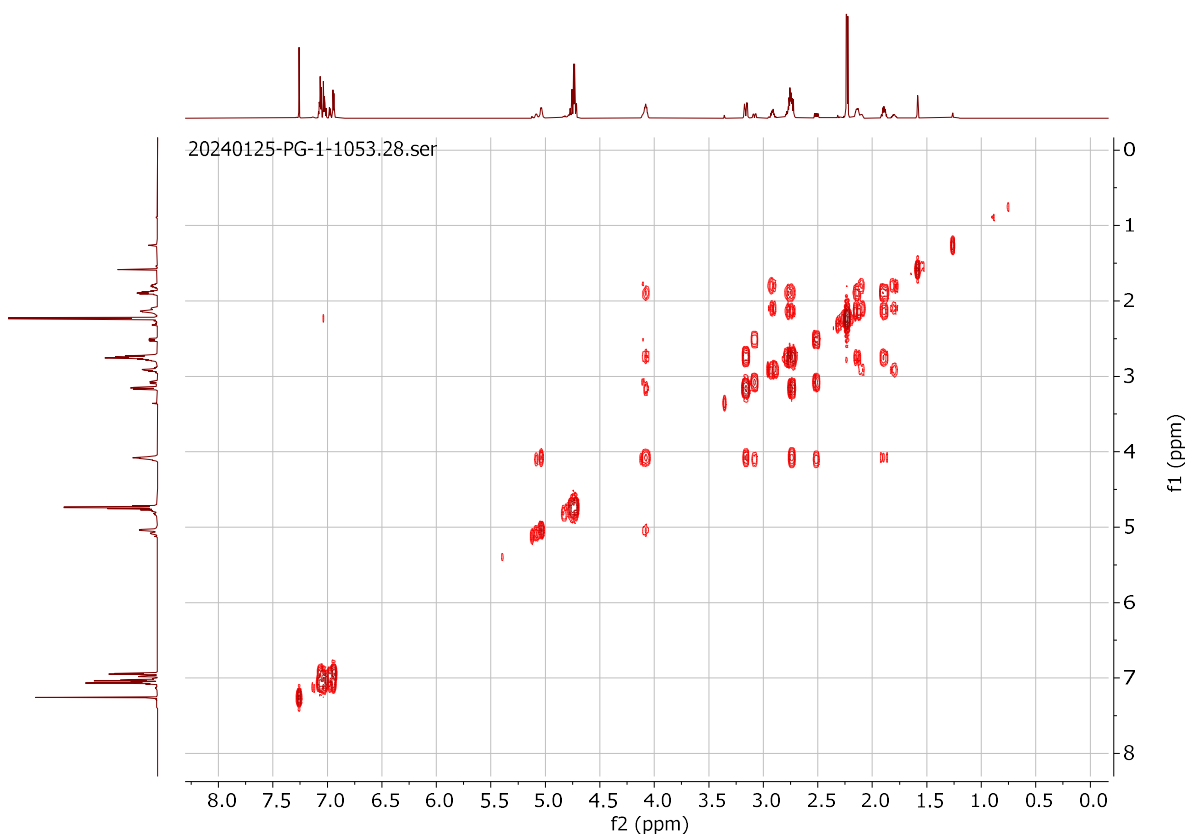
| Peak # | RetTime [min] | Type | Width [min] | Area [mAU*s] | Height [mAU] | Area % |
|--------|---------------|------|-------------|--------------|--------------|---------|
| 1 | 9.389 | VV R | 0.1981 | 8540.25586 | 659.27283 | 86.7633 |
| 2 | 11.875 | BV R | 0.2057 | 1302.91284 | 75.37483 | 13.2367 |

Totals : 9843.16870 734.64766

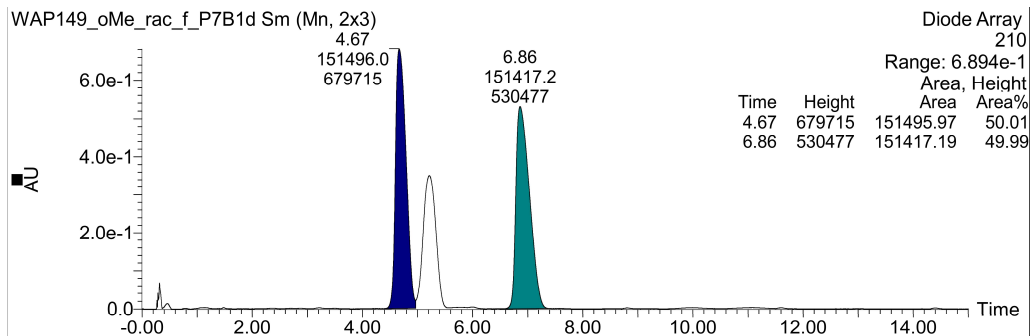
2,2,2-trichloroethyl (R)-(5-methyl-1,2,3,4-tetrahydronaphthalen-2-yl)carbamate (**4.50**) and 2,2,2-trichloroethyl (R)-(8-methyl-1,2,3,4-tetrahydronaphthalen-2-yl)carbamate (**4.50'**):



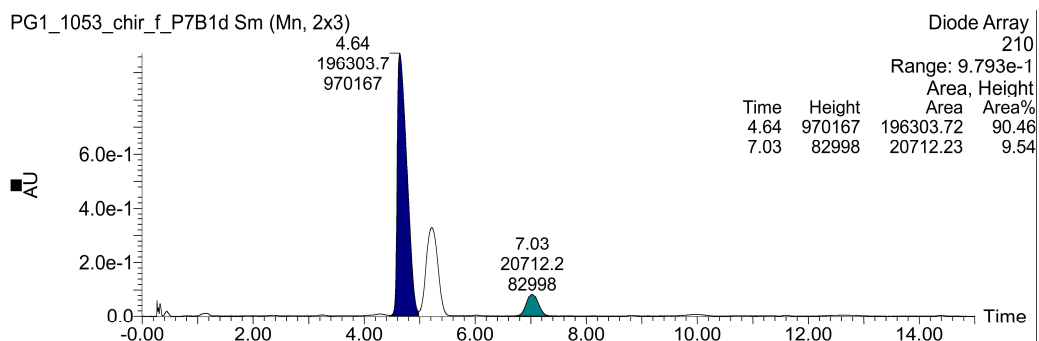
(4.50) and (4.50'):



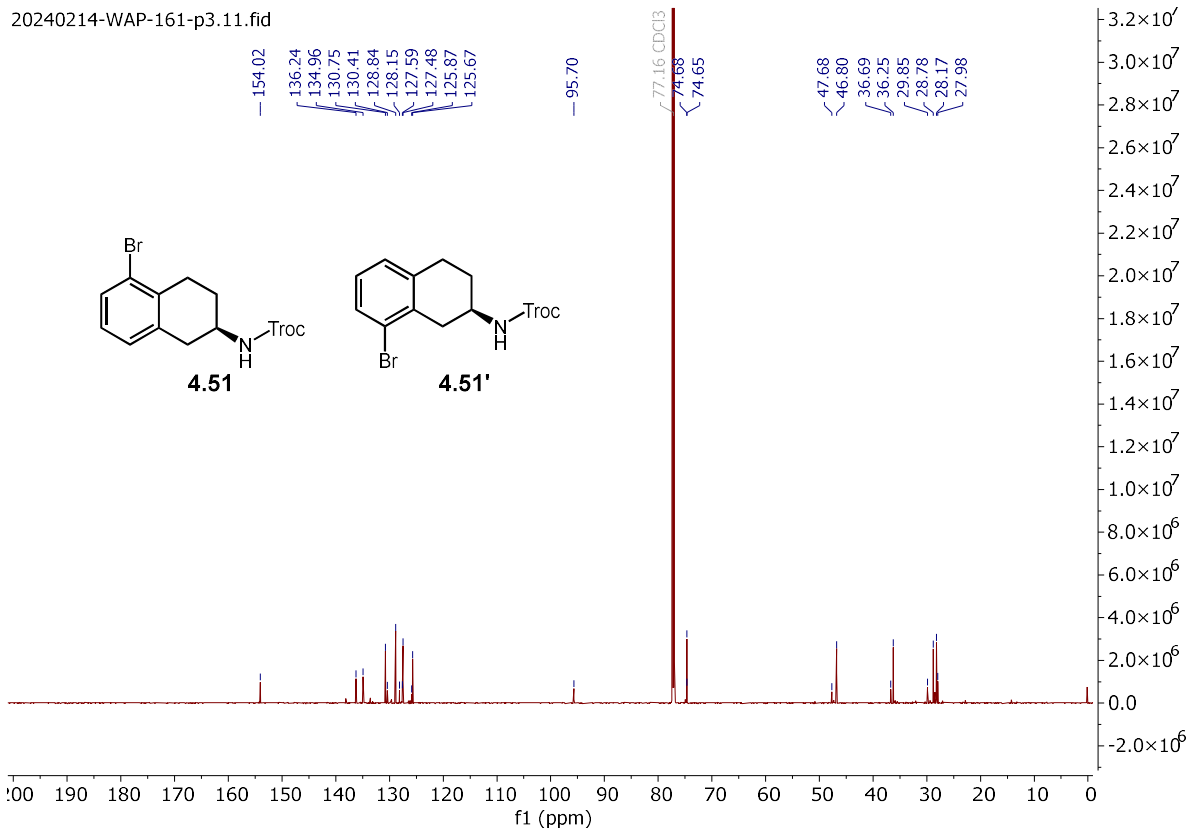
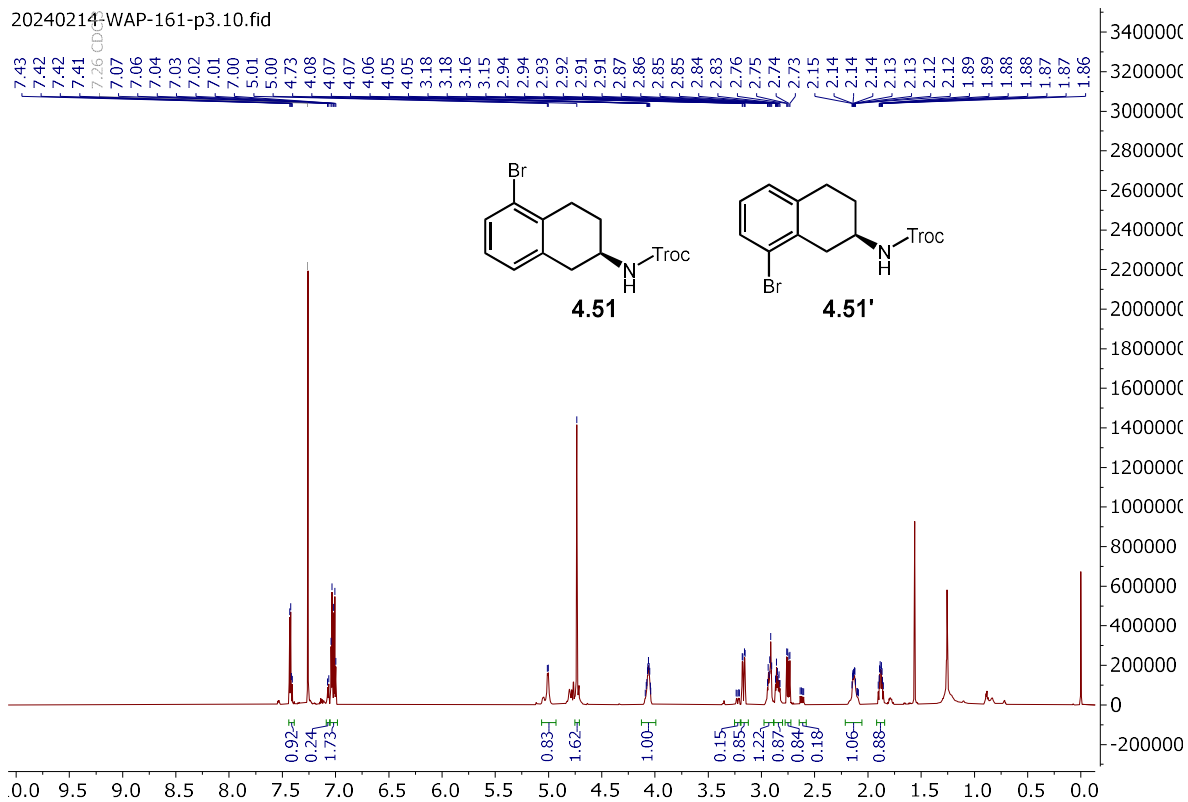
2,2,2-trichloroethyl (5-methyl-1,2,3,4-tetrahydronaphthalen-2-yl)carbamate (\pm -4.50):



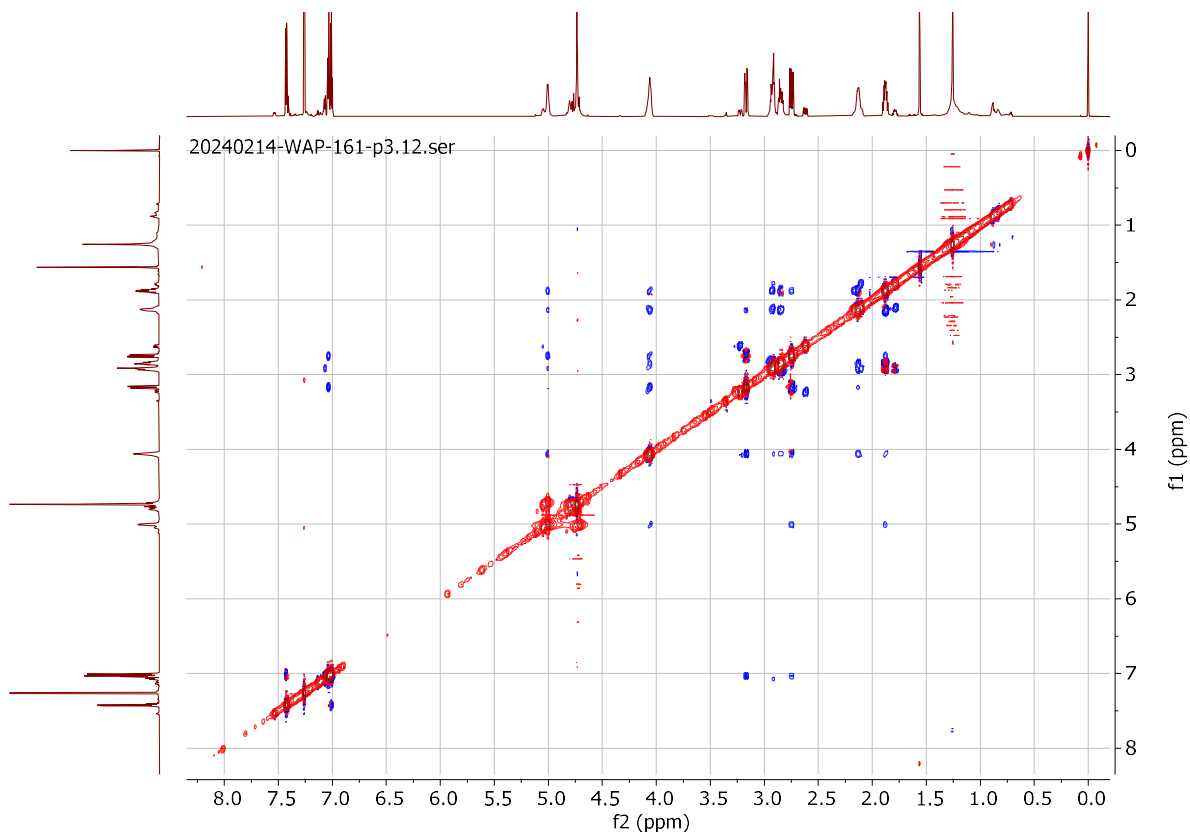
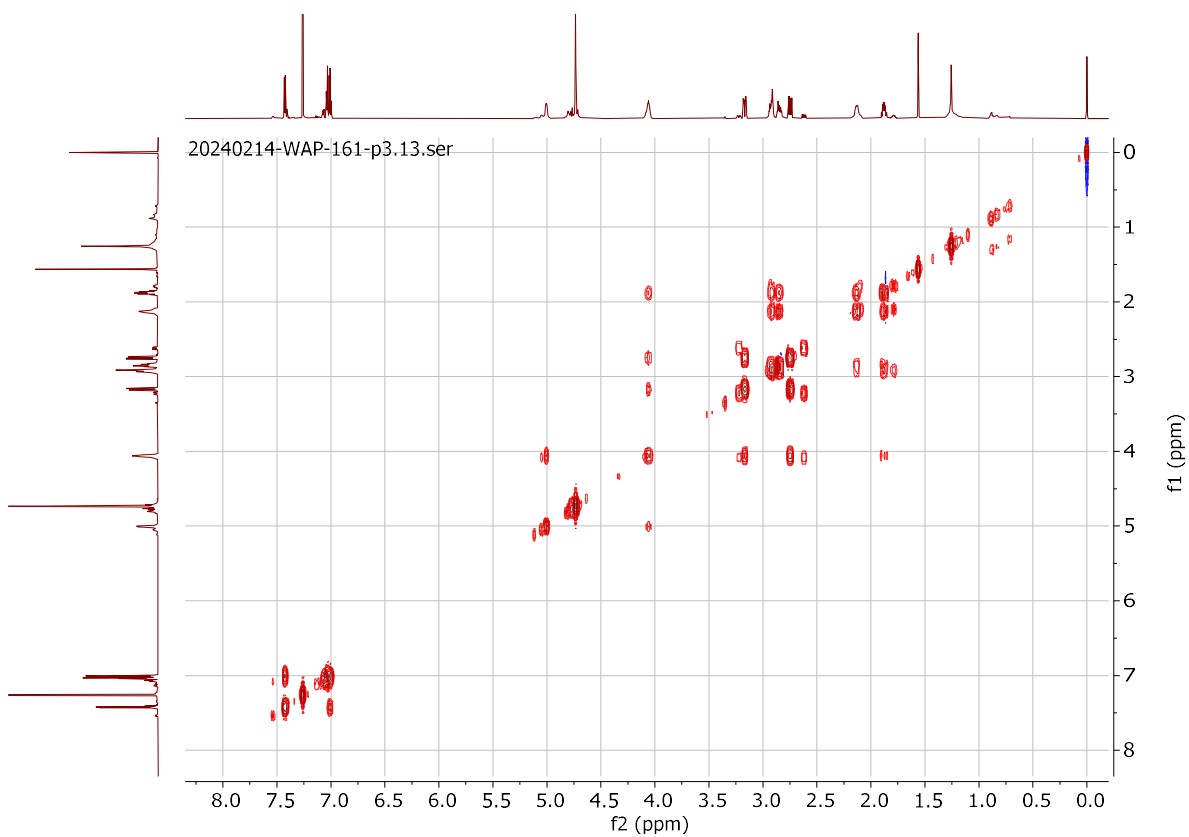
2,2,2-trichloroethyl (R)-(5-methyl-1,2,3,4-tetrahydronaphthalen-2-yl)carbamate (4.50):



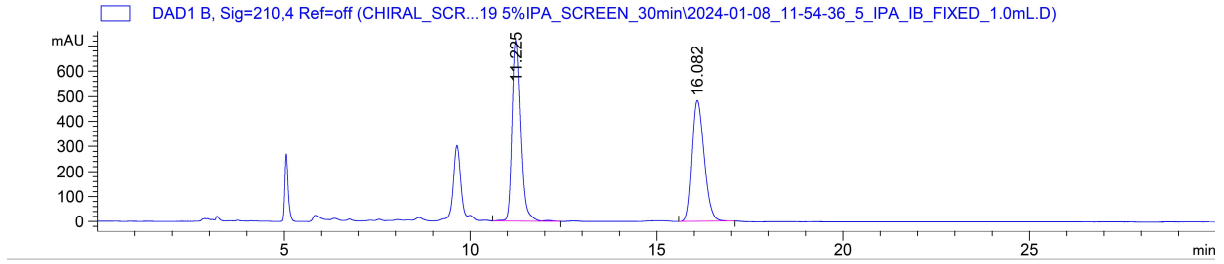
2,2,2-trichloroethyl (R)-(5-bromo-1,2,3,4-tetrahydronaphthalen-2-yl)carbamate (**4.51**) and 2,2,2-trichloroethyl (R)-(8-bromo-1,2,3,4-tetrahydronaphthalen-2-yl)carbamate (**4.51'**):



(4.51) and (4.51'):



2,2,2-trichloroethyl (5-bromo-1,2,3,4-tetrahydronaphthalen-2-yl)carbamate (\pm -4.51):

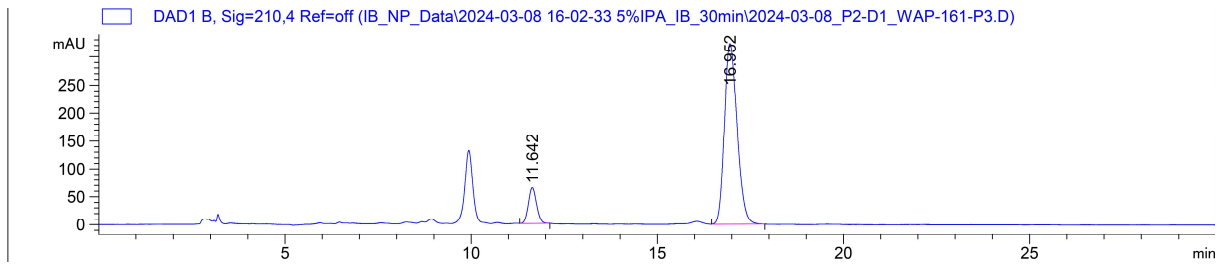


Signal 2: DAD1 B, Sig=210,4 Ref=off

| Peak # | RetTime [min] | Type | Width [min] | Area [mAU*s] | Height [mAU] | Area % |
|--------|---------------|------|-------------|--------------|--------------|---------|
| 1 | 11.225 | VV R | 0.2354 | 1.12944e4 | 721.33508 | 50.8184 |
| 2 | 16.082 | BV R | 0.2855 | 1.09306e4 | 483.89395 | 49.1816 |

Totals : 2.22250e4 1205.22903

2,2,2-trichloroethyl (R)-(5-bromo-1,2,3,4-tetrahydronaphthalen-2-yl)carbamate (4.51):

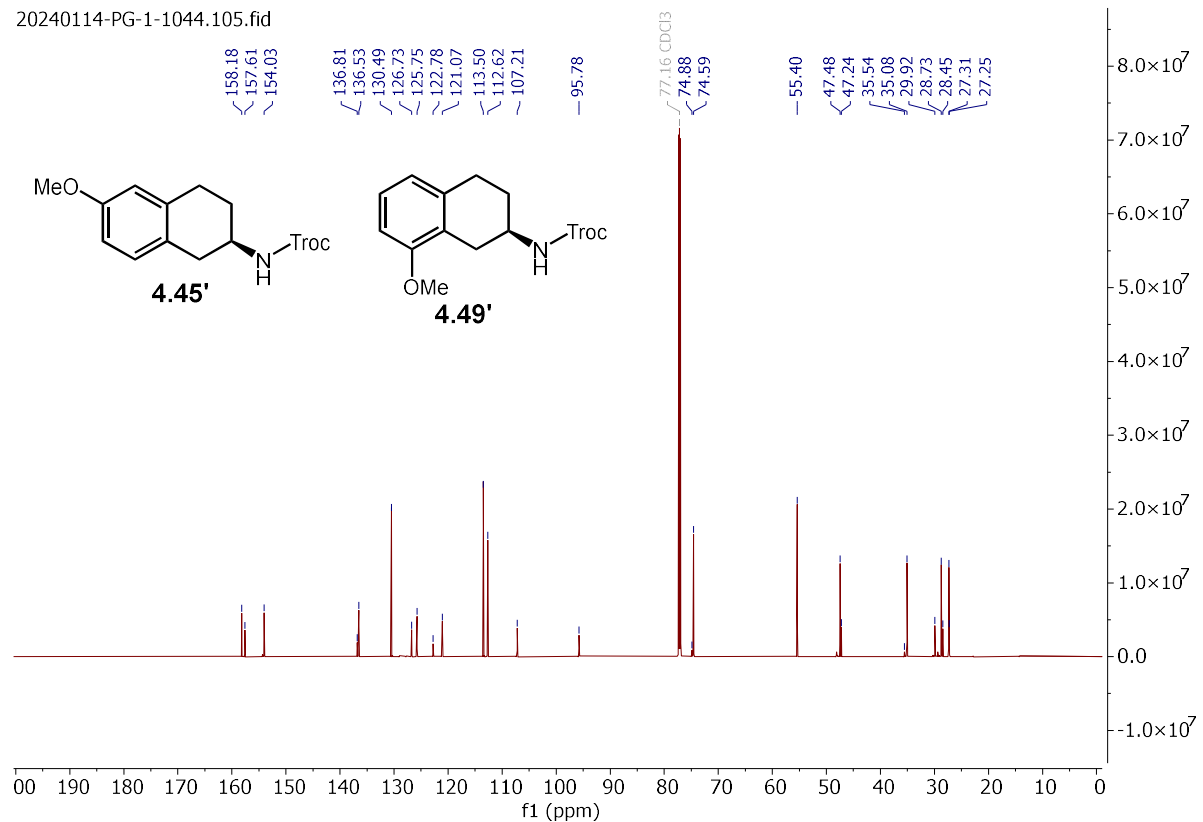
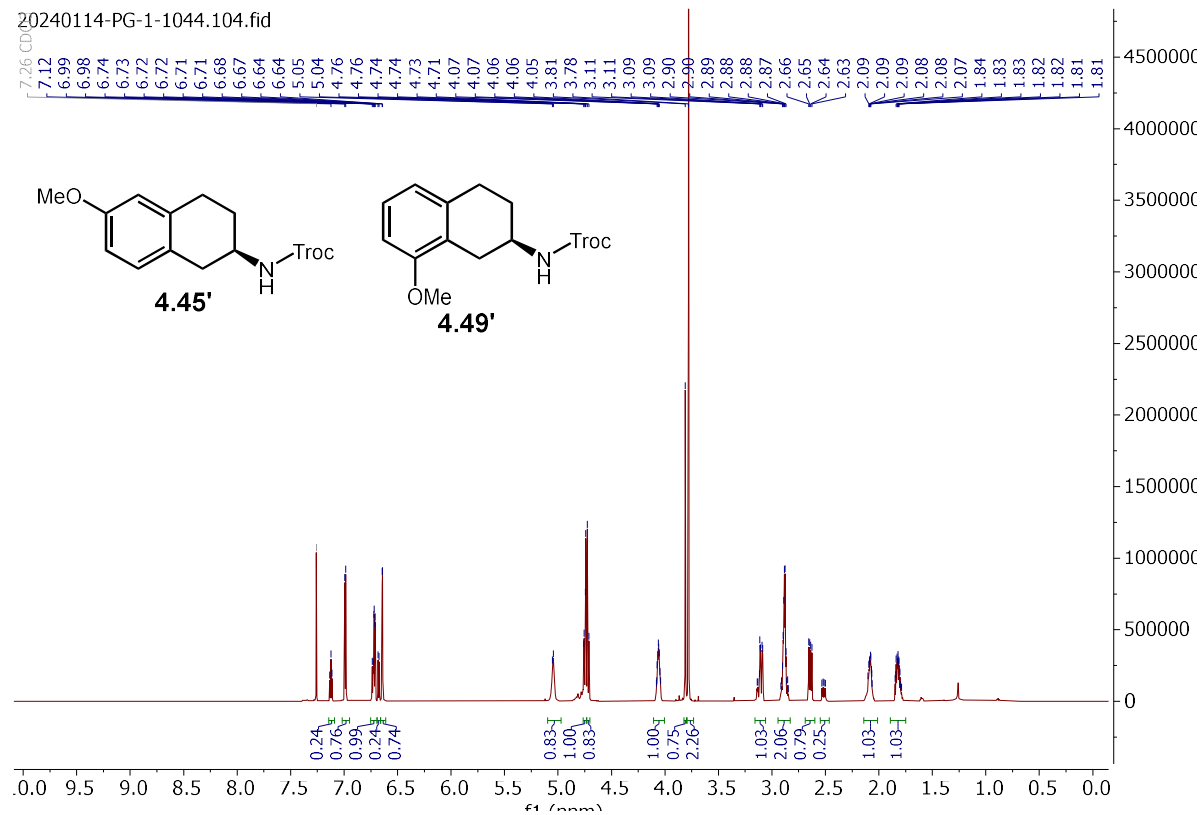


Signal 2: DAD1 B, Sig=210,4 Ref=off

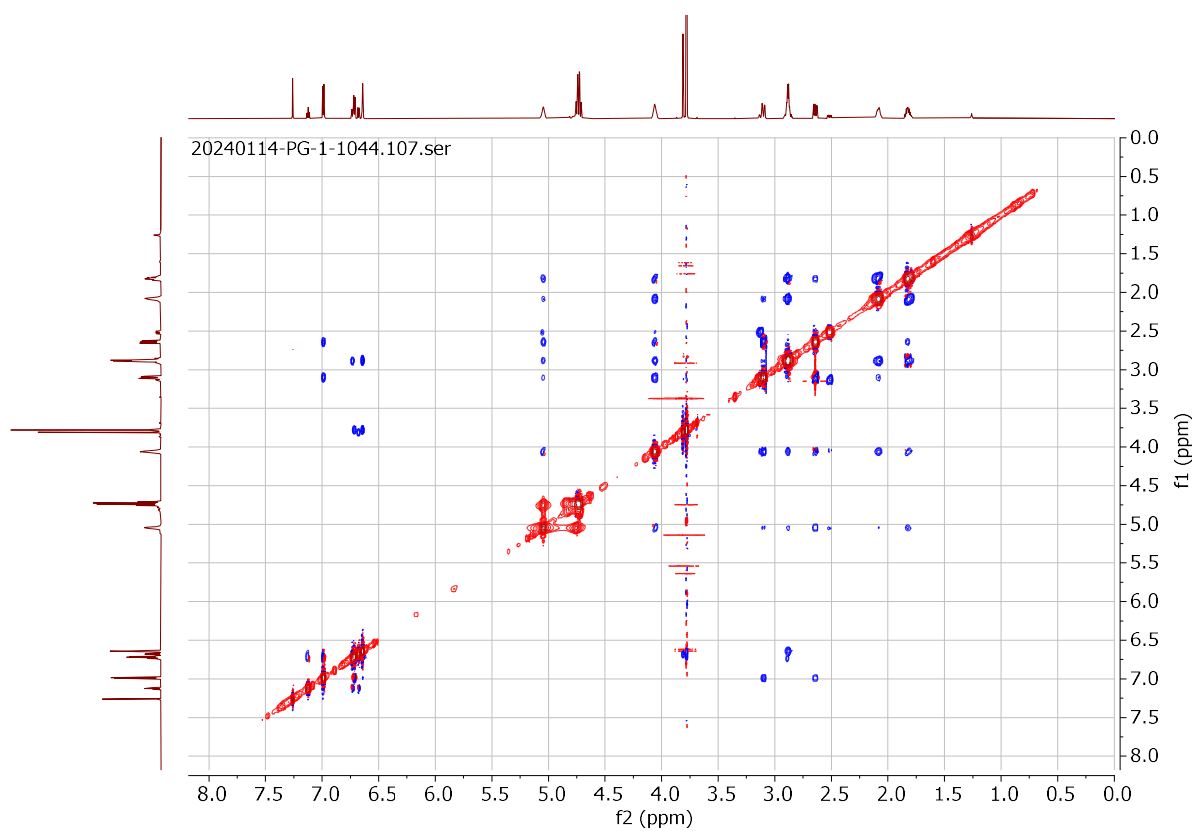
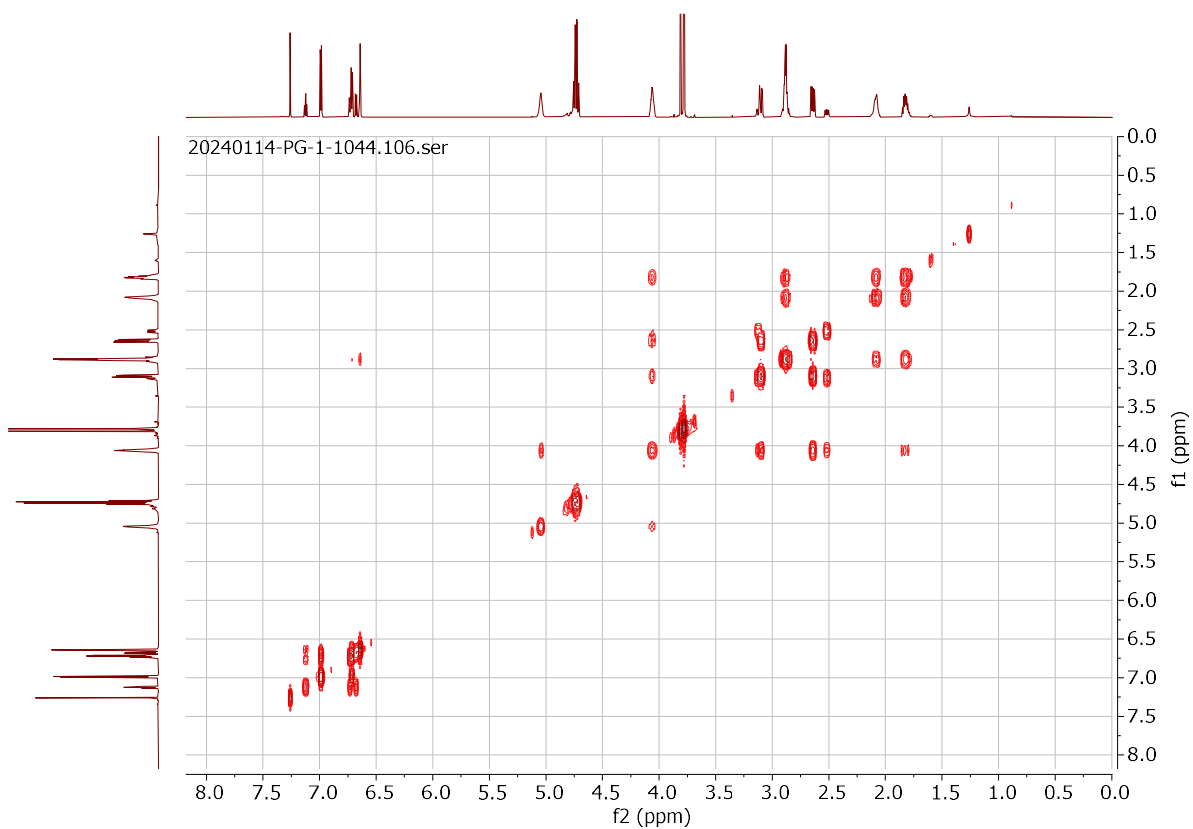
| Peak # | RetTime [min] | Type | Width [min] | Area [mAU*s] | Height [mAU] | Area % |
|--------|---------------|------|-------------|--------------|--------------|---------|
| 1 | 11.642 | BV R | 0.1801 | 980.41797 | 64.21804 | 11.3562 |
| 2 | 16.952 | BB | 0.2793 | 7652.92725 | 322.51056 | 88.6438 |

Totals : 8633.34521 386.72860

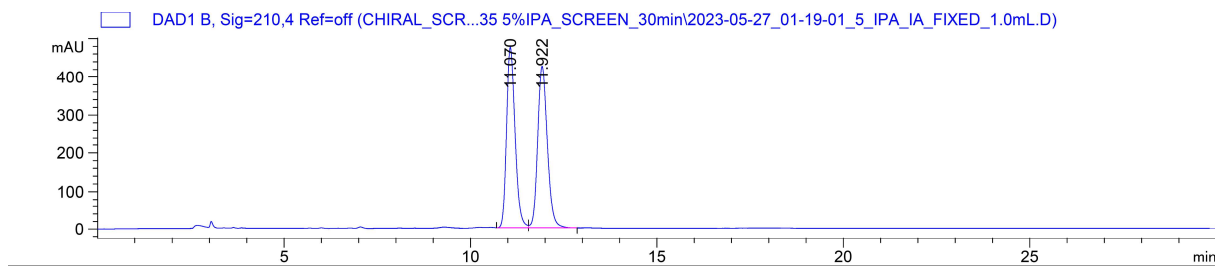
2,2,2-trichloroethyl (R)-(6-methoxy-1,2,3,4-tetrahydronaphthalen-2-yl)carbamate (**4.45'**) and 2,2,2-trichloroethyl (R)-(8-methoxy-1,2,3,4-tetrahydronaphthalen-2-yl)carbamate (**4.49'**):



(4.45') and (4.49')



2,2,2-trichloroethyl (6-methoxy-1,2,3,4-tetrahydronaphthalen-2-yl)carbamate (\pm -4.45'):

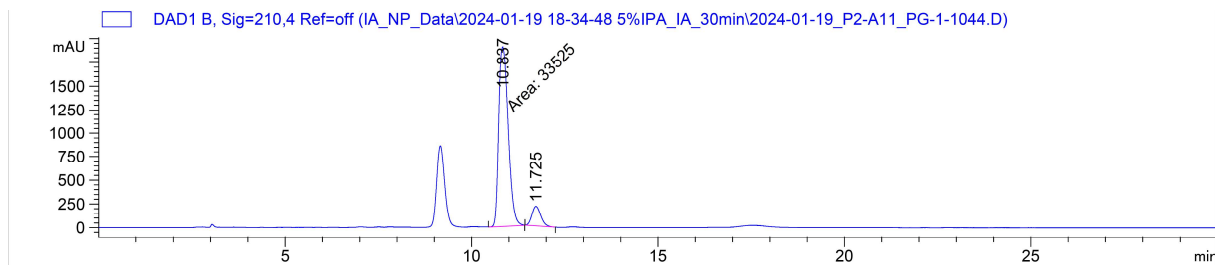


Signal 2: DAD1 B, Sig=210,4 Ref=off

| Peak # | RetTime [min] | Type | Width [min] | Area [mAU*s] | Height [mAU] | Area % |
|--------|---------------|------|-------------|--------------|--------------|---------|
| 1 | 11.070 | BV | 0.2391 | 7528.36133 | 474.48944 | 49.5182 |
| 2 | 11.922 | VB | 0.2683 | 7674.84766 | 425.82767 | 50.4818 |

Totals : 1.52032e4 900.31711

2,2,2-trichloroethyl (R)-(6-methoxy-1,2,3,4-tetrahydronaphthalen-2-yl)carbamate (4.45'):

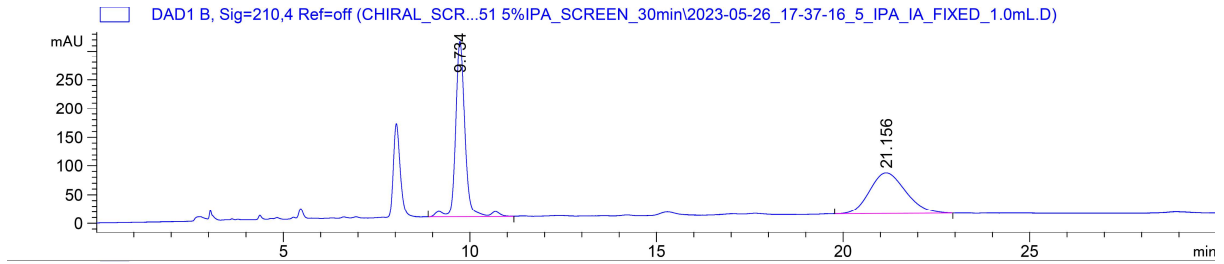


Signal 2: DAD1 B, Sig=210,4 Ref=off

| Peak # | RetTime [min] | Type | Width [min] | Area [mAU*s] | Height [mAU] | Area % |
|--------|---------------|------|-------------|--------------|--------------|---------|
| 1 | 10.837 | MM T | 0.2934 | 3.35250e4 | 1904.11755 | 90.7335 |
| 2 | 11.725 | BB | 0.2218 | 3423.86914 | 207.72342 | 9.2665 |

Totals : 3.69488e4 2111.84097

2,2,2-trichloroethyl (8-methoxy-1,2,3,4-tetrahydronaphthalen-2-yl)carbamate (\pm -4.49'):

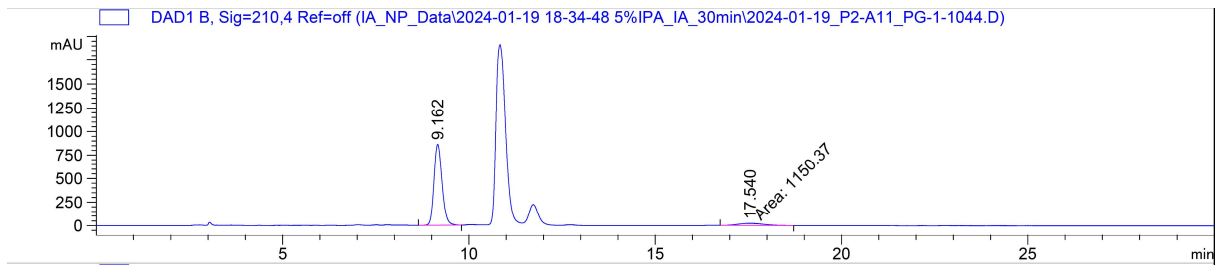


Signal 2: DAD1 B, Sig=210,4 Ref=off

| Peak # | RetTime [min] | Type | Width [min] | Area [mAU*s] | Height [mAU] | Area % |
|--------|---------------|------|-------------|--------------|--------------|---------|
| 1 | 9.734 | VV R | 0.2519 | 5403.88330 | 306.12808 | 53.0699 |
| 2 | 21.156 | BV R | 0.7940 | 4778.69287 | 70.52479 | 46.9301 |

Totals : 1.01826e4 376.65287

2,2,2-trichloroethyl (R)-(8-methoxy-1,2,3,4-tetrahydronaphthalen-2-yl)carbamate (4.49'):

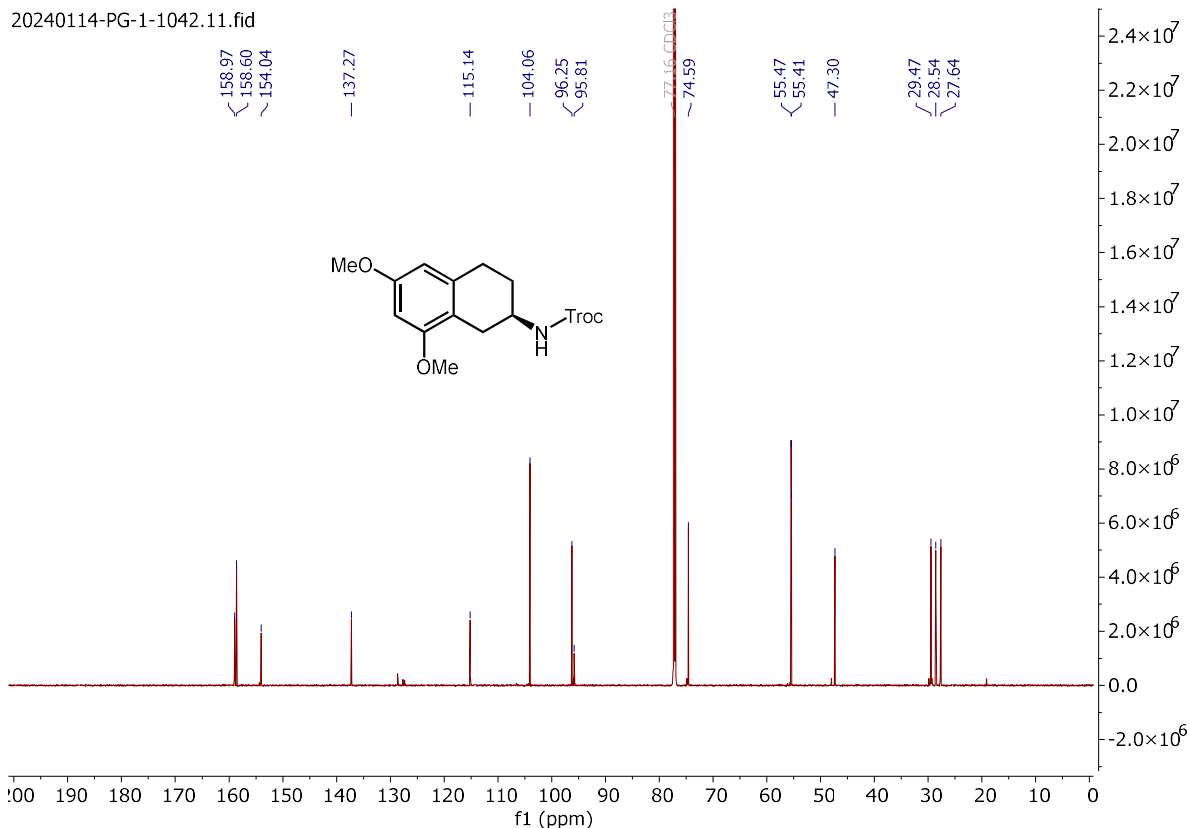
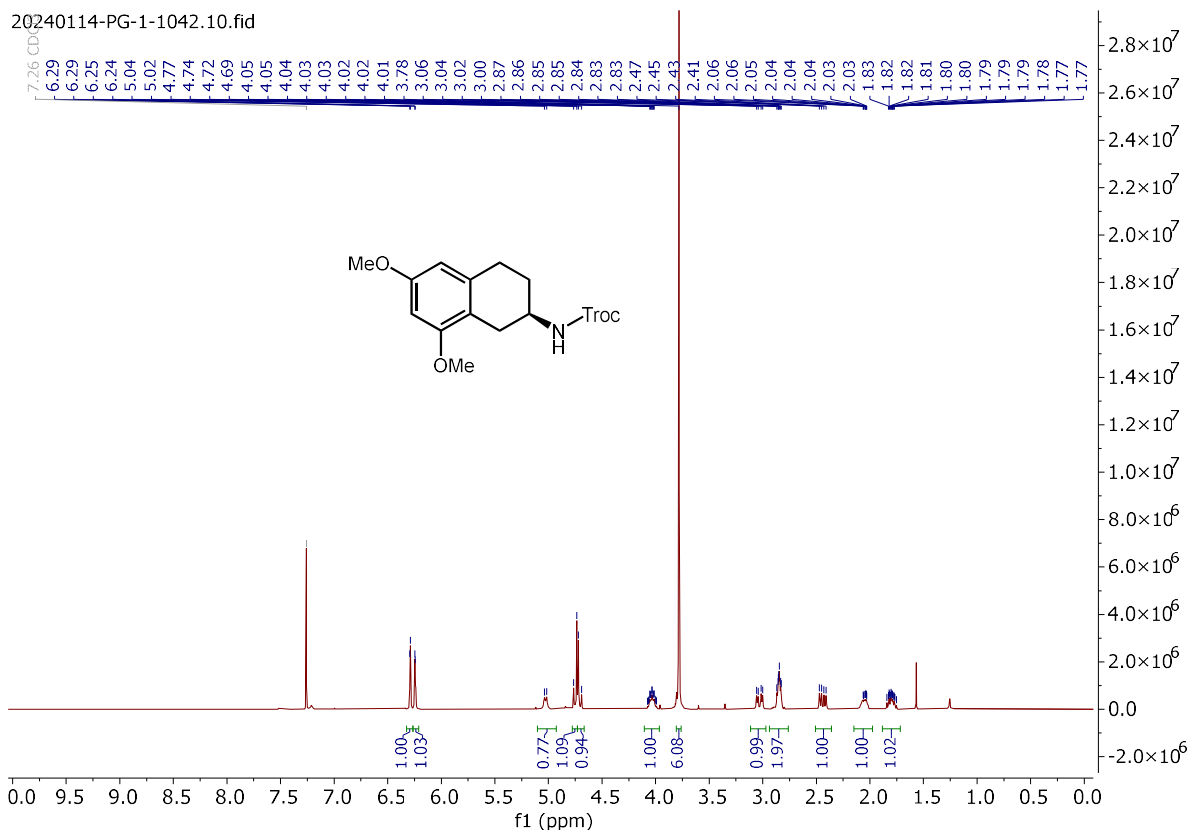


Signal 2: DAD1 B, Sig=210,4 Ref=off

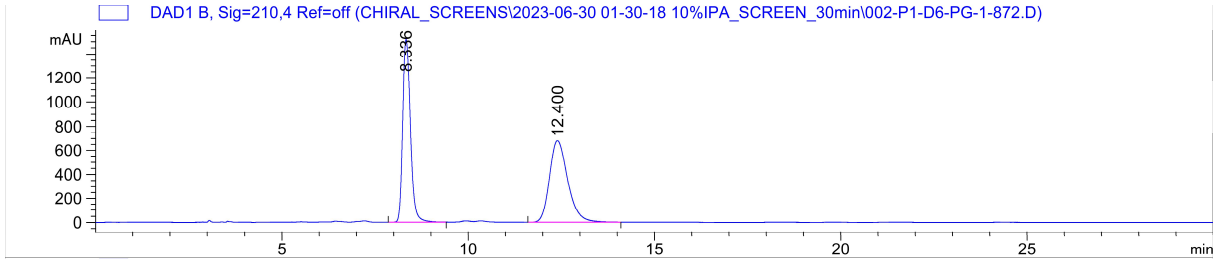
| Peak # | RetTime [min] | Type | Width [min] | Area [mAU*s] | Height [mAU] | Area % |
|--------|---------------|------|-------------|--------------|--------------|---------|
| 1 | 9.162 | BB | 0.2231 | 1.29499e4 | 863.01361 | 91.8415 |
| 2 | 17.540 | MM T | 0.8418 | 1150.37000 | 22.77640 | 8.1585 |

Totals : 1.41003e4 885.79001

2,2,2-trichloroethyl (R)-(6,8-dimethoxy-1,2,3,4-tetrahydronaphthalen-2-yl)carbamate (**4.53**):



2,2,2-trichloroethyl (6,8-dimethoxy-1,2,3,4-tetrahydronaphthalen-2-yl)carbamate (\pm -4.53):

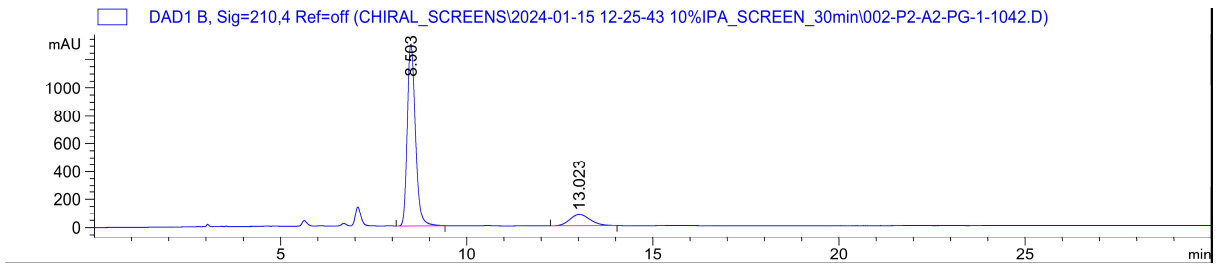


Signal 2: DAD1 B, Sig=210,4 Ref=off

| Peak # | RetTime [min] | Type | Width [min] | Area [mAU*s] | Height [mAU] | Area % |
|--------|---------------|------|-------------|--------------|--------------|---------|
| 1 | 8.336 | BB | 0.2056 | 2.18494e4 | 1516.03369 | 48.6000 |
| 2 | 12.400 | BB | 0.4063 | 2.31082e4 | 680.35248 | 51.4000 |

Totals : 4.49576e4 2196.38617

2,2,2-trichloroethyl (R)-(6,8-dimethoxy-1,2,3,4-tetrahydronaphthalen-2-yl)carbamate (4.53):

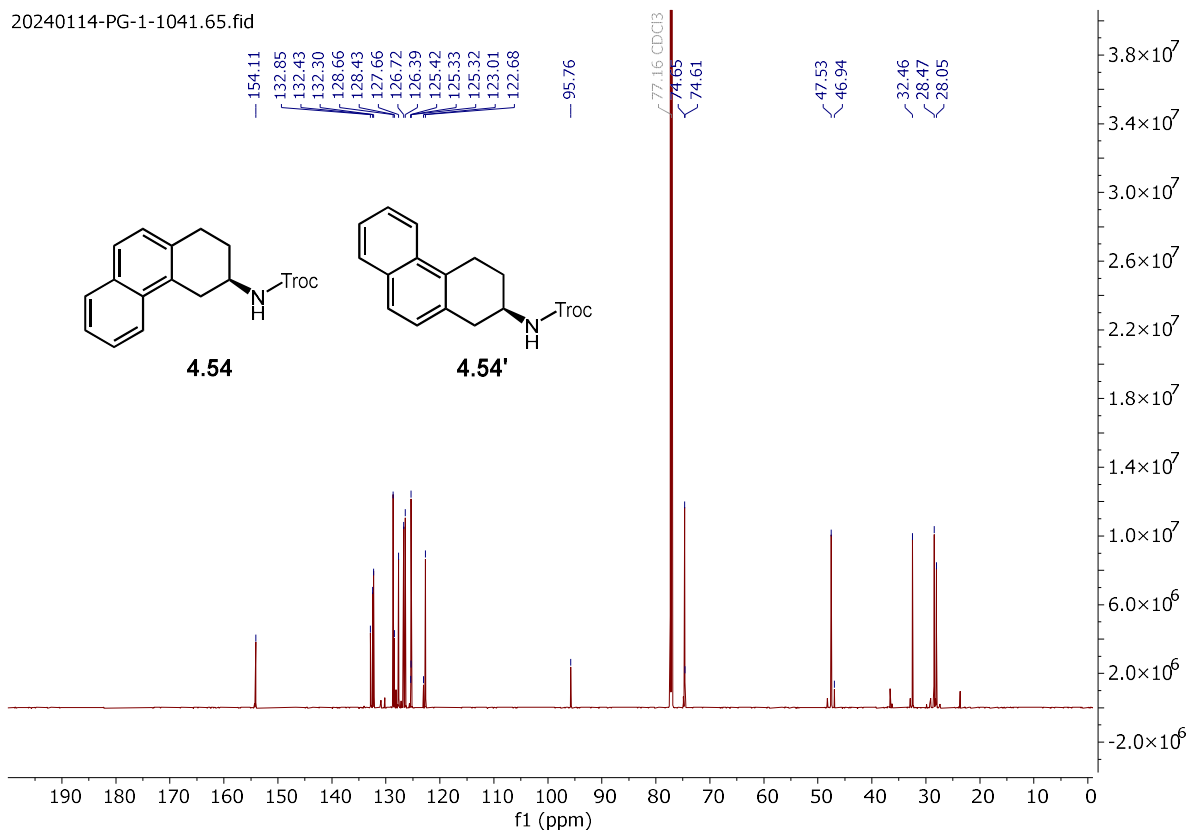
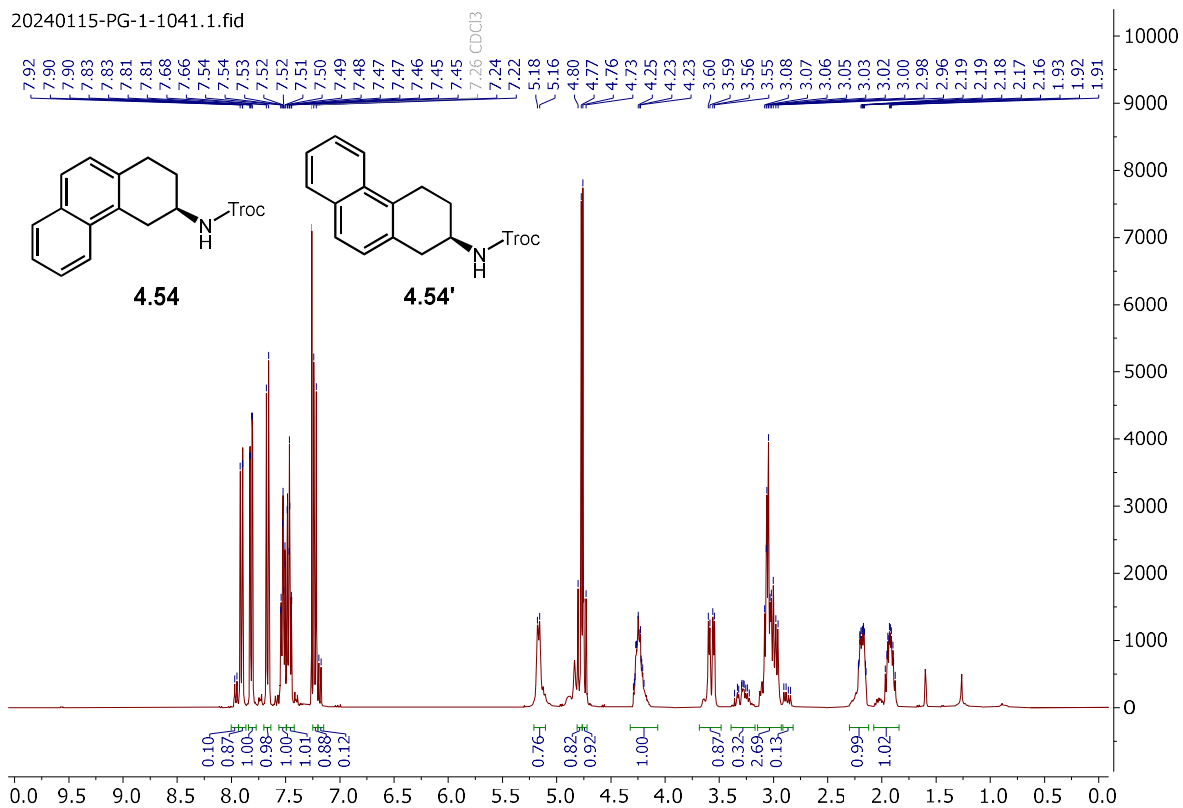


Signal 2: DAD1 B, Sig=210,4 Ref=off

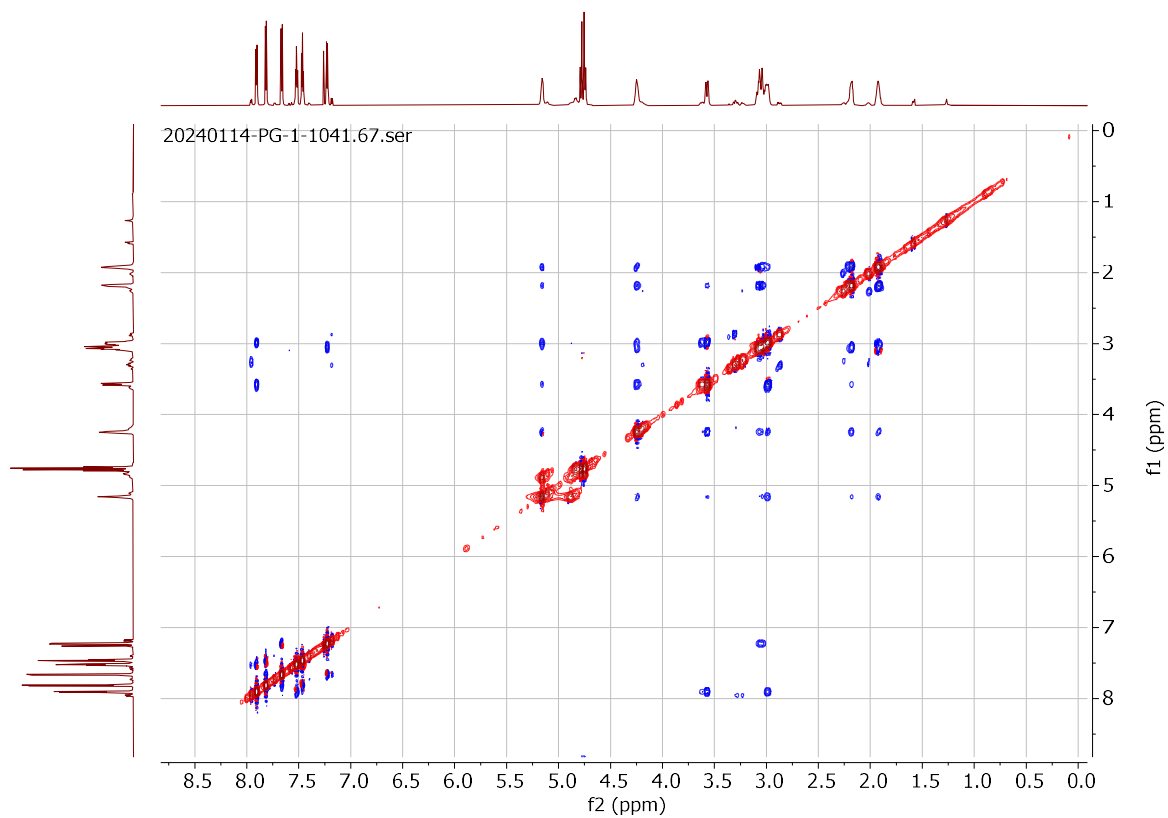
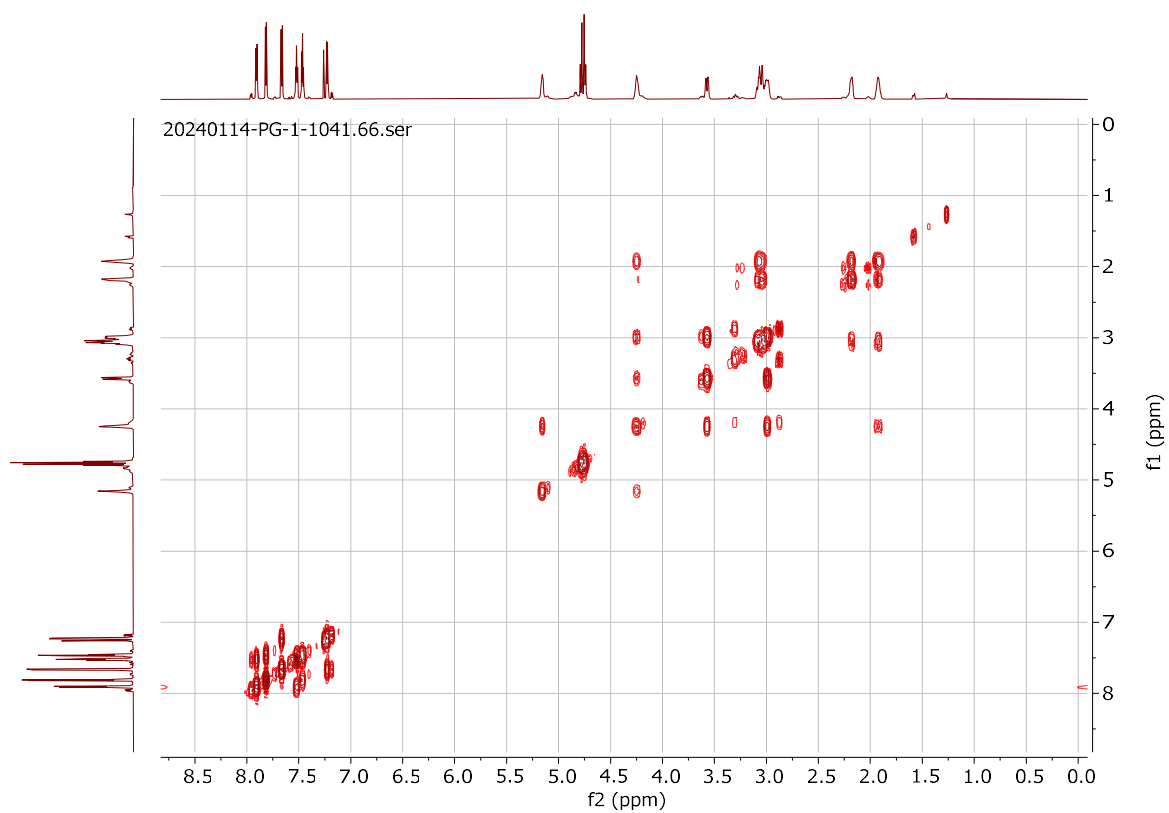
| Peak # | RetTime [min] | Type | Width [min] | Area [mAU*s] | Height [mAU] | Area % |
|--------|---------------|------|-------------|--------------|--------------|---------|
| 1 | 8.503 | BV R | 0.1974 | 1.97550e4 | 1302.82568 | 87.0335 |
| 2 | 13.023 | VV R | 0.4447 | 2943.16187 | 77.56516 | 12.9665 |

Totals : 2.26982e4 1380.39084

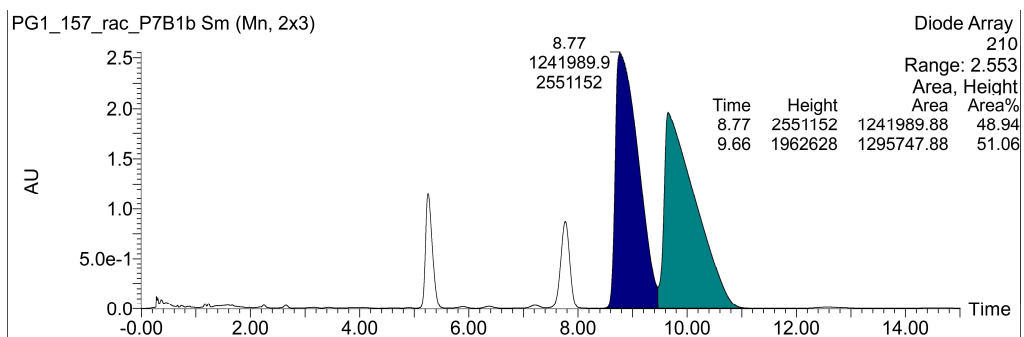
2,2,2-trichloroethyl (*R*)-(1,2,3,4-tetrahydrophenanthren-3-yl)carbamate (**4.54**) and 2,2,2-trichloroethyl (*R*)-(1,2,3,4-tetrahydrophenanthren-2-yl)carbamate (**4.54'**):



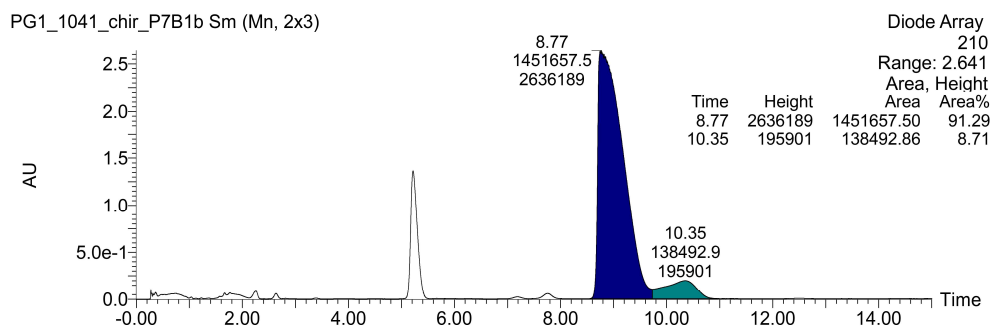
(4.54) and (4.54'):



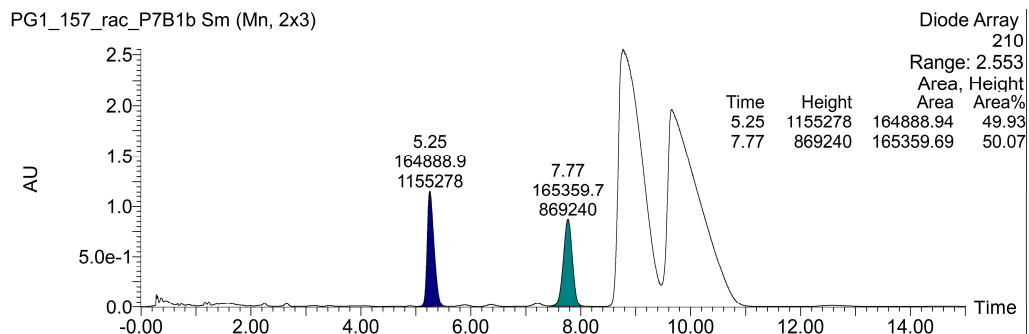
2,2,2-trichloroethyl (1,2,3,4-tetrahydrophenanthren-3-yl)carbamate (\pm -4.54):



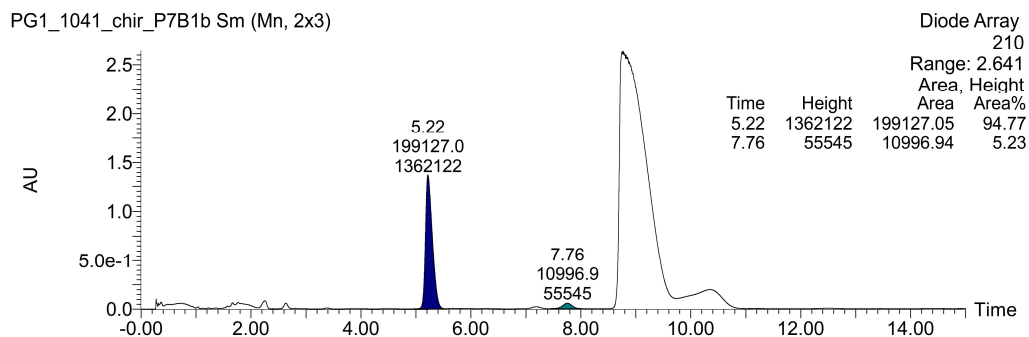
2,2,2-trichloroethyl (R)-(1,2,3,4-tetrahydrophenanthren-3-yl)carbamate (4.54):



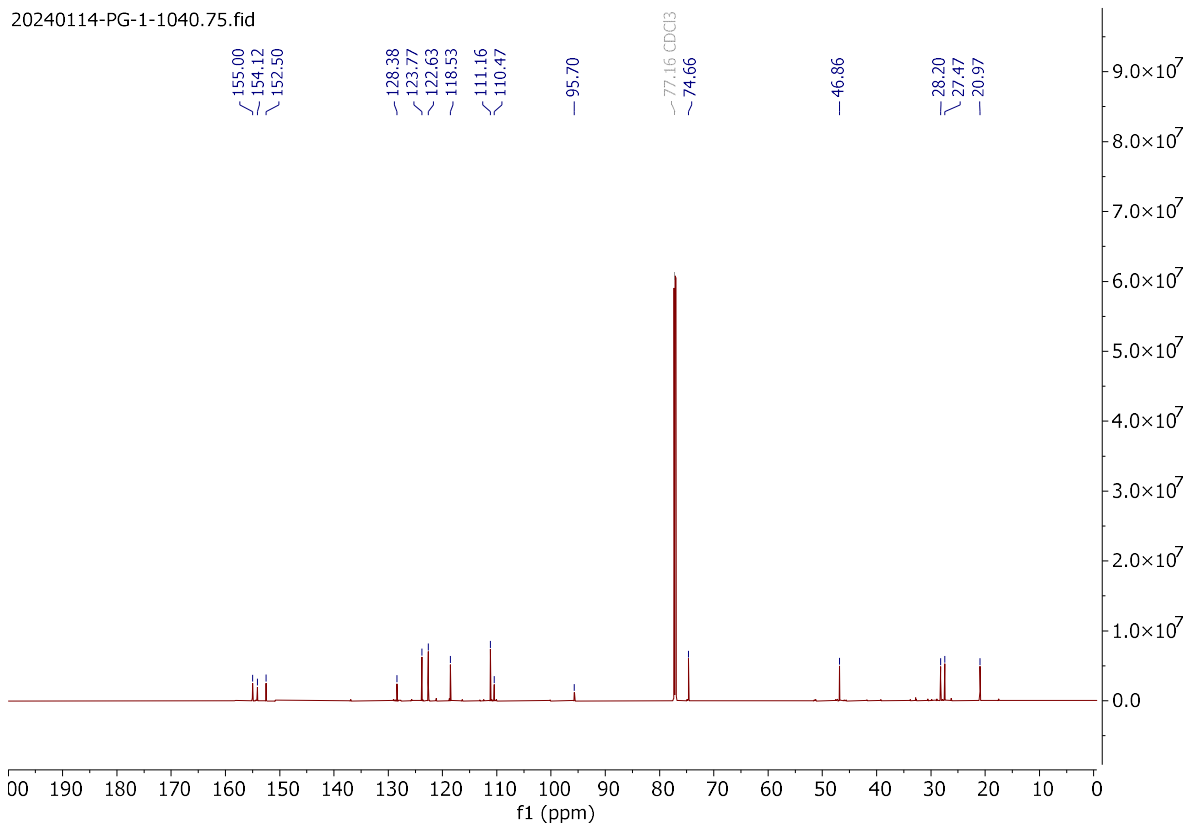
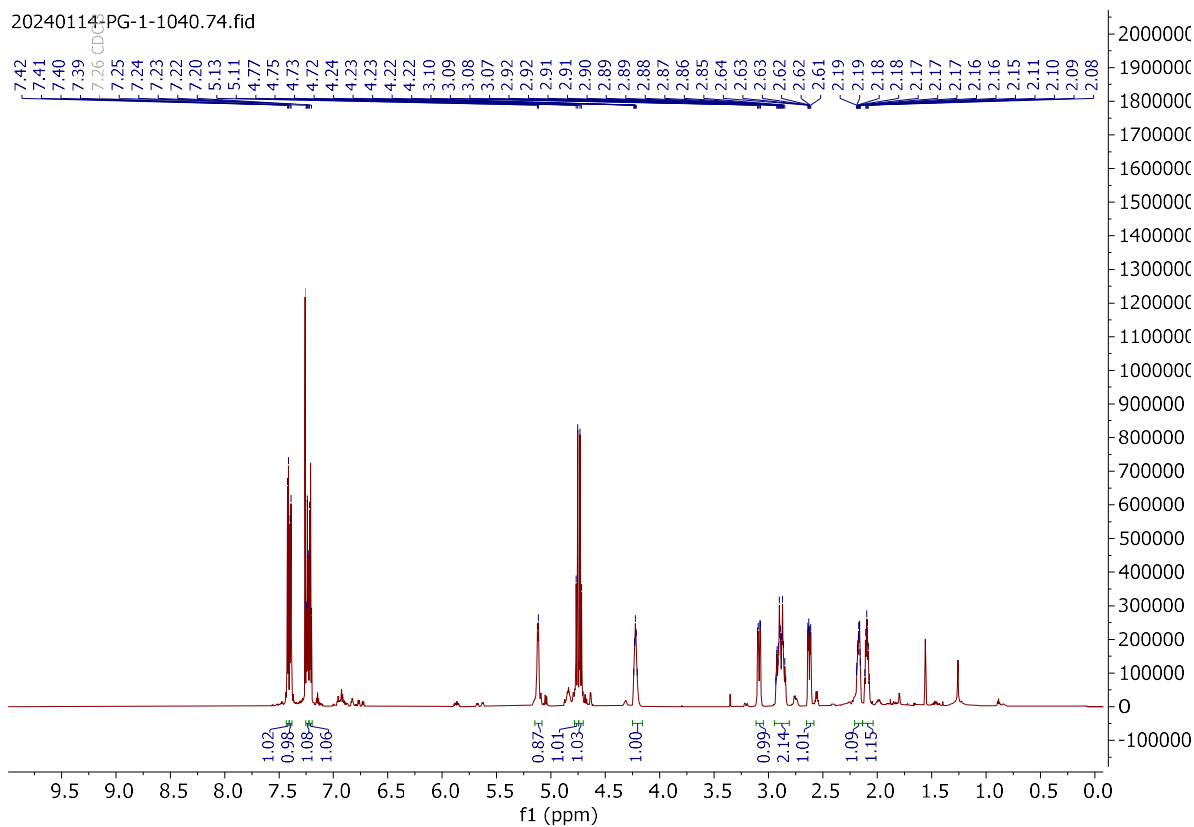
2,2,2-trichloroethyl (R)-(1,2,3,4-tetrahydrophenanthren-2-yl)carbamate (\pm -4.54[']):



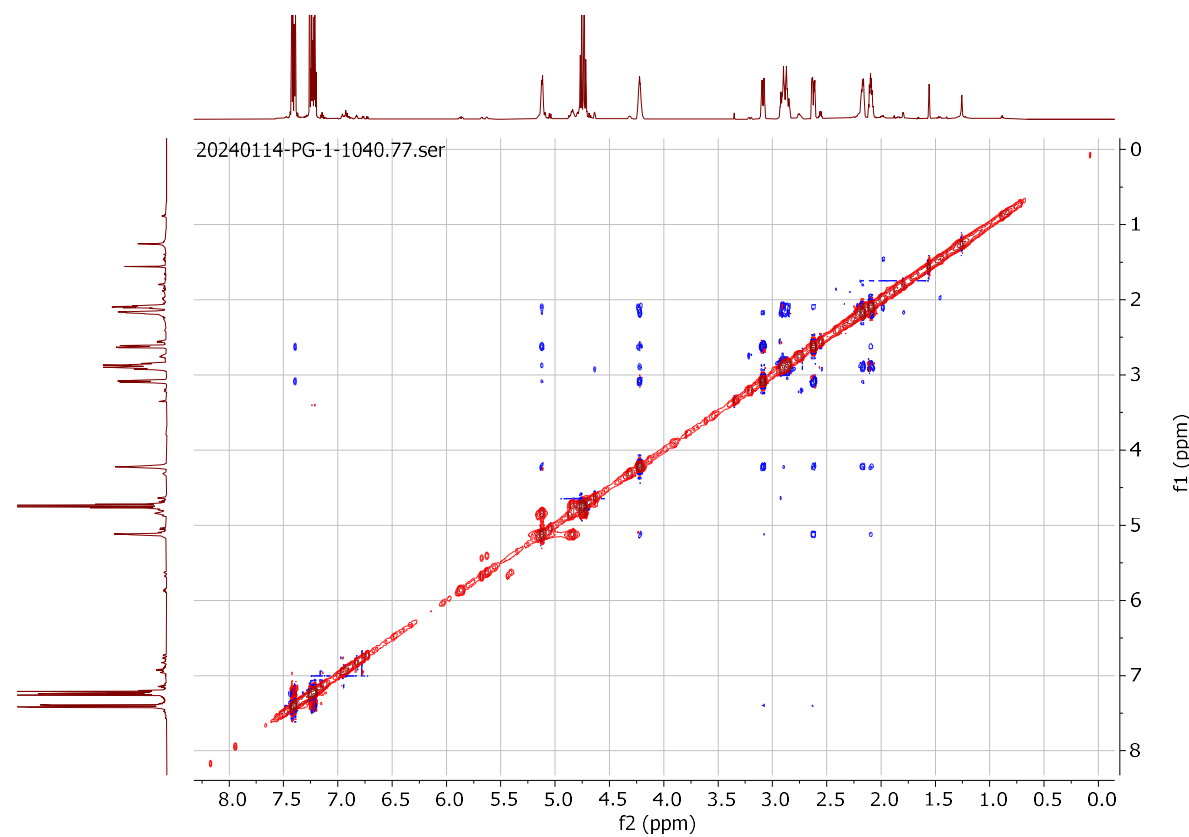
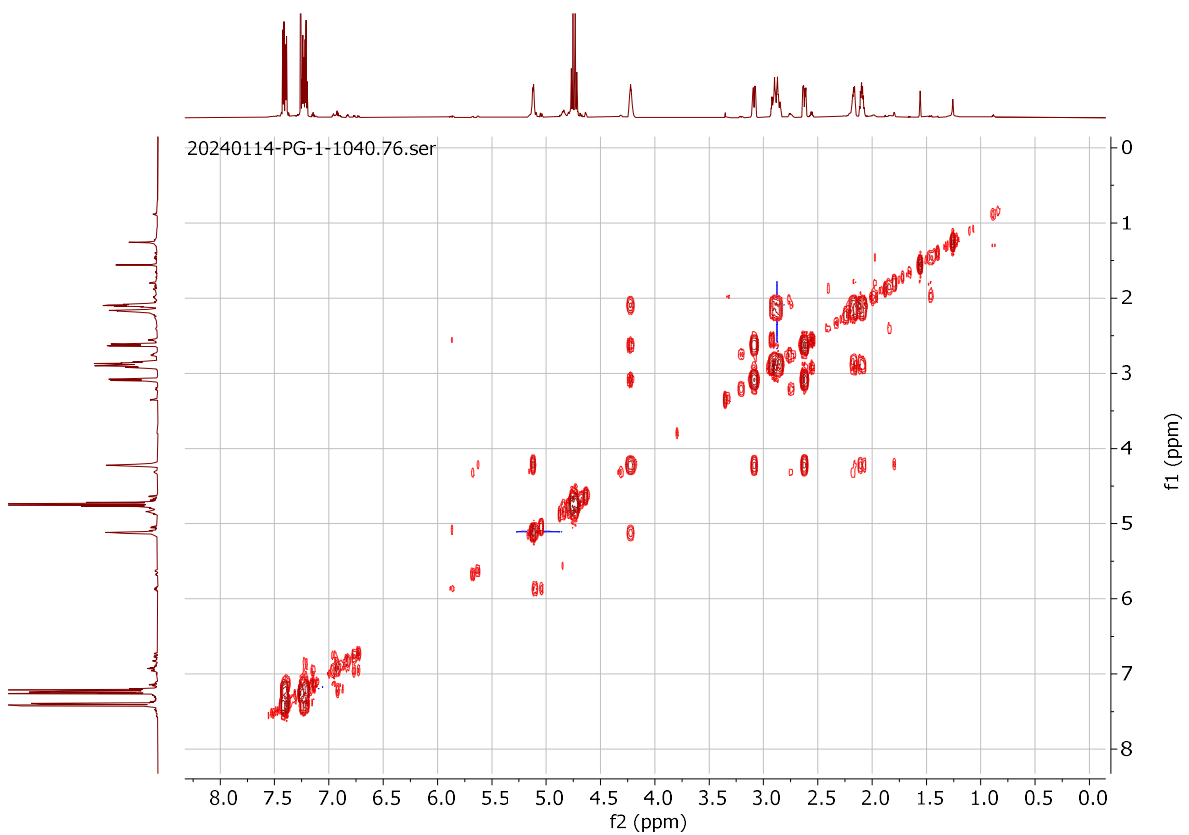
2,2,2-trichloroethyl (R)-(1,2,3,4-tetrahydrophenanthren-2-yl)carbamate (4.54[']):



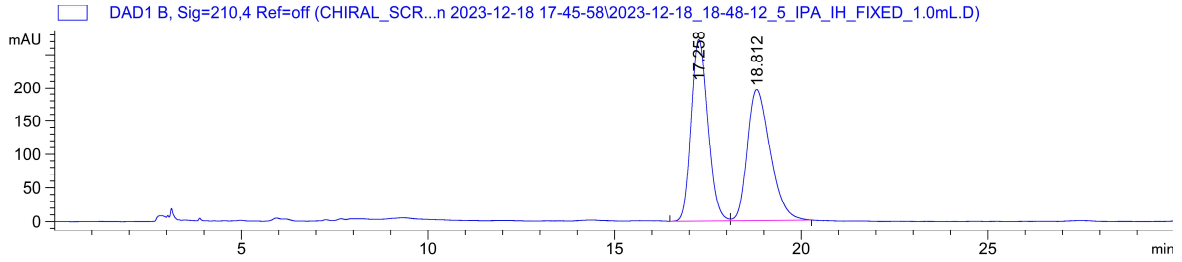
2,2,2-trichloroethyl (R)-(1,2,3,4-tetrahydrodibenzo[b,d]furan-2-yl)carbamate (4.55):



(4.55):



2,2,2-trichloroethyl (1,2,3,4-tetrahydrodibenzo[b,d]furan-2-yl)carbamate (\pm -4.55):

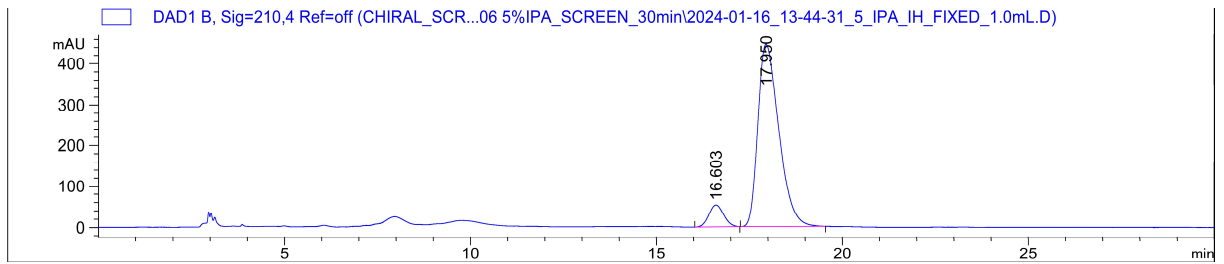


Signal 2: DAD1 B, Sig=210,4 Ref=off

| Peak # | RetTime [min] | Type | Width [min] | Area [mAU*s] | Height [mAU] | Area % |
|--------|---------------|------|-------------|--------------|--------------|---------|
| 1 | 17.258 | VV R | 0.3623 | 8411.32813 | 271.97485 | 50.2865 |
| 2 | 18.812 | VV R | 0.4986 | 8315.49414 | 195.37236 | 49.7135 |

Totals : 1.67268e4 467.34721

2,2,2-trichloroethyl (R)-(1,2,3,4-tetrahydrodibenzo[b,d]furan-2-yl)carbamate (4.55):

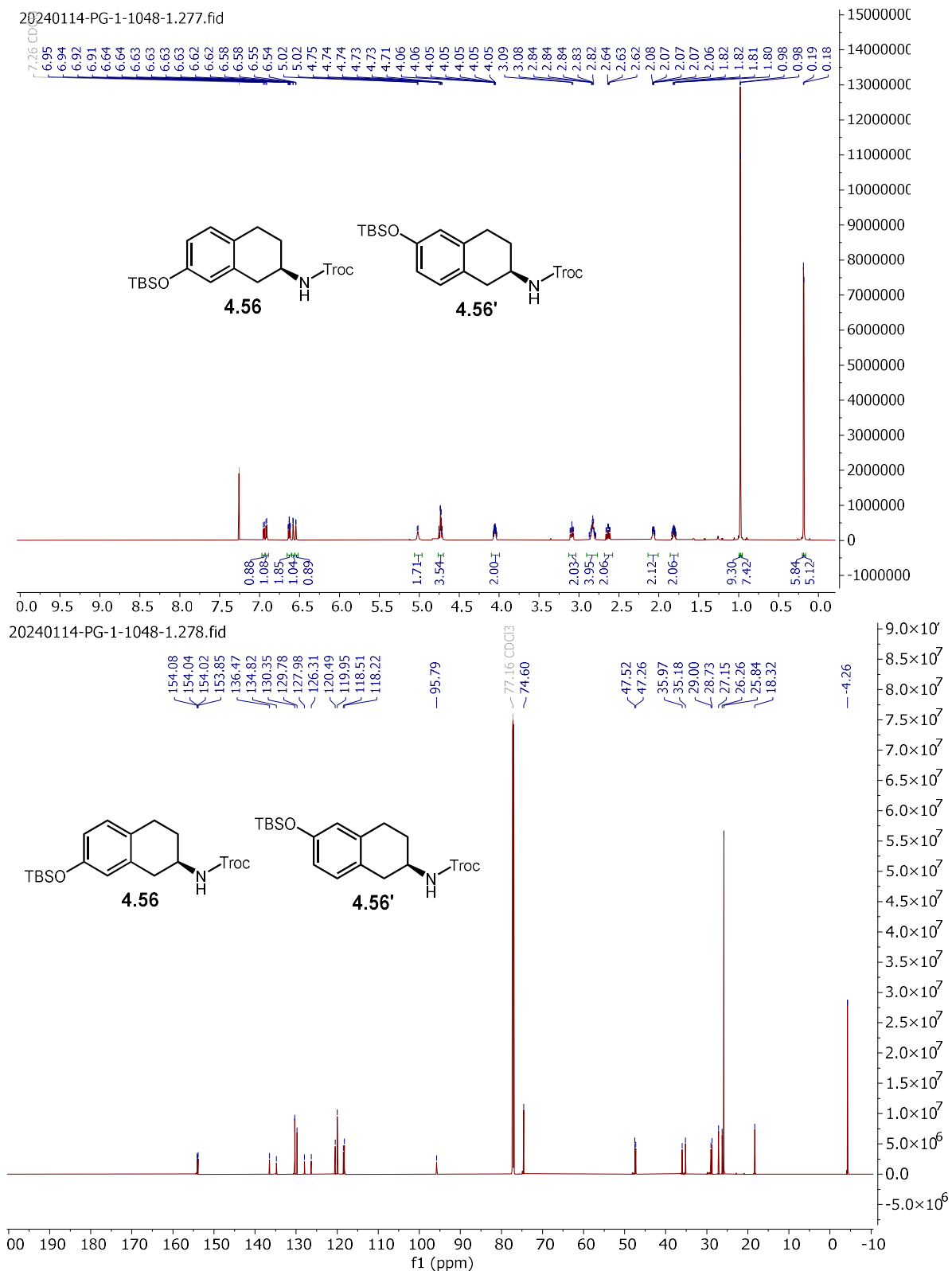


Signal 2: DAD1 B, Sig=210,4 Ref=off

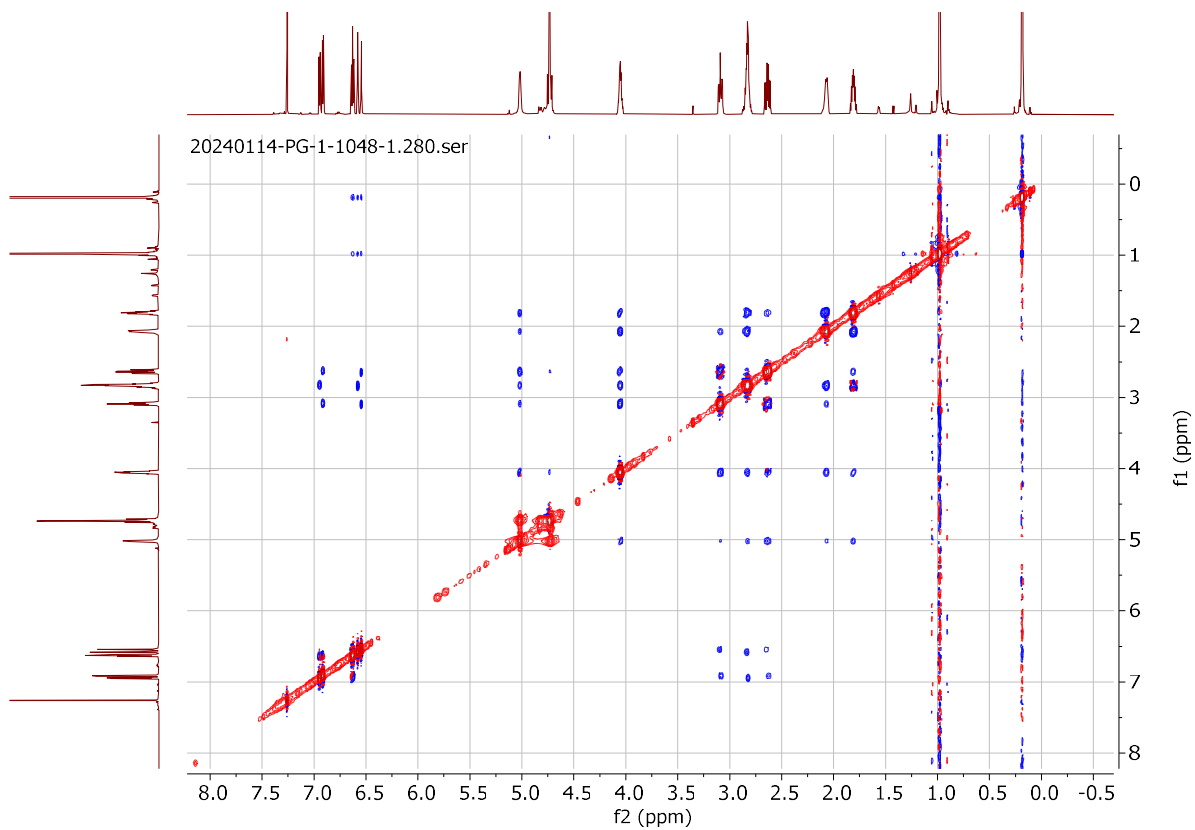
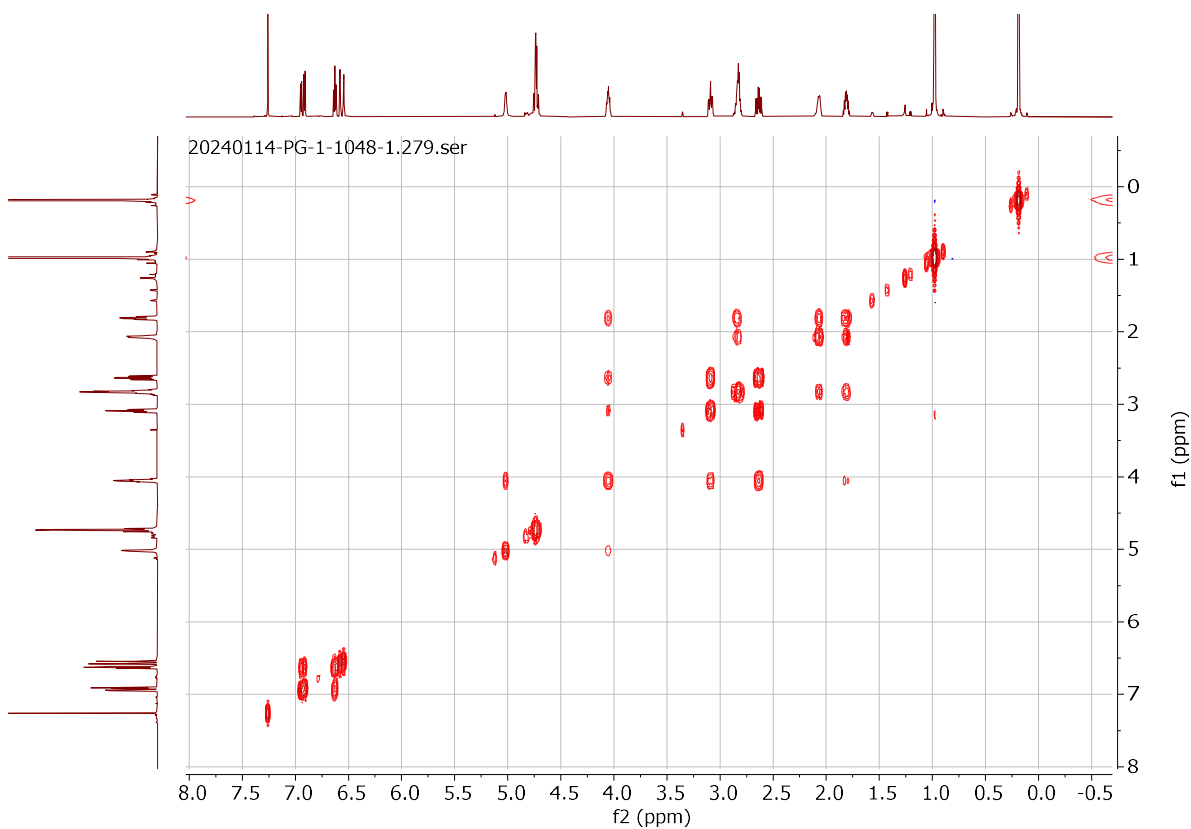
| Peak # | RetTime [min] | Type | Width [min] | Area [mAU*s] | Height [mAU] | Area % |
|--------|---------------|------|-------------|--------------|--------------|---------|
| 1 | 16.603 | BB | 0.3248 | 1463.62378 | 52.97777 | 7.7664 |
| 2 | 17.950 | BV R | 0.4572 | 1.73819e4 | 445.93954 | 92.2336 |

Totals : 1.88455e4 498.91731

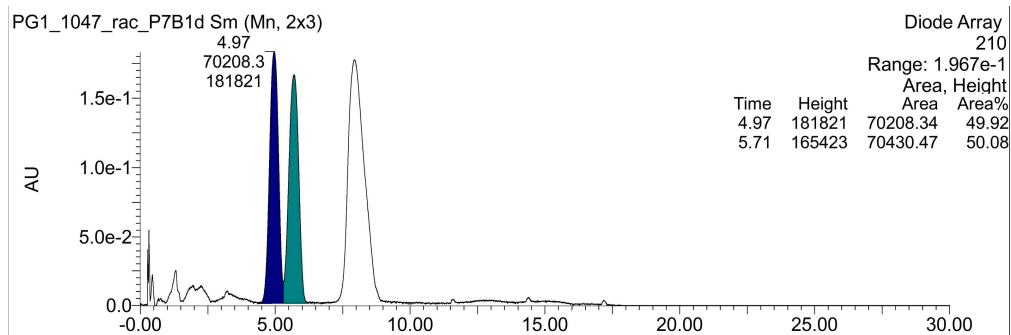
2,2,2-trichloroethyl (*R*)-(7-((*tert*-butyldimethylsilyl)oxy)-1,2,3,4-tetrahydronaphthalen-2-yl)carbamate (**4.56**) and 2,2,2-trichloroethyl (*R*)-(6-((*tert*-butyldimethylsilyl)oxy)-1,2,3,4-tetrahydronaphthalen-2-yl)carbamate (**4.56'**):



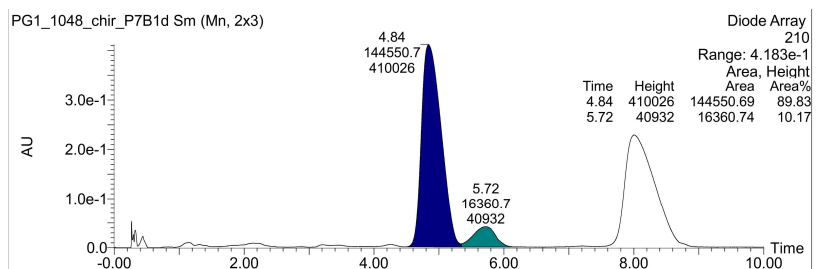
(4.56) and (4.56'):



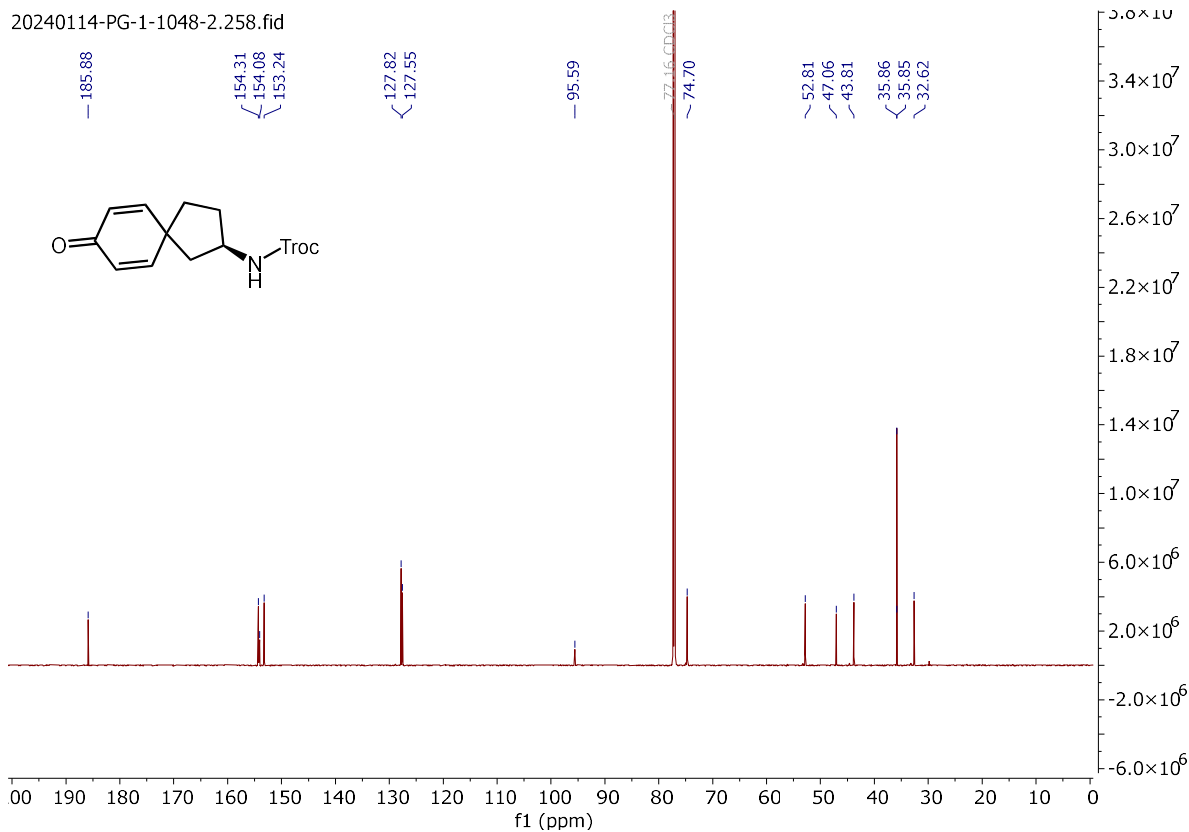
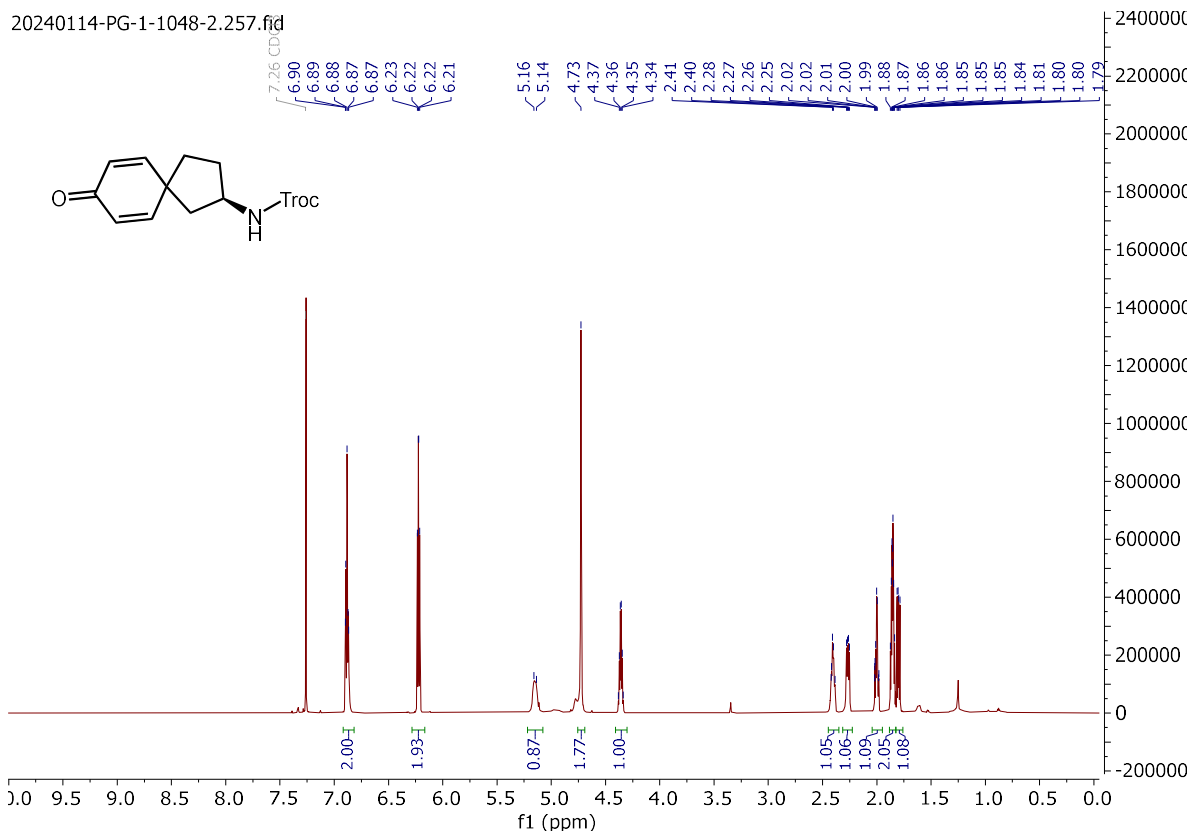
2,2,2-trichloroethyl (7-((tert-butyldimethylsilyl)oxy)-1,2,3,4-tetrahydronaphthalen-2-yl)carbamate
 (±-4.56):



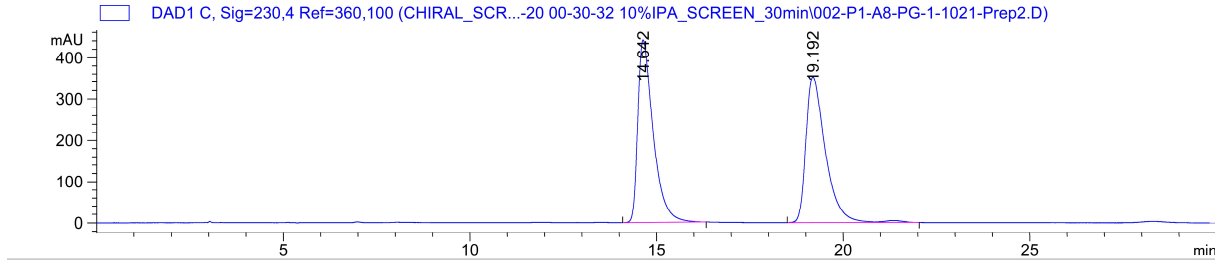
2,2,2-trichloroethyl (R)-(7-((tert-butyldimethylsilyl)oxy)-1,2,3,4-tetrahydronaphthalen-2-yl)carbamate
 (4.56):



2,2,2-trichloroethyl (R)-(8-oxospiro[4.5]deca-6,9-dien-2-yl)carbamate (4.57):



2,2,2-trichloroethyl (8-oxospiro[4.5]deca-6,9-dien-2-yl)carbamate (\pm -4.57):

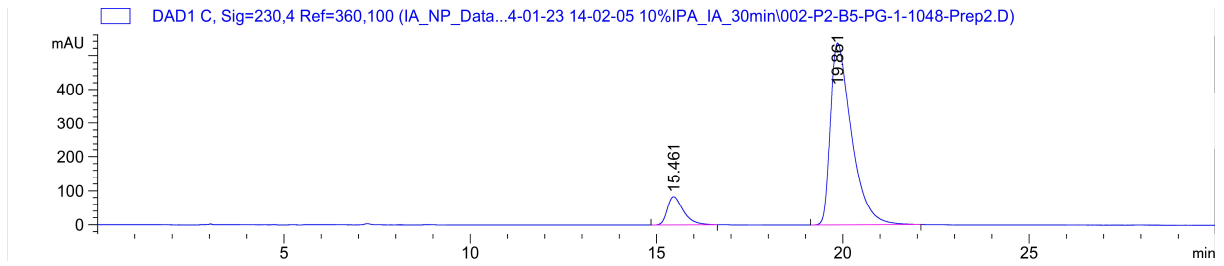


Signal 3: DAD1 C, Sig=230,4 Ref=360,100

| Peak # | RetTime [min] | Type | Width [min] | Area [mAU*s] | Height [mAU] | Area % |
|--------|---------------|------|-------------|--------------|--------------|---------|
| 1 | 14.642 | BV R | 0.3926 | 1.26219e4 | 441.36261 | 49.5520 |
| 2 | 19.192 | VV R | 0.4398 | 1.28501e4 | 352.37262 | 50.4480 |

Totals : 2.54720e4 793.73523

2,2,2-trichloroethyl (R)-(8-oxospiro[4.5]deca-6,9-dien-2-yl)carbamate (4.57):

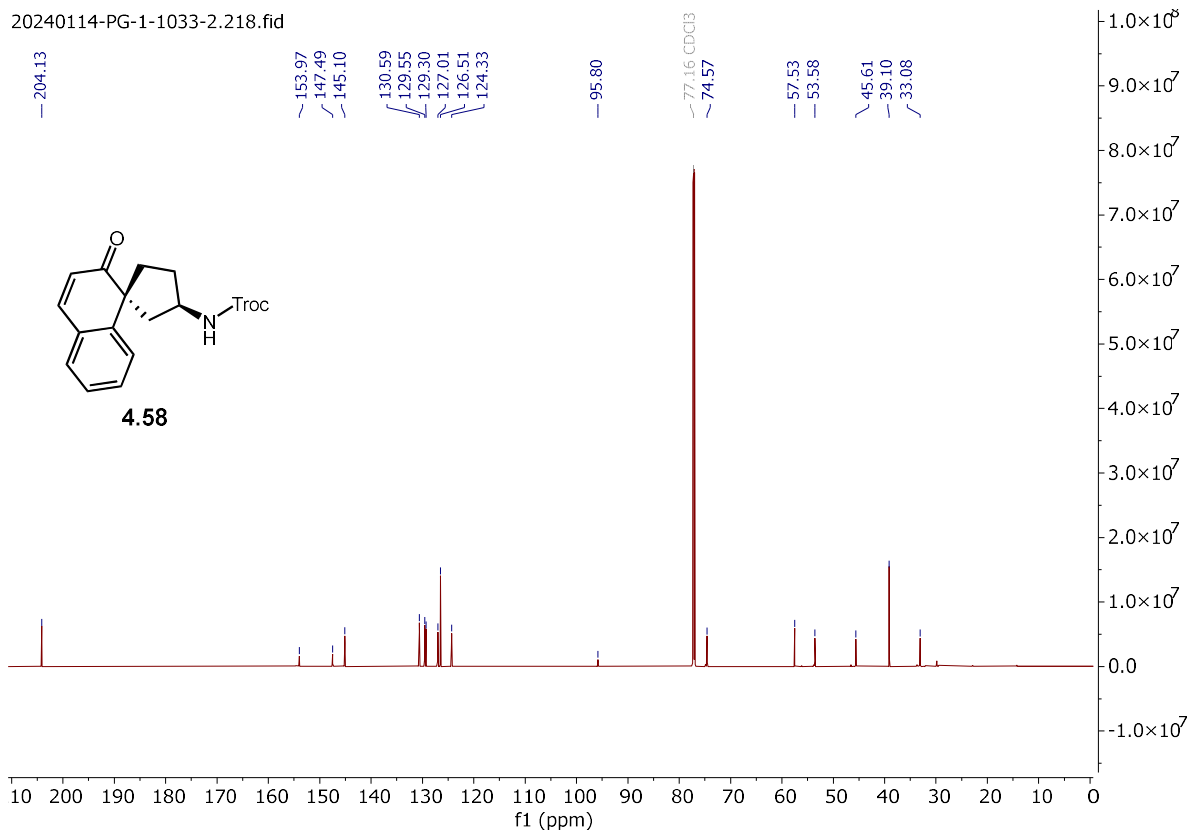
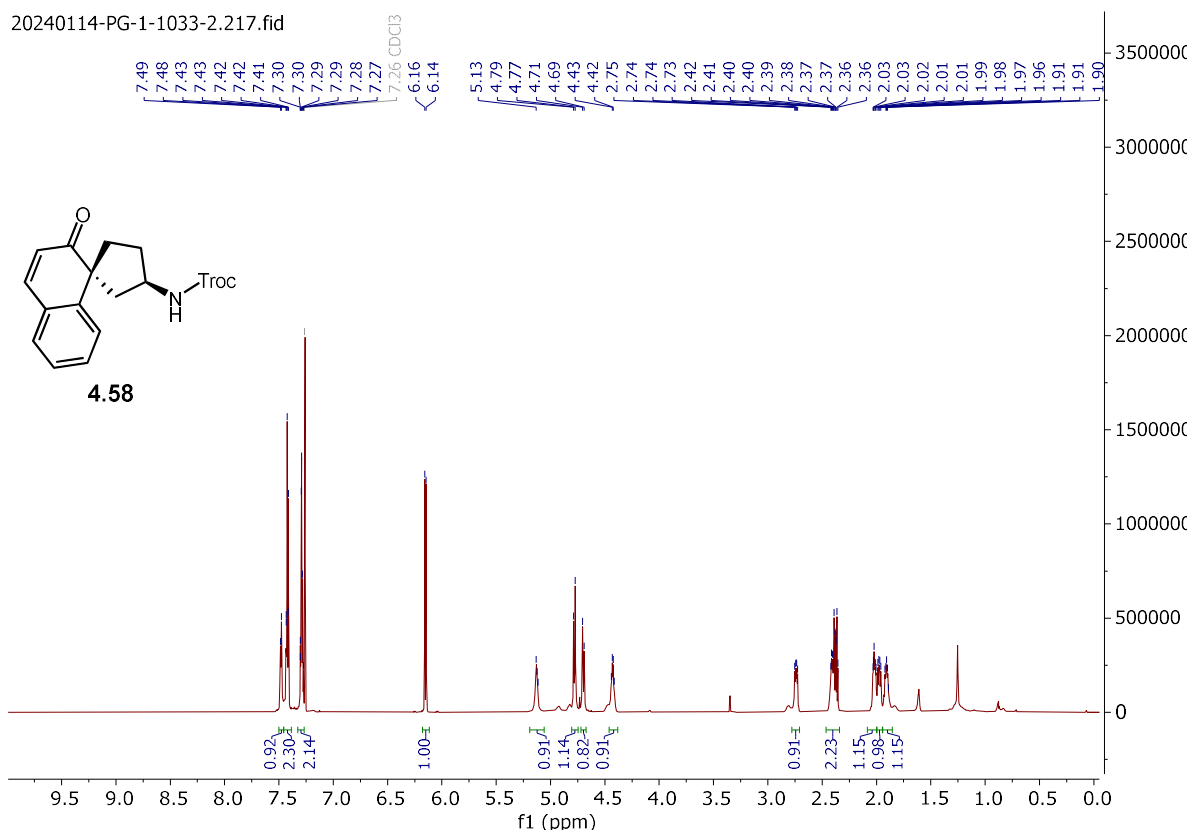


Signal 3: DAD1 C, Sig=230,4 Ref=360,100

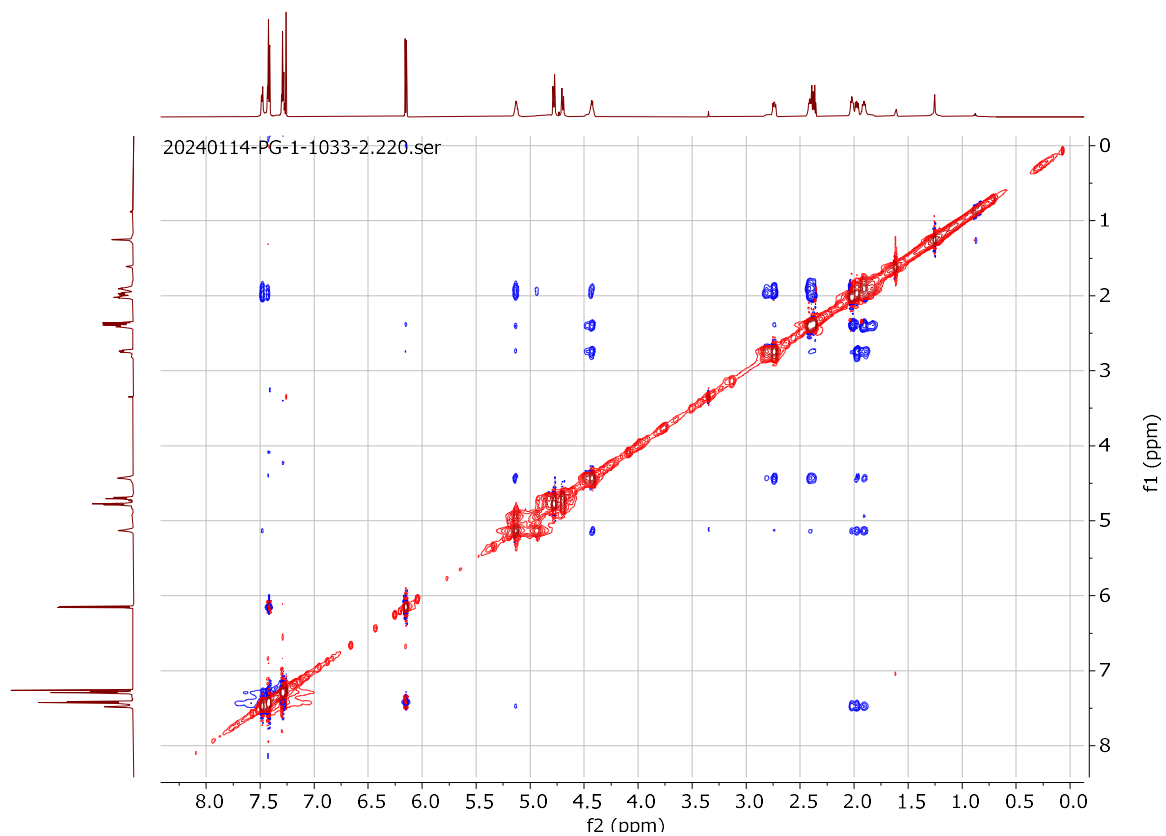
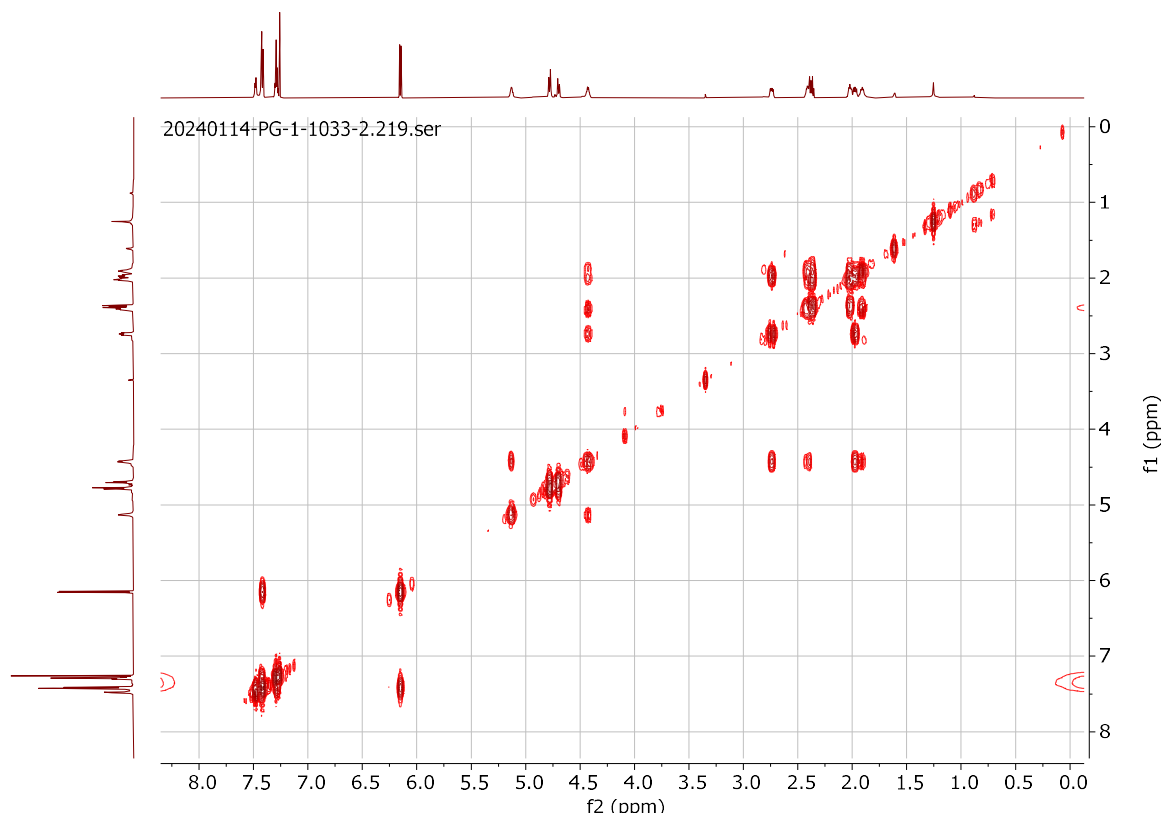
| Peak # | RetTime [min] | Type | Width [min] | Area [mAU*s] | Height [mAU] | Area % |
|--------|---------------|------|-------------|--------------|--------------|---------|
| 1 | 15.461 | BB | 0.3499 | 2481.91553 | 83.11046 | 10.5321 |
| 2 | 19.861 | BB | 0.4951 | 2.10833e4 | 535.13440 | 89.4679 |

Totals : 2.35652e4 618.24486

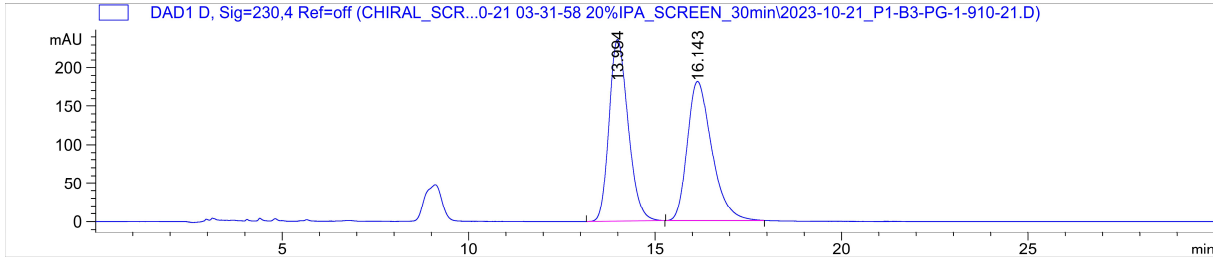
2,2,2-trichloroethyl ((1R,3R)-2'-oxo-2'H-spiro[cyclopentane-1,1'-naphthalen]-3-yl)carbamate (**4.58**):



(4.58):



2,2,2-trichloroethyl ((1R,3R)-2'-oxo-2'H-spiro[cyclopentane-1,1'-naphthalen]-3-yl)carbamate (\pm -4.58):

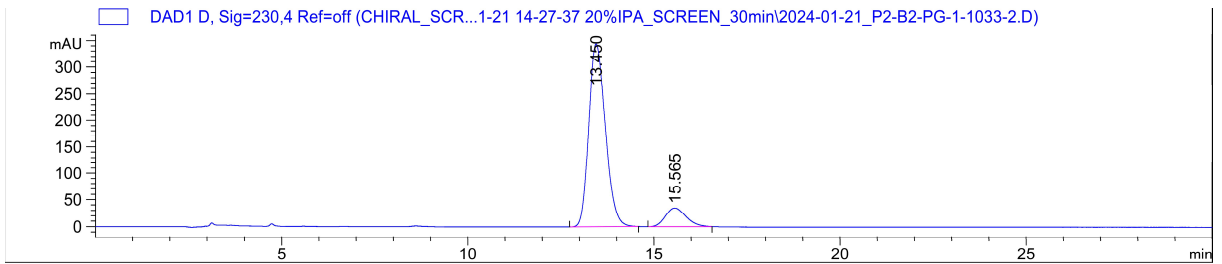


Signal 4: DAD1 D, Sig=230,4 Ref=off

| Peak # | RetTime [min] | Type | Width [min] | Area [mAU*s] | Height [mAU] | Area % |
|--------|---------------|------|-------------|--------------|--------------|---------|
| 1 | 13.994 | BB | 0.4373 | 8360.22461 | 236.01596 | 50.3765 |
| 2 | 16.143 | BB | 0.5380 | 8235.26074 | 179.92947 | 49.6235 |

Totals : 1.65955e4 415.94543

2,2,2-trichloroethyl ((1R,3R)-2'-oxo-2'H-spiro[cyclopentane-1,1'-naphthalen]-3-yl)carbamate (4.58):

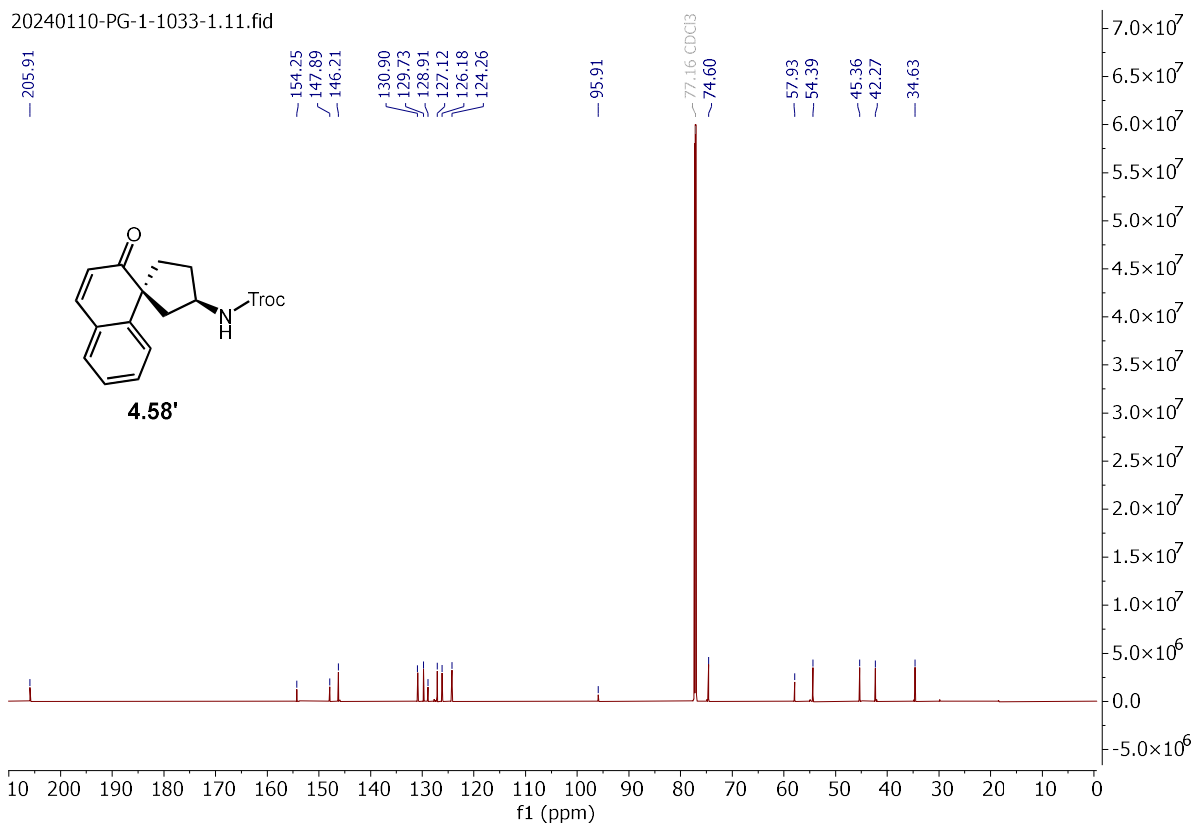
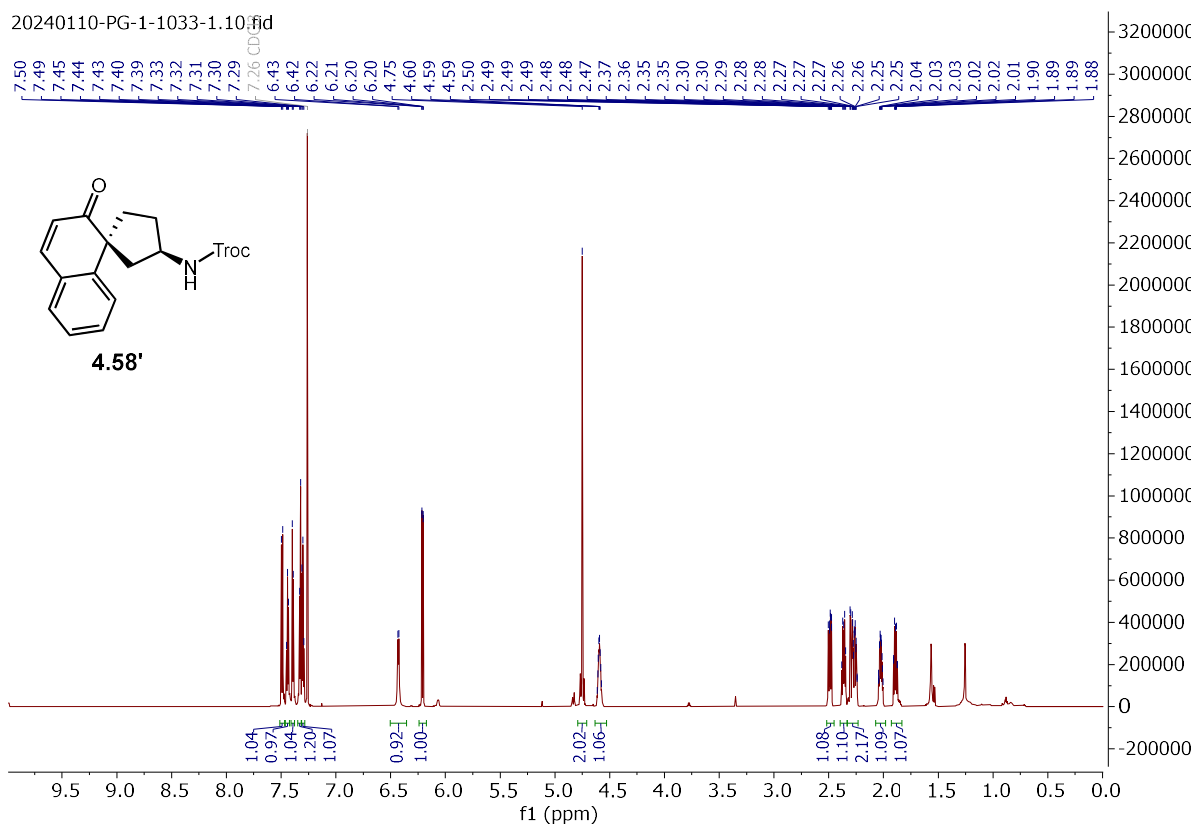


Signal 4: DAD1 D, Sig=230,4 Ref=off

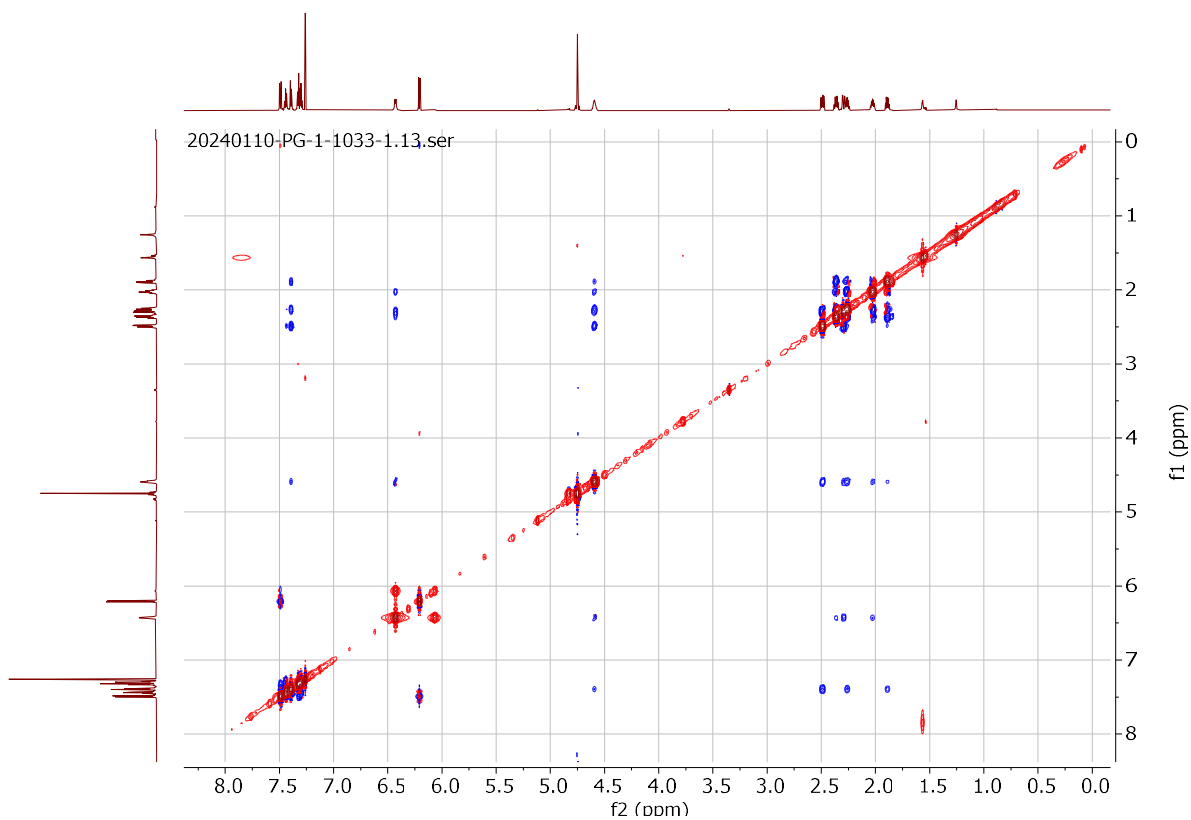
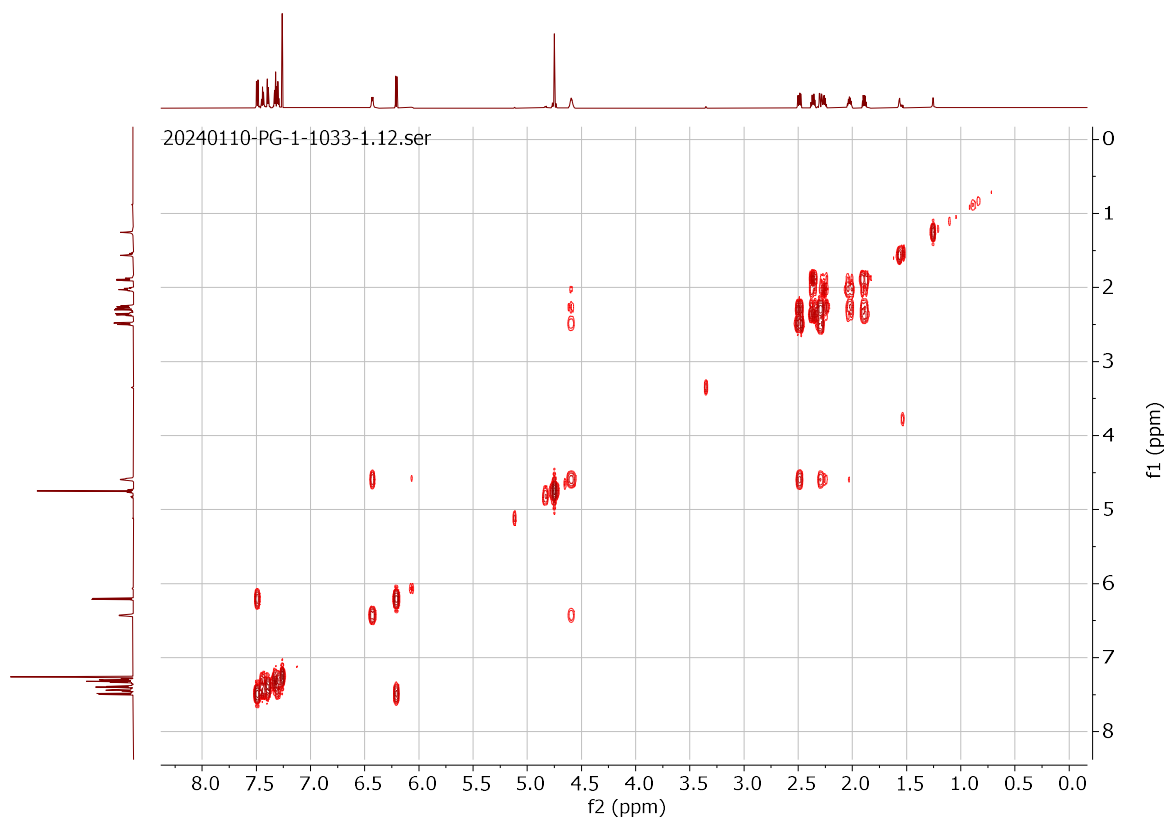
| Peak # | RetTime [min] | Type | Width [min] | Area [mAU*s] | Height [mAU] | Area % |
|--------|---------------|------|-------------|--------------|--------------|---------|
| 1 | 13.450 | BB | 0.4065 | 1.06456e4 | 344.05215 | 88.8895 |
| 2 | 15.565 | VV R | 0.4525 | 1330.62378 | 34.45852 | 11.1105 |

Totals : 1.19762e4 378.51067

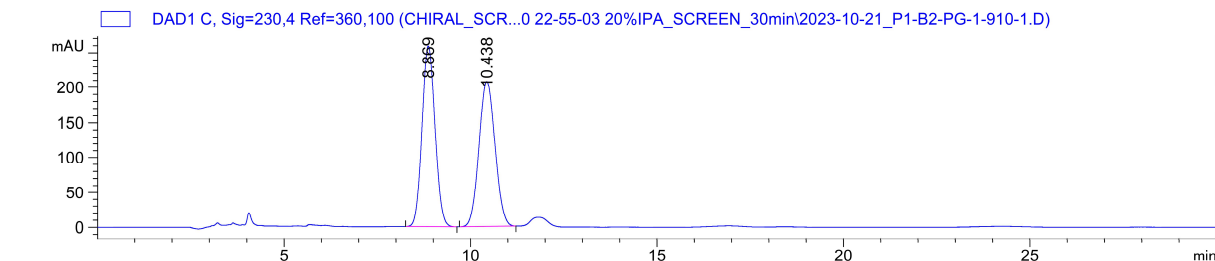
2,2,2-trichloroethyl ((1S,3R)-2'-oxo-2'H-spiro[cyclopentane-1,1'-naphthalen]-3-yl)carbamate (**4.58'**):



(4.58')



2,2,2-trichloroethyl ((1S,3R)-2'-oxo-2'H-spiro[cyclopentane-1,1'-naphthalen]-3-yl)carbamate (\pm -4.58')

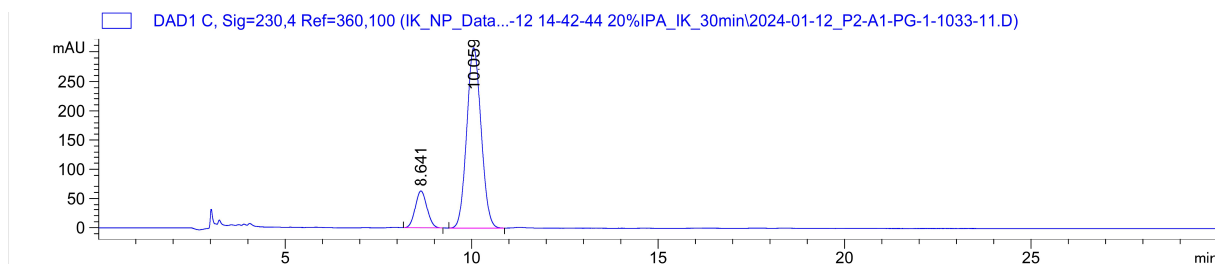


Signal 3: DAD1 C, Sig=230,4 Ref=360,100

| Peak # | RetTime [min] | Type | Width [min] | Area [mAU*s] | Height [mAU] | Area % |
|--------|---------------|------|-------------|--------------|--------------|---------|
| 1 | 8.869 | BB | 0.3284 | 6275.72217 | 258.78503 | 50.1898 |
| 2 | 10.438 | BB | 0.3588 | 6228.25781 | 207.75491 | 49.8102 |

Totals : 1.25040e4 466.53995

2,2,2-trichloroethyl ((1S,3R)-2'-oxo-2'H-spiro[cyclopentane-1,1'-naphthalen]-3-yl)carbamate (4.58')

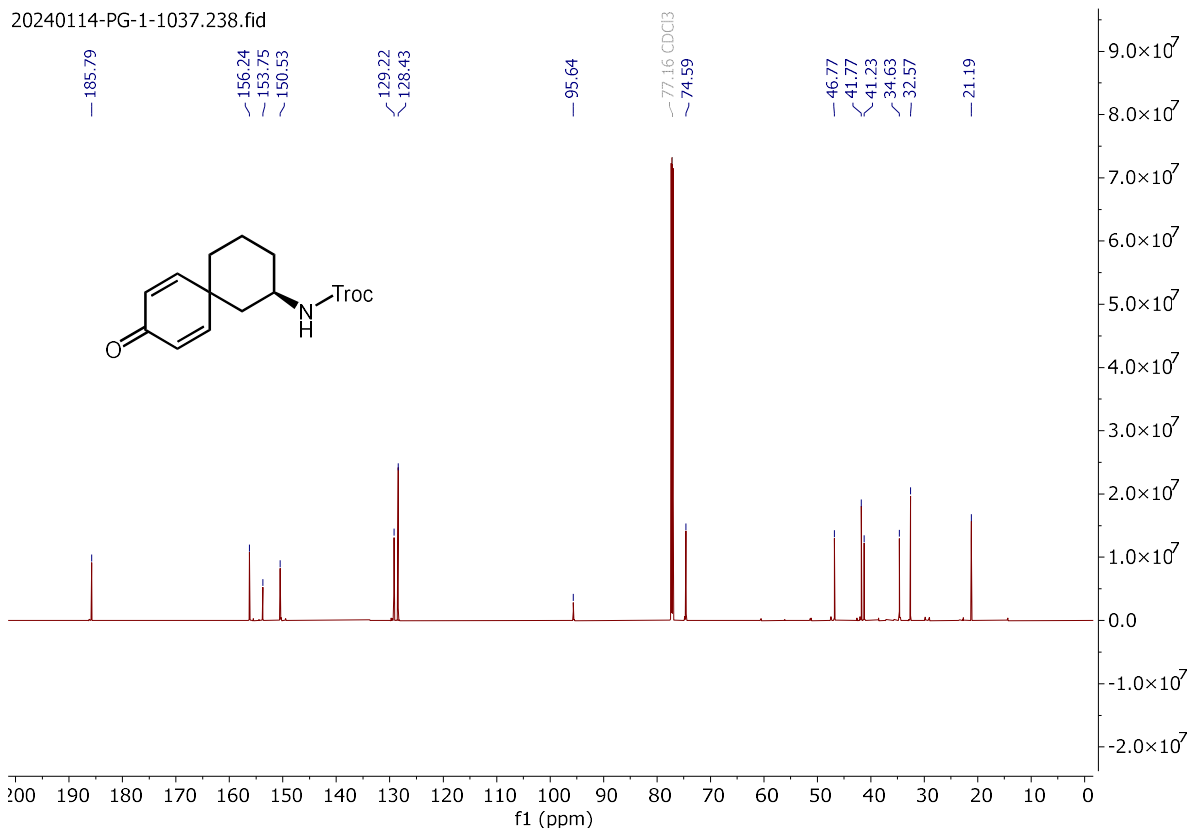
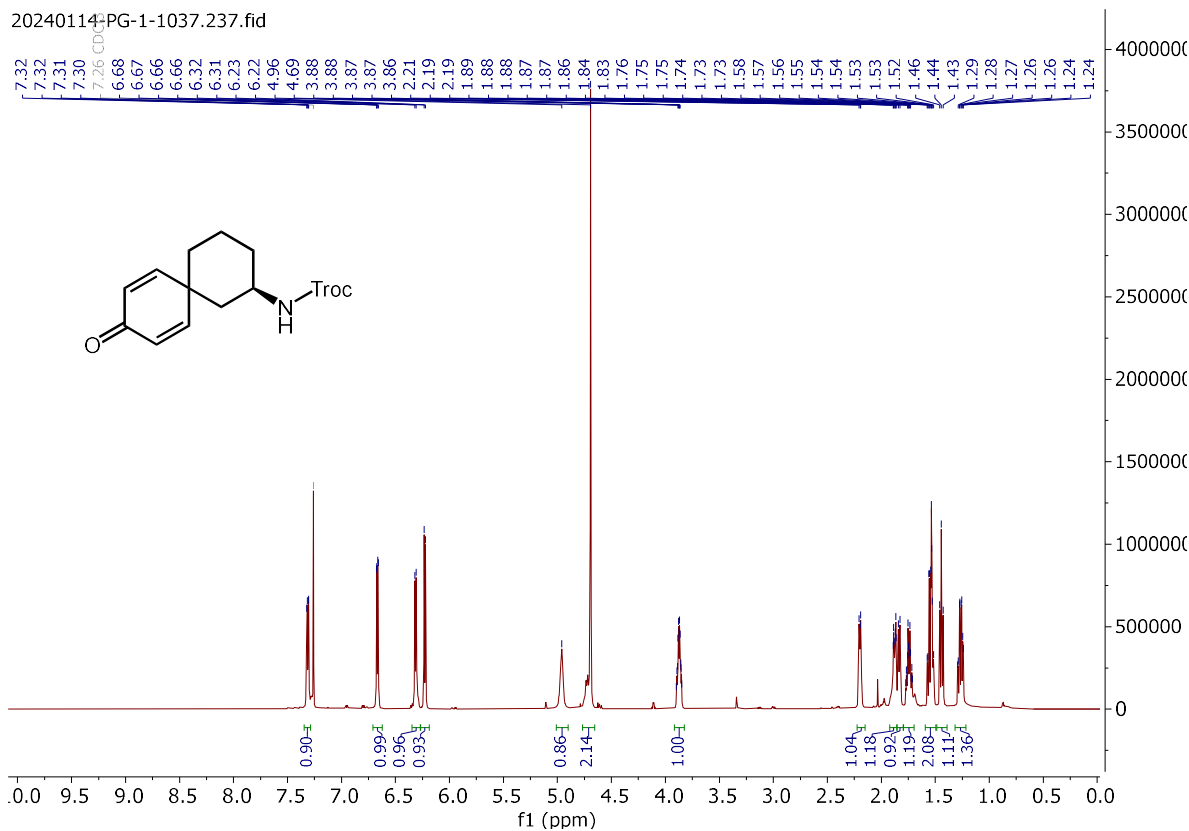


Signal 3: DAD1 C, Sig=230,4 Ref=360,100

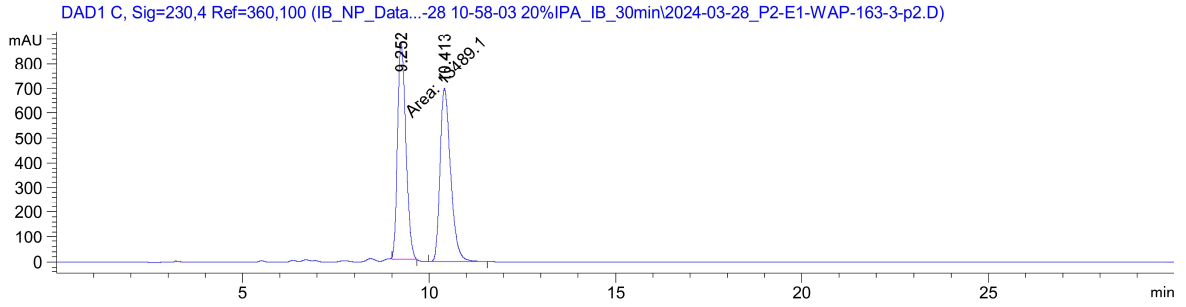
| Peak # | RetTime [min] | Type | Width [min] | Area [mAU*s] | Height [mAU] | Area % |
|--------|---------------|------|-------------|--------------|--------------|---------|
| 1 | 8.641 | BB | 0.2550 | 1359.03430 | 62.55727 | 14.1970 |
| 2 | 10.059 | BB | 0.3244 | 8213.65332 | 306.76489 | 85.8030 |

Totals : 9572.68762 369.32216

2,2,2-trichloroethyl (R)-(9-oxospiro[5.5]undeca-7,10-dien-2-yl)carbamate (4.59):



2,2,2-trichloroethyl (9-oxospiro[5.5]undeca-7,10-dien-2-yl)carbamate (\pm -4.59):

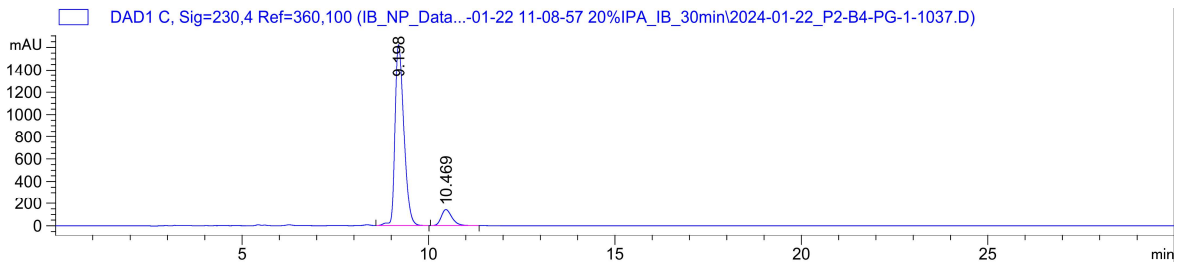


Signal 3: DAD1 C, Sig=230,4 Ref=360,100

| Peak # | RetTime [min] | Type | Width [min] | Area [mAU*s] | Height [mAU] | Area % |
|--------|---------------|------|-------------|--------------|--------------|---------|
| 1 | 9.252 | MM | 0.2565 | 1.34891e4 | 876.44525 | 49.5070 |
| 2 | 10.413 | BV R | 0.2945 | 1.37577e4 | 699.34204 | 50.4930 |

Totals : 2.72468e4 1575.78729

2,2,2-trichloroethyl (R)-(9-oxospiro[5.5]undeca-7,10-dien-2-yl)carbamate (4.59):

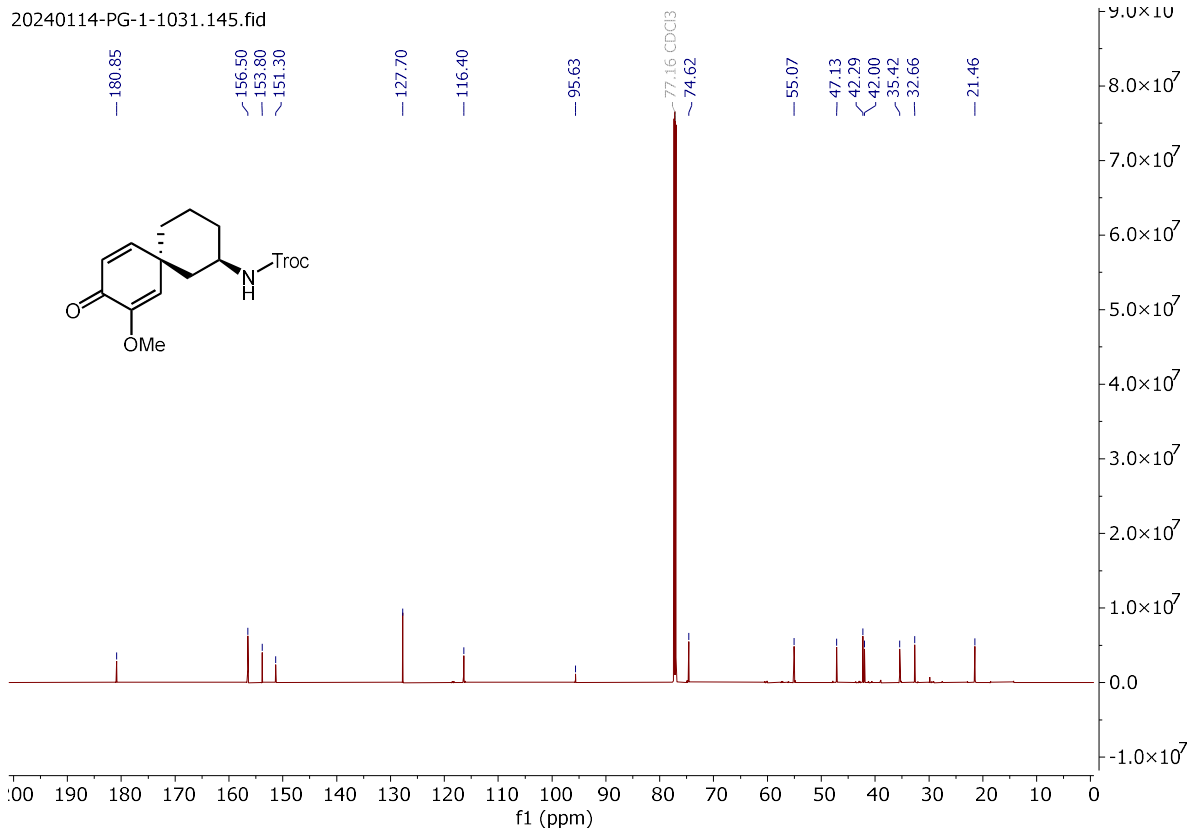
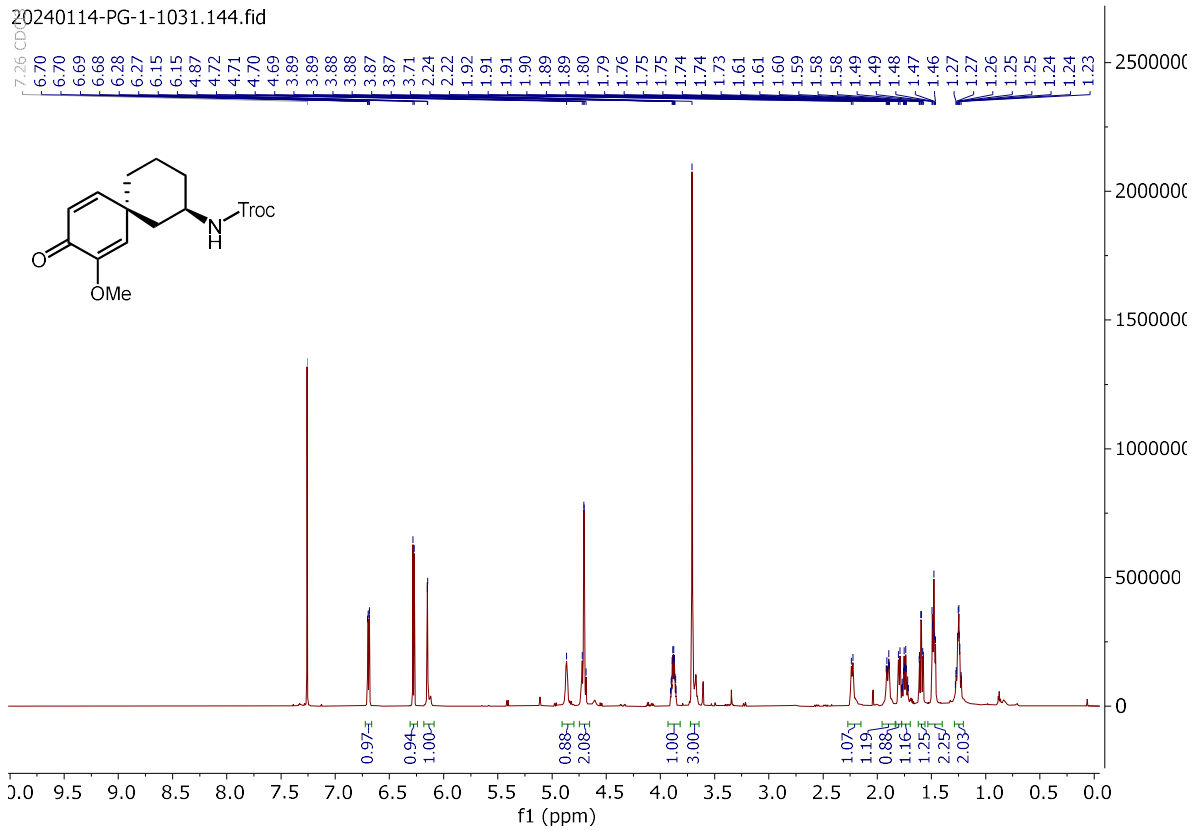


Signal 3: DAD1 C, Sig=230,4 Ref=360,100

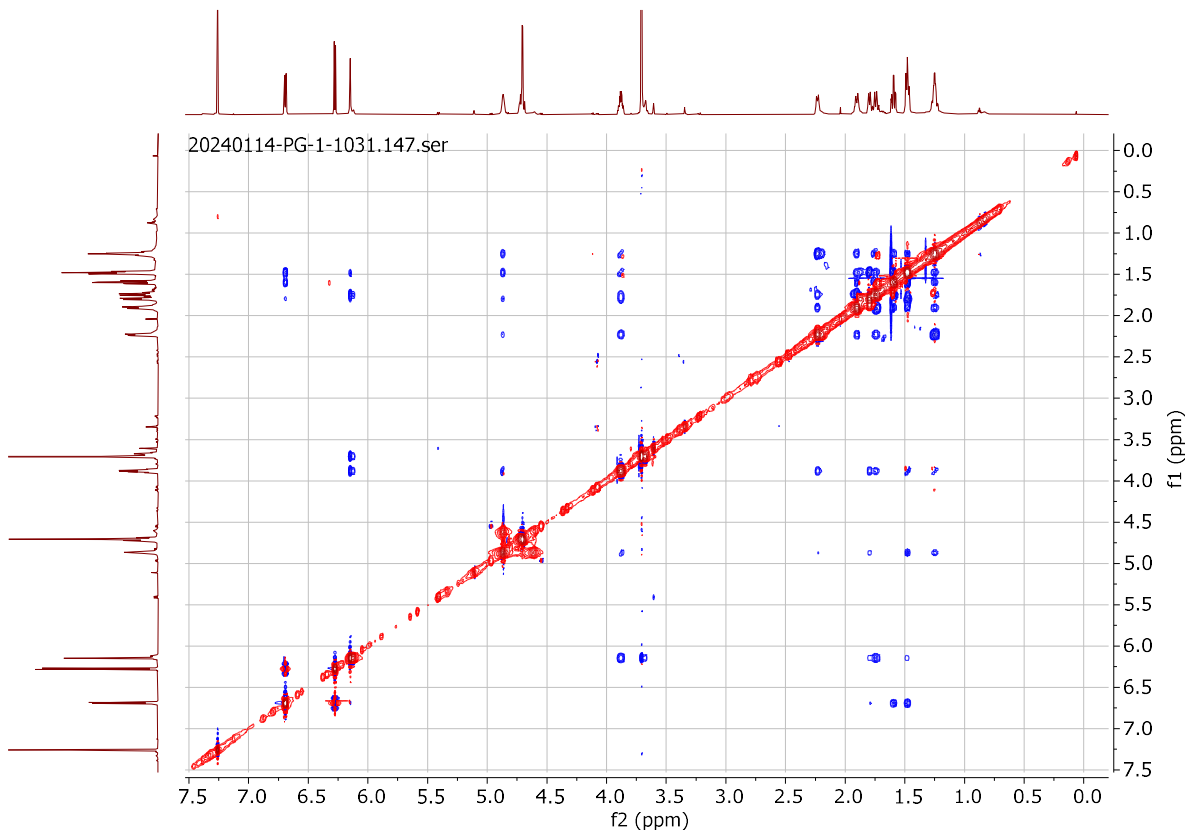
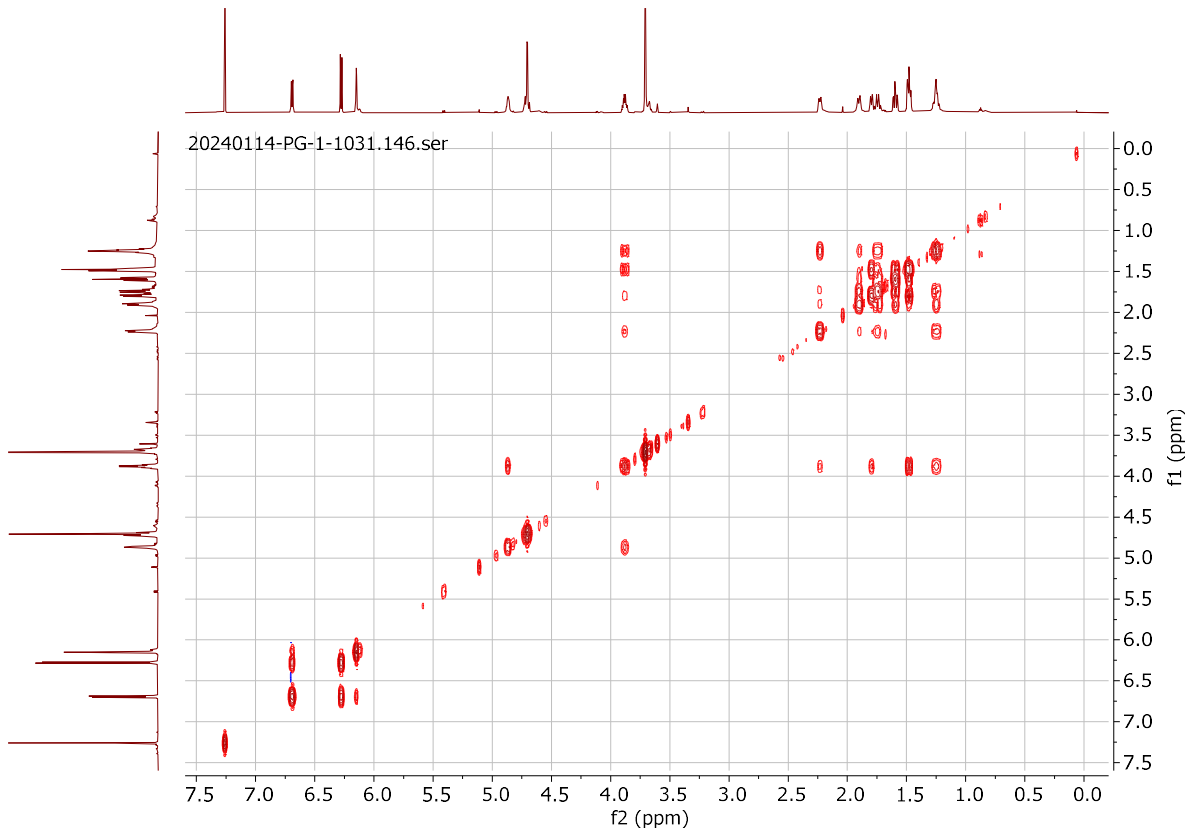
| Peak # | RetTime [min] | Type | Width [min] | Area [mAU*s] | Height [mAU] | Area % |
|--------|---------------|------|-------------|--------------|--------------|---------|
| 1 | 9.198 | VB R | 0.2308 | 2.68146e4 | 1620.85364 | 90.4624 |
| 2 | 10.469 | BB | 0.2716 | 2827.10815 | 142.10719 | 9.5376 |

Totals : 2.96417e4 1762.96083

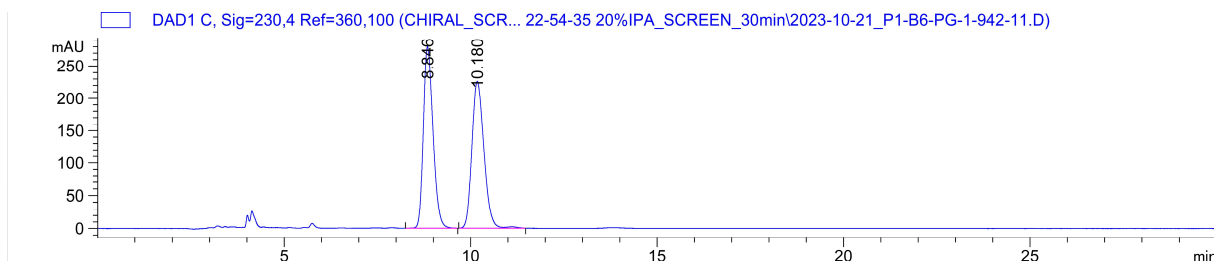
2,2,2-trichloroethyl ((2R,6R)-8-methoxy-9-oxospiro[5.5]undeca-7,10-dien-2-yl)carbamate (**4.60**):



4.60



2,2,2-trichloroethyl ((2R,6R)-8-methoxy-9-oxospiro[5.5]undeca-7,10-dien-2-yl)carbamate (\pm -4.60):

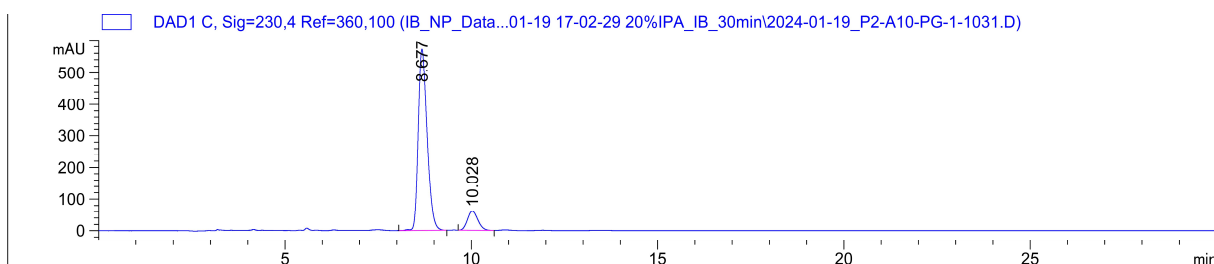


Signal 3: DAD1 C, Sig=230,4 Ref=360,100

| Peak # | RetTime [min] | Type | Width [min] | Area [mAU*s] | Height [mAU] | Area % |
|--------|---------------|------|-------------|--------------|--------------|---------|
| 1 | 8.846 | BB | 0.2710 | 5008.08105 | 278.82919 | 49.8599 |
| 2 | 10.180 | BV R | 0.3215 | 5036.21826 | 225.72603 | 50.1401 |

Totals : 1.00443e4 504.55522

2,2,2-trichloroethyl ((2R,6R)-8-methoxy-9-oxospiro[5.5]undeca-7,10-dien-2-yl)carbamate (4.60):

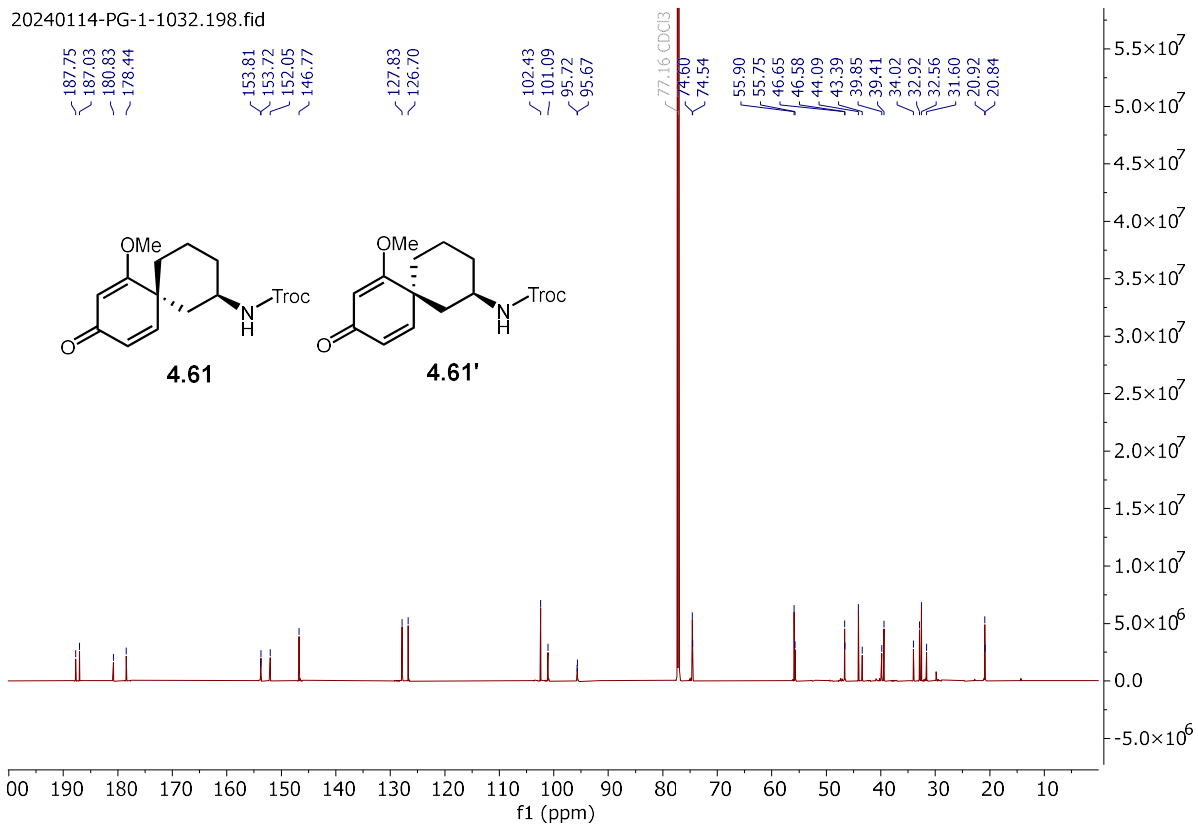
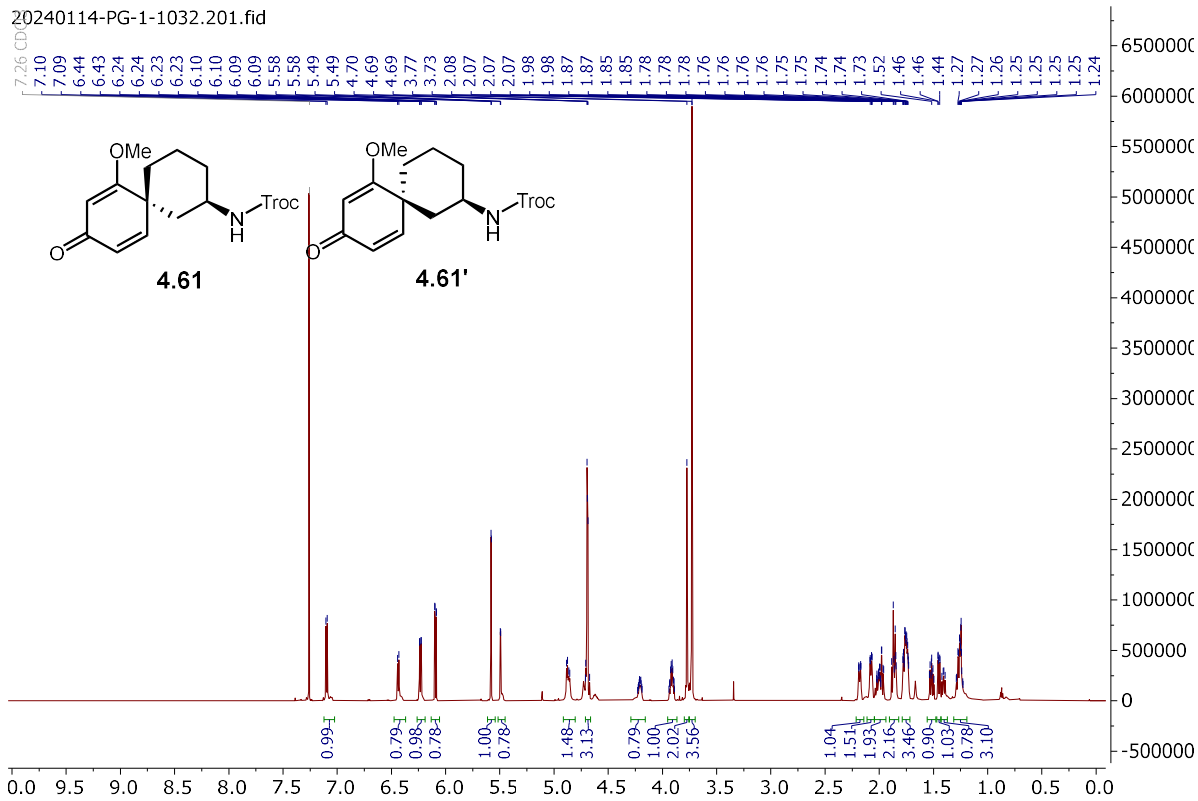


Signal 3: DAD1 C, Sig=230,4 Ref=360,100

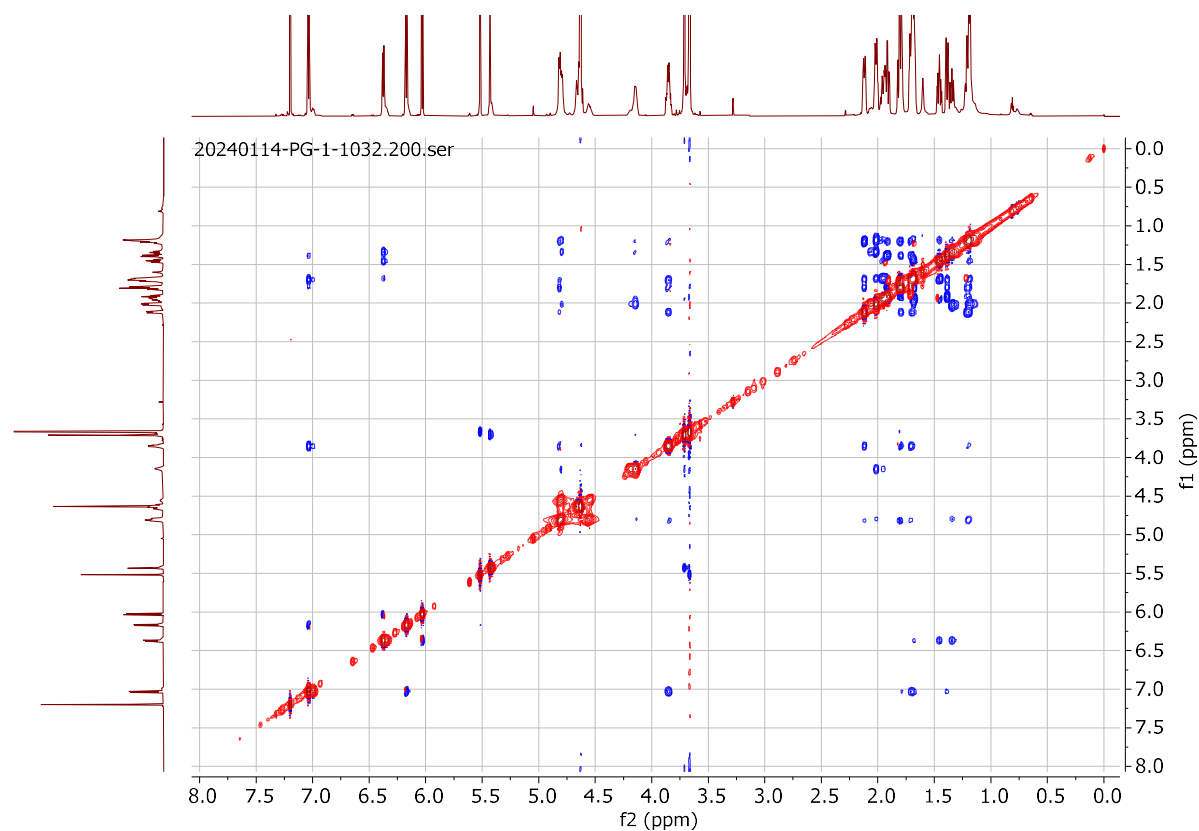
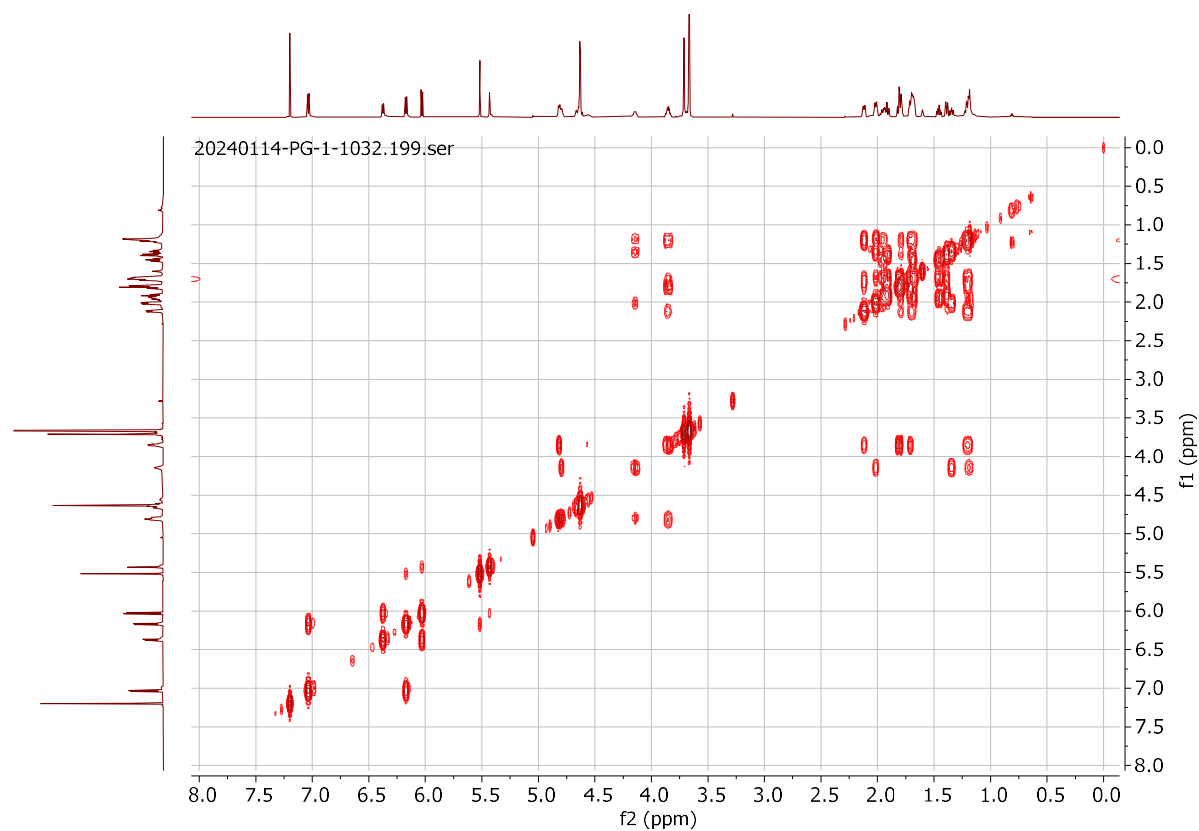
| Peak # | RetTime [min] | Type | Width [min] | Area [mAU*s] | Height [mAU] | Area % |
|--------|---------------|------|-------------|--------------|--------------|---------|
| 1 | 8.677 | VB R | 0.2491 | 9455.07324 | 571.04541 | 89.0630 |
| 2 | 10.028 | BV R | 0.2463 | 1161.08948 | 59.98688 | 10.9370 |

Totals : 1.06162e4 631.03229

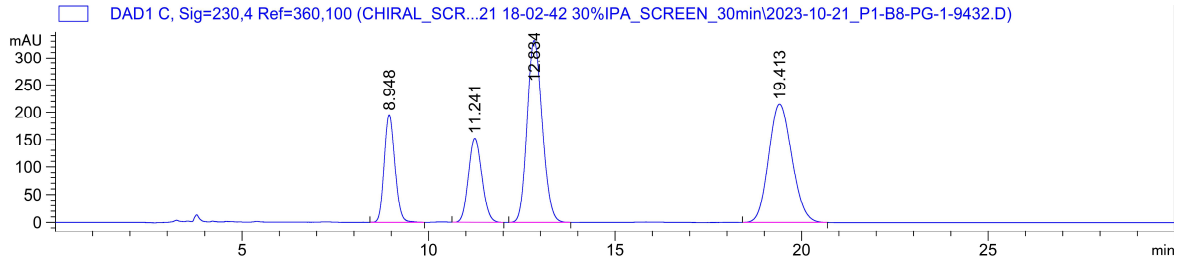
2,2,2-trichloroethyl ((2R,6R)-7-methoxy-9-oxospiro[5.5]undeca-7,10-dien-2-yl)carbamate (**4.61**) and 2,2,2-trichloroethyl ((2R,6S)-7-methoxy-9-oxospiro[5.5]undeca-7,10-dien-2-yl)carbamate (**4.61'**):



(4.61) and (4.61')



2,2,2-trichloroethyl ((2R,6R)-7-methoxy-9-oxospiro[5.5]undeca-7,10-dien-2-yl)carbamate (\pm -4.61):

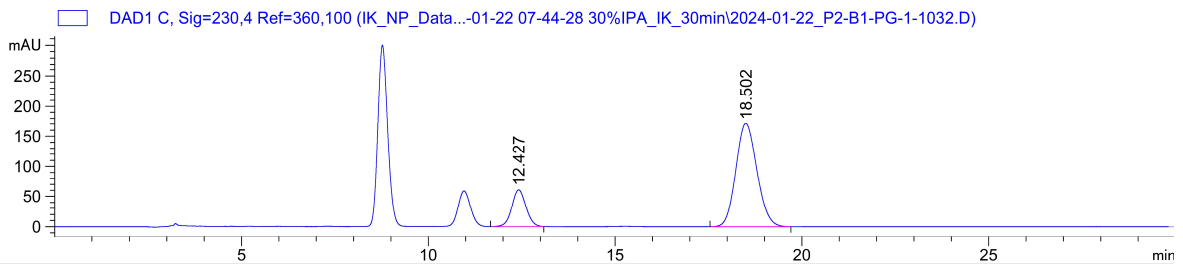


Signal 3: DAD1 C, Sig=230,4 Ref=360,100

| Peak # | RetTime [min] | Type | Width [min] | Area [mAU*s] | Height [mAU] | Area % |
|--------|---------------|------|-------------|--------------|--------------|---------|
| 1 | 8.948 | BB | 0.2813 | 3882.78125 | 195.42876 | 14.7403 |
| 2 | 11.241 | BB | 0.3405 | 3818.19800 | 152.29341 | 14.4951 |
| 3 | 12.834 | BB | 0.3649 | 9345.39160 | 331.48193 | 35.4780 |
| 4 | 19.413 | BB | 0.5059 | 9294.97559 | 215.19852 | 35.2866 |

Totals : 2.63413e4 894.40262

2,2,2-trichloroethyl ((2R,6R)-7-methoxy-9-oxospiro[5.5]undeca-7,10-dien-2-yl)carbamate (4.61):

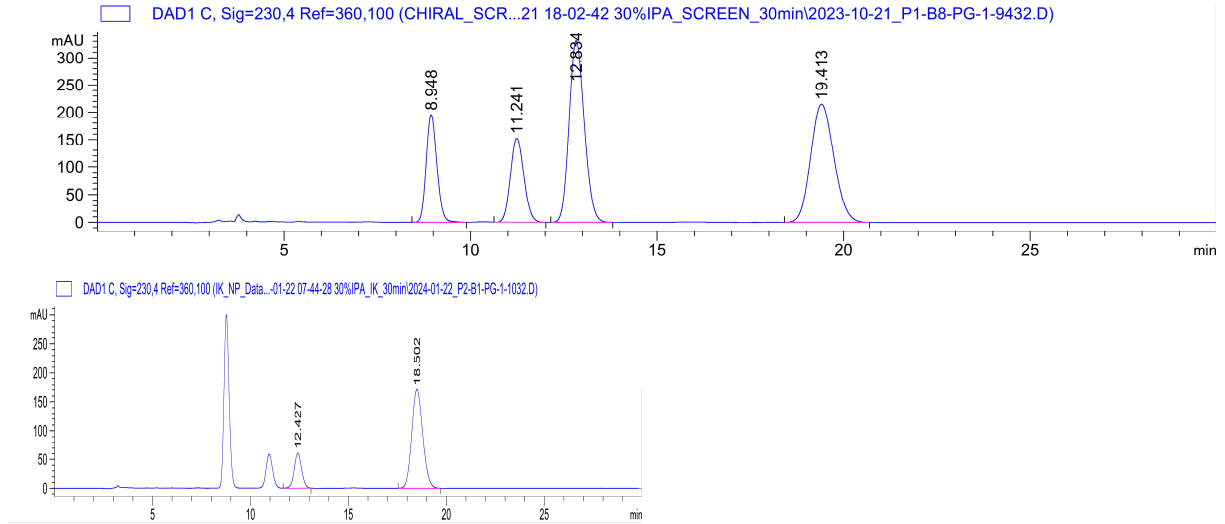


Signal 3: DAD1 C, Sig=230,4 Ref=360,100

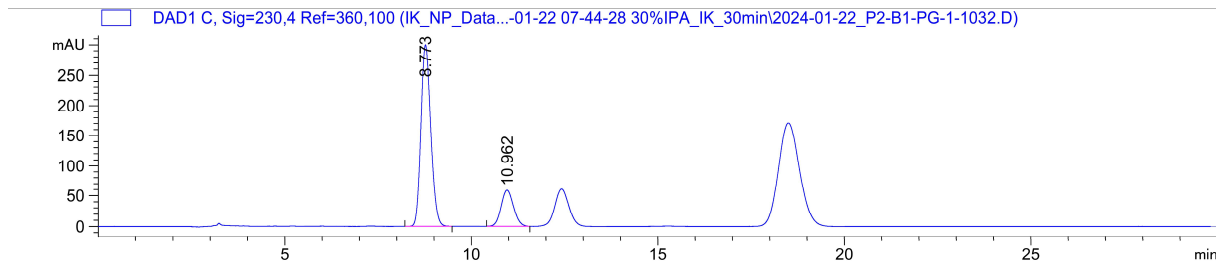
| Peak # | RetTime [min] | Type | Width [min] | Area [mAU*s] | Height [mAU] | Area % |
|--------|---------------|------|-------------|--------------|--------------|---------|
| 1 | 12.427 | BV R | 0.3101 | 1592.13757 | 60.58779 | 19.2001 |
| 2 | 18.502 | VB R | 0.4610 | 6700.19141 | 171.05046 | 80.7999 |

Totals : 8292.32898 231.63825

2,2,2-trichloroethyl ((2R,6S)-7-methoxy-9-oxospiro[5.5]undeca-7,10-dien-2-yl)carbamate (\pm -4.61'):



2,2,2-trichloroethyl ((2R,6S)-7-methoxy-9-oxospiro[5.5]undeca-7,10-dien-2-yl)carbamate (4.61'):

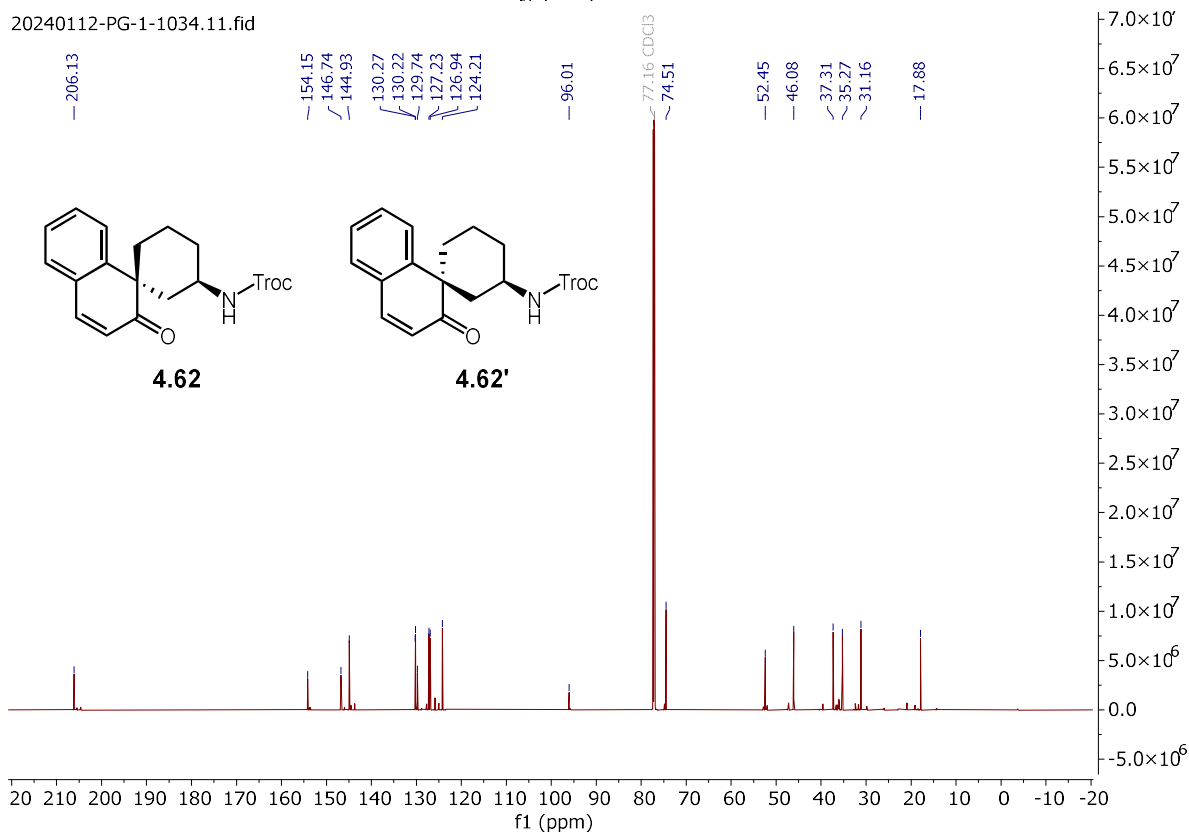
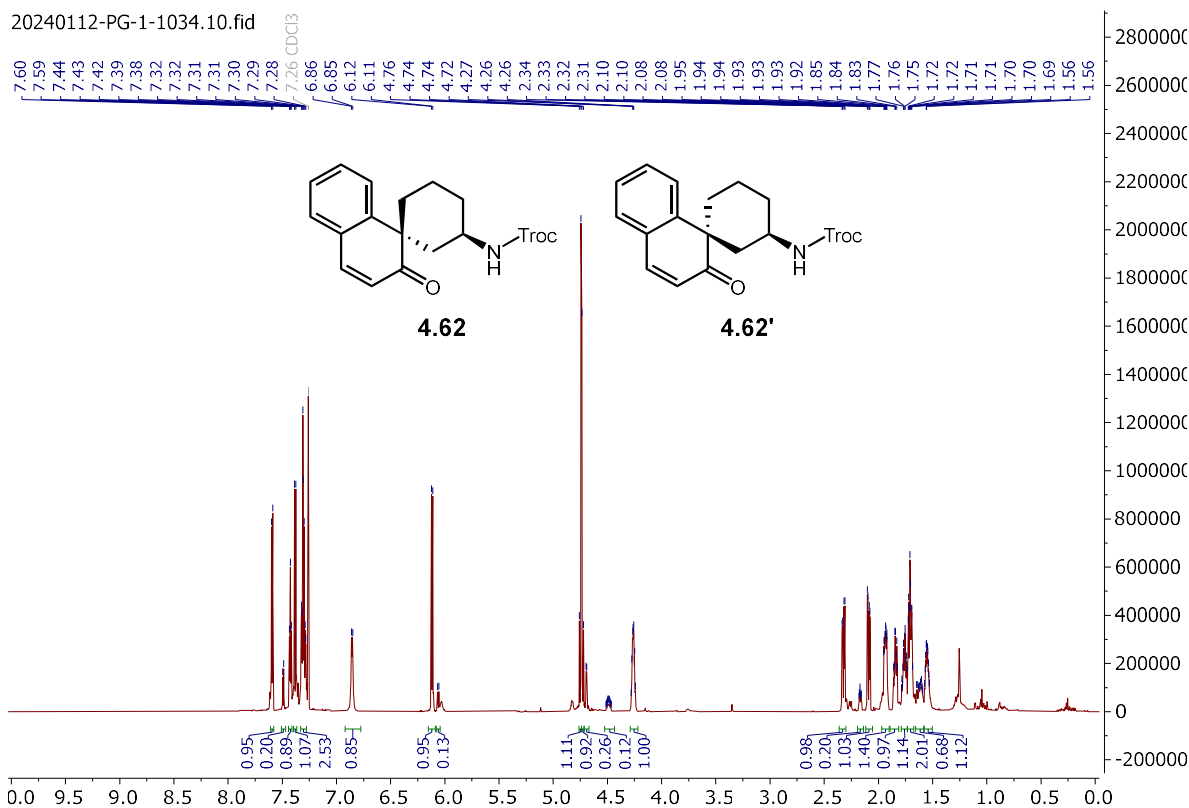


Signal 3: DAD1 C, Sig=230,4 Ref=360,100

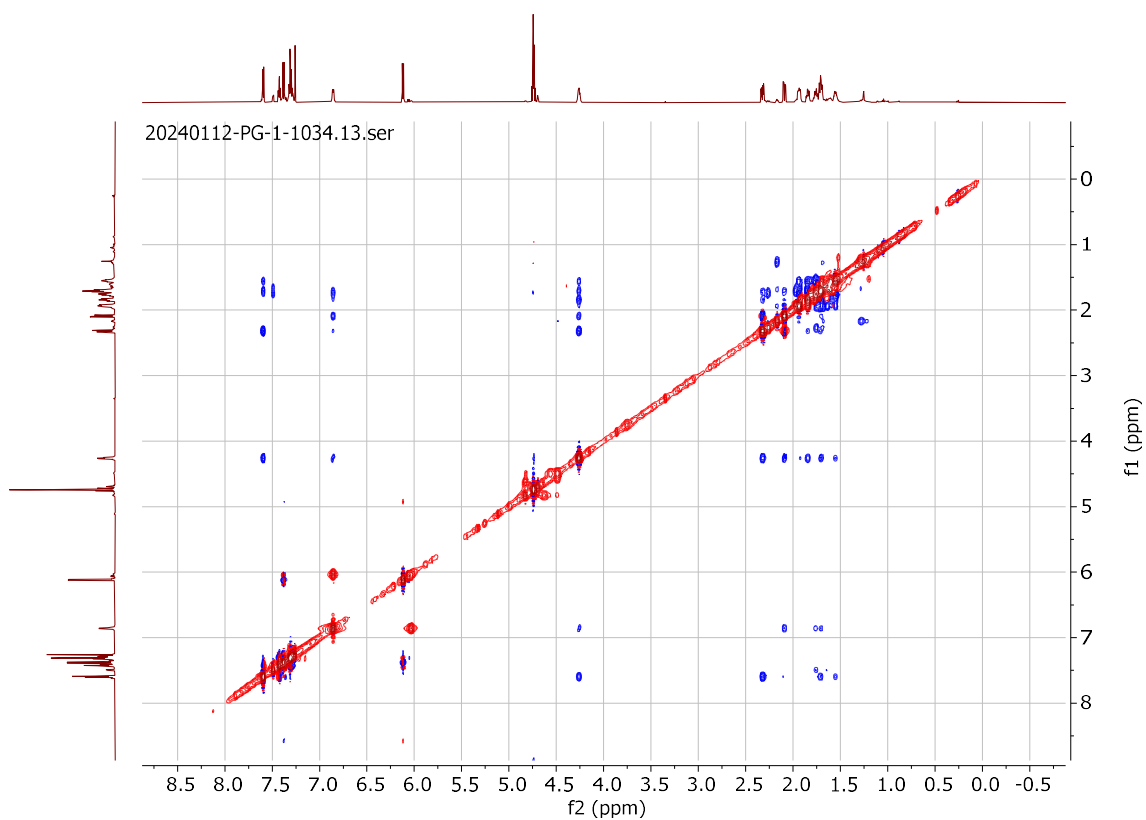
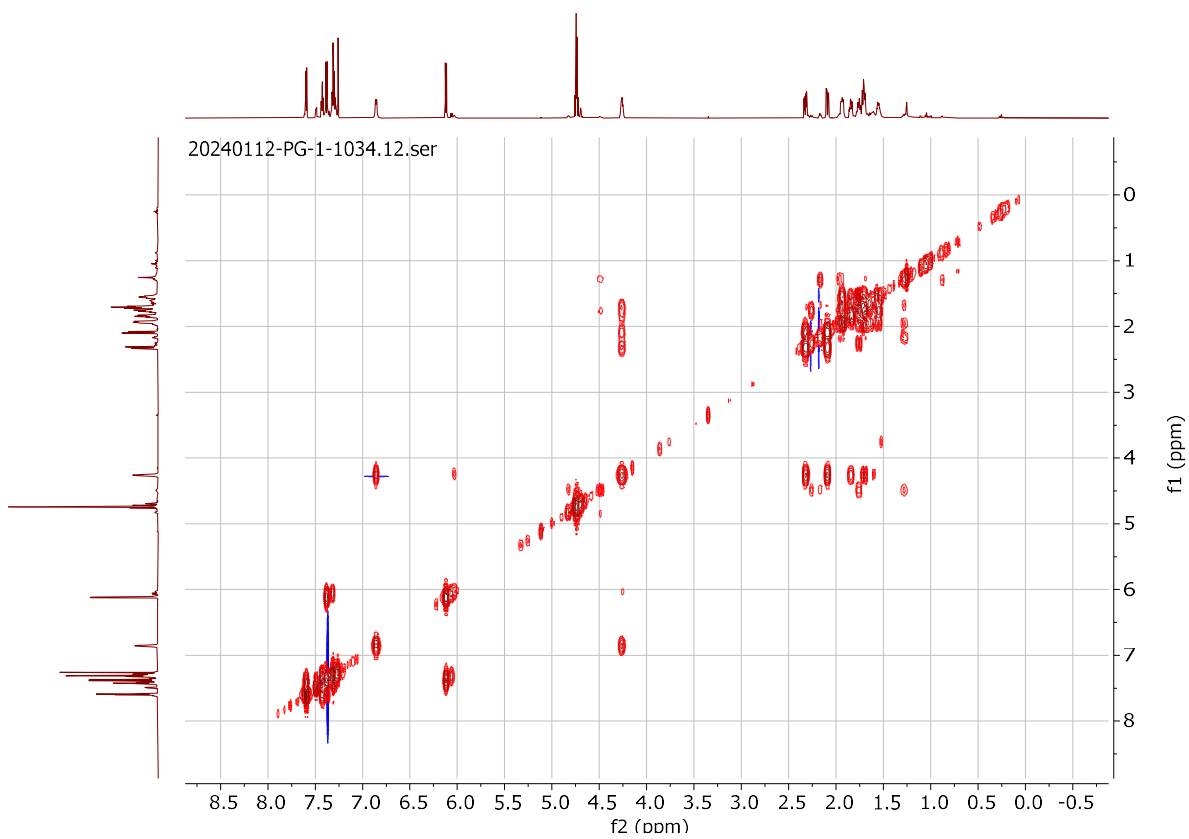
| Peak # | RetTime [min] | Type | Width [min] | Area [mAU*s] | Height [mAU] | Area % |
|--------|---------------|------|-------------|--------------|--------------|---------|
| 1 | 8.773 | BV R | 0.2657 | 5483.44824 | 300.02490 | 80.1786 |
| 2 | 10.962 | BV R | 0.2733 | 1355.59644 | 58.72931 | 19.8214 |

Totals : 6839.04468 358.75422

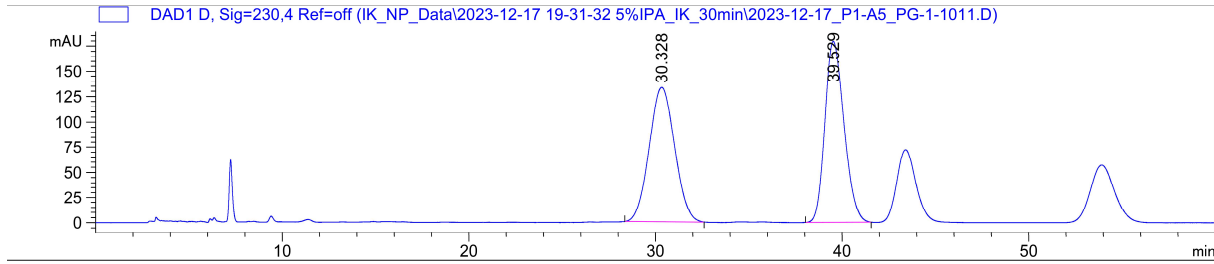
2,2,2-trichloroethyl ((1*S*,3*R*)-2'-oxo-2'*H*-spiro[cyclohexane-1,1'-naphthalen]-3-yl)carbamate (**4.62**) and 2,2,2-trichloroethyl ((1*R*,3*R*)-2'-oxo-2'*H*-spiro[cyclohexane-1,1'-naphthalen]-3-yl)carbamate (**4.62'**):



(4.62) and (4.62'):



2,2,2-trichloroethyl ((1S,3R)-2'-oxo-2'H-spiro[cyclohexane-1,1'-naphthalen]-3-yl)carbamate (\pm -4.62):

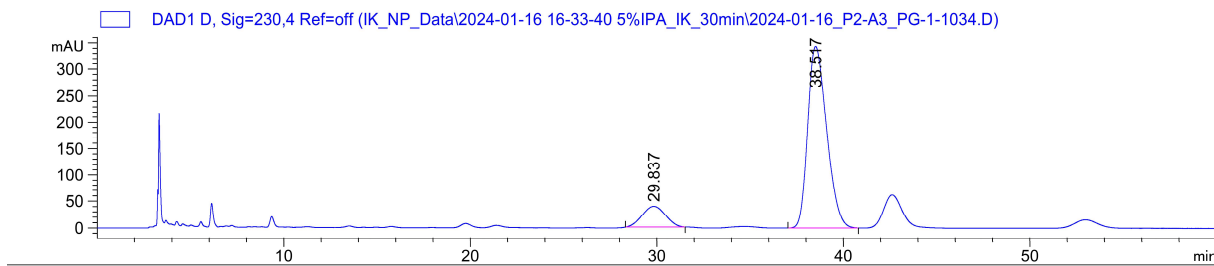


Signal 4: DAD1 D, Sig=230,4 Ref=off

| Peak # | RetTime [min] | Type | Width [min] | Area [mAU*s] | Height [mAU] | Area % |
|--------|---------------|------|-------------|--------------|--------------|---------|
| 1 | 30.328 | BB | 1.1113 | 1.26442e4 | 132.91623 | 49.7966 |
| 2 | 39.529 | BB | 0.8334 | 1.27475e4 | 179.31085 | 50.2034 |

Totals : 2.53917e4 312.22708

2,2,2-trichloroethyl ((1S,3R)-2'-oxo-2'H-spiro[cyclohexane-1,1'-naphthalen]-3-yl)carbamate (4.62):

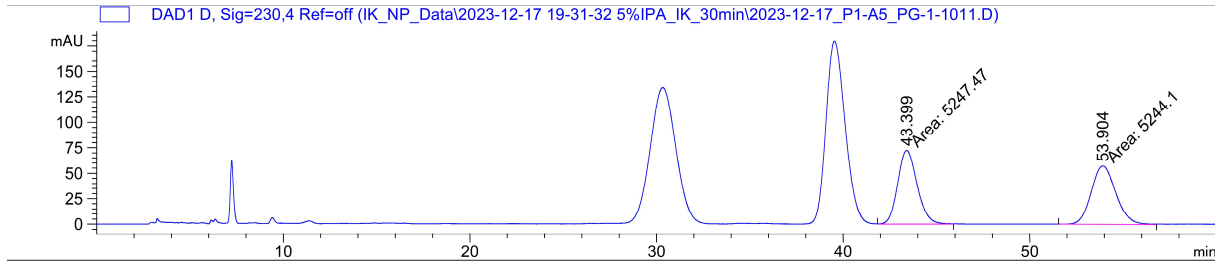


Signal 4: DAD1 D, Sig=230,4 Ref=off

| Peak # | RetTime [min] | Type | Width [min] | Area [mAU*s] | Height [mAU] | Area % |
|--------|---------------|------|-------------|--------------|--------------|---------|
| 1 | 29.837 | BB | 1.0125 | 3344.14697 | 38.59244 | 12.1706 |
| 2 | 38.517 | VV R | 0.8216 | 2.41332e4 | 343.51312 | 87.8294 |

Totals : 2.74774e4 382.10556

2,2,2-trichloroethyl ((1R,3R)-2'-oxo-2'H-spiro[cyclohexane-1,1'-naphthalen]-3-yl)carbamate (\pm -4.62'):

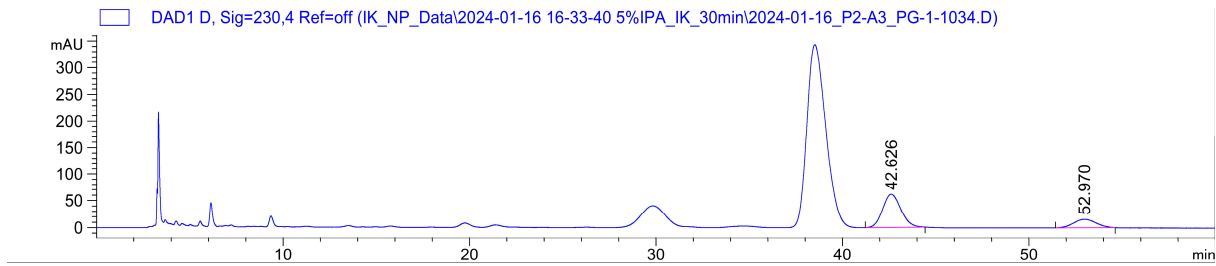


Signal 4: DAD1 D, Sig=230,4 Ref=off

| Peak # | RetTime [min] | Type | Width [min] | Area [mAU*s] | Height [mAU] | Area % |
|--------|---------------|------|-------------|--------------|--------------|---------|
| 1 | 43.399 | MM | 1.2078 | 5247.46826 | 72.41349 | 50.0161 |
| 2 | 53.904 | MM | 1.5274 | 5244.09717 | 57.22234 | 49.9839 |

Totals : 1.04916e4 129.63583

2,2,2-trichloroethyl ((1R,3R)-2'-oxo-2'H-spiro[cyclohexane-1,1'-naphthalen]-3-yl)carbamate (4.62'):

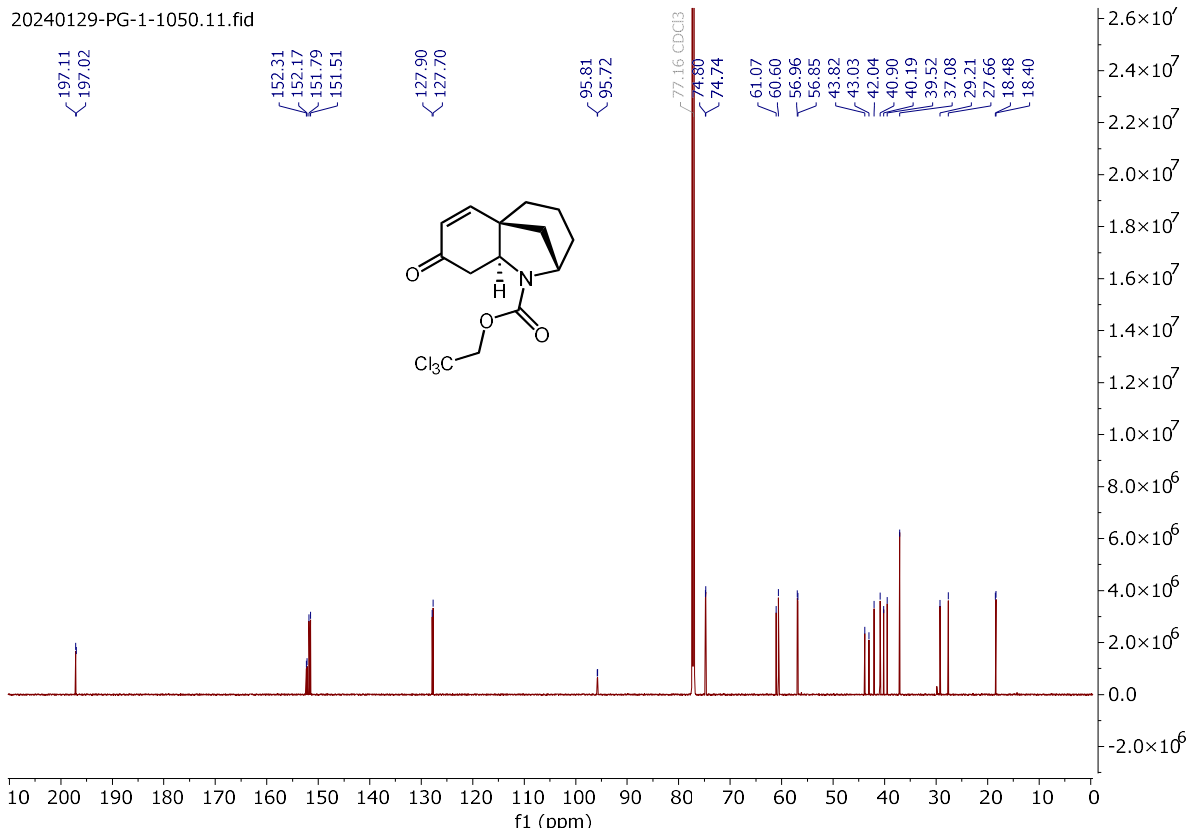
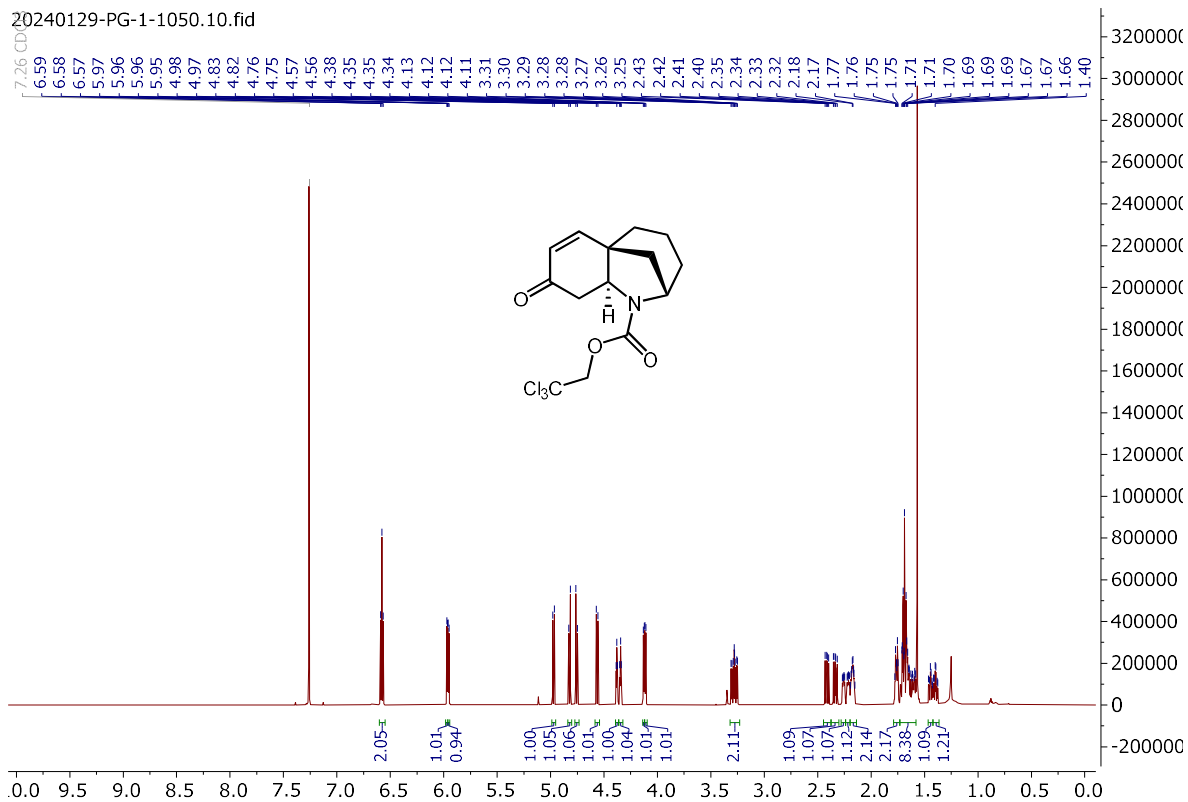


Signal 4: DAD1 D, Sig=230,4 Ref=off

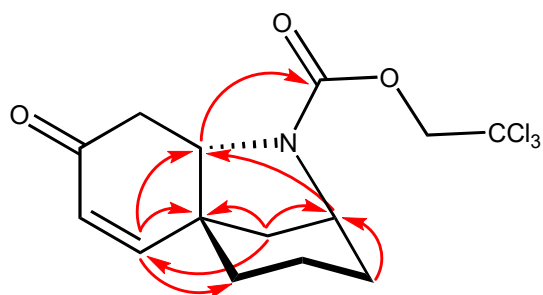
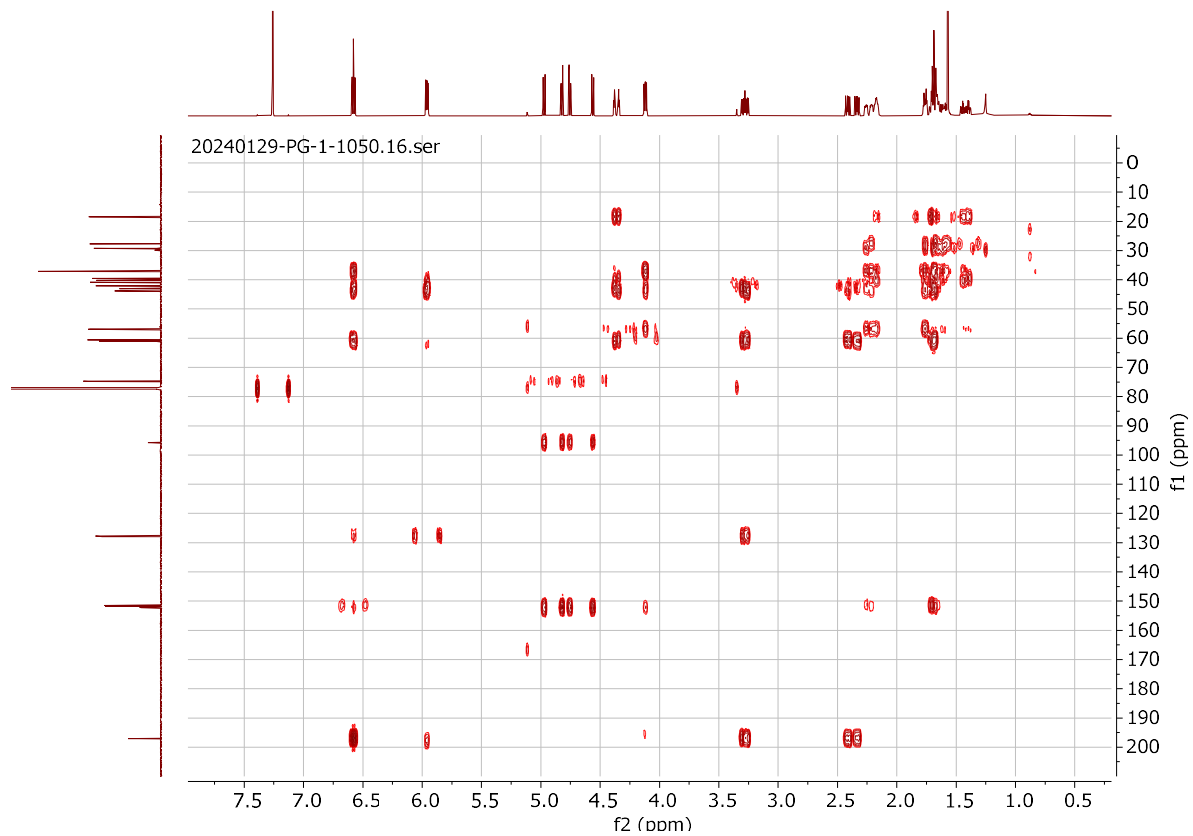
| Peak # | RetTime [min] | Type | Width [min] | Area [mAU*s] | Height [mAU] | Area % |
|--------|---------------|------|-------------|--------------|--------------|---------|
| 1 | 42.626 | BV R | 0.7925 | 4138.69336 | 61.04314 | 76.2606 |
| 2 | 52.970 | BB | 0.9757 | 1288.34912 | 15.42955 | 23.7394 |

Totals : 5427.04248 76.47270

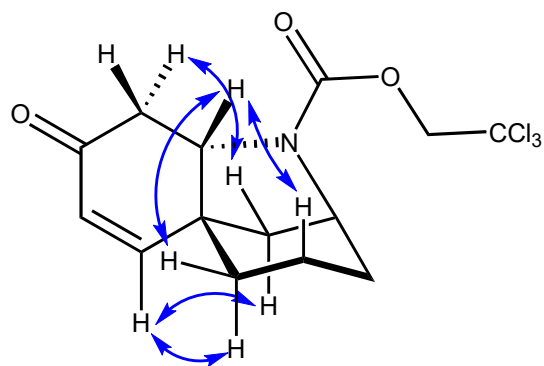
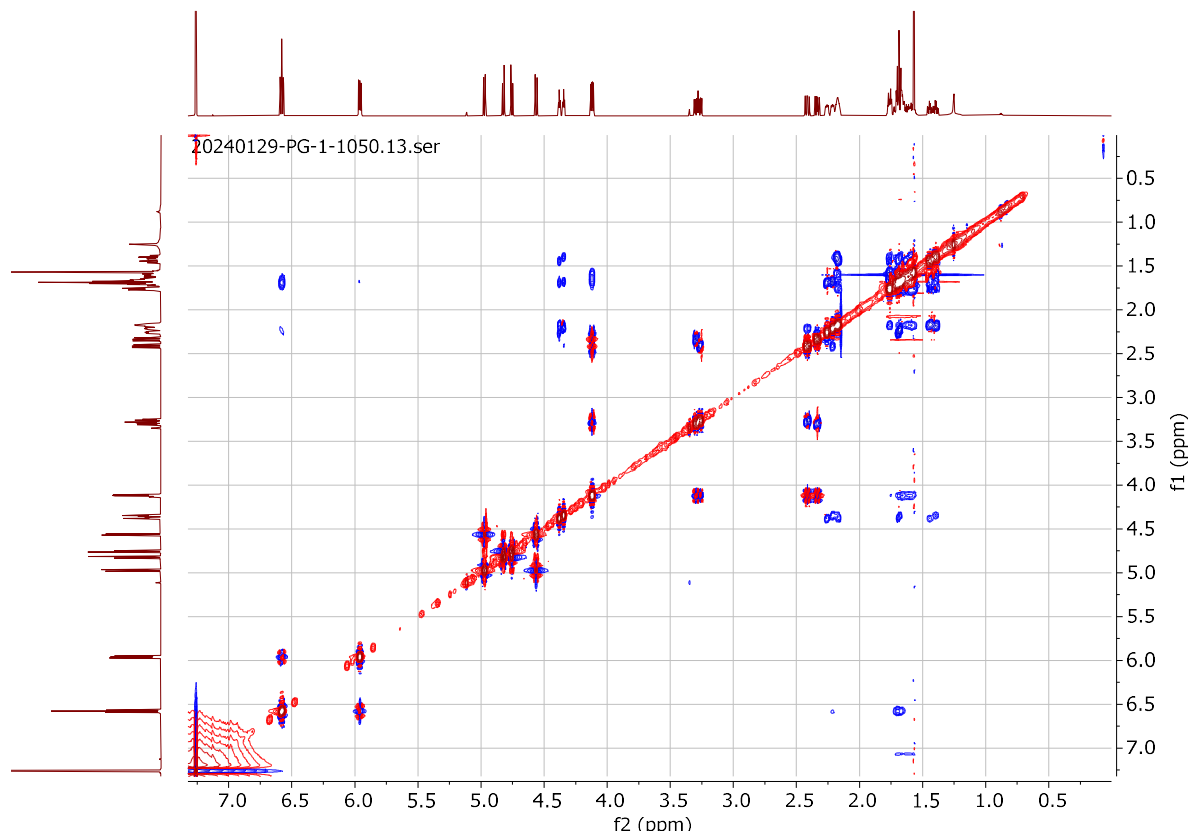
2,2,2-trichloroethyl-8-oxo-2,3,4,5,9,9a-hexahydro-2,5a-methanobenzo[b]azepine-1(8H)-carboxylate (4.66):



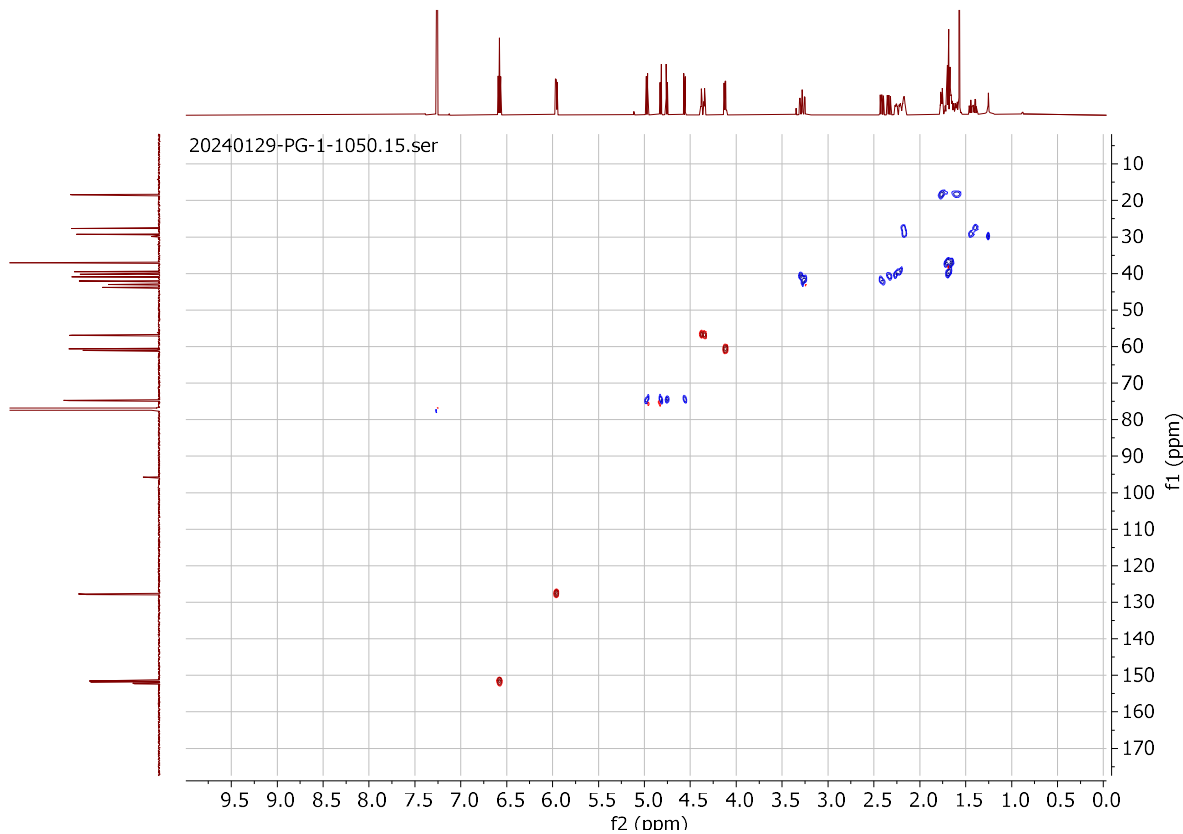
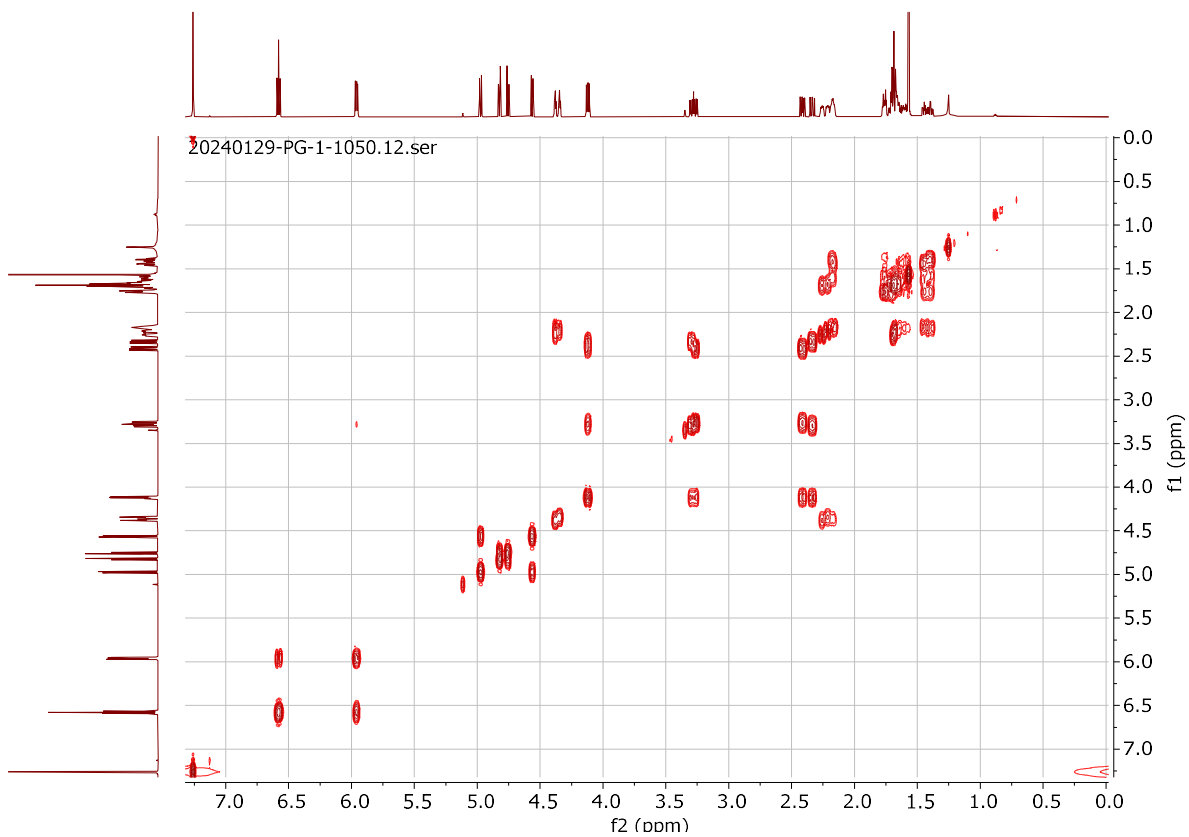
Key HMBC (^1H - ^{13}C) correlations used to assign the structure of **4.66**:



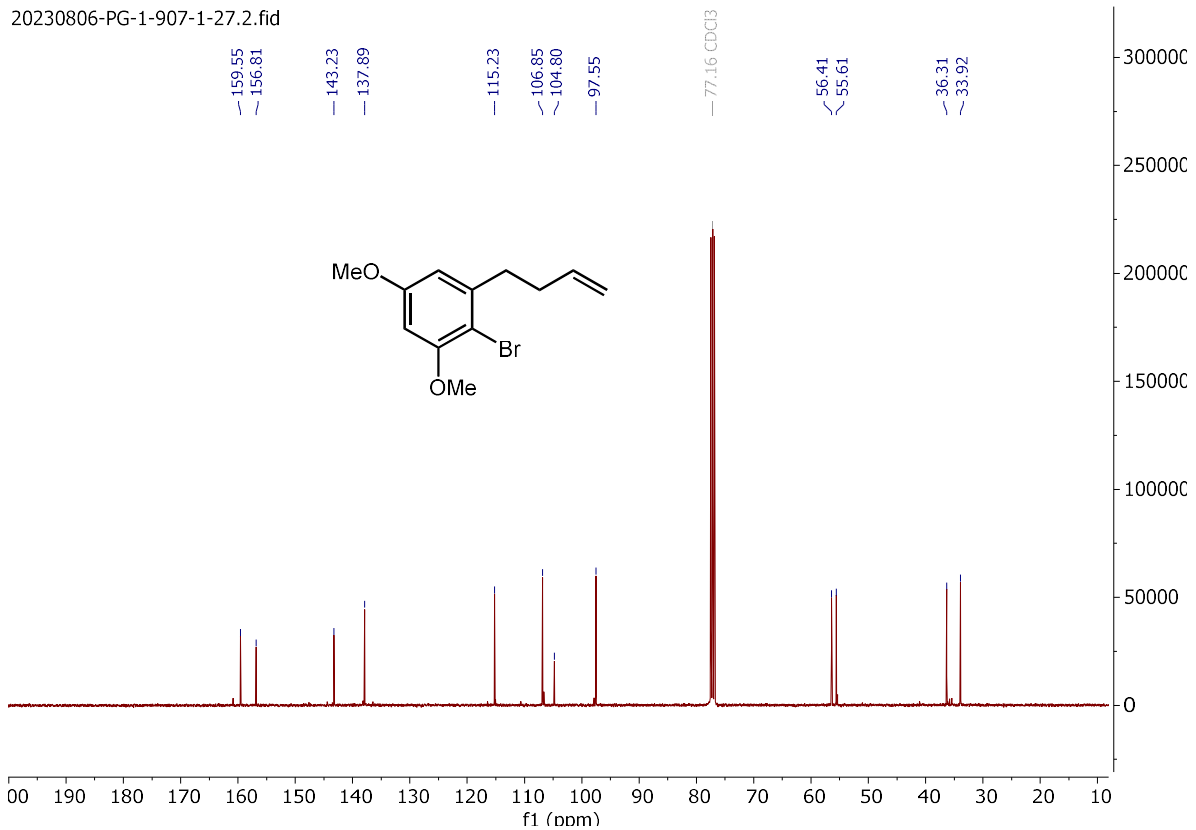
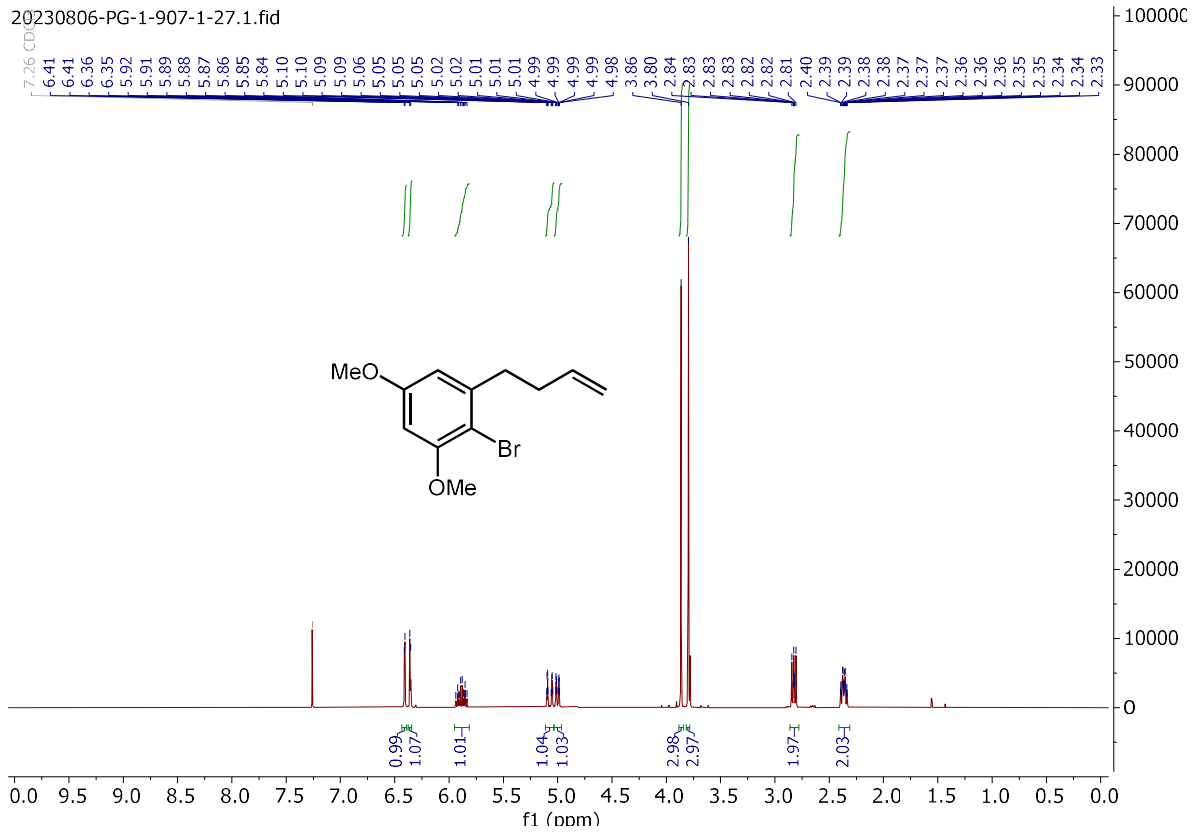
Key NOESY (^1H - ^1H) correlations used to assign the structure of **4.66**:



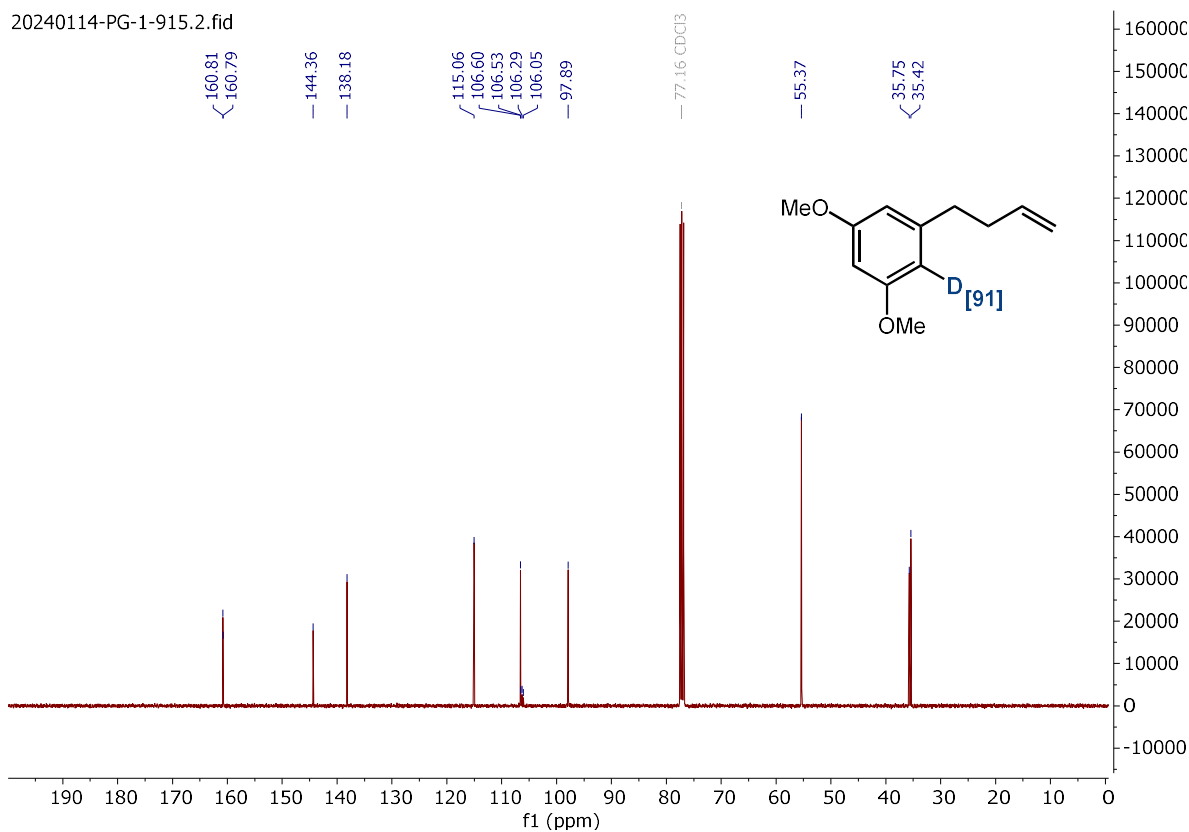
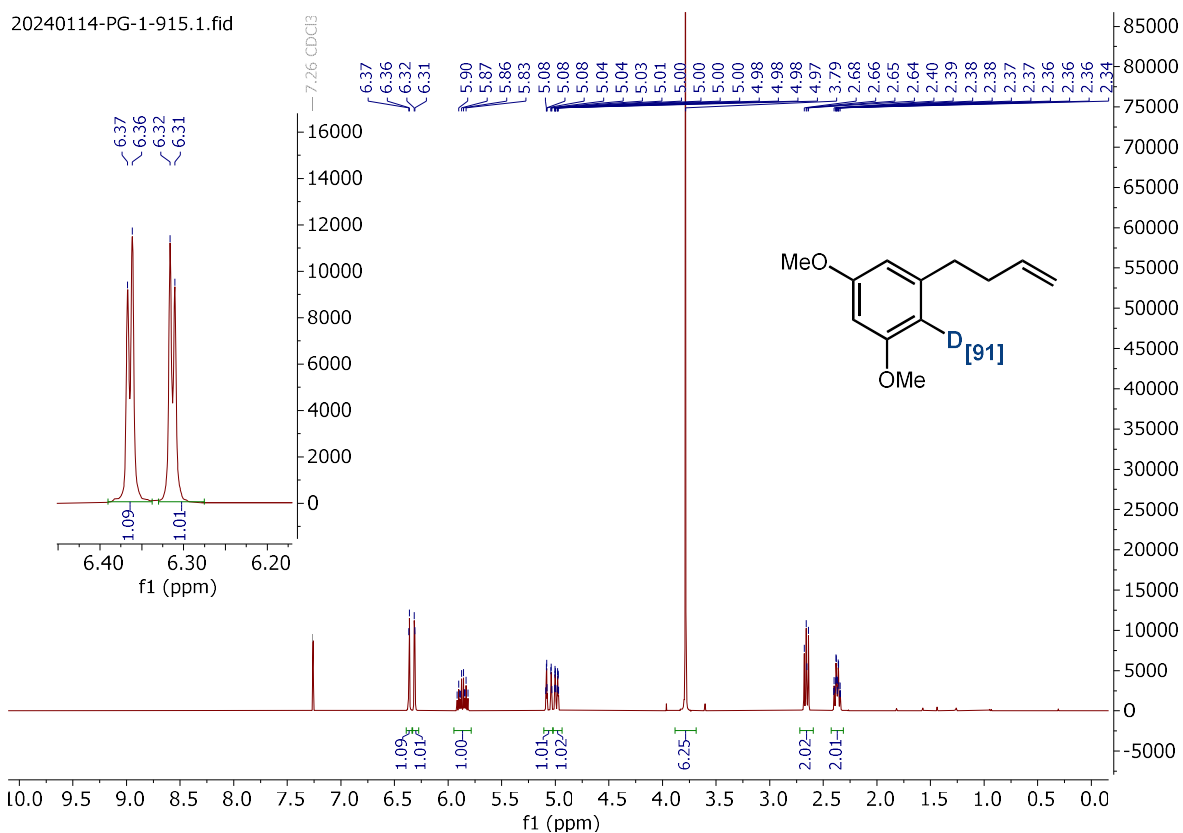
COSY and HSQC used to assign the structure of 4.66



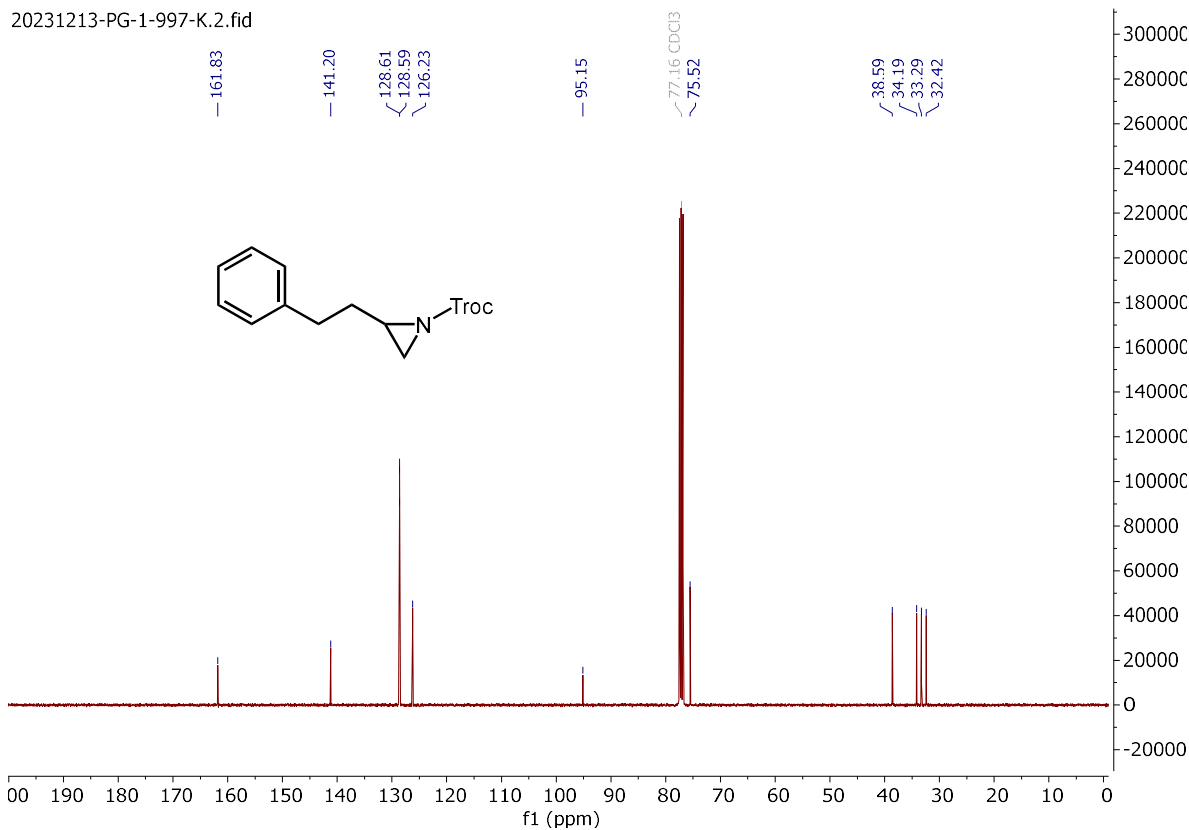
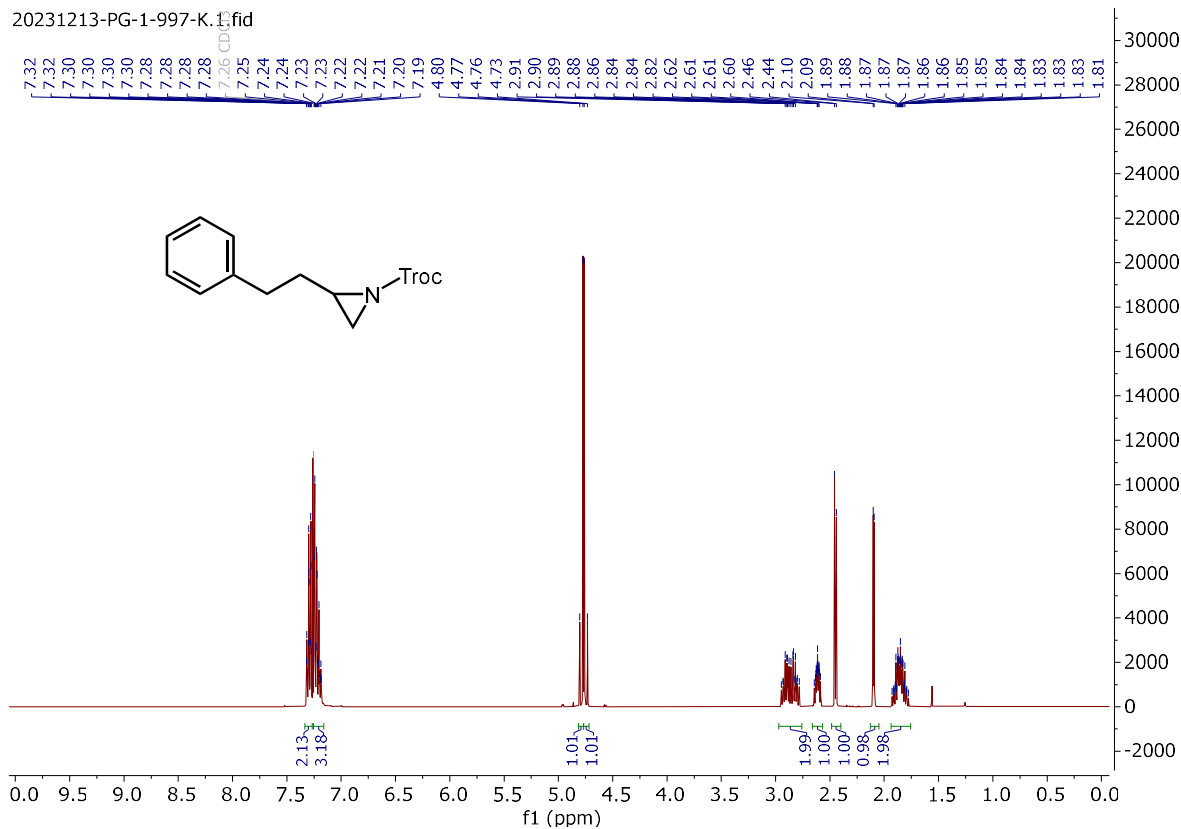
2-bromo-1-(but-3-en-1-yl)-3,5-dimethoxybenzene (S21):



1-(but-3-en-1-yl)-3,5-dimethoxybenzene-2-d (4.67-d₁):

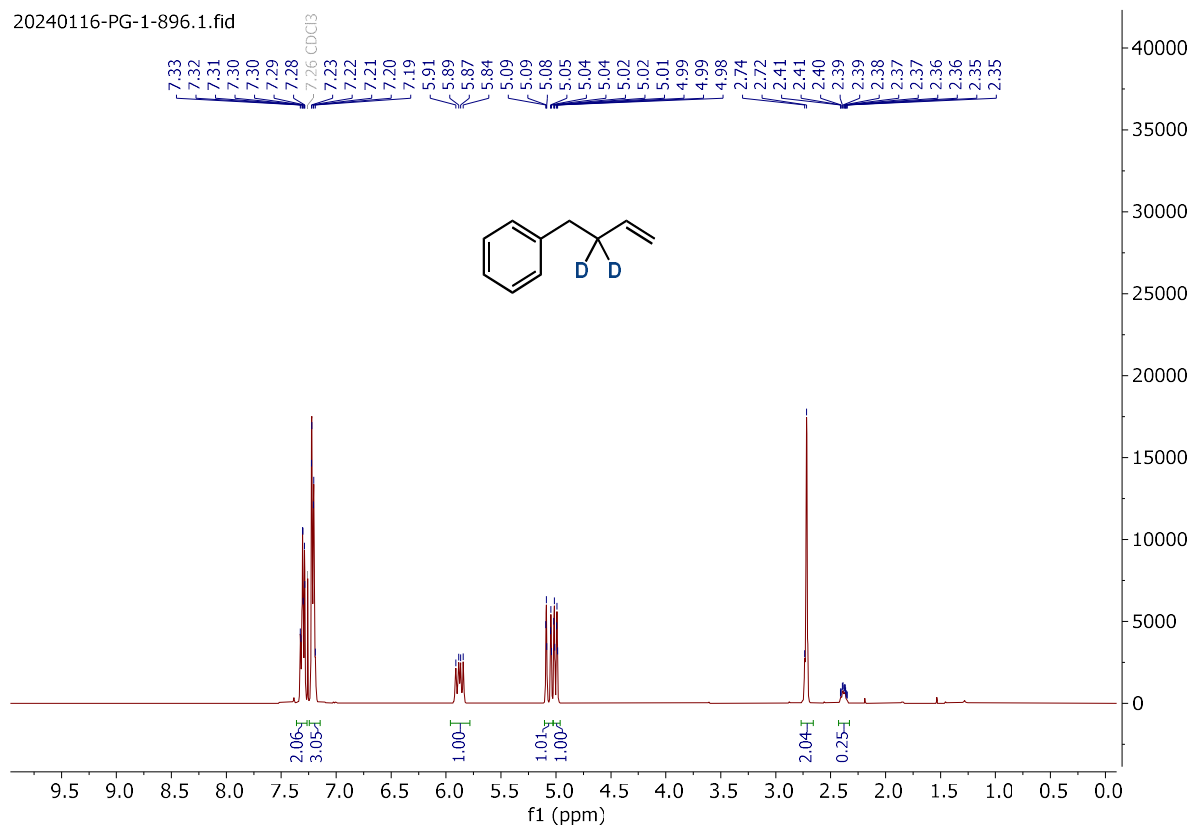


2,2,2-trichloroethyl 2-phenethylaziridine-1-carboxylate (4.68):

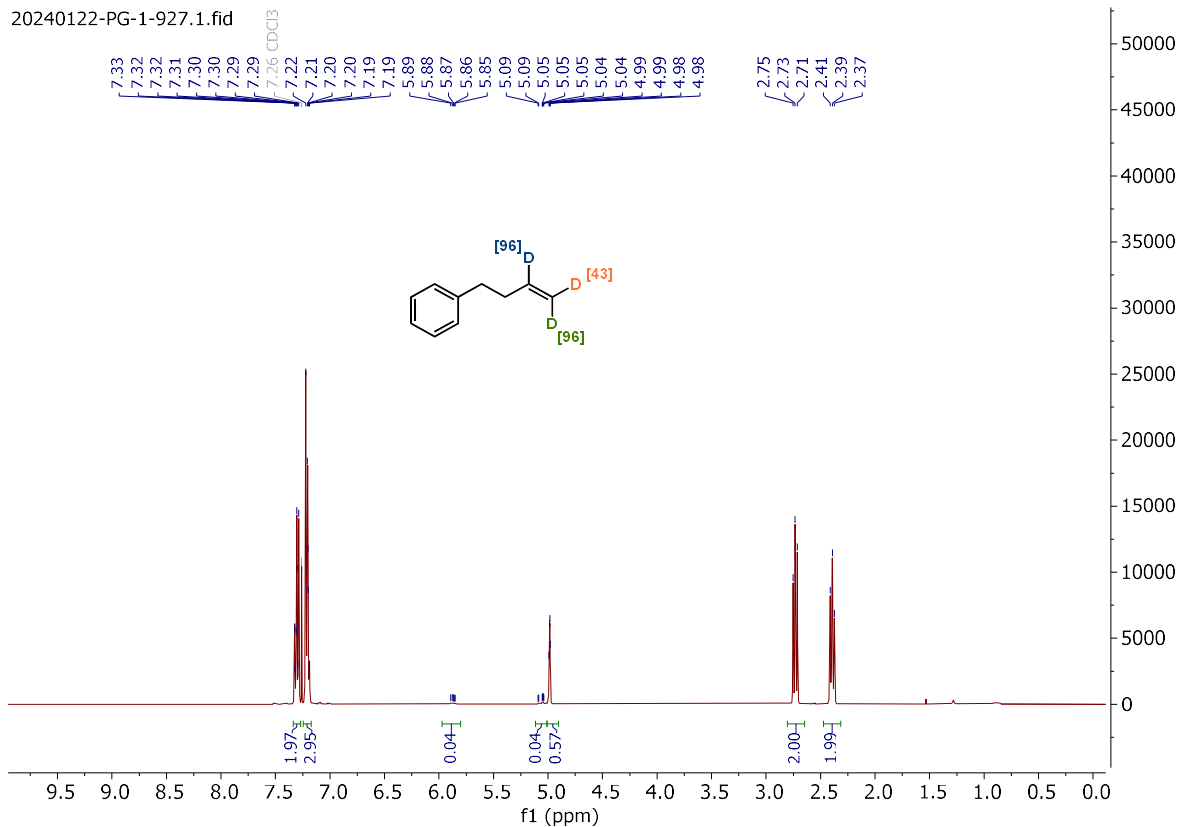


(but-3-en-1-yl-2,2-d2)benzene (4.28-d₂):

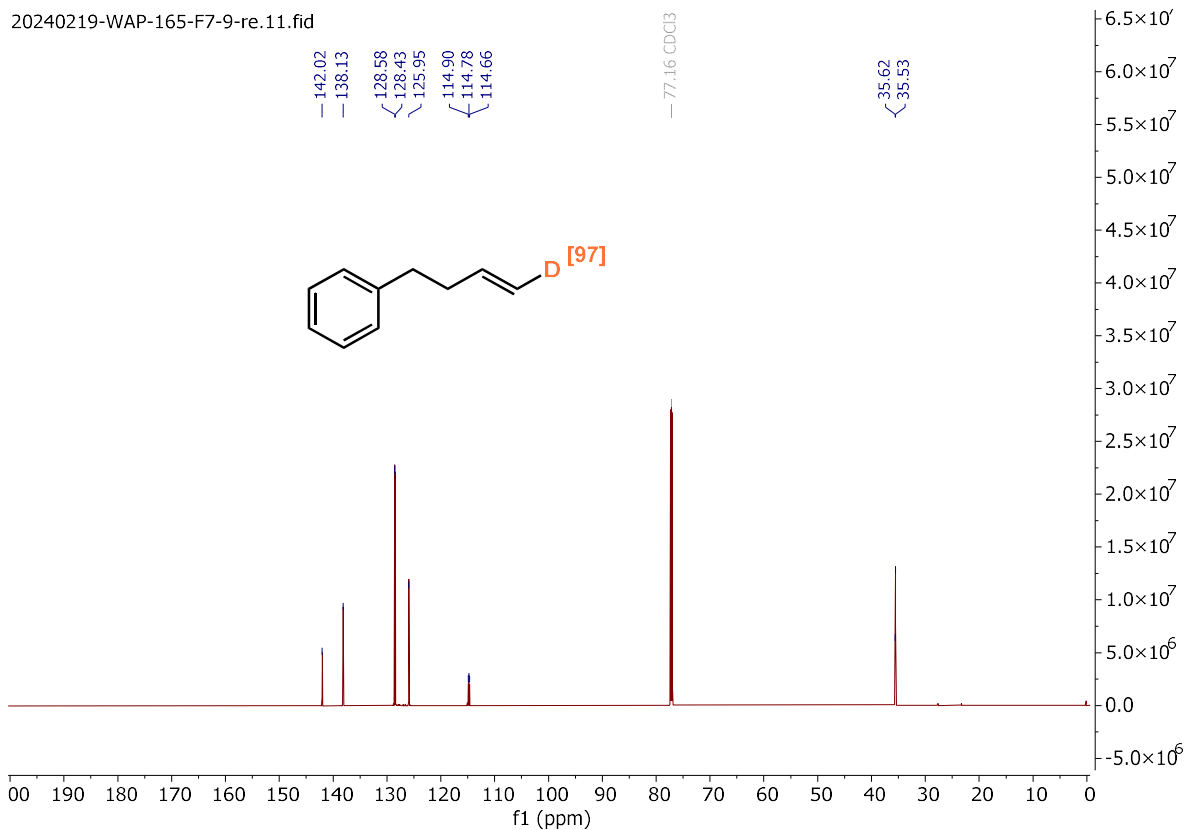
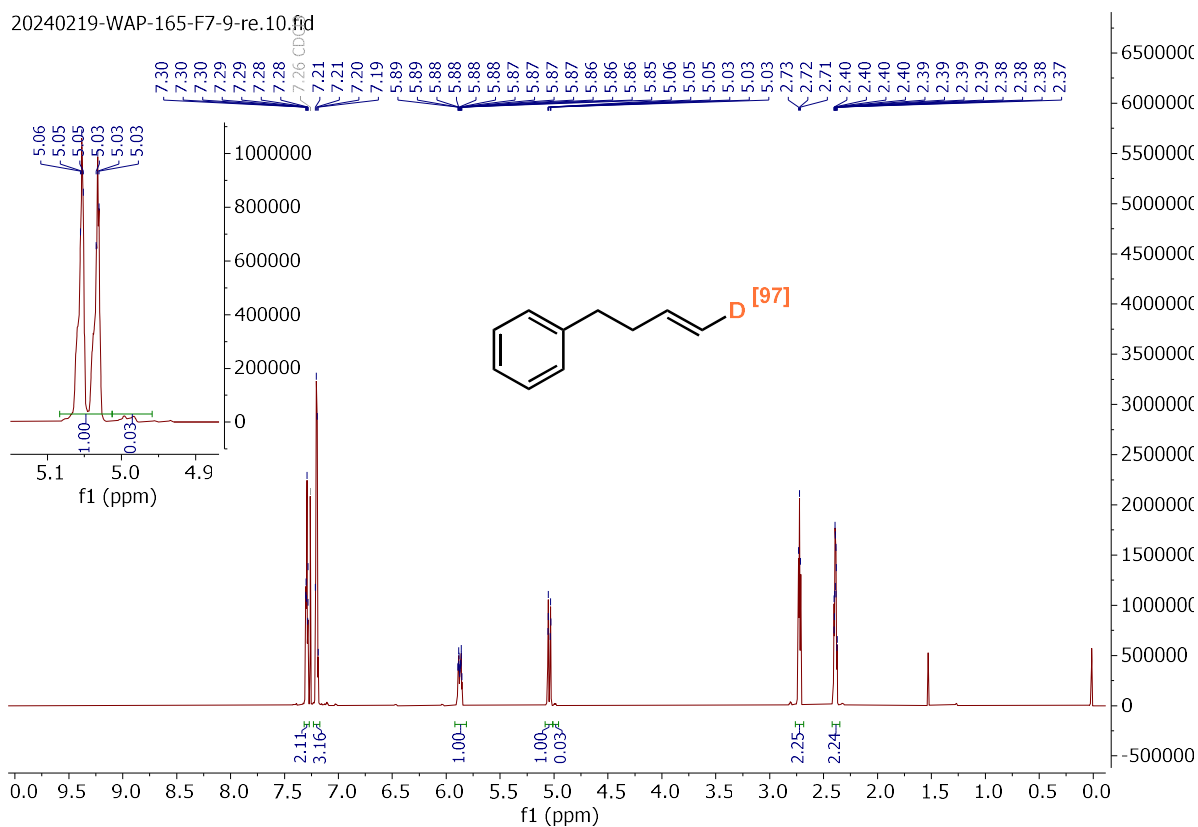
20240116-PG-1-896.1.fid



(but-3-en-1-yl-3,4,4-d3)benzene (4.28-d₃):

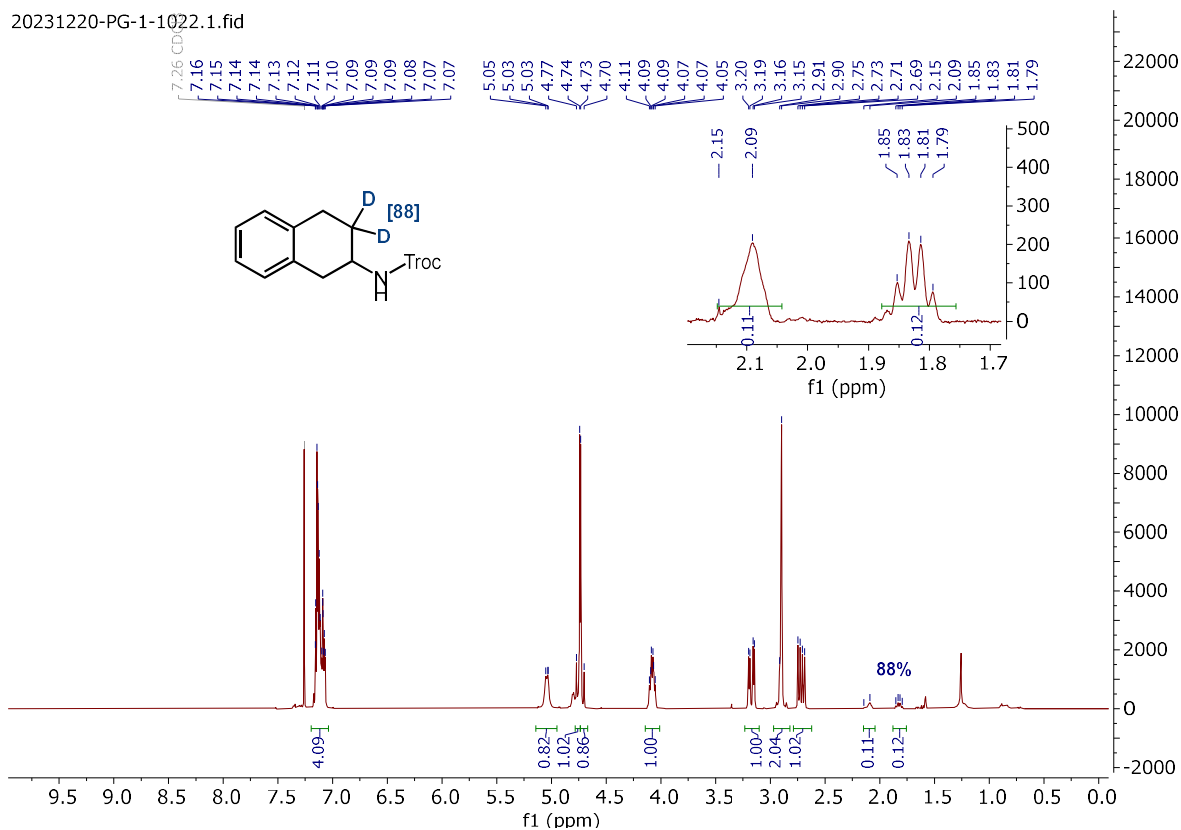


(E)-(but-3-en-1-yl-4-d)benzene (*E*-4.28-d₁):

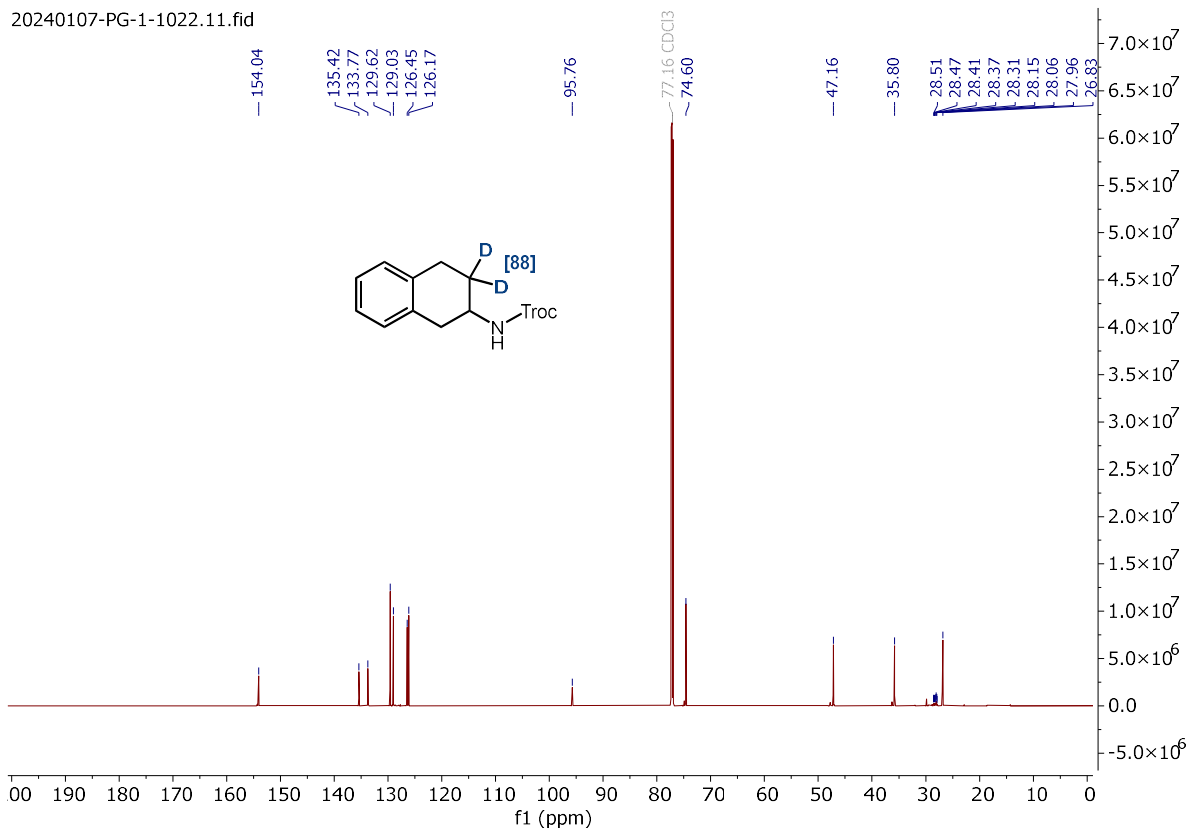


2,2,2-trichloroethyl (1,2,3,4-tetrahydronaphthalen-2-yl-3,3-d2)carbamate (**4.31-d2**):

20231220-PG-1-1022.1.fid

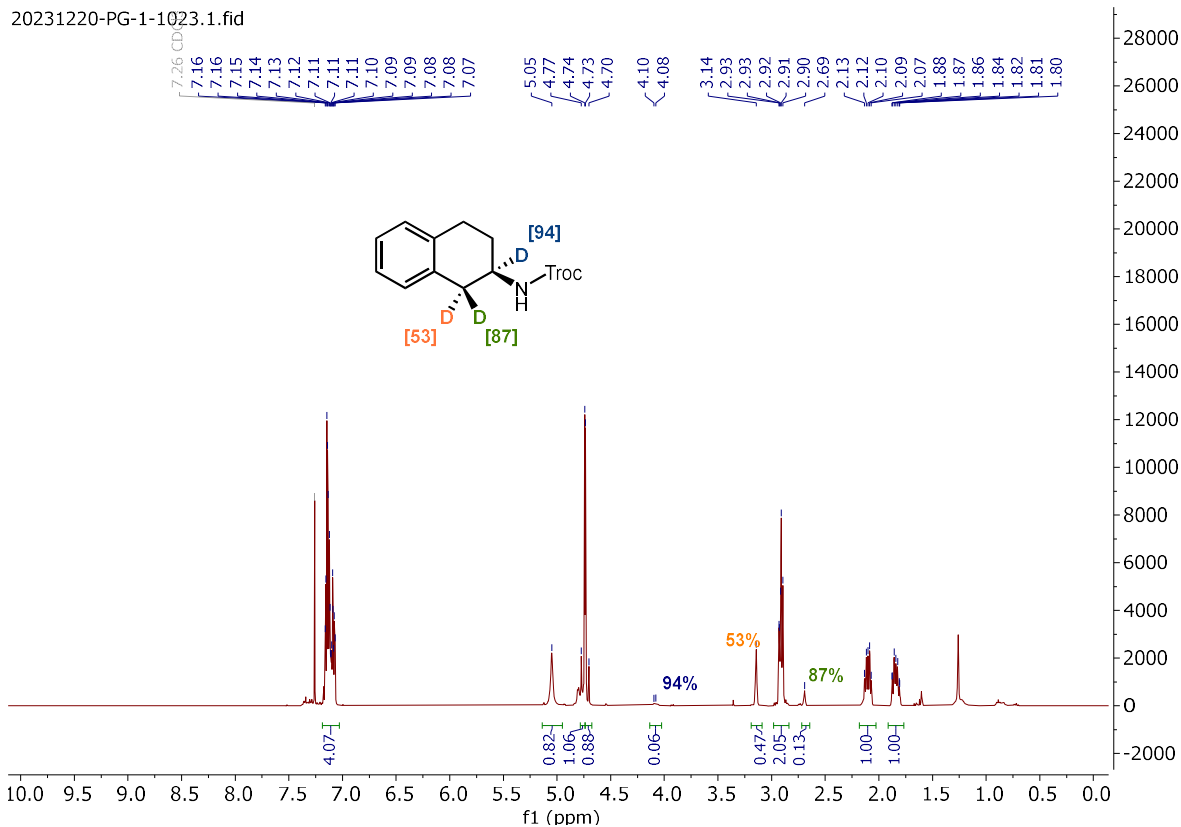


20240107-PG-1-1022.11.fid

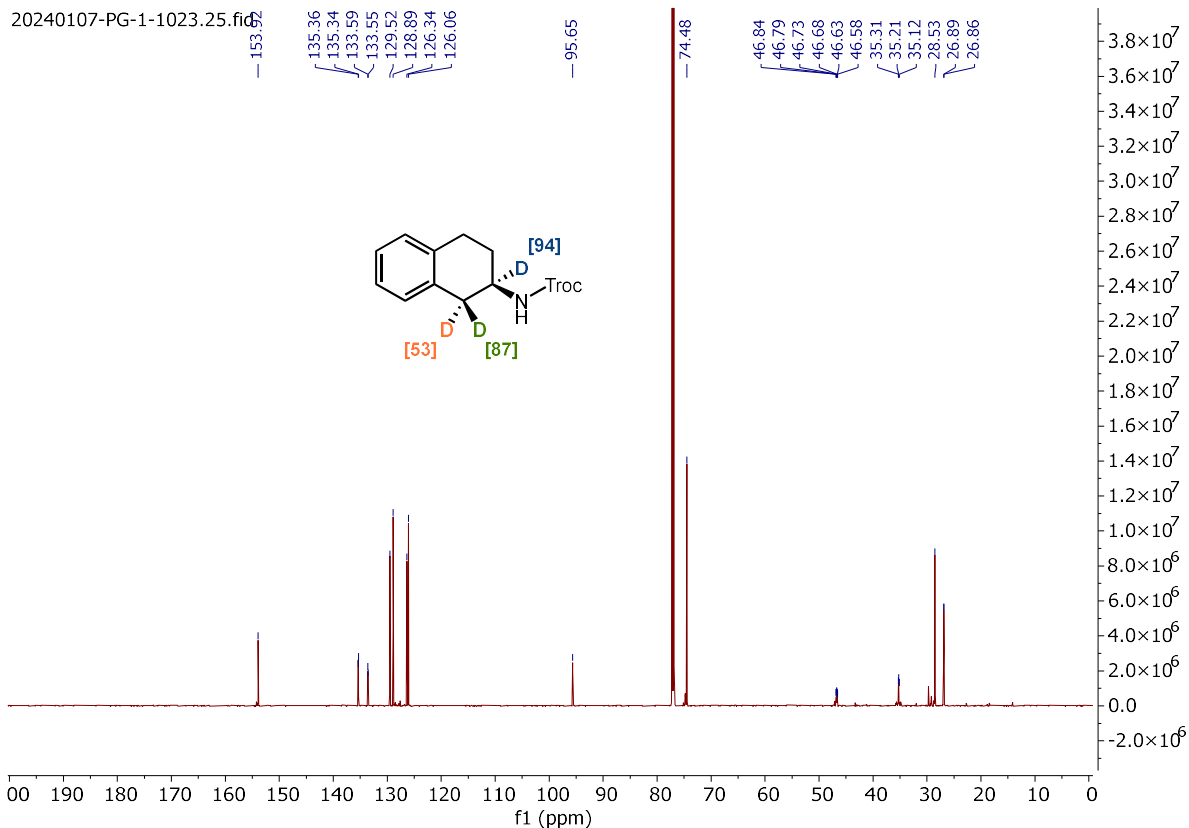


2,2,2-trichloroethyl (1,2,3,4-tetrahydronaphthalen-2-yl-1,1,2-d3)carbamate (**4.31-d3**):

20231220-PG-1-1023.1.fid



20240107-PG-1-1023.25.fid



22,2,2-trichloroethyl (1,2,3,4-tetrahydronaphthalen-2-yl-1-d)carbamate (**4.31-d₁**):

